HANDBOOK OF SPACE ASTRONOMY AND ASTROPHYSICS

By
MARTIN V. ZOMBECK

This page intentionally left blank

HANDBOOK OF SPACE ASTRONOMY AND ASTROPHYSICS

Third Edition

Fully updated and including data from space-based observations, this Third Edition is a comprehensive compilation of the facts and figures relevant to astronomy and astrophysics. As well as a vast number of tables, graphs, diagrams, and formulae, it also includes a comprehensive index and bibliography, allowing readers to easily find the information they require. The book covers a diverse range of topics in addition to astronomy and astrophysics, including atomic physics, nuclear physics, relativity, plasma physics, electromagnetism, mathematics, probability and statistics, and geophysics.

This handbook contains the most frequently used information in modern astrophysics, and is an essential reference for graduate students, researchers and professionals working in astronomy and the space sciences. A website containing extensive supplementary information and databases, maintained by the author, can be found at www.cambridge.org/9780521782425.

MARTIN ZOMBECK was a senior scientist at the High Energy Astrophysics Division of the Harvard-Smithsonian Center for Astrophysics in Cambridge, Massachusetts. He is co-editor of *High Resolution X-ray Spectroscopy of Cosmic Plasmas* (Cambridge University Press, 1990).

HANDBOOK OF SPACE ASTRONOMY AND ASTROPHYSICS

Third Edition

MARTIN V. ZOMBECK

Smithsonian Astrophysical Observatory, Cambridge, USA

CAMBRIDGE
UNIVERSITY PRESS

CAMBRIDGE UNIVERSITY PRESS
Cambridge, New York, Melbourne, Madrid, Cape Town, Singapore, São Paulo

Cambridge University Press
The Edinburgh Building, Cambridge CB2 8RU, UK
Published in the United States of America by Cambridge University Press, New York

www.cambridge.org
Information on this title: www.cambridge.org/9780521782425

First published in print format 2006

ISBN-13 978-0-511-34872-3 eBook (EBL)

ISBN-13 978-0-521-78242-5 hardback

Contents

Some weeks later the Einsteins were taken to the Mt. Wilson Observatory in California. Mrs. Einstein was particularly impressed by the giant telescope. 'What on Earth do they use it for?, she asked. Her host explained that one of its chief purposes was to find out the shape of the Universe. "Oh", said Mrs. Einstein, "my husband does that on the back of an envelope. - Bennett Cerf in "Try and Stop Me".

Foreword

Modern astrophysics requires the use of observations over the broadest range of wavelengths to fully understand the physical nature of the objects and processes we wish to study in the universe.

Data are obtained from ground-based and space-based observations operating in radio, infrared, visible, ultraviolet, x-rays and gamma rays. The design and operation of the instrumentation used to gather this information, the telescopes and detectors themselves, depend on the interaction between matter and radioactivity at the different wavelengths and requires in-depth knowledge of the findings of molecular, atomic, nuclear, and particle physics.

The observer needs to have the data at hand to understand the properties and the limitations of the instrumentation and their relevance to data reduction, analysis, and interpretation.

The theorist who is seeking new models to interpret the findings from the most sensitive and sophisticated observatories that ever existed needs, from time to time, a reality check with what is known.

The *Handbook of Space Astronomy and Astrophysics* gathers in one place the most frequently-used information in modern astrophysics and presents it in the most useful fashion to the non-specialist in a particular field.

I always loved the chapter on relativistic astrophysics and I am glad it has been retained and improved. I am also glad for the new chapters on experimental subjects that bring the Handbook up-to-date.

I am certain that some young person will find here, as I did, useful food for thought and inspiration that he or she will need to design the next generation of telescopes.

Washington, DC
May, 2005

Riccardo Giacconi
Nobel laureate, 2002
Physics

Preface

I have compiled the tables, graphs, diagrams, and formulae in this book in order to provide a ready reference and working tool for the practicing space astronomer and astrophysicist. Ground-based astronomers, students, and advanced amateur astronomers will find much here of interest, too. The material represents a diversified selection based upon the circumstance that the space astronomer and astrophysicist must draw upon knowledge of atomic physics, nuclear physics, relativity, plasma physics, electromagnetism, mathematics, probability and statistics, geophysics, experimental physics, *et cetera,* in addition to the classical branches of astronomy. My hope is that this book will replace hunting through many separate works or a trip to the reference library or to the World Wide Web. In that spirit, I welcome suggestions of material for inclusion in a later edition and, of course, corrections or criticism.

There are 21 chapters in the book. The first chapter contains physical, astronomical, and numerical constants, and unit conversions. Chapters 2-8 cover general astronomy and astrophysics, radio, infrared, ultraviolet, X-ray, and gamma-ray astronomy, and cosmic rays. Chapter 9 contains information on the Earth's atmosphere and environment relevant to space science. Chapter 10 covers special and general relativity and chapter 11 provides relevant information in atomic physics. Electromagnetic radiation and plasma physics are the subjects of chapters 12 and 13. The remaining chapters deal with the tools of the trade, *viz.*, information on radiation and particle interactions, detectors, astronautics, useful mathematical relations, probability and statistics formulae, laboratory radiation safety, a comprehensive list of astronomical catalogs, and computer science. Each chapter ends with a bibliography for further reading on the subject of the chapter and for more extensive reference material. The last chapter contains a glossary of abbreviations and symbols. 11 Appendices contain material that is of a tutorial nature, not suitable for inclusion in the main text, and material suggested recently by reviewers. The book has a complete index.

The question of units is always a problem in a book of this type; sticking to one consistent set (SI, for example) is not very useful to the practitioner; distance to a galaxy in meters, the energy of an X-ray photon in joules, or the pressure of a gas in newton m^{-2} would leave most scientists frustrated. I have tried to use the unit systems common to the particular field. Thus I have used SI (International System of Units), c.g.s., and Gaussian (e.s.u. c.g.s. units); whatever is customary. What is being used is usually noted and whenever the units are not noted, any consistent system will do. If in doubt, perform a numerical check. Besides a complete set of fundamental constants in SI units, I have also provided a subset in c.g.s. units, which are commonly used in the formulae in this book, and unit conversion tables.

I have established and will maintain a Web site at http://www.astrohandbook.com, where I will provide links to supplementary information for each chapter and a list of *errata,* if any. The links will provide extensive data bases, complete online texts and scientific journal articles, tutorials, online interactive programs for converting units, calculating astronomical coordinates, plotting X-ray absorption and reflectivity, symbolic mathematics, and much more. I have avoided, with a few exceptions, listing the URLs (uniform resource locator) of online source material since locations and file names often change.

I wish to acknowledge colleagues for their useful suggestions and encouragement, especially Gerald Austin, Daniel Fabricant, George Field, who suggested that I first publish the handbook as a Smithsonian Astrophysical Observatory Special Report, Jonathan Grindlay, Paul Gorenstein, F. Rick Harnden, Almus Kenter, Ralph Kraft, Jeffrey McClintock, Gary Meehan, Stephen Murray, who first suggested that I publish my set of notes in handbook form, and Daniel Schwartz of the Harvard-Smithsonian Center for Astrophysics, Joachim Truemper of the Max-Planck-Institut für Extraterrestrische Physik (MPE), and Rashid Sunyaev of the Max-Plank-Institut für Astrophysik.

The typesetting in Latex was initially done by Instill Technologies, BE 277 Salt Lake, Kolkata 700064, India. The partners for this company, Sutanu Ghosh and Pijush K. Maiti did a superior job in typesetting the extensive tables and complex formulae of the handbook. The majority of the typesetting and the completion of the project was accomplished by Gautami Maiti and Pijush K. Maiti of Anin, BC 97 Salt Lake, Kolkata 700064, India. I thank Himel Ghosh, formerly of the Harvard-Smithsonian Center for Astrophysics, for suggesting that I work with Drs. Ghosh and Maiti. The fact that they are physicists helped matters considerably.

My son, Richard, provided substantial technical assistance in the last minute preparations of the book for submission to the publisher.

Now that the book is in electronic format, updated versions will be more easily prepared. A searchable, online version of the book is in the works.

Many of the quotations are from “Physically Speaking, a Dictionary of

Quotations on Physics and Astronomy", Carl C. Gaither and Alma E. Cavazos-Gaither, Institute of Physics Publishing, 1997.

Please cite the original source, if you are referencing any of the material in the *Handbook* in research publications.

I have made every effort to cite the sources for the material presented in this book and to obtain permissions, wherever necessary. If I have omitted a citation, please bring it to my attention.

Naples, Florida
March, 2006

Martin V. Zombeck
mvz@alum.mit.edu

Chapter 1

General data

Facts themselves are meaningless. It's only the interpretation we give those facts which counts. - Earl Stanley Gardner

International system of units (SI)

Physical quantity	Name of unit	Symbol
	Base units	
length	meter	m
mass	kilogram	kg
time	second	s
electric current	ampere	A
thermodynamic temperature	kelvin	K
amount of substance	mole	mol
luminous intensity	candela	cd
	Derived units with special names	
plane angle	radian	rad
solid angle	steradian	sr
frequency	hertz	Hz
energy	joule	J
force	newton	N
pressure	pascal	Pa
power	watt	W
electric charge	coulomb	C
electric potential	volt	V
electric resistance	ohm	Ω
electric conductance	siemens	S
electric capacitance	farad	F
magnetic flux	weber	Wb
inductance	henry	H
magnetic flux density	tesla	T
luminous flux	lumen	lm
illuminance	lux	lx
celsius temperature	degree celsius	°C
activity (of a radioactive source)	becquerel	Bq
absorbed dose (of ionizing radiation)	gray	Gy
dose equivalent	sievert	Sv

Fundamental physical constants (SI)

(1986 recommended values of the fundamental physical constants. The digits in parentheses are the one-standard-deviation uncertainty in the last digits of the given value. For the latest recommended values see: http://physics.nist.gov/constants.)

Quantity	Symbol	Value	Units	Relative uncertainty (ppm)
GENERAL CONSTANTS				
UNIVERSAL CONSTANTS				
speed of light in vacuum	c	299 792 458	$\mathrm{m\,s^{-1}}$	(exact)
permeability of vacuum	μ_0	$4\pi \times 10^{-7}$	$\mathrm{N\,A^{-2}}$	
		$= 12.566\,370\,614\ldots$	$10^{-7}\ \mathrm{N\,A^{-2}}$	(exact)
permittivity of vacuum	ϵ_0	$1/\mu_0 c^2$		
		$= 8.854\,187\,817\ldots$	$10^{-12}\ \mathrm{F\,m^{-1}}$	(exact)
Newtonian constant of gravitation	G	6.672 59(85)	$10^{-11}\ \mathrm{m^3\,kg^{-1}\,s^{-2}}$	128
Planck constant	h	6.626 075 5(40)	$10^{-34}\ \mathrm{J\,s}$	0.60
in electron volts, $h/\{e\}$		4.135 669 2(12)	$10^{-15}\ \mathrm{eV\,s}$	0.30
$h/2\pi$	$\hbar$	1.054 572 66(63)	$10^{-34}\ \mathrm{J\,s}$	0.60
in electron volts, $\hbar/\{e\}$		6.582 122 0(20)	$10^{-16}\ \mathrm{eV\,s}$	0.30
Planck mass, $(\hbar c/G)^{\frac{1}{2}}$	m_P	2.176 71(14)	$10^{-8}\ \mathrm{kg}$	64
Planck length, $\hbar/m_P c = (\hbar G/c^3)^{\frac{1}{2}}$	l_P	1.616 05(10)	$10^{-35}\ \mathrm{m}$	64
Planck time, $l_P/c = (\hbar G/c^5)^{\frac{1}{2}}$	t_P	5.390 56(34)	$10^{-44}\ \mathrm{s}$	64

Fundamental physical constants (SI) (*cont.*)

Quantity	Symbol	Value	Units	Relative uncertainty (ppm)
ELECTROMAGNETIC CONSTANTS				
elementary charge	e	1.602 177 33(49)	10^{-19} C	0.30
	e/h	2.417 988 36(72)	10^{14} A J^{-1}	0.30
magnetic flux quantum, $h/2e$	Φ_0	2.067 834 61(61)	10^{-15} Wb	0.30
Josephson frequency-voltage ratio	$2e/h$	4.835 976 7(14)	10^{14} Hz V^{-1}	0.30
quantized Hall conductance	e^2/h	3.874 046 14(17)	10^{-5} S	0.045
quantized Hall resistance, $h/e^2 = \frac{1}{2}\mu_0 c/\alpha$	R_H	25 812.805 6(12)	Ω	0.045
Bohr magneton, $e\hbar/2m_e$	μ_B	9.274 015 4(31)	10^{-24} J T^{-1}	0.34
in electron volts, $\mu_B/\{e\}$		5.788 382 63(52)	10^{-5} eV T^{-1}	0.089
in hertz, μ_B/h		1.399 624 18(42)	10^{10} Hz T^{-1}	0.30
in wavenumbers, μ_B/hc		46.686 437(14)	m^{-1} T^{-1}	0.30
in kelvins, μ_B/k		0.671 709 9(57)	K T^{-1}	8.5
nuclear magneton, $e\hbar/2m_p$	μ_N	5.050 786 6(17)	10^{-27} J T^{-1}	0.34
in electron volts, $\mu_N/\{e\}$		3.152 451 66(28)	10^{-8} eV T^{-1}	0.089
in hertz, μ_N/h		7.622 591 4(23)	MHz T^{-1}	0.30
in wavenumbers, μ_N/hc		2.542 622 81(77)	10^{-2} m^{-1} T^{-1}	0.30
in kelvins, μ_N/k		3.658 246(31)	10^{-4} K T^{-1}	8.5

Fundamental physical constants (SI) (*cont.*)

Quantity	Symbol	Value	Units	Relative uncertainty (ppm)
ATOMIC CONSTANTS				
ATOM				
fine structure constant, $\frac{1}{2}\mu_0 ce^2/h$	α	7.297 353 08(33)	10^{-3}	0.045
inverse fine-structure constant	α^{-1}	137.035 989 5(61)		0.045
Rydberg constant, $\frac{1}{2}m_e c\alpha^2/h$	R_∞	10 973 731.534(13)	m^{-1}	0.0012
in hertz, $R_\infty c$		3.289 841 949 9(39)	10^{15} Hz	0.0012
in joules, $R_\infty hc$		2.179 874 1(13)	10^{-18} J	0.60
in electron volts, $R_\infty hc/\{e\}$		13.605 698 1(40)	eV	0.30
Bohr radius, $\alpha/4\pi R_\infty$	a_0	0.529 177 249(24)	10^{-10} m	0.045
Hartree energy, $e^2/4\pi\epsilon_0 a_0 = 2R_\infty hc$	E_h	4.359 748 2(26)	10^{-18} J	0.60
in electron volts, $E_h/\{e\}$		27.211 396 1(81)	eV	0.30
quantum of circulation	$h/2m_e$	3.636 948 07(33)	10^{-4} $m^2\,s^{-1}$	0.089
	h/m_e	7.273 896 14(65)	10^{-4} $m^2\,s^{-1}$	0.089
ELECTRON				
electron mass	m_e	9.109 389 7(54)	10^{-31} kg	0.59
		5.485 799 03(13)	10^{-4} u	0.023
in electron volts, $m_e c^2/\{e\}$		0.510 999 06(15)	MeV	0.30

Fundamental physical constants (SI) (*cont.*)

Quantity	Symbol	Value	Units	Relative uncertainty (ppm)
electron-muon mass ratio	m_e/m_μ	4.836 332 18(71)	10^{-3}	0.15
electron-proton mass ratio	m_e/m_p	5.446 170 13(11)	10^{-4}	0.020
electron-deuteron mass ratio	m_e/m_d	2.724 437 07(6)	10^{-4}	0.020
electron-α-particle mass ratio	m_e/m_α	1.370 933 54(3)	10^{-4}	0.021
electron specific charge	$-e/m_e$	−1.758 819 62(53)	10^{11} C kg^{-1}	0.30
electron molar mass	$M(e), M_e$	5.485 799 03(13)	10^{-7} kg mol^{-1}	0.023
Compton wavelength, $h/m_e c$	λ_C	2.426 310 58(22)	10^{-12} m	0.089
$\lambda_C/2\pi = \alpha a_0 = \alpha^2/4\pi R_\infty$	$\lambda\!\!\!^{-}_C$	3.861 593 23(35)	10^{-13} m	0.089
classical electron radius, $\alpha^2 a_0$	r_e	2.817 940 92(38)	10^{-15} m	0.13
Thomson cross-section, $(8\pi/3)r_e^2$	σ_e	0.665 246 16(18)	10^{-28} m^2	0.27
electron magnetic moment	μ_e	928.477 01(31)	10^{-26} J T^{-1}	0.34
in Bohr magnetons	μ_e/μ_B	1.001 159 652 193(10)		1×10^{-5}
in nuclear magnetons	μ_e/μ_N	1838.282 000(37)		0.020
electron magnetic moment anomaly, $\mu_e/\mu_B - 1$	a_e	1.159 652 193(10)	10^{-3}	0.0086
electron g-factor, $2(1 + a_e)$	g_e	2.002 319 304 386(20)		1×10^{-5}
electron-muon magnetic moment ratio	μ_e/μ_μ	206.766 967(30)		0.15
electron-proton magnetic moment ratio	μ_e/μ_p	658.210 688 1(66)		0.010

Fundamental physical constants (SI) (*cont.*)

Quantity	Symbol	Value	Units	Relative uncertainty (ppm)
MUON				
muon mass	m_μ	1.883 532 7(11)	10^{-28} kg	0.61
		0.113 428 913(17)	u	0.15
in electron volts, $m_\mu c^2/\{e\}$		105.658 389(34)	MeV	0.32
muon-electron mass ratio	m_μ/m_e	206.768 262(30)		0.15
muon molar mass	$M(\mu), M_\mu$	1.134 289 13(17)	10^{-4} kg mol^{-1}	0.15
muon magnetic moment	μ_μ	4.490 451 4(15)	10^{-26} J T^{-1}	0.33
in Bohr magnetons	μ_μ/μ_B	4.841 970 97(71)	10^{-3}	0.15
in nuclear magnetons	μ_μ/μ_N	8.890 598 1(13)		0.15
muon magnetic moment anomaly, $[\mu_\mu/(e\hbar/2m_\mu)]-1$	a_μ	1.165 923 0(84)	10^{-3}	7.2
muon g-factor, $2(1+a_\mu)$	g_μ	2.002 331 846(17)		0.0084
muon-proton magnetic moment ratio	μ_μ/μ_p	3.183 345 47(47)		0.15
PROTON				
proton mass	m_p	1.672 623 1(10)	10^{-27} kg	0.59
		1.007 276 470(12)	u	0.012
in electron volts, $m_p c^2/\{e\}$		938.272 31(28)	MeV	0.30
proton-electron mass ratio	m_p/m_e	1836.152 701(37)		0.020

Fundamental physical constants (SI) *(cont.)*

Quantity	Symbol	Value	Units	Relative uncertainty (ppm)
proton-muon mass ratio	m_p/m_μ	8.880 244 4(13)		0.15
proton specific charge	e/m_p	9.578 830 9(29)	10^7 C kg^{-1}	0.30
proton molar mass	$M(p), M_p$	1.007 276 470(12)	10^{-3} kg mol^{-1}	0.012
proton Compton wavelength, h/m_pc	$\lambda_{C,p}$	1.321 410 02(12)	10^{-15} m	0.089
$\lambda_{C,p}/2\pi$	$\bar{\lambda}_{C,p}$	2.103 089 37(19)	10^{-16} m	0.089
proton magnetic moment	μ_p	1.410 607 61(47)	10^{-26} J T^{-1}	0.34
in Bohr magnetons	μ_p/μ_B	1.521 032 202(15)	10^{-3}	0.010
in nuclear magnetons	μ_p/μ_N	2.792 847 386(63)		0.023
diamagnetic shielding correction for protons in pure water, spherical sample, 25°C, $1-\mu'_p/\mu_p$	σ_{H_2O}	25.689(15)	10^{-6}	–
shielded proton moment (H_2O, sph., 25°C)	μ'_p	1.410 571 38(47)	10^{-26} J T^{-1}	0.34
in Bohr magnetons	μ'_p/μ_B	1.520 993 129(17)	10^{-3}	0.011
in nuclear magnetons	μ'_p/μ_N	2.792 775 642(64)		0.023
proton gyromagnetic ratio	γ_p	26 752.2128(81)	10^4 s^{-1} T^{-1}	0.30
	$\gamma_p/2\pi$	42.577 469(13)	MHz T^{-1}	0.30
uncorrected (H_2O, sph., 25°C)	γ'_p	26 751.5255(81)	10^4 s^{-1} T^{-1}	0.30
	$\gamma'_p/2\pi$	42.576 375(13)	MHz T^{-1}	0.30

Fundamental physical constants (SI) (*cont.*)

Quantity	Symbol	Value	Units	Relative uncertainty (ppm)
NEUTRON				
neutron mass	m_n	1.674 928 6(10)	10^{-27} kg	0.59
		1.008 664 904(14)	u	0.014
in electron volts, $m_n c^2/\{e\}$		939.565 63(28)	MeV	0.30
neutron-electron mass ratio	m_n/m_e	1838.683 662(40)		0.022
neutron-proton mass ratio	m_n/m_p	1.001 378 404(9)		0.009
neutron molar mass	$M(n), M_n$	1.008 664 904(14)	10^{-3} kg mol^{-1}	0.014
neutron Compton wavelength, $h/m_n c$	$\lambda_{C,n}$	1.319 591 10(12)	10^{-15} m	0.089
$\lambda_{C,n}/2\pi$	$\lambdabar_{C,n}$	2.100 194 45(19)	10^{-16} m	0.089
neutron magnetic moment[(a)]	μ_n	0.966 237 07(40)	10^{-26} J T^{-1}	0.41
in Bohr magnetons	μ_n/μ_B	1.041 875 63(25)	10^{-3}	0.24
in nuclear magnetons	μ_n/μ_N	1.913 042 75(45)		0.24
neutron-electron magnetic moment ratio	μ_n/μ_e	1.040 668 82(25)	10^{-3}	0.24
neutron-proton magnetic moment ratio	μ_n/μ_p	0.684 979 34(16)		0.24
DEUTERON				
deuteron mass	m_d	3.343 586 0(20)	10^{-27} kg	0.59
		2.013 553 214(24)	u	0.012
in electron volts, $m_d c^2/\{e\}$		1875.613 39(57)	MeV	0.30
deuteron-electron mass ratio	m_d/m_e	3670.483 014(75)		0.020

Fundamental physical constants (SI) (*cont.*)

Quantity	Symbol	Value	Units	Relative uncertainty (ppm)
deuteron-proton mass ratio	m_d/m_p	1.999 007 496(6)		0.003
deuteron molar mass	$M(d), M_d$	2.013 553 214(24)	10^{-3} kg mol^{-1}	0.012
deuteron magnetic moment[(a)]	μ_d	0.433 073 75(15)	10^{-26} J T^{-1}	0.34
in Bohr magnetons	μ_d/μ_B	0.466 975 447 9(91)	10^{-3}	0.019
in nuclear magnetons	μ_d/μ_N	0.857 438 230(24)		0.028
deuteron-electron magnetic moment ratio	μ_d/μ_e	0.466 434 546 0(91)	10^{-3}	0.019
deuteron-proton magnetic moment ratio	μ_d/μ_p	0.307 012 203 5(51)		0.017
PHYSICO-CHEMICAL CONSTANTS				
Avogadro constant	N_A, L	6.022 136 7(36)	10^{23} mol^{-1}	0.59
atomic mass constant, $m_u = \frac{1}{12}m(^{12}C)$	m_u	1.660 540 2(10)	10^{-27} kg	0.59
in electron volts, $m_u c^2/\{e\}$		931.494 32(28)	MeV	0.30
Faraday constant	F	96 485.309(29)	C mol^{-1}	0.30
molar Planck constant	$N_A h$	3.990 313 23(36)	10^{-10} J s mol^{-1}	0.089
	$N_A hc$	0.119 626 58(11)	J m mol^{-1}	0.089
molar gas constant	R	8.314 510(70)	J mol^{-1} K^{-1}	8.4

[(a)] The scalar magnitude of the deuteron moment is listed here. The neutron magnetic dipole is directed oppositely to that of the proton, and corresponds to the dipole associated with a spinning negative charge distribution. The vector sum, $\mu_d = \mu_p + \mu_n$, is approximately satisfied.

Fundamental physical constants (SI) (*cont.*)

Quantity	Symbol	Value	Units	Relative uncertainty (ppm)
Boltzmann constant, R/N_A	k	1.380 658(12)	10^{-23} J K^{-1}	8.5
in electron volts, $k/\{e\}$		8.617 385(73)	10^{-5} eV K^{-1}	8.4
in hertz, k/h		2.083 674(18)	10^{10} Hz K^{-1}	8.4
in wavenumbers, k/hc		69.503 87(59)	m^{-1} K^{-1}	8.4
molar volume (ideal gas), RT/p				
$T = 273.15$ K, $p = 101\,325$ Pa	V_m	22.414 10(19)	L mol^{-1}	8.4
Loschmidt constant, N_A/V_m	n_0	2.686 763(23)	10^{25} m^{-3}	8.5
$T = 273.15$ K, $p = 100$ kPa	V_m	22.711 08(19)	L mol^{-1}	8.4
Sackur-Tetrode constant (absolute entropy constant),(b) $\frac{5}{2} + \ln\{(2\pi m_u kT_1/h^2)^{\frac{3}{2}} kT_1/p_0\}$				
$T_1 = 1$ K, $p_0 = 100$ kPa	S_0/R	−1.151 693(21)		18
$p_0 = 101\,325$ Pa		−1.164 856(21)		18
Stefan-Boltzmann constant, $(\pi^2/60)k^4/\hbar^3 c^2$	σ	5.670 51(19)	10^{-8} W m^{-2} K^{-4}	34
first radiation constant, $2\pi hc^2$	c_1	3.741 774 9(22)	10^{-16} W m^2	0.60
second radiation constant, hc/k	c_2	0.014 387 69(12)	m K	8.4
Wien displacement law constant, $b = \lambda_{\max} T = c_2/4.965\,114\,23\ldots$	b	2.897 756(24)	10^{-3} m K	8.4

(b) The entropy of an ideal monoatomic gas of relative atomic weight A_r is given by $S = S_0 + \frac{3}{2} R \ln A_r - R \ln(p/p_0) + \frac{5}{2} R \ln(T/K)$.

Fundamental physical constants (SI) (*cont.*)

MAINTAINED UNITS AND STANDARD VALUES

A summary of 'maintained' units and 'standard' values and their relationship to SI units, based on a least-squares adjustment with 17 degrees of freedom. The digits in parentheses are the one-standard-deviation uncertainty in the last digits of the given value.

Quantity	Symbol	Value	Units	Relative uncertainty (ppm)
electron volt, $(e/C)\ \mathrm{J} = \{e\}\ \mathrm{J}$	eV	1.602 177 33(49)	10^{-19} J	0.30
(unified) atomic mass unit,				
$1\ \mathrm{u} = m_\mathrm{u} = \frac{1}{12}m(^{12}C)$	u	1.660 540 2(10)	10^{-27} kg	0.59
standard atmosphere	atm	101 325	Pa	(exact)
standard acceleration of gravity	g_n	9.806 65	$\mathrm{m\,s^{-2}}$	(exact)
'AS-MAINTAINED' ELECTRICAL UNITS				
BIPM[a] maintained ohm, $\Omega_{69-\mathrm{BI}}$				
$\Omega_{\mathrm{BI85}} \equiv \Omega_{69-\mathrm{BI}}$ (1 Ja 1985)	Ω_{BI85}	$1 - 1.563(50) \times 10^{-6}$	Ω	
		$= 0.999\,998\,437(50)$	Ω	0.050
drift rate of $\Omega_{69-\mathrm{BI}}$	$\frac{d\Omega_{69-\mathrm{BI}}}{dt}$	$-0.0566(15)$	$\mu\Omega/a$	–
BIPM maintained volt,	$V_{76-\mathrm{BI}}$	$1 - 7.59(30) \times 10^{-6}$	V	
$V_{76-\mathrm{BI}} = 483\,594\ \mathrm{GHz}(h/2e)$		$= 0.999\,992\,41(30)$	V	0.30

Fundamental physical constants (SI) (*cont.*)

Quantity	Symbol	Value	Units	Relative uncertainty (ppm)
BIPM maintained ampere,	A_{BI85}	$1 - 6.03(30) \times 10^{-6}$	A	
$A_{\mathrm{BIPM}} = V_{76-\mathrm{BI}}/\Omega_{69-\mathrm{BI}}$		$= 0.999\,993\,97(30)$	A	0.30
X-RAY STANDARDS				
Cu x-unit: $\lambda(\mathrm{CuK}\alpha_1) \equiv 1537.400$ xu	$\mathrm{xu}(\mathrm{CuK}\alpha_1)$	$1.002\,077\,89(70)$	10^{-13} m	0.70
Mo x-unit: $\lambda(\mathrm{MoK}\alpha_1) \equiv 707.831$ xu	$\mathrm{xu}(\mathrm{MoK}\alpha_1)$	$1.002\,099\,38(45)$	10^{-13} m	0.45
Å*:$\lambda(\mathrm{WK}\alpha_1) \equiv 0.209\,100$ Å*	Å*	$1.000\,014\,81(92)$	10^{-10} m	0.92
lattice spacing of Si				
(in vacuum, 22.5°C)[b]	a	$0.543\,101\,96(11)$	nm	0.21
$d_{220} = a/\sqrt{8}$	d_{220}	$0.192\,015\,540(40)$	nm	0.21
molar volume of Si,				
$M(\mathrm{Si})/\rho(\mathrm{Si}) = N_A a^3/8$	$V_m(\mathrm{Si})$	$12.058\,817\,9(89)$	$\mathrm{cm^3\,mol^{-1}}$	0.74

[a] BIPM: Bureau International des Poids et Mésures.

[b] The lattice spacing of single-crystal Si can vary by parts in 10^7 depending on the preparation process. Measurements at Physikalisch-Technische Bundesanstalt (FRG) indicate also the possibility of distortions from exact cubic symmetry of the order of 0.2 ppm.

A short list of fundamental physical constants (c.g.s.)

Speed of light in vacuum	$c = 2.997\,924\,58 \times 10^{10}$ cm s^{-1}
Gravitational constant	$G = 6.672\,59 \times 10^{-8}$ dyn cm^2 g^{-2}
Planck's constant	$h = 6.626\,075\,5 \times 10^{-27}$ erg s
Electron charge	$e = 4.803\,206\,8 \times 10^{-10}$ esu
Mass of electron	$m_e = 9.109\,389\,7 \times 10^{-28}$ g
Mass of proton	$m_p = 1.672\,623\,1 \times 10^{-24}$ g
Mass of neutron	$m_n = 1.674\,928\,6 \times 10^{-24}$ g
Atomic mass unit (amu)	$m_u = 1.660\,540\,2 \times 10^{-24}$ g
Proton-electron mass ratio	$m_p/m_e = 1\,836.152\,701$
Fine structure constant	$hc/2\pi e^2 = 1/\alpha = 137.035\,989\,5$
Classical electron radius	$e^2/m_e c^2 = r_e = 2.817\,940\,92 \times 10^{-13}$ cm
Bohr radius	$h^2/4\pi^2 m_e e^2 = a_0$ $= 0.529\,177\,249 \times 10^{-8}$ cm
Electron Compton wavelength	$h/m_e c = \lambda_c = 2.426\,310\,58 \times 10^{-10}$ cm
Rydberg constant	$2\pi^2 m_e e^4/ch^3 = R_\infty = 109\,737.315\,34$ cm^{-1}
Boltzmann constant	$k = 1.380\,658 \times 10^{-16}$ erg K^{-1}
Stefan-Boltzmann constant	$\sigma = 2\pi^5 k^4/15h^3c^2$ $= 5.670\,51 \times 10^{-5}$ erg cm^{-2} K^{-4} s^{-1}
Thomson cross-section	$8\pi r_e^2/3 = {}_e\sigma = 0.665\,246\,16 \times 10^{-24}$ cm^2
Bohr magneton	$eh/4\pi m_e = \mu_B$ $= 9.274\,015\,4 \times 10^{-21}$ gauss cm^3
Permeability of vacuum	$\mu_0 = 1$
Permittivity of vacuum	$\varepsilon_0 = 1$
Magnetic flux quantum $h/2e$	$\Phi_0 = 2.067\,834\,61 \times 10^{-7}$ M (maxwell)
Quantized Hall conductance e^2/h	$G_0 = 3.482\,767\,48 \times 10^7$ statS
Avogadro constant	$N_A,\ L = 6.022\,136\,7 \times 10^{23}$ mol^{-1}
Faraday constant $N_A e$	$F = 2.892\,556\,8 \times 10^{14}$ esu mol^{-1}
Molar gas constant	$R = 8.314\,510 \times 10^7$ erg mol^{-1} K^{-1}
Electron volt	eV $= 1.602\,177\,33 \times 10^{-12}$ erg
(unified) atomic mass unit	$1\ u = m_u = \mathrm{m}(^{12}\mathrm{C})/12$ $= 1.660\,540\,2 \times 10^{-24}$ g

(Based on constants recommended by the 1986 CODATA Committee in previous table.)

Sun-Earth system constants

Sun (Best Estimate)	
Radius	6.96×10^8 m
Semidiameter at mean distance	$15'59''.63 = 959''.63$
Mass	1.9891×10^{30} kg
Mean density	1.41×10^3 kg m^{-3}
Surface gravity	2.74×10^2 m s^{-2}
Motion relative to nearby stars	1.94×10^4 m s^{-1}
Period of synodic rotation (ϕ = latitude)	$26.90 + 5.2 \sin^2 \phi$ days
Period of sidereal rotation	25.38 days
Earth (IAU System)	
Equatorial radius for Earth	$a = 6378140$ m
Dynamical form-factor for Earth	$J_2 = 0.001\,082\,63$
Flattening of Earth	$1/f = 298.257$
Polar radius	$b = 6356755$ m
Mass of the Earth	$M = 5.9742 \times 10^{24}$ kg
Mean density	5.52×10^3 kg m^{-3}
Normal gravity (g) (ϕ = latitude)	$9.806\,21 - 0.025\,93 \cos 2\phi + 0.000\,03 \cos 4\phi$ m s^{-2}
Rotation period with respect to fixed stars	
in mean sidereal time	$24^{\rm h}00^{\rm m}00^{\rm s}.008\,4$
in mean solar time	$23^{\rm h}56^{\rm m}04^{\rm s}.098\,9$
Rate of rotation	$15''.041\,067\,178\,669\,10$ s^{-1}
Annual rate of precession (T in centuries from J2000.0)	
general precession in longitude	$50''.290\,966 + 0''.022\,222\,6$T
Constant of nutation (J2000.0)	$N = 9''.202\,5$
Solar parallax	$8''.794\,148$
Constant of Aberration (J2000.0)	$20''.495\,52$
Light-time for 1 AU	499.004 782 s
1 AU	$1.495\,787\,0 \times 10^{11}$ m
Mean eccentricity of orbit	0.016 708 617
Obliquity of the ecliptic (T in centuries from J2000.0)	$23°26'21''.448 - 46''.815$T
Mean Earth-Sun distance	1.000 001 017 8 AU
Mean orbital speed	$29.785\,9 \times 10^3$ m s^{-1}
Sun/Earth mass ratio	332946.0
Moon/Earth mass ratio	0.012 300 2
Mean lunar distance	3.844×10^8 m
Time	
1 day = 24 hours = 1440 minutes = 86400 seconds	
1 Julian year = 365.25 days = 8766 hours = 525960 minutes = 31557600 seconds	
Tropical year (J2000.0) (equinox to equinox)	365.242 days

The Earth-Sun Lagrange points are discussed in Chapter 15.

(From Seidelmann, P.K., *Explanatory Supplement to the Astronomical Almanac,* University Science Books, Mill Valley, CA, 1990)

Additional data can be found in Chapters 2 and 9.

Cosmological data

Hubble constant	$H_0 = 70 \pm 7 \text{ km s}^{-1} \text{ Mpc}^{-1}$ (1999, HST Key Project Team) $= (2.3 \pm 0.2) \times 10^{-18} \text{ s}^{-1}$
Hubble time	$1/H_0 = (4.3 \pm 0.4) \times 10^{17} \text{ s}$ $= (14 \pm 1) \times 10^9$ years
Hubble distance	$R = c/H_0 = (4.3 \pm 0.4) \times 10^3 \text{ Mpc}$ $= (1.3 \pm 0.1) \times 10^{26} \text{ m}$
Critical density	$\rho_c = 3H_0^2/8\pi G$ $= (9.5 \pm 1) \times 10^{-27} \text{ kg m}^{-3}$
Volume	$4\pi R^3/3 = (3.3 \pm 0.3) \times 10^{11} \text{ Mpc}^3$ $= (9.2 \pm 0.9) \times 10^{78} \text{ m}^3$
Smoothed density of galactic material throughout universe (Allen 1973)	$2 \times 10^{-31} \text{ g cm}^{-3}$ $= 2 \times 10^{-28} \text{ kg m}^{-3}$ $1 \times 10^{-7} \text{ atom cm}^{-3}$ $= 1 \times 10^{-1} \text{ atom m}^{-3}$ $3 \times 10^9 \text{ M}_\odot \text{ Mpc}^{-3}$
Space density of galaxies	0.02 Mpc^{-3}
Luminous emission from galaxies	$3 \times 10^8 \text{ L}_\odot \text{ Mpc}^{-3}$
Mean sky brightness from galaxies	$1.4\ (m_v = 10) \text{ deg}^{-2}$
Cosmic background thermodynamic temperature	2.728 ± 0.002 K (COBE)
Energy density of cosmic background radiation (CBR)	$0.261\,53(T/2.728)^4 \text{ eV cm}^{-3}$ $4.190\,17 \times 10^{-14}(T/2.728)^4$ joule m^{-3}
Number density of CBR	$411.87 \text{ cm}^{-3} = 4.118\,7 \times 10^8 \text{ m}^{-3}$
Energy density of relativistic particles	$0.439\,72 \text{ eV cm}^{-3}$ $= 7.045\,09 \times 10^{-14}$ joule m^{-3}
Weak coupling constant	$g_{wk} = 1.435 \times 10^{-49} \text{ erg cm}^3$ $= 1.435 \times 10^{-62}$ joule m^3

(See Chapter 10 and http://pdg.lbl.gov/2002/astrorpp.pdf for additional data.)

Unit conversions

1 keV: $hc/E = 12.398\,54 \times 10^{-8}$ cm
1 keV: $E/h = 2.417\,965 \times 10^{17}$ Hz
1 keV: $E/k = 11.6048 \times 10^{6}$ K
1 keV $= 1.602177 \times 10^{-9}$ erg $= 1.602\,177 \times 10^{-16}$ joule
1 joule $= 10^{7}$ erg
1 calorie $= 4.184$ joule
1.0 EHz: $h\nu = 4.135\,71$ keV
1 parsec $= 3.261\,633$ light years $= 3.085\,678 \times 10^{18}$ cm $= 3.085\,678 \times 10^{16}$ m
1 light year $= 9.460\,530 \times 10^{17}$ cm $= 9.460\,530 \times 10^{15}$ m
1 XU $= 1.002\,09 \times 10^{-11}$ cm $= 1.002\,09 \times 10^{-13}$ m
1 Ångstrom $\equiv 1 \times 10^{-8}$ cm $= 1 \times 10^{-10}$ m
1 amu: $Mc^2 = 1.492\,41 \times 10^{-3}$ erg $= 931.494$ MeV $= 1.492\,41 \times 10^{-10}$ joule
760 torr $= 1.013 \times 10^{6}$ dyn cm^{-2} $= 1$ atmos. $= 1.013$ bars $= 1.013 \times 10^{5}$ pascals
1 Rayleigh $\equiv (1/4\pi) \times 10^{6}$ photons cm^{-2}s^{-1}sr^{-1}
1 Uhuru ct s^{-1} $= 1.7 \times 10^{-11}$ erg cm^{-2} s^{-1} (2 – 6 keV) $= 2.4 \times 10^{-11}$ erg cm^{-2} s^{-1} (2 – 10 keV)
X-ray source intensity in millicrabs =

$$10^3 \int_{E_1}^{E_2} E(dN/dE)dE \Big/ \int_{E_1}^{E_2} E(dN/dE)_{\mathrm{Crab}} dE$$

dN/dE and $(dN/dE)_{\mathrm{Crab}}$ are the source and Crab Nebula photon spectral flux density, respectively.

For $E_2 = 10$ keV and $E_1 = 2$ keV,

$$\int_{E}^{E_2} E(dN/dE)_{\mathrm{Crab}} dE = 2.3 \times 10^{-8} \text{ erg cm}^{-2} \text{ s}^{-1}$$

Crab spectrum is from Chapter 6.

1 flux unit $\equiv 10^{-26}$ watt m^{-2}Hz^{-1} $\equiv 1$ Jansky
1.0 μJy $= 10^{-11}$ erg cm^{-2} s^{-1} EHz^{-1} $= 0.242 \times 10^{-11}$ erg cm^{-2} s^{-1} keV^{-1} $= 1.509 \times 10^{-3}$ keV cm^{-2} s^{-1} keV^{-1}
1 curie: amount of material undergoing 3.7×10^{10} disintegrations s^{-1}
1 nautical mile $= 1852$ m
1 statute mile $= 1609.344$ m
intensity (erg cm^{-2} s^{-1} Hz^{-1}) $= 3.33 \times 10^{-19}\lambda^2$ (Å) intensity (erg cm^{-2} s^{-1} Å^{-1})
1 barn $= 10^{-24}$ cm^2 $= 10^{-28}$ m^2
1 tesla $= 10^{4}$ gauss
$0°$C $= 273.15$ K

Conversion tables

(A given amount of a physical quantity, expressed in the units of one system, is expressed as an equivalent number of units in another system.)

Quantity	Amount	Unit		Amount	Unit
LENGTH					
	1	meter (SI)	=	1.000 00E + 02	centimeter (cgs)
	1	light year	=	9.460 53E + 15	meter (SI)
	1	parsec	=	3.085 68E + 16	meter (SI)
	1	Ångstrom	=	1.000 01E − 10	meter (SI)
	1	Ångstrom	=	1.000 01E − 08	centimeter (cgs)
	1	micron	=	1.000 00E − 06	meter (SI)
	1	nanometer	=	1.000 00E − 09	meter (SI)
	1	XU	=	1.002 09E − 13	meter (SI)
	1	fermi	=	1.000 00E − 15	meter (SI)
	1	nautical mile	=	1.852 00E + 03	meter (SI)
	1	statute mile	=	1.609 34E + 03	meter (SI)
	1	astron. unit (AU)	=	1.495 98E + 11	meter (SI)
	1	solar radius	=	6.959 90E + 08	meter (SI)
	1	centimeter (cgs)	=	3.240 78E − 19	parsec
	1	centimeter (cgs)	=	6.684 56E − 14	astron. unit (AU)
	1	meter (SI)	=	3.240 78E − 17	parsec
	1	meter (SI)	=	6.684 54E − 12	astron. unit (AU)
	1	inch (Eng)	=	2.540 00E − 02	meter (SI)
VOLUME					
	1	fluid ounce (US)	=	2.957 353E − 05	$meter^3$ (SI)
	1	ft^3	=	2.831 685E − 02	$meter^3$ (SI)
	1	in^3	=	1.638 706E − 05	$meter^3$ (SI)
	1	gallon (US)	=	3.785 412E − 03	$meter^3$ (SI)
	1	gallon (US)	=	3.785 412E00	liter

Conversion tables (*cont.*)

Quantity	Amount	Unit	Amount	Unit
	1	gallon (US) =	4.000	quart
	1	quart =	2.000	pint
	1	liter =	1.000 000E − 03	meter^3 (SI)
	1	barrel =	1.589 873E − 01	meter^3 (SI)
	1	cup =	2.366E + 02	mL
	1	yd^3 =	7.645 549E − 01	meter^3 (SI)
MASS				
	1	kilogram (SI) =	1.000 00E + 03	gram (cgs)
	1	at. mass unit (amu) =	1.660 54E − 24	gram (cgs)
	1	at. mass unit (amu) =	1.660 54E − 27	kilogram (SI)
	1	solar mass =	1.989 10E + 33	gram (cgs)
	1	solar mass =	1.989 10E + 30	kilogram (SI)
	1	gram (cgs) =	6.02214E + 23	at. mass unit (amu)
	1	gram (cgs) =	5.027 40E − 34	solar mass
	1	kilogram (SI) =	6.022 14E + 26	at. mass unit (amu)
	1	kilogram (SI) =	5.027 40E − 31	solar mass
	1	kilogram (SI) =	2.204 62E + 00	pound (avdp.)
	1	kilogram (SI) =	3.527 40E + 01	ounce (avdp.)
	1	pound (avdp.) =	4.535 92E − 01	kilogram (SI)
	1	pound (avdp.) =	1.600 00E + 01	ounce (avdp.)
	1	ounce (avdp.) =	2.834 95E + 01	gram (cgs)
	1	gram (cgs) =	3.527 40E − 02	ounce (avdp.)
	1	ounce (troy) =	3.110 35E + 01	gram (cgs)
	1	gram (cgs) =	3.215 07E − 02	ounce (troy)
ENERGY				
	1	joule (SI) =	1.000 00E + 07	erg (cgs)
	1	joule (SI) =	6.241 51E + 18	electron volt (eV)

Conversion tables *(cont.)*

Quantity	Amount	Unit		Amount	Unit
	1	erg (cgs)	=	1.000 00E − 07	joule (SI)
	1	erg (cgs)	=	6.241 51E + 11	electron volt
	1	electron volt	=	1.602 18E − 12	erg (cgs)
	1	amu × c^2	=	9.314 95E + 08	electron volt
	1	gm (cgs) × c^2	=	5.609 59E + 32	electron volt
	1	calorie	=	4.184 00E + 00	joule (SI)
FORCE					
	1	newton (SI)	=	1.000 00E + 05	dyne (cgs)
	1	dyne (cgs)	=	1.000 00E − 05	newton (SI)
	1	pound force	=	4.448 22E + 00	newton (SI)
	1	newton (SI)	=	2.248 09E − 01	pound force
PRESSURE					
	1	pascal (SI)	=	1.000 00E + 00	newton m^{-2} (SI)
	1	bar	=	1.000 00E + 06	dyne cm^{-2} (cgs)
	1	bar	=	9.869 23E − 01	atmosphere
	1	torr	=	1.333 22E − 03	bar
	1	psi	=	6.894 76E + 03	pascal (SI)
	1	pascal	=	1.450 38E − 04	psi
	1	psi	=	6.894 76E − 02	bar
	1	psi	=	5.171 49E + 01	torr
POWER					
	1	watt (SI)	=	1.000 00E + 07	erg s^{-1} (cgs)
	1	horsepower	=	7.457 00E + 02	watt (SI)
	1	Btu s^{-1} (Eng)	=	1.055 80E + 03	watt (SI)

Conversion tables *(cont.)*

Quantity	Amount	Unit Amount	Unit
TIME			
	1	second (SI) = 1	second (cgs)
	1	minute = 6.000 00E + 01	second
	1	hour = 3.600 00E + 03	second
	1	day = 8.640 00E + 04	second
	1	tropical year = 3.155 69E + 07	second
	1	tropical year = 3.652 42E + 02	day
	1	second = 3.168 88E − 08	tropical year
	1	sidereal second = 9.972 70E − 01	second (SI)
	1	sidereal year = 3.652 56E + 02	day
TEMPERATURE			
	T	kelvin = $T - 273.15$	celsius
	T	kelvin = $(9/5) \times (T - 273.15) + 32$	fahrenheit
	T	celsius = $T + 273.15$	kelvin
	T	fahrenheit = $(5/9) \times (T - 32) + 273.15$	kelvin
	T	celsius = $(9/5) \times T + 32$	fahrenheit
	T	fahrenheit = $(5/9) \times (T - 32)$	celsius
Energy equivalence	1	electron volt : 1.160 48E + 04	kelvin
Temperature equivalence	1	kelvin : 8.617 12E − 05	electron volt
ELECTRICITY AND MAGNETISM			
Charge	1	coulomb = 2.997 92E + 09	statcoulomb
Charge density	1	coulomb m^{-3} = 2.997 92E + 03	statcoul cm^{-3}
Current	1	ampere (coul s^{-1}) = 2.997 92E + 09	statampere
Current density	1	ampere m^{-2} = 2.997 92E + 05	statamp cm^{-2}
Electric field	1	volt m^{-1} = 3.335 65E − 05	statvolt cm^{-1}
Potential	1	volt = 3.335 65E − 03	statvolt

Conversion tables *(cont.)*

Quantity	Amount	Unit Amount	Unit
Resistance	1	ohm = 1.112 65E − 12	s cm^{-1}
Resistivity	1	ohm m = 1.112 65E − 10	s
Conductance	1	siemens, mho = 8.987 52E + 11	cm s^{-1}
Conductivity	1	mho m^{-1} = 8.987 52E + 09	s^{-1}
Capacitance	1	farad = 8.987 52E + 11	cm
Magnetic flux	1	weber = 1.000 00E + 08	gauss cm^2 (maxwell)
Magnetic flux density	1	tesla = 1.000 00E + 04	gauss
Magnetic field	1	ampere-turn m^{-1} = 1.256 64E − 02	oersted
Inductance	1	henry = 1.112 65E − 12	s^2 cm^{-1}
MISCELLANEOUS			
Radio-activity	1	curie (SI) = 3.700 00E + 10	disinteg. s^{-1}
Intensity	1	rayleigh = 7.957 75E + 04	ph cm^{-2} s^{-1} sr^{-1}
Flux density	1	fu or jansky = 1.000 00E − 26	watt m^{-2} Hz^{-1}
Flux density	1	jansky = 1.000 00E − 05	erg cm^{-2} s^{-1} EHz^{-1}
Flux density	1	jansky = 2.417 97E − 06	erg cm^{-2} s^{-1} keV^{-1}
Flux density	1	jansky = 1.509 00E + 03	keV cm^{-2} s^{-1} keV^{-1}
Energy equivalence	1	eV : 1.239 85E + 04	Ångstrom
Energy equivalence	1	eV : 2.417 97E + 14	Hz
Wavelength equivalence	1	Ångstrom : 1.239 85E + 04	eV
Angle	1	arcsec = 4.848 14E − 06	radian
Angle	1	arcmin = 2.908 88E − 04	radian
Angle	1	degree = 1.745 33E − 02	radian
Solid angle	1	$arcsec^2$ = 2.350 40E − 11	steradian
Solid angle	1	$arcmin^2$ = 8.461 70E − 08	steradian
Solid angle	1	deg^2 = 3.046 20E − 04	steradian

Energy unit conversion

TO → FROM ↓	λ(Å)	$\lambda(\mu m)$	λ(cm)	ν(Hz)	E(keV)	$\tilde{\nu}(cm^{-1})$	E(erg)
λ(Å)	1	$10^{-4}\lambda$	$10^{-8}\lambda$	$3.00 \times 10^{18}/\lambda$	$12.4/\lambda$	$10^{8}/\lambda$	$1.99 \times 10^{-8}/\lambda$
$\lambda(\mu m)$	$10^{4}\lambda$	1	$10^{-4}\lambda$	$3.00 \times 10^{14}/\lambda$	$1.24 \times 10^{-3}/\lambda$	$10^{4}/\lambda$	$1.99 \times 10^{-12}/\lambda$
λ(cm)	$10^{8}\lambda$	$10^{4}\lambda$	1	$3.00 \times 10^{10}/\lambda$	$1.24 \times 10^{-7}/\lambda$	$1/\lambda$	$1.99 \times 10^{-16}/\lambda$
ν(Hz)	$3.00 \times 10^{18}/\nu$	$3.00 \times 10^{14}/\nu$	$3.00 \times 10^{10}/\nu$	1	$4.14 \times 10^{-18}\nu$	$3.34 \times 10^{-11}\nu$	$6.63 \times 10^{-27}\nu$
E(keV)	$12.4/E$	$1.24 \times 10^{-3}/E$	$1.24 \times 10^{-7}/E$	$2.42 \times 10^{17}E$	1	$8.07 \times 10^{6}E$	$1.60 \times 10^{-9}E$
$\tilde{\nu}(cm^{-1})$	$10^{8}/\tilde{\nu}$	$10^{4}/\tilde{\nu}$	$1/\tilde{\nu}$	$3.00 \times 10^{10}\tilde{\nu}$	$1.24 \times 10^{-7}\tilde{\nu}$	1	$1.99 \times 10^{-16}\tilde{\nu}$
E(erg)	$1.99 \times 10^{-8}/E$	$1.99 \times 10^{-12}/E$	$1.99 \times 10^{-16}/E$	$1.51 \times 10^{26}E$	$6.24 \times 10^{8}E$	$5.03 \times 10^{15}E$	1

(Reprinted with permission from Eureka Scientific, Inc., Oakland, CA)

Note: 1 Å = 0.1 nanometer.

Conversion factors for natural units; $c = \hbar = 1$.

	s^{-1}	cm^{-1}	K	eV	amu	erg	g
s^{-1}	1	0.334×10^{10}	0.764×10^{-11}	0.658×10^{-15}	0.707×10^{-24}	1.055×10^{-27}	1.173×10^{-48}
cm^{-1}	2.998×10^{10}	1	0.229	1.973×10^{-5}	2.118×10^{-14}	3.161×10^{-17}	0.352×10^{-37}
K	1.310×10^{11}	4.369	1	0.862×10^{-4}	0.962×10^{-13}	1.381×10^{-16}	1.537×10^{-37}
eV	1.519×10^{15}	0.507×10^{5}	1.160×10^{4}	1	1.074×10^{-9}	1.602×10^{-12}	1.783×10^{-33}
amu	1.415×10^{24}	0.472×10^{14}	1.081×10^{13}	0.931×10^{9}	1	1.492×10^{-3}	1.661×10^{-24}
erg	0.948×10^{27}	0.316×10^{17}	0.724×10^{16}	0.624×10^{12}	0.670×10^{3}	1	1.113×10^{-21}
g	0.852×10^{48}	2.843×10^{37}	0.651×10^{37}	0.561×10^{33}	0.602×10^{24}	0.899×10^{21}	1

Flux Density Conversion (E in keV; λ in Å)

TO → FROM ↓	S_ν(Jy)	f_E $\left(\frac{\text{photons}}{\text{cm}^2\,\text{s}\,\text{keV}}\right)$	f_λ $\left(\frac{\text{photons}}{\text{cm}^2\,\text{s}\,\text{Å}}\right)$	F_λ $\left(\frac{\text{ergs}}{\text{cm}^2\,\text{s}\,\text{Å}}\right)$	F_ν $\left(\frac{\text{ergs}}{\text{cm}^2\,\text{s}\,\text{Hz}}\right)$
S_ν(Jy)	S_ν(Jy)	$1.51 \times 10^3 S_\nu/E$	$1.51 \times 10^3 S_\nu/\lambda$	$3.00 \times 10^{-5} S_\nu/\lambda^2$	$10^{-23} S_\nu$
f_E $\left(\frac{\text{photons}}{\text{cm}^2\,\text{s}\,\text{keV}}\right)$	$6.63 \times 10^{-4} E f_E$	f_E	$8.07 \times 10^{-2} E^2 f_E$	$1.29 \times 10^{-10} E^3 f_E$	$6.63 \times 10^{-27} E f_E$
f_λ $\left(\frac{\text{photons}}{\text{cm}^2\,\text{s}\,\text{Å}}\right)$	$6.63 \times 10^{-4} \lambda f_\lambda$	$8.07 \times 10^{-2} \lambda^2 f_\lambda$	f_λ	$1.99 \times 10^{-8} f_\lambda/\lambda$	$6.63 \times 10^{-27} \lambda f_\lambda$
F_λ $\left(\frac{\text{ergs}}{\text{cm}^2\,\text{s}\,\text{Å}}\right)$	$3.34 \times 10^4 \lambda^2 F_\lambda$	$4.06 \times 10^6 \lambda^3 F_\lambda$	$5.03 \times 10^7 \lambda F_\lambda$	F_λ	$3.34 \times 10^{-19} \lambda^2 F_\lambda$
F_ν $\left(\frac{\text{ergs}}{\text{cm}^2\,\text{s}\,\text{Hz}}\right)$	$10^{23} F_\nu$	$1.51 \times 10^{26} F_\nu/E$	$1.51 \times 10^{26} F_\nu/\lambda$	$3.00 \times 10^{18} F_\nu/\lambda^2$	F_ν

(Reprinted with permission from Eureka Scientific, Inc., Oakland, CA)

Numerical constants

$\pi = 3.141\,592\,7$
$e = 2.718\,281\,8$
$\ln 2 = 0.693\,147\,2$
$\log_{10} 2 = 0.301\,030\,0$

$\ln 10 = 2.302\,585\,1$
$\log_{10} e = 0.434\,294\,5$
$(2\pi)^{1/2} = 2.506\,628$
$\pi^2 = 9.869\,604$
$2^{10} = 1024$
$e^{-1} = 0.367\,879\,4$
$\Gamma(1/2) = \pi^{1/2}$
Feigenbaum's constants:
$\delta = 4.669\,201\,6$
$\alpha = 2.502\,907\,875\,0$
Euler-Mascheroni: 0.577 215 664 9
Golden mean = 0.618 033 988 7...

rad = 57.295 78 deg
$= 3.437\,747 \times 10^3$ arcmin
$= 2.062\,648 \times 10^5$ arcsec
steradian $= 32\,400/\pi^2$
$= 3.2828 \times 10^3\ \mathrm{deg}^2$
$= 1.1818 \times 10^7\ \mathrm{arcmin}^2$
$= 4.2545 \times 10^{10}\ \mathrm{arcsec}^2$
degree = 0.017 453 3 rad
arcmin $= 2.908\,88 \times 10^{-4}$ rad
arcsec $= 4.848\,137 \times 10^{-6}$ rad
$\mathrm{deg}^2 = 3.0462 \times 10^{-4}$ steradian
$\mathrm{arcmin}^2 = 8.4617 \times 10^{-8}$ steradian
$\mathrm{arcsec}^2 = 2.3504 \times 10^{-11}$ steradian
Fibonacci numbers:
$F_1 = 1 \quad F_2 = 1$
$F_{n+2} = F_n + F_{n+1},\ n \geq 1$

Powers of 2:

n	2^n	$\log 2^n$
0	1	0.00
1	2	0.30
2	4	0.60
3	8	0.90
4	16	1.20
5	32	1.51
6	64	1.81
7	128	2.11
8	256	2.41
9	512	2.71
10	1024	3.01
11	2048	3.31
12	4096	3.61
13	8192	3.91
14	16 384	4.21
15	32 768	4.52
20	1 048 576	6.02
25	33 554 432	7.53
n		$0.301n$

Number system conversions:

Decimal	Octal	Binary	Hexadecimal
0	0	0000	0
1	1	0001	1
2	2	0010	2
3	3	0011	3
4	4	0100	4
5	5	0101	5
6	6	0110	6
7	7	0111	7
8	10	1000	8
9	11	1001	9
10	12	1010	A
11	13	1011	B
12	14	1100	C
13	15	1101	D
14	16	1110	E
15	17	1111	F
16	20	10000	10

Mathematical formulae

$$(a+x)^n = a^n + na^{n-1}x + \frac{n(n-1)}{2!}a^{n-2}x^2 + \frac{n(n-1)(n-2)}{3!}a^{n-3}x^3 + \cdots + nax^{n-1} + x^n,$$ where n is any positive integer.

$$e^x = 1 + x + \frac{x^2}{2!} + \frac{x^3}{3!} + \cdots.$$

$$\ln(1+x) = x - \frac{x^2}{2} + \frac{x^3}{3} - \frac{x^4}{4} + \cdots \text{ for } -1 < x \le 1.$$

$$\sin x = x - \frac{x^3}{3!} + \frac{x^5}{5!} - \frac{x^7}{7!} + \cdots, \qquad \cos x = 1 - \frac{x^2}{2!} + \frac{x^4}{4!} - \frac{x^6}{6!} + \cdots.$$

$$\int u\,dv = uv - \int v\,du + C, \qquad \int_0^\pi \sin^2 nx\,dx = \int_0^\pi \cos^2 nx\,dx = \frac{\pi}{2} \text{ for an integer, } n \neq 0.$$

$$\int_0^\infty e^{-a^2x^2}dx = \pi^{1/2}/2a, \qquad \int_0^\infty x^n e^{-ax}dx = \Gamma(n+1)/a^{n+1}.$$

$$F(u) = \int_{-\infty}^{\infty} f(x)e^{-2\pi iux}dx \leftrightarrow f(x) = \int_{-\infty}^{\infty} F(u)e^{2\pi iux}.$$

The factorial $n!$ is defined for a positive integer n as $n! \equiv n(n-1)\cdots 2\cdot 1$.

$n! \approx (2\pi)^{1/2}n^{n+1/2}e^{-n}$ (for large n).

The functional equation of the Gamma Function:

$\Gamma(x+1) = x\Gamma(x)$, for $x > 0$. $\Gamma(n+1) = n!$, for integer $n > 0$.

$$\int_a^b f(x)dx = -\int_b^a f(x)dx, \qquad \int_a^b f(x)dx = \int_a^c f(x)dx + \int_c^b f(x)dx.$$

$$\frac{d}{dx}f[u(x)] = \frac{df}{du}\frac{du}{dx}, \qquad \frac{d}{dx}[u(x)v(x)] = v\frac{du}{dx} + u\frac{dv}{dx}.$$

$$\frac{d}{dx}\ln y(x) = y'(x)/y(x), \qquad 2.30\log_{10} x = \log_e x$$

$$\frac{d}{dx}[\log(u(x)/v(x))] = v(x)[u'(x)/v(x) - u(x)v'(x)/v(x)^2]/\ln(10)u(x),$$

where $'$ denotes $\frac{d}{dx}$.

$\sin(A+B) = \sin A\cos B + \cos A\sin B$, $\sin 2A = 2\sin A\cos A$

$\cos(A+B) = \cos A\cos B - \sin A\sin B$, $\cos 2A = \cos^2 A - \sin^2 A$.

$e^{ix} = \cos x + i\sin x$.

$(\cos\theta + i\sin\theta)^n = \cos n\theta + i\sin n\theta$.

Elementary particles (short list)

Particle	Charge	Mass (amu)	Spin	Magnetic moment	Mean life[a] (s)
Photon	0	0	1	0	stable
π-meson	+1, −1	0.149 84	1	0	2.60×10^{-8}
	0	0.144 90	0	0	0.83×10^{-16}
Neutrino	0	$< 10^{-6}$	1/2	~ 0	stable
Electron, positron	−1, +1	0.000 548 6	1/2	$1.001\,160\ \mu_{\mathrm{B}}$[b]	stable
μ-meson	−1, +1	0.1134	1/2	$0.004\,842\ \mu_{\mathrm{B}}$	2.20×10^{-6}
Proton	+1, −1	1.007 276	1/2	$2.792\,85\ \mu_{\mathrm{B}}$[c]	stable
Neutron	0	1.008 665	1/2	$-1.913\,04\ \mu_N$	917 ± 14

[a] half-life = mean life × ln 2

[b] $\mu_{\mathrm{B}} = eh/4\pi m_e c = 9.274\,015\,4(31) \times 10^{-24}\ \mathrm{J\,T^{-1}}$

[c] $\mu_N = eh/4\pi m_p c = 5.050\,786\,6(17) \times 10^{-27}\ \mathrm{JT^{-1}}$.

(Data from ‘Reviews of Particle Properties’, *Rev. Mod. Phys.* **52**, No. 2, April 1980)

Short List of Elementary Particles

(The second column is the isospin t, while the next column is the spin and parity, J^P. Masses and lifetimes have generally been rounded; see the original reference for error bars and a complete listing of particle properties.)

Particle	t	J^P	Mass (MeV)	Mean life (s)
LEPTONS				
e		$\frac{1}{2}$	0.511 003	Stable
μ		$\frac{1}{2}$	105.6594	$2.197\,14 \times 10^{-6}$
τ		$\frac{1}{2}$	1784	5×10^{-13}
NONSTRANGE BARYONS				
p	$\frac{1}{2}$	$\frac{1}{2}^+$	938.280	Stable
n	$\frac{1}{2}$	$\frac{1}{2}^+$	939.573	925
Δ	$\frac{3}{2}$	$\frac{3}{2}^+$	1232	6×10^{-24}
STRANGENESS = −1 BARYONS				
Λ	0	$\frac{1}{2}^+$	1115.60	2.63×10^{-10}
Σ^+	1	$\frac{1}{2}^+$	1189.36	8.00×10^{-11}
Σ^0	1	$\frac{1}{2}^+$	1192.46	6×10^{-20}
Σ^-	1	$\frac{1}{2}^+$	1197.34	1.48×10^{-10}
STRANGENESS = −2 BARYONS				
Ξ^0	$\frac{1}{2}$	$\frac{1}{2}^+$	1314.9	2.9×10^{-10}
Ξ^-	$\frac{1}{2}$	$\frac{1}{2}^+$	1321.3	1.64×10^{-10}
STRANGENESS = −3 BARYON				
Ω^-	0	$\frac{3}{2}^+$	1672.5	8.2×10^{-11}
NONSTRANGE CHARMED BARYON				
Λ_c^+	0	$\frac{1}{2}^+$	2282	1×10^{-13}
NONSTRANGE MESONS				
$\pi^\pm$	1	0^-	139.567	2.603×10^{-8}
π^0	1	0^-	134.963	8.3×10^{-17}
η	0	0^-	548.8	8×10^{-19}
ρ	1	1^-	769	4.3×10^{-24}
ω	0	1^-	782.6	6.6×10^{-23}
η'	0	0^-	957.6	2.4×10^{-21}
ϕ	0	1^-	1019.6	1.6×10^{-22}
J/Ψ	0	1^-	3096.9	1.0×10^{-20}
Υ		1^-	9456	1.6×10^{-20}
STRANGENESS = −1 MESONS				
$K^\pm$	$\frac{1}{2}$	0^-	493.67	1.237×10^{-8}
$K^0,\ \bar{K}^0$	$\frac{1}{2}$	0^-	497.7	K_S : 8.92×10^{-11} K_L : 5.18×10^{-8}
CHARMED NONSTRANGE MESONS				
$D^\pm$	$\frac{1}{2}$	0^-	1869.4	9×10^{-13}
$D^0,\ \bar{D}^0$	$\frac{1}{2}$	0^-	1864.7	5×10^{-13}
CHARMED STRANGE MESON				
$F^\pm$	0	0^-	2021	2×10^{-13}

(From Shapiro, S.L. & Teukolsky, S.A., *Black Holes, White Dwarfs,* and *Neutron Stars,* John Wiley and Sons, 1983, with permission.) For a complete list of elementary particles see http://pdg.lbl.gov/.

Energy conversions

1 erg	= 1 dyne-centimeter = 10^{-7} joule
1 joule	= 1 newton-meter
1 foot-pound	= 1.356 joule
1 calorie	= 4.184 joule
1 Btu	= 1.055×10^3 joule
1 horsepower-hour	= 2.6845×10^6 joule
1 kilowatt-hour	= 3.6×10^6 joule = 3.413×10^3 Btu
1 MeV	= 1.6×10^{-13} joule
Energy of fission of 1 atom of ^{235}U	= 199 MeV = 3.2×10^{-11} joule
Energy equivalent of 1 ton of TNT	= 4.2×10^9 joule
Energy of fission of 1 kilogram of ^{235}U	= 20 kilotons of TNT
Hydrogen fusion:	$D + T \rightarrow {}_2\text{He}^4 + n + 17.6$ MeV
Energy equivalent of 1 gram of matter	= 9×10^{13} joule
High heat value of 1 ton of coal	= 26×10^6 Btu
High heat value of 1 cord of red oak	= 30×10^6 Btu
High heat value of 100 gallons of fuel oil	= 15×10^6 Btu
High heat value of 20 000 cu ft natural gas	= 20×10^6 Btu
US energy consumption	= 10^{20} joule yr^{-1} (proj. 1970–2000)
Earth's daily receipt of solar energy	= 1.49×10^{22} joule = 4.2×10^{12} Mwh
Earth's rotational energy	= 2.2×10^{29} joule
Earth's total heat content	= 3×10^{31} joule
1 D-cell flashlight battery	= 10^4 watt-s = 10^4 joule

Prefixes and symbols

(used with SI units to indicate decimal multiples and submultiples)

Multiples			Submultiples		
Factor	Prefix	Symbol	Factor	Prefix	Symbol
10^{24}	yotta	Y	10^{-1}	deci	d
10^{21}	zetta	Z	10^{-2}	centi	c
10^{18}	exa	E	10^{-3}	milli	m
10^{15}	peta	P	10^{-6}	micro	μ
10^{12}	tera	T	10^{-9}	nano	n
10^{9}	giga	G	10^{-12}	pico	p
10^{6}	mega	M	10^{-15}	femto	f
10^{3}	kilo	k	10^{-18}	atto	a
10^{2}	hecto	h	10^{-21}	zepto	z
10	deca	da	10^{-24}	yocto	y

Periodic table of the elements

PERIODIC TABLE
OF THE ELEMENTS

KEY: ATOMIC NUMBER 30; ATOMIC WEIGHT 65.37; BOILING POINT, °C 906; MELTING POINT, °C 419.5; DENSITY (g/ml) 7.14; SYMBOL Zn; NAME ZINC

GROUP IA	IIA	IIIB	IVB	VB	VIB	VIIB	VIII	VIII	VIII
1 H 1.00797 -252.7 / -259.2 / 0.071 HYDROGEN									
3 Li 6.939 1330 / 180.5 / 0.53 LITHIUM	4 Be 9.0122 2770 / 1277 / 1.85 BERYLLIUM								
11 Na 22.9898 892 / 97.8 / 0.97 SODIUM	12 Mg 24.312 1107 / 650 / 1.74 MAGNESIUM								
19 K 39.102 760 / 63.7 / 0.86 POTASSIUM	20 Ca 40.08 1440 / 838 / 1.55 CALCIUM	21 Sc 44.956 2730 / 1539 / 3.0 SCANDIUM	22 Ti 47.90 3260 / 1668 / 4.51 TITANIUM	23 V 50.942 3450 / 1900 / 6.1 VANADIUM	24 Cr 51.996 2665 / 1875 / 7.19 CHROMIUM	25 Mn 54.938 2150 / 1245 / 7.43 MANGANESE	26 Fe 55.847 3000 / 1536 / 7.86 IRON	27 Co 58.933 2900 / 1495 / 8.9 COBALT	28 Ni 58.71 2730 / 1453 / 8.9 NICKEL
37 Rb 85.47 688 / 38.9 / 1.53 RUBIDIUM	38 Sr 87.62 1380 / 768 / 2.6 STRONTIUM	39 Y 88.905 2927 / 1509 / 4.47 YTTRIUM	40 Zr 91.22 3580 / 1852 / 6.49 ZIRCONIUM	41 Nb 92.906 3300 / 2468 / 8.4 NIOBIUM	42 Mo 95.94 5560 / 2610 / 10.2 MOLYBDENUM	43 Tc (98) — / 2140 / 11.5 TECHNETIUM	44 Ru 101.07 4900 / 2500 / 12.2 RUTHENIUM	45 Rh 102.905 4500 / 1966 / 12.4 RHODIUM	46 Pd 106.4 3980 / 1552 / 12.0 PALLADIUM
55 Cs 132.905 690 / 28.7 / 1.90 CESIUM	56 Ba 137.34 1640 / 714 / 3.5 BARIUM	57 La 138.91 3470 / 920 / 6.17 LANTHANUM	72 Hf 178.49 5400 / 2222 / 13.1 HAFNIUM	73 Ta 180.948 5425 / 2996 / 16.6 TANTALUM	74 W 183.85 5930 / 3410 / 19.3 WOLFRAM	75 Re 186.2 5900 / 3180 / 21.0 RHENIUM	76 Os 190.2 5500 / 3000 / 22.6 OSMIUM	77 Ir 192.2 5300 / 2454 / 22.5 IRIDIUM	78 Pt 195.09 4530 / 1769 / 21.4 PLATINUM
87 Fr (223) — / (27) / — FRANCIUM	88 Ra (226) — / 700 / 5.0 RADIUM	89 Ac (227) — / 1050 / — ACTINIUM	104						

58 Ce 140.12 3468 / 795 / 6.67 CERIUM	59 Pr 140.907 3127 / 935 / 6.77 PRASEODYMIUM	60 Nd 144.24 3027 / 1024 / 7.00 NEODYMIUM	61 Pm (147) — / (1027) / — PROMETHIUM	62 Sm 150.35 1900 / 1072 / 7.54 SAMARIUM	63 Eu 151.96 1439 / 826 / 5.26 EUROPIUM	64 Gd 157.25 3000 / 1312 / 7.89 GADOLINIUM
90 Th 232.038 3850 / 1750 / 11.7 THORIUM	91 Pa (231) — / (1230) / 15.4 PROTACTINIUM	92 U 238.03 3818 / 1132 / 19.07 URANIUM	93 Np (237) — / 637 / 19.5 NEPTUNIUM	94 Pu (242) 3235 / 640 / — PLUTONIUM	95 Am (243) — / — / 11.7 AMERICIUM	96 Cm (247) — / — / — CURIUM

VALUES FOR GASEOUS ELEMENTS ARE FOR LIQUIDS AT THE BOILING POINT.

OUTLINE - SYNTHETICALLY PREPARED.

Periodic table of the elements (*cont.*)

IB	IIB	IIIA	IVA	VA	VIA	VIIA	VIIIA
							2 4.0026 -268.9 -269.7 0.126 He HELIUM
		5 10.811 — (2030) 2.34 B BORON	6 12.01115 4830 3727g 2.26 C CARBON	7 14.0067 -195.8 -210 0.81 N NITROGEN	8 15.9994 -183 -218.8 1.14 O OXYGEN	9 18.9984 -188.2 -219.6 1.505 F FLUORINE	10 20.183 -246 -248.6 1.20 Ne NEON
		13 26.9815 2450 660 2.70 Al ALUMINUM	14 28.086 2680 1410 2.33 Si SILICON	15 30.9738 280w 44.2w 1.82w P PHOSPHORUS	16 32.064 444.6 119.0 2.07 S SULFUR	17 35.453 -34.7 -101.0 1.56 Cl CHLORINE	18 39.948 -185.8 -189.4 1.40 Ar ARGON
29 63.54 2595 1083 8.96 Cu COPPER	30 65.37 906 419.5 7.14 Zn ZINC	31 69.72 2237 29.8 5.91 Ga GALLIUM	32 72.59 2830 937.4 5.32 Ge GERMANIUM	33 74.922 613 817 5.72 As ARSENIC	34 78.96 685 217 4.79 Se SELENIUM	35 79.909 58 -7.2 3.12 Br BROMINE	36 83.80 -152 -157.3 2.6 Kr KRYPTON
47 107.870 2210 960.8 10.5 Ag SILVER	48 112.40 765 320.9 8.65 Cd CADMIUM	49 114.82 2000 156.2 7.31 In INDIUM	50 118.69 2270 231.9 7.30 Sn TIN	51 121.75 1380 630.5 6.62 Sb ANTIMONY	52 127.60 989.8 449.5 6.24 Te TELLURIUM	53 126.904 183 113.7 4.94 I IODINE	54 131.30 -108.0 -111.9 3.06 Xe XENON
79 196.967 2970 1063 19.3 Au GOLD	80 200.59 357 -38.4 13.6 Hg MERCURY	81 204.37 1457 303 11.85 Tl THALLIUM	82 207.19 1725 327.4 11.4 Pb LEAD	83 208.980 1560 271.3 9.8 Bi BISMUTH	84 (210) — 254 (9.2) Po POLONIUM	85 (210) — (302) — At ASTATINE	86 (222) (-61.8) (-71) — Rn RADON

65 158.924 2800 1356 8.27 Tb TERBIUM	66 162.50 2600 1407 8.54 Dy DYSPROSIUM	67 164.930 2600 1461 8.80 Ho HOLMIUM	68 167.26 2900 1497 9.05 Er ERBIUM	69 168.934 1727 1545 9.33 Tm THULIUM	70 173.04 1427 824 6.98 Yb YTTERBIUM	71 174.97 3327 1652 9.84 Lu LUTETIUM
97 (247) — — — Bk BERKELIUM	98 (249) — — — Cf CALIFORNIUM	99 (254) — — — Es EINSTEINIUM	100 (253) — — — Fm FERMIUM	101 (256) — — — Md MENDELEVIUM	102 254) — — — No NOBELIUM	103 (257) — — — Lw LAWRENCIUM

Greek alphabet

A	α	Alpha	N	ν	Nu
B	β	Beta	Ξ	ξ	Xi
Γ	γ	Gamma	O	o	Omicron
Δ	δ	Delta	Π	π	Pi
E	ϵ	Epsilon	P	ρ	Rho
Z	ζ	Zeta	Σ	σ	Sigma
H	η	Eta	T	τ	Tau
Θ	θ	Theta	Υ	υ	Upsilon
I	ι	Iota	Φ	ϕ	Phi
K	κ	Kappa	X	χ	Chi
Λ	λ	Lambda	Ψ	ψ	Psi
M	μ	Mu	Ω	ω	Omega

Bibliography

BETA Mathematics Handbook, Rade, L. and Westergren, B., CRC Press, Inc. (1990).

CODATA recommended values of the fundamental physical constants: 1998, P.J. Mohr and B.N. Taylor, Rev. Mod. Phys., **72**, No. 2, 2000.

Handbook of Chemistry and Physics, CRC Press, Inc.

International Critical Tables of Numerical Data, Physics, Chemistry, and Technology, McGraw-Hill Book Company.

Landolt-Bornstein: Zahlenwerte und Funktionen aus Physik, Chemie, Astronomie, Geophysik, und Technik, Springer-Verlag.

Reviews of Particle Properties, C. Caso, *et al.*, The European Physical Journal C3 (1998).

Standard Mathematical Tables and Formulae, D. Zwillinger, ed., CRC Press, Inc. (1996).

Note: Links to WWW resources which supplement the material in this chapter can be found at:

http://www.astrohandbook.com

Chapter 2

Astronomy and astrophysics

. . . to observe is not enough. We must use our observations, and to do that we must generalize. - Henri Poincaré

The Solar System

The Sun

Global parameters	
Mass	1.989×10^{30} kg
Radius	6.955×10^{8} m
Surface area	6.079×10^{18} m^2
Volume	1.409×10^{27} m^3
Moment of inertia	5.7×10^{46} kg m^2
Mean density	1.412×10^{3} kg m^{-3}
Gravity at surface	2.740×10^{2} m s^{-2}
Escape velocity at surface	6.177×10^{5} m s^{-1}
Magnetic field strengths (typical)	
Sunspots	2000–4000 $\times 10^{-4}$ tesla
Polar field	1×10^{-4}
Bright, chromospheric network	25×10^{-4}
Ephemeral (unipolar) active regions	20×10^{-4}
Chromospheric plages	200×10^{-4}
Prominences	10–100 $\times 10^{-4}$
Sidereal rotation (func. of lat.)	$14^\circ.4 - 3^\circ.0 \sin^2 \phi$ per day[(1)]
Sidereal period for helio. long.	25.38 days
Sunspot cycle	~ 11.4 y
Luminosity	3.842×10^{26} W (var.)[(2)]
Radiation emittance at Sun's surface	6.319×10^{7} W m^{-2} (var.)
Mean radiation intensity of Suns's disk	2.012×10^{7} W m^{-2} sr^{-1} (var.)
Specific mean energy production	1.932×10^{-4} W kg^{-1} (var.)
Standard Model parameters[(3)]	
Central density	1.5×10^{5} kg m^{-3}
Central temperature	15.7×10^{6} K
Central pressure	2.33×10^{16} Pascal
Central hydrogen content by mass, X_c	0.355
Density at 1 $R_\odot$	2.18×10^{-4} kg m^{-3}
Temperature at 1 $R_\odot$	6000 K
Pressure at 1 $R_\odot$	8.27×10^{3} Pascal
Photospheric abundances[(4)]	
X(H)	0.706
Y(He)	0.274
Z(Li–U)	0.019

The Sun (cont.)

Earth dependent parameters	
1 Astronomical Unit (AU)	$1.4959787066 \times 10^{11}$ m
Light-time for 1 AU	499.00478 s
Mean distance from Earth	1.000001057 AU
Perihelion distance	1.4710×10^{11} m
Aphelion distance	1.5210×10^{11} m
Inclination of equator to ecliptic	$7°15'$
Solar parallax	$8''.794144$
Semidiameter of Sun at mean distance	$959''.63$
Solid angle of Sun at mean distance	6.8000×10^{-5} sr
Oblateness: semidiam. equator-pole diff.	$0''.0086$
Solar constant	$1.365 - 1.367 \times 10^{3}$ W m^{-2}
Synodic rotation (func. of lat.)	$13°.4 - 3°.0 \sin^2 \phi$ per day
Synodic period for helio. long.	27.28 days
The Sun as a star	
V	−26.75
B	−26.10
U	−25.91
m_{bol}	−26.83
M_V	+4.82
M_B	+5.47
M_U	+5.66
M_{bol}	+4.74
Bolometric correction, BC	−0.08
T_{eff}	5777 K
Spectral type	G2 V
Age of Sun	$(4.5 - 4.7) \times 10^{9}$ yr
Velocity relative to nearby stars	19.7 km s^{-1}
Solar apex	$\alpha = 271°, \delta = 30°$
Velocity relative to CBR	370 km s^{-1}
Velocity around galactic center	220 km s^{-1}
Distance from galactic center	8.5 kpc
Mean magnetic field (photosphere)	10 – 15 G*
Frequency of flares (solar max.)	1000 – 2000 y^{-1}
Frequency of flares (solar min.)	20 – 60 y^{-1}
Coronal mass ejection (CME) avg. mass	3×10^{12} kg
Coronal mass ejection (CME) avg. k.e.	2×10^{23} J
X-ray luminosity (excluding flares)	$3 - 100 \times 10^{15}$ W

*Time and spatial average; from S. Saar, Harvard-Smithsonian Center for Astrophysics, 2005.

The Sun (cont.)

[1] Based upon sunspot groups as tracers.
[2] approx. 0.1% peak-to-peak variation; 11 year cycle.
[3] Guenther, D.B., et al., Ap J, **387**, 372, 1992.
[4] Anders, E. and Grevesse, N., Geo. Cosm. Acta, **53**, 197, 1989.
[5] Hα importance ≥ 1.

1 pascal = 1 newton m^{-2} = 10 dyne cm^{-2}
1 tesla = 1×10^4 Gauss
1 watt = 1 J s^{-1} = 1×10^7 erg s^{-1}
1 kg m^{-3} = 1×10^{-3} g cm^{-3}

(Except where noted, data is from: W.C. Livingston in, *Allen's Astrophysical Quantities*, A.N. Cox, ed., Springer, 2000 and the *Explanatory Supplement to the Astronomical Almanac*, P.K. Seidelmann, University Science Books, 1992.)

The Sun (cont.)

Temperature and density as a function of distance from the solar surface. (Courtesy of G. Withbroe, Harvard/Smithsonian Center for Astrophysics.

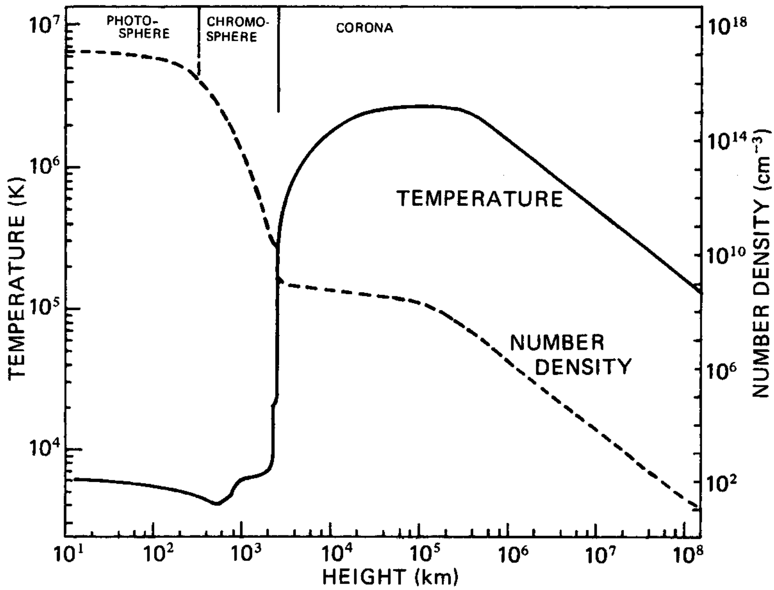

Solar temperature and electron density. (Adapted from Carrigan, A.L. & Skrivanek, R.A., *Aerospace Environment*, Air Force Cambridge Research Laboratories, Massachusetts, 1974.)

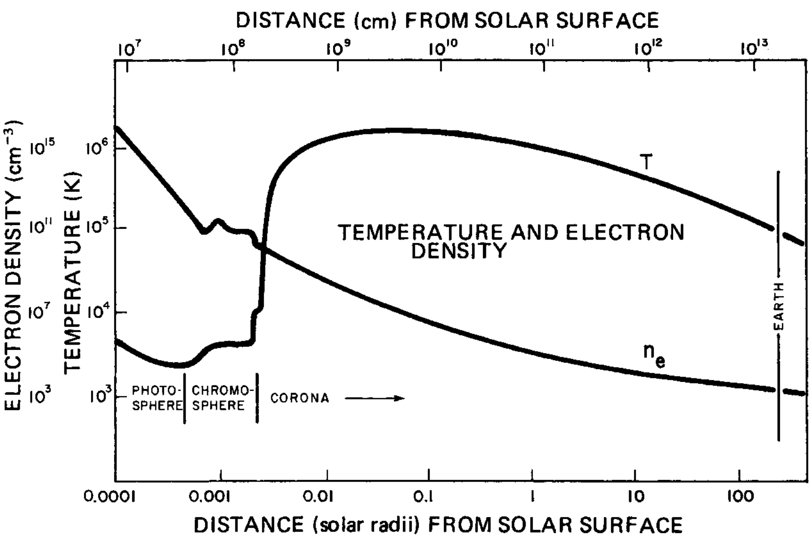

The Sun (cont.)

Solar spectral irradiance. (Adapted from Carrigan, A.L. & Skrivanek, R.A., *Aerospace Environment*, Air Force Cambridge Research Laboratories, Massachusetts. 1974.)

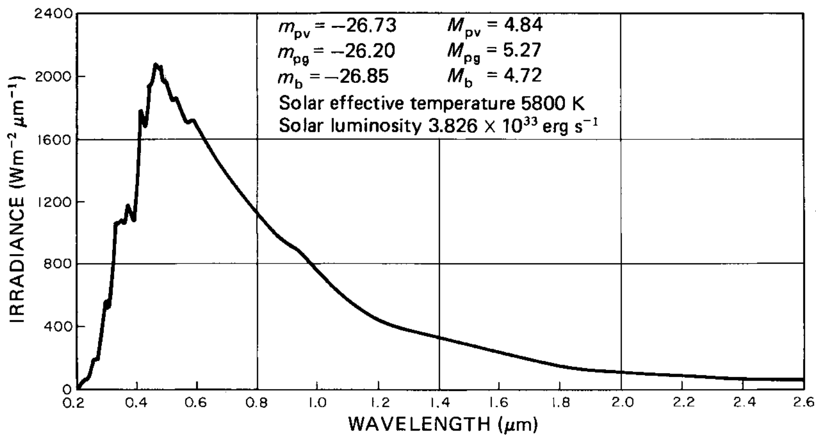

The solar spectral irradiance at 1 AU between 10 and 300 Å. Three states of solar activity are shown for the region 10–30 Å. The vertical extent of the shaded areas is representative of the variability of the spectral irradiance for changing solar conditions. (Adapted from Manson, J.E. in *The Solar Output and Its Variation*, O.R. White, ed., Colorado Associated University Press, Boulder, 1977.)

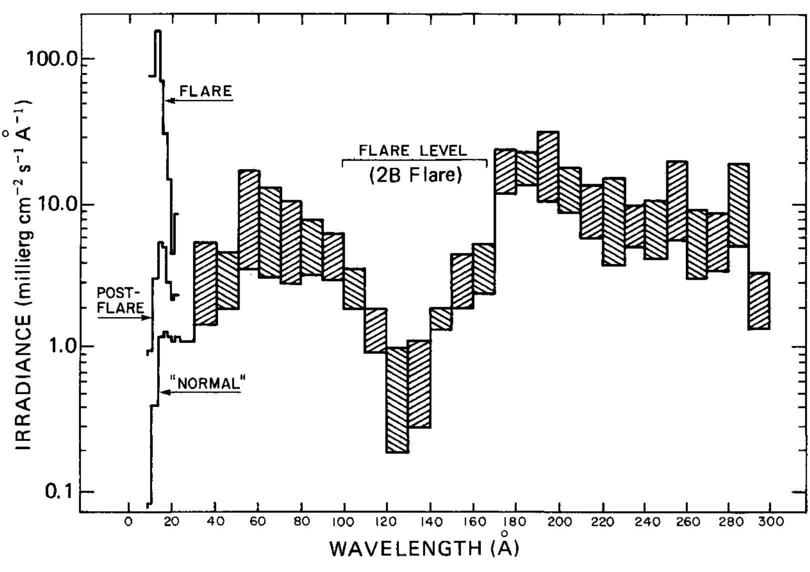

The Sun (cont.)

Solar EUV flux distribution incident on Earth's atmosphere (moderately active, non-flaring sun). (Adapted from Carrigan, A.L. & Skrivanek, R.A., *Aerospace Environment*, Air Force Cambridge Research Laboratories, Massachusetts, 1974.)

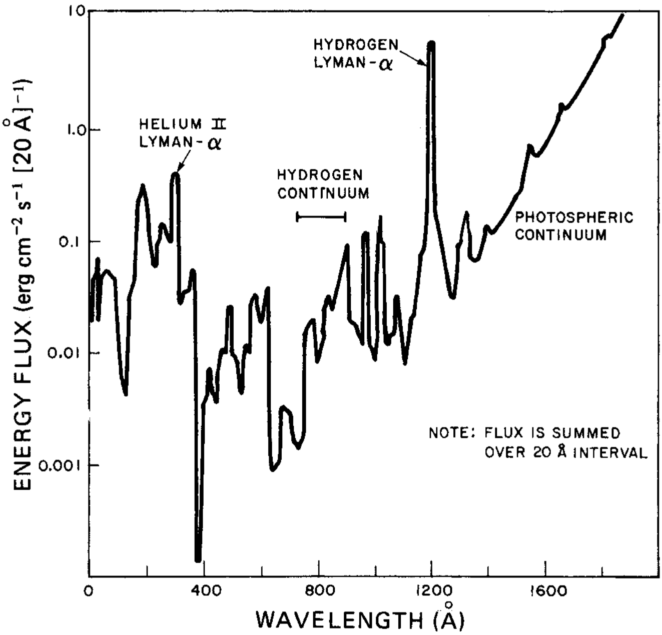

Daily mean values of the Sun's total irradiance from 1979 to 1997. (Adapted from the Encyclopedia of Astronomy and Astrophysics, Institute of Physics Publishing, 2001.)

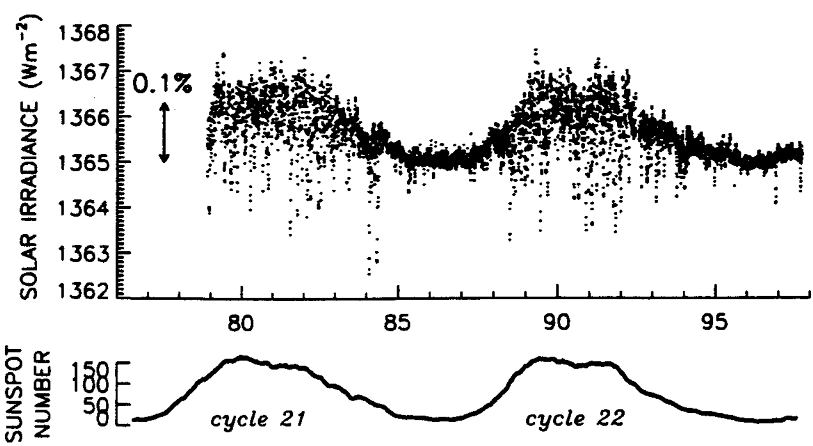

The Sun (cont.)

Overall structure of the solar interior.

(From Kivelson, M.G. and Russell, C.T., eds., *Introduction to Space Physics,* Cambridge University Press, 1995, with permission.)

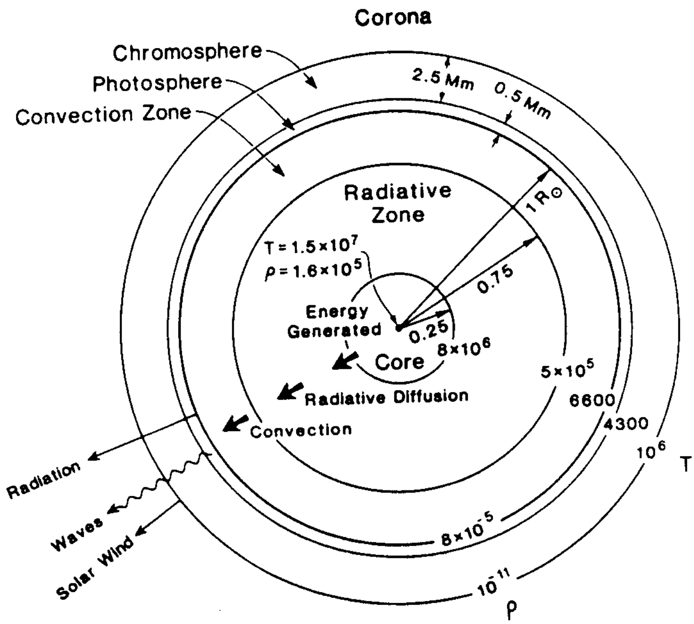

Solar-wind flux densities and fluxes near the orbit of the Earth

	Flux Density	Flux Through Sphere at 1 AU
Protons	3.0×10^8 cm^{-2} s^{-1}	8.4×10^{35} s^{-1}
Mass	5.8×10^{-16} g cm^{-2} s^{-1}	1.6×10^{12} g s^{-1}
Radial momentum	2.6×10^{-9} pascal (Pa)	7.3×10^{14} newton (N)
Kinetic energy	0.6 erg cm^{-2} s^{-1}	1.7×10^{27} erg s^{-1}
Thermal energy	0.02 erg cm^{-2} s^{-1}	0.05×10^{27} erg s^{-1}
Magnetic energy	0.01 erg cm^{-2} s^{-1}	0.025×10^{27} erg s^{-1}
Radial magnetic flux	5×10^{-9} tesla (T)	1.4×10^{15} weber (Wb)

(From Kivelson, M.G. and Russell, C.T., eds., *Introduction to Space Physics,* Cambridge University Press, 1995, with permission.)

The Sun (cont.)

Monthly averages of the sunspot numbers. The sunspot number is calculated by first counting the number of sunspot groups and then the number of individual sunspots. The "sunspot number" is then given by the sum of the number of individual sunspots and ten times the number of groups. Since most sunspot groups have, on average, about ten spots, this formula for counting sunspots gives reliable numbers even when the observing conditions are less than ideal and small spots are hard to see. (D.H. Hathaway, NASA/MSFC, 2001.)

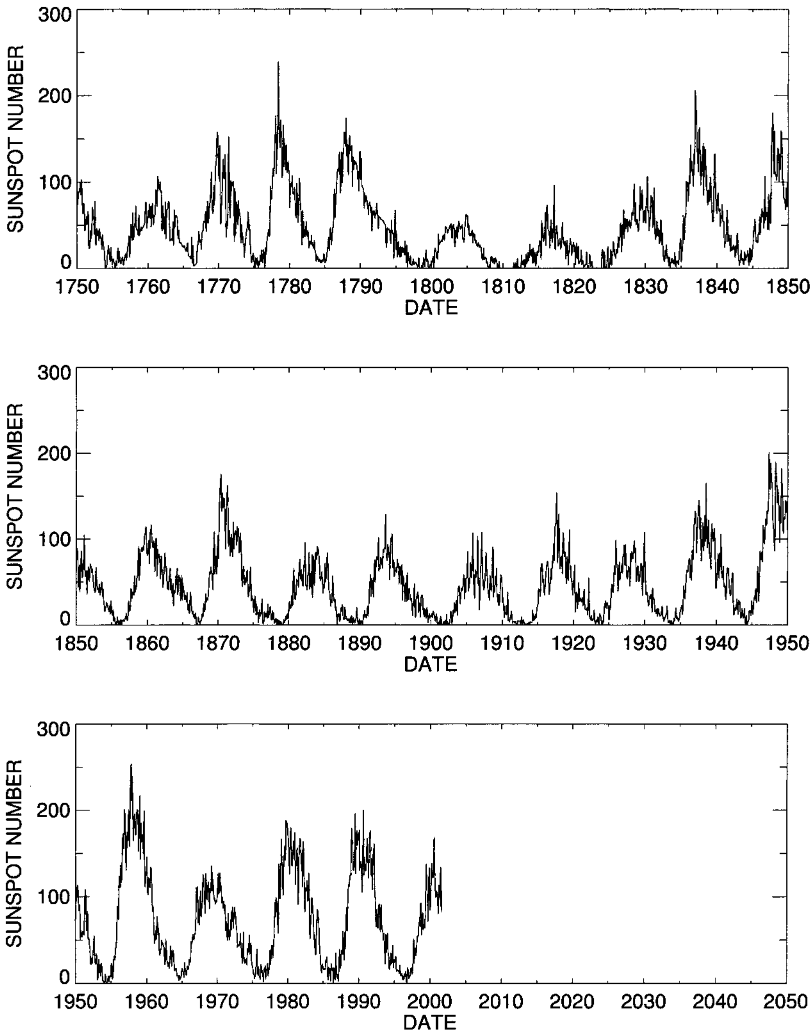

The Sun (cont.)

Sunspots do not appear at random over the surface of the sun but are concentrated in two latitude bands on either side of the equator. A butterfly diagram shows the positions of the spots for each rotation of the Sun and shows that these bands first form at mid-latitudes, widen, and then move toward the equator as each cycle progressess. (D.H. Hathaway, NASA/MSFC, 2001.)

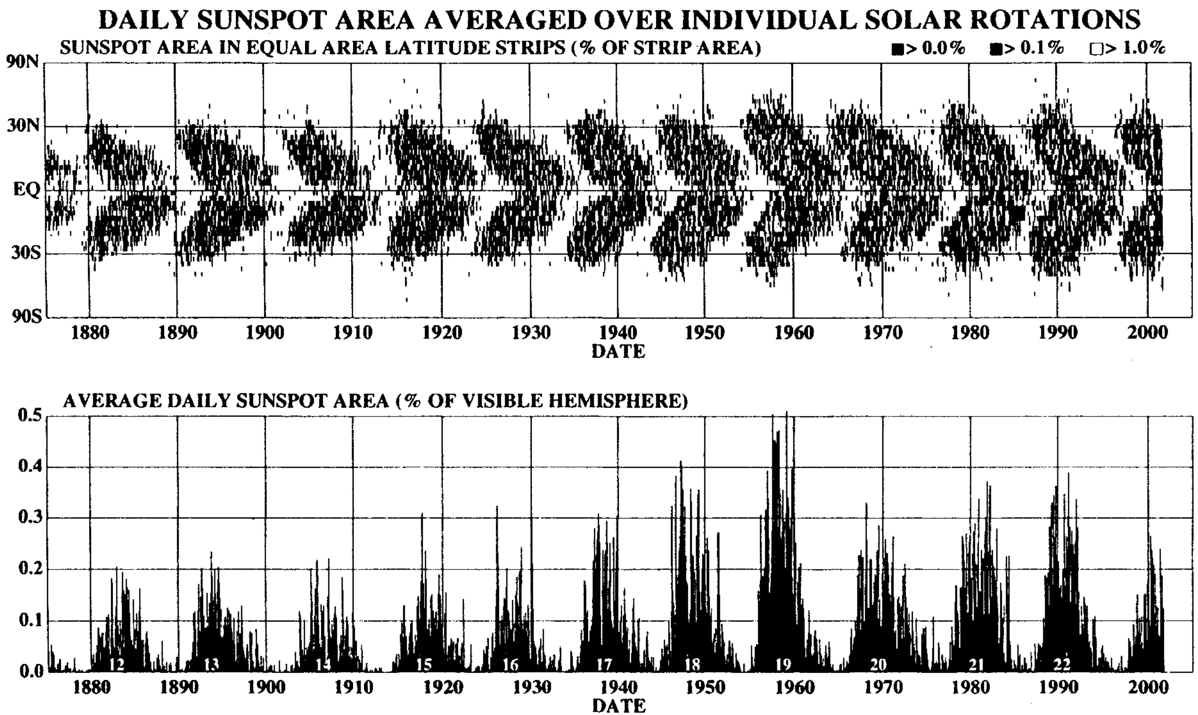

Fraunhofer lines in the solar spectrum

λ(Å)	Element	W(Å)	λ (Å)	Element	W (Å)
3581.21	Fe I	2.14	4920.51	Fe I	0.43
3719.95	Fe I	1.66	4957.61	Fe I	0.45
3734.87	Fe I	3.03	5167.33	Mg I	0.65
3749.50	Fe I	1.91	5172.70	Mg I	1.26
3758.24	Fe I	1.65	5183.62	Mg I	1.58
3770.63	H_{11}	1.86	5232.95	Fe I	0.35
3797.90	H_{10}	3.46	5269.55	Fe I	0.41
3820.44	Fe I	1.71	5324.19	Fe I	0.32
3825.89	Fe I	1.52	5238.05	Fe I	0.38
3832.31	Mg I	1.68	5528.42	Mg I	0.29
3835.39	H_9	2.36	5889.97	Na I	0.63
3838.30	Mg I	1.92	5895.94	Na I	0.56
3859.92	Fe I	1.55	6122.23	Ca I	0.22
3889.05	H_8	2.35	6162.18	Ca I	0.22
3933.68	Ca II	20.25	6562.81	Hα	4.02
3968.49	Ca II	15.47	6867.19	O_2	Tell*
4045.82	Fe I	1.17	7593.70	O_2	Tell*
4101.75	H_δ	3.13	8194.84	Na I	0.30
4226.74	Ca I	1.48	8498.06	Ca II	1.46
4310 ± 10	CH	G band	8542.14	Ca II	3.67
4340.48	H_7	2.86	8662.17	Ca II	2.60
4383.56	Fe I	1.01	8688.64	Fe I	0.27
4361.34	H_β	3.68	8736.04	Mg I	0.29
4891.50	Fe I	0.31			

*Tell - Telluric. Absorption lines produced by the Earth's atmosphere.
Note: The equivalent width W is the width of a rectangle with the height of the continuum adjacent to the absorption line and the same area as the absorption line.

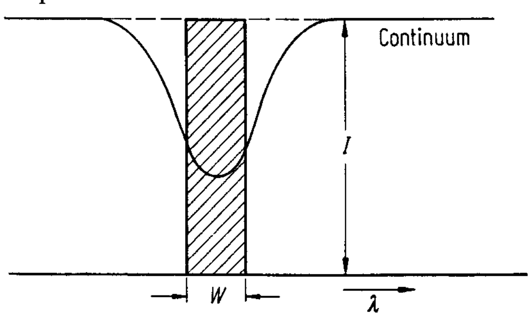

$W \equiv \int_{\lambda_1}^{\lambda_2} [(F_c - F_\lambda)/F_c] d\lambda$, where F_λ is the spectral flux at wavelength λ in the line, F_c = the continuum flux, and $F_\lambda = F_c$ for $\lambda \geq \lambda_2$ and $\lambda \leq \lambda_1$.

(Data from Lang, K., *Astrophysical Formulae,* Vol. I, Springer-Verlag, 1999.)

Solar eclipses, 2001-2010

Date	Eclipse Type	Eclipse[1] Magnitude	Central[2] Duration	Geographic Region of Eclipse Visibility[3]
2001 Jun 21	Total	1.050	04m57s	e S. America, Africa [Total: s Atlantic, s Africa, Madagascar]
2001 Dec 14	Annular	0.968	03m53s	N. & C. America, nw S. America [Annular: c Pacific, Costa Rica]
2002 Jun 10	Annular	0.996	00m23s	e Asia, Australia, w N. America [Annular: n Pacific, w Mexico]
2002 Dec 04	Total	1.024	02m04s	s Africa, Antarctica, Indonesia, Australia [Total: s Africa, s Indian, s Australia]
2003 May 31	Annular	0.938	03m37s	Europe, Asia, nw N. America [Annular: Iceland, Greenland]
2003 Nov 23	Total	1.038	01m57s	Australia, N. Z., Antarctica, s S. America [Total: Antarctica]
2004 Apr 19	Partial	0.736	–	Antarctica, s Africa
2004 Oct 14	Partial	0.927	–	ne Asia, Hawaii, Alaska
2005 Apr 08	Hybrid[4]	1.007	00m42s	N. Zealand, N. & S. America [Hybrid: s Pacific, Panama, Colombia, Venezuela]
2005 Oct 03	Annular	0.958	04m32s	Europe, Africa, s Asia [Annular: Portugal, Spain, Libya, Sudan, Kenya]
2006 Mar 29	Total	1.052	04m07s	Africa, Europe, w Asia [Total: c Africa, Turkey, Russia]
2006 Sep 22	Annular	0.935	07m09s	S. America, w Africa, Antarctica [Annular: Guyana, Suriname, F. Guiana, s Atlantic]
2007 Mar 19	Partial	0.874	–	Asia, Alaska
2007 Sep 11	Partial	0.749	–	S. America, Antarctica
2008 Feb 07	Annular	0.965	02m12s	Antarctica, e Australia, N. Zealand [Annular: Antarctica]
2008 Aug 01	Total	1.039	02m27s	ne N. America, Europe, Asia [Total: n Canada, Greenland, Siberia, Mongolia, China]
2009 Jan 26	Annular	0.928	07m54s	s Africa, Antarctica, se Asia, Australia [Annular: s Indian, Sumatra, Borneo]
2009 Jul 22	Total	1.080	06m39s	e Asia, Pacific Ocean, Hawaii [Total: India, Nepal, China, c Pacific]
2010 Jan 15	Annular	0.919	11m08s	Africa, Asia [Annular: c Africa, India, Malymar, China]
2010 Jul 11	Total	1.058	05m20s	s S. America [Total: s Pacific, Easter Is., Chile, Argentina]

[1]**Eclipse magnitude** is the fraction of the Sun's diameter obscured by the Moon. For annular eclipses, the eclipse magnitude is always less than 1. For total eclipses, the eclipse magnitude is always greater than or equal to 1. For both annular and total eclipses, the value listed is actually the ratio of diameters between the Moon and the Sun.

[2]**Central Duration** is the duration of a total or annular eclipse at Greatest Eclipse.

Greatest Eclipse is the instant when the axis of the Moon's shadow passes closest to Earth's center.

[3]**Geographic Region of Eclipse Visiblity** is the portion of Earth's surface where a partial eclipse can be seen. The central path of a total or annular eclipse covers a much smaller region of Earth and is described in brackets [ ].

[4]**Hybrid** eclipses are also known as **annular/total** eclipses. Such an eclipse is both total and annular along different sections of its umbral path.

(From F. Espenak, NASA/GSFC, 2001)

Solar eclipses (cont.)

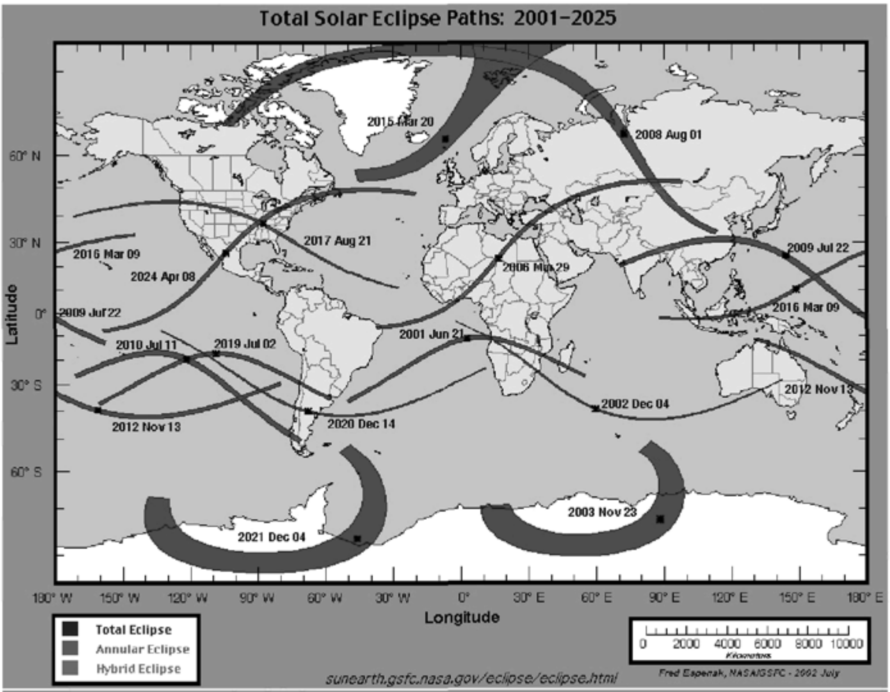

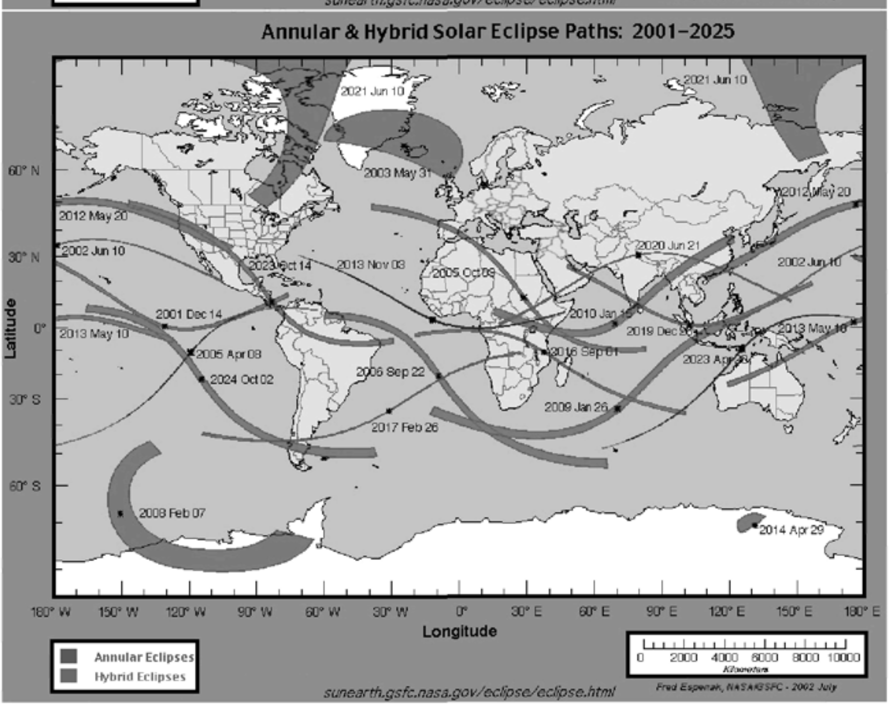

Solar system elemental abundances (log $N_H = 12.00$)

Element	Photosphere*	Meteorites†	Element	Photosphere	Meteorites
1 H	12.00	[12.00]	44 Ru	1.84 ±0.07	1.82 ±0.02
2 He	[10.99 ±0.035]	[10.99]	45 Rh	1.12 ±0.12	1.09 ±0.03
3 Li	1.16 ±0.1	3.31 ±0.04	46 Pd	1.69 ±0.04	1.70 ±0.03
4 Be	1.15 ±0.10	1.42 ±0.04	47 Ag	(0.94 ±0.25)	1.24 ±0.01
5 B	(2.6 ±0.3)	2.88 ±0.04	48 Cd	1.86 ±0.15	1.76 ±0.03
6 C	8.56 ±0.04	[8.56]	49 In	(1.66 ±0.15)	0.82 ±0.03
7 N	8.05 ±0.04	[8.05]	50 Sn	2.0 ±(0.3)	2.14 ±0.04
8 O	8.93 ±0.035	[8.93]	51 Sb	1.0 ±(0.3)	1.04 ±0.07
9 F	4.56 ±0.3	4.48 ±0.06	52 Te	–	2.24 ±0.04
10 Ne	[8.09 ±0.10]	[8.09 ±0.10]	53 I	–	1.51 ±0.08
11 Na	6.33 ±0.03	6.31 ±0.03	54 Xe	–	2.23 ±0.08
12 Mg	7.58 ±0.05	7.58 ±0.02	55 Cs	–	1.12 ±0.02
13 Al	6.47 ±0.07	6.48 ±0.02	56 Ba	2.13 ±0.05	2.21 ±0.03
14 Si	7.55 ±0.05	7.55 ±0.02	57 La	1.22 ±0.09	1.20 ±0.01
15 P	5.45 ±(0.04)	5.57 ±0.04	58 Ce	1.55 ±0.20	1.61 ±0.01
16 S	7.21 ±0.06	7.27 ±0.05	59 Pr	0.71 ±0.08	0.78 ±0.01
17 Cl	5.5 ±0.3	5.27 ±0.06	60 Nd	1.50 ±0.06	1.47 ±0.01
18 Ar	[6.56 ±0.10]	[6.56 ±0.10]	62 Sm	1.00 ±0.08	0.97 ±0.01
19 K	5.12 ±0.13	5.13 ±0.03	63 Eu	0.51 ±0.08	0.54 ±0.01
20 Ca	6.36 ±0.02	6.34 ±0.03	64 Gd	1.12 ±0.04	1.07 ±0.01
21 Sc	3.10 ±(0.09)	3.09 ±0.04	65 Tb	(−0.1 ±0.3)	0.33 ±0.01
22 Ti	4.99 ±0.02	4.93 ±0.02	66 Dy	1.1 ±0.15	1.15 ±0.01
23 V	4.00 ±0.02	4.02 ±0.02	67 Ho	(0.26 ±0.16)	0.50 ±0.01
24 Cr	5.67 ±0.03	5.68 ±0.03	68 Er	0.93 ±0.06	0.95 ±0.01
25 Mn	5.39 ±0.03	5.53 ±0.04	69 Tm	(0.00 ±0.15)	0.13 ±0.01
26 Fe	7.67 ±0.03	7.51 ±0.01	70 Yb	1.08 ±(0.15)	0.95 ±0.01
27 Co	4.92 ±0.04	4.91 ±0.03	71 Lu	(0.76 ±0.30)	0.12 ±0.01
28 Ni	6.25 ±0.04	6.25 ±0.02	72 Hf	0.88 ±(0.08)	0.73 ±0.01
29 Cu	4.21 ±0.04	4.27 ±0.05	73 Ta	–	0.13 ±0.01
30 Zn	4.60 ±0.08	4.65 ±0.02	74 W	(1.11 ±0.15)	0.68 ±0.02
31 Ga	2.88 ±(0.10)	3.13 ±0.03	75 Re	–	0.27 ±0.04
32 Ge	3.41 ±0.14	3.63 ±0.04	76 Os	1.45 ±0.10	1.38 ±0.03
33 As	–	2.37 ±0.05	77 Ir	1.35 ±(0.10)	1.37 ±0.03
34 Se	–	3.35 ±0.03	78 Pt	1.8 ±0.3	1.68 ±0.03
35 Br	–	2.63 ±0.08	79 Au	(1.01 ±0.15)	0.83 ±0.06
36 Kr	–	3.23 ±0.07	80 Hg	–	1.09 ±0.05
37 Rb	2.60 ±(0.15)	2.40 ±0.03	81 Tl	(0.9 ±0.2)	0.82 ±0.04
38 Sr	2.90 ±0.06	2.93 ±0.03	82 Pb	1.85 ±0.05	2.05 ±0.03
39 Y	2.24 ±0.03	2.22 ±0.02	83 Bi		0.71 ±0.03
40 Zr	2.60 ±0.03	2.61 ±0.03	90 Th	0.12 ±(0.06)	0.08 ±0.02
41 Nb	1.42 ±0.06	1.40 ±0.01	92 U	(< −0.47)	−0.49 ±0.04
42 Mo	1.92 ±0.05	1.96 ±0.02			

* Values in parentheses are uncertain.
† Values in brackets are based upon solar or other astronomical data.
(From Anders, A. and Grevesse, N., *Geochim. Cosmochim. Acta*, **53**, 197, 1989.)

The planets (physical elements)

Planet	Mass	Radius (equ.)	Angular Diameter	Distance from Earth	Flattening (geom.)	Mean Density	Sidereal Period of Rotation	Inclination of Equator to orbit	Equatorial surface gravity	Equatorial escape velocity
	10^{24} kg	km		AU		g/cm^3	*d*	°	(Earth = 1)	(km s^{-1})
Mercury	0.33022	2439.7	11.″0	0.613	0	5.43	58.6462	0.0	0.387	4.3
Venus	4.8690	6051.9	60.″2	0.277	0	5.24	−243.01	177.3	0.879	10.3
Earth	5.9742	6378.140	–	–	0.00335364	5.515	0.99726968	23.45	1.000	11.2
(Moon)	0.073483	1738	31.′08	0.00257	0	3.34	27.32166	6.68	0.166	2.38
Mars	0.64191	3397	17.″9	0.524	0.00647630	3.94	1.02595675	25.19	0.380	5.0
Jupiter	1898.8	71492	46.″8	4.203	0.0648744	1.33	0.41354 (System III)	3.12	2.339	59.5
Saturn	568.50	60268	19.″4	8.539	0.0979624	0.70	0.4375 (System III)	26.73	0.925	35.6
Uranus	86.625	25559	3.″9	18.182	0.0229273	1.30	−0.65	97.86	0.794	21.22
Neptune	102.78	24764	2.″3	29.06	0.0171	1.76	0.768	29.56	1.125	23.6
Pluto	0.015	1151	0.″1	38.44	0	1.1	−6.3867	118?	0.77	1.32

The angular diameters correspond to the distances from the Earth (in AU) given in the adjacent column. The distances from the Earth refer to inferior conjunction for Mercury and Venus and to mean opposition for the other planets.

1 AU = 1.495979×10^{11} m.

System III refers to the apparent rate of rotation derived from radio emissions.

Equatorial surface gravity, $g = GM/R_{eq}^2$ ($g_{earth} = 9.80$ m s^{-2}).

Equatorial escape velocity = $(2MGR_{eq})^{1/2}$

M, mass of planet; G, universal gravitational constant; R_{eq}, equatorial radius of planet.

Earth-Moon mean distance = 3.84401×10^5 km.

(Adapted from the *Explanatory Supplement to the Astronomical Almanac*, Seidelmann, P.K., University Science Books, 1992.) A number of astronomers consider Pluto to be a minor planet along with the recently discovered (2005) 2003 UB313. Minor planet is the official term for asteroids and trans-Neptunian objects (TNOs). Physical elements for 2003 UB313: mass = ?, radius = at least 1200 km, mean density = ?, absolute magnitude = −1.1.

The planets (mean orbital elements)

Planet	Inclination (i)	Eccentricity (e)	Mean Longitude of Node (Ω)	Mean Longitude of Perihelion (ϖ)	Mean Longitude at Epoch (L)
Mercury	7°00′17.″95051	0.2056317524914	48°19′51.″21495	77°27′22.″02855	252°15′03.″25985
Venus	3°23′40.″07828	0.0067718819142	76°40′47.″71268	131°33′49.″34607	181°58′47.″28304
Earth	0.0	0.0167086171540	0.0	102°56′14.″45310	100°27′59.″21464
Mars	1°50′59.″01532	0.0934006199474	49°33′29.″13554	336°03′36.″84233	355°25′59.″78866
Jupiter	1°18′11.″77079	0.0484948512199	100°27′51.″98631	14°19′52.″71326	34°21′05.″34211
Saturn	2°29′19.″96115	0.0555086217172	113°39′55.″88533	93°03′24.″43421	50°04′38.″89695
Uranus	0°46′23.″50621	0.0462958985125	74°00′21.″41002	173°00′18.″57320	314°03′18.″01840
Neptune	1°46′11.″82795	0.0089880948652	130°47′02.″60528	48°07′25.″28581	304°20′55.″19574
Pluto	17°08′31.″8	0.249050	110°17′49.″7	224°08′05.″5	238°44′38.″2

	Sidereal Period (Julian years)	Synodic Period (d)	Mean Daily Motion (n) (°)	Mean Orbital Velocity (km/s)	Mean Distance (AU)	Mean Distance (10^{11} m)
Mercury	0.24084445	115.8775	4.°09237706	47.8725	0.3870983098	0.579090830
Venus	0.61518257	583.9214	1.°60216874	35.0214	0.7233298200	1.08208601
Earth	0.99997862		0.°98564736	29.7859	1.0000010178	1.49598023
Mars	1.88071105	779.9361	0.°52407109	24.1309	1.5236793419	2.27939186
Jupiter	11.85652502	398.8840	0.°08312944	13.0697	5.2026031913	7.78298361
Saturn	29.42351935	378.0919	0.°03349791	9.6724	9.5549095957	14.29394133
Uranus	83.74740682	369.6560	0.°01176904	6.8352	19.2184460618	28.75038615
Neptune	163.7232045	367.4867	0.°006020076	5.4778	30.1103868694	45.04449769
Pluto	248.0208	366.7207	0.°003973966	4.7490	39.544674	59.157990

The mean orbital elements are for the epoch J2000.0 = JD2451545.0 = 2000 January 1.5 except for Pluto.

The elements for Pluto are based on a fit over one century.

The sidereal period is the period of revolution measured with respect to the fixed stars; the synodic period is the interval between successive oppositions of a superior planet or successive inferior conjunctions of an inferior planet.

1 AU = $1.49597870 \times 10^{11}$ m.

(Adapted from the *Explanatory Supplement to the Astronomical Almanac*, Seidelmann, P.K., University Science Books, 1992.) A number of astronomers consider Pluto to be a minor planet along with the recently discovered (2005) 2003 UB313. Minor planet is the official term for asteroids and trans-Neptunian objects (TNOs). Orbital elements (JD 2453600.5) for 2003 UB313: inclination = 44.177°, eccentricity = 0.4416129, longitude of the ascending node = 35.8750°, argument of perihelion = 151.3115°, orbital period = 203,500 d, mean orbital velocity = 3.436 km s^{-1}, semi-major axis = 67.7091 AU, perihelion = 37.808 AU, aphelion = 97.610 AU, mean anomaly = 197.5379°.

The planets (additional data)

Planet	Perihelion Distance (AU)	Aphelion Distance (AU)	V_{max}	Magnetic Dipole Moment[b]	Solar Constant (Wm^{-2})	T_{BB} (K)	Oblateness
Mercury	0.31	0.47	−1.2	3×10^{19}	9936.9	445	0.0
Venus	0.72	0.73	−4.28	$< 8\times10^{17}$	2613.9	325	0.0
Earth	0.98	1.02	−3.86[a]	8.02×10^{22}	1367.6	277	0.00335
Mars	1.38	1.67	−2.52	1×10^{18}	589.0	225	0.006476
Jupiter	4.95	5.45	−2.7	1.56×10^{27}	50.5	123	0.064874
Saturn	9.00	10.4	−0.6	4.72×10^{25}	15.04	90	0.097962
Uranus	18.27	20.06	+5.3	3.83×10^{24}	3.71	63	0.022927
Neptune	29.71	30.34	+7.50	2.16×10^{24}	1.47	50	0.0182
Pluto	29.7	49.1	+13.8			44	

1 AU = 1.496×10^{11} m.

V_{max}, maximum visual apparent magnitude.

[a] As seen from the Sun.

[b] Units are A m^2.

The theoretical value (ignoring dipole offset) for the planetary surface magnetic field at the magnetic equator is

$$B_0 = \mu_0 M / 4\pi R^3 \text{ weber m}^{-2} \text{ (or tesla} = 1 \times 10^4 \text{ gauss)}$$

where

M = the magnetic dipole moment

R = the radius of the planet at the magnetic equator.

$\mu_0 = 4\pi \times 10^{-7}$ H m^{-1}, the vacuum magnetic permeability.

For the Earth, the surface field is 3.1×10^{-5} T = 0.31 gauss.

T_{BB}, blackbody temperature.

Oblateness, $(R_{eq} - R_{pol})/R_{eq}$

Natural satellites in the solar system (orbital data)

Planet		Satellite	Orbital Period[1] (R = Retrograde) d	Semimajor Axis $\times 10^3$ km	Orbital Eccentricity	Inclination of Orbit to Planet's Equator °
Earth		Moon	27.321 661	384.400	0.054 900 489	18.28–28.58
Mars	I	Phobos	0.318 910 23	9.378	0.015	1.0
	II	Deimos	1.262 440 7	23.459	0.000 5	0.9–2.7
Jupiter	I	Io	1.769 137 786	422	0.004	0.04
	II	Europa	3.551 181 041	671	0.009	0.47
	III	Ganymede	7.154 552 96	1 070	0.002	0.21
	IV	Callisto	16.689 018 4	1 883	0.007	0.51
	V	Amalthea	0.498 179 05	181	0.003	0.40
	VI	Himalia	250.566 2	11 480	0.157 98	27.63
	VII	Elara	259.652 8	11 737	0.207 19	24.77
	VIII	Pasiphae	735 R	23 500	0.378	145
	IX	Sinope	758 R	23 700	0.275	153
	X	Lysithea	259.22	11 720	0.107	29.02
	XI	Carme	692 R	22 600	0.206 78	164
	XII	Ananke	631 R	21 200	0.168 70	147
	XIII	Leda	238.72	11 094	0.147 62	26.07
	XIV	Thebe	0.674 5	222	0.015	0.8
	XV	Adrastea	0.298 26	129		
	XVI	Metis	0.294 780	128		
Saturn	I	Mimas	0.942 421 813	185.52	0.020 2	1.53
	II	Enceladus	1.370 217 855	238.02	0.004 52	0.00
	III	Tethys	1887 802 160	294.66	0.000 00	1.86
	IV	Dione	2.736 914 742	377.40	0.002 230	0.02
	V	Rhea	4.517 500 436	527.04	0.001 00	0.35
	VI	Titan	15.945 420 68	1 221.83	0.029 192	0.33
	VII	Hyperion	21.276 608 8	1 481.1	0.104	0.43
	VIII	Iapetus	79.330 182 5	3 561.3	0.028 28	14.72
	IX	Phoebe	550.48 R	12 952	0.163 26	177[2]
	X	Janus	0.694 5	151.472	0.007	0.14

Natural satellites in the solar system (orbital data, cont.)

Planet		Satellite	Orbital Period[1] (R = Retrograde) d	Semimajor Axis $\times 10^3$ km	Orbital Eccentricity	Inclination of Orbit to Planet's Equator °
	XI	Epimetheus	0.694 2	151.422	0.009	0.34
	XII	Helene	2.736 9	377.40	0.005	00
	XIII	Telesto	1.887 8	294.66		
	XIV	Calypso	1.887 8	294.66		
	XV	Atlas	0.601 9	137.670	0.000	0.3
	XVI	Prometheus	0.613 0	139.353	0.003	0.0
	XVII	Pandora	0.628 5	141.700	0.004	0.0
	XVIII	Pan	0.575 0	133.583		
Uranus	I	Ariel	2.520 379 35	191.02	0.003 4	0.3
	II	Umbriel	4.144 177 2	266.30	0.005 0	0.36
	III	Titania	8.705 871 7	435.91	0.002 2	0.14
	IV	Oberon	13.463 238 9	583.52	0.000 8	0.10
	V	Miranda	1.413 479 25	129.39	0.002 7	4.2
	VI	Cordelia	0.335 033	49.77	< 0.001	0.1
	VII	Ophelia	0.376 409	53.79	0.010	0.1
	VIII	Bianca	0.434 577	59.17	< 0.001	0.2
	IX	Cressida	0.463 570	61.78	< 0.001	0.0
	X	Desdemona	0.473 651	62.68	< 0.001	0.2
	XI	Juliet	0.493 066	64.35	< 0.001	0.1
	XII	Portia	0.513 196	66.09	< 0.001	0.1
	XIII	Rosalind	0.558 459	69.94	< 0.001	0.3
	XIV	Belinda	0.623 525	75.26	< 0.001	0.0
	XV	Puck	0.761 832	86.01	< 0.001	0.31
Neptune	I	Triton	5.876 854 1 R	354.76	0.000 016	157.345
	II	Nereid	360.136 19	5 513.4	0.751 2	27.6[3]
	III	Naiad	0.294 396	48.23	< 0.001	4.74
	IV	Thalassa	0.311 485	50.07	< 0.001	0.21
	V	Despina	0.334 655	52.53	< 0.001	0.07
	VI	Galatea	0.428 745	61.95	< 0.001	0.05
	VII	Larissa	0.554 654	73.55	0.001 4	0.20
	VIII	Proteus	1.122 315	117.65	< 0.001	0.55
Pluto	I	Charon	6.387 25	19.6	< 0.001	99[3]

[1] Sidereal periods, except that tropical periods are given for satellites of Saturn.

[2] Relative to ecliptic plane.

[3] Referred to equator of 1950.0.

(From the 1999 *Astronomical Almanac*, USNO, Government Printing Office.) As of August, 2005, the current number of natural satellites is Mercury = 0, Venus = 0, Earth = 1, Mars = 2, Jupiter = 63, Saturn = 47, Uranus = 27, Neptune = 13, Pluto = 1.

Natural satellites in the Solar System (physical and photometric data)

		Satellite	Mass (Planet = 1)	Radius km	V_0^*
Earth		Moon	0.01230002	1738	−12.74
Mars	I	Phobos	1.5×10^{-8}	$13.5 \times 10.8 \times 9.4$	11.3
	II	Deimos	3×10^{-9}	$7.5 \times 6.1 \times 5.5$	12.40
Jupiter	I	Io	4.68×10^{-5}	1815	5.02
	II	Europa	2.52×10^{-5}	1569	5.29
	III	Ganymede	7.80×10^{-5}	2631	4.61
	IV	Callisto	5.66×10^{-5}	2400	5.65
	V	Amalthea	38×10^{-10}	$135 \times 83 \times 75$	14.1
	VI	Himalia	50×10^{-10}	93	14.84
	VII	Elara	4×10^{-10}	38	16.77
	VIII	Pasiphae	1×10^{-10}	25	17.03
	IX	Sinope	0.4×10^{-10}	18	18.3
	X	Lysithea	0.4×10^{-10}	18	18.4
	XI	Carme	0.5×10^{-10}	20	18.0
	XII	Ananke	0.2×10^{-10}	15	18.9
	XIII	Leda	0.03×10^{-10}	8	20.2
	XIV	Thebe	4×10^{-10}	55×45	15.7
	XV	Adrastea	0.0×10^{-10}	$12.5 \times 10 \times 7.5$	19.1
	XVI	Metis	0.5×10^{-10}	20	17.5
Saturn	I	Mimas	8.0×10^{-8}	196	12.9
	II	Enceladus	1.3×10^{-7}	250	11.7
	III	Tethys	1.3×10^{-6}	530	10.2
	IV	Dione	1.85×10^{-6}	560	10.4
	V	Rhea	4.4×10^{-6}	765	9.7
	VI	Titan	2.38×10^{-4}	2575	8.28
	VII	Hyperion	3×10^{-8}	$205 \times 130 \times 110$	14.19
	VIII	Iapetus	3.3×10^{-6}	730	11.1
	IX	Phoebe	7×10^{-10}	110	16.45
	X	Janus		$110 \times 100 \times 80$	14:

Natural satellites in the Solar System (physical and photometric data, cont.)

		Satellite	Mass (Planet = 1)	Radius km	V_0^*
	XI	Epimetheus		$70 \times 60 \times 50$	15 :
	XII	Helene		$18 \times 16 \times 15$	18 :
	XIII	Telesto		$17 \times 14 \times 13$	18.5:
	XIV	Calypso		$17 \times 11 \times 11$	18.7:
	XV	Atlas		20×10	18 :
	XVI	Prometheus		$70 \times 50 \times 40$	16 :
	XVII	Pandora		$55 \times 45 \times 35$	16 :
	XVIII	Pan		10	
Uranus	I	Ariel	1.56×10^{-5}	579	14.16
	II	Umbriel	1.35×10^{-5}	586	14.81
	III	Titania	4.06×10^{-5}	790	13.73
	IV	Oberon	3.47×10^{-5}	762	13.94
	V	Miranda	0.08×10^{-5}	240	16.3
	VI	Cordelia		13	24.1
	VII	Ophelia		15	23.8
	VIII	Bianca		21	23.0
	IX	Cressida		31	22.2
	X	Desdemona		27	22.5
	XI	Juliet		42	21.5
	XII	Portia		54	21.0
	XIII	Rosalind		27	22.5
	XIV	Belinda		33	22.1
	XV	Puck		77	20.2
Neptune	I	Triton	2.09×10^{-4}	1353	13.47
	II	Nereid	$2 \quad \times 10^{-7}$	170	18.7
	III	Naiad		29:	24.7
	IV	Thalassa		40:	23.8
	V	Despina		74	22.6
	VI	Galatea		79	22.3
	VII	Larissa		104×89	22.0
	VIII	Proteus		$218 \times 208 \times 201$	20.3
Pluto	I	Charon	0.22	593	16.8

*V_0 = visual magnitude at opposition.

23 small irregular jovian satellites have been discovered in the period 1999–2001.

(From the 1999 *Astronomical Almanac*, USNO, Government Printing Office.) As of August, 2005, the current number of natural satellites is Mercury = 0, Venus = 0, Earth = 1, Mars = 2, Jupiter = 63, Saturn = 47, Uranus = 27, Neptune = 13, Pluto = 1.

Selected comets

Number	Name	Orbital Period	Perihelion Date	Perihelion Distance	Semi-Major Axis	Orbital Eccentricity	Orbital Inclination	Absolute Magnitude*
1P	Halley	76.1 yr	1986-02-09	0.587 AU	17.94 AU	0.967	162.2	5.5
2P	Encke	3.30	2003-12-28	0.340	2.21	0.847	11.8	9.8
6P	d'Arrest	6.51	2008-08-01	1.346	3.49	0.614	19.5	8.5
9P	Tempel 1	5.51	2005-07-07	1.500	3.12	0.519	10.5	12.0
19P	Borrelly	6.86	2001-09-14	1.358	3.61	0.624	30.3	11.9
21P	Giacobini-Zinner	6.52	1998-11-21	0.996	3.52	0.706	31.8	9.0
26P	Grigg-Skjellerup	5.09	1992-07-22	0.989	2.96	0.664	21.1	12.5
27P	Crommelin	27.89	1984-09-01	0.743	9.20	0.919	29.0	12.0
45P	Honda-Mrkos -Pajdusakova	5.29	1995-12-25	0.528	3.02	0.825	4.3	13.5
46P	Wirtanen	5.46	2013-10-21	1.063	3.12	0.652	11.7	9.0
55P	Tempel-Tuttle	32.92	1998-02-28	0.982	10.33	0.906	162.5	9.0
73P	Schwassmann -Wachmann 3	5.36	2006-06-02	0.937	3.06	0.694	11.4	11.7
75P	Kohoutek	6.24	1973-12-28	1.571	3.4	0.537	5.4	12.1
76P	West-Kohoutek -Ikemura	6.46	2000-06-01	1.596	3.45	0.540	30.5	10.5
81P	Wild 2	6.39	2003-09-25	1.583	3.44	0.540	3.2	6.5
95P	Chiron	50.7	1996-02-14	8.46	13.7	0.383	7	
107P	Wilson-Harrington	4.29	2001-03-26	1.000	2.64	0.623	2.8	9.0
	Hale-Bopp	4000.	1997-03-31	0.914	250.	0.995	89.4	−1.0
	Hyakutake	~ 40000.	1996-05-01	0.230	~ 1165.	0.9998	124.9	

*Absolute magnitude: This is the brightness a comet would exhibit if placed 1 AU from both the Earth and Sun.

The comets were selected for historical interest or are subjects for flybys. (NASA/Goddard, 2000)

Periodic comets, periods under 200 yr

Desig.	Name	Discovery	Last T	Next T	Period	Inclin.
2P	Encke	1786	2000	2003	3.3 yr	11.8°
107P	Wilson-Harrington	1949	1996	2001	4.3	2.8
26P	Grigg-Skjellerup	1902	1997	2002	5.11	21.1
79P	du Toit-Hartley	1945	1987	2003	5.21	2.9
141P	Machholz 2	1994	1999	2005	5.22	12.8
96P	Machholz 1	1986	1996	2001	5.24	60.1
45P	Honda-Markos-Pajdusakova	1948	1995	2001	5.27	4.2
73P	Schwassmann-Wachmann 3	1930	1995	2001	5.34	11.4
25D	Neujmin 2	1916	1927	Lost	5.43	10.6
46P	Wirtanen	1948	1997	2002	5.46	11.7
5D	Brorsen	1846	1879	Lost	5.46	29.4
41P	Tuttle-Giacobini-Kresak	1858	1995	2001	5.46	9.2
10P	Tempel 2	1873	1999	2005	5.47	12.0
9P	Tempel 1	1867	2000	2005	5.51	10.5
71P	Clark	1973	2000	2006	5.52	9.5
125P	Spacewatch	1991	1996	2002	5.56	10.0
88P	Howell	1981	1998	2004	5.57	4.4
133P	Elst-Pizarro	1996	1996	2001	5.61	1.4
124P	Mrkos	1991	1996	2002	5.64	31.5
11D	Tempel-Swift	1869	1908	Lost	5.68	5.4
100P	Hartley 1	1985	1997	2003	6.02	25.7
83P	Russell 1	1979	1985	2006	6.1	22.7
37P	Forbes	1929	1999	2005	6.13	9.9
116P	Wild 4	1990	1996	2003	6.16	3.7
104P	Kowal 2	1979	1998	2004	6.18	15.5
54P	de Vico-Swift	1844	1965	Lost	6.31	3.6
127P	Holt-Olmstead	1990	1997	2003	6.33	14.4
7P	Pons-Winnecke	1819	1996	2002	6.37	22.3
103P	Hartley 2	1986	1997	2004	6.39	13.6
57P	du Toit-Neujmin-Delporte	1941	1996	2002	6.39	2.8
81P	Wild 2	1978	1997	2003	6.39	3.2
31P	Schwassmann-Wachmann 2	1929	1994	2002	6.39	3.8
76P	West-Kohoutek-Ikemura	1975	1993	2000	6.41	30.5
105P	Singer Brewster	1986	1999	2005	6.44	9.2
22P	Kopff	1906	1996	2002	6.45	4.7
43P	Wolf-Harrington	1924	1997	2004	6.46	18.5
6P	d'Arrest	1851	1995	2002	6.51	19.5
118P	Shoemaker-Levy 4	1991	1997	2003	6.51	8.5
87P	Bus	1981	2000	2007	6.52	2.6
94P	Russell 4	1984	1997	2003	6.58	6.2
67P	Churyumov-Gerasimenko	1969	1996	2002	6.59	7.1
49P	Arend-Rigaux	1951	1998	2005	6.61	18.3
21P	Giacobini-Zinner	1900	1998	2005	6.61	31.9
3D	Biela	1772	1852	Broke up	6.62	12.6
62P	Tsuchinshan 1	1965	1998	2004	6.64	10.5
44P	Reinmnuth 2	1947	1994	2001	6.64	7.0
112P	Urata-Niijima	1986	2000	2006	6.65	24.2
114P	Wiseman-Skiff	1986	2000	2006	6.66	18.3
75P	Kohoutek	1975	1994	2001	6.67	5.9
130P	McNaught-Hughes	1991	1998	2004	6.69	7.3

Periodic comets, periods under 200 yr (cont.)

Desig.	Name	Discovery	Last T	Next T	Period	Inclin.
18D	Perrine-Mrkos	1896	1968	Lost?	6.72 yr	17.8°
15P	Finlay	1886	1995	2002	6.76	3.7
51P	Harrington	1953	1994	2001	6.78	8.7
60P	Tsuchinshan 2	1965	1999	2005	6.79	6.7
65P	Gunn	1970	1996	2003	6.83	10.4
110P	Hartley 3	1988	1994	2001	6.88	11.7
19P	Borrelly	1904	1994	2001	6.88	30.3
138P	Shoemaker-Levy 7	1991	1998	2005	6.89	10.1
16P	Brooks 2	1889	1994	2001	6.89	5.5
86P	Wild 3	1980	1994	2001	6.91	15.5
84P	Giclas	1978	1999	2006	6.95	7.3
48P	Johnson	1949	1997	2004	6.97	13.7
69P	Taylor	1915	1997	2004	6.97	20.5
77P	Longmore	1975	1995	2002	6.98	24.4
148P	Anderson-LINEAR	1963	1963	2001	7.04	3.7
70P	Kojima	1970	2000	2007	7.04	6.6
131P	Mueller 2	1990	1997	2004	7.05	7.4
33P	Daniel	1909	1992	2008	7.06	20.1
17P	Holmes	1892	2000	2007	7.07	19.2
113P	Spitaler	1890	1994	2001	7.1	5.8
78P	Gehrels 2	1973	1997	2004	7.2	6.3
98P	Takamizawa	1984	1998	2006	7.21	9.5
108P	Ciffreo	1985	2000	2007	7.25	13.1
129P	Shoemaker-Levy 3	1991	1998	2005	7.25	5.0
102P	Shoemaker 1	1984	1991	2006	7.26	26.3
106P	Schuster	1977	1999	2007	7.29	20.1
30P	Reinmuth 1	1928	1995	2002	7.31	8.1
4P	Faye	1843	1999	2006	7.34	9.1
89P	Russell 2	1980	1994	2002	7.38	12.0
147P	Kushida-Muramatsu	1993	1993	2001	7.44	2.4
47P	Ashbrook-Jackson	1948	1993	2001	7.49	12.5
91P	Russell 3	1983	1997	2005	7.49	14.1
61P	Shajn-Schaldach	1949	1993	2001	7.49	6.1
135P	Shoemaker-Levy 8	1992	1999	2007	7.49	6.1
52P	Harrington-Abell	1955	1999	2006	7.53	10.2
144P	Kushida	1994	1994	2001	7.58	4.1
123P	West-Hartley	1989	1996	2003	7.59	15.3
150P	2000 WT168	2000	2001	2008	7.66	18.5
97P	Metcalf-Brewington	1906	1991	2001	7.76	13.0
146P	Shoemaker-LINEAR	1984	2000	2008	7.88	21.6
39P	Oterma	1942	1958	Lost?	7.88	4.0
121P	Shoemaker-Holt 2	1989	1996	2004	8.05	17.7
82P	Gehrels 3	1975	1993	2001	8.11	1.1
80P	Peters-Hartley	1846	1998	2006	8.12	29.9
111P	Helin-Roman-Crockett	1989	1996	2004	8.16	4.2
14P	Wolf	1884	2000	2009	8.21	27.9
24P	Schaumasse	1911	1993	2001	8.22	11.8
58P	Jackson-Neujmin	1936	1995	2004	8.24	13.5
50P	Arend	1951	1999	2007	8.24	19.2
132P	Helin-Roman-Alu 2	1989	1997	2006	8.24	5.8
120P	Mueller 1	1987	1996	2004	8.41	8.8

Periodic comets, periods under 200 yr (cont.)

Desig.	Name	Discovery	Last T	Next T	Period	Inclin.
36P	Whipple	1933	1994	2003	8.53 yr	9.9°
74P	Smirnova-Chernykh	1975	1992	2001	8.57	6.6
145P	Shoemaker-Levy 5	1991	2000	2009	8.69	11.8
136P	Mueller 3	1990	1999	2007	8.71	9.4
115P	Maury	1985	1994	2002	8.74	11.7
32P	Comas Sola	1926	1996	2005	8.83	12.9
119P	Parker-Hartley	1989	1996	2005	8.89	5.2
143P	Kowal-Mrkos	1984	2000	2009	8.95	4.7
149P	Muller 4	1992	1992	2001	9.01	29.7
72P	Denning-Fujikawa	1881	1978	2005	9.01	8.6
93P	Lovas 1	1980	1998	2007	9.15	12.2
64P	Swift-Gehrels	1889	1991	2009	9.21	9.3
137P	Shoemaker-Levy 2	1990	2000	2009	9.37	4.7
59P	Keams-Kwee	1963	1999	2009	9.47	9.4
128P	Shoemaker-Holt 1	1987	1997	2007	9.51	4.4
139P	Väisälä-Oterma	1939	1998	2008	9.54	2.3
117P	Helin-Roman-Alu 1	1989	1997	2005	9.57	9.7
42P	Neujmin 3	1929	1993	2004	10.63	4.0
40P	Väisälä 1	1939	1993	2004	10.78	11.6
68P	Klemola	1965	1998	2009	10.82	11.1
34P	Gale	1927	1938	Lost	10.99	11.7
142P	Ge-Wang	1988	1999	2010	11.17	12.2
85P	Boethin	1975	1986	2008	11.23	5.8
56P	Slaughter-Burnham	1958	1993	2005	11.59	8.2
53P	Van Biesbroeck	1954	1991	2003	12.43	6.6
92P	Sanguin	1977	1990	2002	12.5	18.7
63P	Wild 1	1960	1999	2013	13.24	19.9
126P	IRAS	1983	1996	2010	13.29	46.0
8P	Tuttle	1790	1994	2008	13.51	54.7
101P	Chernykh	1977	1992	2005	13.96	5.1
29P	Schwassmann-Wachmann 1	1927	1989	2004	14.85	9.4
66P	du Toit	1944	1974	2003	14.97	18.7
99P	Kowal 1	1977	1992	2007	15.02	4.4
90P	Gehrels 1	1972	1987	2002	15.06	9.6
134P	Kowal-Vavrova	1983	1998	2014	15.58	4.3
140P	Bowell-Skiff	1983	1999	2015	16.18	3.8
28P	Neujmin 1	1913	1984	2002	18.19	14.2
27P	Crommelin	1818	1984	2011	27.41	29.1
55P	Tempel-Tuttle	1865	1998	2031	33.22	162.5
38P	Stephan-Oterma	1867	1980	2018	37.71	18.0
95P	Chiron	1977	1996	2046	50.78	6.9
20D	Westphal	1852	1913	Lost?	61.86	40.9
13P	Olbers	1815	1956	2024	69.56	44.6
23P	Brorsen-Metcalf	1847	1989	2059	70.54	19.3
12P	Pons-Brooks	1812	1954	2024	70.92	74.2
122P	de Vico	1846	1995	2069	74.41	85.4
1P	Halley	240 BC	1986	2061	76.01	162.2
109P	Swift-Tuttle	1862	1992	2126	135	113.4
35P	Herschel-Rigollet	1788	1939	2092	154.91	64.2

Last T, year of last perihelion passage.

Next T, next predicted perihelion year.

Period, orbital period taken from last observed apparition.

Inclin., inclination with respect to the ecliptic.

Orbital element may change due to perturbations, especially encounters with Jupiter.

Selected asteroids

Asteroid Number	Name	Diameter (km)	~Mass 10^{15} kg	Rotation Period hr	Orbital period yr	Semimajor Axis AU	Orbital Eccentricity	Orbital Inclination°
1	Ceres	960 × 932	870,000	9.075	4.60	2.767	0.0789	10.58
2	Pallas	570 × 525 × 482	318,000	7.811	4.61	2.774	0.2299	34.84
3	Juno	240	20,000	7.210	4.36	2.669	0.2579	12.97
4	Vesta	530	300,000	5.342	3.63	2.362	0.0895	7.14
45	Eugenia	226	6,100	5.699	4.49	2.721	0.0831	6.61
140	Siwa	103	1,500	18.5	4.51	2.734	0.2157	3.19
216	Kleopatra	217 × 94		5.385	4.67	2.793	0.2535	13.14
243	Ida	58 × 23	100	4.633	4.84	2.861	0.0451	1.14
253	Mathilde	66 × 48 × 46	103.3	417.7	4.31	2.646	0.2660	6.71
433	Eros	33 × 13 × 13	6.69	5.270	1.76	1.458	0.2229	10.83
951	Gaspra	19 × 12 × 11	10	7.042	3.29	2.209	0.1738	4.10
1566	Icarus	1.4	0.001	2.273	1.12	1.078	0.8269	22.86
1620	Geographos	2.0	0.004	5.222	1.39	1.245	0.3356	13.34
1862	Apollo	1.6	0.002	3.063	1.81	1.471	0.5600	6.36
2060	Chiron	180	4,000	5.9	50.7	13.633	0.3801	6.94
2530	Shipka				5.25	3.019	0.1237	10.10
2703	Rodari				3.25	2.194	0.0572	6.04
3352	McAuliffe	2 − 5			2.57	1.879	0.3686	4.77
3840	Mimistrobell				3.38	2.249	0.0831	3.92
4179	Toutatis	4.6 × 2.4 × 1.9	0.05	130.	3.98	2.512	0.6339	0.47
4660	Nereus	2			1.82	1.490	0.3603	1.42
4769	Castalia	1.8 × 0.8	0.0005		1.10	1.063	0.4831	8.89
4979	Otawara	5.5	0.2		3.19	2.168	0.1449	0.91
9969	Braille	2.2 × 1.0			3.58	2.341	0.4336	29.0
1998	SF36	~1			1.52	1.324	0.2789	1.71

1 Ceres– The largest and first discovered asteroid, by G. Piazzi on January 1, 1801. Ceres comprises over one-third the 2.3×10^{21} kg estimated total mass of all the asteroids.

2 Pallas– The 2nd largest asteroid and second asteroid discovered, by H. Olbers in 1802.

3 Juno– The 3rd asteroid discovered, by K. Harding in 1804.

4 Vesta– The 3rd largest asteroid.

The asteroids were selected for historical interest, are subjects for flybys, or because of peculiarities (near-Earth, odd shape, double object).

(NASA/Goddard, 2000)

Asteroid distribution histogram

This histogram shows the primary Kirkwood gaps in the main asteroid belt. These gaps (labeled “3:1”, “5:2”, “7:3”, “2:1”) are caused by mean-motion resonances between an asteroid and Jupiter. For example, the 3:1 Kirkwood gap is located where the ratio of an asteroid's orbital period to that of Jupiter is 3/1 (the asteroid completes 3 orbits for every 1 orbit of Jupiter). The effect of these mean-motion resonances is a change in the asteroid's orbital elements (particularly semi-major axis) sufficient to create the gaps in semi-major axis space.

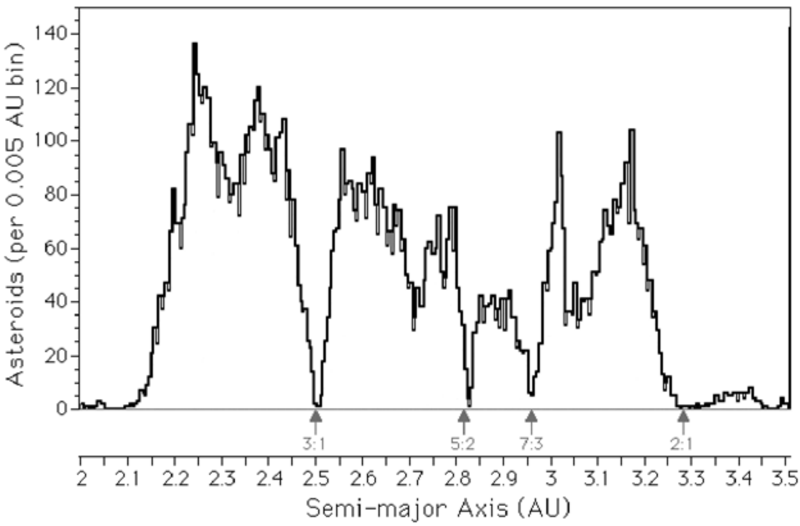

(NASA/JPL, 1999)

Estimated total mass of asteroids = 1.8×10^{24} g.

Estimated densities (most asteroids): 1.0 – 3.5 g cm^{-3}.

Typical rotation period, approx. 9 h (range: 2 to greater than 1000 h).

Annual major meteor showers

			Radiant				
Shower	Activity	Max	λ	α	δ	V	ZHR
Quadrantids	Dec 28-Jan 07	Jan 3/4	283	229	+49	41	45-200
Lyrids	Apr 16-Apr 22	Apr 21/22	032	271	+33	49	10
η Aquarids	Apr 21-May 12	May 05	046	337	−01	66	10
α Capricornids	Jul 15-Sep 11	Aug 1	129	307	−08	25	6-14
Southern δ Aquarids	Jul 14-Aug 18	Jul 29	125	339	−17	34	15-20
Northern δ Aquarids	Jul 16-Sep 10	Aug 13	139	344	+02	42	10
Perseids	Jul 23-Aug 22	Aug 11/12	140	047	+57	59	80
Orionids	Oct 15-Oct 29	Oct 20/21	208	095	+16	66	20
Southern Taurids	Sep 17-Nov 27	Nov 1-7	216	053	+12	27	5
Northern Taurids	Oct 12-Dec 02	Nov 4-7	221	054	+21	29	7
Leonids	Nov 14-Nov 21	Nov 17	235	153	+22	71	10-15
Geminids	Dec 09-Dec 19	Dec 13/14	262	112	+33	35	80
Ursids	Dec 17-Dec 24	Dec 22/23	271	217	+76	33	10-15

α, δ: Coordinates for a shower's radiant position, at maximum; α is right ascension, δ is declination. Radiants drift across the sky each day due to the Earth's own orbital motion around the Sun.

λ: Solar longitude at maximum, a precise measure of the Earth's position on its orbit which is not dependent on the vagaries of the calendar. All λ's are given for the equinox J2000.0.

V: Atmospheric or apparent meteoric velocity given in $\mathrm{km\,s^{-1}}$. Velocities range from about 11 $\mathrm{km\,s^{-1}}$ (very slow) to 72 $\mathrm{km\,s^{-1}}$ (very fast). 40 $\mathrm{km\,s^{-1}}$ is roughly medium speed.

ZHR: Zenith Hourly Rate, a calculated maximum number of meteors an ideal observer would see in perfectly clear skies with the shower radiant overhead. This figure is given in terms of meteors per hour.

Meteoroid flux density

Cumulative flux density of meteroids that are larger than a given mass *vs* the meteoroid mass for meteoroids near the Earth. (From *The Astronomy and Astrophysics Encyclopedia*, Cambridge University Press, 1991.)

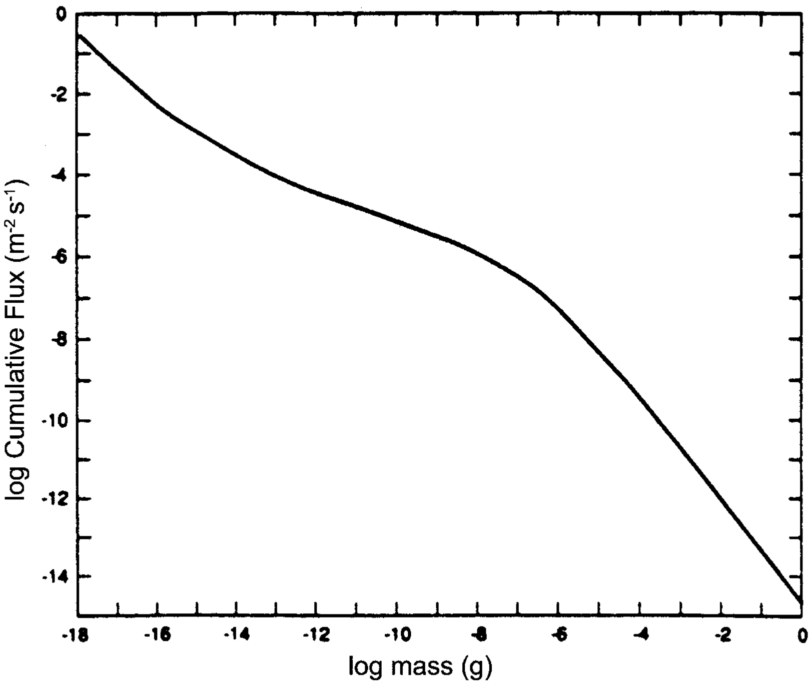

An analytical expression for the meteoroid flux density in the vicinity of the Earth-Moon system is given by

$$F = 7.9\ m^{-1.16} 10^6\ km^{-2}\ yr^{-1},\ 10^{-10} < m < 10^5\ kg$$

Where F is the number of meteoroids with mass greater than m (kg) per 10^6 km^2 per year. Meteoroids with masses greater than 6 kg will arrive in the vicinity of the Earth-Moon system at a rate of approximately 1 per 10^6 km^2 per year.

(From Schubert, G. and Walterschied, R.L, in *Allen's Astrophysical Quantities*, Cox, A.N., Editor, Springer, 1999.)

Glossary of meteor astronomy

Asteroid
One of a number of objects ranging in size from sub-km to about 1000 km, most of which lie between the orbits of Mars and Jupiter; also called 'minor planet'. The preliminary designations consist of the year of discovery, an upper case letter to indicate the half month in that year (A = Jan 1–15, B = Jan 16–31,..., Y = Dec 16–31, the letter I being omitted), and a second upper case letter in sequence. When this sequence of 25 letters (with I again being omitted) has been completed it is repeated and followed by a sequential number. Permanent designations consist of numbers and names, beginning with (1) Ceres, given to asteroids for which orbits are accurately determined. Names are generally proposed by the discoverer.
Comet
A diffuse body of solid particles and gas, which orbits the Sun. The orbit is usually highly elliptical or even parabolic. Comets are unstable bodies with masses of the order of 10^{18} g whose average lifetime is about 100 perihelion passages. Periodic comets comprise only $\sim 4\%$ of all known comets. Periodic comets are designated by a number, followed by "P/" and its name; e.g. Halley's comet has the designation 1P/Halley, the parent body of the Perseids, 109P/Swift-Tuttle.
Fireball
A bright meteor with an apparent visual magnitude of -4 mag. or brighter.
Meteor
In particular, the light phenomenon which results from the entry into the Earth's atmosphere of a solid particle from space.
Meteorite
A natural object of extraterrestrial origin (meteoroid) that survives passage through the atmosphere and hits the ground.
Meteoroid
A solid object moving in interplanetary space, of a size considerably smaller than a asteroid and considerably larger than an atom or molecule.
Meteoroid Stream
Stream of solid particles released from a parent body such as a comet or asteroid, moving on similar orbits. Various ejection directions and velocities for individual meteoroids cause the width of a stream and the gradual distribution of meteoroids over the entire average orbit.
Meteor Shower
A number of meteors with approximately parallel trajectories. The meteors belonging to one shower appear to emanate from their radiant.
Micrometeorite
A small extraterrestrial particle that has survived entry into the Earth's

atmosphere. The actual size is not rigorously constrained but is operationally defined by the collection procedure. Micrometeorites found on the Earth's surface are smaller than 1 mm, those collected in the stratosphere are rarely as large as 50 μm.

Persistent train

Remaining glow due to ionization in the upper atmosphere after the passage of a meteoroid. The intensity and duration depend on the meteoroid's atmospheric entry velocity, its size, and its composition. Bright fireballs occasionally caused trains visible for several minutes.

Radiant

The point where the backward projection of the meteor trajectory intersects the celestial sphere. More generally, the point in the sky where meteors from a specific shower seem to come from.

Radio observations

Two main methods are used, forward scatter observations and radar observations. The first are easy to carry out, but deliver only data on the general meteor activity; showers cannot be associated. The last is carried out by professional astronomers. Meteor radiants and meteoroid orbits can be determined.

Solar longitude

Angular distance along the Earth's orbit measured from the intersection of the ecliptic and the celestial equator where the Sun moves from south to north. It gives the position of the Earth on its orbit and, hence, is a more appropriate information on a meteor shower's maximum than the date.

(Adapted from the International Meteor Organization)

Contents of the solar system

Contents of the planetary system (mass, energy, and momentum)	
Total mass of planets	2.669×10^{27} kg
Total mass of satellites	6.2×10^{23} kg
Total mass of asteroids	1.8×10^{21} kg
Total mass of meteoric and cometary matter	6.0×10^{15} kg
Total mass of entire planetary system	2.670×10^{27} kg
Total angular momentum of planetary system	3.148×10^{43} kg m^2 s^{-1}
Total translational kinetic energy of the planetary system	1.99×10^{35} Joule
Total rotational energy of planets	0.7×10^{35} Joule
For comparison:	
Mass of the Sun	1.989×10^{30} kg
Solar angular momentum (based on surface rotation)	1.63×10^{41} kg m^2 s^{-1}
Contents of comet source regions (mass and number)	
Estimated total mass of Oort Cloud of comets	$10^{25} - 10^{27}$ kg
Estimated number of Oort cloud comets	$10^{11} - 10^{13}$
Estimated distance of the Oort cloud	$10^{3} - 10^{5}$ AU
Estimated total mass of Kuiper belt of comets	$10^{22} - 10^{26}$ kg
Estimated number of Kuiper belt comets	$10^{8} - 10^{12}$
Estimated distance of the Kuiper belt	$30 - 1000$ AU

(From Allen's Astrophysical Quantities, Cox, A.N., ed., Springer-Verlag, 2000.)

Extrasolar planets

	Star	$M_p \sin i$	P	a	e	K	M	α	δ
1	HD83443b	0.35	2.986	0.04	0.00	57.0	0.79	09 37 11.8	−43 16 20
2	HD46375	0.25	3.024	0.04	0.02	35.2	1.00	06 33 12.6	5 27 47
3	HD179949	0.93	3.092	0.04	0.00	112.0	1.24	19 15 33.2	−24 10 46
4	HD187123	0.54	3.097	0.04	0.01	72.0	1.06	19 46 58.1	34 25 10
5	τ Boo	4.14	3.313	0.05	0.02	474.0	1.30	13 47 15.7	17 27 25
6	BD-103166	0.48	3.487	0.05	0.05	60.6	1.10	10 58 28.8	−10 46 13
7	HD75289	0.46	3.508	0.05	0.01	56.0	1.15	08 47 40.4	−41 44 12
8	HD209458	0.63	3.524	0.05	0.02	82.0	1.05	22 03 10.8	18 53 4
9	51Peg	0.46	4.231	0.05	0.01	55.2	1.06	22 57 28.0	20 46 8
10	ν Andb	0.68	4.617	0.06	0.02	70.2	1.30	01 36 47.8	41 24 20
11	HD68988	1.90	6.276	0.07	0.14	187.0	1.20	08 18 22.2	61 27 39
12	HD168746	0.24	6.400	0.07	0.00	28.0	0.92	18 21 49.8	−11 55 22
13	HD217107	1.29	7.130	0.07	0.14	139.7	0.98	22 58 15.5	−2 23 43
14	HD162020	13.73	8.420	0.07	0.28	1813.0	0.70	17 50 38.4	−40 19 6
15	HD130322	1.15	10.720	0.09	0.05	115.0	0.89	14 47 32.7	0 16 53
16	HD108147	0.35	10.880	0.10	0.56	37.0	1.05	12 25 46.3	−64 01 20
17	HD38529	0.79	14.310	0.13	0.12	53.6	1.39	05 46 34.9	1 10 5
18	55Cnc	0.93	14.660	0.12	0.03	75.8	1.03	08 52 35.8	28 19 51
19	GJ86	4.23	15.800	0.12	0.04	379.0	0.86	02 10 25.9	−50 49 25
20	HD195019	3.55	18.200	0.14	0.02	271.0	1.02	20 28 18.6	18 46 10
21	HD6434	0.48	22.090	0.15	0.30	37.0	0.99	01 04 40.2	−39 29 18
22	HD192263	0.81	24.350	0.15	0.22	68.2	0.79	20 13 59.8	0 52 1
23	HD83443c	0.17	29.830	0.17	0.42	14.0	0.79	09 37 11.8	−43 16 20
24	GJ876c	0.56	30.120	0.13	0.27	81.0	0.32	22 53 16.7	−14 15 49
25	ρ CrB	0.99	39.810	0.22	0.07	61.3	0.95	16 01 2.7	33 18 12
26	HD74156b	1.55	51.600	0.28	0.65	108.0	1.05	08 42 25.1	4 34 41
27	HD168443b	7.64	58.100	0.29	0.53	470.0	1.01	18 20 3.9	−9 35 45
28	GJ876b	1.89	61.020	0.21	0.10	210.0	0.32	22 53 16.7	−14 15 49
29	HD121504	0.89	64.620	0.32	0.13	45.0	1.02	13 57 17.2	−56 02 24
30	HD178911B	6.46	71.500	0.33	0.14	343.0	0.90	19 09 3.1	34 35 59
31	HD16141	0.22	75.800	0.35	0.00	10.8	1.00	02 35 19.9	−3 33 38
32	HD114762	10.96	84.030	0.35	0.33	615.0	0.82	13 12 19.7	17 31 2
33	HD80606	3.43	111.800	0.44	0.93	414.0	0.90	09 22 37.6	50 36 13
34	70Vir	7.42	116.700	0.48	0.40	316.2	1.10	13 28 25.8	13 46 44
35	HD52265	1.14	119.000	0.49	0.29	45.4	1.13	07 00 18.0	−5 22 2
36	HD1237	3.45	133.800	0.51	0.51	164.0	0.96	00 16 12.7	−79 51 4
37	HD37124	1.13	154.800	0.55	0.31	48.0	0.91	05 37 2.5	20 43 51
38	HD82943c	0.88	221.600	0.73	0.54	34.0	1.05	09 34 50.7	−12 07 46
39	HD8574	2.23	228.800	0.76	0.40	76.0	1.10	01 25 12.5	28 34 0
40	HD169830	2.95	230.400	0.82	0.34	83.0	1.40	18 27 49.5	−29 49 1
41	ν Andc	2.05	241.300	0.83	0.24	58.0	1.30	01 36 47.8	41 24 20
42	HD12661	2.84	250.500	0.80	0.19	89.1	1.07	02 04 34.3	25 24 51
43	HD89744	7.17	256.000	0.88	0.70	257.0	1.40	10 22 10.6	41 13 46
44	HD202206	14.68	258.900	0.77	0.42	554.0	0.90	21 14 57.8	−20 47 21
45	HD134987	1.63	265.000	0.82	0.37	53.7	1.05	15 13 28.7	−25 18 34

See end of the table for explanation of column headings.

Extrasolar planets (cont.)

Star	$M_P \sin i$	P	a	e	K	M	α	δ
46 HD17051	2.12	312.000	0.91	0.15	63.0	1.03	02 42 33.5	−50 48 1
47 HD92788	3.88	337.000	0.97	0.28	113.0	1.07	10 42 48.5	−2 11 2
48 HD142	1.00	337.100	0.98	0.38	29.6	1.10	00 06 19.2	−49 04 31
49 HD28185	5.59	385.000	1.00	0.06	168.0	0.90	04 26 26.3	−10 33 3
50 HD177830	1.24	391.000	1.10	0.40	34.0	1.17	19 05 20.8	25 55 14
51 HD4203	1.64	406.000	1.09	0.53	51.0	1.06	00 44 41.2	20 26 56
52 HD27442	1.32	415.000	1.16	0.06	32.0	1.20	04 16 29.0	−59 18 8
53 HD210277	1.29	436.600	1.12	0.45	39.1	0.99	22 09 29.9	−7 32 55
54 HD82943b	1.63	444.600	1.16	0.41	46.0	1.05	09 34 50.7	−12 07 46
55 HD19994	1.66	454.000	1.19	0.20	42.0	1.10	03 12 46.4	−1 11 46
56 HD114783	0.99	501.000	1.20	0.10	27.0	0.92	13 12 43.8	−2 15 54
57 HD222582	5.18	576.000	1.35	0.71	179.6	1.00	23 41 51.5	−5 59 9
58 HD23079	2.54	627.300	1.48	0.06	56.7	1.10	03 39 43.1	−52 54 57
59 HD141937	9.67	658.800	1.48	0.40	247.0	1.00	15 52 17.5	−18 26 10
60 HD160691	1.99	743.000	1.65	0.62	54.0	1.08	17 44 8.7	−51 50 3
61 HD213240	3.75	759.000	1.60	0.31	91.0	0.95	22 31 0.4	−49 25 60
62 16CygB	1.68	796.700	1.69	0.68	50.0	1.01	19 41 52.0	50 31 3
63 HD4208	0.81	829.000	1.69	0.04	18.3	0.93	00 44 26.7	−26 30 56
64 HD10697	6.08	1074.000	2.12	0.11	114.0	1.10	01 44 55.8	20 04 59
65 47UMab	2.56	1090.500	2.09	0.06	49.7	1.03	10 59 28.0	40 25 49
66 HD190228	5.01	1127.000	2.25	0.43	96.0	1.20	20 03 0.8	28 18 25
67 HD50554	4.49	1296.000	2.36	0.51	94.9	1.04	06 54 42.8	24 14 44
68 ν Andd	4.29	1308.500	2.56	0.31	70.4	1.30	01 36 47.8	41 24 20
69 HD33636	7.71	1553.000	2.62	0.39	148.0	0.99	05 11 46.4	4 24 13
70 HD106252	7.10	1722.000	2.77	0.57	150.7	0.96	12 13 29.5	10 02 30
71 HD168443c	16.96	1770.000	2.87	0.20	289.0	1.01	18 20 3.9	−9 35 45
72 HD145675	4.05	1775.000	2.93	0.37	70.4	1.06	16 10 24.3	43 49 3
73 HD39091	10.37	2115.200	3.34	0.62	196.2	1.10	05 37 9.9	−80 28 9
74 HD74156c	7.46	2300.000	3.47	0.40	121.0	1.05	08 42 25.1	4 34 41
75 ϵ Eri	0.88	2518.000	3.36	0.60	19.0	0.80	03 32 55.8	−9 27 30
76 47UMac	0.76	2640.000	3.78	0.00	11.0	1.03	10 59 28.0	40 25 49

i, inclination of the planetary orbit with respect to the plane of the sky in degrees.
M_P, mass of the planet (in Jupiter masses).
P, period of the planetary orbit in days.
a, semimajor axis of the orbit in AU.
e, eccentricity of the orbit.
K, semi-amplitude of the radial velocity of the star in m s^{-1}.
M, mass of the star (in solar masses).
α, δ star's right ascension and declination, International Celestial Reference System coordinates (2000.0); hh mm ss, dd mm ss.
$M_P \sin i = 4.92 \times 10^{-3}\ KM^{2/3}\ P^{1/3}$, $a = 1.96 \times 10^{-2}\ P^{2/3}\ M^{1/3}$.
(University of California Planet Search Project, list as of 19 November 2001)
See http://exoplanets.org/ for an up-to-date list of extrasolar planets.

Star charts

NORTH POLE

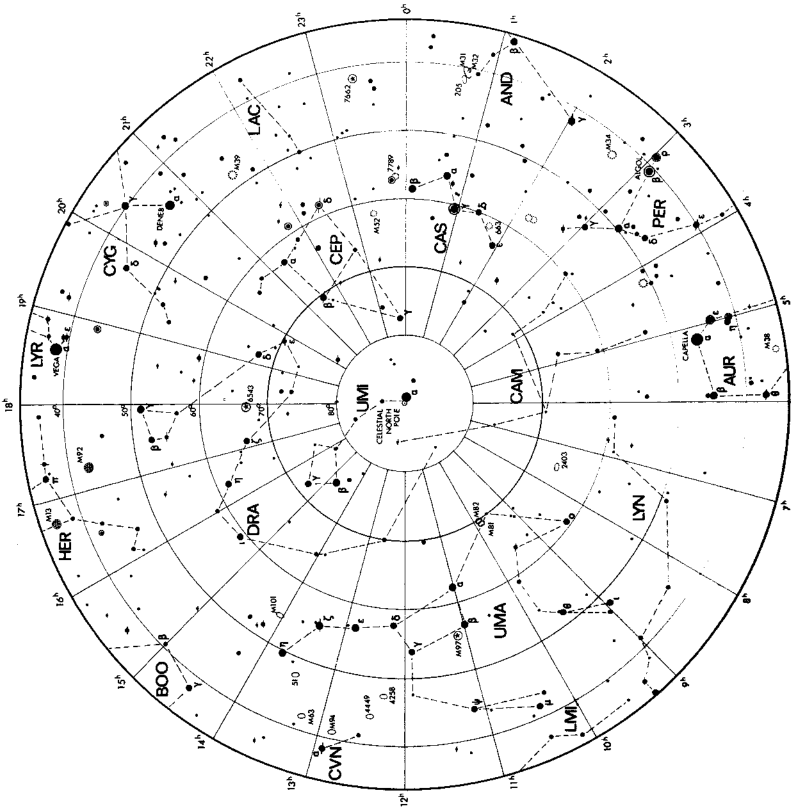

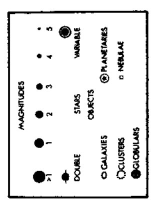

Star charts (con

Star charts (cont.)

SOUTH POLE

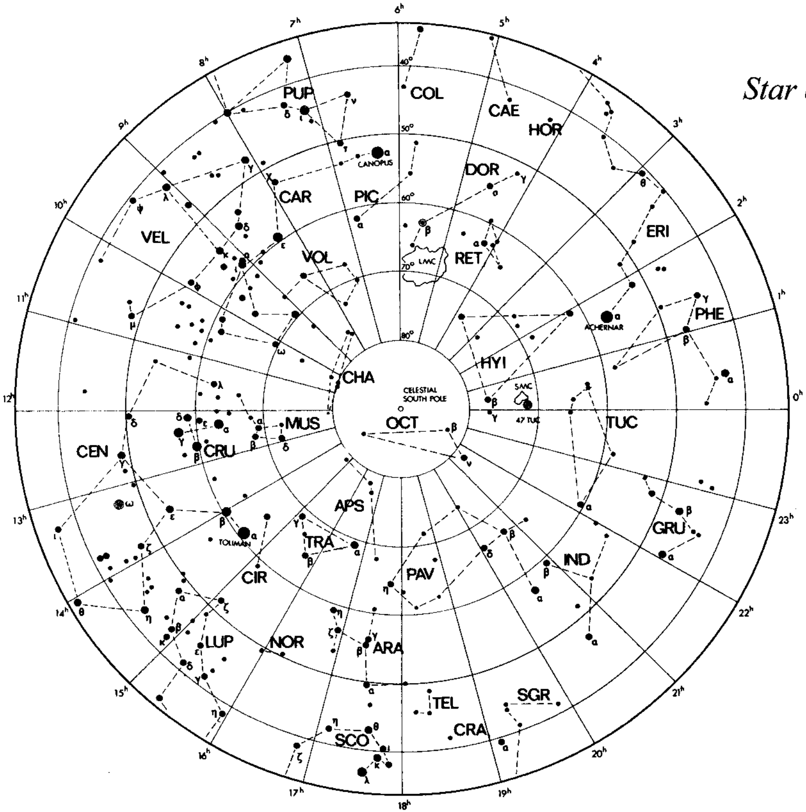

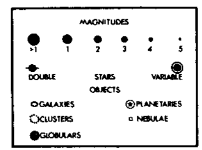

(Adapted from Vehrenberg, H. and Blank, D., *Handbook of the Constellations*, Treugesell-Verlag, 1973.)

Constellations

Constellation	Gen. ending	Contr.	Description	α	δ	Area[a] (sq. deg.)	Order of size
Andromeda	-dae	And	the chained maiden[b]	1^h	40° N	722.278	19
Antlia	-liae	Ant	the air pump	10	35 S	238.901	62
Apus	-podis	Aps	the bird of paradise	16	75 S	206.327	67
Aquarius	-rii	Aqr	the water pourer	23	15 S	979.854	10
Aqulia	-lae	Aql	the eagle	20	5 N	652.473	22
Ara	-rae	Ara	the altar	17	55 S	237.057	63
Aries	-ietis	Ari	the ram	3	20 N	441.395	39
Auriga	-gae	Aur	the wagoner	6	40 N	657.438	21
Boötes	-tis	Boo	the ploughman	15	30 N	906.831	13
Caelum	-aeli	Cae	the burin	5	40 S	124.865	81
Camelopardalis	-di	Cam	the giraffe	6	70 N	756.828	18
Cancer	-cri	Cnc	the crab	9	20 N	505.872	31
Canes Venatici	-num -corum	CVn	the hunting dogs	13	40 N	465.194	38
Canis Major	-is -ris	CMa	the large dog	7	20 S	380.118	43
Canis Minor	-is -ris	CMi	the small dog	8	5 N	183.367	71
Capricornum	-ni	Cap	the goat	21	20 S	413.947	40
Carina	-nae	Car	the keel	9	60 S	494.184	34
Cassiopeia	-peiae	Cas	Cassiopeia	1	60 N	598.407	25
Centaurus	-ri	Cen	the centaur	13	50 S	1060.422	9
Cepheus	-phei	Cep	King Cepheus	22	70 N	587.787	27
Cetus	-ti	Cet	the sea monster	2	10 S	1231.411	4
Chamaeleon	-ntis	Cha	the chamaeleon	11	80 S	131.592	79
Circinus	-ni	Cir	the pair of compasses	15	60 S	93.353	85
Columba	-bae	Col	the dove	6	35 S	270.184	54
Coma Berenices	-mae -cis	Com	the hair of Berenice	13	20 N	386.475	42
Corona Australis	-nae -lis	CrA	the southern crown	19	40 S	127.696	80
Corona Borealis	-nae -lis	CrB	the northern crown	16	30 N	178.710	73
Corvus	-vi	Crv	the crow	12	20 S	183.801	70
Crater	-eris	Crt	the cup	11	15 S	182.398	53
Crux	-ucis	Cru	the southern cross	12	60 S	68.447	88
Cygnus	-gni	Cyg	the swan	21	40 N	803.983	16
Delphinus	-ni	Del	the dolphin	21	10 N	188.5499	69
Dorado	-dus	Dor	the swordfish	5	65 S	179.173	72
Draco	-onis	Dra	the dragon	17	65 N	1082.952	8
Equuleus	-lei	Equ	the foal	21	10 N	71.641	87
Eridanus	-ni	Eri	the river	3	20 S	1137.919	6
Formax	-acis	For	the furnace	3	30 S	397.502	41
Gemini	-norum	Gem	the twins	7	20 N	513.761	30
Grus	-ruis	Gru	the crane	22	45 S	365.513	45
Hercules	-lis	Her	Hercules	17	30 N	1225.148	5
Horologium	-gii	Hor	the clock	3	60 N	248.885	58
Hydra	-drae	Hya	the water snake	10	20 S	1302.844	1
Hydrus	-dri	Hyi	the sea serpent	2	75 S	243.035	61
Indus	-di	Ind	the Indian	21	55 S	294.006	49
Lacerta	-tae	Lac	the lizard	22	45 N	200.688	68
Leo	-onis	Leo	the lion	11	15 N	946.964	12
Leo Minor	-onis -ris	LMi	the small lion	10	35 N	231.956	64
Lepus	-poris	Lep	the hare	6	20 S	290.291	51
Libra	-rae	Lib	the balance	15	15 S	538.052	29
Lupus	-pi	Lup	the wolf	15	45 S	333.683	46
Lynx	-ncis	Lyn	the lynx	8	45 N	545.386	28
Lyra	-rae	Lyr	the lyre	19	40 N	286.476	52
Mensa	-sae	Men	the table[c]	5	80 S	153.484	75
Microscopium	-pii	Mic	the microscope	21	35 S	209.513	66
Monoceros	-rotis	Mon	the unicorn	7	5 S	481.569	35

Constellations (cont.)

Constellation	Gen. ending	Contr.	Description	α	δ	Area[(a)] (sq. deg.)	Order of size
Musca	-cae	Mus	the fly	12°	70°S	138.355	77
Norma	-mae	Nor	the square	16	50 S	165.290	74
Octans	-ntis	Oct	the octant	22	85 S	291.045	50
Ophiuchus	-chi	Oph	the serpent bearer	17	0	948.340	11
Orion	-nis	Ori	the hunter	5	5 N	594.120	26
Pavo	-vonis	Pav	the peacock	20	65 S	377.666	44
Pegasus	-si	Peg	the winged horse	22	20 N	1120.794	7
Perseus	-sei	Per	Perseus	3	45 N	614.997	24
Phoenix	-nisis	Phe	the Phoenix	1	50 S	469.319	37
Pictor	-ris	Pic	the easel	6	55 S	246.739	59
Pisces	-cium	Psc	the fishes	1	15 N	889.417	14
Piscis Austrinus	-is -ni	PsA	the southern fish	22	30 N	245.375	60
Puppis	-ppis	Pup	the poop	8	40 S	673.434	20
Pyxis (= Malus)	-xidis	Pyx	the compass	9	30 S	220.833	65
Reticulum	-li	Ret	the net	4	60 S	113.936	82
Sagitta	-tae	Sge	the arrow	20	10 N	79.923	86
Sagittarius	-rii	Sgr	the archer	19	25 S	867.432	15
Scorpius	-pii	Sco	the scorpion	17	40 S	496.783	33
Sculptor	-ris	Scl	the sculptor	0	30 S	474.764	36
Scutum	-ti	Sct	the shield[(d)]	19	10 S	109.114	84
Serpens (Caput and Cauda)	-ntis	Ser	the serpent	18	5 S	639.928	23
Sextans	-ntis	Sex	the sextant	10	0	313.515	47
Taurus	-ri	Tau	the bull	4	15 N	797.249	17
Telescopium	-pii	Tel	the telescope	19	50 S	251.512	57
Triangulum	-li	Tri	the triangle	2	30 N	131.847	78
Triangulum Australe	-li -lis	TrA	the southern triangle	16	65 S	109.978	83
Tucana	-nae	Tuc	the toucan	0	65 S	294.557	48
Ursa Major	-sae -ris	UMa	the great bear	11	50 N	1279.660	3
Ursa Minor	-sae -ris	UMi	the little bear	15	70 N	255.864	56
Vela	-lorum	Vel	the sails	9	50 S	499.649	32
Virgo	-ginis	Vir	the virgin	13	0	1294.428	2
Volans	-ntis	Vol	the flying fish	8	70 S	141.354	76
Vulpecula	-lae	Vul	the little fox	20	25 N	268.165	55

(a) From *Sky and Telescope*, June 1983.
(b) Daughter of Cepheus and Cassiopeia.
(c) After Table Mountain in South Africa.
(d) Of John Sobieski, the Polish hero.

The 50 visually brightest stars (in order of brightness)

Rank	Classical Name	Star Name	α 2000	δ 2000	V	d	σ_{rel}	M_V	Spec. Type	HIP
0	Sun				−26.75	4.85×10^{-6}		4.82	G2 V	
1	Sirius	9 α CMa	06 45 08.9	−16 42 58	−1.46	2.64	0.4	143	A1 Vm	32349
2	Canopus	α Car	06 23 57.1	−52 41 45	−0.72	95.8	5.1	−5.63	F0 II	30438
3	Arcturus	16 α Boo	14 15 39.7	+19 10 57	−0.04	11.25	0.8	−0.3	K2 IIIFe-0.5	69673
4	Rigil Kentaurus	α^1 Cen	14 39 35.9	−60 50 07	−0.01	1.35	0.2	4.34	G2 V	71683
5	Vega	3 α Lyr	18 36 56.3	+38 47 01	0.03	7.76	0.4	0.58	A0 Va	91262
6	Capella	13 α Aur	05 16 41.4	+45 59 53	0.08	12.94	1.2	−0.48	G5 IIIe + G0 III	24608
7	Rigel	19 β Ori	05 14 32.3	−08 12 06	0.12	236.8	19.2	−6.75	B8 Ia:	24436
8	Procyon	10 α CMi	07 39 18.1	+05 13 30	0.38	3.49	0.3	2.66	F5 IV-V	37279
9	Achernar	α Eri	01 37 42.9	−57 14 12	0.46	44.0	2.5	−2.76	B3 Vpe	7588
10	Betelgeuse	58 α Ori	05 55 10.3	+07 24 25	0.5	131	21.5	−5.09	M1-2 Ia-Iab	27989
11	Hadar	Beta Cen	14 03 49.4	−60 22 23	0.61	161	9	−5.42	B1 III	68702
12	Altair	53 α Aql	19 50 47.0	+08 52 06	0.77	5.15	0.5	2.21	A7 V	97649
13	Aldebaran	87 α Tau	04 35 55.2	+16 30 33	0.85	20.0	1.9	−0.65	K5 III	21421
14	Antares	21 α Sco	16 29 24.4	−26 25 55	0.96	185	31.1	−5.38	M1.5 Iab-ab + B4 Ve	80763
15	Spica	67 α Vir	13 25 11.6	−11 09 41	0.98	80	6.9	−3.55	B1 III-IV + B2 V	65474
16	Pollux	78 β Gem	07 45 18.9	+28 01 34	1.14	10.3	0.9	1.07	K0 IIIb	37826
17	Fomalhaut	24 α PsA	22 57 39.1	−29 37 20	1.16	7.69	0.7	1.73	A3 V	113368
18	Mimosa	β Cru	12 47 43.2	−59 41 19	1.25	108	6.6	−3.92	B0.5 III	62434
19	Deneb	50 α Cyg	20 41 25.9	+45 16 49	1.25	989	56.4	−8.73	A2 Ia	102098
20	Acrux	α^1 Cru	12 26 35.9	−63 05 57	1.33	98	6.6	−3.63	B0.5 IV	60718
21	Regulus	32 α Leo	10 08 22.3	+11 58 02	1.35	23.8	1.9	−0.53	B7 V	49669
22	Adhara	21 ε CMa	06 58 37.5	−28 58 20	1.5	132	7.5	−4.1	B2 II	33579

See end of the table for explanation of column headings.

The 50 visually brightest stars (cont.)

Rank	Classical Name	Star Name	α 2000	δ 2000	V	d	σ_{rel}	M_V	Spec. Type	HIP
23	Gacrux	γ Cru	12 31 09.9	−57 06 48	1.63	26.9	1.8	−0.52	M3.5 III	61084
24	Shaula	35 λ Sco	17 33 36.5	−37 06 14	1.63	215	19.4	−5.04	B2 IV + B	85927
25	Bellatrix	24 γ Ori	05 25 07.9	+06 20 59	1.64	74	7.3	−2.72	B2 III	25336
26	El Nath	112 β Tau	05 26 17.5	+28 36 27	1.65	40	3.5	−1.37	B7 III	25428
27	Miaplacidus	β Car	09 13 12.0	−69 43 02	1.68	34.1	1.6	−0.98	A2 IV	45238
28	Alnilan	46 ε Ori	05 36 12.8	−01 12 07	1.7	411	37.4	−6.37	B0 Ia	26311
29	Al Na'ir	α Gru	22 08 14.0	−46 57 40	1.74	31.1	2.5	−0.72	B7 IV	109268
30	Alioth	77 ε UMa	12 54 01.7	+55 57 35	1.77	24.8	1.5	−0.2	A0 pCr	62956
31		γ^2 Vel	08 09 32.0	−47 20 12	1.78	258	13.7	−5.28	WC8 + O9 I	39953
32	Mirfak	33 α Per	03 24 19.4	+49 51 40	1.79	181	12	−4.5	F5 Ib	15863
33	Dubhe	50 α UMa	11 03 43.7	+61 45 03	1.79	37.9	2	−1.1	K0 IIIa	54061
34	Wezen	25 δ CMa	07 08 23.5	−26 23 36	1.84	549	30.8	−6.86	F8 Ia	34444
35	Kaus Australis	20 ε Sgr	18 24 10.3	−34 23 05	1.85	44.3	4.5	−138	B9.5 III	90185
36	Avior	ε Car	08 22 30.8	−59 30 35	1.86	194	9.5	−4.58	K3 III + B2: V	41037
37	Alkaid	85 η UMa	13 47 32.4	+49 18 48	1.86	30.8	2.3	−0.59	B3 V	67301
38	Sargas	θ Sco	17 37 19.2	−42 59 52	1.87	83	7	−2.74	F1 II	86228
39	Menkaliman	34 β Aur	05 59 31.7	+44 56 51	1.9	25.2	2	−0.1	A2 IV	28360
40	Atria	α TrA	16 48 39.9	−69 01 40	1.92	127	8	−3.61	K2 IIb-IIIa	82273
41	Alhena	24 γ Gem	06 37 42.7	+16 23 57	1.93	32	7.5	−0.6	A0 IV	31681
42	Peacock	α Pav	20 25 38.9	−56 44 06	1.94	56	3.9	−1.81	B2 IV	100751
43		δ Vel	08 44 42.2	−54 42 30	1.96	24.4	0.9	0.02	A1 V	42913

The 50 visually brightest stars *(cont.)*

Rank	Classical Name	Star Name	α2000	δ2000	V	d	σ_{rel}	M_V	Spec. Type	HIP
44	Mirzam	2 β CMa	06 22 42.0	−17 57 21	1.98	153	10.1	−3.95	Bl II-III	30324
45	Castor	66 α Gem	07 34 36.0	+31 53 18	1.98	15.8	1.9	0.99	A1 V	36850
46	Alphard	30 α Hya	09 27 35.2	−08 39 31	1.98	54.3	4.2	−1.7	K3 II-III	46390
47	Hamal	13 α Ari	02 07 10.4	+23 27 45	2	20.2	2	0.47	K2 III	9884
48	Polaris	1 α UMi	02 31 48.7	+89 15 51	2.02	132	6.3	−3.59	F7: Ib-IIv	11767
49	Nunki	34 α Sgr	18 55 15.9	−26 17 48	2.02	69	6.1	−2.17	B2.5 V	92855
50	Deneb Kaitos	16 β Cet	00 43 35.2	+52 59 12	2.04	29.4	2.4	−0.3	K0 III	3419

Column headings:
Star name: Flamsteed number, Bayer letter, and constellation abbreviation.
α : right ascension for equator, equinox, and epoch 2000.0; hh mm ss.
δ : declination for equator, equinox, and epoch 2000.0; dd, mm ss.
V: visual magnitude in the U,B, V system.
d: distance to the star in parsecs (pc); 1 pc = 3.086×10^{16} m = 3.262 lyr.
σ_{rel} : relative uncertainty in the distance in percent.
M_V : absolute visual magnitude.
Spec. Type: spectral type and luminosity class in the MKK system.
HIP: Hipparcos catalog number.
For updated parallaxes, absolute magnitudes, and proper motions see:
The 150 Stars in the Hipparcos Catalogue with Highest Apparent Magnitude,

The 100 visually brightest stars (limiting magnitude, $V = 2.59$)

Star name	α2000	δ 2000	$\mu(\alpha)$	$\mu(\delta)$	V	$B-V$	M_V	Spec	RV ($\mathrm{km\,s^{-1}}$)	d (pc)	Notes
21 α And	$0^h08^m23^s.2$	$+29°05'26''$	$+0^s.010$	$-0''.16$	2.06	−0.11	0.3	A0 p	−12	22 mn	Alpheratz, m
11 β Cas	0 09 10.6	+59 08 59	+0.068	−0.18	2.27	0.34	1.9	F2 IV	+12	13 ts	Caph, m
α Phe	0 26 17.0	−42 18 22	+0.019	−0.39	2.39	1.09	0.2	K0 III	+75	24 s	(Ankaa), m
18 α Cas	0 40 30.4	+56 32 15	+0.006	−0.03	2.23	1.17	−0.9	K0 II-III	−4	37 s	Schedar, m
16 β Cet	0 43 35.3	−17 59 12	+0.016	+0.04	2.04	1.02	0.2	K0 III	+13	21 ts	Deneb Kait, Diphda
27 γ Cas	0 56 42.4	+60 43 00	+0.003	0.00	2.47	−0.15	−4.6	B0 IV e	−7	240 s	Cih, m, v
43 β And	1 09 43.8	+35 37 14	+0.015	−0.11	2.06	1.58	−0.4	M0 III	0	27 ts	Mirach, m
α Eri	1 37 42.9	−57 14 12	+0.013	−0.03	0.46	−0.16	−1.6	B5 IV	+19	26 s	Achernar
57 γ^1 And	2 03 53.9	+42 19 47	+0.004	−0.05	2.18	1.20	−0.1	K2 III	−12	37 mn	Almach
57 γ^2 And	2 03 54.7	+42 19 51	+0.003	−0.05	5.03			A0 p	−14	37 mn	m
13 α Ari	2 07 10.3	+23 27 45	+0.014	−0.14	2.00	1.15	−0.1	K2 III	−14	26 ts	Hamal
68 o Cet	1 19 20.6	−2 58 39	−0.001	−0.23	2.0	1.7	−0.3	Md	+64	29 mn	Mira, m, v
1 α UMi	2 31 50.4	+89 15 51	+0.232	−0.01	2.02	0.60	−4.6	F8 Ib	−17		Polaris, m
92 α Cet	3 02 16.7	+4 05 23	−0.001	−0.07	2.53	1.64	−0.5	M2 III	−26	40 mn	Menkar
26 β Per	3 08 10.1	+40 57 21	0.000	0.00	2.12	−0.05	−0.2	B8 V	+4	29 ts	Algol, m, v
33 α Per	3 24 19.3	+49 51 40	+0.003	−0.02	1.80	0.48	−4.6	F5 Ib	−2	190 s	Mirfak, m
87 α Tau	4 35 55.2	+16 30 33	+0.005	−0.19	0.85	1.54	−0.3	K5 III	+54	21 ts	Aldebaran, m
13 α Aur	5 16 41.3	+45 59 53	+0.008	−0.42	0.08	0.80	+0.3	G8 III	+30	13 t	Capella, m
19 β Ori	5 14 32.2	−8 12 06	0.000	0.00	0.12	−0.03	−7.1	B8 Ia	+21	280 s	Rigel, m
24 γ Ori	5 25 07.8	+6 20 59	−0.001	−0.01	1.64	−0.22	−3.6	B2 III	+18	110 s	Bellatrix, m
112 β Tau	5 26 17.5	+28 36 27	+0.002	−0.17	1.65	−0.13	−1.6	B7 III	+8	40 mx	El Nath, m
34 δ Ori	5 32 00.3	−0 17 57	0.000	0.00	2.23	−0.22		O9.5 II	+16		Mintaka, m
11 α Lep	5 32 43.7	−17 49 20	0.000	0.00	2.58	0.21	−4.7	F0 Ib	+25	290 s	Arneb, m

*See end of the table for explanation of column headings.

The 100 visually brightest stars (cont.)

Star name	α2000	δ 2000	μ(α)	μ(δ)	V	B − V	M_V	Spec	RV (km s^{-1})	d (pc)	Notes
46 ε Ori	$5^h36^m12^s.7$	−1°12′07″	$0^s.000$	0″.00	1.70	−0.19	−6.2	B0 Ia	+26	370 s	Alnilam, m
50 ζ Ori	5 40 45.5	−1 56 34	0.000	0.00	1.77	−0.21	−5.9	09.5 Ib	+18	340 s	Alnitak, m
53 κ Ori	5 47 45.3	−9 40 11	0.000	−0.01	2.06	−0.17	0.4	B0.5 Ia	+21	21 mn	Saiph
58 α Ori	5 55 10.2	+7 24 26	+0.002	+0.01	0.50	1.85	−4.4	M2 Iab	+21	95 s	Betelgeuse, m
34 β Aur	5 59 31.7	+44 56 51	−0.005	0.00	1.90	0.03	0.6	A2 IV	−18	22 ts	Menkalinan, m
2 β CMa	6 22 41.9	−17 57 22	−0.001	0.00	1.98	−0.23	−4.8	B1 II-III	+34	220 s	Mirzam, m
α Car	6 23 57.1	−52 41 44	+0.003	+0.02	−0.72	0.15	−8.5	F0 Ia	+21	360 s	Canopus
24 γ Gem	6 37 42.7	+16 23 57	+0.003	−0.04	1.93	0.00	0.0	A0 IV	−13	26 ts	Alhena, m
9 α CMa	6 45 08.9	−16 42 58	−0.038	−1.21	−1.46	0.01	1.4	A1 V	−8	2.7 t	Sirius, m
21 ε CMa	6 58 37.5	−28 58 20	0.000	0.00	1.50	−0.21	−4.4	B2 II	+27	150 s	Adhara, m
25 δ CMa	7 08 23.4	−26 23 36	−0.001	0.00	1.86	0.65	−8.0	F8 Ia	+34	940 s	Wezen
31 η CMa	7 24 05.6	−29 18 11	−0.001	0.00	2.44	−0.07	−7.0	B5 Ia	+41	760 s	Aludra, m
66 α Gem	7 34 35.9	+31 53 18	−0.013	−0.10	1.58	0.04	1.2	A1 V	−1	14 ts	Castor, m
10 α CMi	7 39 18.1	+5 13 30	−0.047	−1.03	0.38	0.42	2.6	F5 IV	−3	3.5 t	Procyon, m
78 β Gem	7 45 18.9	+28 01 34	−0.047	−0.05	1.14	1.00	0.2	K0 III	+3	11 ts	Pollux, m
ζ Pup	8 03 35.0	−40 00 12	−0.003	+0.01	2.25	−0.26		O5.8	−24		Naos
γ Vel	8 09 31.9	−47 20 12	−0.001	0.00	1.78	−0.22		WC7	+35		m
ε Car	8 22 30.8	−59 30 34	−0.003	+0.01	1.86	1.27	−2.1	K0 II	+12	62 s	(Avior)
δ Vel	8 44 42.2	−54 42 30	+0.003	−0.08	1.96	0.04	0.3	A0 V	+2	21 ts	m
λ Vel	9 07 59.7	−43 25 57	−0.002	+0.01	2.21	1.66	−4.4	K5 Ib	+18	150 ts	Suhail
β Car	9 13 12.2	−69 43 02	−0.029	+0.10	1.68	0.00	−0.6	A0 III	−5	26 s	Miaplacidus
ι Car	9 17 05.4	−59 16 13	−0.002	0.00	2.25	0.18	−4.7	F0 Ib	+13	250 s	Aspidiske, Scutulum
κ Vel	9 22 06.8	−55 00 38	−0.001	+0.01	2.50	−0.18	−2.9	B2 IV	+22	120 s	m
30 α Hya	9 27 35.2	−8 39 31	−0.001	+0.03	1.98	1.44	−0.2	K3 III	−4	26 mn	Alphard

The 100 visually brightest stars (cont.)

Star name	α2000	δ 2000	$\mu(\alpha)$	$\mu(\delta)$	V	$B-V$	M_V	Spec	RV (km s^{-1})	d (pc)	Notes
32 α Leo	$10^h08^m22^s.2$	+11°58′02″	$-0^s.017$	0″.00	1.35	−0.11	−0.7	B7 V	+4	26 ts	Regulus, m
41 γ^1 Leo	10 19 58.3	+19 50 30	+0.022	−0.15	2.28	1.08	0.2	K0 III	−37		Algieba, m
41 γ^2 Leo	10 19 58.6	+19 50 25	+0.022	−0.17	3.58			G7 III	−36		m
48 β UMa	11 01 50.4	+56 22 56	+0.010	+0.03	2.37	−0.02	1.0	A1 V	−12	19 ts	Merak
50 α UMa	11 03 43.6	+61 45 03	−0.017	−0.07	1.79	1.07	0.0	K0 III	−9	23 ts	Dubhe, m
68 δ Leo	11 14 06.4	+20 31 25	+0.010	−0.14	2.56	0.12	1.5	A4 V	−21	16 s	Zosma, m
94 β Leo	11 49 03.5	+14 34 19	−0.034	−0.12	2.14	0.09	1.7	A3 V	0	12 mx	Denebolan, m
64 γ UMa	11 53 49.7	+53 41 41	+0.011	+0.01	2.44	0.00	0.6	A0 V	−13	23 s	Phecda
4 γ Crv	12 15 48.3	−17 32 31	−0.011	+0.02	2.59	−0.11	−1.2	B8 III	−4	57 s	Gienah
α^1 Cru	12 26 35.9	−63 05 56	−0.004	−0.02	1.41	0.1	−3.8	B1 IV	−11	110 s	Acrux, m
α^2 Cru	12 26 36.5	−62 05 58	−0.005	−0.02	1.88	0.0	−3.3	B3 n	−1	110 s	m
γ Cru	12 31 09.9	−57 06 47	+0.003	−0.27	1.63	1.59	−0.5	M3 III	+21	27 s	(Gacrux), m
γ Cen	12 41 30.9	−48 57 34	−0.019	−0.01	2.17	−0.01	−0.5	A0 III	−8	34 s	Muhlifain, m
β Cru	12 47 43.2	−59 41 19	−0.005	−0.02	1.25	−0.23	−4.3	B0 III	+20	130 mx	Mimosa
77 ε UMa	12 54 01.7	+55 57 35	+0.013	−0.01	1.77	−0.02	0.4	A0 p	−9	19 mn	Alioth
79 ζ UMa	13 23 55.5	+54 55 31	+0.014	−0.02	2.27	0.02	1.4	A2 V	−9	18 ts	Mizar, m
67 α Vir	13 25 11.5	−11 09 41	−0.003	-0.03	0.98	−0.23	−3.5	B1 V	+1	79 s	Spica, m, v
ε Cen	13 39 53.2	−53 27 58	−0.002	−0.02	2.30	−0.22	−3.5	B1 V	+6	150 s	m
85 η UMa	13 47 32.3	+49 18 48	−0.013	−0.01	1.86	−0.19	−1.7	B3 V	−11	33 mx	Alkaid
ζ Cen	13 55 32.3	−47 17 17	−0.006	−0.04	2.55	−0.22	−3.0	B2 IV	+7	110 mx	m
β Cen	14 03 49.4	−60 22 22	−0.003	−0.02	0.61	−0.24	−5.1	B1 II		140 s	Hadar, m
5 θ Cen	14 06 40.9	−36 22 12	−0.043	−0.52	2.06	1.01	1.7	K0 III-IV	+1	14 ts	(Menkent)
16 α Boo	14 15 39.6	+19 10 57	−0.077	−2.00	−0.04	1.23	−0.2	K2 III p	−5	11 t	Arcturus
η Cen	14 35 30.3	−42 09 28	−0.003	−0.04	2.31	−0.19	−2.9	B3 III	0	110 s	
α^2 Cen	14 39 35.4	−60 50 13	−0.494	+0.69	1.39		5.8	K1 V	−21	1.3 t	m
α^1 Cen	14 39 36.7	−60 50 02	−0.494	+0.69	0.00	0.68	4.4	G2 V	−25	1.3 t	Rigil Kent, m
α Lup	14 41 55.7	−47 23 17	−0.002	−0.02	2.30	−0.20	−4.4	B1 III	+7	210 s	m

The 100 visually brightest stars (cont.)

Star name	α2000	δ 2000	μ(α)	μ(δ)	V	B − V	M_V	Spec	RV (km s^{-1})	d (pc)	Notes
36 ε Boo	$14^h44^m59^s.1$	+27°04′27″	$-0^s.004$	+0″.02	2.37	0.97	−0.9	K0 II-III	−17	46 s	Izar
7 β UMi	14 50 42.2	+74 09 19	−0.009	+0.01	2.08	1.47	−0.3	K4 III	+17	29 ts	Kochab
5 α CrB	15 34 41.2	+26 42 53	+0.009	−0.09	2.23	−0.02	0.6	A0 V	+2	24 s	Alphecca, m
7 δ Sco	16 00 19.9	−22 37 18	−0.001	−0.03	2.32	−0.12	−4.1	B0 V	−14	170 s	Dzuba
8 β^1 Sco	16 05 26.1	−19 48 19	0.000	−0.02	2,64	−0.07	−4.3	B0.5 V	−7	250 s	Acrab, m
8 β^2 Sco	16 05 26.4	−19 48 07	−0.001	−0.02	4.92	−0.02	−2.5	B2 V	−5	250 s	
21 α Sco	16 29 24.3	−26 25 55	0.000	−0.02	0.96	1.83	−4.7	M1 Ib	−3	100 s	Antares, m, v
13 ζ Oph	16 37 09.4	−10 34 02	+0.001	+0.02	2.56	0.02	−4.4	09.5 V	−19	170 s	
α TrA	16 48 39.8	−69 01 39	−0.005	−0.03	1.92	1.44	−0.1	K2 III	−4	17 s	(Atria)
26 ε Sco	16 50 09.7	−34 17 36	−0.049	−0.25	2.29	1.15	−0.1	K2 III	−3	20 mx	
35 ζ Oph	17 10 22.5	−15 43 30	+0.003	+0.09	2.43	0.06	1.4	A2 V	−1	18 ts	Sabik, m
35 λ Sco	17 33 36.4	−37 06 14	0.000	−0.03	1.63	−0.22	−3.0	B2 IV	0	84 s	Shaula, m
55 α Oph	17 34 55.9	+12 33 36	+0.008	−0.23	2.08	0.15	0.3	A5 III	+13	19 s	Ras-Alhague
θ Sco	17 37 19.0	−42 59 52	+0.001	0.00	1.87	0.40	−5.6	F0 I-II	+1	280 s	
κ Sco	17 42 29.0	−39 01 48	−0.001	−0.03	2.41	−0.22	−3.0	B2 IV	−10	120 s	
33 γ Dra	17 56 36.2	+51 29 20	−0.001	−0.02	2.23	1.52	−0.3	K5 III	−28	31 s	Eltanin, m
20 ε Sgr	18 24 10.2	−34 23 05	−0.003	−0.13	1.85	−0.03	−0.3	B9 IV	−11	26 s	Kaus Australis, m
3 α Lyr	18 36 56.2	+38 47 01	+0.017	+0.28	0.03	0.00	0.5	A0 V	−14	8.1 t	Vega, m
34 σ Sgr	18 55 15.7	−26 17 48	+0.001	−0.05	2.02	−0.22	−2.0	B3 IV-V	−11	64 s	Nunki, m
53 α Aql	19 50 46.8	+8 52 06	+0.036	+0.39	00.77	0.22	2.2	A7 IV-V	−26	5.1 t	Altair, m
37 γ Cyg	20 22 13.5	+40 15 24	0.000	0.00	2.20	0.68	−4.6	F8 Ib	−8	230 s	Sadir, m
α Pav	20 25 38.7	−56 44 06	+0.002	−0.08	1.94	−0.20	−2.3	B3 IV	+2	71 s	(Peacock), m
50 α Cyg	20 41 25.8	+45 16 49	0.000	+0.01	1.25	0.09	−7.5	A2 Ia	−5	560 s	Deneb, m
53 ε Cyg	20 46 12.5	+33 58 13	+0.028	+0.33	2.46	1.03	0.2	K0 III	−10	25 ts	Gienar, m
5 α Cep	21 18 34.6	+62 35 08	+0.022	+0.05	2.44	0.22	1.7	A7 IV-V	−10	145 s	Alderamin, m
8 ε Peg	21 44 11.0	+9 52 30	+0.002	0.00	2.38	1.52	−3.6	K2 Ib	+5	160 s	Enif, m

The 100 visually brightest stars (cont.)

Star name	α2000	δ 2000	$\mu(\alpha)$	$\mu(\delta)$	V	$B-V$	M_V	Spec	RV ($\mathrm{km\,s^{-1}}$)	d (pc)	Notes
α Gru	$22^h08^m13^s.8$	$-46°57'40''$	$+0^s.013$	$-0''.15$	1.74	−0.13	0.1	B5 V	+12	21 mx	(Al Na'ir), m
β Gru	22 42 39.9	−46 53 05	+0.014	−0.01	2.11	1.62	−2.4	M3 II	+2	53 mx	
24 α PsA	22 57 38.9	−29 37 20	+0.026	−0.16	1.16	0.09	2.0	A3 V	+7	6.7 t	Fomalhaut
53 β Peg	23 03 46.3	+28 04 58	+0.014	+0.14	2.42	1.67	−1.4	M2 II-III	+9	54 s	Scheat, m, v
54 α Peg	23 04 45.5	+15 12 19	+0.004	−0.04	2.49	−0.04	0.2	B9 V	−4	31 ts	Markab

Column headings

Star name: the Flamsteed number, Bayer letter, and constellation abbreviation.
α 2000: right ascension for equator, equinox, and epoch 2000.0.
δ 2000: declination for equator, equinox, and epoch 2000.0
$\mu(\alpha)$: proper motion in right ascension in seconds of time per year.
$\mu(\delta)$: proper motion in declination in seconds of arc per year.
V : visual magnitude in the standard U, B, V photometric system.
$B-V$: the color index in the U, B, V system.
M_v : the absolute visual magnitude ($M_v = v + 5 - 5\log d$ (pc)).
Spec: the spectral type and luminosity class in the MKK system.
RV : radial velocity. Positive means receding from the Solar System.
d (pc): distance to the star in parsecs. 't' denotes the distance is based on a trigonometric parallax; 's' denotes spectroscopic parallax; 'mn' denotes a minimum likely value; 'mx' denotes a maximum likely value.

Notes: the classical names are given here; 'm' means the star is part of a multiple system; 'v' means the star is variable. Only the dominant star is listed. If more than one member of a multiple system is visually bright, all the visually bright members are listed ($V < 8.0$). The combined magnitude of a pair of close stars in given by:

$m = m_2 - 2.5\log(R+1)$ where $R = 10^{0.4(m_2 - m_1)}$, m_1 is the magnitude of the brightest component, and m_2 is that of the fainter star.

(Data are from *Sky catalogue 2000.00*, Hirshfeld, A. & Sinnott, R., eds., Sky Publishing Corp., 1982.)

For updated parallaxes, absolute magnitudes, and proper motions see:
The 150 Stars in the Hipparcos Catalogue with Highest Apparent Magnitude,
http://astro.estec.esa.nl/Hipparcos/table365-new.html.

Stars within 5 pc

No.	Name	α 1950	δ 1950	Trig. parallax, π	Proper motion, $\mu''\mathrm{yr}^{-1}$	Radial velocity v_r km s^{-1}	Spec	V	$B-V$	$U-B$	$R-I$	M_V	Luminosity ($L_\odot = 1$)
1	Sun						G2 V	−26.72	0.65	0.10		4.85	1.0
2	Proxima Cen	$14^{\mathrm{h}}26^{\mathrm{m}}.3$	$-62°28'$	$0''.772 \pm 0''.007$	3.85	−16	dM5 e	11.05	1.97		1.65	15.49	0.000 06
	α Cen A	14 36.2	−60 38	0.750 ± 0.010	3.68	−22	G2 V	−0.01	0.68		0.22	4.37	1.6
	α Cen B						K0 V	1.33	0.88		0.24	5.71	0.45
3	Barnard's star	17 55.4	+4 33	0.545 ± 0.003	10.31	−108	M5 V	9.54	1.74	1.29	1.25	13.22	0.00045
4	Wolf 359	10 54.1	+7 19	0.421 ± 0.006	4.70	+13	dM8 e	13.53	2.01	1.54	1.85	16.65	0.000 02
5	BD +36°2147	11 00.6	+36 18	0.397 ± 0.004	4.78	−84	M2 V	7.50	1.51	1.12	0.91	10.50	0.0055
6	L 726 − 8 = *A*	1 36.4	−18 13	0.387 ± 0.012	336	+29	dM6 e	12.52	1.85	1.09:	1.6	15.46	0.000 06
	UV Cet = B					+32	dM6 e	13.02				15.96	0.000 04
7	Sirius A	6 42.9	−16 39	0.277 ± 0.006	1.33	−8	A1 V	−1.46	0.00	−0.04	0.12	1.42	23.5
	Sirius B						DA	8.3:	−0.12:	−1.03:		11.2	0.003
8	Ross 154	18 46.7	−23 53	0.345 ± 0.012	0.72	−4	dM5 e	10.45	1.70	1.17	1.30	13.14	0.000 48
9	Ross 248	23 39.4	+43 55	0.314 ± 0.004	1.60	−81	dM6 e	12.29	1.91	1.48	1.56	14.78	0.000 11
10	ε Eri	3 30.6	−9 38	0.303 ± 0.004	0.98	+16	K2 V	3.73	0.88	0.58	0.30	6.14	0.30
11	Ross 128	11 45.1	+1 06	0.298 ± 0.006	1.38	−13	dM5	11.10	1.76	1.30	1.30	13.47	0.000 36
12	61 Cyg A	21 04.1	+38 30	0.294 ± 0.006	5.22	−64	K5 V	5.22	1.17	1.11	0.47	7.56	0.082
	61 Cyg B						K7 V	6.03	1.37	1.23	0.60	8.37	0.039
13	ε Ind	21 59.6	−57 00	0.291 ± 0.010	4.70	−40	K5 V	4.68	1.05	1.00	0.40	7.00	0.14
14	BD +43° 44A	0 15.5	+43 44	0.290 ± 0.006	2.90	+13	M1 V	8.08	1.56	1.24	0.88	10.39	0.0061
	+43 44B					+20	M6 V e	11.06	1.80	1.40	1.22	13.37	0.000 39
15	L 789 − 6	22 35.7	−15 36	0.290 ± 0.007	3.26	−60	dM7 e	12.18	1.96	1.54	1.66	14.49	0.000 14
16	Procyon A	7 36.7	+5 21	0.285 ± 0.006	1.25	−3	F5 IV-V	0.37	0.42	0.03	0.14	2.64	7.65
	Procyon B						DF	10.7				13.0	0.000 55
17	BD +59°1915A	18 42.2	+59 33	0.282 ± 0.004	2.29	0	dM4	8.90	1.54	1.11	1.07	11.15	0.0030
	+59 1915B				2.27	+10	dM5	9.69	1.59	1.14	1.14	11.94	0.0015
18	CD −36°15693	23 02.6	−36 09	0.279 ± 0.024	6.90	+10	M2 V	7.35	1.48	1.18	0.85	9.58	0.013
19	G 51 − 15	8 26.9	+26 57	0.278 ± 0.004	1.27			14.81	2.06		1.79	17.03	0.000 01

Stars within 5 pc (cont.)

No.	Name	α 1950	δ 1950	Trig. parallax, π	Proper motion, $\mu''\text{yr}^{-1}$	Radial velocity v_r km s^{-1}	Spec	V	$B-V$	$U-B$	$R-I$	M_V	Luminosity ($L_\odot = 1$)
20	τ Cet	$1^h41^m.7$	$-16°12'$	$0''.277 \pm 0''.007$	1.92	−16	G8 V	3.50	0.72	0.22	0.26	5.72	0.45
21	BD +5°1668	7 24.7	+5 23	0.266 ± 0.006	3.77	+26	dM5	9.82	1.56	1.12	1.19	11.94	0.0015
22	L 725 − 32	09.9	−17 16	0.261 ± 0.012	1.32	+28	dM5 e	12.04	1.83	1.46	1.44	14.12	0.000 20
23	CD −39°14192	21 14.3	−39 04	0.260 ± 0.012	3.46	+21	M0 V	6.66	1.40	1.20	0.69	8.74	0.028
24	Kapteyn's star	5 09.7	−45 00	0.256 ± 0.010	8.72	+245	sdM0 pec	8.84	1.56	1.05	0.77	10.88	0.0039
25	Krüger 60A	22 26.2	+57 27	0.253 ± 0.004	0.86	−26	dM3	9.85	1.62	1.25	1.14	11.87	0.0016
	Krüger 60B						dM5 e	11.3	1.8	1.3		13.3	0.0004
26	BD −12°4523	16 27.5	−12 32	0.247 ± 0.007	1.18	−13	dM5	10.11	1.60	1.16	1.20	12.07	0.0013
27	Ross 614 A	6 26.8	−2 46	0.246 ± 0.004	1.00	+24	dM7 e	11.10 }	1.71	1.15	1.40	13.12	0.000 49
	Ross 614 B							14 }				16	0.000 04
28	Van Maanen's star	0 46.5	+5 09	0.232 ± 0.004	2.99	+54	DG	12.37	0.56	0.02	0.16	14.20	0.000 18
29	Wolf 424 A	12 30.9	+9 18	0.230 ± 0.006	1.76	−5	dM6 e	13.16 }	1.80	1.18	1.62	14.97	0.000 09
	Wolf 424 B						dM6 e	13.4 }				15.2	0.000 07
30	CD −37°15492	0 02.5	−37 36	0.225 ± 0.012	6.11	+23	M4 V	8.56	1.46	1.03	0.92	10.32	0.0065
31	L 1159 − 16	1 57.5	+12 50	0.224 ± 0.004	2.09		dM8 e	12.26	1.82	1.35	1.35	14.01	0.000 22
32	BD +50°1725	10 08.3	+49 42	0.222 ± 0.010	1.45	−26	K7 V	6.59	1.36	1.28	0.60	8.32	0.041
33	CD −46°11540	17 24.9	−46 51	0.216 ± 0.012	1.06		dM4	9.37	1.53	1.21	1.03	11.04	0.0033
34	G 158 − 27	0 04.2	−7 48	0.214 ± 0.007	2.04		dM	13.74	1.95		1.52	15.39	0.000 06
35	CD−49°13515	21 30.2	−49 13	0.214 ± 0.010	0.81	+8	M1 V	8.67	1.46	1.05	0.93	10.32	0.0065
36	CD−44°11909	17 33.5	−44 17	0.213 ± 0.007	1.16		M5	10.96	1.65	1.20	1.26	12.60	0.000 79
37	BD+68°946	17 36.7	+68 23	0.213 ± 0.006	1.31	−22	M3.5 V	9.15	1.50	1.08	1.10	10.79	0.0042
38	G 208 − 44 =A	19 52.3	+44 18	0.211 ± 0.004	0.74			13.41	1.90			15.03	0.000 08
	G 208 − 45 =B							13.99	1.98			15.61	0.000 05
39	BD−15°6290	22 50.6	−14 31	0.209 ± 0.007	1.14	+9	dM5	10.17	1.60	1.15	1.22	11.77	0.0017
40	o(40)Eri A	4 13.0	−7 44	0.207 ± 0.003	4.08	−42	K1 V	4.43	0.82	0.44	0.31	6.01	0.34
40	Eri B	4 13.1	−7 44		4.07	−21	DA	9.52	0.03	−0.68	−0.10	11.10	0.0032
40	Eri C					−45	dM4 e	11.17	1.66	0.83	1.31	12.75	0.000 69

Stars within 5 pc (cont.)

No.	Name	α 1950	δ 1950	Trig. parallax, π	Proper motion, $\mu'' \mathrm{yr}^{-1}$	Radial velocity v_r km s^{-1}	Spec	V	$B-V$	$U-B$	$R-I$	M_V	Luminosity ($L_\odot = 1$)
41	BD+20°2465	$10^{\mathrm{h}}16^{\mathrm{m}}.9$	+20°07′	$0''.206 \pm 0''.006$	0.49	+11	M4.5 V e	9.43	1.54	1.06	1.12	11.00	0.0035
42	L 145 − 141	11 43.0	−64 33	0.206 ± 0.012	2.68		DC	11.50	0.19	−0.60	0.04	13.07	0.000 52
43	70 Oph A	18 02.9	+2 31	0.203 ± 0.006	1.12	−7	K0 V	4.22	0.86 (A+B)	0.51 (A+B)	0.30 (A+B)	5.76	0.43
	70 Oph B						K5 V	6.00				7.54	0.084
44	BD+43°4305	22 44.7	+44 05	0.200 ± 0.004	0.83	−2	dM5 e	10.2	1.6	1.1	1.15	11.7	0.0018
45	Altair	19 48.3	+8 44	0.198 ± 0.006	0.66	−26	A7 IV-V	0.76	0.22	0.08	0.02	2.24	11.1
46	AC+79°3888	11 44.6	+78 58	0.193 ± 0.007	0.89	−119	sdM4	10.8	1.60		1.18	12.23	0.0011
47	G9 − 38 = A	8 55.4	+19 57	0.192 ± 0.004	0.89		m	14.06	1.84			15.48	0.000 06
	LP426 − 40 =B						m	14.92	1.93			16.34	0.000 025
48	BD+15°2620	13 43.2	+15 10	0.192 ± 0.007	2.30	+15	M4 V	8.49	1.44	1.10	0.86	9.91	0.0095

: denotes approximate value.

For updated parallaxes, absolute magnitudes, and proper motions see:
The 150 Start in the Hipparcos Catalogue Closest to the Sun,
http://astro.estec.esa.nl/Hipparcos/table 361.html.
(Adapted from Landolt-Börnstein, V1/2C, Springer-Verlag, 1982.)

Stars of large proper motion

Star Name	α 2000	δ 2000	V	B−V	Spec	μ	Con
Barnard's Star	17 57.9	+04.6	9.54	+1.74	M5 V	10.27	OPH
Kapteyn's Star	05 11.2	−44.9	8.81	+1.59	M0 V	8.73	PIC
Groombridge 1830	11 52.7	+37.8	6.45	+0.75	G8 Vp	7.04	UMA
Lacaille 9352	23 05.4	−35.8	7.33	+1.48	M2 V	6.90	PSA
Cordoba 32416	00 05.0	−37.3	8.96	+1.46	M4 V	6.08	SCL
Ross 619	08 11.9	+08.8	12.5	+1.7	dM5	5.30	CNC
61 CYG A	21 06.6	+38.7	5.19	+1.19	K5 V	5.20	CYG
61 CYG B	21 06.6	+38.7	6.02	+1.38	K7 V	5.20	CYG
Lalande 21185	11 03.5	+36.0	7.47	+1.52	M2 V	4.78	UMA
Wolf 359	10 56.7	+07.0	13.66	+1.75	M6e	4.71	LEO
ε IND	22 03.0	−56.8	4.74	+1.07	K5 V	4.69	IND
Lalande 21258	11 05.8	+43.5	8.66	+1.52	M2 V	4.53	UMA
WX UMA	11 05.8	+43.5	14.8	+1.2	dM5.5e	4.53	UMA
o^2 ERI A	04 15.5	−07.6	4.42	+0.81	K1 V	4.08	ERI
o^2 ERI B	04 15.5	−07.6	9.50	+0.11	DA	4.08	ERI
o^2 ERI C	04 15.5	−07.6	11.2	+1.5	M4e	4.08	ERI
Wolf 489	13 36.9	+03.7	14.8	+0.96	DC	3.87	VIR
Proxima Centauri	14 30.2	−62.7	10.68	+2.72	M5e	3.85	CEN
BD +5 1668	07 27.4	+05.4	9.82	+1.56	M5	3.76	CMI
μ CAS	01 07.9	+55.0	5.12	+0.69	G2 VI	3.75	CAS
α Centauri A	14 40.0	−60.8	0.33	+0.60	G2 V	3.69	CEN
α Centauri B	14 40.0	−60.8	1.70	+0.85	K0 V	3.69	CEN
Washington 5584	15 10.3	−16.3	9.05	+0.78	K0 VI	3.68	LIB
Washington 5583	15 10.3	−16.4	9.44	+0.86	dK0	3.68	LIB
LP 9 − 231	17 50.7	+82.7	14.8	+0.6	g	3.59	UMI
Lacaille 8760	21 17.5	−38.9	6.70	+1.42	M0 V	3.46	MIC
Luyten 726 − 8A	01 38.8	−17.9	12.5	+1.7	M6e	3.36	CET
Luyten 726 − 8B	01 38.8	−17.9	12.95	+1.76	M6e	3.36	CET
Luyten 789 − 6	22 38.4	−15.3	12.2	+1.7	M6	3.25	AQR
Ross 451	11 40.4	+67.3	12.23	+1.45	sdM0	3.20	DRA
82 ERI	03 19.7	−43.1	4.26	+0.70	G5 V	3.14	ERI
Ross 578	03 38.2	−11.4	13.1	+1.5	M2	3.06	ERI
van Maanen 1	00 49.1	+05.4	12.4	+0.56	DG	2.98	PSC

Column headings:
α2000: right ascension for equator, equinox, and epoch 2000.0; hh mm.m.
δ2000: declination for equator, equinox, and epoch 2000.0; dd.d.
V: visual magnitude in the U, B, V system.
B-V: color index.
Spec. Type: spectral type and luminosity class in the MKK system.
μ: proper motion in arcsec y^{-1}.
Con: constellation.

For updated parallaxes, absolute magnitudes, and proper motions see: *The 150 Stars in the Hipparcos Catalogue with Largest Proper Motion*, http://astro.estec.esa.nl/Hipparcos/table362.html.

Bright white dwarfs

Star Name	Con	α 2000	δ 2000	V	d
Sirius B	CMA	06 45.1	−16.7	8.3	2.6
40 ERI B	ERI	04 15.4	−07.7	9.5	4.8
Procyon B	CMI	07 39.3	+05.2	10.7	3.5
Feige 34	UMA	10 39.6	+43.1	11.1	17
W1346	CYG	20 34.4	+25.1	11.5	14
EG247	CAM	05 05.5	+52.8	11.8	43
He3 (EG50)	AUR	06 47.6	+37.5	12.0	18
EG62 (LP 532 − 81)	PYX	08 41.5	−32.9	12.0	9.1
EG3 68	DRA	16 48.4	+59.1	12.2	12
van Maanen's star	PSC	00 49.2	+05.4	12.4	4.3
EG180	CAM	04 31.2	+59.0	12.4	5.5
AC + 70 5824	UMI	13 38.9	+70.3	12.8	31
EG15	ARI	02 08.8	+25.2	13.2	31

Column headings:
Con: constellation
α 2000: right ascension for equator, equinox, and epoch 2000.0; hh mm.m.
δ 2000: declination for equator, equinox, and epoch 2000.0; dd.d.
V: visual magnitude in the U, B, V system.
d: distance in parsec.
D: diameter in km.

Pulsars

Galactic distribution of pulsars. 0° latitude corresponds to the Galactic plane, while 0° longitude, 0° latitude corresponds to the direction of the Galactic center. (From the Australia Telescope National Facility Catalog of 1529 pulsars, 2005.)

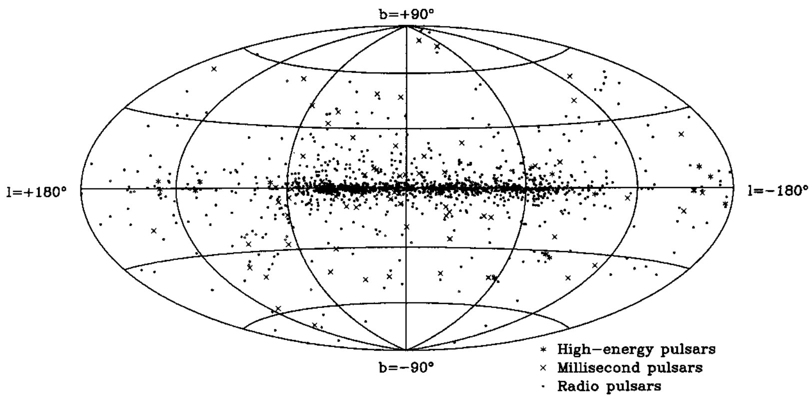

Period distribution of pulsars. (From the Australia Telescope National Facility Catalog of 1529 pulsars, 2005.)

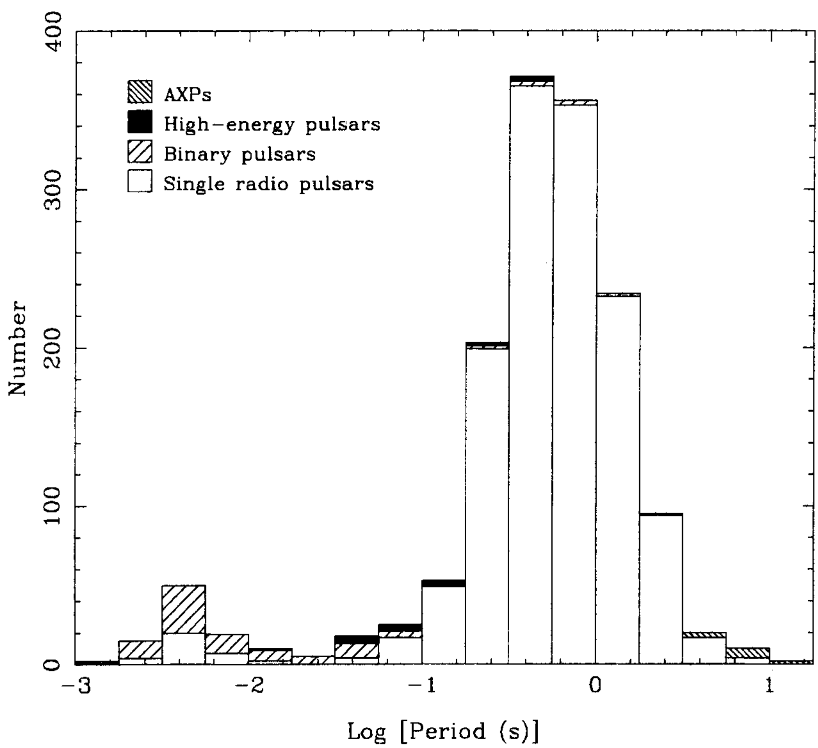

The 20 fastest radio pulsars (as of February 2002)

Pulsar Name	α J2000	δ J2000	P(s)	dP/dt	Epoch (MJD)	DM(pc cm^{-3})	d (kpc)
J1939+2134	$19^h39^m38.56^s$	$+21°34'59.1''$	0.0015578064924327	1.05110E-04	50100.000000	71.0370	9.65
J1959+2048	19 59 36.77	+20 48 15.1	0.0016074016848063	1.68515E-05	48196.000000	29.1168	1.53
J0034−0534	00 34 21.83	−05 34 36.6	0.0018771818543796	5.06000E-06	49550.000000	13.7630	0.98
J0023−7203J	00 23 59.40	−72 03 58.8	0.0021006335458588	−9.78420E-06	51000.000000	24.5845	5.00
J1701−3006F	17 01 13	−30 06 43	0.0022950000000000		52247.000000	115.6400	4.16
J0218+4232	02 18 06.35	+42 32 17.5	0.0023230904564000	7.50000E-05	49150.608600	61.2500	5.85
J0024−7204W	00 24	−72 04	0.0023520000000000			24.3000	5.00
J0024−7204F	00 24 03.85	−72 04 42.8	0.0026235793491669	6.45070E-05	51000.000000	24.3819	5.00
J0024−7204O	00 24 04.65	−72 04 53.7	0.0026433432956678	3.03800E-05	51000.000000	24.3000	5.00
J0024−7204S	00 24 03.98	−72 04 42.3	0.0028304059560080	−1.20470E-04	51779.744510	24.3000	5.00
J1908−3741	19 08 52.0	−37 41 35	0.0029471094385460		52055.870432	10.3500	0.55
J2229+2643	22 29 50.89	+26 43 57.8	0.0029778192947192	1.90000E-06	49440.000000	23.0190	1.43
J1824−2452	18 24 32.01	−24 52 10.8	0.0030543146293258	1.61845E-03	47953.500000	119.8289	5.50
J1807−2459	18 07 21	−24 59 51	0.0030594487974000	−7.00000E-04	51734.975100	134.0000	3.27
J0613−0200	06 13 43.97	−02 00 47.1	0.0030618440367440	9.57200E-06	50315.000000	38.7792	2.19
J1640+2224	16 40 16.75	+22 24 09.0	0.0031633158173403	2.90000E-06	49360.000000	18.4150	1.18
J0024−7204H	00 24 06.70	−72 04 06.8	0.0032103407094388	1.64000E-06	51000.000000	24.3700	5.00
J1701−3006E	17 01 13	−30 06 43	O.0032340000000000		52247.000000	115.6400	4.16
J1910−5958	19 10 52	−59 58 54	0.0032661820000000		51745.000000	33.5200	2.18
J1701−3006D	17 01 13	−30 06 43	0.0034180000000000		52247.000000	115.6400	4.16

α, δ = position of pulsar, P = pulse period, dP/dt = pulse period derivative in unit of 10^{-15} s s^{-1},
Epoch = modified Julian date of the epoch of observation,

DM = dispersion measure = $\int_0^d N_e$ dl where d = distance of the pulsar from the Sun, N_e = electron number density in interstellar space.

The pulse arrival time for two different observing frequencies f_1 and f_2 differs by: $t_2 - t_1 = \frac{e^2}{2\pi m_e c}\left(\frac{1}{f_2^2} - \frac{1}{f_1^2}\right) DM$.

d = Pulsar distance in most cases estimated using the Taylor & Cordes (1993) model for N$_e$. (Data from the Australia National Facility Catalog of 1323 Pulsars, 2002.)

Binary pulsars in the Galaxy

Pulsar	P (ms)	P_b (d)	e^a	$f(M)^b$ $(M_\odot)$	M_2^c $(M_\odot)$	$\log(B)^d$ (G)	$P/(2\dot{P})$ (y)
J0045−7319	926.3	51	0.808	2.169	~ 10	12.3	3×10^6
1259−63	47.8	1237	0.870	1.53	~ 10	11.5	3×10^5
1820−11	279.8	358	0.794	0.068	(0.8)	11.8	3×10^6
1534+12	37.9	0.42	0.274	0.315	1.34	10.0	2×10^8
1913+16	59.0	0.32	0.617	0.132	1.39	10.4	1×10^8
2303+46	1066.4	12.3	0.658	0.246	1.4	11.9	3×10^7
J2145−0750	16.0	6.8	0.000021	0.0241	(0.51)	<8.9	$>8\times10^9$
0655+64	195.7	1.03	7×10^{-6}	0.071	(0.8)	10.1	5×10^9
0820+02	864.8	1232	0.0119	0.0030	(0.23)	11.5	1×10^8
J1803−2712	334	407	0.00051	0.0013	(0.17)	10.9	3×10^8
1953+29	6.1	117	0.00033	0.0024	(0.21)	8.6	3×10^9
J2019+2425	3.9	76.5	0.000111	0.0107	(0.37)	8.3	1×10^{10}
J1713+0747	4.6	67.8	0.000075	0.0079	(0.33)	8.3	9×10^9
1855+09	5.4	12.3	0.000022	0.0056	0.26	8.5	5×10^9
J0437−4715	5.8	5.7	0.000018	0.0012	(0.17)	8.7	2×10^9
J1045−4509	7.5	4.1	0.000019	0.00177	(0.19)	8.6	6×10^9
J2317+1439	3.4	2.46	< 0.000002	0.0022	(0.21)	8.1	1×10^{10}
J0034−0534	1.9	1.6	< 0.0001	0.0012	(0.17)	8.0	4×10^9
J0751+18	3.5	0.26	< 0.01	(0.15)			
1718−19	1004	0.26	< 0.005	0.00071	(0.14)	12.2	1×10^7
1831−00	520.9	1.8	< 0.004	0.00012	(0.07)	10.9	6×10^8
1957+20	1.6	0.38	$< 4\times10^{-5}$	5×10^{-6}	0.02	8.1	2×10^9

[a] Eccentricity.
[b] Mass function, $f(M) = (M_2 \sin i)^3/(M_1 + M_2)^2$, where M_1 and M_2 are the masses of the pulsar and companion, respectively; i, the orbital inclination, is the angle between the plane of the orbit and the plane of the sky.
$M_\odot$ represent's the Sun's mass as a unit of measurement.
[c] Mass of pulsar's companion. Values in parentheses are estimated from f(M), assuming a pulsar mass of 1.4 $M_\odot$ and $i = 60°$.
[d] Dipole surface field, $B = 3.2 \times 10^{19} (P\dot{P})^{1/2}$ gauss.
(Adapted from Phinney, E.S and Kulkarni, S.R., Annu. Rev. Astron. Astrophys, **32**: 591, 1994.)

Binary pulsar PSR 1913+16

A schematic diagram showing the binary pulsar PSR 1913+16. (Longair, M.S., *High Energy Astrophysics*, Cambridge University Press, 1994, with permission)

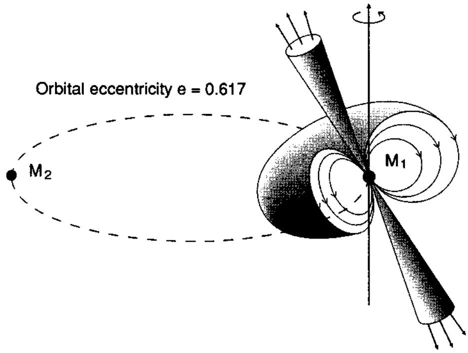

Binary period = 7.751939337 hours
Pulsar period = 59 milliseconds
Neutron star mass M_1 = 1.4411(7) $M_\odot$
Neutron star mass M_2 = 1.3874(7) $M_\odot$

Parameters of PSR 1913+16

Parameter	Symbol (units)	Value
(i) "Physical" parameters		
Right Ascension	α	$19^h 15^m 28.00018(15)$
Declination	δ	$16°06'27''.4043(3)$
Pulsar Period	P_p (ms)	59.029997929613(7)
Derivative of Period	$\dot{P}_p$	$8.62713(8)\times 10^{-18}$
(ii) "Keplerian" parameters		
Projected semimajor axis	α_p sin i(s)	2.3417592(19)
Eccentricity	e	0.6171308(4)
Orbital Period	P_b (day)	0.322997462736(7)
Longitude of periastron	$\omega_0(°)$	226.57528(6)
Julian date of periastron	T_0 (MJD)	46443.99588319(3)
(iii) "Post-Keplerian" parameters		
Mean rate of periastron advance	$(\dot{\omega})$ (° yr^{-1})	4.226621(11)
Redshift/time dilation	γ' (ms)	4.295(2)
Orbital period derivative	$\dot{P}_b(10^{-12})$	−2.422(6)

(Will, C.M., *The Confrontation between General Relativity and Experiment*, http://www.livingreviews.org/Articles/Volume4/2001-4will/, 2002.)

Pulsars (cont.)

Distribution of periods and period derivatives for 353 pulsars. The seven known binary pulsars, indicated by circles around the dots, have unusually small period derivatives and hence relatively weak magnetic fields. (Dewey, R. J. *et al.*, *Nature*, **322**, 712, 1986, with permission.)

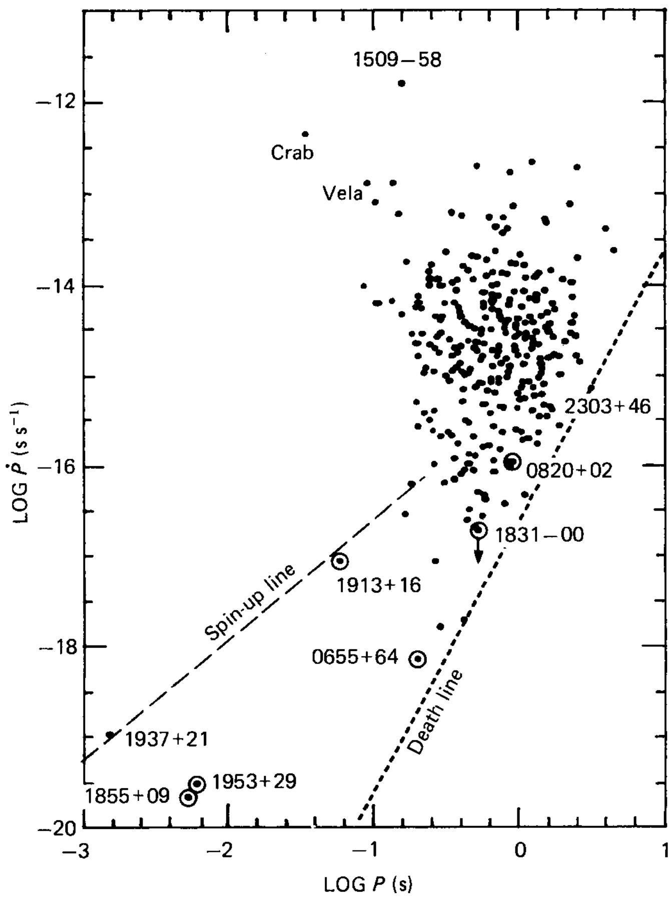

A selection of globular clusters

Name	Equatorial Coord.		Galactic Coord.		V	Diameter
	$\alpha(2000)$	$\delta(2000)$	l	b		D(arcmin)
NGC 104 = 47 Tuc	$0^h24^m_.1$	$-72°05'$	$305°_.9$	$-44°_.9$	4.0	30
NGC 362	1 03.2	−70 51	301.5	−46.3	6.6	13
NGC 3201 = Dun 445	10 17.6	−46 25	277.2	+8.6	6.8	18
NGC 4833 = LacI−4	12 59.6	−70 53	303.6	−8.0	7.4	14
NGC 5024 = M 53	13 12.9	+18 10	333.0	+79.8	7.7	13
NGC 5139 = ω Cen	13 26.8	−47 29	309.1	+15.0	3.6	36
NGC 5272 = M 3	13 42.2	+28 23	42.2	+78.7	6.4	16
NGC 5286 = Dun 388	13 46.4	−51 22	311.6	+10.6	7.6	9
NGC 5904 = M 5	15 18.6	+ 2 05	3.9	+46.8	5.8	17
NGC 5986 = Dun 552	15 46.1	−37 47	337.0	+13.3	7.1	10
NGC 6093 = M 80	16 17.0	−22 59	352.7	+19.5	7.2	9
NGC 6121 = M 4	16 23.6	−26 32	351.0	+16.0	5.9	26
NGC 6205 = M 13	16 41.7	+36 28	59.0	+40.9	5.9	17
NGC 6218 = M 12	16 47.2	− 1 57	15.7	+26.3	6.6	14
NGC 6254 = M 10	16 57.1	− 4 06	15.1	+23.1	6.6	15
NGC 6266 = M 62	17 01.2	−30 07	353.6	+7.3	6.6	14
NGC 6273 = M 19	17 02.6	−26 16	356.9	+9.4	7.2	14
NGC 6341 = M 92	17 17.1	+43 08	68.4	+34.9	6.5	11
NGC 6388	17 36.3	−44 44	345.5	−6.7	6.8	9
NGC 6397	17 40.7	−53 40	338.2	−12.0	5.6	26
NGC 6402 = M 14	17 37.6	− 3 15	21.3	+14.8	7.6	12
NGC 6441	17 50.2	−37 03	353.5	−5.0	7.4	8
NGC 6626 = M 28	18 24.5	−24 52	7.8	−5.6	7.0	11
NGC 6637 = M 69	18 31.4	−32 21	1.7	−10.3	7.7	7
NGC 6656 = M 22	18 36.4	−23 54	9.9	−7.6	5.1	24
NGC 6715 = M 54	18 55.1	−30 29	5.6	−14.1	7.7	9
NGC 6723 = Dun 573	18 59.6	−36 38	0.1	−17.3	7.3	11
NGC 6752 = Dun 295	19 10.9	−59 59	336.5	−25.6	5.4	20
NGC 6809 = M 55	19 40.0	−30 58	8.8	−23.3	6.9	19
NGC 7078 = M 15	21 30.0	+12 10	65.0	−27.3	6.4	12
NGC 7089 = M 2	21 33.5	− 0 49	53.4	−35.8	6.5	13
NGC 7099 = M 30	21 40.4	−23 11	27.2	−46.8	7.5	11

V = integrated apparent visual magnitude.

(Data from Roth, G.D., ed., *Compendium of Practical Astronomy*, Vol. 3, Springer-Verlag, 1994.)

For a catalog of galactic globular clusters see Harris, W.E. 1996, AJ, **112**, 1487 or http://www.physics.mcmaster.ca/Globular.html

Prominent OB associations

Name	α 2000	δ 2000	Diameter (′)	Distance (pc)	O stars	B stars	*RV* ($km\,s^{-1}$)	Clusters	Stars
Cas OB4	$0^h28^m.4$	$+62°42'$		2880	5	12	−43	103	
Cas OB14	0 28.8	+63 22		1110	0	3	−8		κ Cas
Cas OB1	1 00.8	+61 30	120	2510	0	5	−38	381?	
Cas OB8	1 46.2	+61 19		2880	1	10	−30	581, 663; 654?	
Per OB1	2 14.5	+57 19	360	2290	9	56	−41	h, χ Per	
Cas OB6	2 43.2	+61 23	480	2190	17	8	−47	IC 1805	
Cam OB1	3 31.6	+58 38		1000	3	9	−6	1444? 1502?	
Per OB3	3 27.8	+49 54		170					α, δ Per
Per OB2	3 42.2	+33 26	480×300	400	1	3			ζ, o, χ Per
Aur OB2	5 28.3	+34 54		3160	5	3	−13	1893, IC 410	
Aur OB1	5 21.7	+33 52	360×300	1320	5	5	−3	1912, 60; 1931?	
Gem OB1	6 09.8	+21 35	300	1510	4	13	+13	2175?	χ^2 Ori
Ori OB1	5 31.4	−2 41	960	460	9	6		Trapezium	$\theta, \beta, \gamma, \delta, \varepsilon$ Ori
Mon OB1	6 33.1	+8 50	840×300	550	1	0	+22	2264	S Mon
Mon OB2	6 37.2	+4 50	360×250	1510	10	7	+28	2244	Plaskett's star
CMa OB1	7 07.0	−10 28	240	1320	4	3	+27	2335, 53; 2343?	
Pup OB1	7 54.8	−27 05	240×180	2510	7	0	+43	2467?	
Vel OB2	8 11.8	−47 50		460					Vela pulsar?
Vel OB1	8 49.9	−45 00	360×240	1400	5	11		2659?	
Car OB1	10 46.7	−59 05	120×66	2510	6	15		3293; IC 2581?	
Car OB2	11 06.0	−59 51	330×150	2000	8	6		3572, Tr 18	
Car OB4	11 08.3	−60 31	114×54					3590	
Cen OB2	11 35.3	−62 36	84×48	2500				IC 2944	λ Cen
Cen OB1	13 04.8	−62 04	360	2510	2	19		4755	χ Cru
Nor OB1	15 58.7	−54 30		2500	0	6		6031?	

Prominent OB associations (cont.)

Name	α 2000	δ 2000	Diameter (′)	Distance (pc)	O stars	B stars	*RV* ($km\,s^{-1}$)	Clusters	Stars
Sco-Cen	16^h:	-25°:		160				IC 2602?	α CMa, α Carm α Eri
Ara OB1	16 39.5	−46 46	270 × 180	1380				6169, 93	μ Nor
Sco OB1	16 53.5	−41 57	96 × 66	1910	18	10	−18	6231	ζ^1 Sco
Sco OB2	16 14.9	−25 55		160	0	3			α, β^1, δ Sco
Sgr OB1	18 07.9	−21 28	570 × 240	1580	8	9	−4	6514, 30−1	μ Sgr
Sgr OB4	18 14.4	−19 03		2400	1	6	+3	6603	
Ser OB1	18 20.8	−14 35	300 × 180	2190	9	9	−23	6611	
Ser OB2	18 18.6	−11 58	500:	2000:	9	6	+6	6604?	
Vul OB1	19 44.0	+24 13		2000	5	7	+8	6823	
Cyg OB3	20 04.7	+35 50		2290	9	15	0	6871?	Cyg X−1
Cyg OB1	20 17.8	+37 38	420 × 240	1820	12	28	−7	6913, IC 4996	
Cyg OB9	20 23.3	+39 56		1200	7	7	−20	6910	
Cyg OB2	20 32.4	+41 17	30	1820	13	2			
Cyg OB4	21 13.1	+37 52		1000					
Cyg OB7	21 02.7	+49 43		830	3	6	−10		σ Cyg
Cep OB2	21 47.9	+61 04	480	830	8	9	−20	7160, IC 1396	μ, v, λ Cep
Cep OB1	22 24.6	+55 14	210	3470	7	26	−51	7380?	β Cep
Lac OB1	22 41.2	+39 05	900 × 540	600	1	0			10 Lac
Cep OB3	23 00.4	+64 03		870	3	3	−21		
Cas OB5	23 58.7	+60 22	150	2510	5	10	−46	7788; 7790?	ρ Cas
Cep OB4	23 59.5	+67 35		840	2	0			

: denotes approximate value.

(adapted from *Sky Catalogue 2000.0*, Vol. 2, Sky Publishing Corp., 1985.)

The orbital elements of some binary stars

Name	α 2000	δ 2000	Period, P (mean solar years)	Epoch of periastron, t	Longitude of periastron, $\omega(^\circ)$	Eccen-tricity, e	Semi-major axis of orbit, a (arcsec)	Inclin. orbit, i ($^\circ$)	Position angle of ascending node, Ω ($^\circ$)	Distance, d (pc)
η CrB	$15^{h}23^{m}21^{s}$	$30^\circ 17'$	41.623	1934.008	219.907	0.2763	0.907	59.025	23.717	14
γ Vir	12 41 40	−01 27	171.37	1836.433	252.88	0.8808	3.746	146.05	31.78	11
η Cas	00 49 06	57 49	480	1889.6	268.59	0.497	11.9939	34.76	278.42	5.9
ζ Ori	05 40 46	−01 56	1508.6	2070.6	47.3	0.07	2.728	72.0	155.5	340
α CMa (Sirius)	06 45 09	−16 43	50.09	1894.13	147.27	0.5923	7.500	136.53	44.57	2.7
δ Gem	07 20 07	21 59	1200	1437	57.19	0.1100	6.9753	63.28	18.38	18
α Gem (Castor)	07 34 36	31 53	420.07	1965.3	261.43	0.33	6.295	115.94	40.47	14
α CMi (Procyon)	07 39 18	5 14	40.65	1927.6	269.8	0.40	4.548	35.7	284.3	3.5
α Cen	14 39 36	−60 50	79.920	1955.56	231.560	0.516	17.583	79.240	204.868	1.3
α Sco (Antares)	16 29 24	−26 26	900	1889.0	0.0	0.0	3.21	86.3	273.0	100

a semi-major axis, P period of revolution, M_1, M_2 stellar masses, $\dfrac{a^3}{p^2} = \dfrac{G}{4\pi^2}(M_1+M_2)$, where G is the gravitational constant (Kepler's third law).

If we express masses in solar masses, periods in years, and distances in astronomical units, we have
$(M_1 + M_2)P^2 = a^3$ (a (AU) $= a$ (arcsec) $\times$ d (pc)).

e eccentricity, t epoch of the periastron passage (the closest approach of the stars),

Ω position of the ascending node. The nodes are points of intersection of the relative orbit and a plane tangential to the celestial sphere at the position of the bright component,

ω longitude of the periastron, the angle between the radius vector to the ascending node and that in the direction of the periastron, measured from the node to the periastron in the direction of the orbital motion,

i inclination, the angle between the orbital plane and the plane tangential to the celestial sphere.

(Adapted from Duffett-Smith, P., *Practical Astronomy With Your Calculator*, Cambridge University Press, 1988.)

The classification of variable stars

Main class		Subclass	Brightness variation (mag)	Period (d)	Typical representative	Brightness[(a)] (mag) max	min	Period (d)
Cepheids	C	Classical cepheids	0.1–2.0	1–50 or 70	TW CMa	9.5	11.0 p	6.99
	Cδ	Classical cepheids	0.1–2.0	1–50 or 70	δ Cep	4.1	5.2 p	5.37
	CW	Long-period cepheids	0.1–2.0	1–50 or 70	W Vir	9.9	11.3 p	17.29
	I	Irregular variables	—	—	RX Cep	7.5	7.8 v	—
	Ia	Irregular variables	—	—	V395 Cyg	7.8	8.4 v	—
	Ib	Irregular variables	—	—	CO Cyg	9.6	10.6 v	—
	Ic	Irregular variables	—	—	TZ Cas	9.2	10.5 v	—
Long-period variables	M	Mira Ceti stars	2.5–5.0 and more	80–1000	o Cet	2.0	10.1 v	331.62
Red giant variables	SR	Semiregular variables	1–2.0	30–1000	VW UMa	8.4	9.1 p	125
	SRa	Semiregular variables	< 2.5	—	Z Aqr	9.5	12.0 p	136.9
	SRb	Semiregular variables	—	—	AF Cyg	7.4	9.4 p	94.1
	SRc	Semiregular variables	—	—	μ Cep	3.6	5.1 v	—
	SRd	Semiregular variables	—	—	UU Her	8.5	10.6 p	—
RR Lyrae variables	RR	Cluster variables	$< 1 - 2.0$	0.05–1.2	V756 Oph	12.3	13.7 p	—
	RRa	Cluster variables	< 1.5	0.5 and 0.7	RR Lyr	6.94	8.03 p	0.567
	RRc	Cluster variables	—	0.3	SX UMa	10.6	11.2 p	0.307
RV Tauri variables	RV	Variable supergiants	3	30–150	EP Lyr	10.2	11.6 p	83.43
	RVa	Red-giant variables	3	30–150	AC Her	7.4	9.2 p	75.46
	RVb	Red-giant variables	3	30–150	R Sge	9.0	11.2 p	70.594
	βC	β Cephei V. β Canis Major V.	0.1	0.1–0.3	β Cep	3.3	3.35 p	0.190
	δSc	Scuti variables	< 0.25	1.0	δ Sct	4.9	5.19 p	0.194
	α^2CV	α^2 Canis Ven. variables	< 0.1	1–25	α^2 CVn	3.0	3.1 p	5.47

The classification of variable stars (cont.)

Main class		Subclass	Brightness variation (mag)	Period (d)	Typical representative	Brightness[a] (mag) max	Brightness[a] (mag) min	Period (d)
Eruptive variables	N	Novae	7–16	—	—	—	—	—
	Na	Novae	7–16	—	V603 Aql	−1.1	10.8 p	—
	Nb	Novae	7–16	—	RR Pic	1.2	12.8 p	—
	Nc	Novae	7–16	—	RT Ser	10.6	16 p	—
	Nd	Recurrent novae	7–16	—	T GrB	2.0	10.8 v	29000
	Ne	Nova-like variables	—	—	P Cyg	3.0	6 v	—
	SN	Supernovae	20	—	CM Tau (SN 1054 Crab Nebula)	−6	15.9 p	—
	RCB	R Coronae Borealis variables	1–9	10–100	R CrB	5.8	14.8 v	—
	RW	RW Aurigae variables	—	—	RW Aur	9.6	13.6 p	—
	UG	U Geminorum varibales (SS Cygni variables)	2–6	20–600	U Gem	8.9	14.0 v	103
	UV	UV Ceti variables	1–6	—	UV Cet	7.0	12.9 v	—
	Z	Z Camelopardalis variables	2–5	10–40	—	—	—	—
Eclipsing variables	E	Eclipsing variables	—	—	QX Cas	10.2	10.6 p	—
	EA	Algol variables	—	0.2–10 000	β Per	2.2	3.47 v	2.867
	EB	β Lyrae variables	< 2.0	> 1	β Lyr	3.4	4.34	12.908
	EW	W Ursae Majoris variables	0.8	1	W UMa	8.3	9.03 p	0.334
	Ell	Ellipsoid variables	—	—	b Per	4.6	4.66 p	1.527
Unclassifiable variables		—	—	—	V389 Cyg	5.5	5.69 p	—

[a] P = photographic, v = visual.
(Adapted from Roth, G.D., ed., *Handbuch für Sternfreunde*, springer-Verlag, 1967.)

Position of various classes of variable stars in the H-R diagram. (Adapted from Roth, G.D., Compendium of Practical Astronomy, Springer-Verlag, 1994.)

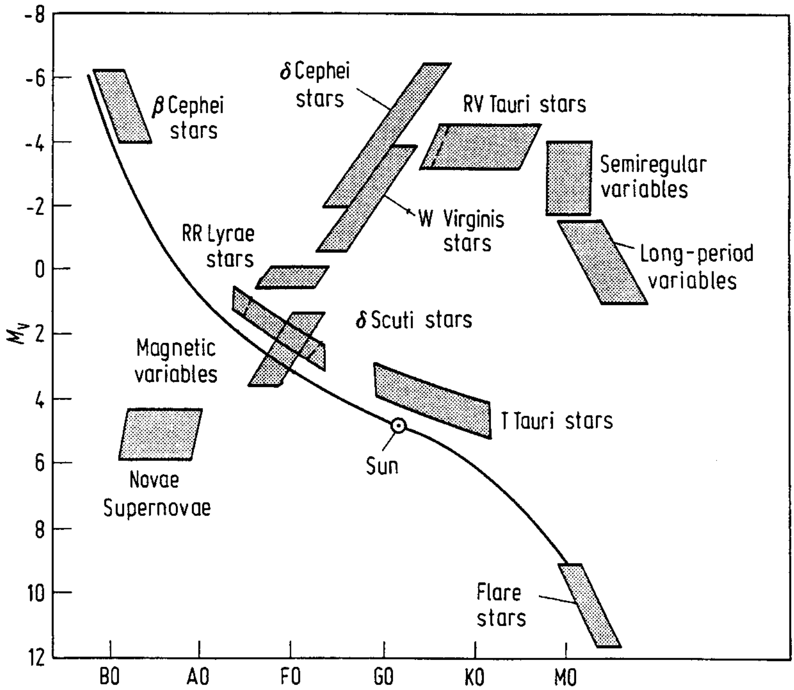

Representative galactic supernova remnants

Name	Galactic coordinates l^{II}, b^{II}	α 1950	δ 1950	Radio size	Optical size
CTA 1	119°.53 +9°.77	$00^h04^m18^s$	+72°04′.5	90′	50′ ×90′
Tycho	120.09 +1.41	00 22 33	+63 51.8	8′	8′
HB 3	132.70 +1.30	02 14	+62 18	140′	...
HB 9	160.39 +2.75	04 57	+46 36	130′ ×155′	90′ ×125′
OA 184	166.07 +4.40	05 15 38	+41 46	70′ ×90′	70′ ×80′
VRO 42.05.01	166.27 +2.53	05 23 21	+43 00	70′ ×75′	35′ ×40′
S 147	180.33 −1.68	05 36 45	+27 44.5	175′	195 ×200′
Crab	184.55 −5.78	05 31 31	+21 58.9	290″ ×420″	290′ ×420″
IC 443	189.01 +3.02	06 14 06	+22 37.2	47′ ×54′	48′
Monoceros	205.62 −0.10	06 35	+06 30	210′	180′ ×200′
Puppis	260.40 −3.42	08 20 30	−42 50	45′ ×65′	50′ ×80′
Vela	263.37 −3.01	08 32	−45 00	300′	270′
MSH 10−53	284.17 −1.78	10 15 40	−58 40.5	33′ ×50′	1′ ×5′
RCW 86	315.44 −2.33	14 39 08	−62 15	55′	8′ ×31′
RCW 89	320.36 −0.97	15 09 30	−58 46	8′:	450″ ×580″
RCW 103	332.43 −0.39	16 13 54	−50 55.8	7′	5′.7 ×9′.5
Kes 45	342.05 +0.13	16 50 11	−43 30.3	30′	··· ×20′
Kepler	004.52 +6.82	17 27 41	−21 26.6	3′	21″ ×64″
W28	006.46 −0.09	17 57 36	−23 25	30′	30′
3C 400.2	053.62 −2.23	19 36 30	+17 08	20′	4′ ×6′
DR 4	078.13 +1.81	20 20 38	+40 03.4	≤ 3′	2′ ×3′
Cygnus	074.27 −8.49	20 49 30	+30 45	160′ ×240′	160′ ×210′
Cas A	111.73 −2.13	23 21 10	+58 32.4	4′	4′
CTB 1	116.94 +0.18	23 56 45	+62 10	35′: ×45′:	32′

: denotes approximate value.

(Adapted from van den Bergh *et al.*, *Ap. J. Suppl.*, **26**, 19, 1973.)

See http://www.mrao.cam.ac.uk/surveys/ for a complete catalog of SNRs.

Typical supernovae light curves

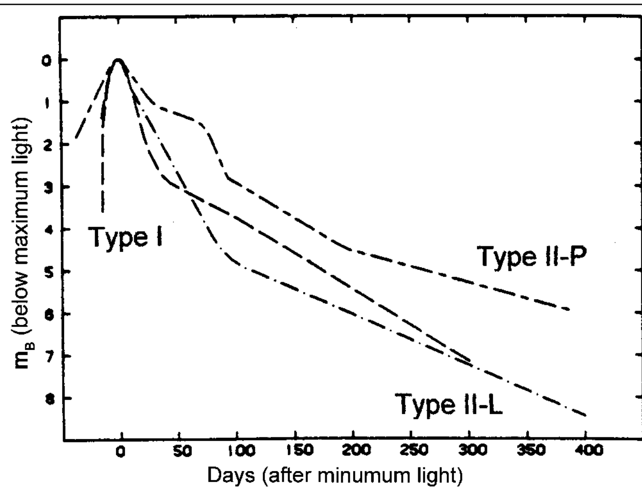

(Adapted from Doggett, J. and Branch, D., Astron. J., 90, 2303, 1985.)

Henry Draper (HD) spectral classification

Class	Class characteristics
O	Hot stars with He II absorption
B	He I absorption; H developing later
A	Very strong H, decreasing later; Ca II increasing
F	Ca II stronger; H weaker; metals developing
G	Ca II strong; Fe and other metals strong; H weaker
K	Strong metallic lines; CH and CN bands developing
M	Very red; TiO bands developing strongly

Spectral type and luminosity class (MK, or Yerke's classification)

Luminosity class		Examples:	Spectral type
Ia	Supergiants	α Boo (Arcturus)	K2 III
Ib	Supergiants	α CMi (Procyon)	F5 IV
II	Bright giants	β Gem (Pollux)	K0 III
III	Giants	α Lyr (Vega)	A0 V
IV	Subgiants	α UMi (polaris)	F8 Ib
V	Main sequence (dwarfs)	α CMa (Sirius)	A1 V
VI	Subdwarfs	α Cyg (Deneb)	A2 Ia
VII	White dwarfs	α Leo (Regulus)	B7 V
		β Ori (Rigel)	B8 Ia
		Sun	G2 V

Spectral type and luminosity class of the MK classification; dependence on color index B−V and visual absolute magnitude M_v.
(Adapted from Unsoeld, A., *The New Cosmos*, Springer-Verlag, 1969.)

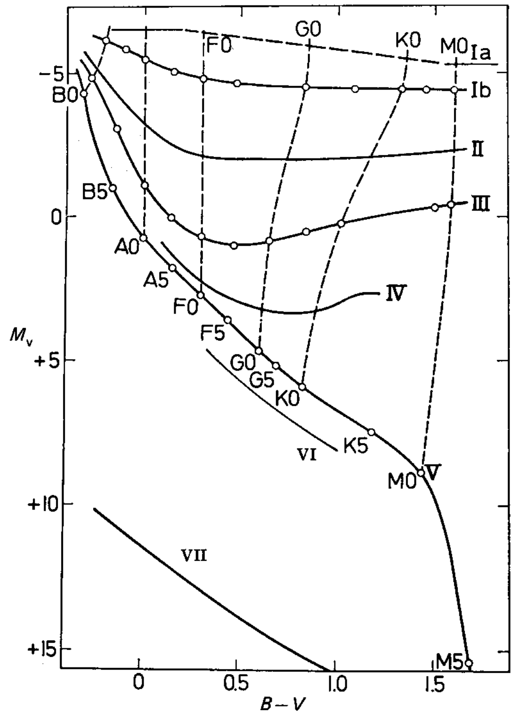

Hertzsprung–Russell diagram

Hertzsprung–Russell or temperature luminosity diagram. (Adapted from Goldberg, L. & Dyer, E. R. in *Science in Space*, L. V. Berkner & H. Odishaw, eds., McGraw-Hill Book Company, 1961.)

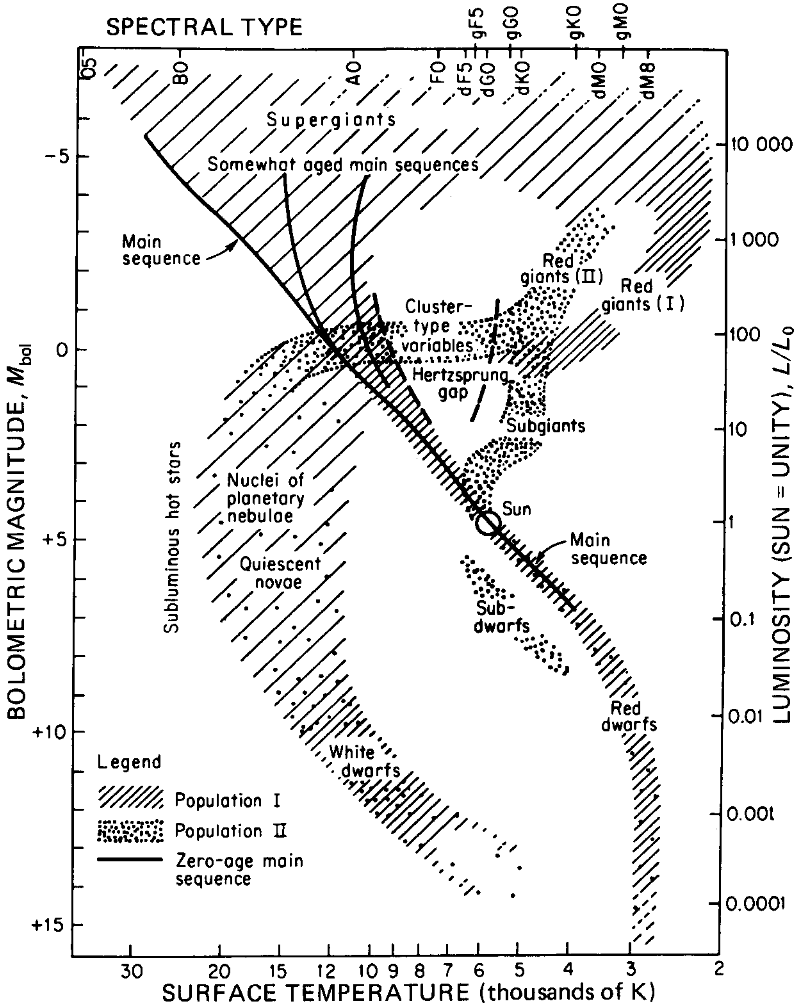

Hertzsprung-Russell diagram with stellar examples.
(From Kaler, J.B., *Stars and their Spectra*, Cambridge University Press, 1989, with permission.)

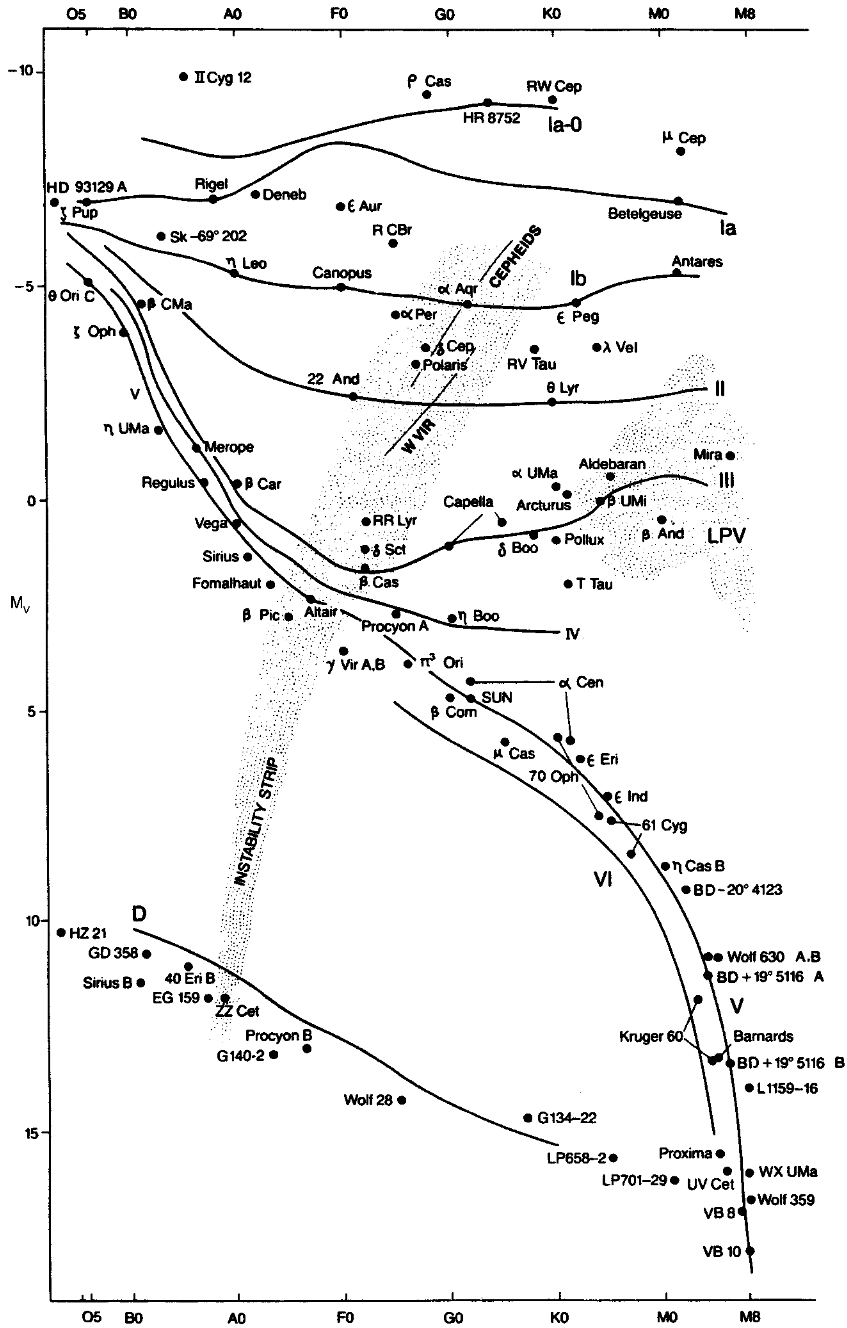

An incomplete list of astrophysically important infrared and visible spectral features

Identification	Wavelength (Å)	Identification	Wavelength (Å)
He I	10 830	O II	4649
C I	10 691	N III	4641
Si I	10 689	N III	4634
Si I	10 627	Mg I	4571
Si I	10 603	He II	4541
Si I	10 371	Mg II	4481
He II	10 124	He I	4472
He II	10 120	He I	4471
Na I	9961	He I	4388
C III	9710	Fe I	4384
O I	8446	[O III]	4363
He II	8237	H I γ	4340
O I	7774	O II	4318
He I	7065	G band[b]	4300
H I α	6563	Ca I	4227
[O I]	6363[a]	He II	4200
[O I]	6300	H I δ	4102
Na I (D)	5896	He II	4100
Na I (D)	5890	N III	4097
He I	5876	Si IV	4089
He II	5412	O II	4073
Fe XIV	5303	He I	4026
Mg I	5175[b]	H I ε	3970
Mg I	5173	Ca II (H)	3968
[O III]	5007	[Ne III]	3968
[O III]	4959	He I	3965
He I	4922	Ca II (K)	3934
H I β	4861	[Ne III]	3869
He II	4686	He I	3820
C IV	4658	O III	3760
O II	4650	[O II]	3727
C II	4650	[Ne V]	3426

†$h\nu$ (eV) = 123 98.54/λ (Å).

[a] Forbidden transitions are noted by brackets.

[b] Superposition of CH band and metallic lines.

Calibration of MK spectral types

Sp	$M(V)$	$B-V$	$U-B$	$V-R$	$R-I$	$T_{\rm eff}$	BC
MAIN SEQUENCE, V							
O5	−5.7	−0.33	−1.19	−0.15	−0.32	42 000	−4.40
O9	−4.5	−0.31	−1.12	−0.15	−0.32	34 000	−3.33
B0	−4.0	−0.30	−1.08	−0.13	−0.29	30 000	−3.16
B2	−2.45	−0.24	−0.84	−0.10	−0.22	20 900	−2.35
B5	−1.2	−0.17	−0.58	−0.06	−0.16	15 200	−1.46
B8	−0.25	−0.11	−0.34	−0.02	−0.10	11 400	−0.80
A0	+0.65	−0.02	−0.02	0.02	−0.02	9 790	−0.30
A2	+1.3	+0.05	+0.05	0.08	0.01	9 000	−0.20
A5	+1.95	+0.15	+0.10	0.16	0.06	8 180	−0.15
F0	+2.7	+0.30	+0.03	0.30	0.17	7 300	−0.09
F2	+3.6	+0.35	0.00	0.35	0.20	7 000	−0.11
F5	+3.5	+0.44	−0.02	0.40	0.24	6 650	−0.14
F8	+4.0	+0.52	+0.02	0.47	0.29	6 250	−0.16
G0	+4.4	+0.58	+0.06	0.50	0.31	5 940	−0.18
G2	+4.7	+0.63	+0.12	0.53	0.33	5 790	−0.20
G5	+5.1	+0.68	+0.20	0.54	0.35	5 560	−0.21
G8	+5.5	+0.74	+0.30	0.58	0.38	5 310	−0.40
K0	+5.9	+0.81	+0.45	0.64	0.42	5 150	−0.31
K2	+6.4	+0.91	+0.64	0.74	0.48	4 830	−0.42
K5	+7.35	+1.15	+1.08	0.99	0.63	4 410	−0.72
M0	+8.8	+1.40	+1.22	1.28	0.91	3 840	−1.38
M2	+9.9	+1.49	+1.18	1.50	1.19	3 520	−1.89
M5	+12.3	+1.64	+1.24	1.80	1.67	3 170	−2.73
GIANTS, III							
G5	+0.9	+0.86	+0.56	0.69	0.48	5 050	−0.34
G8	+0.8	+0.94	+0.70	0.70	0.48	4 800	−0.42
K0	+0.7	+1.00	+0.84	0.77	0.53	4 660	−0.50
K2	+0.5	+1.16	+1.16	0.84	0.58	4 390	−0.61
K5	−0.2	+1.50	+1.81	1.20	0.90	4 050	−1.02
M0	−0.4	+1.56	+1.87	1.23	0.94	3 690	−1.25
M2	−0.6	+1.60	+1.89	1.34	1.10	3 540	−1.62
M5	−0.3	+1.63	+1.58	2.18	1.96	3 380	−2.48

Absolute magnitude, colors, effective surface temperatures, and bolometric corrections for various spectral types and luminosity classes. (From Drilling, J.S. and Landolt, A.U. in *Allen's Astrophysical Quantities*, Cox, A.N., ed., Springer-Verlag, 2000, with permission.)

Calibration of MK spectral types (cont.)

Sp	$M(V)$	$B-V$	$U-B$	$V-R$	$R-I$	T_{eff}	BC
SUPERGIANTS, I							
O9	−6.5	−0.27	−1.13	−0.15	−0.32	32 000	−3.18
B2	−6.4	−0.17	−0.93	−0.05	−0.15	17 600	−1.58
B5	−6.2	−0.10	−0.72	0.02	−0.07	13 600	−0.95
B8	−6.2	−0.03	−0.55	0.02	0.00	11 100	−0.66
A0	−6.3	−0.01	−0.38	0.03	0.05	9 980	−0.41
A2	−6.5	+0.03	−0.25	0.07	0.07	9 380	−0.28
A5	−6.6	+0.09	−0.08	0.12	0.13	8610	−0.13
F0	−6.6	+0.17	+0.15	0.21	0.20	7460	−0.01
F2	−6.6	+0.23	+0.18	0.26	0.21	7 030	−0.00
F5	−6.6	+0.32	+0.27	0.35	0.23	6 370	−0.03
F8	−6.5	+0.56	+0.41	0.45	0.27	5 750	−0.09
G0	−6.4	+0.76	+0.52	0.51	0.33	5 370	−0.15
G2	−6.3	+0.87	+0.63	0.58	0.40	5 190	−0.21
G5	−6.2	+1.02	+0.83	0.67	0.44	4 930	−0.33
G8	−6.1	+1.14	+1.07	0.69	0.46	4 700	−0.42
K0	−6.0	+1.25	+1.17	0.76	0.48	4 550	−0.50
K2	−5.9	+1.36	+1.32	0.85	0.55	4 310	−0.61
K5	−5.8	+1.60	+1.80	1.20	0.90	3 990	−1.01
M0	−5.6	+1.67	+1.90	1.23	0.94	3 620	−1.29
M2	−5.6	+1.71	+1.95	1.34	1.10	3 370	−1.62
M5	−5.6	+1.80	+1.60:	2.18	1.96	2 880	−3.47

Classification and absolute magnitude of stars (M_v)

Sp	Supergiants Ia	Supergiants Ib	Bright giants II	Giants III	Sub-giants IV	Main sequence dwarfs V	ZAMS[(a)] V	White dwarfs VII	Population II: Sub-dwarfs VI	Population II: Red branch	Population II: Horiz. branch
O5	−6.4			−5.4		−5.7					
B0	−6.7	−6.1	−5.4	−5.0	−4.7	−4.1	−3.3	+10.2			
B5	−6.9	−5.7	−4.3	−2.4	−1.8	−1.1	−0.2	+10.7			+2.3
A0	−7.1	−5.3	−3.1	−0.2	+0.1	+0.7	+1.5	+11.3			+0.8
A5	−7.7	−4.9	−2.6	+0.5	+1.4	+2.0	+2.4	+12.2			+0.5
F0	−8.2	−4.7	−2.3	+1.2	+2.0	+2.6	+3.1	+12.9			+0.4
F5	−7.7	−4.7	−2.2	+1.4	+2.3	+3.4	+3.9	+13.6	+4.8	+4.8	+0.4
G0	−7.5	−4.7	−2.1	+1.1	+2.9	+4.4	+4.6	+14.3	+5.7	+4.1	+0.3
G5	−7.5	−4.7	−2.1	+0.7	+3.1	+5.1	+5.2	+14.9	+6.4	+2.0	−0.1
K0	−7.5	−4.6	−2.1	+0.5	+3.2	+5.9	+6.0	+15.3	+7.3	−0.2	−0.6
K5	−7.5	−4.6	−2.2	−0.2		+7.3	+7.3	+15	+8.4	−2.2	−2.2
M0	−7.5	−4.6	−2.3	−0.4		+9.0	+9.0	+15	+10	−3	−3
M2	−7		−2.4	−0.6		+10.0	+10.0		+12		
M5				−0.8		+11.8	+11.8		+14		
M8						+16			+16		

Relation between absolute magnitude M_v and emission line width W (FWHM in $km\,s^{-1}$):

Emission line	*Relation*
Ca II K	$M_v = 27.59 - 14.94 \log W$ (Wilson-Bappu)
Mg II K	$M_v = 34.93 - 15.15 \log W$
H Lα	$M_v = (40.2 \pm 4.5) - (14.7 \pm 1.6) \log W$

[(a)] Zero age main sequence.

(After Allen, C.W., *Astrophysical Quantities*, The Athlone Press, 1973.)

Stellar mass, luminosity, radius and density (luminosity and radius with mass; white dwarfs omitted)

$\log(M/M_\odot)$	$\log(L/L_\odot)$	M_{bol}	M_{v}	M_{B}	$\log(R/R_\odot)$ main seq.
−1.0	−2.9	+12.1	15.5	+17.1	−0.9
−0.8	−2.5	+10.9	13.9	+15.5	−0.7
−0.6	−2.0	+9.7	12.2	+13.9	−0.5
−0.4	−1.5	+8.4	10.2	+11.8	−0.3
−0.2	−0.8	+6.6	7.5	+8.7	−0.14
0.0	0.0	+4.7	4.8	+5.5	0.00
+0.2	+0.8	+2.7	2.7	+3.0	+0.10
+0.4	+1.6	+0.7	1.1	+1.1	+0.32
+0.6	+2.3	−1.1	−0.2	−0.1	+0.49
+0.8	+3.0	−2.9	−1.1	−1.2	+0.58
+1.0	+3.7	−4.6	−2.2	−2.4	+0.72
+1.2	+4.4	−6.3	−3.4	−3.6	+0.86
+1.4	+4.9	−7.6	−4.6	−4.9	+1.00
+1.6	+5.4	−8.9	−5.6	−6.0	+1.15
+1.8	+6.0	−10.2	−6.3	−6.9	+1.3

(After Allen, C. W., *Astrophysical Quantities*, Athlone Press, 1973.)

Stellar mass, luminosity, radius and density (mass, radius, luminosity, and mean density with spectral class)[a]

	$\log(M/M_\odot)$			$\log(R/R_\odot)$			$\log\overline{\rho}$ ($\mathrm{g\,cm^{-3}}$)			$\log(L/L_\odot)$		
Sp	I	III	V	I	III	V	I	III	V	I	III	V
O5	+2.2		+1.6			+1.25			−2.0			+5.7
B0	+1.7		+1.25	+1.3	+1.2	+0.87	−2.1		−1.2	+5.4		+4.3
B5	+1.4		+0.81	+1.5	+1.0	+0.58	−2.9		−0.78	+4.8		+2.9
A0	+1.2		+0.51	+1.6	+0.8	+0.40	−3.5		−0.55	+4.3		+1.9
A5	+1.1		+0.32	+1.7		+0.24	−3.8		−0.26	+4.0		+1.3
F0	+1.1		+0.23	+1.8		+0.13	−4.2		−0.01	+3.9		+0.8
F5	+1.0		+0.11	+1.9	+0.6	+0.08	−4.5		+0.03	+3.8		+0.4
G0	+1.0	+0.4	+0.04	+2.0	+0.8	+0.02	−4.9	−1.8	+0.13	+3.8	+1.5	+0.1
G5	+1.1	+0.5	−0.03	+2.1	+1.0	−0.03	−5.2	−2.4	+0.20	+3.8	+1.7	−0.1
K0	+1.1	+0.6	−0.11	+2.3	+1.2	−0.07	−5.7	−2.9	+0.25	+3.9	+1.9	−0.4
K5	+1.2	+0.7	−0.16	+2.6	+1.4	−0.13	−6.4	−3.4	+0.38	+4.2	+2.3	−0.8
M0	+1.2	+0.8	−0.33	+2.7		−0.20	−6.7	−4	+0.4	+4.5	+2.6	−1.2
M2	+1.3		−0.41	+2.9		−0.3	−7.2		+0.7	+4.7	+2.8	−1.5
M5			−0.67			−0.5			+1.0		+3.0	−2.1
M8			−1.0			−0.9			+1.8			−3.1

[a] I = supergiant, III = giant, V = dwarf.
A single column between III and V represents main sequence.
(After Allen, C. W.., *Astrophysical Quantities*, Athlone Press, 1973.)

Present-day mass function **(PDMF)**

M_v	$\phi(M_v)$ (stars pc^{-3} mag^{-1})	$\log M/M_\odot$	$-\frac{dM_v}{d\log M}$	$2H$ (pc)	$\log T_{MS}$(y)	f_{MS}	$\phi_{MS}(\log M)$ (stars pc^{-2} $\log M^{-1}$)
−6	1.49(−8)*	2.07	3.7	180	6.42	0.40	3.97(−6)*
−5	7.67(−8)	1.80	3.7	180	6.50	0.40	2.04(−5)
−4	3.82(−7)	1.53	3.7	180	6.58	0.41	1.04(−4)
−3	1.80(−6)	1.26	3.7	180	6.84	0.42	5.03(−4)
−2	7.86(−6)	0.99	3.7	180	7.19	0.43	2.25(−3)
−1	3.07(−5)	0.72	3.7	180	7.68	0.46	9.41(−3)
0	1.04(−4)	0.45	10.8	180	8.36	0.50	1.01(−1)
1	2.95(−4)	0.36	10.8	180	8.62	0.56	3.21(−1)
2	6.94(−4)	0.26	10.8	180	8.93	0.64	8.63(−1)
3	1.36(−3)	0.17	10.8	300	9.24	0.78	3.44(+0)
4	2.26(−3)	0.08	10.8	465	9.60	0.98	1.11(+1)
5	3.31(−3)	−0.02	10.8	630	9.83	1.00	2.25(+1)
6	4.41(−3)	−0.11	10.8	650	10.28	1.00	3.10(+1)
7	5.48(−3)	−0.20	10.8	650	—	1.00	3.85(+1)
8	6.52(−3)	−0.29	10.8	650	—	1.00	4.58(+1)
9	7.53(−3)	−0.39	10.8	650	—	1.00	5.29(+1)
10	8.52(−3)	−0.48	10.8	650	—	1.00	5.98(+1)

***Present-day mass function* (PDMF)** (cont.)

M_v	$\phi(M_v)$ (stars pc^{-3} mag^{-1})	$\log M/M_\odot$	$-\dfrac{dM_v}{d\log M}$	$2H$ (pc)	$\log T_{MS}$(y)	f_{MS}	$\phi_{MS}(\log M)$ (stars pc^{-2} $\log M^{-1}$)
11	9.54(−3)	−0.57	10.8	650	—	1.00	6.70(+1)
12	1.06(−2)	−6.67	10.8	650	—	1.00	7.44(+1)
13	1.17(−2)	0.76	10.8	650	—	1.00	8.21(+1)
14	1.29(−2)	−0.85	10.8	650	—	1.00	9.06(+1)
15	1.41(−2)	−0.94	10.8	650	—	1.00	9.90(+1)
16	1.41(−2)	−1.04	10.8	650	—	1.00	9.90(+1)

* Number in parenthesis is power of 10.

$\phi(M_v) \equiv$ luminosity function of field stars.

$\phi_{MS}(\log M) \equiv$ present-day mass function (PDMF) of *main-sequence* field stars in the solar neighborhood is given by

$\phi_{MS}(\log M) + \phi(M_v)\left|\dfrac{dM_v}{d\log M}\right| 2H(M_v) f_{MS}(M_v)$, where $H(M_v)$ is the scale height assuming that stars are distributed as $\exp(-|z|/H)$, where z is the distance measured perpendicular to the Galactic plane.

The factor $f_{MS}(M_v)$ gives the fraction of stars at a given magnitude that are on the main sequence

T_{MS} = the main-sequence lifetime is given by

$$T_{MS} = \frac{\Delta X_{MS} M E}{L} \simeq 13 \times 10^9 (M/M_\odot)^{-2.5}\ \text{yr},\ M \leq 10 M_\odot,$$

where ΔX_{MS} = the mass fraction of hydrogen burned during the main-sequence phase, ~ 0.13.

E = energy released per gram in the nuclear fusion reaction, $H \rightarrow He \simeq 6.4 \times 10^{18}\ \text{erg g}^{-1}$.

L = total luminosity of star.

(Adapted from Shapiro, S.L. & Teukolsky, S. A. *Black Holes, White Dwarfs, and Neutron Stars*, John Wiley and Sons, 1983.)

Star number densities ($\log N_{\mathrm{m}}(pg)$ with galactic latitude [a])

	Galactic latitude									Mean
m_{pg}	0°	±5°	±10°	±20°	±30°	±40°	±50°	±60°	±90°	0° – 90°
0.0		−4.0			−4.3			−4.4		−4.25
1.0		−3.4			−3.75			−3.9		−3.70
2.0		−2.83			−3.20			−3.3		−3.18
3.0		−2.32			−2.69			−2.8		−2.60
4.0	−1.75	−1.83	−1.88	−2.01	−2.16	−2.25	−2.30	−2.32	−2.40	−2.11
5.0	−1.28	−1.36	−1.43	−1.56	−1.69	−1.76	−1.80	−1.83	−1.89	−1.63
6.0	−0.82	−0.90	−0.97	−1.10	−1.22	−1.29	−1.34	−1.37	−1.42	−1.14
7.0	−0.39	−0.46	−0.53	−0.66	−0.77	−0.84	−0.89	−0.92	−0.97	−0.69
8.0	0.05	−0.01	−0.09	−0.22	−0.32	−0.40	−0.45	−0.48	−0.54	−0.25
9.0	0.52	0.43	0.35	0.22	0.12	0.04	−0.01	−0.06	−0.12	0.19
10.0	0.97	0.88	0.80	0.66	0.54	0.46	0.40	0.35	0.27	0.62
11.0	1.43	1.33	1.23	1.08	0.96	0.87	0.80	0.75	0.66	1.05
12.0	1.88	1.77	1.65	1.50	1.37	1.26	1.19	1.12	1.03	1.46
13.0	2.30	2.19	2.07	1.90	1.76	1.64	1.54	1.47	1.39	1.87
14.0	2.72	2.61	2.48	2.28	2.12	1.98	1.88	1.79	1.71	2.26
15.0	3.12	3.00	2.88	2.65	2.46	2.31	2.20	2.10	1.97	2.62
16.0	3.48	3.41	3.24	3.00	2.77	2.61	2.48	2.38	2.24	2.98
17.0	3.83	3.78	3.60	3.33	3.07	2.84	2.75	2.64	2.48	3.33
18.0	4.20	4.10	3.93	3.63	3.35	3.14	2.99	2.87	2.72	3.64
19.0	4.5	4.4	4.3	3.9	3.6	3.4	3.2	3.1	2.9	3.90
20.0	4.7	4.7	4.6	4.2	3.8	3.6	3.4	3.3	3.1	4.17
21.0	5.0	4.9	4.8	4.5	4.0	3.7	3.6	3.4	3.2	4.4

[a] $N_{\mathrm{m}}(pg \approx \mathrm{B})$ = number of stars per square degree brighter than photographic magnitude m_{pg}.

Star number densities ($\log N_{\rm m}$(vis) with galactic latitude [b]) (cont.)

	Galactic latitude									Mean
$m_{\rm vis}$	0°	±5°	±10°	±20°	±30°	±40°	±50°	±60°	±90°	0° – 90°
0.0		−3.9			−4.2			−4.3		−4.1
1.0		−3.3			−3.6			−3.7		−3.56
2.0		−2.7			−3.0			−3.1		−3.00
3.0		−2.14			−2.5			−2.6		−2.43
4.0	−1.55	−1.63	−1.68	−1.81	−1.96	−2.05	−2.10	−2.12	−2.20	−1.90
5.0	−1.08	−1.16	−1.23	−1.36	−1.49	−1.56	−1.60	−1.63	−1.69	−1.41
6.0	−0.60	−0.68	−0.75	−0.88	−1.00	−1.07	−1.12	−1.15	−1.20	−0.93
7.0	−0.16	−0.23	−0.30	−0.43	−0.54	−0.61	−0.66	−0.69	−0.74	−0.46
8.0	0.29	0.23	0.15	0.02	−0.08	−0.16	−0.21	−0.24	−0.30	0.00
9.0	0.78	0.69	0.61	0.48	0.38	0.30	0.25	0.20	0.14	0.45
10.0	1.25	1.16	1.08	0.94	0.82	0.74	0.68	0.63	0.55	0.91
11.0	1.73	1.63	1.53	1.38	1.26	1.17	1.10	1.05	0.96	1.34
12.0	2.18	2.07	1.93	1.80	1.67	1.57	1.49	1.42	1.33	1.76
13.0	2.60	2.49	2.37	2.20	2.08	1.94	1.84	1.77	1.69	2.17
14.0	3.02	2.91	2.78	2.60	2.44	2.28	2.18	2.09	2.01	2.56
15.0	3.42	3.30	3.18	2.95	2.78	2.61	2.50	2.40	2.27	2.94
16.0	3.78	3.71	3.54	3.30	3.09	2.91	2.78	2.68	2.54	3.29
17.0	4.13	4.08	3.90	3.60	3.37	3.19	3.05	2.94	2.78	3.64
18.0	4.50	4.40	4.23	3.93	3.65	3.44	3.29	3.17	3.02	3.95
19.0	4.8	4.7	4.6	4.2	3.9	3.7	3.5	3.4	3.2	4.20
20.0	5.0	5.0	4.9	4.5	4.1	3.9	3.7	3.6	3.4	4.5
21.0	5.3	5.2	5.1	4.8	4.3	4.1	3.9	3.7	3.5	4.7

[b] $N_{\rm m}({\rm vis} \approx V)$ = number of stars per square degree brighter than visual magnitude $m_{\rm vis}$.
(After Allen, C. W., *Astrophysical Quantities*, Athlone Press, 1973.)

Relative numbers of stars in each class (up to $V = 8.5$ in *HD Catalog)*

Sp	O	B	A	F	G	K	M
% stars	1	10	22	19	14	31	3

(After Allen, C. W., *Astrophysical Quantities*, Athlone Press, 1973.)

Integrated star light as a function of galactic latitude

	Star light (10th mag deg^{-2})			Star light (10th mag deg^{-2})			Star light (10th mag deg^{-2})	
Latitude	*pg*	*V*	Latitude	*pg*	*V*	Latitude	*pg*	*V*
0	180	372	20	54	105	60	21	38
5	123	247	30	37	71	70	19	35
10	88	176	40	29	54	80	18	34
15	69	138	50	24	43	90	18	34

Integrated star light from whole sky: 230 zero *pg* mag stars; 460 zero V mag stars. Night sky total brightness (zenith, mean sky) $\approx 1(m_v = 22.5)$ star $arcsec^{-2}$.
(After Allen, C. W., *Astrophysical Quantities*, Athlone Press, 1973.)

Mean star density vs. visual magnitude

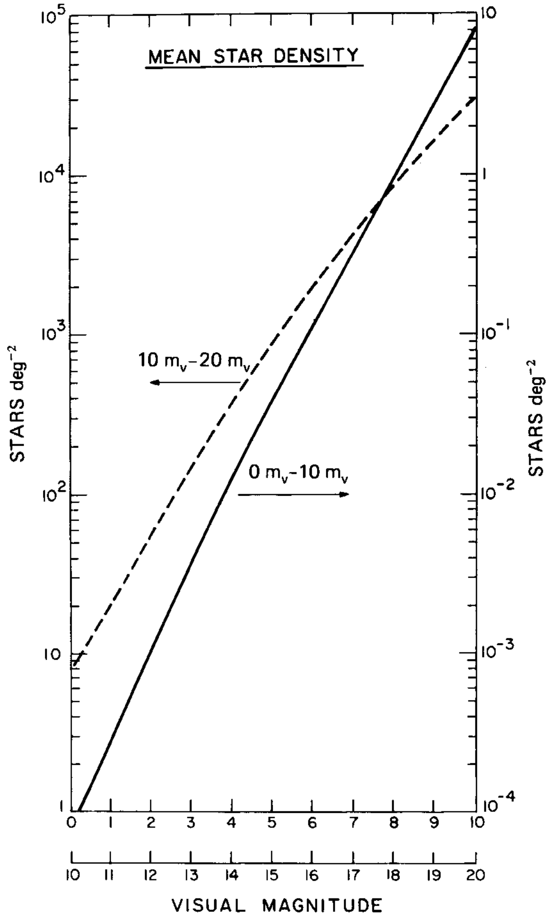

Star counts

A formula for estimating ($\sim$ 15% accuracy) differential A and integral N star counts for a given galactic longitude l, latitude b, and apparent magnitudes V and B over the ranges $b \geq 20°, 5 \leq m \leq 30$ for zero obscuration, $\Delta m = 0$, has been derived by Bahcall & Soniera (*Ap. J. Suppl.*, **44**, 73, 1980). (For non-zero obscuration, replace m by $m - \Delta m$, where $\Delta m_V = 0.15$ csc b and $\Delta m_B = 0.20$ csc b.) The units of A are stars mag^{-1} deg^{-2} and N are stars deg^{-2}.

$$D(l, b, m) = \frac{C_1 10^{\beta(m-m*)}}{[1 + 10^{\alpha(m-m*)}]^{\delta}} \frac{1}{[\sin b(1 - \mu \cot b \cos l)]^{3-5\gamma}} + \frac{C_2 10^{\eta(m-m\dagger)}}{[1 + 10^{\kappa(m-m\dagger)}]^{\lambda}} \frac{1}{(1 - \cos b \cos l)^{\sigma}},$$

where the constants are $\sigma = 1.45 - 0.20 \cos b \cos l$,

Constant	Range of m: $m \leq 12$	$12 < m < 20$	$m \geq 20$
μ	0.03	$0.0075(m - 12) + 0.03$	0.09
γ	0.36	$0.04(12 - m) + 0.36$	0.04

Star count	C_1	C_2	α	β	δ	m^*	κ	η	λ	$m\dagger$
$A_V = D$	200	400	−0.2	0.01	2	15	−0.26	0.065	1.5	17.5
$N_V = D$	925	1050	−0.132	0.035	3.0	15.75	−0.180	0.087	2.5	17.5
$A_B = D$	235	370	−0.227	0.0	1.5	17	−0.175	0.06	2.0	18
$N_B = D$	950	910	−0.124	0.027	3.1	16.60	−0.167	0.083	2.5	18

Luminosity functions

Local stellar luminosity function for the disk in the Visual band. The solid line is an analytic approximation, (Adapted from Bahcall, J. H. & Soneira,R. M., *Ap. J. Suppl.* **44** 73, 1980.)

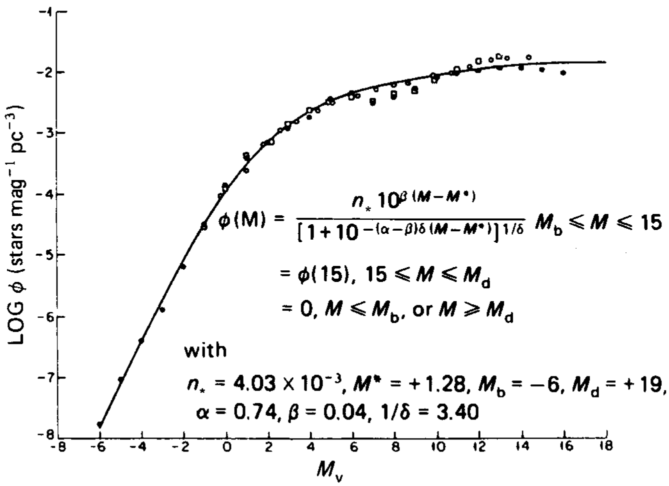

Local stellar luminosity function for the disk in the Blue band. The solid line is an analytic approximation. (Adapted from Bahcall, J. N. & Soneira, R. M., *Ap. J. Suppl.*, **44**, 73, 1980.)

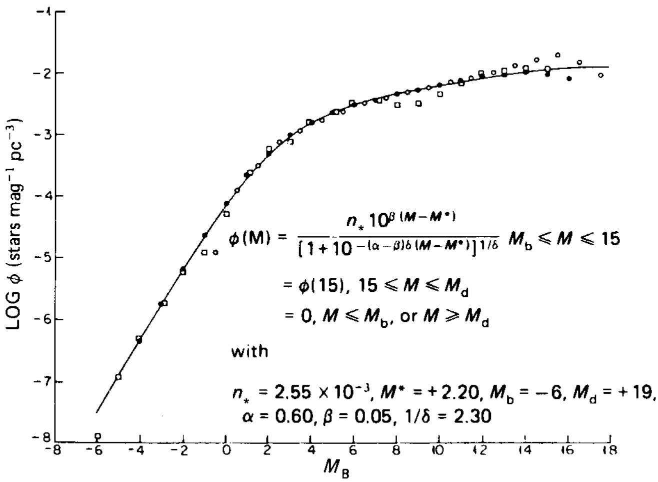

Parameters of the interstellar gas

Mean density ρ	3×10^{-24} g cm^{-3}
Typical particle density	
n (HI) in diffuse clouds	20 cm^{-3}
n (HI) between clouds	0.1 cm^{-3}
n_H in molecular clouds	$10^3 - 10^6$ cm^{-3}
Typical temperature T	
Diffuse HI clouds	80 K
HI between clouds	6000 K
HII photon ionized regions	8000 K
Coronal gas between clouds	6×10^5 K
Root-mean-square random cloud velocity	10 km s^{-1}
Isothermal sound speed C	
HI cloud at 80 K	0.7 km s^{-1}
HII gas at 8000 K	10 km s^{-1}
Magnetic field B	2.5×10^{-6} G
Effective thickness $2H$ of HI cloud layer	250 pc

(Adapted from Spitzer, L., *Physical Processes in the Interstellar Medium*, John Wiley and Sons, 1977.)

Proton-proton chain and the CNO cycle

	Reaction	Neutrino energy (MeV)
The proton-proton chain		
PP-I	$H + H \to D + e^+ + \nu_e$ (99.75%)	0–0.420 spectrum
	or	
	$H + H + e^- \to D + \nu_e$ (0.75%)	1.44 line
	$D + H \to {}^3He + \gamma$	
	${}^3He + {}^3He \to 2H + {}^4He$ (87%)	
PP-II	${}^3He + {}^4He \to {}^7Be + \gamma$ (13%)	0.861 (90%) line
	${}^7Be + e^- \to {}^7Li + \nu_e$	0.383 (10%) line
	${}^7Li + H \to \gamma + {}^8Be \to 2{}^4He$	
PP-III	${}^7Be + H \to {}^8B + \gamma$ (0.017%)	
	${}^8B \to {}^9Be^* + e^+ + \nu_e$, ${}^9Be^* \to 2{}^4He$	0–14.1 spectrum
The carbon-nitrogen cycle		
	$H + {}^{12}C \to {}^{13}N + \gamma$	
	${}^{13}N \to {}^{13}C + e^+ + \nu_e$	0–1.20 spectrum
	$H + {}^{13}C \to {}^{14}N + \gamma$	
	$H + {}^{14}N \to {}^{15}O + \gamma$	
	${}^{15}O \to {}^{15}N + e^+ + \nu_e$	0–1.73 spectrum
	$H + {}^{15}N \to {}^{12}C + {}^4He$	

Stellar structure equations (spherical symmetry)

Equation of hydrostatic equilibrium

$$\frac{dP(r)}{dr} = -\frac{GM(r)\rho(r)}{r^2}$$

Equation of continuity of mass

$$\frac{dM(r)}{dr} = 4\pi r^2 \rho(r)$$

Equation of energy transport

$$\frac{dT(r)}{dr} = -\frac{3\kappa\rho(r)L(r)}{16\pi acr^2 T(r)^3} \quad \text{radiative diffusion}$$

$$\frac{dT(r)}{dr} = \frac{(\gamma - 1)}{\gamma} \frac{T(r)}{P(r)} \frac{dP(r)}{dr} \quad \text{convection}$$

Equation of conservation of energy

$$\frac{dL(r)}{dr} = 4\pi r^2 \rho(r)\varepsilon(r)$$

P = pressure
M(r) = mass interior to a sphere of radius r
G = gravitational constant
ρ = density
T = temperature
L = luminosity
κ = opacity
γ = ratio of specific heats
a = 4σ/c = radiation density constant
σ = Stefan-Boltzmann constant
c = speed of light
ε = energy generation

Galaxies

Properties of the Milky Way Galaxy

Type of galaxy:

Hubble-van den Bergh system	Sb(−Sb$^+$)I−II
de Vaucouleur's system	SAB(rs) bc II
Morgan's system	gkS 7

M_v (mag): –20.5

Diameter: 23 kpc (isophote: 25.0 mag (B) arcsec^{-2})

Scale height of disc: $z_0 = 0.17$ kpc

Period of rotation: 2.5×10^8 yr

Mass:

Visible mass: $2 \times 10^{11} M_\odot$ Total mass: $1 \times 10^{12} M_\odot$(R< 200 kpc)

Gas: 8×10^9 $M_\odot$

Age: 1.2×10^{10} yr

Density in solar neighborhood:

Stars: 0.05 $M_\odot$ pc^{-3}

Total known: 0.08 $M_\odot$ pc^{-3}

Galactic nucleus:

$R < 0.4\,\mathrm{pc} \approx 5 \times 10^6\ M_\odot$

$R < 150\,\mathrm{pc} \approx 1 \times 10^9\ M_\odot$

Central bulge $R(< 2.5$ kpc): $\approx 4 \times 10^{10}\ M_\odot$

Luminosity of the galaxy:		Energy density in the galaxy:	
Radio	3×10^{38} erg s^{-1}	Starlight	0.7×10^{-12} erg cm^{-2}
Infrared	3×10^{41}	Turbulent gas	0.5×10^{-12}
Optical	3×10^{43}	Cosmic rays	2×10^{-12}
X-ray	$10^{39} - 10^{40}$	Magnetic field	2×10^{-12}
γ-ray(> 100 MeV)	5×10^{38}	2.7 K radiation	0.4×10^{-12}

Total luminosity (bolometric): 3.6×10^{10} $L_\odot$

Stellar radiation emission (solar neighborhood):

$1.5 \times 10^{-3}(M_{\mathrm{bol}} = 0)$ stars pc^{-3}

1.5×10^{-23} erg cm^{-3} s^{-1}

Stellar luminous radiation emission (solar neighborhood):

$6.7 \times 10^{-4}(M_v = 0)$ stars pc^{-3}

Distance of the Sun from the galactic center:

8.7 ± 0.6 kpc (IAU, 1985)

7.1 ± 1.2 kpc (courtesy of M. Reid, Harvard/Smithsonian)

Height of Sun above galactic disk: 24 ± 6 pc

Galactic coordinates of the nucleus: $l^{\mathrm{II}} = l = 0,\ b^{\mathrm{II}} = b = 0$

Equatorial coordinates of the nucleus:

$\alpha 2000 = 17^{\mathrm{h}} 45^{\mathrm{m}} 37.1991^{\mathrm{s}}$

$\delta 2000 = -28° 56' 10.221''$

$L_\odot = 3.83 \times 10^{33}$ erg s^{-1}

Note: The mass and energy parameters are representative not definitive; consult the literature for currently accepted values. Additional data on the Milky Way Galaxy can be found in Trible, V., in *Allen's Astrophysical Quantities*, A.N. Cox, ed., Springer-Verlag, 2000.

The local group

Name	α 2000	δ 2000	V (mag)	Dimension	Type	M_V	Distance (kpc)	Diameter (kpc)
Andromeda galaxy	$0^h42^m\!.7$	+41° 16′	3.4	178′ × 63′	Sb	−21.1	730	38
Milky Way	(17 45.6	−28 56)			Sb+:	−20.5	(8.5)	30:
Triangulum galaxy	1 33.9	+30 39	5.7	62 × 39	Sc	−18.9	900	16
Large Magellanic Cloud	5 23.6	−69 45	0.1	650 × 550	S Bm	−18.5	50	9.5
IC 10	0 20.4	+59 18	10.3	5 × 4	Ir+:	−17.6	1300	1.9
Small Magellanic Cloud	0 52.7	−72 50	2.3	280 × 160	S Bmp	−16.8	60	4.9
NGC 205	0 40.4	+41 41	8.0	17 × 10	E6:	−16.4	730	3.6
NGC 221	0 42.7	+40 52	8.2	8 × 6	E2	−16.4	730	1.7
NGC 6822	19 44.9	−14 48	9:	10 × 10	Ir+	−15.7	520	1.5
NGC 185	0 39.0	+48 20	9.2	12 × 10	dE0	−15.2	730	2.5
NGC 147	0 33.2	+48 30	9.3	13 × 8	dE4	−14.9	730	2.8
IC 1613	1 04.8	+2 07	9.3	12 × 11	Ir+	−14.8	740	2.6
WLM system	0 02.0	−15 28	10.9	12 × 4	Ir+	−14.7	1600	5.6
Leo A	9 59.4	+30 45	12.6	5 × 3	Ir+	−14.1	2300	3.3
Fornax dwarf galaxy	2 39.9	−34 32	8:	20: × 14:	dE3	−13.3	130	2.2:
IC 5152	22 02.9	−51 17	11:	5 × 3	Ir+	−13.5	1500	2.2
Pegasus dwarf galaxy	23 28.6	+14 45	12.0	5 × 3	Ir+	−13.4	1300	1.9
Sculptor dwarf galaxy	0 59.9	−33 42	10:		dE3	−11.7	85	1.5:
Leo I	10 08.4	+12 18	9.8	11 × 8	dE3	−11.0	230	0.7
Andromeda I	0 45.7	+38 00	13.2		dE0	−11:	730	
Andromeda II	1 16.4	+33 27	13:		dE0	−11:	730	
Andromeda III	0 35.4	+36 31	13:		dE2	−11:	730	
Aquarius dwarf galaxy	20 46.9	−12 51			Ir	−11:	1500	
Sagittarius dwarf galaxy	19 30.0	−17 41	15:		Ir−	−10:	1100	
Leo II	11 13.5	+22 10	11.5	15 × 13	dE0	−9.4	230	1.0
Ursa Minor dwarf galaxy	15 08.8	+67 12	12:	27 × 16	dE6	−8.8	75	0.6
Draco dwarf galaxy	17 20.2	+57 55	11:	34 × 19	dE3	−8.6:	80	0.8
LGS 3	1 03.8	+21 53	15:	2	Ir	−8.5:	900	0.5
Carina dwarf galaxy	6 41.6	−50 58			dE		170	

: denotes approximate value

(Adapted from *Sky Catalogue 2000.0*, Vol. 2, Sky Publishing (Corp., 1985.)

Hubble's classification of galaxies
The number n behind the symbol E characterizes the ellipticity: $n = 10(a-b)/a$, where a and b are the major and minor diameters of the ellipse. The letters a, b, c following S and SB characterize the increasing degree of opening of the spiral arms. (Adapted from *Landolt–Börnstein, Astronomy and Astrophysics*, 1982.)

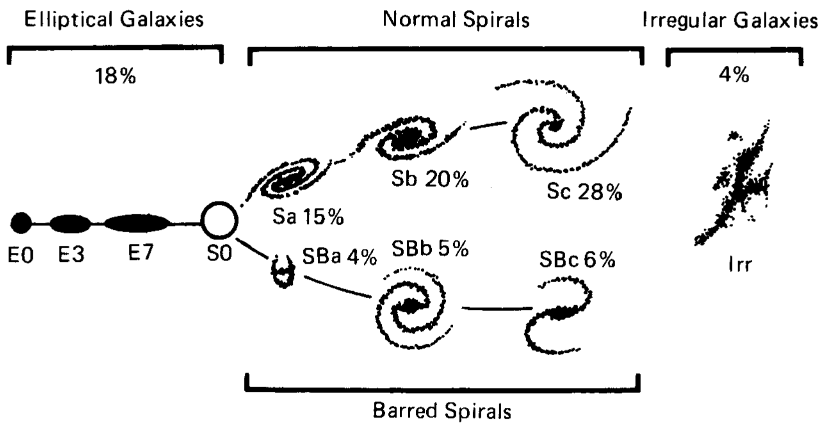

Selected brighter galaxies (B_T < 10; local group excluded)

Galaxy	α J2000	δ J2000	Diam.[a]	b/a[b]	B_T[c]	$(B-V)_0^d$	Type	Dist. (Mpc)	log $\mathcal{M}_{tot}$
NGC 55	00^h15^m	$-39°13'$	32.4	0.17	8.42	0.54	SBc/m III	1.3	9.87
NGC 247	00^h47^m	$-20°46'$	21.4	0.32	9.67	0.54	SABc/d III-IV	2.1	10.02
NGC 253	00^h48^m	$-25°17'$	27.5	0.25	8.04		SABc II	3.0	10.87
NGC 300	00^h54^m	$-37°41'$	21.9	0.71	8.72	0.58	Sc/d II-IV	1.2	9.89
NGC 628 = M74	01^h37^m	$+15°47'$	10.5	0.91	9.95	0.51	SAc II	9.7	
NGC 1068 = M77	02^h43^m	$-00°01'$	7.1	0.85	9.61	0.70	SAb II	14.4	
NGC 1291	03^h17^m	$-41°06'$	9.8	0.83	9.39	0.91	SB0/a	8.6	
NGC 1313	03^h18^m	$-66°30'$	9.1	0.76	9.20	0.48	SBc/d III-IV	3.7	10.31
NGC 1316 (Fornax A)	03^h23^m	$-37°12'$	12.0	0.71	9.42	0.87	SAB0/a pec	16.9	
NGC 2403	07^h37^m	$+65°36'$	21.9	0.56	8.93	0.39	Scd III	4.2	10.67
NGC 2903	09^h32^m	$+21°30'$	12.6	0.48	9.68	0.55	SABbc I-II	6.3	10.91
NGC 3031 = M81	09^h56^m	$+69°04'$	26.9	0.52	7.89	0.82	SAab I-II	1.4	10.73
NGC 3034 = M82	09^h56^m	$+69°41'$	11.2	0.38	9.30	0.79	10/amorphous	5.2	
NGC 3115	10^h05^m	$-07°43'$	7.2	0.84	9.87	0.94	S0	6.7	
NGC 3521	11^h06^m	$-00°02'$	11.0	0.47	9.83	0.68	SABbc II	7.2	10.99
NGC 3627 = M66	11^h20^m	$+13°00'$	9.1	0.46	9.65	0.60	SABb II	6.6	10.74
NGC 4258 = M106	12^h19^m	$+47°18'$	14.8	0.39	9.10	0.55	SABbc II-III	6.8	11.17
NGC 4449	12^h28^m	$+46°06'$	6.2	0.71	9.99	0.41	IB/Sm IV	3.0	
NGC 4472 = M49	12^h30^m	$+08°00'$	10.2	0.81	9.37	0.95	E1-2/S0	16.8	
NGC 4486 = M87	12^h31^m	$+12°23'$	8.3	0.79	9.59	0.93	cD, E0p	16.8	
NGC 4594 = M104 (Sombrero)	12^h40^m	$-11°37'$	8.7	0.41	8.98	0.45	Sa/ab	20.0	11.38
NGC 4631	12^h42^m	$+32°32'$	15.5	0.17	9.75	0.55	SBc/d III	6.9	10.70
NGC 4649 = M60	12^h44^m	$+11°33'$	7.4	0.81	9.81	0.95	S0/E2	16.8	
NGC 4736 = M94	12^h51^m	$+41°07'$	11.2	0.81	8.99	0.72	SAab II	4.3	10.78
NGC 4826 = M64	12^h57^m	$+21°41'$	10.0	0.54	9.36	0.71	Sab II	4.1	
NGC 4945	13^h05^m	$-49°28'$	20.0	0.19	9.3		SBcd IV	5.2	
NGC 5055 = M63	13^h16^m	$+42°02'$	12.6	0.58	9.31	0.64	SAbc II-III	7.2	11.15
NGC 5128 (Cen. A)	13^h25^m	$-43°01'$	25.7	0.79	7.84	0.88	S0p	4.9	
NGC 5194 = M55	13^h30^m	$+47°12'$	11.2	0.62	8.96	0.53	SAbc I-IIp	7.7	
NGC 5236 = M83	13^h37^m	$-29°52'$	12.9	0.89	8.20	0.61	SBc II	4.7	
NGC 5447 = M101	14^h03^m	$+54°21'$	28.8	0.93	8.31	0.44	SABcd I	5.4	
NGC 6744	19^h10^m	$-63°51'$	20.0	0.65	9.14		sBc II	10.4	11.37
NGC 6946	20^h35^m	$+60°09'$	11.5	0.85	9.61	0.40	Scd II	5.5	10.81
NGC 7793	23^h58^m	$-32°35'$	9.3	0.68	9.63		SAd IV	2.8	9.95

α, δ, diameters, b/a, B_T, B-V are from de Vaucouleurs, G., *et al.*, *Third Reference Catalogue of Bright Galaxies* (RC3), University of Texas Press, 1990.

Type from Sandage, A. and Tammann, G.A., *A revised Shapley Ames Catalog of Bright Galaxies*, Carnegie Institution of Washington, 1987 and de Vaucouleurs, G., *et al.*, *Third Reference Catalogue of Bright Galaxies* (RC3), University of Texas Press, 1990.

Distances from Tully, R.B., *Nearby Galaxies Catalog, Cambridge University Press*, 1987.

[a] Arcminutes, isophotal to 25^m arcsec^{-2}

[b] Axial ratio, to to 25^m arcsec^{-2} isophote.

[c] B total magnitude; entire galaxy; not corrected for absorption.

[d] Entire galaxy, corrected for reddening.

(Adapted from Trimble, V. in *Allen's Astrophysical Quantities*, Cox, A.N., ed., Springer-Verlag, 2000.)

Named galaxies

Name	α 2000	δ 2000
Andromeda galaxy = M31 = NGC 224	$00^h42^m.7$	$+41°16'$
Andromeda I	00 45.7	+38 00
Andromeda II	01 16.3	+33 25
Andromeda III	00 35.3	+36 30
Andromeda IV	00 42.5	+40 34
BL Lac	22 02.7	+42 17
Capricorn dwarf = Pal 13†	21 46.8	−21 15
Caraffe galaxy	04 28.0	−47 54
Carina dwarf	06 46.3	−51 03
Cartwhell galaxy	00 37.4	−33 45
Centaurus A = NGC 5128 = Arp 135	13 25.4	−43 02
Circinus galaxy	14 13.2	−65 20
Copeland Septet = NGC 3745/54 = Arp 320	11 37.7	+22 01
Cygnus A	19 59.4	+40 44
Draco dwarf = DDO 208	17 20.0	+57 55
Fath 703	15 13.8	−15 28
Formax A = NGC 1316	03 22.7	−37 12
Fornax dwarf	02 39.9	−34 31
Fourcade-Figueroa object	13 35.2	−33 53
GR8 = DDO 155	12 58.7	+41 13
Hardcastle Nebula	13 13.0	−32 42
Hercules A	16 51.2	+05 01
Holmberg I + DDO 63	09 40.5	+71 12
Holmberg II = DDO 50 = Arp 268	08 19.0	+70 43
Holmberg III	09 14.9	+74 14
Holmberg IV = DDO 185	13 54.6	+53 54
Holmberg V	13 40.7	+54 20
Holmberg VI = NGC 1325 A	03 24.8	−21 20
Holmberg VII = DDO 137	12 34.7	+06 18
Holmberg VIII = DDO 166	13 13.3	+36 13
Holmberg IX = DDO 66	09 57.6	+69 03
Hydra A	09 18.1	−12 06
Large Magellanic Cloud	05 23.5	−69 45
Leo I = Harrington-Wilson No. 1 = Regulus Dwarf = DDO 74	10 08.5	+12 18
Leo II = Harrington-Wilson No. 2 = Leo B = DDO 93	11 13.5	+22 10
Leo A = Leo III = DDO 69	09 59.4	+30 45
Lindsay-Shapley ring	06 43.1	−74 14
Maffei I	02 36.3	+59 39
Maffei II	02 41.9	+59 36
Mayall's Object = Arp 148 = VV 32	11 03.9	+40 51
Mice = NGC 4676 = Arp 242	12 47.1	+30 38
Pegasus dwarf = DDO 216	23 28.5	+14 44
Perseus A = NGC 1275	03 19.8	+41 31
Reticulum dwarf	04 36.2	−58 50
Reinmuth 80 = NGC 4517 A	01 00.0	−33 42

Named galaxies (cont.)

Name	α 2000	δ 2000
Seashell galaxy	$13^h47\overset{m}{.}3$	−30°25′
Serpens dwarf	15 16.0	−00 08
Seyfert's Sextet = NGC 6027 A–D	15 59.2	+20 45
Sextans A = DDO 75	10 11.1	−04 43
Sextans B = DDO 70	10 00.0	+05 20
Sextans C	10 05.5	+00 04
Small Magellanic Cloud	00 52.8	−72 50
Sombrero galaxy = M 104 = NGC 4594	12 40.2	−11 37
Stephan's Quintet = NGC 7317–20 =Arp 319	22 36.0	+33 58
Triangulum galaxy = M33 = NGC 598	01 34.5	+30 39
Ursa Minor dwarf = DDO 199	15 08.8	+67 12
Virgo A = M87 = NGC 4486 = Arp 152	12 30.8	+12 23
Whirlpool galaxy = M51 = NGC 5194	13 29.9	+47 12
Wild's Triplet = Arp 248	11 46.8	−03 50
Wolf–Lundmark–Melotte object = DDO 221	00 02.0	−15 27
Zwicky No. 2 = DDO 105	11 58.5	+38 04
Zwicky's triplet = Arp 103	16 49.5	+45 28

† Probably a distant globular cluster.

(Adapted from Landolt-Börnstein, *Astronomy and Astrophysics*, VI/2C, Springer-Verlag, 1982.)

Representative active galactic nuclei (AGNs)

Object	α 1950	δ 1950	z	m_V
QUASARS				
Q 0002−422	$00^h02^m16^s$	−42°14′	2.758	17.4
PHL 938	00 58 20	01 55	1.95	17.2
4C 25.05	01 23 57	25 44	2.34	17.5
PHL 1093	01 37 23	01 17	0.262	17.1
PHL 1194	01 48 52	09 03	0.298	17.5
RN 8	02 10 49	86 05	0.184	19.0
Q 0242−410	02 42 02	−41 04	2.214	18.1
Q 0324−407	03 24 29	−40 47	3.056	17.6
PKS 0424−13	04 24 48	−13 10	2.16	17.5
Q 0453−423	04 53 48	−42 21	2.661	17.3
Q 0551−366	05 51 02	−36 38	2.307	17.0
OH 471	06 42 53	44 55	3.39	18.5
PKS 0736+01	07 36 43	01 44	0.192	16.5
4C 05.34	08 05 19	04 41	2.86	18.2
0938+119	09 38 32	11 59	3.19	19.0
3C 232	09 55 25	32 38	0.533	15.8
Ton 490	10 11 06	25 04	1.63	15.4
PKS 1217+02	12 17 39	02 20	0.240	16.5
3C 273	12 36 33	02 20	0.158	12.8
Q 1246−057	12 46 29	−05 43	2.212	17.0
B 340	12 04 48	34 40	0.184	17.0
1331+170	13 31 10	17 04	2.08	16.0

Representative active galactic nuclei (cont.)

Object	α 1950	δ 1950	z	m_V
3C 323.1	$15^h45^m31^s$	21°01′	0.264	16.7
4C 29.50	17 02 11	29 51	1.92	19.1
3C 351	17 04 03	60 49	0.371	15.3
Q 2116−358	21 16 22	−35 49	2.341	17.0
PKS 2135−14	21 35 01	−14 46	0.200	15.5
2256+017	22 56 25	01 48	2.66	18.5
SEYFERT GALAXIES				
Seyfert 1 galaxies				
Mrk 335	00 03 45	19 55	0.025	14.2
I Zw 1	00 51 00	12 25	0.061	14.3
Mrk 376	07 10 36	45 47	0.056	16.0
Mrk 79	07 38 47	49 56	0.020	13.4
Mrk 10	07 43 07	61 03	0.029	15.0
Mrk 110	09 21 44	52 30	0.036	16.1
NGC 3227	10 20 47	20 07	0.0033	13.5
NGC 3516	11 03 24	72 50	0.0093	13.1
NGC 4151	12 08 01	39 41	0.0033	12.0
Mrk 236	12 58 18	61 55	0.052	17.0
Mrk 279	13 51 52	69 33	0.0307	15.4
Mrk 290	15 34 45	58 04	0.0308	15.6
Mrk 486	15 35 21	54 43	0.039	15.0
Mrk 509	20 41 26	−10 54	0.0355	13.0
NGC 7469	23 00 44	08 36	0.0167	13.6
Mrk 541	23 53 30	07 15	0.041	15.5
Seyfert 2 galaxies				
Mrk 1	01 13 19	32 50	0.016	16.6
NGC 1068	02 40 07	−00 14	0.003 63	10.5
Mrk 612	03 21 10	−03 19	0.020 22	16.5
III Zw 55	03 38 38	−01 28	0.0246	14.0
Mrk 3	06 09 48	71 03	0.0137	13.8
Mrk 78	07 37 56	65 18	0.0375	15.6
Mrk 622	08 04 21	39 09	0.022 83	15.6
Mrk 34	10 30 52	60 17	0.051	14.8
Mrk 176	11 29 54	53 14	0.0269	15.5
Mrk 270	13 39 41	56 55	0.009	15.0
Mrk 463E	13 53 40	18 37	0.0505	16.0
Mrk 533	23 25 24	08 30	0.028 73	16.0
BL LAC OBJECTS				
PKS 0215+015	02 15 13	01 31		18.3
AO 0235+164	02 35 53	16 24		15.5
PKS 0521−365	05 21 14	−36 30	0.55	15.0
PKS 0548−323	05 48 50	−32 17	0.069	15.5
OJ 287	08 51 57	20 18		14.0
4C 22.25	09 57 34	22 48		18.0
Mkn 421	11 01 41	38 29	0.03	13.5
Mkn 180	11 33 30	70 25	0.0458	15.0
AP Lib	15 14 45	−24 11	0.049	15.0
Mkn 501	16 52 12	39 50	0.034	13.8
BL Lac	22 00 40	42 02	0.0688	14.5

Representative active galactic nuclei *(cont.)*

Object	α 1950	δ 1950	z	m_V
RADIO GALAXIES				
BLRGs				
3C 109	$04^h10^m55^s$	$11°15'$	0.306	18.0
3C 120	04 30 32	05 15	0.033	14.6
3C 227	09 45 07	07 39	0.0855	16.3
3C 234	09 58 57	29 02	0.1846	17.1
3C 287.1	13 29 04	25 24	0.2156	18.5
PKS 1417−19	14 17 02	−19 15	0.1195	17.5
4C 35 37	15 31 45	35 52	0.1565	17.5
3C 332	16 14 44	30 09	0.1515	16.0
3C 381	18 32 28	47 24	0.1614	17.5
3C 382	18 33 12	32 39	0.0586	15.4
3C 390.3	18 45 38.8	79 43	0.0569	15.4
3C 445	22 21 15	−02 21	0.0568	15.8
NLRGs				
3C 33	01 06 14	13 04	0.0595	16.3
3C 98	03 56 10	10 18	0.0306	14.8
3C 178	07 22 33	−09 30	0.0079	16.1
3C 184.1	07 32 20	70 20	0.1182	17
3C 192	08 02 38	24 16	0.0598	16.2
3C 327	15 59 56	02 06	0.1039	16.3
3C 433	21 21 30	24 52	0.1025	15.7
3C 452	22 43 33	39 25	0.082	16.6
PKS 2322−12	23 22 43	−12 24	0.0821	15.8
LINERS				
Mrk 1158	01 32 07	34 47	0.0151	16.2
NGC 1052	02 38 37	−08 28	0.0048	13.2
Ark 160	08 17 52	19 31	0.019	17.6
NGC 2841	09 18 35	51 11	0.0022	13.5
NGC 2911	09 31 05	10 23	0.0106	15.3
NGC 3031	09 51 30	69 18	−0.0001	12.4
NGC 3758	11 33 48	21 52	0.0296	16.6
NGC 3998	11 55 20	55 44	0.0038	13.3
NGC 4036	11 58 54	62 10	0.0046	14.0
NGC 4278	12 17 36	29 34	0.0022	13.6
NGC 5005	13 08 37	37 19	0.0033	14.1
NGC 5077	13 16 53	−12 24	0.0094	14.4
NGC 5371	13 53 33	40 42	0.0086	15.0
Mrk 298	16 03 18	17 56	0.0345	16.2
Mrk 700	17 01 21	31 31	0.034	15
NGC 6764	19 07 01	50 51	0.008	15.5

BLRGs: broad-line radio galaxies; NLRGs: narrow-line radio galaxies; LINERS: low-ionization nuclear emission-line region.

Redshift $z = \Delta\lambda/\lambda$.

m_V = approximate nuclear visual magnitude.

Luminosity distance $D_L(q_0 = 0) = \dfrac{cz}{H_0}(1 + 0.5z)$. For other values of q_0 see chapter on Relativity and Cosmology.

(Adapted from Landolt–Börnstein, *Astronomy and Astrophysics*, V1/2C, Springer-Verlag, 1982.)

Objects with large redshifts ($z > 5.06$)

Object Name*	α J2000	δ J2000	Type	z
SDSS J0338+0021	$03^h38^m29.3^s$	$+00°21'56''$	QSO	5.07
SDSS J120441.72-002149.5	12 04 41.7	−00 21 50	QSO	5.11
TN J0924-2201	09 24 19.9	−22 01 41	G	5.19
SDSSp J120823.82+001027.7	12 08 23.8	+00 10 28	QSO	5.273
SDSS J172341.09+555340.6	17 23 41.1	+55 53 41	QSO	5.30
HDF:[WBD96] 3-0951.0	12 36 59.9	+62 12 19	Gpair	5.34
6C 0140+326:[DS98] RD1	01 43 42.8	+32 54 00	G	5.35
RD J030117+002025	03 01 17.0	+00 20 57	QSO	5.50
HDF:[LYF96] 4-269	12 36 45.9	+62 11 58	G	5.60
CADIS 9H e0580	09 13 59.8	+46 11 47	G	5.69
CADIS 9H e0931	09 13 31.6	+46 13 32	G	5.70
CADIS 9H e0304	09 13 36.2	+46 10 42	G	5.70
CADIS 9H e1359	09 13 58.3	+46 15 37	G	5.70
CADIS 9H e0778	09 13 30.8	+46 12 44	G	5.71
CADIS 9H e1305	09 13 54.8	+46 15 25	G	5.71
CADIS 9H e1090	09 13 32.1	+46 14 20	G	5.72
SSA 22 HCM1	22 17 39.7	+00 13 49	G	5.74
SDSS J1044-0125	10 44 33.0	−01 25 02	QSO	5.80
SDSSp J083643.85+005453.3	08 36 43.8	+00 54 53	QSO	5.82
SDSSp J130608.26+035626.3	13 06 08.3	+03 56 26	QSO	5.99
SDSSp J1030227.10+052455.0	10 30 27.1	+05 24 55	QSO	6.28
SDSS J172201.84+563744.7	17 22 01.8	+56 37 45	QSO	6.50

(List as of the end of 2001)

*6C: Sixth **C**ambridge Catalog of Selected Areas.

CADIS: **C**alar **A**lto **D**eep **I**maging **S**urvey.

SDSS: **S**loan **D**igital **S**ky **S**urvey.

SDSSp: **S**loan **D**igital **S**ky **S**urvey, **p**rovisory.

HDF: **H**ubble **D**eep **F**ield.

RD: SSE2000; **S**tern, **S**pinrad, **E**isenhardt, *et al...*, Astrophys, J., **533**, L75, 2000.

TN: DVR2000; **D**e Brueck, **V**an Breugel, **R**oettgering, *et al.*, Astron. Astrophys. Suppl. Ser., **143**, 303, 2000.

SSA: **S**mall **S**elected **A**rea; Hawaii Deep Survey fields.

DS98: **D**umm and **S**child, New Astronomy, **3**, 137, 1998.

WBD96: **W**illiams, **B**lacker, **D**ickinson, *et al.*, Astron. J., **112**, 1335, 1996.

HCM1: HMC99b; Hu, McMahon, and Cowie, Astrophys, J., **522**, L9, 1999.

LYF98: **L**anzetta, **Y**ahil, and **F**ernandez-Soto, Astron, J., **116**, 1066, 1998.

Prominent clusters of galaxies

Name	Abell No.	α 2000	δ 2000	Diameter (°)	RV (km s^{-1})	RS type	NGC	Radio source	Notes
Haufen A	151	$1^h08^m.9$	$-15°25'$		15 800	cD			
	194	1 25.6	−1 30	0.3	5320	L	541, 5, 7	3C 40	In Perseus supercluster
	400	2 57.6	+6 02		7200	I		3C 75	
Perseus	426	3 18.6	+41 32	4	5460	L	1275	3C 84	In Perseus supercluster; XRS
Fornax II		3 28	−20 45	7	1560		1232		
Fornax I		3 32	−35 20	7	1500		1316	For A	
Gemini	568	7 07.6	+35 03	0.5	23 400	C			
Cancer		8 21	+20 56	3	4800		2563		
Hydra II		8 58	+3 09		60 900				
Leo	1020	10 27.8	+10 25	0.6	19 500				Also Abell 1016?
Hydra I	1060	10 36.9	−27 32		3000	C	3309, 11		XRS
Ursa Major II		10 58	+56 46	0.2	41 000				
Leo A	1185	11 10.9	+28 41		10 500	C	3550		
	1367	11 44.5	+19 50		6150	F	3842, 62	3C 264	In Coma supercluster; XRS
Ursa Major I	1377	11 47.1	+55 44	0.7	15 300	B			
Virgo		12 30	12 23	12	1200		4472, 86	Vir A	In Local supercluster; XRS
Centaurus		12 50	−41 18	2	3200		4696	PKS	XRS
Coma	1656	12 59.8	+27 59	4	6650	B	4889		In Coma supercluster; XRS
Boötes	1930	14 33	31 33	0.3	39 300				
Corona Borealis	2065	15 22.7	+27 43	0.5	21 600	C			
Hercules	2151	16 05.2	+17 45	1.7	11 200	F	6040, 47	4C+17.66	In Hercules supercluster; XRS
	2152	16 05.4	+16 27		11 500	~I			In Hercules supercluster
	2197	16 28.2	+40 54		9100	L	6173		In Hercules supercluster
	2199	16 28.6	+39 31	0.2	9200	cD	6166	3C 338	In Hercules supercluster; XRS
Pegasus II		23 10	+ 7 36	2	12 700		7720	4C+07.61	
Pegasus I		23 22	+ 9 02	1	4000		7619	PKS	

$z = RV/3.00 \times 10^5$; distance (Mpc) $= RV/50$ ($H_0 = 50$ km s^{-1} Mpc^{-1}).

(Adapted from *Sky Catalogue 2000.0*, Vol. 2, Sky Publishing Corp., 1985.)

The Messier catalog

M	NGC	α 2000	δ 2000	Const.	Dim.(′)	V (mag)	Type	Common name
1	1952	$5^h34^m.5$	+22°01′	Tau	6 × 4	8.4:	Di	Crab Nebula
2	7089	21 33.5	−0 49	Aqr	13	6.5	Gb	
3	5272	13 42.2	+28 23	CVn	16	6.4	Gb	
4	6121	16 23.6	−26 32	Sco	26	5.9	Gb	
5	5904	15 18.6	+2 05	Ser	17	5.8	Gb	
6	6405	17 40.1	−32 13	Sco	15	4.2	OC	
7	6475	17 53.9	−34 49	Sco	80	3.3	OC	
8	6523	18 03.8	−24 23	Sgr	90 × 40	5.8:	Di	Lagoon Nebula
9	6333	17 19.2	−18 31	Oph	9	7.9:	Gb	
10	6254	16 57.1	−4 06	Oph	15	6.6	Gb	
11	6705	18 51.1	−6 16	Sct	14	5.8	OC	
12	6218	16 47.2	−1 57	Oph	14	6.6	Gb	
13	6205	16 41.7	+36 28	Her	17	5.9	Gb	Herculus Cluster
14	6402	17 37.6	−3 15	Oph	12	7.6	Gb	
15	7078	21 30.0	+12 10	Peg	12	6.4	Gb	
16	6611	18 18.8	−13 47	Ser	7	6.0	OC	
17	6618	18 20.8	−16 11	Sgr	46 × 37	7:	Di	Omega Nebula
18	6613	18 19.9	−17 08	Sgr	9	6.9	OC	
19	6273	17 02.6	−26 16	Oph	14	7.2	Gb	
20	6514	18 02.6	−23 02	Sgr	29 × 27	8.5:	Di	Trifid Nebula
21	6531	18 04.6	−22 30	Sgr	13	5.9	OC	
22	6656	18 36.4	−23 54	Sgr	24	5.1	Gb	
23	6494	17 56.8	−19 01	Sgr	27	5.5	OC	
24		18 16.9	−18 29	Sgr	90	4.5:		
25	IC 4725	18 31.6	−19 15	Sgr	32	4.6	OC	
26	6694	18 45.2	−9 24	Sct	15	8.0	OC	
27	6853	19 59.6	+22 43	Vul	8 × 4	8.1:	Pl	Dumbbell Nebula
28	6626	18 24.5	−24 52	Sgr	11	6.9:	Gb	
29	6913	20 23.9	+38 32	Cyg	7	6.6	OC	
30	7099	21 40.4	−23 11	Cap	11	7.5	Gb	
31	224	0 42.7	+41 16	And	178 × 63	3.4	S	Andromeda Galaxy
32	221	0 42.7	+40 52	And	8 × 6	8.2	E	
33	598	1 33.9	+30 39	Tri	62 × 39	5.7	S	
34	1039	2 42.0	+42 47	Per	35	5.2	OC	
35	2168	6 08.9	+24 20	Gem	28	5.1	OC	
36	1960	5 36.1	+34 08	Aur	12	6.0	OC	
37	2099	5 52.4	+32 33	Aur	24	5.6	OC	
38	1912	5 28.7	+35 50	Aur	21	6.4	OC	

The Messier catalog *(cont.)*

M	NGC	α 2000	δ 2000	Const.	Dim.(′)	V (mag)	Type	Common name
39	7092	$21^h32^m.2$	$+48°26'$	Cyg	32	4.6	OC	
40		12 22.4	+58 05	UMa		8:		
41	2287	6 47.0	−20 44	CMa	38	4.5	OC	
42	1976	5 35.4	−5 27	Ori	66 × 60	4:	Di	Orion Nebula
43	1982	5 35.6	−5 16	Ori	20 × 15	9:	Di	
44	2632	8 40.1	+19 59	Cnc	95	3.1	OC	Praesepe
45		3 47.0	+24 07	Tau	110	1.2	OC	Pleiades
46	2437	7 41.8	−14 49	Pup	27	6.1	OC	
47	2422	7 36.6	−14 30	Pup	30	4.4	OC	
48	2548	8 13.8	−5 48	Hya	54	5.8	OC	
49	4472	12 29.8	+8 00	Vir	9 × 7	8.4	E	
50	2323	7 03.2	−8 20	Mon	16	5.9	OC	
51	5194−5	13 29.9	+47 12	CVn	11 × 8	8.1	S	Whirlpool Galaxy
52	7654	23 24.2	+61 35	Cas	13	6.9	OC	
53	5024	13 12.9	+18 10	Com	13	7.7	Gb	
54	6715	18 55.1	−30 29	Sgr	9	7.7	Gb	
55	6809	19 40.0	− 30 58	Sgr	19	7.0	Gb	
56	6779	19 16.6	+30 11	Lyr	7	8.2	Gb	
57	6720	18 53.6	+33 02	Lyr	1	9.0:	Pl	Ring Nebula
58	4579	12 37.7	+11 49	Vir	5 × 4	9.8	S	
59	4621	12 42.0	+11 39	Vir	5 × 3	9.8	E	
60	4649	12 43.7	+11 33	Vir	7 × 6	8.8	E	
61	4303	12 21.9	+4 28	Vir	6 × 5	9.7	S	
62	6266	17 01.2	−30 07	Oph	14	6.6	Gb	
63	5055	13 15.8	+42 02	CVn	12 × 8	8.6	S	
64	4826	12 56.7	+21 41	Com	9 × 5	8.5	S	
65	3623	11 18.9	+13 05	Leo	10 × 3	9.3	S	
66	3627	11 20.2	+12 59	Leo	9 × 4	9.0	S	
67	2682	8 50.4	+11 49	Cnc	30	6.9	OC	
68	4590	12 39.5	−26 45	Hya	12	8.2	Gb	
69	6637	18 31.4	−32 21	Sgr	7	7.7	Gb	
70	6681	18 43.2	−32 18	Sgr	8	8.1	Gb	
71	6838	19 53.8	+18 47	Sge	7	8.3	Gb	
72	6981	20 53.3	−12 32	Aqr	6	9.4	Gb	
73	6994	20 58.9	−12 38	Aqr				
74	628	1 36.7	+15 47	Psc	10 × 9	9.2	S	
75	6864	20 06.1	−21 55	Sgr	6	8.6	Gb	
76	650−1	1 42.4	+51 34	Per	2 × 1	11.5:	Pl	
77	1068	2 42.7	−0 01	Cet	7 × 6	8.8	S	
78	2068	5 46.7	+0 03	Ori	8 × 6	8:	Di	
79	1904	5 24.5	−24 33	Lep	9	8.0	Gb	
80	6093	16 17.0	−22 59	Sco	9	7.2	Gb	

The Messier catalog *(cont.)*

M	NGC	α 2000	δ 2000	Const.	Dim.($'$)	V (mag)	Type	Common name
81	3031	$9^h55^m.6$	$+69°04'$	UMa	26 × 14	6.8	S	
82	3034	9 55.8	+69 41	UMa	11 × 5	8.4	Ir	
83	5236	13 37.0	−29 52	Hya	11 × 10	7.6:	S	
84	4374	12 25.1	+12 53	Vir	5 × 4	9.3	E	
85	4382	12 25.4	+18 11	Com	7 × 5	9.2	E	
86	4406	12 26.2	+12 57	Vir	7 × 6	9.2	E	
87	4486	12 30.8	+12 24	Vir	7	8.6	E	Virgo A
88	4501	12 32.0	+14 25	Com	7 × 4	9.5	S	
89	4552	12 35.7	+12 33	Vir	4	9.8	E	
90	4569	12 36.8	+13 10	Vir	10 × 5	9.5	S	
91	4548	12 35.4	+14 30	Com	5 × 4	10.2	S	
92	6341	17 17.1	+43 08	Her	11	6.5	Gb	
93	2447	7 44.6	−23 52	Pup	22	6.2:	OC	
94	4736	12 50.9	+41 07	CVn	11 × 9	8.1	S	
95	3351	10 44.0	+11 42	Leo	7 × 5	9.7	S	
96	3368	10 46.8	+11 49	Leo	7 × 5	9.2	S	
97	3587	11 14.8	+55 01	UMa	3	11.2:	Pl	Owl Nebula
98	4192	12 13.8	+14 54	Com	10 × 3	10.1	S	
99	4254	12 18.8	+14 25	Com	5	9.8	S	
100	4321	12 22.9	+15 49	Com	7 × 6	9.4	S	
101	5457	14 03.2	+54 21	UMa	27 × 26	7.7	S	
102								M101 reobservation
103	581	1 33.2	+60 42	Cas	6	7.4:	OC	
104	4594	12 40.0	−11 37	Vir	9 × 4	8.3	S	Sombrero Galaxy
105	3379	10 47.8	+12 35	Leo	4 × 4	9.3	E	
106	4258	12 19.0	+47 18	CVn	18 × 8	8.3	S	
107	6171	16 32.5	−13 03	Oph	10	8.1	Gb	
108	3556	11 11.5	+55 40	UMa	8 × 2	10.0	S	
109	3992	11 57.6	+53 23	UMa	8 × 5	9.8	S	
110	205	0 40.4	+41 41	And	17 × 10	8.0	E?	

: denotes approximate value.
Types: diffuse nebula (Di), globular cluster (Gb), open cluster (OC), planetary nebula (Pl), or galaxy (E for elliptical, Ir for irregular, S for spiral).
Magnitudes with a colon are approximate visual magnitudes.
(Adapted from *Sky Catalogue 2000.0,* Vol. 2, Sky Publishing Corp., 1985.)

The Universe

Mass-radius-density data for astronomical objects

Class of objects	Examples	log M (g)	log R (cm)	log ρ ($\mathrm{g\,cm^{-3}}$)	log ϕ†
Neutron stars		33.16	5.93	14.75	−0.6?
		32.54	7.44	9.60	−2.5
White dwarfs	L930−80	33.45	8.3:	7.93	−2.7
	αCMaB	33.30	8.77	6.37	−3.2
	vM2	32.90	9.05	4.13	−5.0
Main sequence stars	dM8	32.2	9.95	1.76	−5.6
	Sun	33.30	10.84	0.15	−5.5
	A0	33.85	11.25	−0.55	−4.7
	O5	34.9	12.1:	−2.0	−5.0:
Supergiant stars	F0	34.4	12.65	−4.2	−6.1
	K0	34.4	13.15	−5.7	−6.6
	M2	34.7	13.75	−7.2	−6.9
Protostars	IR	35.3?	16.2?	−13.9?	−8.7?
Compact dwarf elliptical galaxies	M32, core	41.0	19.5?	−18.1	−6.3
	M32, effective	42.5	20.65	−20.0	−5.9
	N4486-B	43.4	20.5	−18.75	−5.0
Spiral galaxies	LMC	43.2	21.75	−22.65	−6.3
	M33	43.5	21.8	−22.5	−6.1
	M31	44.6	22.3	−22.9	−5.5
Giant elliptical galaxies	N3379	44.3	22.0	−22.35	−5.6
	N4486	45.5	22.4	−22.3	−4.7
Compact groups of galaxies	Stephan	45.5	22.6:	−23.1:	−4.7
Small groups of spirals	Scuptor	46.2	24.1	−26.7	−5.7
Dense groups of ellipticals	Virgo E, core Fornax I	46.5	23.7	−25.2	−5.0
Small clouds of galaxies	Virgo S Ursa Major	47.0	24.3	−26.5	−5.1
Small clusters of galaxies	Virgo F	47.2	24.3	−26.3	−4.9
Large clusters of ellipticals	Coma	48.3	24.6	−26.1	−4.9
Superclusters	Local	48.7:	25.5:	−28.4:	−4.7
HMS sample to $m \simeq 12.5$			26.0:	−29.6	−4.6
Lick Observatory counts to $m \simeq 19.0$			26.8	−30.5	−4.1

: denotes approximate value;? denotes large uncertainty

† The filling factor $\phi = \rho/\rho_{\mathrm{m}}$, where $\rho_{\mathrm{m}} = 3c^2/8\pi G R_m^2$; $R_{\mathrm{m}} = 2GM/c^2$.

(Adapted from de Vaucouleurs, G., *Science*, **167**, 1203, 1970.)

Primordial element abundances *(Big Bang Nucleosynthesis, BBN)*

The plot below shows the predicted light element primordial abundances as a function of the present baryon-to-photon ration $\eta = n_B/n_\gamma$.

$\rho_B = 6.86 \times 10^{-22}\eta$ gm cm^{-3}, the current baryon mass density.

Then $\eta = 2.74 \times 10^{-8}\Omega_B h^2$, since $\Omega_B = \rho_B/\rho_c$, the baryon density parameter, where ρ_c is the critical mass density and $\rho_c = 3H_0^2/(8\pi G) = 1.88 \times 10^{-29}$ h^2 g cm^{-3}; $H_0 = 100$h km s^{-1} Mpc^{-1} is the present value of Hubble's constant and G is the gravitational constant.

$Y_P = [^4He/(H + {}^4He]$ is the ^{4}He mass fraction abundance and is plotted on a linear scale.

The abundances for the other isotopes are the ratios by number relative to hydrogen and are plotted logarithmically. N_v corresponds to the assumed number of neutrino species, $N_v = 3$ corresponds to the standard Big Bang. $\tau_{1/2}$ = the half-life of the neutron.

(Adapted from Kolb, E.W. and Turner, *The Early Universe*, Addison-Wesley, 1990.)

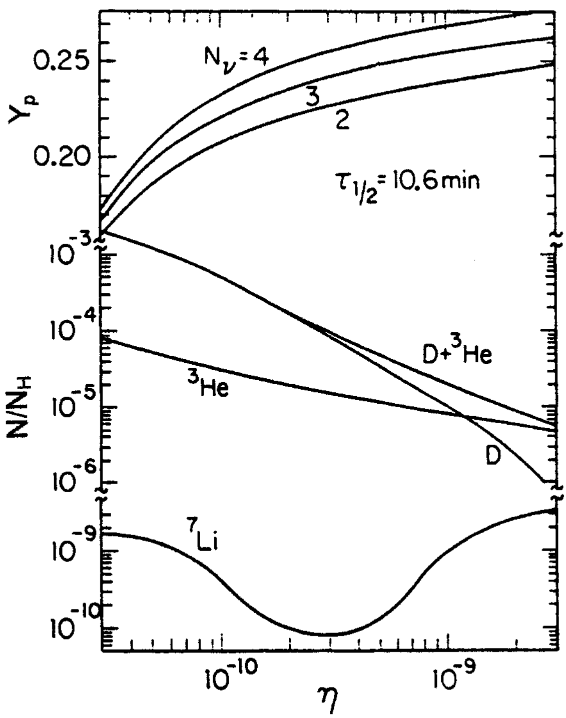

The background radiation spectrum of the Universe

The radio background spectra are from the Galactic pole (lower curve) and the Galactic plane. The interstellar medium photoionization optical depth for 10^{19}, 10^{18}, and 10^{17} H atoms cm^{-2} is shown rather than the EUV background, which is local. (Adapted from Henry, R., *Ap. J.*, **L49**, 516, 1999.)

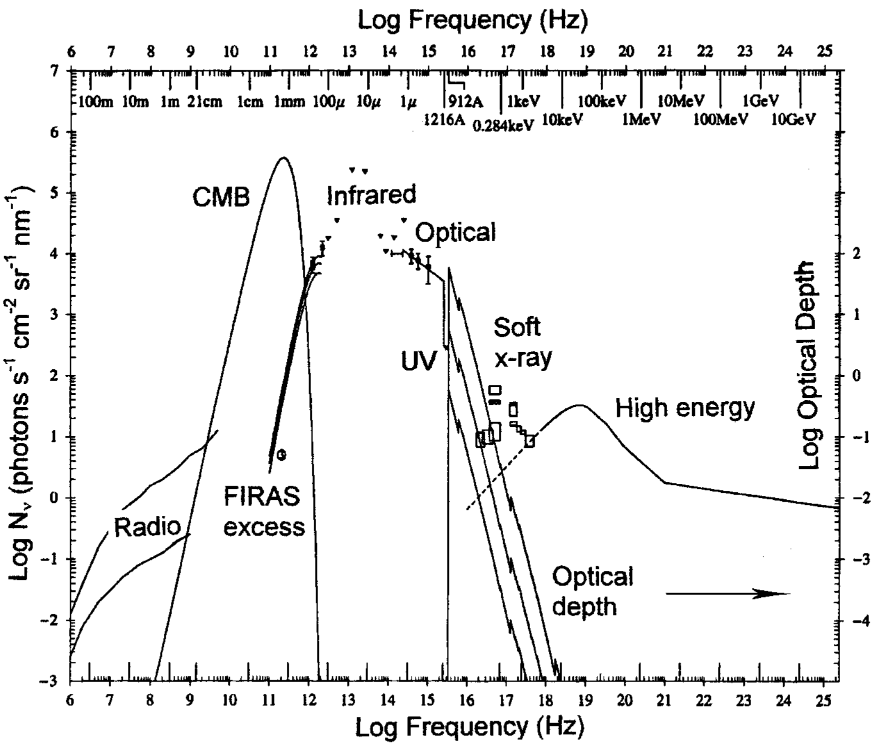

Note: The infrared background is very uncertain; upper limits only are shown.

Redshift survey

The Harvard-Smithsonian Center for Astrophysics Redshift Survey (CFA2).

The redshift distribution of galaxies can be seen in this polar projection of the redshifts for all the galaxies in the survey (about 18,600 galaxies). This is a section of a cylinder in equatorial coordinates looking down from the north pole to the equator with a height of 12,000 km s^{-1} and a radius of 15,000 km s^{-1}. The major structures seen are the Local Supercluster just above the middle of the plot, the Great Wall cutting from 9 hours and 5,500 km s^{-1} to 15 hours and 9,000 km s^{-1} and the Pisces-Perseus supercluster centered around 1 hour and 4,000 km s^{-1}. (Courtesy of John Huchra, CfA, 2001)

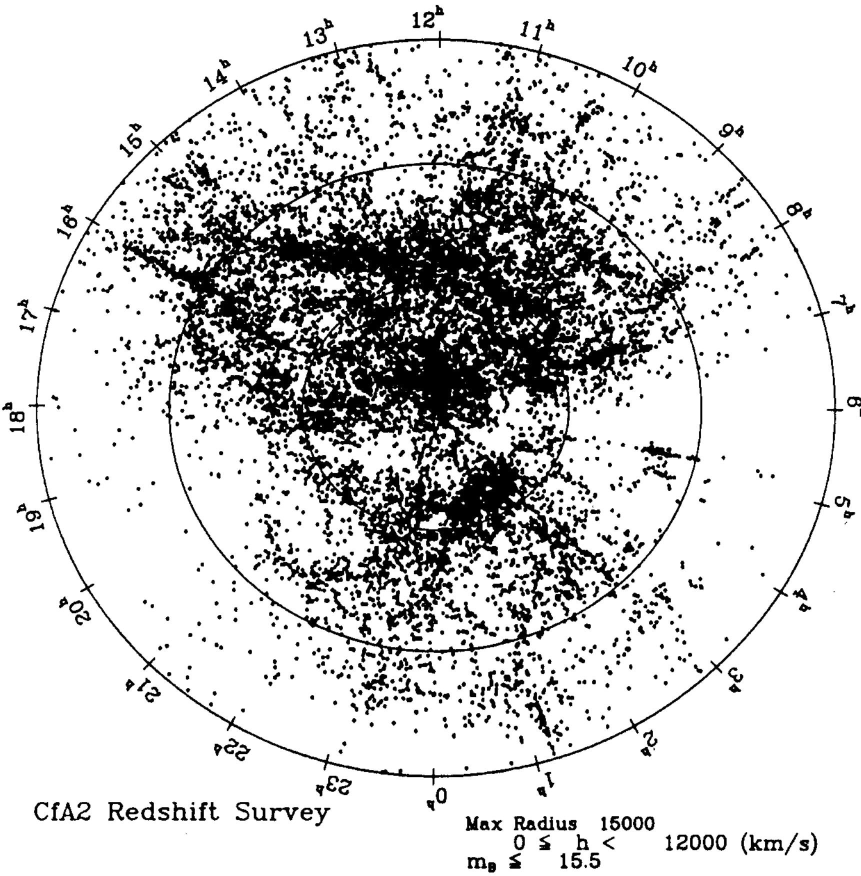

The luminosity distance is given to a good approximation by cz/H_0 for the velocities in the figure above. For a velocity of 12000 km s^{-1} and an $H_0 = 75$ km s^{-1} Mpc^{-1}, the luminosity distance is 160 Mpc.

Astronomical photometry

Following M. Golay (*Introduction to Astronomical Photometry*, D. Reidel Publishing Company, 1974.) we can write the following expression for the apparent magnitude difference on the Earth of two stars:

$$m_1 - m_2 = -2.5 \log \frac{\int_{\lambda_a}^{\lambda_b} \alpha_1^2 I_1(\lambda) T_i(\lambda, d_1) T_a(\lambda, d_1) T_t(\lambda) T_f(\lambda) r(\lambda) d\lambda}{\int_{\lambda_a}^{\lambda_b} \alpha_2^2 I_2(\lambda) T_i(\lambda, d_2) T_a(\lambda, d_2) T_t(\lambda) T_f(\lambda) r(\lambda) d\lambda},$$

where

$I_1(\lambda)$	the spectral radiance of star 1.
$I_2(\lambda)$	the same for star 2.
α_1 and α_2	the apparent diameters of stars 1 and 2, which are assumed to be spherical and emit isotropic radiation.
$T_i(\lambda, d_1)$	the fraction of the radiation of star 1 transmitted by interstellar space in the direction d_1 of star 1.
$T_i(\lambda, d_2)$	the same for star 2.
$T_a(\lambda, d_1)$	the fraction of stellar radiation transmitted by the Earth's atmosphere when star 1 is in direction d_1.
$T_a(\lambda, d_2)$	the same for star 2 when it is in direction d_2.
$T_t(\lambda)$	the fraction of stellar radiation transmitted by the optical system of the telescope t, whose entry pupil is perpendicular to the star's direction.
$T_f(\lambda)$	the fraction of stellar radiation transmitted by a filter f placed in front of the receiver.
$r(\lambda)$	the response of the receiver r which, for simplicity, is assumed to depend only upon λ.

The limits of integration, λ_a and λ_b where $\lambda_b > \lambda_a$ are defined by

$$\lambda \geq \lambda_b \quad T_a \cdot T_t \cdot T_f \cdot r \equiv 0,$$

$$\lambda \leq \lambda_a, \quad T_a \cdot T_t \cdot T_f \cdot r \equiv 0.$$

Let

$$S(\lambda) = T_t(\lambda) T_f(\lambda) r(\lambda),$$

the response of the photometric system and

$$E(\lambda) = \frac{\alpha^2}{4} I(\lambda) T_i(\lambda, d),$$

the stellar spectral irradiance at the top of the Earth's atmosphere, then the difference in apparent magnitudes for two stars outside the Earth's atmosphere is given by the expression:

$$(m_1 - m_2)_0 = -2.5 \log \frac{\int_{\lambda_a}^{\lambda_b} E_1(\lambda) \cdot S(\lambda) d\lambda}{\int_{\lambda_a}^{\lambda_b} E_2(\lambda) \cdot S(\lambda) d\lambda}.$$

We can define three wavelengths for a photometric system:

(1) $$\lambda_0 = \frac{\int_{\lambda_a}^{\lambda_b} \lambda S(\lambda)d\lambda}{\int_{\lambda_a}^{\lambda_b} S(\lambda)d\lambda},$$

the mean wavelength of the pass-band defined by the response function $S(\lambda)$.

(2) $$E(\lambda_i)\int_{\lambda_a}^{\lambda_b} S(\lambda)d\lambda = \int_{\lambda_a}^{\lambda_b} E(\lambda)S(\lambda)d\lambda,$$

where λ_i is the isophotal wavelength

(3) $$\lambda_{\text{eff}} = \frac{\int_{\lambda_a}^{\lambda_b} \lambda E(\lambda)S(\lambda)d\lambda}{\int_{\lambda_a}^{\lambda_b} E(\lambda)S(\lambda)d\lambda},$$

the effective wavelength.

$$\lambda_{\text{eff}} - \lambda_0 = \frac{E'(\lambda_0)}{E(\lambda_0)} \cdot \mu^2 \quad \text{and} \quad \lambda_i - \lambda_0 = \frac{1}{2}\mu^2 \frac{E''(\lambda_0)}{E'(\lambda_0)},$$

where

$$\mu^2 = \frac{\int (\lambda - \lambda_0)^2 S(\lambda)d\lambda}{\int S(\lambda)d\lambda}.$$

E' and E'' are the first and second derivatives of E with respect to the wavelength.

The color index of a star is defined by

$$C_{\text{AB}} \equiv m_A - m_B = -2.5 \log \frac{\int_A E(\lambda)S_A(\lambda)d\lambda}{\int_B E(\lambda)S_B(\lambda)d\lambda} + \text{constant},$$

where A and B represent two different spectral bands.

The relationship between the heterochromatic magnitude m_{λ_0} (obtained with a band of mean wavelength λ_0) and monochromatic magnitudes taken at the isophotal wavelength, $m(\lambda_i)$, at the mean wavelength $m(\lambda_0)$ and at the effective wavelength $m(\lambda_{\text{eff}})$ is given by

$$m_{\lambda_0} = m(\lambda_i) + S, \quad \text{where } S = -2.5 \log \int_{\lambda_a}^{\lambda_b} S(\lambda)d\lambda.$$

$$m(\lambda_i) - m(\lambda_0) = -0.543\mu^2 \left(\frac{E''(\lambda_0)}{E(\lambda_i)}\right)$$

$$m(\lambda_i) - m(\lambda_{\text{eff}}) = -0.543 \left(\frac{\lambda_{\text{eff}} E'(\lambda_{\text{eff}})}{E(\lambda_{\text{eff}})} + 1\right) \frac{\lambda_0 - \lambda_{\text{eff}}}{\lambda_{\text{eff}}}$$

Standard photometric systems

Standard U, B, V, R, I and long wavelength systems

Filter band	$\lambda_0^{(a)}$ (μm)	$\Delta\lambda_0$ (FWHM) (μm)	Absolute spectral irradiance for mag = 0.0 $f_\lambda(0)$ (erg cm^{-2} s^{-1} Å^{-1})	$f_\nu(0)$ (W m^{-2} Hz^{-1})
U	0.365	0.068	4.27×10^{-9}	1.90×10^{-23}
B	0.44	0.098	6.61×10^{-9}	$4.27(4.64)^{(b)}\times10^{-23}$
V	0.55	0.089	3.64×10^{-9}	3.67×10^{-23}
R	0.70	0.22	1.74×10^{-9}	2.84×10^{-23}
I	0.90	0.24	8.32×10^{-10}	2.25×10^{-23}
J	1.25	0.3	3.18×10^{-10}	1.65×10^{-23}
H	1.65	0.4	1.18×10^{-10}	1.07×10^{-23}
K	2.2	0.6	4.17×10^{-11}	6.73×10^{-24}
L	3.6	1.2	6.23×10^{-12}	2.69×10^{-24}
M	4.8	0.8	2.07×10^{-12}	1.58×10^{-24}
N	10.2		1.23×10^{-13}	4.26×10^{-25}

$f^{mks}{}_\lambda(0) = 10^{-2}\times f_\lambda(0)$ W m^{-2} nm^{-1}
$f^{cgs}{}_\nu(0) = 10^3\times f_\nu(0)$ erg s^{-1} cm^{-2} Hz^{-1}
$^{(a)}$ $\lambda_0 = \int \lambda S(\lambda)d\lambda / \int S(\lambda)d\lambda$, where $S(\lambda)$ is the photometer response function.
$^{(b)}$ From S. Kleinmann.
U, B, R, I, N values from Allen. C.W. *Astrophysical Quantities*. The Athlone Press (1973). V, J, H, K, L, M values from Wamsteker, W., *Astron. Astrophys.*, **97**, 329 (1981).

The spectral irradiance for a star of a given magnitude is given either by:

$$\log f_\lambda(m_x) = -0.4m_x + \log f_\lambda(0),$$

where $f_\lambda(m_x)$ is the spectral irradiance in erg cm^{-2} s^{-1} Å^{-1} of a star of magnitude (m_x) in the x filter band at the mean wavelength $\lambda_0(x)$, or

$$\log f_\nu(m_x) = -0.4m_x + \log f_\nu(0),$$

where $f_\nu(m_x)$ is the spectral irradiance in W m^{-2} Hz^{-1}.

The relationships above are for the irradiance at the top of the Earth's atmosphere and are valid for B through M stars.

Photometer response curves for UBVRI and long wavelength systems. (Adapted from Webbink, R.F. & Jeffers, W.Q., *Space Sci. Rev.*, **10**, 191 1969.)

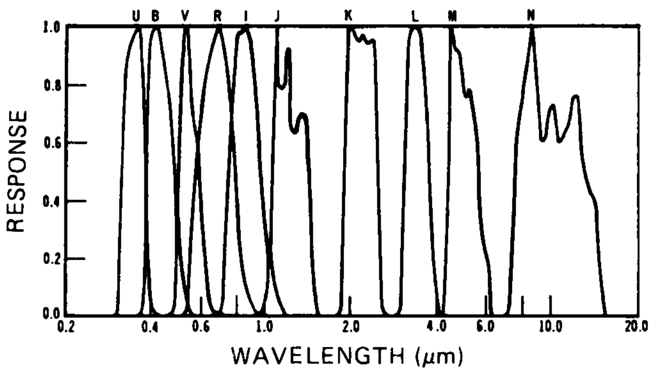

Response curves of photometer plus atmosphere. (Adapted from Webbink, R.F. & Jeffers, W.Q., *Space Sci. Rev.*, **10**, 191, 1969.)

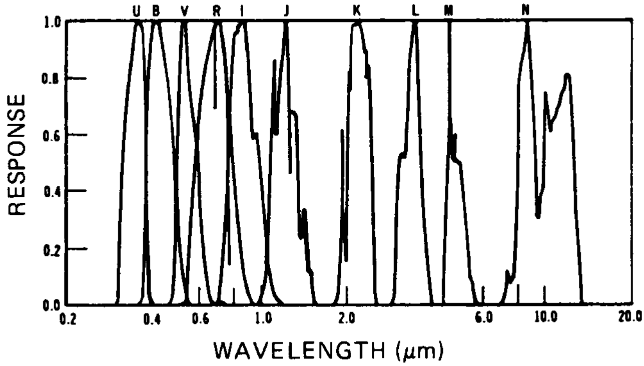

List of UBV primary standard stars

HD No.	Name	V	$B-V$	$U-B$	Spectral type
12 929	α Ari	2.00	+1.151	+1.12	K2 III
18 331	HR 875	5.17	+0.084	+0.05	A1 V
69 267	β Cnc	3.52	+1.480	+1.78	K4 III
74 280	η Hya	4.30	−0.195	−0.74	B3 V
135 742	β Lib	2.61	−0.108	−0.37	B8 V
140 573	α Ser	2.65	+1.168	+1.24	K2 III
143 107	ε CrB	4.15	+1.230	+1.28	K3 III
147 394	τ Her	3.89	−0.152	−0.56	B5 IV
214 680	10 Lac	4.88	−0.203	−0.04	O9 V
219 134	HR 8832	5.57	+1.010	+0.89	K3 V

(List taken from Strand, K. A. A., ed., *Basic Astronomical Data*, University of Chicago Press, Chicago, 1963.)

Standard stars for the JHKLM system

Standard	BS	Spectral type	m_{vis}	J	H	K	L	M
0	519	gM 4	5.49	2.117	1.317	1.078	0.890	1.181
1	721	B5 III	4.25	4.548	4.575	4.604	4.601	4.689
2	1195	G5 III	4.17	2.672	2.233	2.119	2.025	2.156
3	2827	B5 Ia	2.44	2.565	2.548	2.557	2.472	2.542
4	4216	G5 III	2.69	1.148	0.744	0.622	0.530	0.673
5	5530	F5 IV	5.16	4.408	4.194	4.156	4.092	4.134
6	7120	K3 III	4.98	2.822	2.197	2.052	1.910	2.103
7	8204	G4 Ibp	3.74	2.346	1.964	1.865	1.794	1.882
8	8502	K3 III	2.85	0.558	−0.077	−0.091	−0.372	−0.199
9	8728	A3 V	1.16	1.075	1.034	1.019	0.998	1.025

(List taken from Wamstecker, W., *Astron. Astrophys.*, **97**, 329, 1981.)

Kron photographic J and F bands

Sensitivity functions $S_\lambda(\lambda)$ for the J waveband *(left)* and the F waveband *(right)*. (From Kron, R.G., *Ap. J.*, **43**, 305, 1980.)

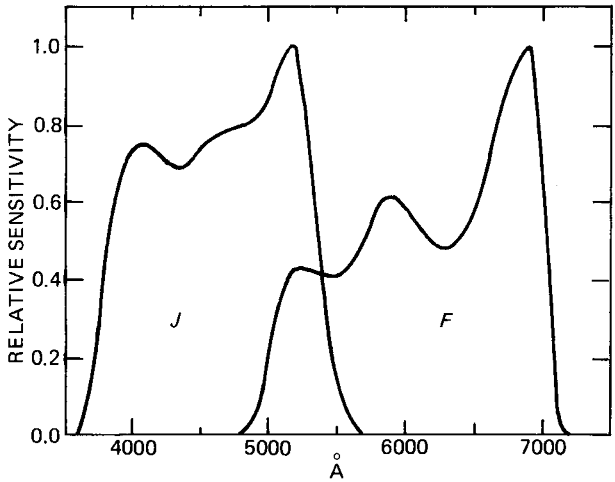

The earlier photovisual (m_{pv}) and photographic (m_{pg}) magnitudes are related to the standard B and V magnitudes by:

$$B \equiv m_{\mathrm{B}} = m_{\mathrm{pg}} + 0.11,$$

$$V \equiv m_{\mathrm{V}} = m_{\mathrm{pv}} + 0.00.$$

Color index,

$$C = m_{\mathrm{pg}} - m_{\mathrm{V}} = B - V - 0.11.$$

Bolometric correction,

$$BC = m_{\mathrm{b}} - m_{\mathrm{v}} = M_{\mathrm{b}} - M_{\mathrm{v}},$$

where $m_{\mathrm{b}}(M_{\mathrm{b}})$ is the apparent (absolute) bolometric magnitude, a measure of the total energy output of a star.

$$M_{\mathrm{b}}^{\mathrm{star}} - 4.72 = -2.5 \log(L_{\mathrm{star}}/L_{\odot}),$$

where L_{star} and $L_{\odot} = 3.83 \times 10^{33}$ erg s^{-1} are the absolute luminosities of the star and the Sun, respectively.

$$L_{\mathrm{star}} = 2.97 \times 10^{35} \times 10^{-0.4 M_{\mathrm{b}}} \ \mathrm{erg\,s^{-1}}.$$

The total irradiance at the top of the Earth's atmosphere is

$$f = 2.48 \times 10^{-5} \times 10^{-0.4 m_{\mathrm{b}}} \ \mathrm{erg\,cm^{-2}\,s^{-1}}$$

for a star apparent bolometric magnitude m_{b}.

Assuming black-body radiation, the spectral photon irradiance from a star of apparent bolometric magnitude m_b is given by:

$$f(\lambda) = \frac{8.48 \times 10^{34} \times 10^{-0.4 m_b}}{T_e^4 \lambda^4 [\exp(1.44 \times 10^8 / \lambda T_e) - 1]} \text{ photons cm}^{-2}\,\text{s}^{-1}\,\text{Å}^{-1}$$

λ in Å; T_e the effective temperature of the star in K (e.g., AO star; $m_v = 0$, $T_e = 10800, BC = -0.40$, $\lambda = 5000$ Å; $f(\lambda) = 10^3$ photons cm^{-2} s^{-1} Å^{-1}).

Interstellar reddening

The observed color index is given by

$$C_{ij} = C_{ij}^0 + [A(\lambda_i) - A(\lambda_j)] \equiv C_{ij}^0 + E_{ij},$$

where

$$A(\lambda) = \text{amount of interstellar absorption at } \lambda,$$

$$C_{ij}^0 = \text{intrinsic color index of the star,}$$

$$E_{ij} \equiv \text{color excess.}$$

In the *UBV* system, the color excesses are

$$E(B-V) \equiv (B-V) - (B-V)_0,$$

$$E(U-B) \equiv (U-B) - (U-B)_0$$

(subscript zero denotes intrinsic values).

$$A_V / E(B-V) = 3.2 \pm 0.2 \text{ (normal regions)}$$

$$\frac{E(U-B)}{E(B-V)} = 0.72 + 0.05 E(B-V).$$

Relationship of reddening $E(B-V)$ to the hydrogen column density:

$$\langle N(\mathrm{HI} + \mathrm{H_2}) / E(B-V) \rangle = 5.8 \times 10^{21} \text{ atoms cm}^{-2} \text{ mag}^{-1},$$

$$\langle N(\mathrm{HI}) / E(B-V) \rangle = 4.8 \times 10^{21} \text{ atoms cm}^{-2} \text{ mag}^{-1}.$$

(Bohlin *et al.*, *Ap. J.*, **224**, 132, 1978).

Visual extinction to the galactic center:

$$A_V \approx 30 \text{ mag}$$

(Becklin *et al.*, *Ap. J.*, **151**, 145, 1968).

The mean color excess $\overline{E}_{B-V}(b)$ at galactic latitude b for objects outside the absorbing layer can be estimated by:

$$\overline{E}_{B-V}(b) = 0.06 \operatorname{cosec} |b| - 0.06$$

(Woltjer, L., *Astron. Astrophys.*, **42**, 109, 1975).

A more general expression giving an estimate of interstellar absorption can be found in de Vaucouleurs *et al.*, *Second Reference Catalogue of Bright Galaxies*, University of Texas Press, 1976.

The interstellar reddening law

λ(Å)	$1/\lambda(\mu^{-1})$	$A_\lambda/E(B-V)$	λ(Å)	$1/\lambda(\mu^{-1})$	$A_\lambda/E(B-V)$
3200	3.13	5.58	5556	1.80	3.12
3250	3.08	5.47	5840	1.71	2.91
3300	3.03	5.38	6050	1.65	2.80
3350	2.98	5.32	6436	1.55	2.65
3400	2.94	5.26	6790	1.47	2.48
3448	2.90	5.18	7100	1.41	2.35
3509	2.85	5.10	7550	1.32	2.18
3571	2.80	5.06	7780	1.28	2.06
3636	2.75	4.99	8090	1.24	1.98
3862	2.59	4.72	8188	1.22	1.94
4036	2.48	4.56	8370	1.20	1.88
4167	2.40	4.39	8446	1.18	1.85
4255	2.35	4.33	8710	1.15	1.72
4464	2.24	4.12	9700	1.03	1.50
4566	2.19	4.04	9832	1.02	1.48
4780	2.09	3.91	10 256	0.95	1.36
5000	2.00	3.70	10 610	0.94	1.28
5263	1.90	3.41	10 796	0.93	1.26
5480	1.82	3.20	10 870	0.92	1.22

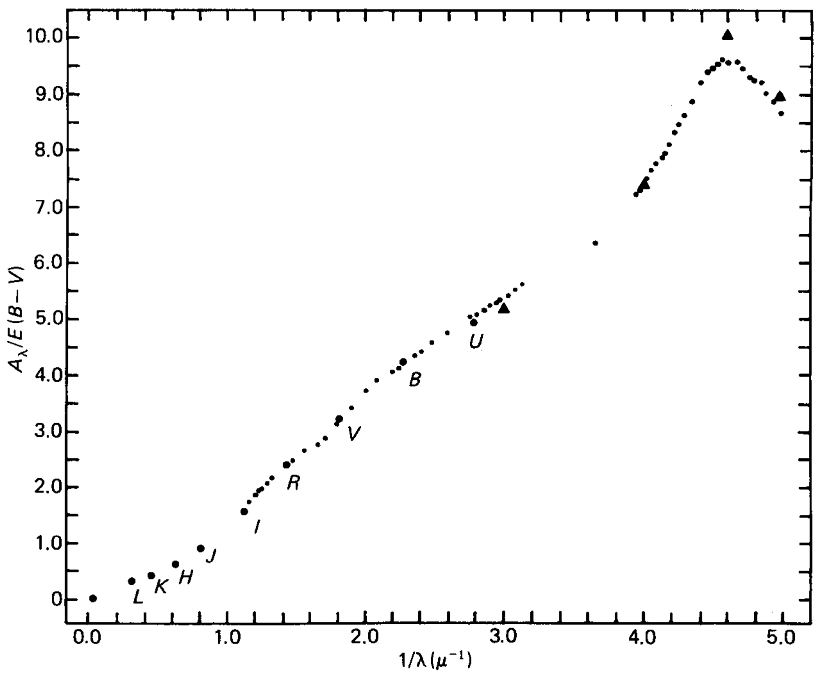

(Courtesy of R. Schild, Harvard-Smithsonian Center for Astrophysics.)

Absolute magnitude

The absolute magnitude M of a star is the apparent magnitude it would have if placed at a distance of 10 parsecs:

$$m - M = 5 \log D - 5 + A.$$

where D is the distance to the star in parsecs and A is a correction for interstellar absorption expressed in magnitude units. $m - M \equiv$ distance modulus. Solving for D:

$$D = 10^{[1+(m-M-A)/5]}.$$

Moon, night sky, sun, and planetary brightness

Moon
$V(R, \phi) = 0.23 + 5 \log R - 2.5 \log P(\phi)$,
$V(R, \phi) =$ the apparent V magnitude of the Moon,
$R =$ the observer–Moon distance in AU, and
$\phi =$ the phase angle $=$ angle between the Sun and the Earth as seen from the Moon.
$P(0°) = 1.000$, $P(40°) = 0.377$, $P(80°) = 0.127$,
$P(120°) = 0.027$, $P(160°) = 0.001$.
Mean lunar distance $= 2.570 \times 10^{-3}$ AU.
The V magnitude of the Moon at the Earth at opposition (full moon) is -12.73.

(Adapted from Wertz, J.R., *Spacecraft Attitude Determination and Control*, D. Reidel, 1980)

The Moon's phase law.

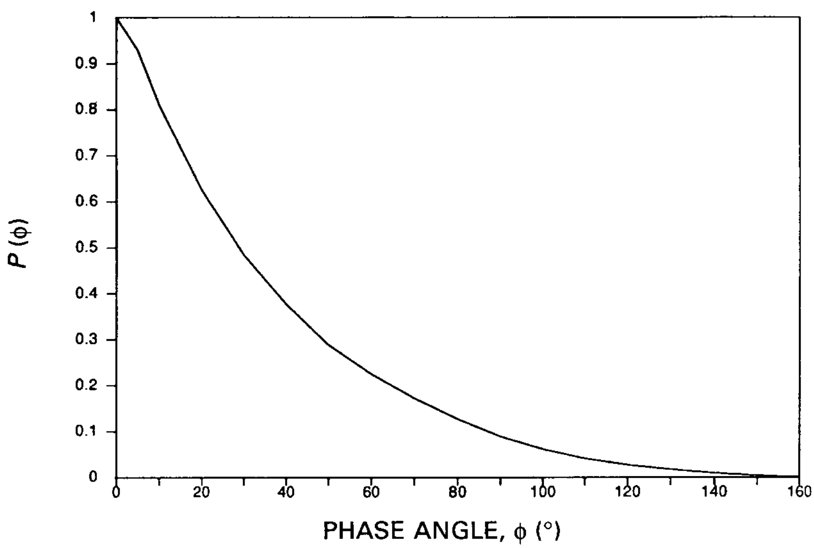

Night sky
Total brightness (zenith, mean sky) ≈ 1 ($m_v = 22.5$) star arcsec^{-2}.

Sun

Apparent magnitude	*Color index*	*Absolute magnitude*
$U = -26.06$	$U - B = +0.10$	$M_U = +5.51$
$B = -26.16$	$B - V = +0.62$	$M_B = +5.41$
$V = -26.78$	$BC = -0.07$	$M_V = +4.79$
$m_b = -26.85$		$M_b = +4.72$

Planetary brightness

The change in the brightness of a planet because of the changing distance from the Sun (r) and the Earth (Δ) is given by:

$$V = V(1,0) + 5\log(r\Delta) + \alpha(p),$$

where
$V(1,0)$ = visual magnitude of planet reduced to a distance of 1 AU from both the Sun and the Earth and phase angle $p = 0$.
α = phase law; change of planet brightness with p,
p = phase angle; angle between Sun and Earth seen from the planet

$$\cos p = \frac{r^2 + \Delta^2 - R^2}{2r\Delta},$$

where R = distance from the Earth to the Sun.

Planet	$V(1,0)^{(a)}$	$\alpha^{(b)}$
Mercury	-0.42 mag	$+0.027p + 2.2 \times 10^{-13}p^6$
Venus	-4.40	$+0.013p + 4.2 \times 10^{-7}p^3$
Mars	-1.52	$+0.016p$
Jupiter	-9.40	$+0.014p$
Saturn	-8.88	$+0.044L - 2.6\sin B + 1.2\sin^2 B$
Uranus	-7.19	$+0.001p$
Neptune	-6.87	$+0.001p$

p in degrees; L = Saturnicentric ring longitude difference of Sun and Earth;
B = Saturnicentric ring latitude of Earth $0° < L < 6°, 0° < |B| < 27°$.

---

[a] (from the *The Nautical Almanac*)
[b] (from Allen, C.W., *Astrophysical Quantities*, The Athlone Press, University of London, 1973)

Spherical astronomy

Time

The *Julian Date* (JD) is a continuous count of days, including the fraction of a day, from 1 January 4713 BC (= −4712 January 1), Greenwich mean noon (= 12h UT). For Example, AD 1978 January 1, 0h UT is JD 2443509.5 and AD 1978 July 21, 15h UT, is JD 2443711.125.

Conversion of the Gregorian calendar date to the Julian date for years AD 1801-2099 can be carried out with the following formula:

$$\mathrm{JD} = 367\mathrm{K} - \langle(7(\mathrm{K}+\langle(\mathrm{M}+9)/12\rangle))/4\rangle + \langle(275\mathrm{M})/9\rangle + \mathrm{I} + 1721013.5 + \mathrm{UT}/24 - 0.5\mathrm{sign}(100\mathrm{K} + \mathrm{M} - 190002.5) + 0.5$$

where K is the year (1801 <= K <= 2099), M is the month (1 <= M <= 12), I is the day of the month (1 <= I = 31), and UT is the universal time in hours ("<=" means "less than or equal to"). The last two terms in the formula add up to zero for all dates after 1900 February 28, so these two terms can be omitted for subsequent dates. This formula makes use of the sign and truncation functions described below:

The sign function serves to extract the algebraic sign from a number. Examples: sign(247) = 1; sign(−6.28 = −1.

The truncation function $\langle\ \rangle$ extracts the integral part of a number. Examples: $\langle 17.835\rangle = 17$; $\langle -3.14\rangle = -3$.

Example: Compute the JD corresponding to 1877 August 11, 7h30m UT.
Substituting K = 1877, M = 8, I = 11 and UT = 7.5,
JD = 688859−3286 + 244 + 11 + 1721013.5 + 0.3125 + 0.5 + 0.5
=2406842.8125

The formula given above was taken from the U.S. Naval Observatory's no-longer-published *Almanac for Computers for year 1990.*

A Modified Julian Date (MJD) is defined as:

$$\mathrm{MJD} = \mathrm{JD} - 2400000.5$$

The Julian Dates for some Besselian years:

B.Y.	Julian Date	B.Y.	Julian Date
B1850.0	2396758.203	B2000.0	2451544.533
B1900.0	2415020.313	B2050.0	2469806.643
B1950.0	2433282.423	B2100.0	2488068.753

Time zones

Time Zone	Add the following to UT
International Date Line East (IDLE) New Zealand Standard Time (NZST) New Zealand Time (NZT)	+12 hours
Guam Standard Time (GST) East Australian Standard Time (EAST)	+10 hours
Japan Standard Time (JST)	+9 hours
China Coast Time (CCT)	+8 hours
West Australian Standard Time (WAST)	+7 hours
India Standard Time (IST)	+5.5 hours
Russian Zone 3	+4 hours
Baghdad Time (BT) Russian Zone 2	+3 hours
Eastern European Time (EET) Russian Zone 1	+2 hours
Central European Time (CET) Middle European Time (MET) Swedish Winter Time (SWT)	+1 hours
Greenwich Mean Time (GMT) Universal Time (UT) Western European Time (WET)	0 hours
West African Time (WAT)	−1 hours
Atlantic Standard Time (AST)	−4 hours
Eastern Standard Time (EST)	−5 hours
Central Standard Time (CST)	−6 hours
Mountain Standard Time (MST)	−7 hours
Pacific Standard Time (PST)	−8 hours
Alaskan Standard Time (AkST)	−9 hours
Hawaiian Standard Time (HST)	−10 hours
International Date Line West (IDLW)	−12 hours

A world time zone map can be found at http://www.worldtimezone.com/.

Definitions

One *Besselian year* is the period of a complete circuit of the mean Sun in right ascension beginning at the instant when its right ascension is $18^h 40^m$. The epochs to which stellar coordinates are referred are in Besselian year numbers. (The epoch 1950.0 started December 31, 1949 at 2209 UT.)

A *mean sidereal day* is the interval between two successive upper culminations or transits of the vernal equinox.

The *civil or mean solar day* is $\frac{1}{365.2422}$ of a *tropical year*, the interval between two successive passages of the Sun through the vernal equinox.

Sidereal time is the hour angle of the vernal equinox.

Apparent solar time is the local hour angle of the Sun, expressed in hours, plus 12 hours.

Mean solar time is the local hour angle, plus 12 hours, of a fictitious *mean Sun* which moves along the equator at a constant rate equal to the average annual rate of the Sun.

Mean solar time at 0° longitude is called *universal time* (UT formerly *Greenwich mean time* or GMT).

In 1999:	1 mean solar day	= 1.002 737 090 35	mean sidereal days
		$= 24^h\, 03^m 56^s.555\ 37$ of	mean sidereal time
	1 mean sidereal day	= 0.997 269 566 33	mean solar days
		$= 23^h 65^m 04^s.090\ 53$ of	mean solar time

The name Greenwich mean time (GMT) is not used in astronomy since it is ambiguous and is now used, in the sense of UTC in addition to the earlier sense of UT; prior to 1925 it was reckoned for astronomical purposes from Greenwich mean noon (12^h UT).

Relationships with local time and hour angle

The following general relationships are used:

Local mean solar time	= universal time + east longitude.
Local mean sideral time	= Greenwich mean sidereal time + east longitude
Local apparent sidereal time	= local mean sidereal time + equation of equinoxes
	= Greenwich apparent sidereal time + east longitude.
Local hour angle	= local apparent sidereal time − apparent right ascension
	= local mean sidereal time − (apparent right ascension − equation of equinoxes).

A further small correction for the effect of polar motion is required in the production of very precise observations.

Notation for time-scales

A summary of the notation for time-scales and related quantities used in the *Astronomical Almance* is given below. Additional information is given in the *Supplement* to the *Almanac.*

UT = UT1; universal time; counted from 0^h at midnight; unit is mean solar day.

UT0 local approximation to universal time; not corrected for polar motion.

GMST Greenwich mean sidereal time; GHA of mean equinox of date.

GAST Greenwich apparent sidereal time; GHA of true equinox of date.

TAI international atomic time; unit is the SI second.

UTC coordinated universal time; differs from TAI by an integral number of seconds, and is the basis of most radio time signals and legal time systems.

ΔUT = UT−UTC; increment to be applied to UTC to give UT.

DUT = predicted value of ΔUT, rounded to $0^s.1$, given in some radio time signals.

ET ephemeris time; was used in dynamical theories and in the Almanac from 1960–83; but is now replaced by TDT and TDB.

TDT terrestrial dynamical time; used as time-scale of ephemerides for observations from the Earth's surface. TDT = TAI + $32^s.184$.

TDB barycentric dynamical time; used as time-scale of ephemerides referred to the barycenter of the solar system.

ΔT = ET−UT (prior to 1984); increment to be applied to UT to give ET.

ΔT = TDT−UT (1984 onwards); increment to be applied to UT to give TDT.

ΔT = TAI + $32^s.184$− UT.

ΔAT = TAI−UTC; increment to be applied to UTC to give TAI.

ΔET = ET−UTC; increment to be applied to UTC to give ET.

ΔTT = TDT−UTC; increment to be applied to UTC to give TDT.

For most purposes. ET up to 1983 December 31 and TDT from 1984 January 1 can be regarded as a continuous time-scale. Values of ΔT for the years 1620 onwards are given in the *Astronomical Almanac.*

From the Astronomical Almanac:

The differences between the terrestrial and barycentric dynamical time-scales (due to the variations in gravitational potential around the Earth's orbit) are given by:

$$\mathrm{TDB} = \mathrm{TDT} + 0^s.001\,658 \sin g + 0^s.000\,014 \sin 2g$$

$$\mathrm{g} = 357^\circ.53 + 0^\circ.985\,600\,28(\mathrm{JD} - 245\;1545.0)$$

where higher-order terms are neglected and g is the mean anomaly of the Earth in its orbit around the Sun.

Equation of time

The difference between local mean time (LMT) and local apparent solar time (LAT) is known as the equation of time (shown below), and is given by

$$\text{LAT} = \text{LHA Sun} + 12^{\text{h}} = \text{LMT} + \text{equation of time},$$

where LHA Sun is the local hour angle of the Sun.

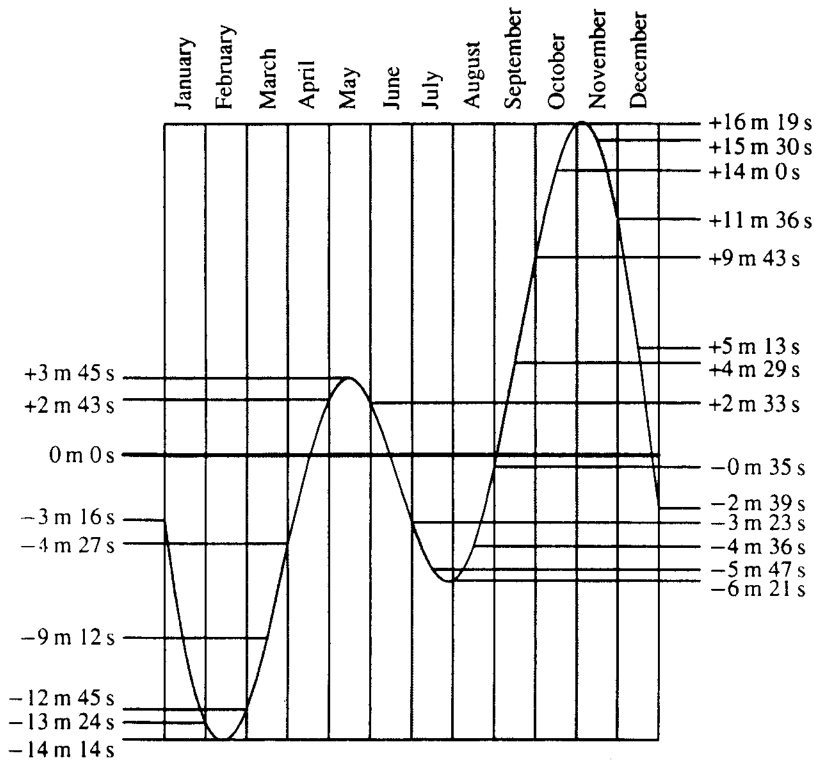

(From the *Explanatory Supplement to the Astronomical Almanac*)

Analemma curve

Plotting the position of the apparent Sun relative to the mean Sun (which moves uniformly along the equator) produces the *Analemma curve.* (From the *Explanatory Supplement to the Astronomical Almanac.*)

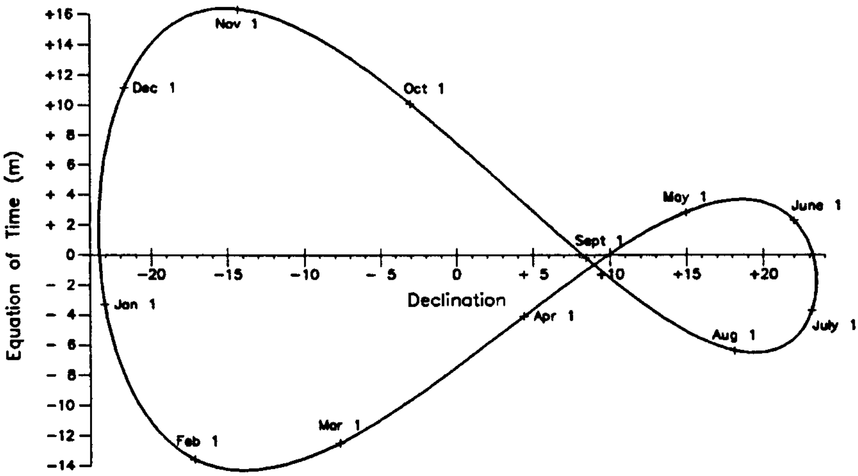

The celestial sphere

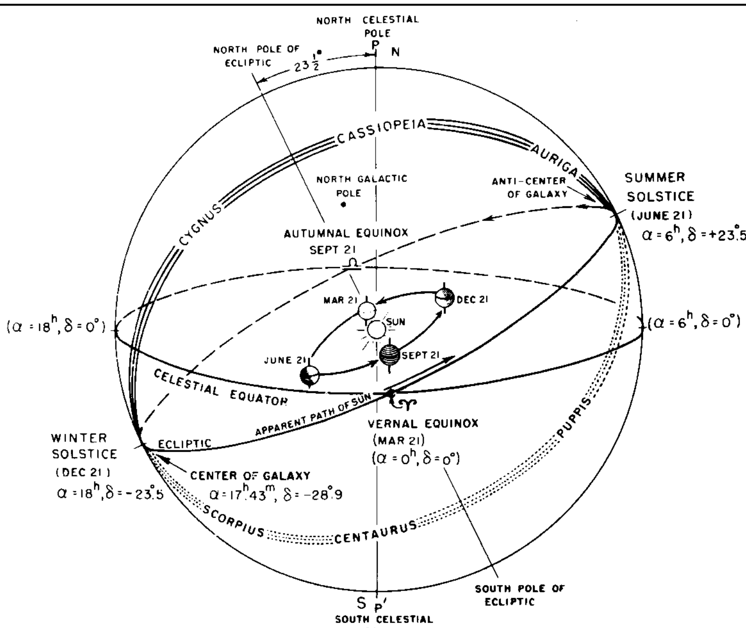

(Adapted from Valley, S.L., ed., *Handbook of Geophysics and Space Environment*, AFCRL, 1965.)

Celestial Coordinates

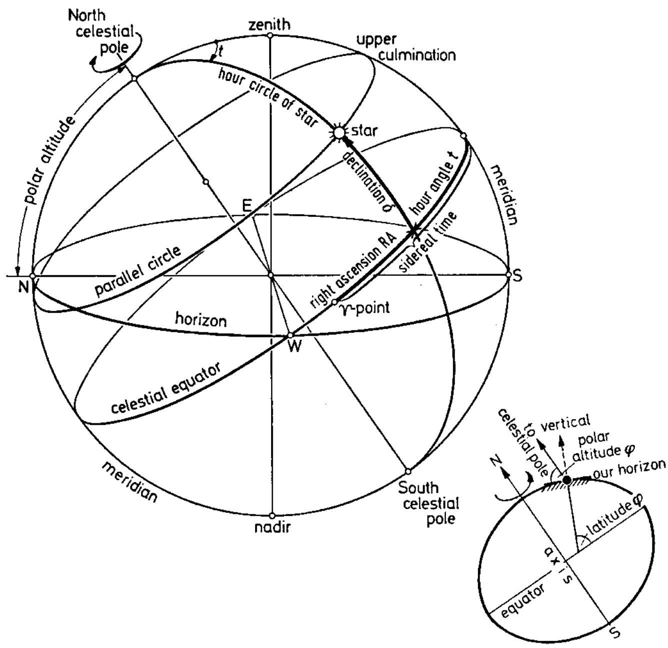

(Unsoeld, A., *The New Cosmos*, Springer-Verlag, 1969, with permission.)

The Zodiac

Path of the Earth around the Sun, seasons, and Zodiac. Perihelion is 2 January and aphelion is 2 July. Right ascension in hours of each constellation is given. (Adapted from Ussoeld, A., *The New Cosmos*, Springer-Verlag, 1969.)

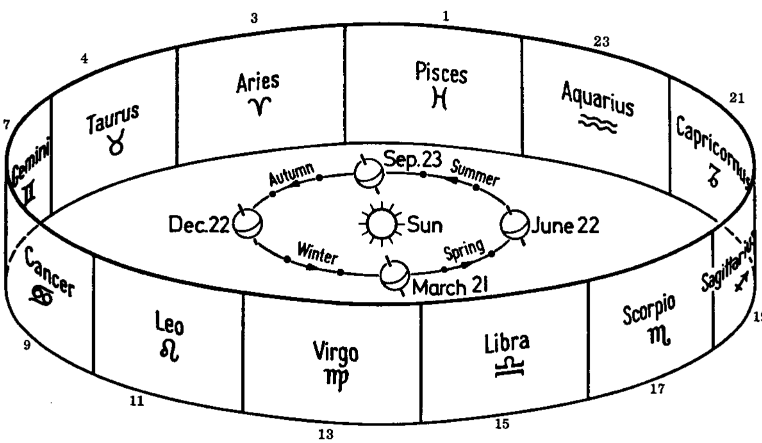

Astronomical coordinate transformations

Horizon–equatorial (*celestial*) *systems*

$\cos h \sin A = + \cos\delta \sin t,$

$\cos h \cos A = - \sin\delta \cos\varphi + \cos\delta \cos t \sin\varphi,$

$\sin h = \sin\delta \sin\varphi + \cos\delta \cos t \cos\varphi,$

$\cos\delta \sin t = \cos a \sin A,$

$\cos\delta \cos t = \sin h \cos\varphi + \cos h \cos A \sin\varphi,$

$\sin\delta = \sin h \sin\varphi - \cos h \cos A \cos\varphi,$

t = local sidereal time $- \alpha$ = local hour angle,

A = azimuth, toward West from South,

h = altitude,

φ = observer's latitude,

α = right ascension,

δ = declination.

Ecliptic–equatorial (celestial) systems

$\cos\delta \cos\alpha = \cos\beta \cos\lambda,$

$\cos\delta \sin\alpha = \cos\beta \sin\lambda \cos\varepsilon - \sin\beta \sin\varepsilon,$

$\sin\delta = \cos\beta \sin\lambda \sin\varepsilon + \sin\beta \cos\varepsilon,$

$\cos\beta \cos\lambda = \cos\delta \cos\alpha,$

$\cos\beta \sin\lambda = \cos\delta \sin\alpha \cos\varepsilon + \sin\delta \sin\varepsilon,$

$\sin\beta = \sin\delta \cos\varepsilon - \cos\delta \sin\alpha \sin\varepsilon,$

α = right ascension, δ = declination,

λ = ecliptic longitude, β = ecliptic latitude,

ε = obliquity of the ecliptic $= 23°27'8''.26 - 46''.845T - 0''.0059T^2 + 0''.001\,81T^3$

where T is the time in centuries from 1900.

Galactic-equatorial (celestial) systems

$\cos b^{\rm II} \cos(l^{\rm II} - 33°) = \cos\delta \cos(\alpha - 282.25°)$

$\cos b^{\rm II} \sin(l^{\rm II} - 33°) = \cos\delta \sin(\alpha - 282.25°) \cos 62.6° + \sin\delta \sin 62.6°.$

$\sin b^{\rm II} = \sin\delta \cos 62.6° - \cos\delta \sin(\alpha - 282.25°) \sin 62.6°,$

$\cos\delta \sin(\alpha - 282.25°) = \cos b^{II} \sin(l^{II} - 33°) \cos 62.6° - \sin b^{II} \sin 62.6°,$

$\sin\delta = \cos b^{II} \sin(l^{II} - 33°) \sin 62.6° + \sin b^{II} \cos 62.6°,$

$l^{\rm II}$ = new galactic longitude,

$b^{\rm II}$ = new galactic latitude,

α = right descension (1950.0),

δ = declination (1950.0),

For example, $l^{\rm II} = b^{\rm II} = 0 : \alpha = 17^{\rm h}42^{\rm m}.4, \delta = -28°55'$ (1950.0);

$b^{\rm II} = +\,90.0$, galactic north pole: $\alpha = 12^{\rm h}49^{\rm m}, \delta = +27°.4$ (1950.0).

Galactic-equatorial (celestial) systems (cont.)

Chart for conversion of equatorial (1950.0) coordinates into new galactic coordinates ($l^{II}b^{II}$) or vice versa. (Kraus, J.D., *Radio Astronomy*, 2nd edn., with permission.)

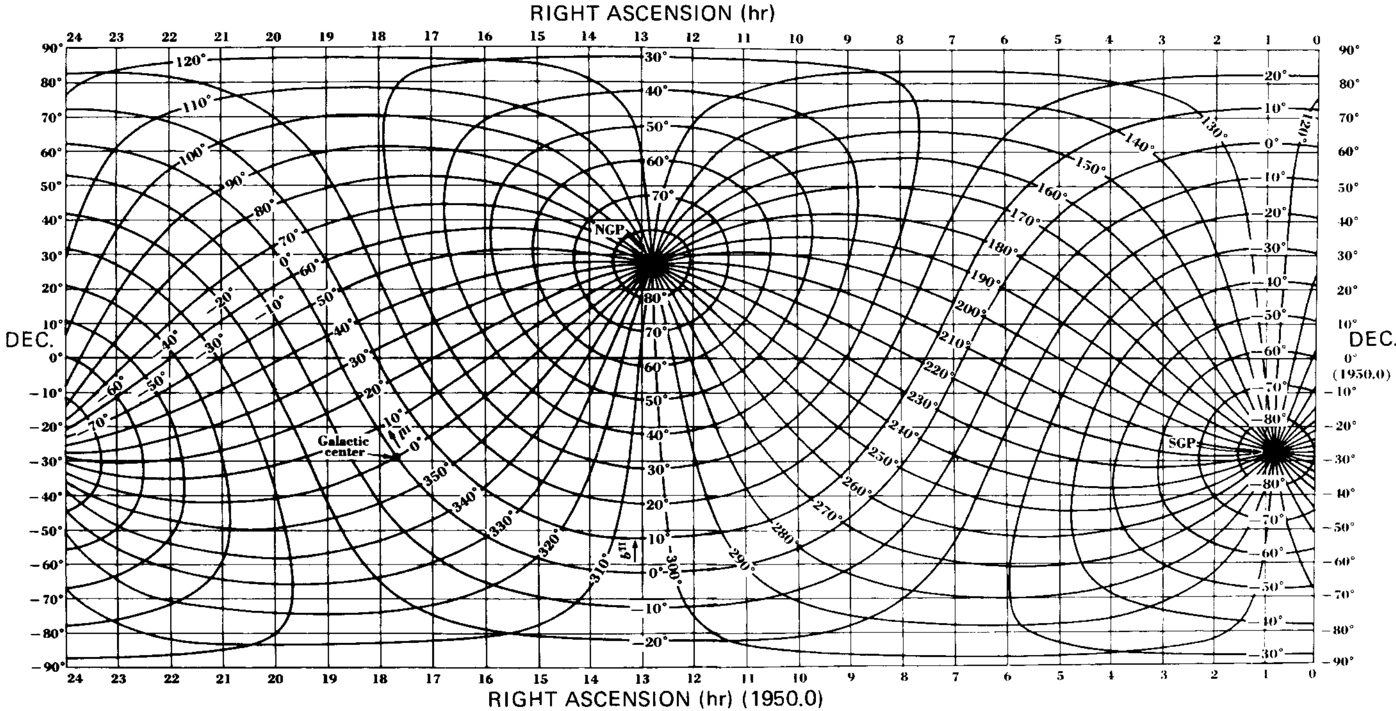

Approximate reduction of astronomical coordinates

Right-ascension precession in seconds of time per year.

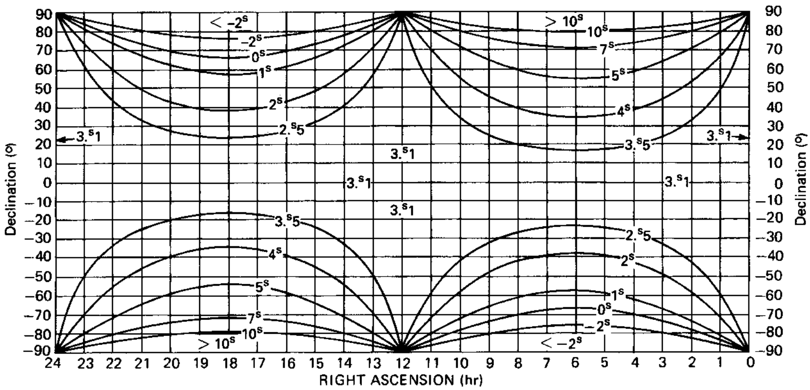

Declination precession in seconds of arc per year (*left*) and minutes of arc as a function of interval in years (*right*).

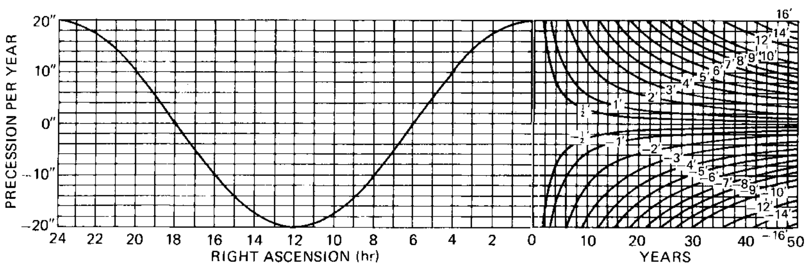

Precession charts: The charts show the precession in right ascension in seconds of time per year and of declination in seconds of arc per year as a function of position as given by the relations

$$\Delta\alpha = 3^{s}.07 + 1^{s}.34 \sin\alpha \tan\delta \quad \text{per year,}$$
$$\Delta\delta = 20'' \cos\alpha \quad \text{per year.}$$

The lower chart also indicates the precession in declination in minutes of arc as a function of the interval in years. For example, to find the precession for an object at RA = $04^{h}00^{m}$ for an 18-year interval one enters the chart at 4 hr, finding a precession of 10 sec of arc per year. Then moving horizontally to the right-hand chart to a point above 18 years the precession is found to be 3 min of arc for the 18-year interval.

The charts are useful for approximate precession determinations for intervals between epochs 1800.0 to 2000.0. (Kraus, J.D., *Radio Astronomy*, 2nd edn., with permission.)

Reduction for precession – approximate formulae

These formulae are from *The Astronomical Almanac*, U.S. Government Printing Office. See the latest volume for procedures for the complete reduction of celestial coordinates, including proper motion, aberration, light-deflection, parallax, precession and nutation.

Approximate formulae for the reduction of coordinates and orbital elements referred to the mean equinox and equator or ecliptic of date (t) are as follows:

For reduction to J2000.0	For reduction from J2000.0
$\alpha_0 = \alpha - M - N \sin\alpha_m \tan\delta_m$	$\alpha = \alpha_0 + M + N \sin\alpha_m \tan\delta_m$
$\delta_0 = \delta - N \cos\alpha_m$	$\delta = \delta_0 + N \cos\alpha_m$
$\lambda_0 = \lambda - a + b\cos(\lambda + c')\tan\beta_0$	$\lambda = \lambda_0 + a - b\cos(\lambda_0 + c)\tan\beta$
$\beta_0 = \beta - b\sin(\lambda + c')$	$\beta = \beta_0 + b\sin(\lambda_0 + c)$

α, δ = right ascension and declination

λ, β = ecliptic longitude and latitude

The subscript zero refers to epoch J2000.0 and α_m, δ_m to the mean epoch; with sufficient accuracy:

$$\alpha_m = \alpha - \frac{1}{2}(M + N \sin\alpha \tan\delta)$$

$$\delta_m = \delta - \frac{1}{2} N \cos\alpha_m$$

or

$$\alpha_m = \alpha_0 + \frac{1}{2}(M + N \sin\alpha_0 \tan\delta_0)$$

$$\delta_m = \delta_0 + \frac{1}{2} N \cos\alpha_m$$

The precessional constants M, N, etc., are given by:

$$M = 1^\circ.281\,2323T + 0^\circ.000\,3879\,T^2 + 0^\circ.000\,0101\,T^3$$

$$N = 0^\circ.556\,7530\,T - 0^\circ.000\,1185\,T^2 - 0^\circ.000\,0116\,T^3$$

$$a = 1^\circ.396\,971\,T + 0^\circ.000\,3086\,T^2$$

$$b = 0^\circ.013\,056\,T - 0^\circ.000\,0092\,T^2$$

$$c = 5^\circ.123\,62 + 0^\circ.241\,614\,T + 0^\circ.000\,1122\,T^2$$

$$c' = 5^\circ.123\,62 - 1^\circ.155\,358\,T - 0^\circ.000\,1964\,T^2$$

where $T = (t - 2000.0)/100 = (\text{JD}-\ 245\ 1545.0)/36\ 525$

Major ground-based astronomical telescopes

Reflecting telescopes

Name	Location	Size	Date	Latitude, Longitude, Altitude
Gran Telescopio de Canarias (GTC)	La Palma, Spain	10	2003	19 49 N, 17 54 W, 2400
Keck Telescope I	Mauna Kea, Hawaii	10	1991	19 49 N, 155 28 W, 4150
Keck Telescope II	Mauna Kea, Hawaii	10	1996	19 49 N, 155 28 W, 4150
Hobby-Eberly Telescope (HET)	Mt. Fowlkes, Texas	9.1	1997	30 41 N, 104 01 W, 2002
South African Large Telescope (SALT)	Sutherland, S. Africa	9.1	2004	32 23 S, 20 49 E, 1798
Large Binocular Telescope (LBT)	Mt. Graham, Arizona	2×8.4	2004	32 42 N, 109 51 W, 3170
Subaru Telescope	Mauna Kea, Hawaii	8.2	1999	19 50 N, 155 29 W, 4139
Antu (VLT 1) (VLT: Very Large Telescope)	Cerro Paranal, Chile	8.2	1998	24 38 S, 70 24 W, 2635
Kueyen (VLT 2)	Cerro Paranal, Chile	8.2	1999	24 38 S, 70 24 W, 2635
Melipal (VLT 3)	Cerro Paranal, Chile	8.2	2000	24 38 S, 70 24 W, 2635
Yepun (VLT 4)	Cerro Paranal, Chile	8.2	2000	24 38 S, 70 24 W, 2635
Gemini Telescope North	Mauna Kea, Hawaii	8.1	1999	19 49 N, 155 28 W, 4214
Gemini Telescope South	Cerro Pachon, Chile	8.1	2001	30 14 S, 70 43 W, 2715
MMT Observatory 6.5 m Telescope	Mt Hopkins, Arizona	6.5	2000	31 41 N, 110 53 W, 2606
Walter Baade Telescope	Las Campanas, Chile	6.5	2000	29 00 S, 70 42 W, 2300
Landon Clay telescope	Las Campanas, Chile	6.5	2002	29 00 S, 70 42 W, 2300
Bolshoi Teleskop Azimutal'ny (BTA)	Mount Pastukhov, Russia	6.0	1975	43 39 N, 41 26 E, 2070
200-in Hale Telescope	Mount Palomar, CA	5.1	1948	33 21 N, 116 52 W, 1706
William Herschel Telescope (WHT)	La Palma, Spain	4.2	1987	28 46 N, 17 53 W, 2332
SOAR 4-m Telescope	Cerro Pachon, Chile	4.2	2002	30 21 S, 70 49 W, 2701
Victor M. Blanco Telescope (CTIO 4 m)	Cerro Tololo, Chile	4.0	1976	30 10 S, 70 49 W, 2215
Large Sky Area Multi-Object Fiber Spectroscopic Telescope (LAMOST)	Xinglong Station, China	40	2004	40 24 N, 117 34 E, 916
Anglo-Australian Telescope (AAT)	Siding Spring, Australia	3.9	1975	31 17 S, 149 04 E, 1130
Nicholas U. Mayall Reflector (Kitt Peak 4 m)	Kitt Peak, Arizona	3.8	1973	31 58 N, 111 36 W, 2120
UK Infrared Telescope (UKIRT 3.8 m)	Mauna Kea, Hawaii	3.8	1978	19 50 N, 155 28 W, 4194
Adv. Electro-Optical System Telescope	Haleakala, Hawaii	3.7	2000	20 42 N, 156 15 W, 3058
Canada-France-Hawaii Telescope (CFHT)	Mauna Kea, Hawaii	3.6	1979	19 49 N, 155 28 W, 4200
Telescopio Nazionale Galileo (Galileo 3.6 m)	La Palma, Spain	3.6	1998	28 45 N, 17 54 W, 2370
ESO 3.6 m Telescope	La Silla, Chile	3.6	1977	29 15 S, 70 43 W, 2387

Size: Clear aperture in meters.
Date: date of completion, dedication ceremony. "first light", or first scientific use.
Latitude: in degrees and arc minutes.
Longitude: in degrees and arc minutes.
Altitude: in meters above sea level.
(*Adapted from Sky & Telescope*, G. Schilling, August 2000, Sky Publishing Company)

Major ground-based astronomical telescopes (cont.)

Refracting telescopes

Name	Location	Size	Date	Latitude, Longitude, Altitude
Yerkes Observatory, University of Chicago	Williams Bay, WI	101	1897	42 34 N, 83 33 W, 334
36-inch Refractor, Lick Observatory	Mt. Hamilton, CA	89.5	1888	37 20 N, 121 39 W, 1284
Observatoire de Paris	Meudon, France	83	1889	48 48 N,02 14 E, 162
Zentralinstitut fuer Astrophysik	Potsdam, Germany	80	1889	52 23 N, 13 04 E, 107
The Thaw Refractor, Allegheny Observatory	Pittsburgh, PA	76	1914	40 29 N, 80 01 W, 370
Lunette Bischoffsheim, Observatorie de Nice	Mont Gros, France	74	1886	43 43 N, 07 18 E, 376
28-inch Visual Refractor, Old Roy. Green. Obs.	Greenwich, UK	71	1894	51 29 N, 00 00, 47
Gross Refraktor, Archenhold-Sternwarte	Berlin, Germany	68	1896	52 29 N, 13 29 E, 41
Gross Refraktor, Institut fuer Astronomie	Vienna, Austria	67	1880	48 14 N, 16 20 E, 240
The Innes Telescope	Johannesburg, South Africa	67	1925	26 11 S, 28 04 E, 1806
Leander McCormick Observatory	Charlotttesville, VA	67	1883	38 02 N, 78 31 W, 259
26-inch Equatorial, U.S. Naval Observatory	Washington, DC	66	1873	38 55 N, 77 04 W, 92
The Thompson Refractor, Royal Greenwich Obs.	Hailsham, UK	66	1899	50 52 N, 00 20 E, 34
Yale-Columbia Refractor	Mt. Stromlo, Australia	66	1925	35 19 S, 149 00 E, 769

Size: Clear aperture in centimeters.

Date: date of completion, dedication ceremony, "first light", or first scientific use.

Latitude: in degrees and arc minutes.

Longitude: in degrees and arc minutes.

Altitude: in meters above sea level.

(*Adapted from Sky & Telescope*, Classen, J. & Sperling, N., **61**, 1981 Sky Publishing Company)

Major ground-based astronomical telescopes (cont.)

Schmidt telescopes

Name	Location	Size	Date	Latitude, Longitude, Altitude
2-meter Telescope (Tautenberg Schmidt)	Tautenberg, Germany	1.3	1960	50 59 N, 11 43 E, 331
Oschin 48 inch Telescope	Palomar Mt., CA	1.2	1948	33 21 N, 116 51 W, 1706
U.K. Schmidt Telescope Unit (U.K. Schmidt)	Siding Spring Mt., Australia	1.2	1973	31 16 S, 149 04 E, 1145
Kiso Schmidt Telescope	Kiso, Japan	1.0	1975	35 48 N, 137 38 E, 1130
3TA-10 Schmidt Telescope (Byurakan Schmidt)	Mt. Aragatz, Armenia	1.0	1961	40 20 N, 44 30 E, 1450
Kvistaberg Schmidt Telescope (Uppsala Schmidt)	Kvistaberg, Sweden	1.0	1963	59 30 N, 17 36 E, 33
ESO 1 meter Schmidt	La Silla, Chile	1.0	1972	29 15 S, 70 44 W, 2318
Venezuela 1-meter Schmidt	Merida, Venezuela	1.0	1978	8 47 N, 70 52 W, 3610
Telescope de Schmidt (Calern Schmidt)	Grasse, France	0.9	1981	43 45 N, 6 56 E, 1270
Telescope Combine de Schmidt	Brussells, Belgium	0.8	1958	50 48, N, 4 21 E, 105
Schmidt Telescope	Riga, Latvia	0.8	1968	56 47 N, 24 24 E, 75
Calar-Alto-Schmidtspiegel	Calar Alto, Spain	0.8	1980	37 13 N, 2 33 W, 2168

Size: Clear aperture in meters.

Date: date of completion, dedication ceremony, "first light", or first scientific use.

Latitude: in degrees and arc minutes.

Longitude: in degrees and arc minutes.

Altitude: in meters above sea level.

(*Adapted from Sky & Telescope*, G. Schilling, August 2000, Sky Publishing Company)

Major ground-based astronomical telescopes (cont.)

Radio telescopes

Name	Location	Aperture	Frequency Range (GHz)	Latitude, Longitude, Altitude
Arecibo Observatory	Arecibo, Puerto Rico	305 m dish*	0.05 - 8	18 21 N,66 45 W, 365
MPI fuer Radioastronomie	Effelsberg, Germany	100 m dish	0.6 - 15	50 32 N, 06 53 E, 366
Westerbork Synthesis Radio Observatory	Hooghalen, Netherlands	14 25 m dishes	0.3, 1.4, 8	52 55 N, 06 36 E, 5
Radio Astronomy Observatory, Parkes	New South Wales, Aus.	64 m	0.5 - 5	33 00 S, 148 16 E, 392
Lovell Telescope	Jodrell Bank, UK	76 m dish	0.0003 - 4	53 14 N, 02 18 W, 78
Mullard Radio Astronomy Observatory	Cambridge, UK	8 el. interferom.	2.7, 5, 15	52 10 N, 00 03 E, 17
Owens Valley Radio Observatory	Big Pine, California	40 m dish	0.5 - 12 18 - 24	37 14 N, 118 17 W, 1216
Millimeter-Wavelength Array		6 10.4 m dishes	mm	
Solar Array		2 27 m dishes	1 - 18	
National Radio Astronomy Observatory	Greenbank, WV	100 m dish	1 - 50	38 26 N, 79 50 W, 825
NRAO Very Large Array (VLA)	San Augustin, NM	27 25 m dishes	1.4, 1.7, 5, 15, 24	34 05 N, 107 37 W, 2124
NRAO Very Long Baseline Array (VLBA)	Virgin Islands - Hw	10 25 m dishes	0.3 - 100	— –
James Clerk Maxwell Telescope (JCMT)	Mauna Kea, Hw	15 m dish	230, 345, 460, 690, 810	19 49 N, 155 28 W, 4092
Submillimeter Array (SMA)	Mauna Kea, Hw	86 m dishes	180 - 900	19 49 N, 155 28 W, 4206
IRAM 30m Telescope	Pico Veleta, Spain	30 m dish	80.1 - 115.5	37 04 N, 3 24 W, 2920
Nobeyama 45 m Telescope	Nobeyama, Japan	45 m dish	20–230	35 56 N, 138 29 E, 1350
Nobeyama Millimeter Array (NMA)	Nobeyama, Japan	6 10 m dishes	100, 150, 230	35 56 N, 138 29 E, 1350
Plateau de Bure Interferometer	Plateau de Bure, Fr.	5 15 m dishes	80 - 115 210 - 245	44 38 N, 05 54 E, 2560

Major ground-based astronomical telescopes (cont.)

Radio telescopes

Name	Location	Aperture	Frequency Range (GHz)	Latitude, Longitude, Altitude
The Large Millimeter Telescope (LMT)**	Sierra Negra, Mexico	50 m dish	75 - 300	18 59 N, 97 19 W, 4560
Berkeley Illinois Maryland Association (BIMA)	Hat Creek, CA	10 6.1 m dishes	70 - 116 210 - 270	40 49 N, 121 28 W, 1043
Australia Telescope Compact Array, Culgoora	New South Wales, Aus.	6 22 m dishes	$\lambda: 3, 12$ mm	30 19 S, 149 34 E, 217
The Five College Radio Astronomy Observatory	New Salem, MA	14 m dish	40 - 300	42 24 N, 72 21 W, 314
DRAO Synthesis Telescope	Penticton, B.C.	7 9 m dishes	0.4, 1.4	49 19 N, 119 37 W, 545

Size: Clear aperture in centimeters.

Date: date of completion ceremony, “first light”, or first scientific use.

Latitude: in degrees and arc minutes.

Longitude: in degrees and arc minutes.

Altitude: in meters above sea level.

* Declination range: -2° to $+38^\circ$

** under construction; completion 2003.

The Hubble Space Telescope (HST)
(Material for this section was taken from the Hubble Space Telescope Primer, 2002.)

The Hubble Space Telescope (HST) is managed by the Space Telescope science Institute (STScI):

Space Telescope Science Institute
3700 San Martin Drive
Baltimore, MD 21218
USA
Tel.: (410)-338-4700
Fax: (410)-338-4767
E-mail: user@stsci.edu

To allow European astronomers to make use to the Hubble Space Telescope, the European Space Agency (ESA) has established the Space Telescope-European Coordinating Facility (ECF). The address of the SF-ECF:

Space Telescope–European Coordinating Facility
European Southern Observatory
Karl-Schwarzschild-Str. 2
D-8046 Garching bei München
Federal Republic of Germany
Tel: + 49-89-320 06-291
Fax: + 49-89-320 06-480
E-mail: stdesk@eso.org (ST Desk)

An overview of the HST dealing with the performance of the telescope and instruments and plans for observations and data reduction and analysis can be found in the NASA publication, *The Space Telescope Observatory*, special session of commission, 44, IAU 18th General Assembly, 1982, NASA CP-2244.

Description of the Hubble Space Telescope (HST)

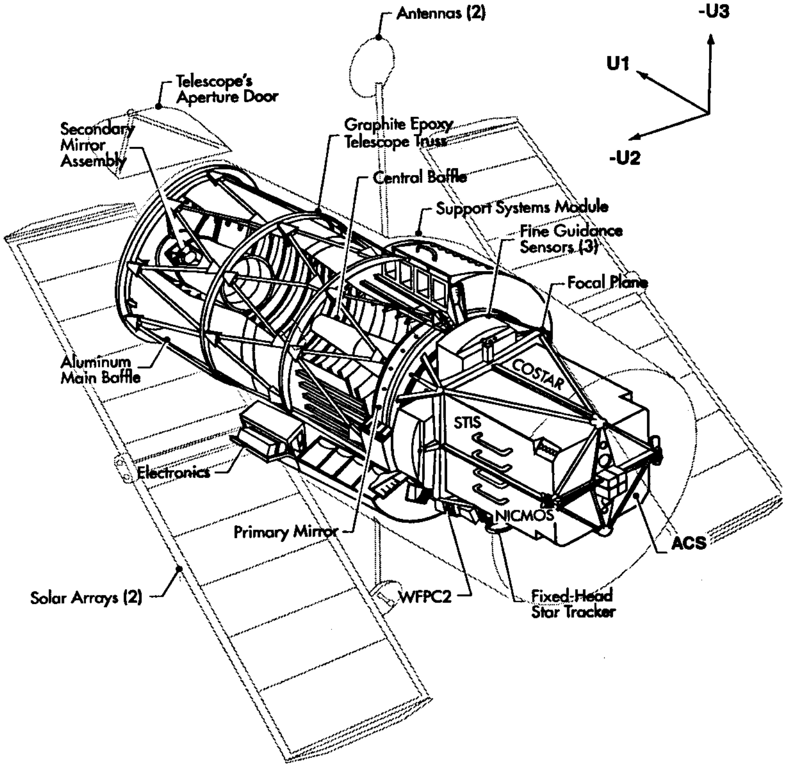

HST nominal orbital parameters

Altitude	600 km
Inclination	28°.5
Orbital period	97 min
Orbital precession period	54 days

HST Optical Characteristics and Performance

Design	Ritchey-Chretien Cassegrain
Aperture	2.4 m
Collecting area	39,000 cm^2
Wavelength Coverage	From 1100 Å(MgF_2 limited)
	To $\sim$ 3 microns (self-emission limited)
Focal Ratio	$f/24$
Plate Scale (on axis)	3.58 arcsec/mm
PSF FWHM at 5000 Å	0.043 arcsec
Encircled Energy within 0.1″ at 5000 Å	87% (60%-80% at the detectors)

Because each SI unique characteristics, the actual encircled energy is instrument dependent, and may also vary with observing techniques.

Description of the Hubble Space Telescope (cont.)

The HST field of view

The scale in arc seconds is indicated.

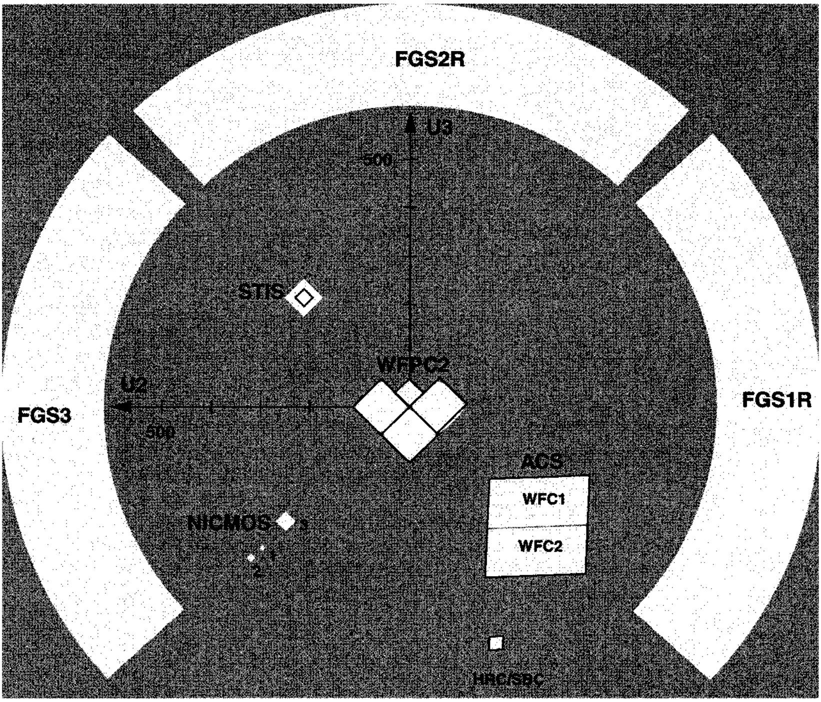

- The AdvancedCamera for Surveys (ACS)
- The Fine Guidance Sensor (FGS1R)
- The Near Infrared Camera and Multi-Object Spectrometer (NICMOS)
- The Space Telescope Imaging Spectrograph (STIS)
- The Wide Field and Planetary Camera 2 (WFPC2)

Description of the Hubble Space Telescope (cont.)

HST Instrument Capabilities: Direct Imaging

SI	Field of View [arcsec]	Projected Pixel Spacing on Sky [arcsec]	Wavelength Range [Å]	Magnitude Limit[2]
ACS/WFC[3]	202×202	∼ 0.05	3700-11,000	28.7
ACS/HRC	29×26	∼ 0.027	2000-11,000	28.2
ACS/SBC	35×31	∼ 0.032	1150-1700	22.6
NICMOS/NIC1	11×11	0.043	8000-19,000	24.5
NICMOS/NIC2	19×19	0.076	8000-25,000	25.0
NICMOS/NIC3	51×51	0.20	8000-25,000	25.0
STIS/CCD	52×52	0.05	2500-11,000	28.5
STIS/NUV	25×25	0.024	1650-3100	24.8
STIS/FUV	25×25	0.024	1150-1700	24.4
WFPC2[4]	150×150	0.10	1200-11,000	27.5
	35×35	0.0455	1200–11,000	27.8

HST Instrument Capabilities: Slit Spectroscopy

SI	Projected Aperture Size	Resolving Power[5]	Wavelength Range [Å]	Magnitude Limit[2]
STIS[6]	$52'' \times (0.05-2)''$ [optical]	**Echelles:**		
		∼ 100, 000	1150−3100	11.8–13.0
	$(25-28)'' \times (0.05-2)''$ [UV first order]	∼ 30, 000	1150−3100	12.7–15.2
		Prism:		
		∼ 150	1150−3100	22.1
	$(0.1-02)'' \times (0.025-0.2)''$ [UV echelle]	**First order:**		
		∼ 8000	1150−10,300	15.2–16.1-19.5
		∼ 700	1150−10,300	18.6–20.1-22.4

Description of the Hubble Space Telescope (cont.)

HST Instrument Capabilities: Slitless Spectroscopy

SI	Field of View [arcsec]	Projected Pixel Spacing on Sky [arcsec]	Resolving Power	Wavelength Range [Å]	Magnitude Limit[2]
ACS/WFC grism G800L	202×202	∼ 0.05	∼ 100	5500−11000	25
ACS/HRC grism G800L	29×26	∼ 0.027	∼ 100	5500−11000	24.2
ACS/HRC prism PR200L	29×26	∼ 0.027	∼ 100	2000−4000	24.7
ACS/SBC prism PR130L	35×31	∼ 0.032	∼ 100	1150−1700	21.5
NICMOS[7]	51×51	0.2	200	8000−25,000	21,20,16
STIS[7]	52×52	0.05	∼ 700 − 8000	2000−11,000	See slit
	25×25	0.024	∼ 700 − 8000	1150−3100	spectroscopy above
WFPC2[7]	150×150	0.1	∼ 100	3700−9800	25

HST Instrument Capabilities: Positional Astrometry

SI	Field of View	Precision (per observation)	Wavelength Range (Å)	Magnitude
FGSIR	69 square arcmin	1-2 mas	4700−7100	< 14.5
		3 mas		< 17.0

HST Instrument Capabilities: Binary Star Resolution and Measurements

SI	Field of View	Separation [mas]	Accuracy [mas]	Delta Magnitude (max)	Primary Star Magnitude
FGSIR	aperture	8	1	0.6	< 14.5
	center	10	1	1.0	< 14.5
	$5'' \times 5''$	15	1	1.0	< 15.5
	IFOV	20	1	2.5	< 14.5
		30	1	4.0	< 15.0

Description of the Hubble Space Telescope (cont.)

Notes for tables

[1] WFPC2 and NICMOS have polarimetric imaging capabilities. STIS and NICMOS have coronographic capabilities.

[2] Limiting V magnitude for an unreddened AO V star in order to achieve a signal-to-noise ratio of 5 in an exposure time of 1 hour assuming low-background conditions.

The limiting magnitude for imaging in the visual is strongly affected by the sky background; under normal observing conditions, the limiting magnitude can be about 0.5 brighter than listed here. Please note that low-sky conditions limit flexibility in scheduling and are not compatible with observing in the CVZ. Single entries refer to wavelengths near the center of the indicated wavelength range. STIS direct imaging entries assume use of a clear filter for the CCD and the quartz filter for the UV (for sky suppression). For STIS spectroscopy to achieve the specified signal-to-noise ratio per wavelength pixel a $0.5''$ slit, multiple value are given corresponding to 1300, 2800 and 6000 Å, respectively (if in range).

The ACS/WFC, ACS/HRC and WFPC2 entries assume filter F606W. The WFPC2 Charge Transfer Efficiency (CTE) loses are negligible for this filter, due to the significant sky background accumulated over 3600 sec in F606W. However, note that WFPC2 images of faint point sources with little sky background can experience significant CTE losses.

[3] With ramp filters, the FOV is $\sim 40'' \times 70''$ for the ACS/WFC.

[4] The WFPC2 has four CCD chips that are exposed simultaneously. Three are "wide-field" chips, each covering a $75''\times 75''$ field and arranged in an "L" shape, and the fourth is a "planetary" chip covering a $35''\times 35''$ field.

[5] The resolving power is lambda/resolution; for STIS it is $\lambda/2\Delta\lambda$ where $\Delta\lambda$ is the dispersion scale in Ångstroms/pixel.

[6] The $25''$ or $28''$ first order slits are for the MAMA detectors, the $52''$ slit is for the CCD. The R $\sim$ 150 entry for the prism on the NUV-MAMA is given for 2300 Å.

[7] All STIS modes can be operated in a slitless manner by replacing the slit by a clear aperture. WFPC2 has a capability of obtaining low-resolution spectra by placing a target successively at various locations in the WFPC2 linear ramp filter. STIS also has a prism for use in the UV. NICMOS has a grism for use in NIC3.

Glossary of astronomical terms

---

aberration: the apparent angular displacement of the observed position of a celestial object from its *geometric position*, caused by the finite velocity of light in combination with the motions of the observer and of the observed object. (See *aberration, planetary.*)

aberration, annual: the component of stellar aberration (see *aberration, stellar*) resulting from the motion of the Earth about the Sun.

aberration, diurnal: the component of stellar aberration (see *aberration, stellar*) resulting from the observer's diurnal motion about the center of the Earth.

aberration, E-terms of: terms of annual aberration (*see aberration, annual*) depending on the *eccentricity* and longitude of *perihelion* of the Earth.

aberration, elliptic: see *aberration, E-terms of.*

aberration, planetary: the apparent angular displacement of the observed position of a celestial body produced by motion of the observer (see *aberration, stellar*) and the actual motion of the observed object (see *correction for light-time*).

aberration, secular: the component of stellar aberration (see *aberration, stellar*) resulting from the essentially uniform and rectilinear motion of the entire solar system in space. Secular aberration is usually disregarded.

aberration, stellar: the apparent angular displacement of the observed position of a celestial body resulting from the motion of the observer. Stellar aberration is divided into diurnal, annual and secular components (see *aberration, diurnal; aberration, annual; aberration, secular*).

altitude: the angular distance of a celestial body above or below the *horizon*, measured along the great circle passing through the body and the *zenith.* Altitude is 90° minus *zenith distance.*

aphelion: the point in a planetary *orbit* that is at the greatest distance from the Sun.

apparent place: the position on a *celestial sphere*, centered at the Earth, determined by removing from the directly observed position of a celestial body the effects that depend on the *topocentric* location of the observer; i.e., *refraction*, diurnal aberration (see *aberration, diurnal*) and geocentric (diurnal) *parallax.* Thus the position at which the object would actually be seen from the center of the Earth. displaced by planetary aberration (except the diurnal part–see *aberration, planetary* and *aberration, diurnal*) and referred to the *true equator and equinox.*

apparent solar time: the measure of time based on the diurnal motion of the true Sun. The rate of diurnal motion undergoes seasonal variation because of the *obliquity* of the *ecliptic* and because of the *eccentricity* of the Earth's *orbit*. Additional small variations result from irregularities in the rotation of the Earth on its axis.

astrometric ephemeris: an ephemeris of a solar system body in which the tabulated positions are essentially comparable to catalog *mean places* of stars at a *standard epoch*. An astrometric position is obtained by adding to the *geometric position*, computed from gravitational theory, the correction for *light-time*. Prior to 1984, the E-terms of annual aberration (see *aberration, annual* and *aberration, E-terms of*) were also added to the geometric position.

astronomical coordinates: the longitude and latitude of a point on the Earth relative to the *geoid*. These coordinates are influenced by local gravity anomalies (see *zenith*,)

astronomical unit (AU): the radius of a circular orbit in which a body of negligible mass, and free of perturbations, would revolve around the Sun in $2\pi/k$ days, where k is the *gaussian gravitational constant*. This is slightly less than the semimajor *axis* of the Earth's *orbit*.

atomic second: see *second, Systeme International*.

augmentation: the amount by which the apparent *semidiameter* of a celestial body, as observed from the surface of the Earth, is greater than the semidiameter that would be observed from the center of the Earth.

azimuth: the angular distance measured clockwise along the *horizon* from a specified reference point (usually north) to the intersection with the great circle drawn from the *zenith* through a body on the *celestial sphere*.

barycenter: the center of mass of a system of bodies; e.g., the center of mass of the solar system or the Earth—Moon system.

barycentric dynamical time (TDB): the independent argument of ephemerides and equations of motion that are referred to the *barycenter* of the solar system. A family of time scales results from the transformation by various theories and metrics of relativistic theories of *terrestrial dynamical time* (TDT). TDB differs from TDT only by periodic variations. In the terminology of the general theory of relativity, TDB may be considered to be a coordinate time. (See *dynamical time*.)

catalog equinox: the intersection of the *hour circle* of zero *right ascension* of a star catalog with the *celestial equator*. (See *dynamical equinox* and *equator*.)

celestial ephemeris pole: the reference pole for *nutation* and *polar motion*; the axis of figure for the mean surface of a model Earth in which the free motion has zero amplitude. This pole has no nearly-diurnal nutation with respect to a space-fixed or Earth-fixed coordinate system.

celestial equator: the projection onto the *celestial sphere* of the Earth's *equator.* (See *mean equator and equinox* and *true equator and equinox.*)

celestial pole: either of the two points projected onto the *celestial sphere* by the extension of the Earth's axis of rotation to infinity.

celestial sphere: an imaginary sphere of arbitrary radius upon which celestial bodies may be considered to be located. As circumstances require, the celestial sphere may be centered at the observer, at the Earth's center, or at any other location.

conjunction: the phenomenon in which two bodies have the same apparent celestial longitude (see *longitude, celestial*) or *right ascension* as viewed from a third body. Conjunctions are usually tabulated as *geocentric* phenomena, however. For Mercury and Venus, geocentric inferior conjunction occurs when the planet is between the Earth and Sun and superior conjunction occurs when the Sun is between the planet and Earth.

constant of aberration (k = 20".49552, J2000.0): the ratio of the mean orbital speed of the Earth to the speed of light.

constellation: a grouping of stars, usually with pictorial or mythical associations, that serves to identify an area of the *celestial sphere.* Also one of the precisely defined areas of the celestial sphere, associated with a grouping of stars, that the International Astronomical Union has designated as a constellation.

coordinated universal time (UTC): the time scale available from broadcast time signals. UTC differs from TAI (*see international atomic time*) by an integral number of seconds; it is maintained within ±0.90 seconds of UT1 (*see universal time*) by the introduction of one second steps (leap seconds).

culmination: passage of a celestial object across the observer's *meridian*, also called 'meridian passage'. More precisely culmination is the passage through the point of greatest *altitude* in the diurnal path. Upper culmination (also called 'culmination above pole' for circumpolar stars and the Moon) or transit is the crossing closer to the observer's *zenith.* Lower culmination (also called 'culmination below pole' for circumpolar stars and the Moon) is the crossing farther from the zenith.

day: an interval of 86 400 SI seconds (*see second, Systeme International*), unless otherwise indicated.

day numbers: quantities that facilitate hand calculations of the reduction of *mean place* to *apparent place.* Besselian day numbers depend solely on the Earth's position and motion; second-order day numbers, used in high precision reductions, depend on the positions of both the Earth and the star.

declination: angular distance on the *celestial sphere* north or south of the *celestial equator.* It is measured along the *hour circle* passing through the celestial object. Declination is usually given in combination with *right ascension* or *hour angle.*

defect of illumination: the angular amount of the observed lunar or planetary disk that is not illuminated to an observer on the Earth.

deflection of light: the angle by which the apparent path of a photon is altered from a straight line by the gravitational field of the Sun. The path is deflected radially away from the Sun by up to 1.″75 at the Sun's limb. Correction for this effect, which is independent of wavelength, is included in the reduction from *mean place* to *apparent place.*

deflection of the vertical: the angle between the astronomical vertical and the geodetic vertical (see *zenith; astronomical coordinates; geodetic coordinates.*)

Delta T (ΔT): the difference between *dynamical time* and *universal time*; specifically the difference between *terrestrial dynamical time* (TDT) and UT1: $\Delta T = TDT - UT1$.

direct motion: for orbital motion in the solar system, motion that is counterclockwise in the orbit as seen from the north pole of the *ecliptic;* for an object observed on the celestial sphere, motion that is from west to east, resulting from the relative motion of the object and the Earth.

ΔUT1: the predicted value of the difference between UT1 and UTC, transmitted in code on broadcast time signals: $\Delta UT1 = UT1 - UTC$. (See *universal time* and *coordinated universal time.*)

dynamical equinox: the ascending *node* of the Earth's mean *orbit* on the Earth's *equator; i.e.*, the intersection of the *ecliptic* with the *celestial equator* at which the Sun's *declination* is changing from south to north (See *catalog equinox* and *equinox.*)

dynamical form factor ($J_2 = 0.00108263$): the second zonal harmonic coefficient in the spherical harmonic expansion of the Earth's gravitational potential.

dynamical time: the family of time scales introduced in 1984 to replace *ephemeris time* as the independent argument of dynamical theories and ephemerides. (See *barycentric dynamical time* and *terrestrial dynamical time.*)

eccentric anomaly: in undisturbed elliptic motion, the angle measured at the center of the ellipse from *pericenter* to the point on the circumscribing auxiliary circle from which a perpendicular to the major axis would intersect the orbiting body. (See *mean anomaly* and *true anomaly.*)

eccentricity: a parameter that specifies the shape of a conic section; one of the standard elements used to describe an elliptic *orbit* (see *elements, orbital.*)

eclipse: the obscuration of a celestial body caused by its passage through the shadow cast by another body.

eclipse, annular: a solar *eclipse* (see *eclipse, solar*) in which the solar disk is never completely covered but is seen as an annulus or ring at maximum eclipse. An annular eclipse occurs when the apparent disk of the Moon is smaller than that of the Sun.

eclipse, lunar: an *eclipse* in which the Moon passes through the shadow cast by the Earth. The eclipse may be total (the Moon passing completely through the Earth's *umbra,*) partial (the Moon passing partially through the Earth's umbra at maximum eclipse), or penumbral (the Moon passing only through the Earth's *penumbra*).

eclipse, solar: an *eclipse* in which the Earth passes through the shadow cast by the Moon. It may be total (observer in the Moon's *umbra*), partial (observer in the Moon's *penumbra*), or annular (see *eclipse, annular*).

ecliptic: the mean plane of the Earth's *orbit* around the Sun.

elements, Besselian: quantities tabulated for the calculation of accurate predictions of an *eclipse* or *occulation* for any point on or above the surface of the Earth.

elements, orbital: parameters that specify the position and motion of a body in *orbit* (see *osculating elements* and *mean elements.*)

elongation, greatest: the instants when the *geocentric* angular distances of Mercury and Venus are at a maximum from the Sun.

elongation (planetary): the *geocentric* angle between a planet and the Sun, measured in the plane of the planet, Earth and Sun. Planetary elongations are measured from 0° to 180°, east or west of the Sun.

elongation (satellite): the *geocentric* angle between a satellite and its primary, measured in the plane of the satellite, planet and Earth. Satellite elongations are measured from 0° east or west of the planet.

ephemeris hour angle: an *hour angle* referred to the *ephemeris meridian.*

ephemeris longitude: longitude (see *longitude, terrestrial*) measured eastward from the *ephemeris meridian.*

ephemeris meridian: a fictitious *meridian* that rotates independently of the Earth at the uniform rate implicitly defined by *terrestrial dynamical time* (TDT). The ephemeris meridian is 1.002 738ΔT east of the Greenwich meridian, where $\Delta T = \text{TDT} - \text{UT1}$.

ephemeris time (ET): the time scle used prior to 1984 as the independent variable in gravitational theories of the solar system. In 1984, ET was replaced by *dynamical time.*

ephemeris transit: the passage of a celestial body or point across the *ephemeris meridian.*

epoch: an arbitrary fixed instant of time or date used as a chronological reference datum for calendars, celestial reference systems, or orbital motions.

Besselian epoch = 1900.0 + (JD− 241 5020.31352)/365.242198781.
B1950.0 is defined to be 1949 Dec 31 22:09 UT.
Julian epoch = 2000.0 + (JD− 2451545.0)/365.25, where JD is the Julian date.
J2000.0 is defined to be 2000 January 1.5 in the TT timescale.

equation of center: in elliptic motion the *true anomaly* minus the *mean anomaly.* It is the difference between the actual angular position in the elliptic *orbit* and the position the body would have if its angular motion were uniform.

equation of the equinoxes: the *right ascension* of the mean *equinox* (see *mean equator and equinox* referred to the *true equator and equinox*; apparent *sidereal time* minus mean sideral time. (See *apparent place* and *mean place.*)

equation of time: the *hour angle* of the true Sun minus the hour angle of the *fictitious mean sun;* alternatively, *apparent solar time* minus *mean solar time.*

equator: the great circle on the surface of a body formed by the intersection of the surface with the plane passing through the center of the body perpendicular to the axis of rotation. (See *celestial equator.*)

equinox: either of the two points on the *celestial sphere* at which the *ecliptic* intersects the *celestial equator;* also the time at which the Sun passes through either of these intersection points; i.e., when the apparent longitude (see *apparent place* and *longitude, celestial*) of the Sun is 0° or 180°. (See *catalog equinox* and *dynamical equinox* for precise usage.)

ficititious mean Sun: an imaginary body introduced to define *mean solar time;* essentially the name of a mathematical formula that defined mean solar time. This concept is no longer used in high precision work.

flattening: a parameter that specifies the degree by which a planet's figure differs from that of a sphere,; the ratio $f = (a - b)/a$, where a is the equatorial radius and b is the polar radius.

Gaussian gravitational constant ($k = 0.017\,202\,098\,95$): the constant defining the astronomical system of units of length (*astronomical unit*), mass (solar mass) and time (*day*), by means of Kepler's third law. The dimensions of k^2 are those of Newton's constant of gravitation: $\mathrm{L^3M^{-1}T^{-2}}$.

geocentric: with reference to, or pertaining to, the center of the Earth.

geocentric coordinates: the latitude and longitude of a point on the Earth's surface relative to the center of the Earth; also celestial coordinates given with respect to the center of the Earth. (See *zenith; latitude, terrestrial; longitude, terrestrial.*)

geodetic coordinates: the latitude and longitude of a point on the Earth's surface determined from the geodetic vertical (normal to the specified spheroid). (See *zenith; latitude, terrestrial; longitude, terrestrial.*)

geoid: an equipotential surface that coincides with mean sea level in the open ocean. On land it is the level surface that would be assumed by water in an imaginary network of frictionless channels connected to the ocean.

geometric position: the *geocentric* position of an object on the *celestial sphere* referred to the *true equator and equinox*, but without the displacement due to planetary aberration. (See *apparent place; mean place; aberration, planetary.*)

Greenwich sidereal date (GSD): the number of *sidereal days* elapsed at Greenwich since the beginning of the Greenwich sidereal day that was in progress at *Julian date* 0.0.

Greenwich sidereal day number: the integral part of the *Greenwich sidereal date.*

Gregorian calendar: the calendar introduced by Pope Gregory XIII in 1582 to replace the *Julian calendar*; the calendar now used as the civil calendar in most countries. Every year that is exactly divisible by four is a leap year, except for centurial years, which must be exactly divisible by 400 to be leap years. Thus 2000 is a leap year, but 1900 and 2100 are not leap years.

heliocentric: with reference to, or pertaining to, the center of the Sun.

horizon: a plane perpendicular to the line from an observer to the *zenith.* The great circle formed by the intersection of the *celestial sphere* with a plane perpendicular to the line from an observer to the zenith is called the astronomical horizon.

horizontal parallax: the difference between the *topocentric* and *geocentric* positions of an object, when the object is on the astronomical *horizon.*

hour angle: angular distance on the *celestial sphere* measured westward along the *celestial equator* from the *meridian* to the *hour circle* that passes thorugh a celestial object.

hour circle: a great circle on the *celestial sphere* that passes through the *celestial poles* and it therefore perpendicular to the *celestial equator.*

inclination: the angle between two planes or their poles; usually the angle between an orbital plane and a reference plane; one of the standard orbital elements (see *elements, orbital*) that specifies the orientation of an *orbit.*

international atomic time (TAI): the continuous scale resulting from analyses by the Bureau International des Poids et Mésures of atomic time standards in many countries. The fundamental unit of TAI is the SI second (see *second*, *Systeme International*), and the epoch is 1958 January 1.

invariable plane: the plane through the center of mass of the solar system perpendicular to the angular momentum vector of the solar system.

irradiation: an optical effect of contrast that makes bright objects viewed against a dark background appear to be larger than they really are.

Julian calendar: the calendar introduced by Julius Caesar in 46 BC to replace the Roman calendar. In the Julian calendar a common year is defined to comprise 365 days, and very fourth year is leap year comprising 366 days. The Julian calendar was superseded by the *Gregorian calendar.*

Julian date (JD): the interval of time in days and fraction of a day since 1 January 4713 BC, Greenwich noon, *Julian proleptic calendar.* In precise work the time scale, e.g., *dynamical time* or *universal time*, should be specified.

Julian date, modified (MJD): the Julian date minus 240 0000.5.

Julian day number (JD): the integral part of the *Julian date.*

Julian proleptic calendar: the calendric system employing the rules of the *Julian calendar*, but extended and applied to dates preceding the introduction of the Julian calendar.

Julian year: a period of 365.25 days. This period served as the basis for the *Julian calendar.*

Laplacian plane: for planets *see invariable plane;* for a system of satellites the fixed plane relative to which the vector sum of the disturbing forces has no orthogonal component.

latitude, celestial: angular distance on the *celestial sphere* measured north or south of the *ecliptic* along the great circle passing through the poles of the ecliptic and the celestial object.

latitude, terrestrial: angular distance on the Earth measured north or south of the *equator* along the *meridian* of a geographic location.

librations: variations in the orientation of the Moon's surface with respect to an observer on the Earth. Physical librations are due to variations in the rate at which the Moon rotates on its axis. The much larger optical librations are due to variations in the rate of the Moon's orbital motion, the *obliquity* of the Moon's *equator* to its orbital plane, and the diurnal changes of geometric perspective of an observer on the Earth's surface.

light-time: the interval of time required for light to travel from a celestial body to the Earth. During this interval the motion of the body in space causes an angular displacement of its *apparent place* from its *geometric position* (see *aberration, planetary*).

light year: the distance that light traverses in a vacuum during one year.

local sidereal time: the local *hour angle* of a *catalog equinox.*

longitude, celestial: angular distance on the *celestial sphere* measured eastward along the *ecliptic* from the *dynamical eqinox* to the great circle passing through the poles of the ecliptic and the celestial object.

longitude, terrestrial: angular distance measured along the Earth's *equator* from the Greenwich *meridian* to the meridian of a geographic location.

lunar phases: cyclically recurring apparent forms of the Moon. New Moon, First Quarter, Full Moon and Last Quarter are defined as the times at which the excess of the apparent celestial longitude (see *longitude, celestial*) of the Moon over that of the Sun is $0°, 90°, 180°$ and $270°$, respectively.

lunation: the period of time between two consecutive New Moons.

magnitude, stellar: a measure on a logarithmic scale of the brightness of a celestial object considered as a point source.

magnitude of a lunar eclipse: the fraction of the lunar diameter obscured by the shadow of the Earth at the greatest phase of a lunar eclipse (see *eclipse, lunar*), measured along the common diameter.

magnitude of a solar eclipse: the fraction of the solar diameter obscured by the Moon at the greatest phase of a solar eclipse (*see eclipse, solar*), measured along the common diameter.

mean anomaly: in undisturbed elliptic motion, the product of the *mean motion* of an orbiting body and the interval of time since the body passed *pericenter.* Thus the mean anomaly is the angle from pericenter of a hypothetical body moving with a constant angular speed that is equal to the mean motion. (See *true anomaly* and *eccentric anomaly.*)

mean distance: the *semimajor axis* of an elliptic *orbit.*

mean elements: elements of a adopted reference *orbital* (see *elements, orbital*) that approximates the actual, perturbed orbit. Mean elements may serve as the basis for calculating *perturbations.*

mean equator and equinox: the celestial reference system determined by ignoring small variations of short period in the motions of the *celestial equator.* Thus the mean equator and equinox are affected only by *precession.* Positions in star catalogs are normally referred to the mean catalog equator and equinox (see *catalog equinox*) of a *standard epoch.*

mean motion: in undisturbed elliptic motion, the constant angular speed required for a body to complete one revolution in a *orbit* of a specified *semimajor axis.*

mean place: the coordinates, referred to the *mean equator and equinox* of a *standard epoch*, of an object on the *celestial sphere* centered at the Sun. A mean place is determined by removing from the directly observed position the effects of *refraction*, geocentric and stellar paralax, and stellar aberration (see *aberration, stellar*), and by referring the coordinates to the mean equator and equinox of a standard epoch. In compiling star catalogs it has been the practice not to remove the secular part of stellar aberration (see *aberration, secular*). Prior to 1984, it was additionally the practice not to remove the elliptic part of annual aberration (see *aberration, annual* and *aberration, E-terms of*).

mean solar time: a measure of time based conceptually on the diurnal motion of the *fictitious mean sun*, under the assumption that the Earth's rate of rotation is constant.

mean Sun: a fictitious Sun used to provide a standard measurements of time; it moves along the celestial equator at a uniform rate equal to the average motion of the actual Sun (see fictitious mean Sun).

meridian: a great circle passing through the *celestial poles* and through the *zenith* of any location of Earth. For planetary observations a meridian is half the great circle passing thorough the planet's poles and through any location on the planet.

moonrise, moonset: the times at which the apparent upper limb of the Moon is on the astronomical *horizon*; i.e., when the true *zenith distance*, referred to the centre of the Earth, of the central point of the disk is $90°34' + s - \pi$, where s is the Moon's semidiameter, π is the *horizontal parallax*, and $34'$ is the adopted value of horizontal *refraction.*

nadir: the point on the *celestial sphere* diametrically opposite to the *zenith.*

node: either of the points on the *celestial sphere* at which the plane of an *orbit* intersects a reference plane. The position of a node is one of the standard orbital elements (see *elements, orbital*) used to specify the orientation of an orbit.

nutation: the short-period oscillations in the motion of the pole of rotation of a freely rotating body that is undergoing torque from external gravitational forces. Nutation of the Earth's pole is discussed in terms of components in *obliquity* and longitude (see *longitude, celestial*).

obliquity: in general the angle between the equatorial and orbital planes of a body or, equivalently, between the rotational and orbital poles. For the Earth the obliquity of the *ecliptic* is the angle between the planes of the *equator* and the ecliptic.

occultation: the obscuration of one celestial body by another of greater apparent diameter; especially the passage of the Moon in front of a star or planet, or the disappearance of a satellite behind the disk of its primary. If the primary source of illumination of a reflecting body is cut off by the occultation, the phenomenon is also called an *eclipse*. The occultation of the Sun by the Moon is a solar eclipse (see *eclipse, solar*).

opposition: a configuration of the Sun, Earth and a planet in which the apparent *geocentric* longitude (see *longitude, celestial*) of the planet differs by 180° from the apparent geocentric longitude of the Sun.

orbit: the path in space followed by a celestial body.

osculating elements: a set of parameters (see *elements, orbital*) that specifies the instantaneous position and velocity of a celestial body in its perturbed *orbit*. Osculating elements describe the unperturbed (two-body) orbit that the body would follow if *perturbations* were to cease instantaneously.

parallax: the difference in apparent direction of an object as seen from two different locations; conversely the angle at the object that is subtended by the line joining two designated points. Geocentric (diurnal) parallax is the difference in direction between a *topocentric* observation and a hypothetical *geocentric* observation. Heliocentric or annual parallax is the difference between hypothetical geocentric and *heliocentric* observations; it is the angle subtended at the observed object by the *semimajor axis* of the Earth's *orbit*. (See also *horizontal parallax*.)

parsec: the distance at which one *astronomical unit* subtends an angle of one second of arc; equivalently the distance to an object having an annual *parallax* of one second of arc.

peculiar velocity: random motions of galaxies relative to the mean Hubble flow.

penumbra: the portion of a shadow in which light from an extended source is partially but not completely cut off by an intervening body; the area of partial shadow surrounding the *umbra.*

pericenter: the point in an *orbit* that is nearest to the center of force. (See *perigee* and *perihelion.*)

perigee: the point at which a body in *orbit* around the Earth most closely approaches the Earth. Perigee is sometimes used with reference to the apparent orbit of the Sun around the Earth.

perihelion: the point at which a body in *orbit* around the Sun most closely approaches the Sun.

period: the interval of time required to complete one revolution in an *orbit* or one cycle of a periodic phenomenon, such as a cycle of *phases.*

perturbations: deviations between the actual *orbit* of a celestial body and an assumed reference orbit; also the forces that cause deviations between the actual and reference orbits. Perturbations, according to the first meaning, are usually calculated as quantities to be added to the coordinates of the reference orbit to obtain the precise coordinates.

phase: the ratio of the illuminated area of the apparent disk of a celestial body to the area of the entire apparent disk taken as a circle. For the Moon, phase designations (see *lunar phases*) are defined by specific configurations of the Sun, Earth and Moon. For eclipses phase designations (total, partial, penumbral, etc.) provide general descriptions of the phenomena (see *eclipse solar; eclipse, annular; eclipse, lunar.*)

phase angle: the angle measured at the center of an illuminated body between the light source and the observer.

photometry: a measurement of the intensity of light usually specified for a specific frequency range.

planetocentric coordinates: coordinates for general use, where the z-axis is the mean axis of rotation, the x-axis is the intersection of the planetary *equator* (normal to the z-axis through the center of mass) and an arbitrary prime *meridian*, and the y-axis completes a right-hand coordinate system. Longitude (see *longitude, celestial*) of a points is measured positive to the prime meridian as defined by rotational elements. Latitude (see *latitude, celestial*) of a point is the angle between the planetary equator and a line of the center of mass. The radius is measured from the center of mass to the surface point.

planetographic coordinates: coordinates for cartographic purposes dependent on an equipotential surface as a reference surface. Longitude (see *longitude, celestial*) of a point is measured in the direction opposite to the rotation (positive to the west for direct rotation) from the cartographic position of the prime *meridian* defined by a clearly observable surface feature. Latitude (see *latitude, celestial*) of a point is the angle between the planetary *equator* (normal to the z-axis and through the center of mass) and normal to the reference surface at the point. The height of a point is specified as the distance above a point with the same longitude and latitude on the reference surface.

polar motion: the irregularly varying motion of the Earth's pole of rotation with respect to the Earth's crust. (See *celestial ephemeris pole.*)

precession: the uniformly progressing motion of the pole of rotation of a freely rotating body undergoing torque from external gravitational forces. In the case of the Earth, the component of precession caused by the Sun and Moon acting on the Earth's equatorial bulge is called lunisolar precession; the component caused by the action of the planets is called planetary precession. The sum of lunisolar and planetary precession is called general precession. (See *nutation.*)

proper motion: the projection onto the *celestial sphere* of the space motion of a star relative to the solar system; thus the transverse component of the space motion of a star with respect to the solar system. Proper motion is usually tabulated in star catalogs as changes in *right ascension* and *declination* per year or century.

quadrature: a configuration in which two celestial bodies have apparent longitudes (see *longitude, celestial*) that differ by 90° as viewed from a third body. Quadratures are usually tabulated with respect to the Sun as viewed from the center of the Earth.

radial velocity: the rate of change of the distance to an object.

refraction, astronomical: the change in direction of travel (bending) of a light ray as it passes obliquely through the atmosphere. As a result of refraction the observed *altitude* of a celestial object is greater than its geometric altitude. The amount of refraction depends on the altitude of the object and on atmospheric conditions.

retrograde motion: for orbital motion in the solar system, motion that is clockwise in the *orbit* as seen from the north pole of the *ecliptic*; for an object observed on the *celestial sphere*, motion that is from east to west, resulting from the relative motion of the object and the Earth. (See *direct motion.*)

right ascension: angular distance on the *celestial sphere* measured eastward along the *celestial equator* from the *equinox* to the *hour circle* passing through the celestial object. Right ascension is usually given in combination with *declination.*

second, Systeme International (SI): the duration of 9 192 631 770 cycles of radiation corresponding to the transition between two hyperfine levels of the ground state of cesium 133.

selenocentric: with reference to, or pertaining to, the center of the Moon.

semidiameter: the angle at the observer subtended by the equatiorial radius of the Sun, Moon or a planet.

semimajor axis: half the length of the major axis of an ellipse; a standard element used to describe an elliptical *orbit* (see *elements, orbital*).

sidereal day: the interval of time between two consecutive *transists* of the *catalog equinox.* (See *sidereal time.*)

sidereal hour angle: angular distance on the *celestial sphere* measured westward along the *celestial equator* from the *catalog equinox* to the *hour circle* passing thorugh the celestial object. It is equal to 360° minus *right ascension* in degrees.

sidereal time: the measure of time defined by the apparent diurnal motion of the *catalog equinox*; hence a measure of the rotation of the Earth with respect to the stars rather than the Sun.

solstice: either of the two points on the *ecliptic* at which the apparent longitude (see *longitude, celestial*) of the Sun is 90° or 270°; also the time at which the Sun is at either point.

spectral types or classes: categorization of stars according to their spectra, primarily due to differing temperatures of the atmosphere. From hottest to coolest, the spectral types are O, B, A, F, G, K and M.

standard epoch: a date and time that specific the reference system to which celestial coordinates are referred. Prior to 1984 coordinates of star catalogs were commonly referred to the *mean equator and equinox* of the beginning of a Besselian year (see *year, Besselian*). Beginning with 1984 the *Julian year* has been used, as denoted by the prefix J, e.g., J2000.0.

stationary point (of a planet): the position at which the rate of change of the apparent *right ascension* (see *apparent place*) of a planet is momentarily zero.

sunrise, sunset: the times at which the apparent upper limb of the Sun is on the astronomical *horizon;* i.e., when the true *zenith distance*, referred to the center of the Earth, of the central point of the disk is $90^{\circ}50'$ based on adopted values of $34'$ for horizontal *refraction* and $16'$ for the Sun's *semidiameter.*

surface brightness (or a planet): the visual magnitude of an average square arc-second area of the illuminated portion of the apparent disk.

synodic period: for planets, the mean interval of time between successive *conjunctions* of a pair of planets, as observed from the Sun; for satellites, the mean interval between successive conjunctions of a satellite with the Sun, as observed from the satellite's primary.

terrestrial dynamical time (TDT): the independent argument for apparent *geocentric* ephemerides. At 1977 January $1^{d}00^{h}00^{m}00^{s}$ TAI, the value of TDT was exactly 1977 January $1^d.000\,3725$. The unit of TDT is 86 400 SI seconds at mean sea level. For practical purposes TDT = TAI + $32^s.184$. (See *barycentric dynamical time*; *dynamical time; international atomic time.*)

terrestrial time (TT): identical to terrestrial dynamical time (TDT).

terminator: the boundary between the illuminated and dark areas of the apparent disk of the Moon, a planet or a planetary satellite.

topocentric: with reference to, or pertaining to, a point on the surface of the Earth, usually with reference to a coordinate system.

transit: the passage of a celestial object across a *meridian*; also the passage of one celestial body in front of another of greater apparent diameter (e.g., the passage of Mercury or Venus across the Sun or Jupiter's satellites across its disk); however, the passage of the Moon in front of the larger apparent Sun is called an annular eclipse (see *eclipse*, *annular*). The passage of a body's shadow across another body is called a shadow transit; however, the passage of the Moon's shadow across the Earth is called a solar eclipse (see *eclipse*, *solar*).

true anomaly: the angle, measured at the focus nearest the *pericenter* of an elliptical *orbit*, between the pericenter and the radius vector from the focus to the orbiting body; one of the standard orbital elements (see *elements*, *orbital*). (See also *eccentric anomaly*, *mean anomaly.*)

true equator and equinox: the celestial coordinate system determined by the instantaneous positions of the *celestial equator* and *ecliptic.* The motion of this system is due to the progressive effect of *precession* and the short-term, periodic variations of *nutation.* (See mean *equator and equinox.*)

twilight: the interval of time preceding sunrise and following sunset (*see sunrise*, *sunset*) during which the sky is partially illuminated. Civil twilight comprises the interval when the *zenith distance*, referred to the center of the Earth, of the central point of the Sun's disk is between $90°50'$ and $96°$, nautical twilight comprises the interval from $96°$ to $102°$, astronomical twilight comprises the interval from $102°$ to $108°$.

umbra: the portion of a shadow cone in which none of the light from an extended light source (ignoring *refraction*) can be observed.

universal time (UT): a measure of time that conforms, within a close approximation, to the mean diurnal motion of the Sun and serves as the basis of all civil timekeeping. UT is formally defined by a mathematical formula as a function of *sidereal time.* Thus UT is determined from observations of the diurnal motions of the stars. The time scale determined directly from such observations is designated UT0; it is slightly dependent on the place of observation. When UT0 is corrected for the shift in longitude of the observing station caused by *polar motion*, the time scale UT1 is obtained.

vernal equinox: the ascending *node* of the *ecliptic* on the *celestial equator*; also the time at which the apparent longitude (*see apparent place* and *longitude, celestial*) of the Sun is 0°. (See *equinox.*)

vertical: apparent direction of gravity at the point of observation (normal to the plane of a free level surface).

year: a period of time based on the revolution of the Earth around the Sun. The calendar year (*see Gregorian calendar*) is an approximation to the tropical year (*see year, tropical*). The anomalistic year is the mean interval between successive passages of the Earth through *perihelion.* The sidereal year is the mean period of revolution with respect to the background stars. (See *Julian year* and *year, Besselian.*)

year, Besselian: the period of one complete revolution in *right ascension* of the *fictitious mean sun*, as defined by Newcomb. The beginning of a Besselian year, traditionally used as a *standard epoch*, is denoted by the suffix '.0'. Since 1984 standard epochs have been defined by the *Julian year* rather than the Besselian year. For distinction, the beginning of a Besselian year is now identified by the prefix B (e.g., B1950.0).

year tropical: the period of one complete revolution of the mean longitude of the Sun with respect to the *dynamical equinox.* The tropical year is longer than the Besselian year (see *year, Besselian*) by $0^{s}.148T$, where T is centuries from B1900.0.

zenith: in general, the point directly overhead on the *celestial sphere.* The astronomical zenith is the extension to infinity of a plumb line. The geocentric zenith is defined by the line from the center of the Earth through the observer. The geodetic zenith is the normal to the geodetic ellipsoid or spheroid at the observer's location. (See *deflection of the vertical.*)

zenith distance: angular distance on the *celestial sphere* measured along the great circle from the zenith to the celestial object. Zenith distance is 90° minus *altitude.*

Bibliography

Allen's Astrophysical Quantities, Cox, A.N., ed., Springer-Verlag, 2000.

The Astronomical Almanac, US Government Printing Office.

The Astronomy and Astrophysics Encyclopedia, Cambridge University Press, 1991.

Astronomy and Astrophysics, Landolt-Bornstein, Springer Verlag.

Astrophysical Formulae, Lang, K.R., Springer-Verlag, 1999.

Astrophysical Quantities, Allen, C.W., The Athlone Press, University of London, 1973.

Compendium of Practical Astronomy, Roth, G.D., Springer-Verlag, 1994.

Computational Spherical Astronomy, Taff, L.G., Wiley and Sons, 1981.

An Introduction to Astronomical Photometry, Golay, M.D., Reidel Publishing Company, 1974.

Spherical Astronomy, Green R.M., Cambridge University Press, 1985.

Note: Links to WWW resources supplement the material in this chapter can be found at:

http://www.astrohandbook.com

Chapter 3

Radio astronomy

To the optical astronomer, radio data serves like a good dog on a hunt. - Sir Fred Hoyle

Major radio surveys

Observatory	Survey	ν (MHz)	Sources	Limit (Jy)[a]
Cambridge	3C	159	471	8
	3CR	178	–	9
	4C	178	4843	2
	5C	408	276	0.025
	6CI	151	1761	–
	6CII	151	8278	–
	6CIII	151	8749	–
	6CIV	151	5421	–
	WKB	38	1069	14
	RN	178	87	0.25
	NB	81.5	558	1
Mills Cross	MSH	86	2270	7
Parkes	PKS	408, 1410, 2650	297	4
	PKS	408, 1410	247	0.5
	PKS	408, 1410	564	0.3
	PKS	408, 1410	628	0.4
	PKS	635, 1410, 2650	397	1.5
Owens Valley	CTA	906	106	–
	CTB, CTBR	960	110	–
	CTD	1421	–	1.15
National Radio	NRAO	750, 1400	726	(3C and 3CR)
Observatory	NRAO	750, 1400	458	0.5
Bologna	B1	408	629	1
	B2	408	3235	0.2
Ohio State	O	1415	128	2, 0.5
	O	1415	236	0.37
	O	1415	1199	0.3
	O	1415	2101	0.2
Vermillion	VRO	610.5	239	0.8
River	VRO	610.5	625	0.8
Dominion Radio Observatory	DA	1420	615	2
Dwingeloo-NRAO	DW	1417	188	2.3
Arecibo	AO	430	25	–
Green Bank	87GB	4.85 GHz	54,579	–
	B2	408	9929	–
	B3	408	13354	–
MIT-Green Bank	MG1	5 GHz	5974	–
	MG2	5 GHz	6182	–
	MG3	5 GHz	3427	–
	MG4	5 GHz	4621	–
Texas		365	~68,000	–
RATAN		7.6 cm	884	–

[a] 1 jansky (Jy) = 10^{-26} W m^{-2} Hz^{-1}.

Microwave background

Measurement of the surface brightness, I_ν of the cosmic background radiation. The spectrum of a 2.73 K blackbody emitter is also shown. (Courtesy of T. Wilkinson, Princeton University.)

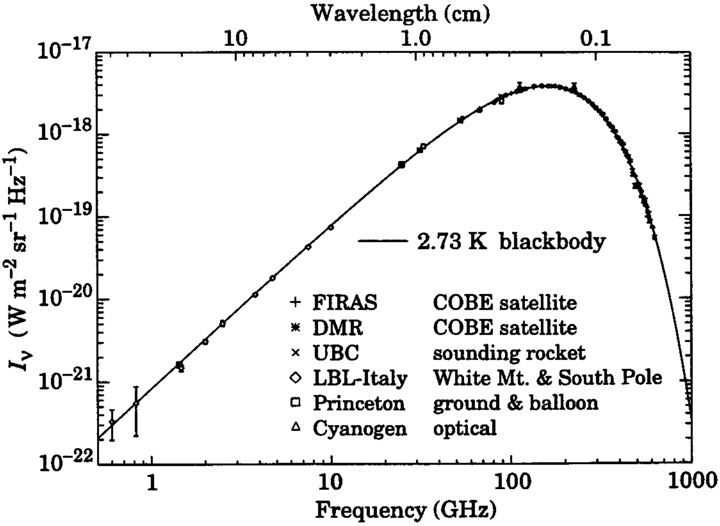

Spectrum of the cosmic microwave background (CMB) from spectrometer observations of the COBE satellite (Mather, et al., 1994, in *An Introduction to Radio Astronomy*, by Bernard F. Burke and Francis Graham-Smith, Cambridge University Press, 1997, with permission.)

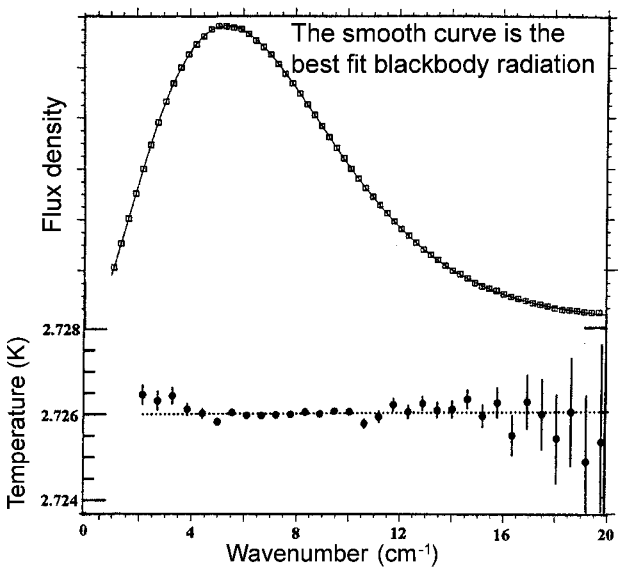

Microwave background (*cont.*)

Terrestrial microwave window. (From NASA SP–419, *The Search for Extraterrestrial Intelligence, SETI.)*

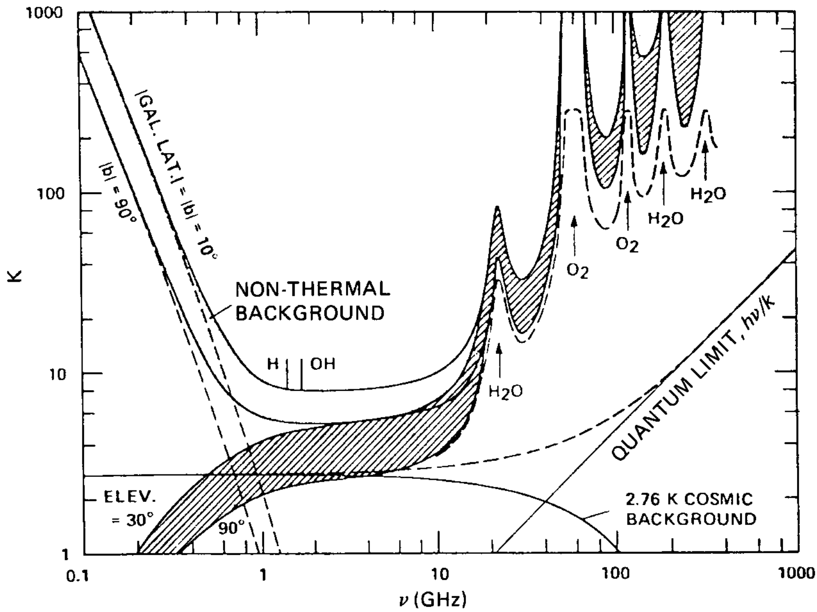

Free space microwave window. (From NASA SP–419, *op. cit.*)

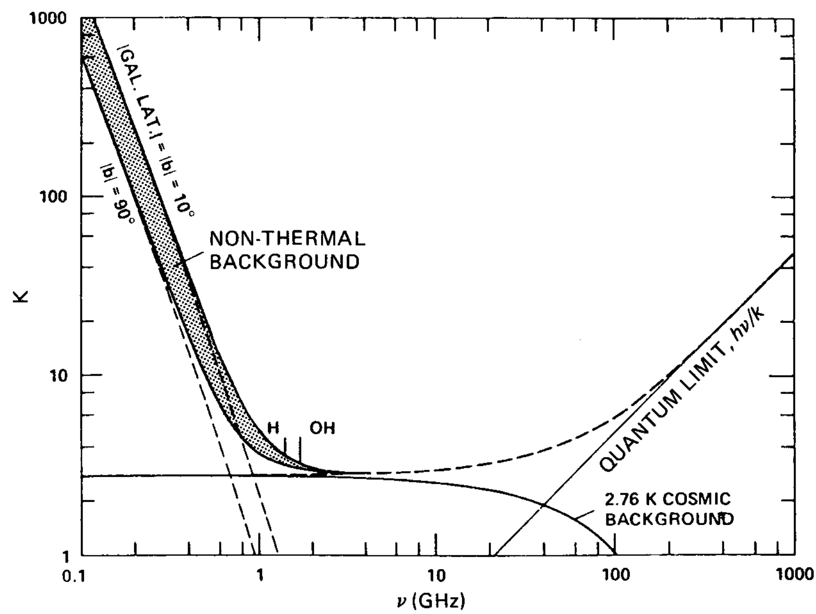

Selected discrete radio sources

Source	J2000.0 α	J2000.0 δ	Spectral flux density (fu)[(a)] 100	1000 (MHz)	10 000	Size (arcmin)	Log distance (pc)	Identification
Cas B	00^h26^m	$+64°09'$	250	56		7	3.5	Tycho SN I, 1572
And A	00 43	+41 16	190	60		140	5.8	Andr. Galaxy, M31
	00 56	−72 44	400	100				
	02 26	+62 04	100	100				Mult. H II region OH em
Per A	03 19	+41 30	130	20		2	7.9	Seyfert Galaxy, NGC 1275
For A	03 22	−37 11	400	120		Large		Pec. Galaxy, NGC 1316?
Per 3C 123	04 37	+29 40	280	70		1		
	05 02	+46 30	120	150		$60 + h(alo)$		Gal. Nebula SN II
Pic A	05 19	−45 46	400	80		Large		
	05 21	−68 57	3000	700				
Tau A	05 35	+22 01	1700	955	560	5	3.3	Crab Nebula SN I 1054
Ori Neb.	05 35	−05 22	40	340	400	10	2.7	Orion Nebula, M42
Gem 3C 157	06 18	+22 37	400	180		$30 + h$	3.1	IC 443, SN II
Mon	06 32	+04 52	400	250		70	3.0	Rosette Nebula
Pup A	08 23	−43 07	600	150		$40 + h$	2.7	
	08 34	−45 47	500	200				Vela X (?)

Selected discrete radio sources (*cont.*)

Source	J2000.0 α	J2000.0 δ	Spectral flux density (fu)$^{(a)}$ 100	1000 (MHz)	10 000	Size (arcmin)	Log distance (pc)	Identification
Hya A	09^h18^m	$-12°05'$	400	60	10	1	8.4	Pec. Galaxy
Car	10 45	−59 46	500	800			3.1	Carina Nebula
3C 273	12 30	+02 02	140	50		1		Quasar
Vir A	12 30	+12 23	1800	263	40	5	7.1	Pec. Jet Galaxy, M87
Cen A	13 25	−43 02	3000	2000		$5+h$	6.8	Pec. Galaxy, NGC 5128
Cen B	13 33	−60 15	600	80				
Boo 3C 295	14 12	+52 12	100	30		1		Distant galaxy
Tr A	16 14	−60 55	800	80				
3C 338	16 29	+39 32	80	7		1		4 Galaxies, NGC 6161
Her A	16 50	+04 59	700	70	8	3	8.6	Pec. Galaxy
	17 14	−38 28	400	100				
2C 1473	17 18	−00 58	400	80	10	4		Galaxy
	17 25	−34 17	400	400	500			
2C 1485	17 31	−21 22	80	20		1	2.9	Kepler SN I, 1604
Sgr A	17 46	−28 57	4000	2000	200	70	3.9	Galactic center
Trifid	18 01	−23 24	800	300			3.0	Galactic nebula, M20
Lagoon	18 04	−24 22	70	150			3.1	Galactic nebula, M8

Selected discrete radio sources (*cont.*)

Source	J2000.0 α	J2000.0 δ	Spectral flux density (fu)[a] 100	1000 (MHz)	10 000	Size (arcmin)	Log distance (pc)	Identification
	18^h05^m	$-21°30'$	200	150				
Omega	18 21	−16 09	200	800	500	10	3.2	Galactic nebula, M17
	18 48	−02 03	500	300	250			
3C 392	18 56	+01 20	500	210		16		Shell source, SN
3C 398	19 10	+09 06	40	70		3		SN II region, OH em
3C 400	19 23	+14 26	400	400		60		
Cyg A	20 00	+40 43	13 800	2340	163	1.2	8.5	Radio galaxy
Cyg X	20 23	+40 22	200	400		60		
Cyg X	20 36	+41 50	150	500	50	40	3.1	? γ Cyg complex
2C 1725	20 46	+50 11	400	150		100		SN II
Cyg Loop	20 51	+30 11	400	200		150	2.7	Loops SN II
America	20 54	+44 05	700	500		150	2.9	Galactic nebula
3C 446	22 26	−04 57	30	6				Quasar
Cas A	23 23	+58 48	19 500	3300	490	4	3.4	Galactic nebula SN II

[a] Flux unit, fu = 10^{-26} W m^{-2} Hz^{-1}.

(After Allen, C.W., *Astrophysical Quantities*, The Athlone Press, 1973, but with J2000 coordinates.)

The brightest radio sources visible in the northern hemisphere
(based on observations at the 20 cm wavelength)

Name	α 1950	δ 1950	Intensity (fu)	Identification
3C 10	$00^h22^m37^s$	$63°51'41''$	44	Supernova remnant[a]– Tycho's supernova
3C 20	00 40 20	51 47 10	12	Galaxy
3C 33	01 06 13	13 03 28	13	Elliptical Galaxy
3C 48	01 34 50	32 54 20	16	Quasar
3C 58	02 01 52	64 35 17	34	Supernova remnant[a]
3C 84	03 16 30	41 19 52	14	Seyfert Galaxy
Fornax A	03 20 42	−37 25 00	115	Spiral Galaxy
NRAO 1560	04 00 00	51 08 00	26	
NRAO 1650	04 07 08	50 58 00	19	
3C 111	04 15 02	37 54 29	15	
3C 123	04 33 55	29 34 14	47	Galaxy
Pictor A	05 18 18	−45 49 39	66	D Galaxy[b]
3C 139.1	05 19 21	33 25 00	40	Emission nebula[a]
NRAO 2068	05 21 13	−36 30 19	19	N Galaxy[c]
3C 144	05 31 30	21 59 00	875	Supernova remnant[a]– Crab Nebula–Taurus A
3C 145	05 32 51	−05 25 00	520	Emission nebula[a]– Orion A–NGC 1976
3C 147	05 38 44	49 49 42	23	Quasar
3C 147.1	05 39 11	−01 55 42	65	Emission nebula[a]– Orion B–NGC 2024
3C 153.1	06 06 53	20 30 40	29	Emission nebula[a]
3C 161	06 24 43	−05 51 14	19	
3C 196	08 09 59	48 22 07	14	Quasar
3C 218	09 15 41	−11 53 05	43	D Galaxy[b]
3C 270	12 16 50	06 06 09	18	Elliptical Galaxy
3C 273	12 26 33	02 19 42	46	Quasar
3C 274	12 28 18	12 40 02	198	Elliptical Galaxy– M87–Virgo A
3C 279	12 53 36	− 5 31 08	11	Quasar
Centaurus A	13 22 32	−42 45 24	1330	Elliptical Galaxy– NGC 5128
3C 286	13 28 50	30 45 58	15	Quasar
3C 295	14 09 33	52 26 13	23	D Galaxy[b]
3C 348	16 48 41	05 04 36	45	D Galaxy[b]
3C 353	17 17 56	−00 55 53	57	D Galaxy[b]
3C 358	17 27 41	−21 27 11	15	Supernova remnant[a]– Kepler's supernova
3C 380	18 28 13	48 42 41	14	Quasar
NRAO 5670	18 28 51	−02 06 00	12	
NRAO 5690	18 32 41	−07 22 00	90	
NRAO 5720	18 35 33	−06 50 18	30	
3C 387	18 38 35	−05 11 00	51	

The brightest radio sources visible in the northern hemisphere (*cont.*)

Name	α 1950	δ 1950	Intensity (fu)	Identification
NRAO 5790	$18^h43^m30^s$	$-02°46'39''$	19	
3C 390.2	18 44 25	−02 33 00	80	
3C 390.3	18 45 53	79 42 47	12	N Galaxy
3C 391	18 46 49	−00 58 58	21	
NRAO 5840	18 50 52	01 08 18	15	
3C 392	18 53 38	01 15 10	171	Supernova remnant[a]
NRAO 5890	18 59 16	01 42 31	14	
3C 396	19 01 39	05 21 54	14	
3C 397	19 04 57	07 01 50	29	
NRAO 5980	19 07 55	08 59 09	47	
3C 398	19 08 43	08 59 49	33	
NRAO 6010	19 11 59	11 03 30	10	
NRAO 6020	19 13 19	10 57 00	35	
NRAO 6070	19 15 47	12 06 00	11	
3C 400	19 20 40	14 06 00	576	
NRAO 6107	19 32 20	−46 27 32	13	
3C 403.2	19 52 19	32 46 00	75	
3C 405	19 57 44	40 35 46	1495	D Galaxy[b]–Cygnus A
NRAO 6210	19 59 49	33 09 00	55	
3C 409	20 12 18	23 25 42	14	
3C 410	20 18 05	29 32 41	10	
NRAO 6365	20 37 14	42 09 07	20	Emission nebula[a]
NRAO 6435	21 04 25	−25 39 06	12	Elliptical Galaxy
NRAO 6500	21 11 06	52 13 00	46	
3C 433	21 21 31	24 51 18	12	D Galaxy[b]
3C 434.1	21 23 26	51 42 14	12	
NRAO 6620	21 27 41	50 35 00	37	
NRAO 6635	21 34 05	00 28 26	10	Quasar
3C 452	22 43 33	39 25 28	11	Elliptical Galaxy
3C 454.3	22 51 29	15 52 54	11	Quasar
3C 461	23 21 07	58 32 47	2477	Supernova remnant[a]–Cassiopeia A

fu = 10^{-26} W m^{-2} Hz^{-1}.

[a] Supernova remnants and emission nebulae lie within our own galaxy.

[b] Galaxy refers to a Dumbell-shaped galaxy.

[c] N Galaxy refers to a galaxy with a bright nucleus.

(Adapted from Verschuur, G.L., *The Invisible Universe*, Springer–Verlag, 1974.)

Broad classification scheme for H II regions

Name of the object observed	Observed characteristics	Diameter [pc]	N_e [cm^{-3}]	Stage of development	Examples
Compact infrared source at $\approx 20\mu m$	Continuous emission at $\simeq 20$ μm, but not at 2 μm; no radio continuum; optically not detectable	$\lesssim 0.05$	$> 5 \times 10^3$	Pre-Main Sequence O-star in a shell, opaque to optical radiation, including UV ("cocoon star")	IRS 5 in W 3
Compact H II region	Thermal radiocontinuum; infrared continuum; usually not detectable in the visible	0.05…1	$\gtrsim 10^3$	Earliest phase of development of an H II region	Components in W 75, DR 21 and in NGC 7538 (see Table 4.10)
Complex H II region of intermediate density	Continuous and line radiation in the optical, infrared and radio-frequency regions (both rows)	1…100	$10 \ldots 10^3$	Expanding H II region	M 42, M 17
Large diffuse H II region		> 100	$\lesssim 10$	Very far expanded H II region	NGC 7000 (North America Nebula)

(From *Physics of the Galaxy and Interstellar Matter*, Scheffler, H. & Elsaesser, H., Springer-Verlag, 1987, with permission.)

Compact HII regions (contained in larger objects)

Extended object	Compact components	α_{1950}	δ_{1950}	Angular diameter [arcsec]	Distance [kpc]	Linear diameter [pc]
W3 (with	A1–A5	$2^h21^m56^s.6$	$+61°52'43''$	28 . . . 35	3.1	0.4 . . . 0.5
opt. nebula	C	$2^h21^m43^s.6$	$+61°52'46''$	5		0.071
IC 1795)	W3(OH), comp. *A*	$2^h23^m16^s.5$	$+61°38'57''$	1.5		0.024
M42	Ori *A*, G 209.0–19.4	$5^h32^m50^s.$	$-5°25'15''$	240	0.5	0.6
M8	A1 (Ring)	$18^h00^m37^s.0$	$-24°22'50''$	15	1.4	0.10
	A4	$18^h00^m36^s.3$	$-24°22'52''$	46		0.32
M17	S	$18^h17^m34^s.$	$-16°13'24''$	220	2.1	2.3
	N	$18^h17^m39^s.$	$-16°10'30''$	280		2.9
	E	$18^h17^m51^s.$	$-16°11'30''$	190		2.0
W51	G49.5–0.4d	$19^h21^m22^s.3$	$+14°25'15''$	11	7.3	0.4
	e	$19^h21^m24^s.4$	$+14°24'43''$	19		0.7
W75	DR 21 A	$20^h37^m13^s.7$	$+42°08'55''$	5.7	3.0	0.083
	B	$20^h37^m14^s.0$	$+42°09'03''$	4.0		0.058
	C	$20^h37^m14^s.1$	$+42°08'54''$	7.1		0.101
	D	$20^h37^m14^s.2$	$+42°09'15''$	4.2		0.062
NGC 7538	A1	$23^h11^m30^s.3$	$+61°12'56''$	110	2.5	1.4
= S 158	A2	$23^h11^m20^s.8$	$+61°13'45''$	10		0.12
	B	$23^h11^m36^s.7$	$+61°12'00''$	12		0.15
	C	$23^h11^m36^s.7$	$+61°11'50''$	1.0		0.013

(From *Physics of the Galaxy and Interstellar Matter*, Scheffler, H. & Elsaesser, H., Springer-Verlag, 1987, with permission.)

Compact HII regions (which are also observed as infrared sources)

Extended	Compact components		$\Phi(20\ \mu m)$	$\frac{\Phi(20\ \mu m)}{\Phi(6\ cm)}$	L_{IR}
object	Radio source	IR source	[Jy]		$[L_\odot]$
W3	A1–A5	IRS 1	2×10^3	70	3×10^5
	C	IRS 4	3×10^3	500	–
	W3 (OH)	IRS 8	2×10^2	300	2×10^5
M42	G209.0–19.4	IRe 1	1.4×10^5	500	4×10^5
M8	A1–A4		1.3×10^3	30	5×10^4
M17	S	IRe 1	5×10^4	220	5×10^6
	N	IRe 2a	3×10^4	140	
W51	G49.5–0.4d	IRS 2	1.5×10^3	140	5×10^6
	c	IRS 1	–	–	
W75	DR 21 D	DR 21 N	1×10^2	50	6×10^4
NGC 7538	B	IRS 2	7×10^2	500	3×10^4
= S 158	C	IRS 1	2×10^2	1700	

The measured radiation flux at the earth at $\lambda = 20\ \mu m$ and $\lambda = 6$ cm ($\nu = 5$ GHz) are denoted by $\Phi(20\ \mu m)$ and $\Phi(6\ cm)$, respectively. L_{IR} is the total infrared luminosity of the source in units of solar luminosity $L_\odot = 4 \times 10^{26}$ W. 1 jansky (Jy) = 10^{-26} $W\,m^{-2}\,Hz^{-1}$.

(From *Physics of the Galaxy and Interstellar Matter*, Scheffler, H. & Elsaesser, H., Springer-Verlag, 1987, with permission.)

Compact HII regions (physical parameters)

Object	T_e [K]	E [pc cm^{-6}]	$\overline{(N_e^2)}^{1/2}$ [cm^{-3}]	u [pc cm^{-2}]	L_e [s^{-1}]	$\mathcal{M}$(H II) [$\mathcal{M}_\odot$]
W3, A1–A5	8400	2×10^7	6×10^3	83	4×10^{49}	10
W3(OH)	10000	1×10^9	2×10^5	54	3×10^{48}	0.1
M42	8200	6×10^6	5×10^3	55	7×10^{48}	10
NGC2237–46	8000	3×10^4	20	80	2×10^{49}	1×10^4
M20	8000	5×10^4	1×10^2	50	5×10^{48}	2×10^2
M8	8000	4×10^5	6×10^2	64	1×10^{49}	2×10^2
M17, main source (S)	7700	5×10^6	2×10^3	170	2×10^{50}	10^2
M16	8000	4×10^5	2×10^2	120	7×10^{49}	7×10^2
W51, main source	7300	5×10^7	8×10^2	190	3×10^{50}	10^2
W75, DR21 A	8400	5×10^7	2×10^4	36	2×10^{48}	0.2
B		5×10^7	3×10^4	27	7×10^{47}	0.1
C		9×10^7	3×10^4	49	4×10^{48}	0.4
D		4×10^7	3×10^4	27	7×10^{47}	0.1
NGC 7538 A1	7900	8×10^5	1×10^3	60	8×10^{48}	33
A2		2×10^6	4×10^3	14	1×10^{47}	0.1
B		7×10^6	6×10^3	26	7×10^{47}	0.3
C		1×10^7	1×10^5	12	7×10^{46}	0.002
NGC 7000	7000	4×10^3	10	100	4×10^{49}	2×10^4

Mean electron temperature T_e, emission measure E, root mean square electron density $\overline{(N_e^2)}^{1/2}$, excitation parameter u, total number of Lyman continuum photons per s L_c and total mass of ionised hydrogen $\mathcal{M}$(H II) for a selection of H II regions.

(From *Physics of the Galaxy and Interstellar Matter*, Scheffler, H. & Elsaesser, H., Springer-Verlag, 1987, with permission)

Radio spectra

Spectra of typical radio sources. (Adapted from Kraus, J.D., *Radio Astronomy*, McGraw-Hill Co., 1966.)

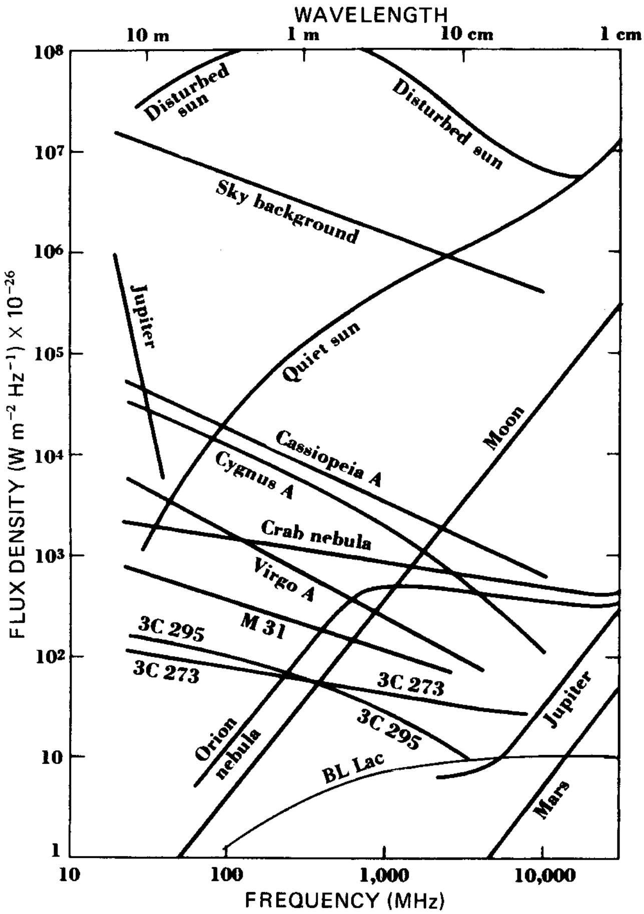

Radio flux calibrators

(a) Spectral parameters of telescope calibrators

Source	Frequency interval	Spectral parameters $\log S\,[Jy] = a + b \cdot \log \nu\,[\mathrm{MHz}] + c \cdot \log^2 \nu\,[\mathrm{MHz}]$					
		a		b		c	
3 C 48	405 MHz…15 GHz	2.345	±0.030	+0.071	±0.001	−0.138	±0.001
3 C 123	405 MHz…15 GHz	2.921	±0.025	−0.002	±0.0001	−0.124	±0.001
3 C 147	405 MHz…15 GHz	1.766	±0.017	+0.447	±0.006	−0.184	±0.001
3 C 161	405 MHz…10.7 GHz	1.633	±0.016	+0.498	±0.008	−0.194	±0.001
3 C 218	405 MHz…10.7 GHz	4.497	±0.038	−0.910	±0.011	–	–
3 C 227	405 MHz…15 GHz	3.460	±0.055	−0.827	±0.016	–	–
3 C 249.1	405 MHz…15 GHz	1.230	±0.027	+0.288	±0.007	−0.176	±0.003
3 C 286	405 MHz…15 GHz	1.480	±0.018	+0.292	±0.006	−0.124	±0.001
3 C 295	405 MHz…15 GHz	1.485	±0.013	+0.759	±0.009	−0.255	±0.001
3 C 348	405 MHz…10.7 GHz	4.963	±0.045	−1.052	±0.014	–	
3 C 353	405 MHz…10.7 GHz	2.944	±0.031	−0.034	±0.001	−0.109	±0.001
DR 21	7 GHz…31 GHz	1.81	±0.05	−0.122	±0.010	–	–
NGC 7027	10 GHz…31 GHz	1.32	±0.08	−0.127	±0.012	–	–

(b) Characteristics, position, and flux densities of telescope calibrators (J2000.0)

Source	α [h m s]	δ [° ′ ″]	b^{II} [°]	S_{400} [J_y]	S_{750} [J_y]	S_{1400} [J_y]	S_{1665} [J_y]	S_{2700} [J_y]	S_{5000} [J_y]
3 C 48	1 37 41.299	+33 09 35.41	−29	39.4	25.6	15.9	13.9	9.20	5.24
3 C 123	4 37 04.4	+29 40 15	−12	119.2	77.7	48.7	42.4	28.5	16.5
3 C 147	5 42 36.127	+49 51 07.23	+10	48.2	33.9	22.4	19.8	13.6	7.98
3 C 161	6 27 10.0	− 5 53 07	− 8	41.2	28.9	19.0	16.8	11.4	6.62
3 C 218	9 18 06.0	−12 05 45	+25	134.6	76.0	43.1	36.8	23.7	13.5
3 C 227	9 47 46.4	+ 7 25 12	+42	20.3	12.1	7.21	6.25	4.19	2.52
3 C 249.1	11 04 11.5	+76 59 01	+39	6.1	4.0	2.48	2.14	1.40	0.77
3 C 274	12 30 49.6	+12 23 21	+74	625.0	365.0	214	184	122	71.9
3 C 286	13 31 08.284	+30 30 32.94	+81	25.1	19.7	14.8	13.6	10.5	7.30
3 C 295	14 11 20.7	+52 12 09	+61	54.1	36.3	22.3	19.2	12.2	6.36
3 C 348	16 51 08.3	+ 4 59 26	+29	168.1	86.8	45.0	37.5	22.6	11.8
3 C 353	17 20 29.5	− 0 58 52		131.1	88.2	57.3	50.5	35.0	21.2
DR 21	20 39 01.2	+42 19 45	+ 1	–	–	–	–	–	–
NGC 7027$^{(d)}$	21 07 01.6	+42 14 10	− 3	–	–	1.35	1.65	3.5	5.7

(b) Characteristics, position, and flux densities of telescope calibrators (J2000.0) *(cont.)*

Source	S_{8000} $[J_y]$	$S_{10\,700}$ $[J_y]$	$S_{15\,000}$ $[J_y]$	$S_{22\,235}$ $[J_y]$	Spec.	Ident.	Polar. (at 5 GHz) [%]	Ang. size (at 1.4 GHz) [″]
3 C 48	3.31	2.46	1.72	1.11	C^-	QSS	5	< 1
3 C 123	10.6	7.94	5.63	3.71	C^-	GAL	2	20
3 C 147	5.10	3.80	2.65	1.71	C^-	QSS	< 1	< 1
3 C 161	4.18	3.09	2.14	–	C^-	GAL	5	< 3
3 C 218	8.81	6.77	–	–	S	GAL	1	core 25 halo 200
3 C 227	1.71	1.34	1.02	0.73	S	GAL	7	180
3 C 249.1	0.47	0.34	0.23	–	S	QSS	–	15
3 C 274	48.1	37.5	28.1	20.0	S	GAL	1	halo 400[(a)]
3 C 286	5.38	4.40	3.44	2.55	C^-	QSS	11	< 5
3 C 295	3.65	2.53	1.61	0.92	C^-	GAL	0.1	4
3 C 348	7.19	5.30	–	–	S	GAL	8	115[(b)]
3 C 353	14.2	10.9	–	–	C^-	GAL	5	150
DR 21	21.6	20.8	20.0	19.0	Th	HII	–	20[(c)]
NGC 7027[(d)]	–	6.43	6.16	5.86	Th	PN	< 1	10

[(a)] Halo has steep spectral index, so for $\lambda \leq 6$ cm, more than 90% of the flux is in the core.

[(b)] Angular distance between the two components.

[(c)] Angular size at 2 cm, but consists of 5 smaller components.

[(d)] Data up to 5 GHz are the direct measurements, not calculated from fit.

Systematic errors over the frequency range 0.4–15 GHz are less than 4%.

(From Baars, J. W. M., Genzel, R., Pauliny-Toth, I. I. K., Witzel, A., *Astron. Astrophys.* **61**, 99 (1977).)

Radio propagation effects

The Earth's atmosphere (> 25 MHz)

$$S(z) = S_0 d^{-X(z)}$$

where

$$S(z) = \text{the flux measured at zenith distance } z,$$
$$S_0 = \text{flux outside the atmosphere},$$
$$d = \text{the attenuation at the zenith for airmass 1},$$
$$X(z) = \text{relative airmass in units of the airmass at the zenith.}$$

For a plane parallel atmospheric model:

$$X(z) = \sec z = \frac{1}{\cos z}$$

Taking into account the Earth's and troposphere's curvature:

$$X(z) = \frac{1}{H}\int_R^{R+H} \frac{\rho(r)/\rho(R)}{\left[1 - \left(\frac{R}{r}\frac{n_0}{n}\right)^2 \sin^2 z\right]^{1/2}} dr$$

where

$$R = \text{radius of Earth},$$
$$H = \text{height of atmosphere},$$
$$\rho(r) = \text{gas density of the atmosphere at radius } r,$$
$$n = \text{index of refraction at radius } r.$$
$$n_0 = \text{index of refraction at radius } R.$$

Up to $X = 5.2$ the following equation gives $X(z)$, with an error less than 6.4×10^{-4}.

$$X(z) = -0.0045 + 1.006\,72 \sec z - 0.002\,234 \sec^2 z - 0.000\,624\,7 \sec^3$$

(After K. Rohlfs, *Tools of Radio Astronomy*, Springer-Verlag, 1986.)

Interplanetary medium

The electron density as a function of distance from the Sun:

$$\mathcal{N}_e = [1.55r^{-6} + 2.99r^{-16}] \times 10^{14}\ (\mathrm{m}^{-3}),\ r < 4,$$

where r is the radial distance from the Sun in units of the solar radius,

$$\mathcal{N}_e = 5 \times 10^{11} r^{-2}\ (\mathrm{m}^{-3}),\ 4 < r < 20.$$

The scattering angle due to the interplanetary medium may be approximated by:

$$\theta_s \simeq 50 \left(\frac{\lambda}{p}\right)^2 \quad (\text{arcmin}),$$

where λ is in meters and p, the solar impact parameter, is in solar radii.

Interstellar medium (delay and Faraday rotation)

The smooth, ionized component of the interstellar medium of the Galaxy affects propagation by introducing delay and Faraday rotation. The time of arrival of a pulse of radiation is:

$$t_p = \int_0^L \frac{dz}{v_g},$$

where L is the propagation path, v_g is the group velocity;

$$\frac{dt_p}{d\nu} \simeq -\frac{e^2}{4\pi\epsilon_0 m c \nu^3} \int_0^L \mathcal{N}_e\, dz.$$

The integral of $\mathcal{N}_e$ over the path length is called the *dispersion measure*,

$$D_m = \int_0^L \mathcal{N}_e\, dz,$$

The magnetic field of the Galaxy causes Faraday rotation of the polarization plane of radiation from extragalactic radio sources.

$$\Delta\psi = \lambda^2 R_m,$$

where R_m is the *rotation measure* given by

$$R_m = 8.1 \times 10^5 \int \mathcal{N}_e B_{\|}\, dz.$$

Here R_m is in radians per square meter, λ is in meters, $B_{\|}$ is the longitudinal component of magnetic field in gauss (1 gauss $= 10^{-4}$ tesla), $\mathcal{N}_e$ is in centimeters^{-3}, dz is in parsecs (pc) (1 pc $= 3.1 \times 10^{16}$ m), and $\Delta\psi$ is the change in position angle of the electric field:

$$B_{\|} \simeq 2\mu G,$$

$$R_m \simeq -18|\cot b| \cos(l - 94°),$$

where l and b are the galactic longitude and latitude, respectively.

Interstellar medium (scintillation)

Approximate formulae for interstellar scintillation:

$$\begin{aligned} \theta_s &\simeq 7.5\lambda^{11/5} && \text{(arcsec)}, && |b| \leq {}^\circ 6 \\ &\simeq 0.5|\sin b|^{-3/5}\lambda^{11/5} && \text{(arcsec)}, && 0^\circ < |b| < 3^\circ - 5^\circ \\ &\simeq 13|\sin b|^{-3/5}\lambda^{11/5} && \text{(milliarcsec)}, && |b| \geq 3^\circ - 5^\circ \\ &\simeq \frac{15}{\sqrt{(|\sin b|)}}\lambda^2 && \text{(milliarcsec)}, && |b| > 15^\circ, \end{aligned}$$

where b is the galactic latitude and λ is the wavelength in meters.

The accuracy of the approximations above decreases with decreasing $|b|$. In particular, the scattering angle at low latitudes, $|b| < 1^\circ$, can take on a large range of values.

(Adapted from Thompson, A.R., Moran, J.M. & Swenson, G.W., *Interferometry and Synthesis in Radio Astronomy*, Wiley-Interscience, 1986.)
(For propagation effects in the neutral lower atmosphere, see Thompson *et al.*, *op. cit.*)

Atmospheric opacity

Atmospheric zenith opacity. The absorption from narrow ozone lines has been omitted. (From Thompson, A.R. *et al.*, *op. cit.*)

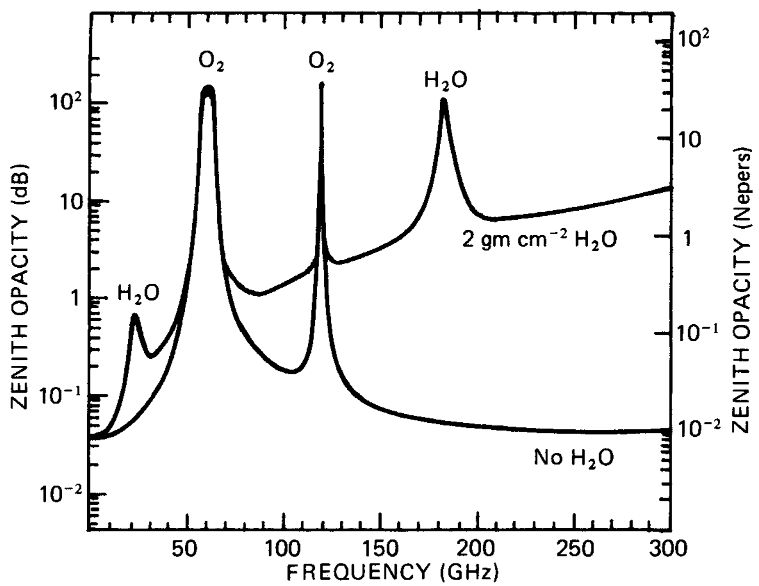

Rotation measures of extragalactic sources

The magnitudes and signs of the rotations measures of 976 extragalactic radio sources plotted in galactic coordinates. (1992 data; figure from P. P. Kronberg; private communication.)

If θ is the observed and θ_0 is the intrinsic polarization angle measured in rad, and λ the wavelength in meters,

$$\theta = \theta_0 + R_m \lambda^2$$

The differential rotation $d\theta$ across a bandwidth dv centered at frequency ν is given by:

$$d\theta = -2 R_m \lambda^2 d\nu / \nu$$

The rotation measure R_m (rad m^{-2}) depends on the properties of the medium:

$$R_m = 8.1 \times 10^5 \int N_e B_{\|} dz.$$

where N_e is the electron density in cm^{-3}, $B_{\|}$ is the magnetic field alnong the line-of-sight in Gauss, and z is the distance to the source in parsecs.

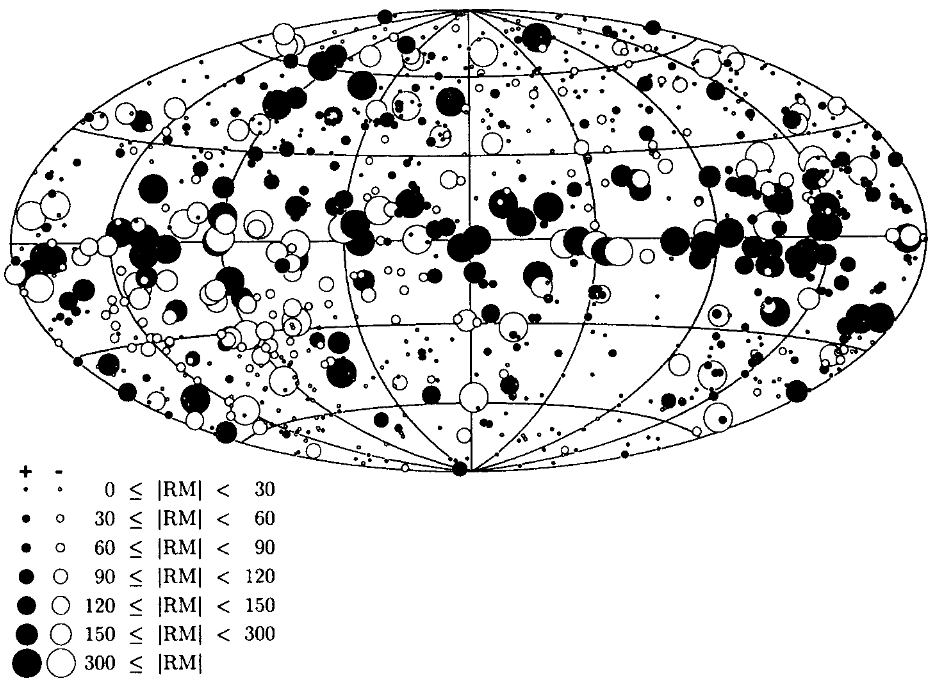

Ionospheric electron density

Idealized electron density distribution in the Earth's ionosphere. The curves drawn indicate the densities to be expected at sunspot maximum in temperate latitudes. (From Evans & Hagfors, 1968.)

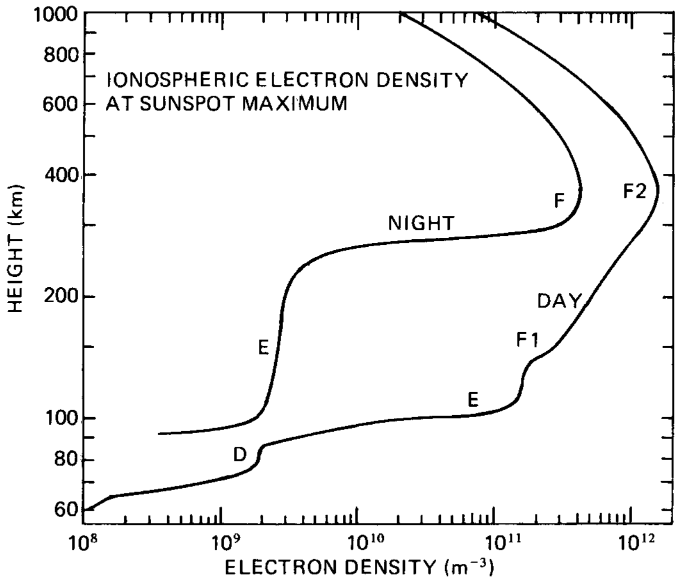

Letter designations of microwave bands

Band	Frequency (GHz)	Wavelength (cm)	Wavenumber (cm^{-1})
L-Band	1–2	30–15	0.033–0.067
S-Band	1–4	15–7.5	0.067–0.133
C-Band	4–8	7.5–3.7	0.133–0.267
X-Band	8–12	3.7–2.5	0.267–0.4
Ku-Band	12–18	2.5–1.7	0.4–0.6
K-Band	18–27	1.7–1.1	0.6–0.9
Ka-Band	27–40	1.1–0.75	0.9–1.33

Radio-frequency lines of importance to astrophysics

Substance	Rest frequency
Deuterium (DI)	327.384 MHz
Hydrogen (HI)	1420.406 MHz
Hydroxyl radical (OH)	1612.231 MHz
Hydroxyl radical (OH)	1665.402 MHz
Hydroxyl radical (OH)	1667.359 MHz
Hydroxyl radical (OH)	1720.530 MHz
Methyladyne (CH)	3263.794 MHz
Methyladyne (CH)	3335.481 MHz
Methyladyne (CH)	3349.193 MHz
Formaldehyde (H_2CO)	4829.660 MHz
Methanol (CH_3OH)	6668.518 MHz
Ionized helium isotope (^{3}HeII)	8665.650 MHz
Methanol (CH_3OH)	12.178 GHz
Formaldehyde (H_2CO)	14.488 GHz
Cyclopropenylidene (C_3H_2)	18.343 GHz
Water vapour (H_2O)	22.235 GHz
Ammonia (NH_3)	23.694 GHz
Ammonia (NH_3)	23.723 GHz
Ammonia (NH_3)	23.870 GHz
Silicon monoxide (SiO)	42.821 GHz
Silicon monoxide (SiO)	43.122 GHz
Carbon monosulphide (CS)	48.991 GHz
Deuterated formylium (DCO^+)	72.039 GHz
Silicon monoxide (SiO)	86.243 GHz
Formylium ($H^{13}CO^+$)	86.754 GHz
Silicon monoxide (SiO)	86.847 GHz
Ethynyl radical (C_2H)	87.300 GHz
Hydrogen cyanide (HCN)	88.632 GHz
Formylium (HCO^+)	89.189 GHz
Hydrogen isocyanide (HNC)	90.664 GHz
Diazenylium (N_2H)	93.174 GHz
Carbon monosulphide (CS)	97.981 GHz
Carbon monoxide ($C^{18}O$)	109.782 GHz
Carbon monoxide (^{13}CO)	110.201 GHz
Carbon monoxide ($C^{17}O$)	112.359 GHz
Carbon monoxide (CO)	115.271 GHz
Formaldehyde ($H_2{}^{13}CO$)	137.450 GHz
Formaldehyde (H_2CO)	140.840 GHz
Carbon monosulphide (CS)	146.969 GHz
Water vapour (H_2O)	183.310 GHz
Carbon monoxide ($C^{18}O$)	219.560 GHz

Radio-frequency lines of importance to astrophysics (*cont.*)

Substance	Rest frequency
Carbon monoxide (^{13}CO)	220.399 GHz
Carbon monoxide (CO)	230.538 GHz
Carbon monosulphide (CS)	244.953 GHz
Hydrogen cyanide (HCN)	265.886 GHz
Formylium (HCO^+)	267.557 GHz
Hydrogen isocyanide (HNC)	271.981 GHz
Diazenylium (N_2H^+)	279.511 GHz
Carbon monoxide ($C^{18}O$)	329.330 GHz
Carbon monoxide (^{13}CO)	330.587 GHz
Carbon monosulphide (CS)	342.883 GHz
Carbon monoxide (CO)	345.796 GHz
Hydrogen cyanide (HCN)	354.484 GHz
Formylium (HCO^+)	356.734 GHz
Diazenylium (N_2H^+)	372.672 GHz
Water vapour (H_2O)	380.197 GHz
Carbon monoxide ($C^{18}O$)	439.088 GHz
Carbon monoxide (^{13}CO)	440.765 GHz
Carbon monoxide (CO)	461.041 GHz
Heavy water (HDO)	464.925 GHz
Carbon (CI)	492.162 GHz
Water vapour ($H_2{}^{18}O$)	547.676 GHz
Water vapour (H_20)	556.936 GHz
Ammonia ($^{15}NH_3$)	572.113 GHz
Ammonia (NH_3)	572.498 GHz
Carbon monoxide (CO)	691.473 GHz
Hydrogen cyanide (HCN)	797.433 GHz
Formylium (HCO^+)	802.653 GHz
Carbon monoxide (CO)	806.652 GHz
Carbon (CI)	809.350 GHz

$\lambda(m) = 0.2997925/f(GHz)$.

(From the *IAU Information Bulletin*, January 1992.)

Known interstellar molecules (March 1999)

Number of Atoms							
2	3	4	5	6	7	8	9
H_2	H_2O	NH_3	SiH_4	CH_3OH	CH_3CHO	CH_3CO_2H	CH_3CH_2OH
OH	H_2S	H_3O^+	CH_4	NH_2CHO	CH_3NH_2	CH_3C_2CN	$(CH_3)_2O$
SO	SO_2	H_2CO	CHOOH	CH_3CN	CH_3CCH	C_7H	CH_3CH_2CN
SO^+	HN_2^+	H_2CS	HC≡CCN	CH_3NC	CH_2CHCN	H_2C_6	$H(C{\equiv}C)_3CN$
SiO	HNO	HNCO	CH_2NH	CH_3SH	HC_4CN	C_8^-	$H(C{\equiv}C)_2CH_3$
SiS	SiH_2?	HNCS	NH_2CN	C_5H	C_6H		C_8H
NO	NH_2	CCCN	H_2CCO	HC_2CHO	c-CH_2OCH_2		C_9^-
NS	H_3^+	HCO_2^+	C_4H	$CH_2 = CH_2$	C_7^-		10
HCl	NNO	CCCH	c-C_3H_2	H_2CCCC			
NaCl	HCO	c-CCCH	CH_2CN	HC_3NH^+			CH_3COCH_3
KCl	HCO^+	CCCO	C_5	C_5N			$CH_3(C{\equiv}C)_2CN$?
AlCl	OCS	CCCS	SiC_4	C_6^-			
AlF	CCH	HCCH	H_2CCC	C_5S?			11
PN	HCS^+	$HCNH^+$	HCCNC				
SiN	c-SiCC	HCCN	HNCCC				$H(C{\equiv}C)_4CN$
NH	CCO	H_2CN	H_3CO^+				
HF	CCS	c-SiC_3					13
CH^+	C_3	CH_2D^+?					
CN	MgNC						$H(C{\equiv}C)_5CN$
CO	NaCN						
CS	CH_2						
C_2	MgCN						
SiC	HOC^+						Total: 123
CP	HCN						
CO^+	HNC						
CH	KCN?						

(Courtesy of P. Thaddeus, Center for Astrophysics.)

Radio pulsars

Neutron star masses from observations of radio pulsars in binary systems. In two cases, the average neutron star mass in a system is known with much better accuracy than the individual masses; these masses are indicated with open circles. Vertical lines are drawn at $m = 1.35 \pm 0.04$ solar masses.

(From Thorsett, S.E. and Chakrabarty, D., Ap. J., **512**, 288, 1999.)

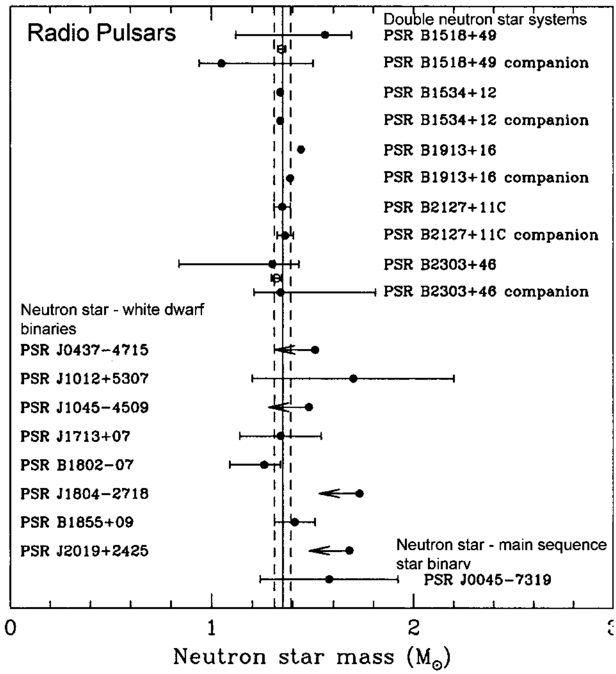

Bibliography

A Handbook of Radio Sources, Pacholczyk, A.G., Pachart Publishing House, 1977.

Interferometry and Synthesis in Radio Astronomy, Thompson, A.R., Moran, J.M. & Swenson, G.W., Wiley-Interscience, 1986.

An Introduction to Radio Astronomy, Burke, B. & Graham-Smith, F., Cambridge University Press, 1997.

Loves, F.J. *et al.*, 1979, *Ap, J.* (*Suppl.*), **41**, 451.

Radio Astronomy, 2nd edn., Kraus, J.O., Cygnus-Quasar Books.

Tools of Radio Astronomy, Rohlfs, K., Springer Verlag, 1986.

Note: Links to WWW resources which supplement the material in this chapter can be found at: **http://www.astrohandbook.com**

Chapter 4

Infrared and submillimeter astronomy

A telescope in the void recently found cosmic "maternity wards" where clouds of interstellar gas and dust appear to be in various stages giving birth to stars. - William J. Brood

Infrared sources

The brightest members of the seven classes of infrared sources (Jy = jansky = fu = 10^{-26} W m^{-2} Hz^{-1}).

1. *Stars*

α 1950	δ 1950	20μ flux den. (Jy)	Name
1^h 04^m	12° 19′	0.83×10^3	CIT 3
2 17	−3 12	1.9	ö Cet
3 51	11 14	1.3	NML Tau
4 57	56 07	1.0	TY Cam
5 52	7 25	2.1	α Ori
7 21	−25 41	11	VY C Ma
9 45	11 39	1.1	R Leo
9 45	13 30	~ 25	IRC + 10216
10 13	30 49	0.83	RW LMi
10 43	−59 25	~ 50	η Car
12 01	−32 04	2.7	IRC −30187
13 46	−28 07	1.9	W Hya
16 26	−26 19	1.0	α Sco
18 05	−22 16	2.1	VY Sgr
18 36	−6 51	2.5	EW Sct
18 45	−2 03	2.5	AB Agl
19 24	11 16	3.3	IRC +10420
20 08	−6 25	1.4	IRC −10529
20 20	37 22	1.1	BC Cyg
20 45	39 56	4.8	NML Cyg
21 42	58 33	0.69	μ Cep

2. *Planetary nebula*

α 1950	δ 1950	20μ flux den. (Jy)	Name
21^h 00^m	36° 30′	2.5×10^3	'Egg Nebula'
21 05	42 02	0.6	NGC 7027

3. *H II Regions*

α 1950	δ 1950	20μ flux den. (Jy)	Name
2^h 22^m	61° 52′	5.6×10^3	W3
5 33	−5 27	5.9	M42
5 39	−1 57	3.3	NGC 2024
17 44	−28 33	0.7	Sgr B2
18 01	−24 21	3.3	M8
18 06	−20 19	3.0	W31
18 11	−17 58	1.4	HFE50
18 16	−13 46	1.4	M16

Infrared sources (*cont.*)

3. *H II Regions*

α 1950	δ 1950	20μ flux den. (Jy)	Name
$18^h\ 18^m$	$-16^\circ\ 13'$	20×10^3	M17
18 43	−2 42	1.1	HFE 56
18 59	1 08	1.0	W48
19 08	9 02	1.7	HFE 58
19 11	10 48	1.2	?
19 20	13 59	1.2	HFE 59
19 21	14 24	1.7	HFE 60
20 00	33 25	1.4	NGC 6857
20 26	37 13	1.2	Sharp 106
23 12	61 12	3.6	NGC 7358

4. *Molecular clouds*

α 1950	δ 1950	100μ flux den. (Jy)	Name
$2^h\ 22^m$	$61^\circ\ 52'$	$\sim 10^4$	W3 IRS 5
5 33	−5 27	1×10^5	KL Neb
6 05	−6 23	5×10^4	Mon R2
16 23	−24 17	3×10^4	ρ Oph DK.Cl.
20 37	42 12	$\sim 10^4$	W75 S OH

5. *Galactic nucleus*

α 1950	δ 1950	20μ flux den. (Jy)	Name
$17^h\ 43^m$	$-28^\circ\ 54'$	2.6×10^3	Sgr A

6. *Galactic nuclei*

α 1950	δ 1950	20μ flux den. (Jy)	Name
$00^h\ 45^m$	$-25^\circ\ 34'$	30	NGC 253
2 40	00 20	60	NGC 1068
9 52	69 55	100	M 82
12 55	56 15	6	MK 231

7. *Active galactic nuclei*

α 1950	δ 1950	10μ flux den. (Jy)	Name
$08^h\ 53^m$	$20^\circ\ 15'$	$0.04 \rightarrow 0.07$	OJ 287
12 27	2 20	$0.2 \rightarrow 0.5$	3C 273
22 01	42 12	$0.2 \rightarrow 0.7$	BL Lac

(Adapted from Low, F. in *Symposium on Infrared and Submillimeter Astronomy*, G.G. Fazio, ed., D. Reidel Publishing Company, 1977.)

Atmospheric transmission

Transmission of the atmosphere at infrared wavelengths at four altitudes. (Adapted from Fazio, G.G. in *Frontiers of Astrophysics*, E.H. Avrett, ed., Harvard University Press, Cambridge, 1976.)

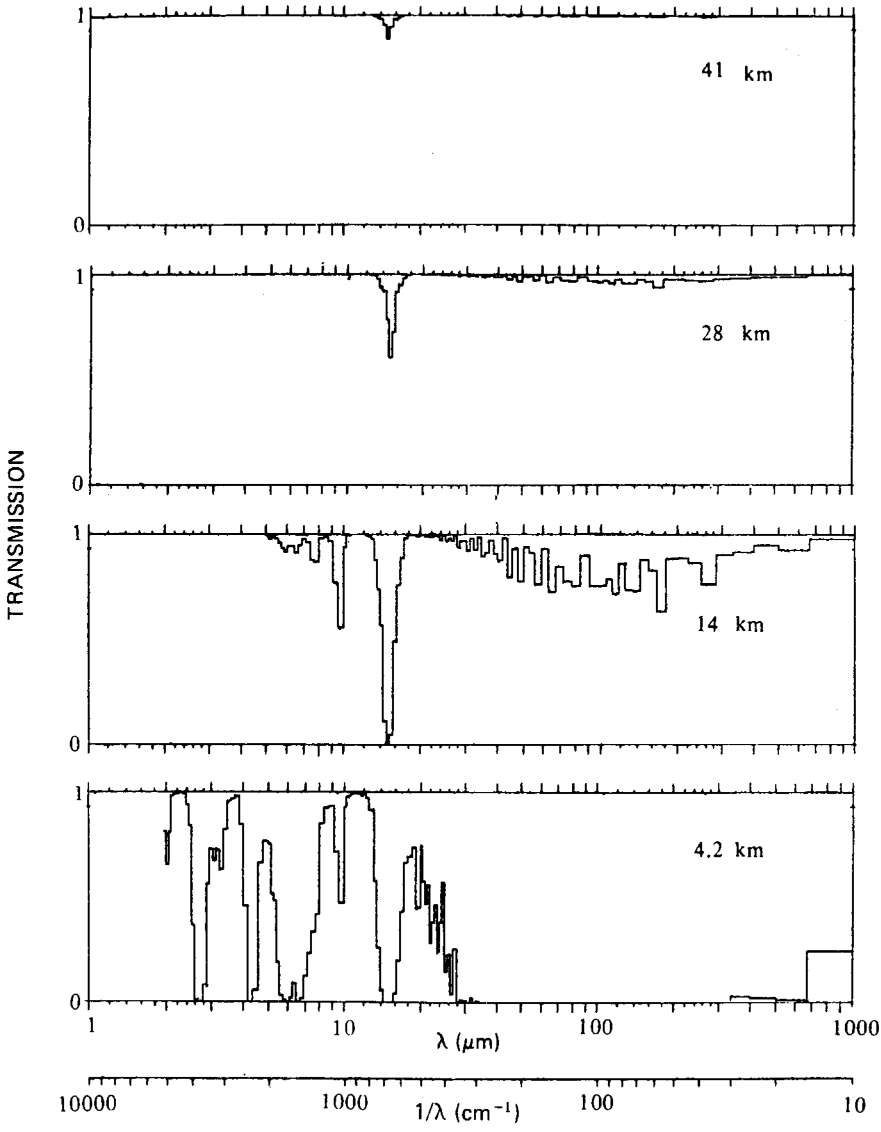

Diffuse emission from the night sky

Specific intensity (times ν) of diffuse emission from the night sky, observed away from the galactic and ecliptic planes, from high in the Earth's atmosphere. (From *Handbook of Infrared Astronomy*, Glass, I.S., Cambridge University Press, 1999, with permission.)

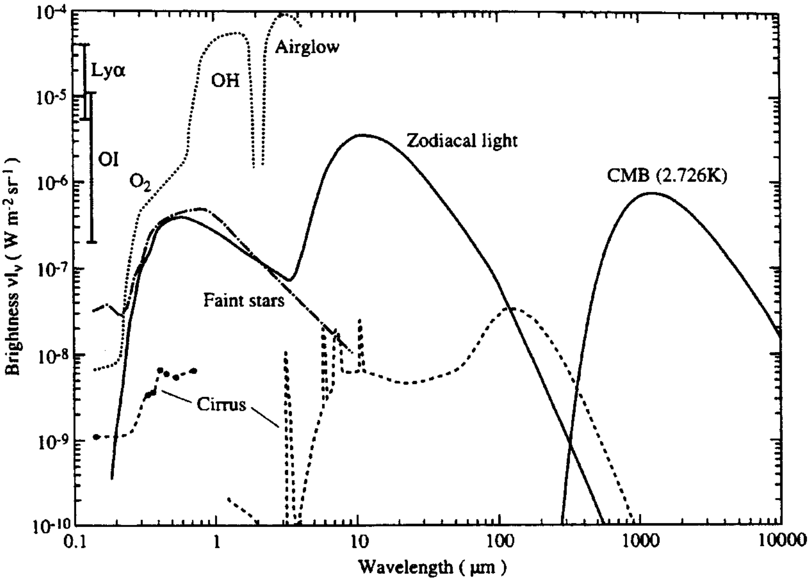

(Note: wisp-like clouds in the infrared are called *cirrus*)

Diffuse emission from the night sky (*cont.*)

Probable spectral irradiance from one-square-degree starfield in or near the galactic plane.

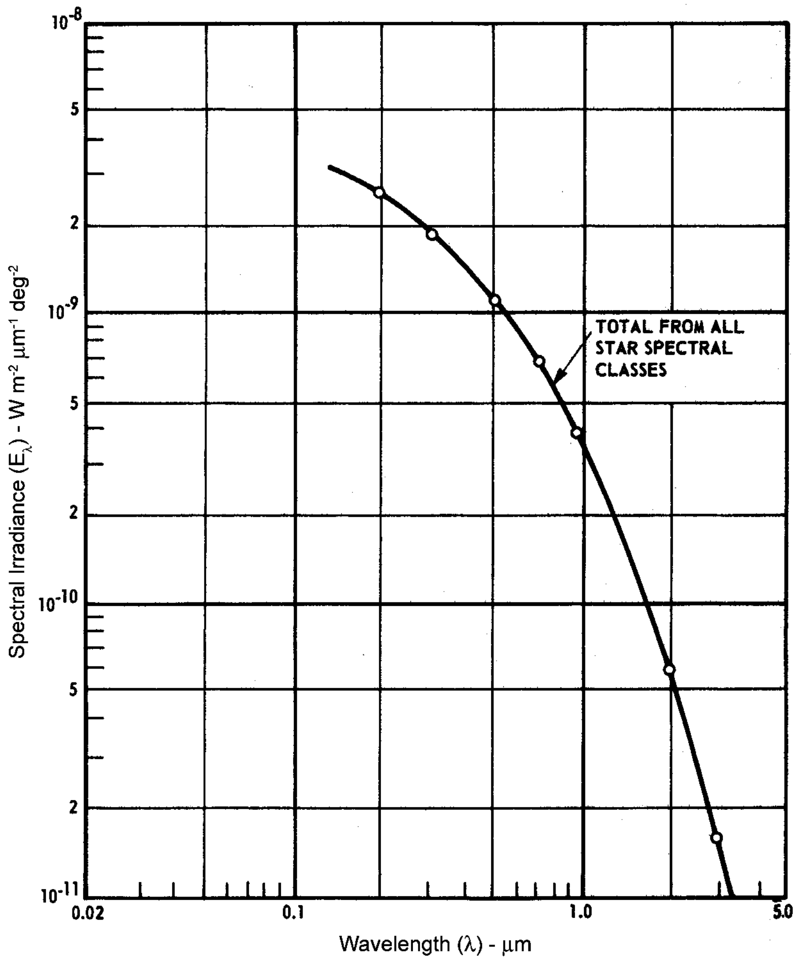

(From the *RCA Electro-Optics Handbook*, 1974.)

Spectral irradiance of the Sun

Spectral irradiance E_λ of the sun at mean earth-sun separation. Shaded areas indicate absorption at sea level due to the atmospheric constituents shown.

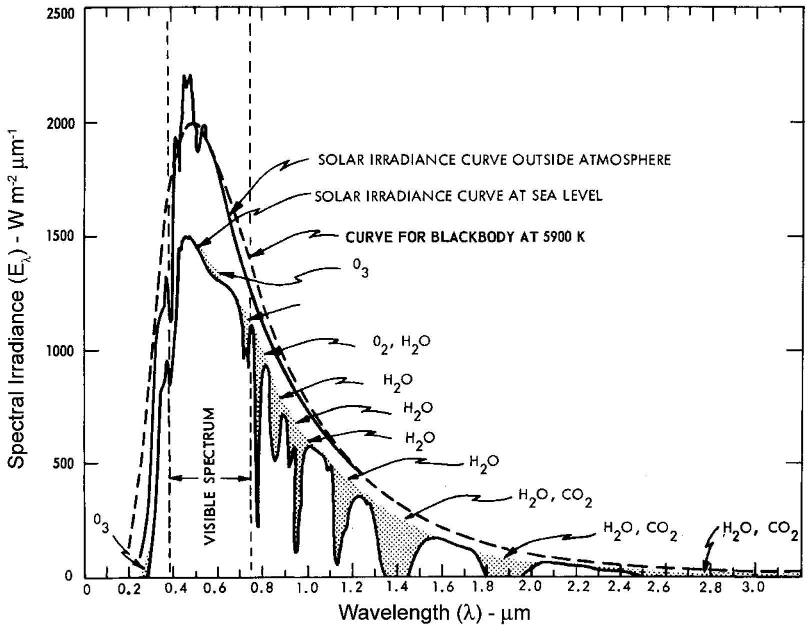

(From the *RCA Electro-Optics Handbook*, 1974.)

Spectral irradiance from the planets and brightest stars

Calculated spectral irradiance from planets at the top of the atmosphere; * = calculated irradiance from planets at brightest due only to sun reflectance; GF = inferior planet at greatest elongation; OPP = superior planet at opposition; QUAD = superior planet at quadrature; # = calculated irradiance from planets due only to self emission; m_ν = visual magnitude at maximum spectral irradiance

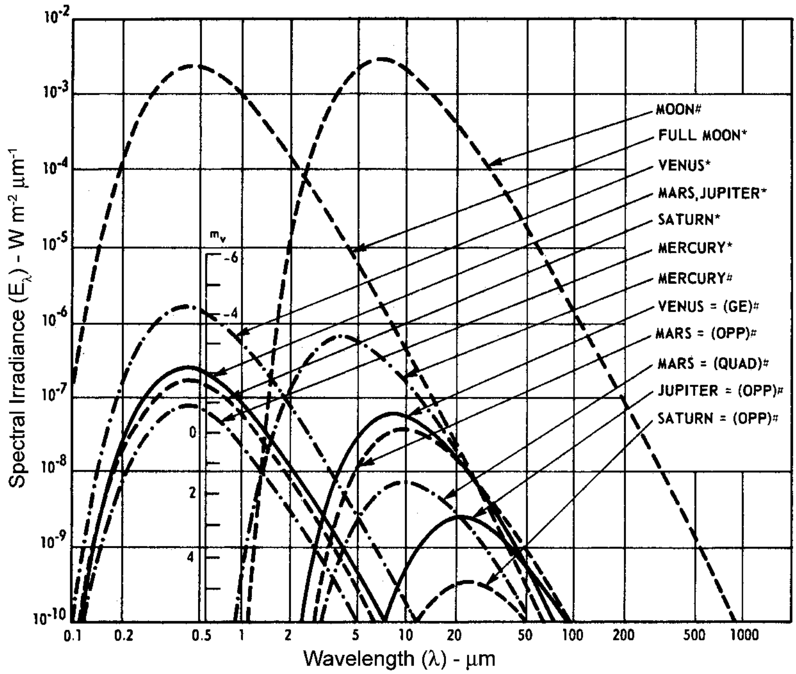

Calculated spectral irradiance from the brightest stars outside of the earth's atmosphere; m_v = visual magnitude at maximum spectral irradiance.

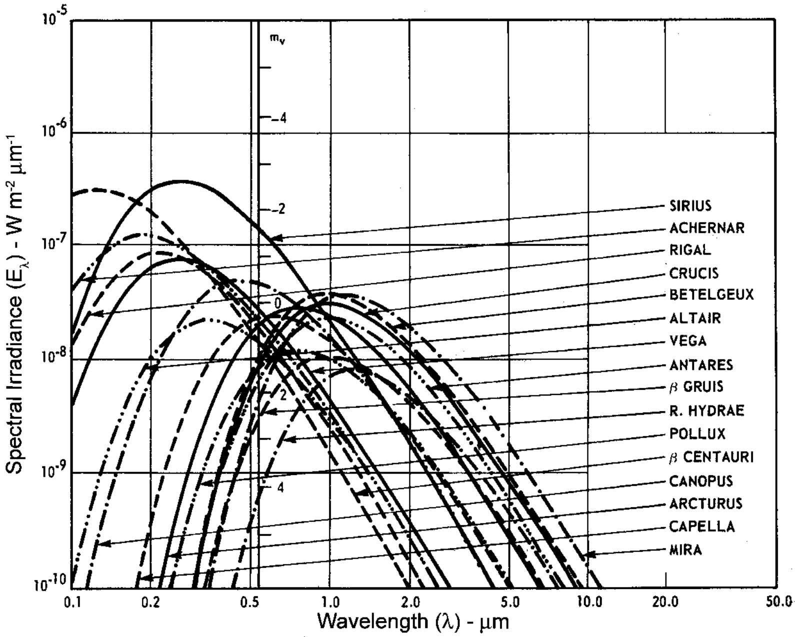

(From the *RCA Electro-Optics Handbook*, 1974.)

Emission from galaxies

Schematic overview of spectral energy distributions in galaxies

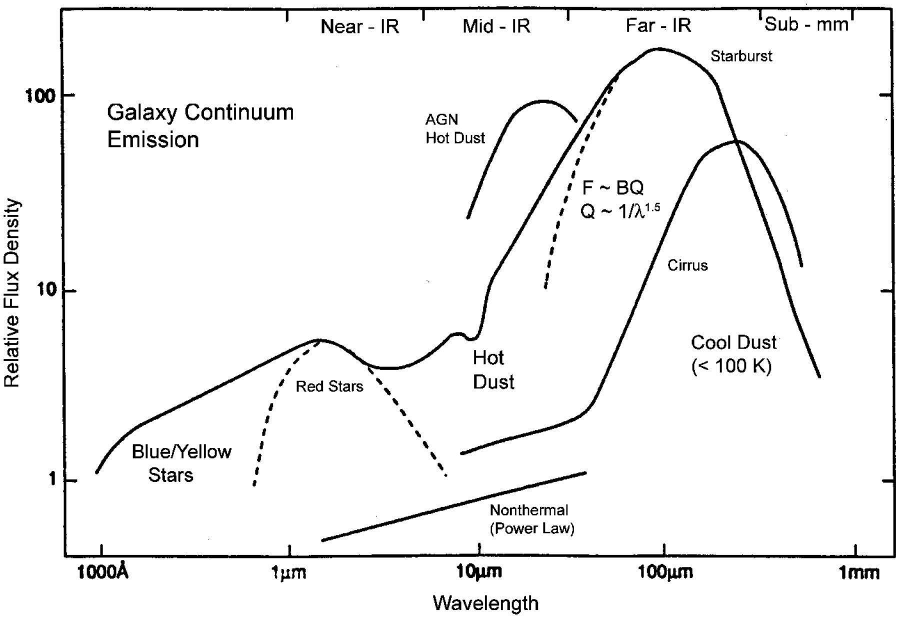

Near-IR colors and CO index for stars

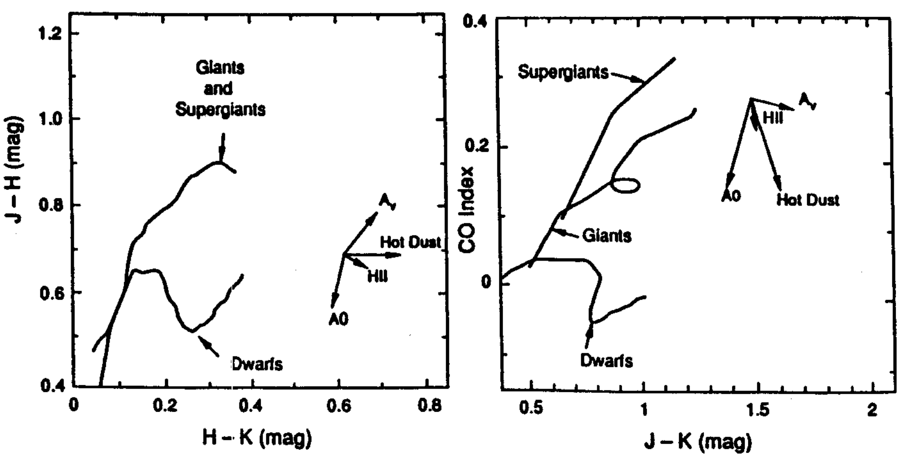

Emission from galaxies (*cont.*)

IR energy distributions for a sample of galaxies.

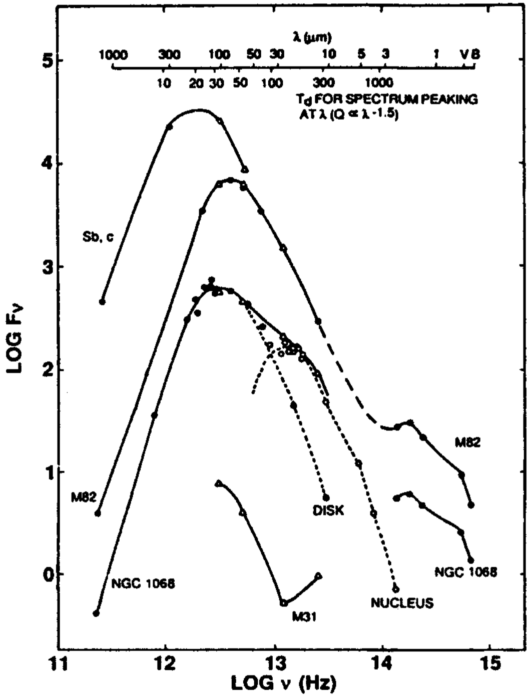

IRAS two-color diagram for non-AGN galaxies

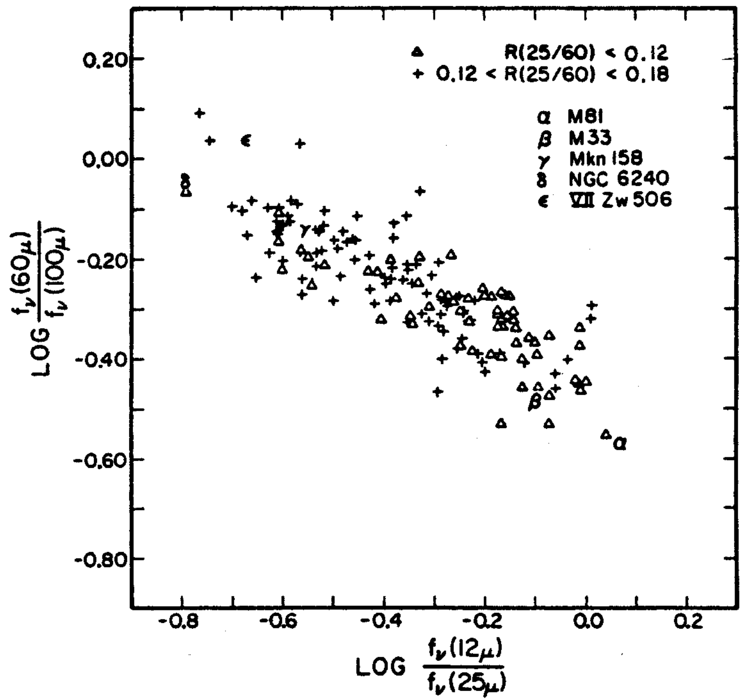

(From C.M. Telesco in *Infrared Astronomy*, Mampaso, A., Prieto, M., and Sanchez, F., Cambridge University Press, 1993, with permission.)

Broad-band infrared colors

Blackbodies

Temp (K)	*J-H*	*H-K*	*K-L*	*L-N*
300	9.37	6.92	7.69	8.59
400	7.03	5.20	5.66	6.14
500	5.62	4.14	4.43	4.69
600	4.67	3.42	3.60	3.75
800	3.45	2.50	2.56	2.60
1000	2.70	1.93	1.94	1.94
3000	0.63	0.43	0.41	0.42
5000	0.25	0.17	0.16	0.17
10000	0.00	0.00	0.00	0.00

Power-law energy spectral distributions

Exponent	$J - H$	$H - K$	$K - L$	$L - N$
−2	1.11	1.13	1.80	4.63
−1	0.78	0.82	1.31	3.39
0	0.46	0.50	0.83	2.19
1	0.13	0.18	0.34	1.00
2	−0.20	−0.14	−0.14	−0.16

Calculated for the JHKL filters used in the SAAO (Carter, B.S., Mon. Not. R. astr. Soc., **242**, 1, 1990.) photometric system. The color zero points for each index have been adjusted to be 0.0 for a 10000K blackbody. (From *Handbook of Infrared Astronomy*, Glass, I.S., Cambridge University Press, 1999, with permission.)

Standard Photometric System

Band	λ_{eff} μm	ν_0 Hz	F_λ W cm^{-2} μm^{-1}	F_ν W m^{-2} Hz^{-1}	$\log F_\nu$	$\log \nu_0$
U	0.366	8.19×10^{14}	4.175×10^{-12}	1.790×10^{-23}	−22.75	14.913
B	0.438	6.84×10^{14}	6.32×10^{-12}	4.063×10^{-23}	−22.39	14.835
V	0.545	5.50×10^{14}	3.631×10^{-12}	3.636×10^{-23}	−22.44	14.740
R_C	0.641	4.68×10^{14}	2.177×10^{-12}	3.064×10^{-23}	−22.51	14.670
I_C	0.798	3.79×10^{14}	1.126×10^{-12}	2.416×10^{-23}	−22.62	14.575
J	1.22	2.46×10^{14}	3.15×10^{-13}	1.59×10^{-23}	−22.80	14.390
H	1.63	1.84×10^{14}	1.14×10^{-13}	1.02×10^{-23}	−23.01	14.26
K	2.19	1.37×10^{14}	3.96×10^{-14}	6.4×10^{-24}	−23.21	14.14
L	3.45	8.7×10^{13}	7.1×10^{-15}	2.9×10^{-24}	−23.55	13.94
M	4.8	6.3×10^{13}	2.2×10^{-15}	1.70×10^{-24}	−23.77	13.80
N	10.6	2.8×10^{13}	9.6×10^{-17}	3.60×10^{-25}	−24.44	13.55
Q	21	1.43×10^{13}	6.4×10^{-18}	9.4×10^{-26}	−25.03	13.15

Absolute spectral irradiance for mag = 0.0 star. Sources for **UBVR$_\mathbf{C}$I$_\mathbf{C}$JHKL** are Bessell, M.S., Castelli, F., and Plez, B., Astron. Astrophys., **333**, 231, 1998. **V** = 0.03 for Vega on this system. The **JHKL** colors are on the Bessell and Brett (Bessell, M.S. and Brett, J.M., PASP, **100**, 1134, 1988) system; **M**, Campins, H., Rieke, G.H., and Lebofsky, M.J., Astron. J., **90**, 896, 1985; **NQ**, Rieke, G.H., Lebofsky, M., and Low, F.J., Astron. J., **90**, 900, 1985. (From *Handbook of Infrared Astronomy*, Glass, L.S., Cambridge University Press, 1999, with permission.)

Spectrophotometric standards in the infrared

Star	Spectral Types
Vega = α Lyr	A0V
Sirius = α CMa	A1V
α^1 Cen	G2V
α TrA	K2III
ϵ Car	K3III
α Boo	K1III
γ Dra	K5III
α Cet	M1.5III
γ Cru	M3.3III
μ UMa	M0III
β Peg	M2.5II-III
β And	M0III
β Gem	K0III
α Hya	K3II-III

(From *Handbook of Infrared Astronomy*, Glass, I.S., Cambridge University Press, 1999, with permission.)

Intrinsic colors of stars

Dwarfs

MK	$V-K$	$J-H$	$H-K$	$J-K$	$K-L$	$K-M$
B8	−0.35	−0.05	−0.035	−0.09	−0.03	−0.05
A0	0.00	0.00	0.00	0.00	0.00	0.00
A2	0.14	0.02	0.005	0.02	0.01	0.01
A5	0.38	0.06	0.015	0.08	0.02	0.03
A7	0.50	0.09	0.025	0.11	0.03	0.03
F0	0.70	0.13	0.03	0.16	0.03	0.03
F2	0.82	0.165	0.035	0.19	0.03	0.03
F5	1.10	0.23	0.04	0.27	0.04	0.02
F7	1.32	0.285	0.045	0.34	0.04	0.02
G0	1.41	0.305	0.05	0.36	0.05	0.01
G2	1.46	0.32	0.052	0.37	0.05	0.01
G4	1.53	0.33	0.055	0.385	0.05	0.01
G6	1.64	0.37	0.06	0.43	0.05	0.00
K0	1.96	0.45	0.075	0.53	0.06	−0.01
K2	2.22	0.50	0.09	0.59	0.07	−0.02
K4	2.63	0.58	0.105	0.68	0.09	−0.04
K5	2.85	0.61	0.11	0.72	0.10	
K7	3.16	0.66	0.13	0.79	0.11	
M0	3.65	0.695	0.165	0.86	0.14	
M1	3.87	0.68	0.20	0.87	0.15	
M2	4.11	0.665	0.21	0.87	0.16	
M3	4.65	0.62	0.25	0.87	0.20	
M4	5.26	0.60	0.275	0.88	0.23	
M5	6.12	0.62	0.32	0.94	0.29	
M6	7.30	0.66	0.37	1.03	0.36	

Giants

MK	$V-K$	$J-H$	$H-K$	$J-K$	$K-L$	$K-M$
G0	1.75	0.37	0.065	0.45	0.04	0.0
G4	2.05	0.47	0.08	0.55	0.05	−0.01
G6	2.15	0.50	0.085	0.58	0.06	−0.02
G8	2.16	0.50	0.085	0.58	0.06	−0.02
K0	2.31	0.54	0.095	0.63	0.07	−0.03
K1	2.50	0.58	0.10	0.68	0.08	−0.04
K2	2.70	0.63	0.115	0.74	0.09	−0.05
K3	3.00	0.68	0.14	0.82	0.10	−0.06
K4	3.26	0.73	0.15	0.88	0.11	−0.07
K5	3.60	0.79	0.165	0.95	0.12	−0.08
M0	3.85	0.83	0.19	1.01	0.12	−0.09
M1	4.05	0.85	0.205	1.05	0.13	−0.10
M2	4.30	0.87	0.215	1.08	0.15	−0.12
M3	4.64	0.90	0.235	1.13	0.17	−0.13
M4	5.10	0.93	0.245	1.17	0.18	−0.14
M5	5.96	0.95	0.285	1.23	(0.20)	−0.15
M6	6.84	0.96	0.30	1.26		0.0:
M7	7.8	0.96	0.31	1.27		0.0:

Bessell and Brett (Bessell, M.S. and Brett, J.M., PASP, **100**, 1134, 1988) system. (From *Handbook of Infrared Astronomy*, Glass, I.S., Cambridge University Press, 1999, with permission.)

Statistics of galaxies at infrared wavelengths

Number counts at 2.2 μm

$$dN/dK = 4000 \times 10^{\alpha(\mathrm{K}-17)} \text{ galaxies per square degree per unit magnitude,}$$

where $\alpha = 0.67$ for $10 < \mathrm{K} < 17$, $\alpha = 0.26$ for $17 < \mathrm{K} < 23$, K = 2.2 μm magnitude.

Luminosity function at 60 μm

$$\log(\rho) = -3.2 - \alpha\{\log[\nu \mathrm{L}_\nu(60\ \mu\mathrm{m})] - 10.2\} \text{ galaxies per cubic megaparsec per unit magnitude at } 60\ \mu\mathrm{m},$$

where $\nu \mathrm{L}_\nu(60\ \mu\mathrm{m})$ is given in units of $\mathrm{L}_\odot$, and $\alpha = 0.8$ for $\log[\nu \mathrm{L}_\nu(60\ \mu\mathrm{m})] < 10.2$ and $\alpha = 2.0$ for $\log[\nu \mathrm{L}_\nu\ (60\ \mu\mathrm{m})] > 10.2$. $\mathrm{H}_0 = 75$ km s^{-1} Mpc^{-1}

Energy density

The total infrared energy density of the local universe from 8 to 1000 μm is

$$1.24 \times 10^8 \mathrm{L}_\odot\ \mathrm{Mpc}^{-3}.$$

(From Tokunaga, A.T., in *Allen's Astrophysical Quantities*, Cox, A.N., ed., Springer-Verlag, 2000)

Near IR and mid IR diagnostic lines

Line Designation	Wavelength (μm)	Utility
H I Brβ	2.63	UV luminosity
Sulfates/bisulfates	2.3, 4.5, 9	Solar system studies
PAH/hydrocarbons	3.4	Dust, low UV
H I Brα	4.05	UV luminosity
CO_2 ice	4.26	Dust, solar system studies
[Mg VII]	5.51	Hot gas coolant
[Mg V]	5.60	General coolant, shocks
[Si VII]	6.50	Hot gas coolant, shocks
[Ar II]	6.99	Radiation intensity
[Ne VI]	7.63	Spectral index
Methane	7.7	Solar system studies
[Ar V]	7.90	Spectral index, reddening
[Mg VII]	8.95	Hot gas coolant
[Ar III]	8.99	Spectral index, reddening
Silicates	9.7	Dust
[S IV]	10.5	General coolants
[Ne II]	12.8	Radiation intensity, shocks
[Ar V]	13.1	Spectral index, reddening
[Mg V]	13.5	Spectral index, hot gas
[Ne V]	14.3	Spectral index, density
[CO_2 ice]	15.2	Dust, solar system studies
[Ne III]	15.6	Metallicity
H_2 (0-0) S(1,2,etc)	17.0, 12.3, etc.	Shock conditions
[S III]	18.7	General coolant
[Ne V]	24.2	Spectral index, reddening
[O IV]	25.9	Spectral index
[S III]	33.5	General coolant
OH	34.6	Radiative pumping
[Si II]	35	Shocks
[Ne III]	15.6, 36	Spectral index, density
[O I]	63	Shocks
[O III]	52, 88	FIR reddening, density

(From NASA)

Extensive lists of infrared lines can be found at the web site noted at the end of this chapter.

Selected submillimeter lines

Species	Transition	Frequency (GHz)
CH	$F_1 \to F_2;\ J = 3/2^- \to 1/2^+$	536.76
$H_2{}^{18}O$	$1_{10} \to 1_{01}$	547.68
NH_3	$1_0 \to 0_0$	572.50
$H_2{}^{18}O$	$2_{11} \to 2_{02}$	745.32
NH	$N = 1 \to 0;\ J = 2 \to 1$	974.48
H_3O^+	$0_0^- \to 1_0^+$	984.66
NH^+	$3/2^+ \to 1/2^-$	998.90
HF	$1 \to 0$	1232.48
H_2D^+	$1_{01} \to 0_{00}$	1370.09
N^+	$^3P\ J = 1 \to 0$	1461.13
^{16}OH	$^2\prod_{1/2}\ J = 3/2^+ \to 1/2^-$	1837.82
C^+	$^2P\ J = 3/2 \to 1/2$	1900.54
CH_2	$1_{10} \to 1_{01}$	1917.66
CO	$18 \to 17$	1956.02

(From the California Institute of Technology's Caltech Submillimeter Interstellar Medium Investigations Receiver (CASIMIR) group, 2000.)

Source temperatures

Brightness temperature

$T_b(\nu) = \dfrac{c^2 B_\nu}{2\nu^2 k}$ (Rayleigh-Jeans approximation).

T_b is the temperature of a blackbody which would have the same spectral radiance B_ν at frequency ν as the source.

Color temperature

$$\frac{B_{\lambda_1}}{B_{\lambda_2}} = \left(\frac{\lambda_2}{\lambda_1}\right)^5 \frac{e^{hc/\lambda_2 k T_c} - 1}{e^{hc/\lambda_1 k T_c} - 1}.$$

B_λ is the spectral radiance of source at wavelength λ.

Effective temperature

$L = 4\pi R^2 \sigma T_{\text{eff}}^4$,

where

L = source power,
R = radius of source,
σ = Stefan-Boltzmann constant.

Blackbody spectral flux densities for stars

The blackbody spectral flux density for a star is given by,

$F_\lambda = \dfrac{1.9 \times 10^{-11} \lambda^{-5} p^2 R^2}{e^{14388/\lambda T} - 1}$ (W cm$^{-2}\mu$m^{-1})

where

R = radius of star (in units of the Sun's radius),
p = parallax (arcsec),
T = temperature (K),
λ = wavelength (μm).

(Johnson, H.M. & Wright, C.D., *Ap. J. Suppl.*, **53**, 643, 1983),

Space Infrared Telescope Facility (SIRTF)

Note: **SIRTF** has been renamed the **Spitzer Space Telescope**

SIRTF consists of a 0.85-meter telescope and three cryogenically-cooled science instruments capable of performing imaging and spectroscopy in the 3 to 180 micron wavelength range. The three instruments are the Infrared Array Camera (IRAC), the Infrared Spectrograph (IRS), and the Multiband Imaging Photometer for SIRTF (MIPS).

SIRTF focal plane

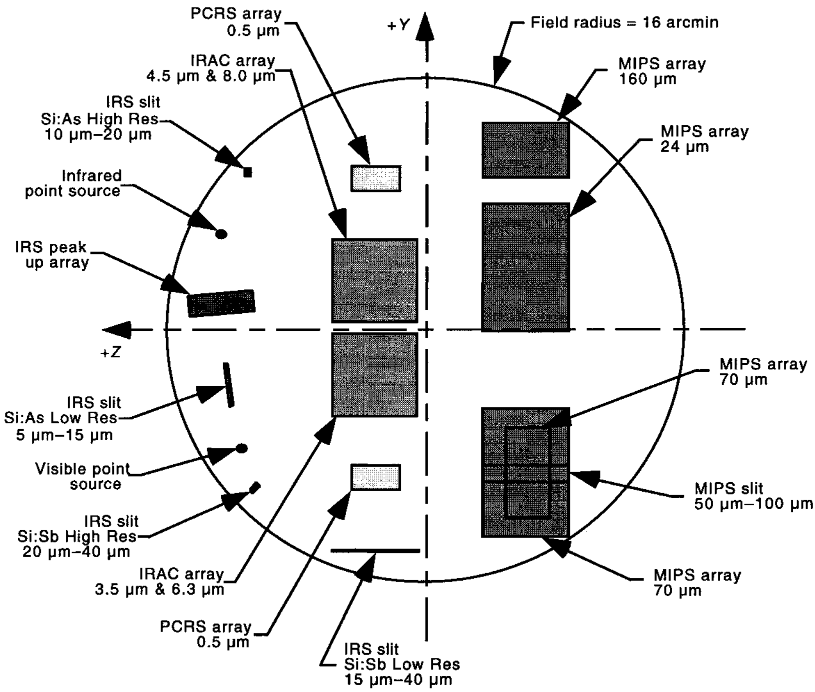

SIRTF Instrumentation summary

Wavelength (μm)	**Array Type**	**Resolving Power**	**Field of View**	**Pixel size (arcsec)**	**Sensitivity (μJy) (5 sigma in 500s, incl. confusion)**
		IRAC: InfraRed Array Camera			
3.6	InSb	4.7	$5.12' \times 5.12'$	1.2	4.1
4.5	InSb	4.4	$5.12' \times 5.12'$	1.2	5.4
5.8	Si:As (IBC)	4.0	$5.12' \times 5.12'$	1.2	18
8.0	Si:As (IBC)	2.8	$5.12' \times 5.12'$	1.2	18
		MIPS: Multiband Imaging Photometer for SIRTF			
24	Si:As (IBC)	5	$5.2' \times 5.2'$	2.45	185
			$2.6' \times 2.6'$	4.9	3000
70	Ge:Ga	4	$5.3' \times 5.3'$	9.9	1410
55-96	Ge:Ga	15-25	$0.32' \times 3.8'$	9.9	11 mjy at 55 micron 14 mjy at 95 micron
160	Ge:Ga (stressed)	5	$0.5' \times 5.3'$	15.8	22.5 mJy
		IRS: Infrared Spectrograph			
5.3-14	Si:As (IBC)	62-124	$3.6'' \times 54.6''$	1.8	550
13.5-18.5 18.5-26	Si:As (IBC) (peak-up)	~ 3	$1' \times 1.2'$	1.8	
10-19.5	Si:As (IBC)	600	$5.3'' \times 11.8''$	2.4	3×10^{-18} W/m^2
14-40	Si-Sb (IBC)	62-124	$9.7'' \times 151.3''$	4.8	1500
19-37	Si:Sb (IBC)	600	$11.1'' \times 22.4''$	4.8	3×10^{-18} W/m^2

(From NASA, 2000)

Bibliography

Handbook of Infrared Astronomy, Glass, I.S., Cambridge University Press, 1999.

Infrared Astronomy, Mampaso, A., Prieto, M., and Sanchez, F., eds., Cambridge University Press, 1993.

Infrared Astronomy, Setti, G. and Fazio, G., eds., D. Reidel Publishing Co., 1977.

Infrared Astronomy, Tokunaga, A.T., in *Allen's Astrophysical Quantities*, Cox, A.N., ed., Springer-Verlag, 2000.

The *Infrared Handbook*, Wolfe, W.I., and Zissis, G.J., eds., Office of Naval Research, Department of the Navy, Washington DC, 1978.

Note: Links to WWW resources which supplement the material in this chapter can be found at:

http://www.astrohandbook.com

Chapter 5

Ultraviolet astronomy

The stars are majestic laboratories, gigantic crucibles, such as no chemist could dream. - Henri Poincaré

UV stellar spectra

Spectral features in stars of different spectral types and luminosities. (Courtesy of A.K. Dupree, Center for Astrophysics, 1982.)

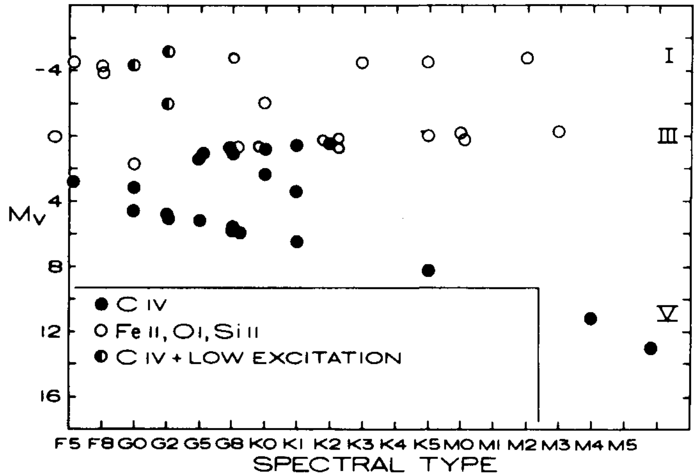

IUE short wavelength spectra of dwarf stars. (Courtesy of A.K. Dupree, Center for Astrophysics, 1982.)

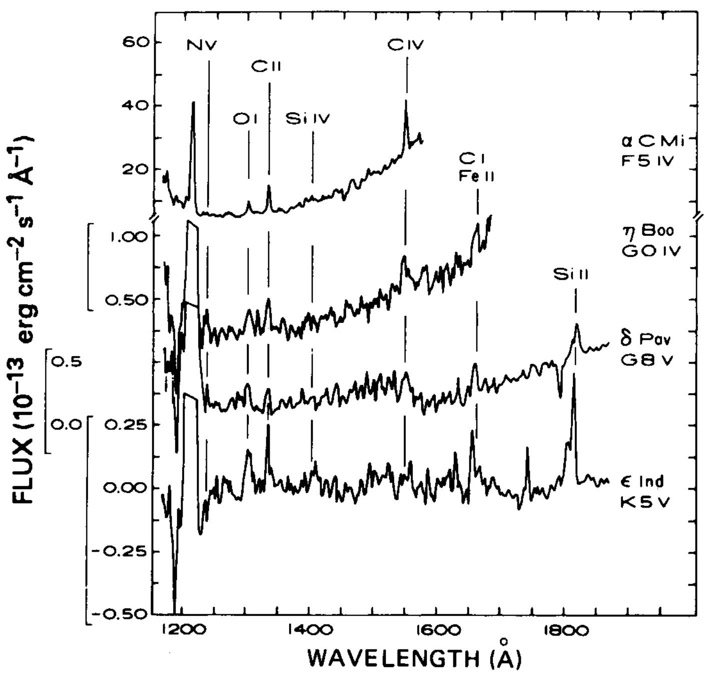

UV stellar spectra (*cont.*) IUE short wavelength spectra of giant and supergiant stars. (Courtesy of A.K. Dupree, Harvard/Smithsonian Center for Astrophysics, 1982.)

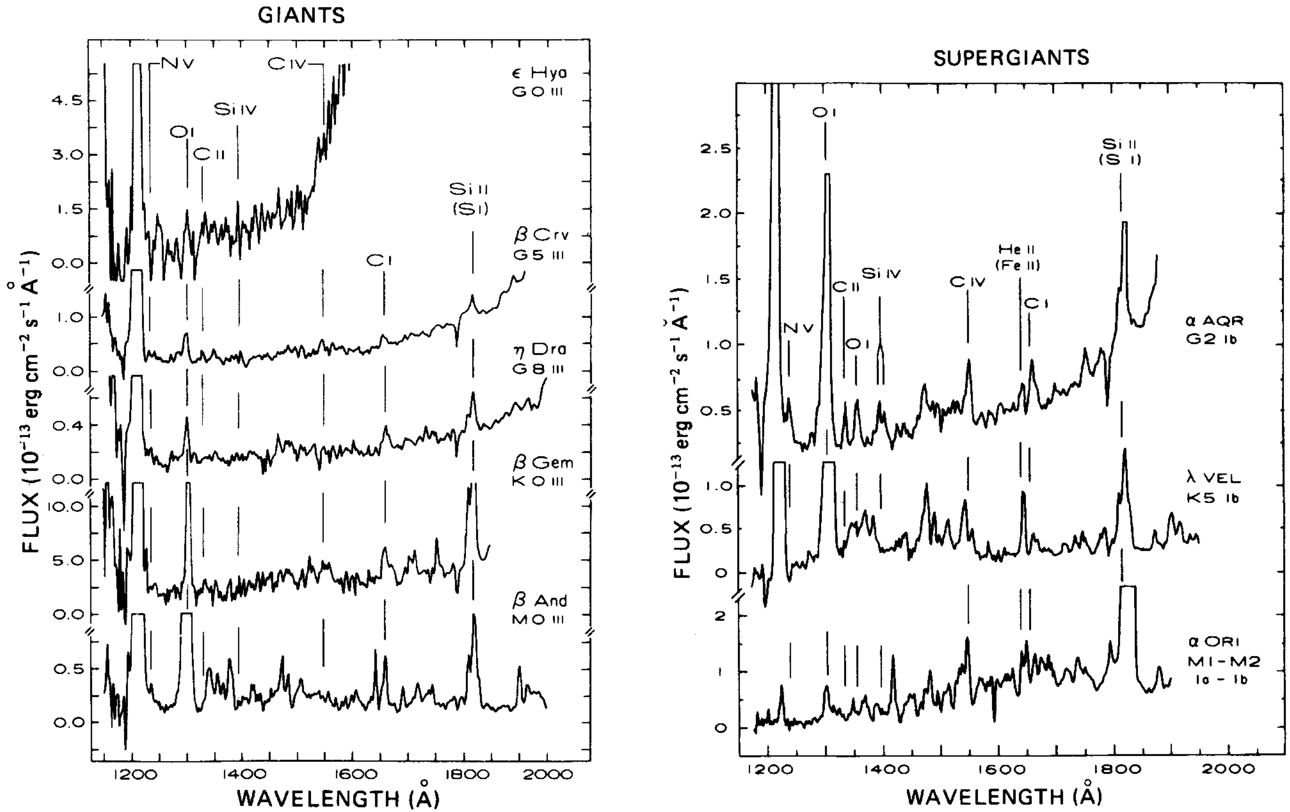

Stellar surface fluxes

The ratio of stellar surface flux to the corresponding solar value for emission lines formed at various temperatures. (Courtesy of A.K. Dupree, Harvard/Smithsonian Center for Astrophysics, 1982.)

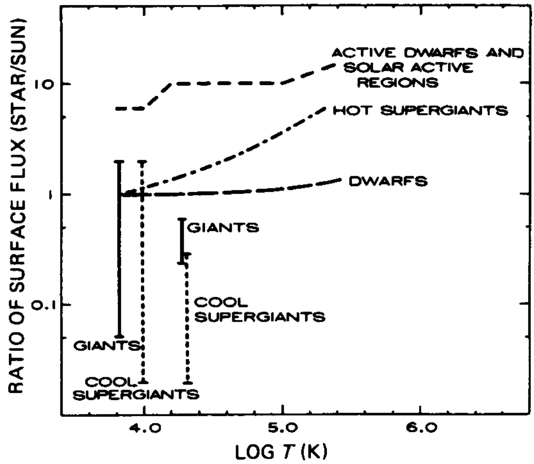

Mass loss rates

Characteristics of mass loss rates and winds (temperatures and terminal velocities) in stars of various luminosities. (Courtesy of A.K. Dupree, Harvard/Smithsonian Center for Astrophysics, 1982.)

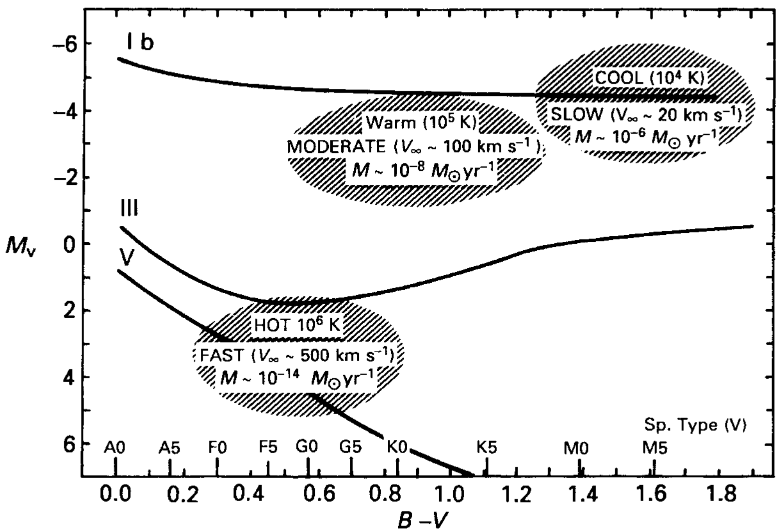

EUV sources

EUV sources from the 2nd EUVE (Extreme Ultraviolet Explorer) catalog. The 737 sources observed are displayed in galactic coordinates. (Courtesy of Roger Malina, The Center for Extreme Ultraviolet Astrophysics, 1999.)

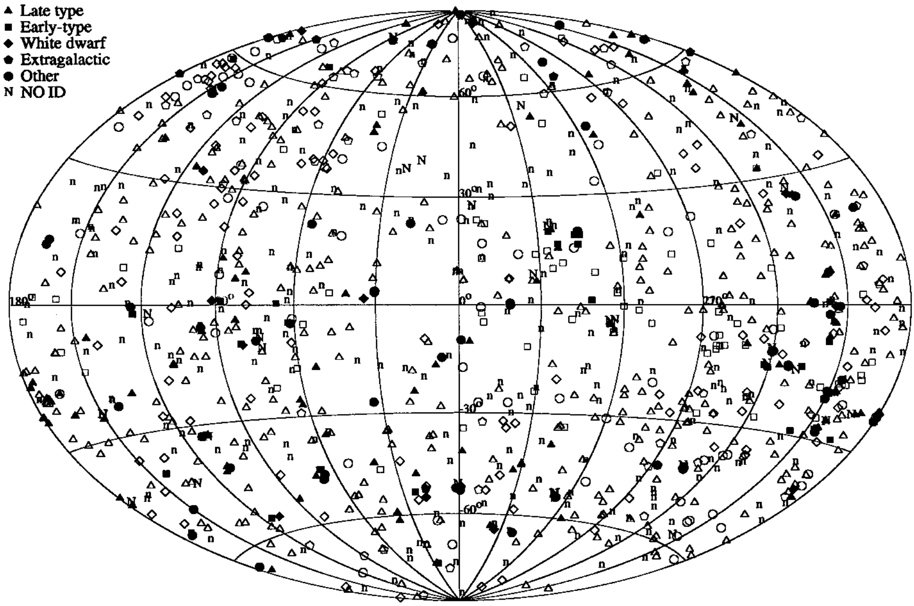

Second EUVE Catalog-list of objects detected

Type	CAT2[a]
Early-type Stars (O, B, A)	24
Late-type Stars (F, G, K, M)	275
White Dwarfs	105
Cataclysmic Variables	14
Low Mass X-ray Binaries	2
Extragalactic	37
Other	35
No Identification	245
TOTAL	737

[a]Bowyer *et al.* 1996, ApJS, 102, 129, *Second EUVE All-sky Catalog.*

Extragalactic EUVE sources

NAME	RA 2000 h m s	Dec 2000 d m	c/ks* 100 Å	ID Name	Type
EUVE J0425−572	04 25 50	−57 12.8	34.0	1H 0419−577	Seyfert
EUVE J1015+494	10 15 04	+49 26.0	28.1	1H1013+498	BL Lac
EUVE J1034+396	10 34 36	+39 38.0	9.3	RE J1034+393	Seyfert
EUVE J1104+382	11 04 33	+38 12.6	56.0	Mrk 421	BL Lac
EUVE J1114+406	11 14 39	+40 37.0	1.4	3C 254	QSO
EUVE J1119+213	11 19 08	+21 19.6	17.0	PG 1116+215	QSO
EUVE J1203+445	12 03 10	+44 31.9	19.3	NGC 4051	Seyfert
EUVE J1229+020	12 29 07	+02 03.1	79.2	3C 273	QSO
EUVE J1236+456	12 36 49	+45 38.9	2.4	CGCG 244−033	AGN
EUVE J1352+692	13 52 56	+69 17.6	33.0	Mrk 279	Seyfert
EUVE J1417+449	14 17 01	+44 56.0	5.2	PG 1415+451	QSO
EUVE J1417+251	14 17 59	+25 08.2	23.6	NGC 5548	Seyfert
EUVE J1421+477	14 21 30	+47 47.0	3.4	CG 0912	QSO
EUVE J1428+426	14 28 33	+42 40.4	32.7	H1426+427	BL Lac
EUVE J1442+354	14 42 08	+35 27.7	56.0	Mrk 478	Seyfert
EUVE J1556+452	15 56 42	+45 13.9	4.3	MS 1555.1+4522	AGN
EUVE J1617+323	16 17 42	+32 22.9	3.5	3C 332	Seyfert
EUVE J1653+397	16 53 52	+39 45.0	30.0	Mrk 501	BL Lac
EUVE J2132+101	21 32 31	+10 07.9	2.0	Mrk 1513	Seyfert
EUVE J2158−302	21 58 51	−30 13.6	297.0	PKS 2155−304	BL Lac
EUVE J2209−471	22 09 17	−47 10.0	23.0	NGC 7213	Seyfert
EUVE J2343−149	23 43 32	−14 55.8	3.0*	1E 2340.9−1511	Seyfert
EUVE J2359−306	23 59 08	−30 37.7	14.7	1H 2354−315	BL Lac

*Count rate from EUVE Deep Survey Telescope; counts per kilosecond. (From Bowyer, S. and Malina, R.F., in *New Developments in X-ray and Ultraviolet Astronomy*, Drew, J.E., ed., Adv. Space. Res. **16**, No. 3, 25, 1995.)

25 Brightest EUVE sources

Name	α 2000			δ 2000		ID 1	ID 2	Sg typ	V mag	Q
EUVE J0658−289	6^h	58^m	43^s	-28°	$56.9'$	ε CMa	RE J0658−285	B2Iab	1.50	U
EUVE J1316+290	13	16	24	+29	5.4	WD 1314+293	PG 1314+293	DAw	12.56	1
EUVE J0505+528	5	5	35	+52	49.7	WD 0501+527	RE J0505+524	DAw	11.78	1
EUVE J0645−167	6	45	13	−16	42.0	α CMa B	WD 0642−166	DA	8.44	1
						α CMa A	TD1 8027	A1V	−1.47	2
EUVE J0457−281	4	57	16	−28		WD 0455−28	RE J0457−281	DA	14.00	1
EUVE J1502+661	15	2	6	+66	11.7	WD 1501+664	RE J1502+661	DZ		1
EUVE J0622−179	6	22	40	−17	58.5	β CMa	RE J0622−175	B1II/III	1.98	U
EUVE J0235+037	2	35	9	+3	44.9	WD 0232+035	PG 0232+035	DA+dM1.5	12.40	1
EUVE J2214−493	22	14	10	−49	19.9	RE J2214−491		DA	11.70	1
EUVE J1816+498	18	16	14	+49	51.7	AM Her	1H 1814+498	CV	12.40	1
EUVE J1257+220	12	57	4	+22	1.2	WD 1254+223	PG 1254+223	DAw	13.40	1
EUVE J0503−288	5	3	56	−28	53.8	RE J0503−285		DO	13.90	1
EUVE J2312+107	23	12	24	+10	46.7	WD 2309+105	PG 2309+105	DAw	13.11	1
EUVE J1032+534	10	32	13	+53	29.0	RE J1032+532		DA	14.50	1
EUVE J2009−604	20	9	2	−60	26.3	RE J2009−602		DA	13.40	1
EUVE J2156−546	21	56	20	−54	39.0	RE J2156−543		DA	14.30	1
EUVE J0515+326	5	15	27	+32	41.2	RE J0515+324	HD 33959 C	A2	7.95	1
						KW Aur	TD1 4235	A9IV	5.05	1
EUVE J0623−376	6	23	14	−37	40.9	RE J0623−374		DA	12.00	1
EUVE J0053−330	0	53	16	−33		WD 0050−332	RE J0053−325	DA	13.38	1
EUVE J1629+780	16	29	1	+78	4.5	WD 1631+78	RE J1629+781	DA	13.00	1
EUVE J0552+158	5	52	30	+15	53.9	WD 0549+158	RE J0552+155	DAw	13.06	1
EUVE J0715−704	7	15	10	−70	24.6	RE J0715−702		DA	14.40	1
EUVE J0228−613	2	28	22	−61	18.4	RE J0228−611	HD 15638	F3IV/V	8.80	1
EUVE J0335−257	3	35	30	−25	43.6	UZ For	EXO 0333.3−2554	CV	18.20	1
EUVE J1059+514	10	59	19	+51	24.2	RE J1059+512	LB 1919	DA	16.80	1

The list is sorted by count rate (highest first, irrespective of the 100, 200, 400, and 600 A detector band passes).
The “Q” column indicates a level of confidence in each source identification. 1: likely, 2: positional coincidence but no supporting evidence, U: some of the counts originate in the known UV leak.
(From the *Second EUVE Source Catalog*, Bowyer S., Lampton M., Lewis J., Wu X., Jelinsky P., Malina R.F., 1996, Astrophys. J. Suppl. Ser. **102**, 129.)

Background fluxes

Cosmic background

Soft X-ray and EUV background fluxes. (Adapted from Stern, R. & Bowyer, S., *Ap. J.*, **230**, 755, 1979.)

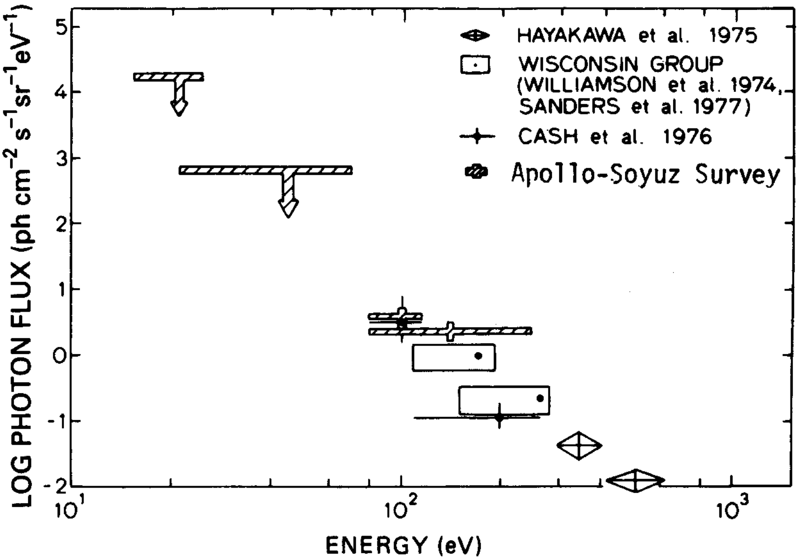

Geocoronal vacuum ultraviolet emission

		Photon radiance (ph cm^{-2} s^{-1} sr^{-1})	
λ (Å)	Line	Day	Night
304	He II	8.0×10^5	8.0×10^5
584	He I	8.0×10^7	8.0×10^5
834	O II	8.0×10^7	2.0×10^6
1025	H I	1.6×10^8	1.6×10^8
1216	H I	8.0×10^8	8.0×10^8
1304-1356	O I	8.0×10^8	8.0×10^6
1356-1600	N_2	2.4×10^7	2.4×10^7

$$1 \text{ Rayleigh} = \frac{1}{4\pi} \times 10^6 \text{ ph cm}^{-2} \text{ s}^{-1} \text{ sr}^{-1}.$$

EUV plasma spectra

EUV (100 – 1000Å) spectrum of an optically thin plasma. Line fluxes are normalized assuming a line width of 1 Å. Logarithmic abundances: H ≡ 12.00, He = 10.93, C = 8.52, N = 7.96, O = 8.82, Ne = 7.92, Mg = 7.42, Si = 7.52, S = 7.20, Fe = 7.60. Dashed curve: free-free continuum; dotted curve: two-photon continuum; solid curve: total continuum including free-bound radiation. (Adapted from Stern, R., Wang, E. and Bowyer, S., *Ap. J. Suppl.*, **37**, 195, 1978.)

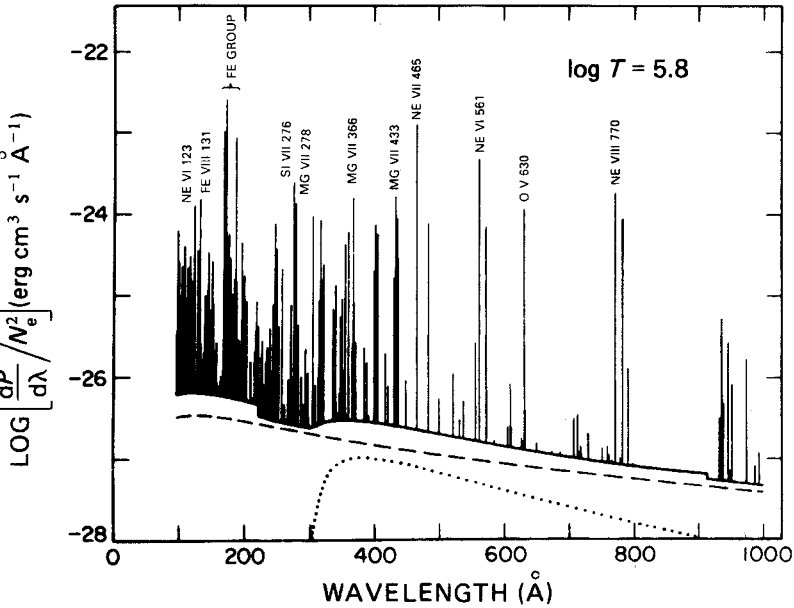

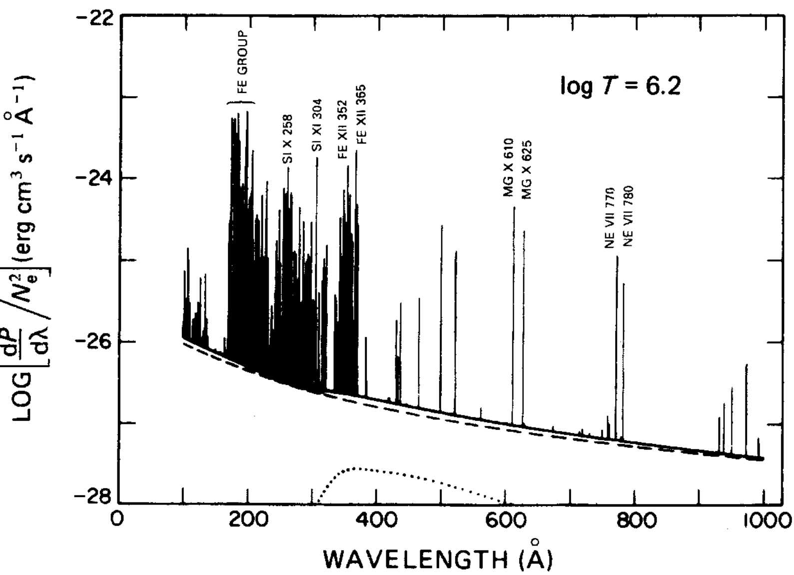

EUV plasma spectra (*cont.*)

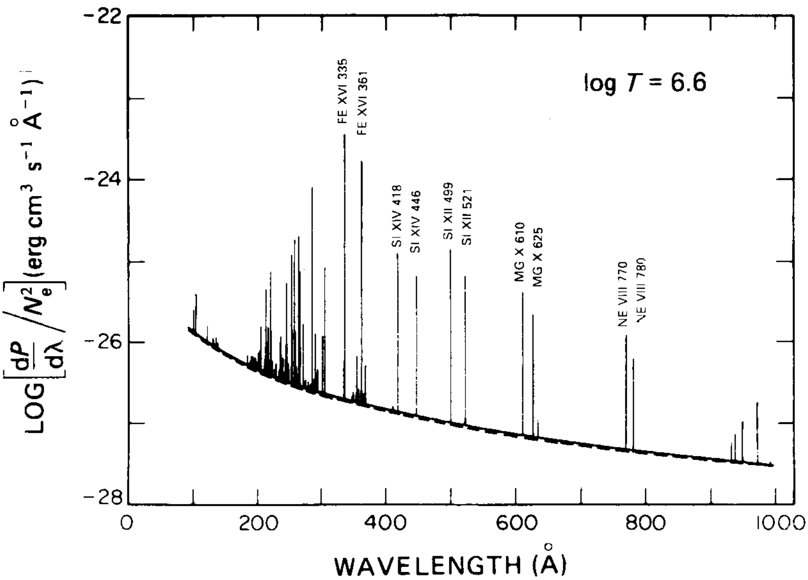

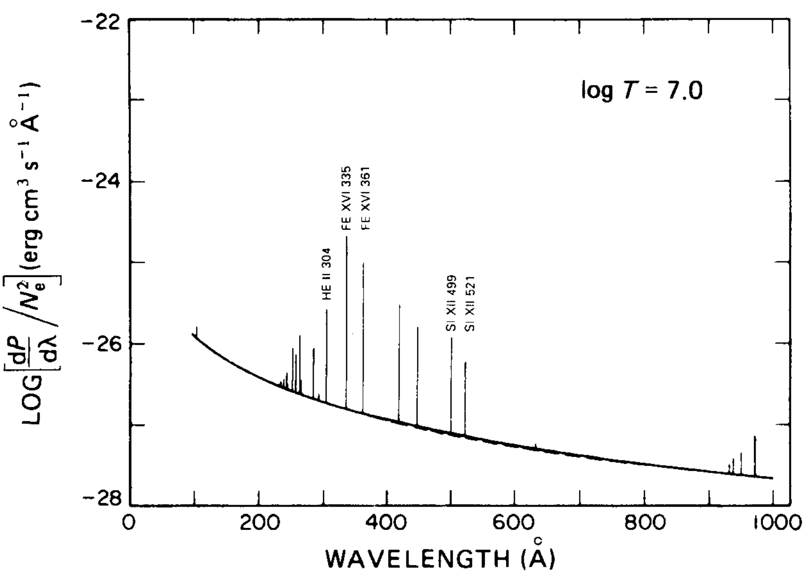

EUV plasma spectra (*cont.*)

X-ray and EUV (1 – 2000 Å) spectrum of an optically thin plasma. The power spectral distribution per unit emission measure and 5 Å band (erg cm^3 s^{-1} (5Å)$^{-1}$) at 3×10^4 and 1×10^6 K are shown. The contributions to continuum radiation from free-free (ff), free-bound (fb), and the two-photon process (2ph) from H-like ions are indicated. The most important lines are labeled.

The following cosmic abundances relative to H ($\log n_{\mathrm{E}}/n_{\mathrm{H}}$) are used: H = 0.0; He = −1.07; C = −3.48; N = −4.04; O = −3.18; Ne = −4.08; Na = −5.72; Mg = −4.58; Si = −4.48; Al = −5.61; S = −4.80; Ar = −5.20; Ca = −5.70; Fe = −4.40; and Ni = −5.70.

(From Landini, M. and Monsignori-Fossi, B., in *Extreme Ultraviolet Astronomy*, Malina, R.F. and Bowyer, S., ed., Pergamon Press, 1989.)

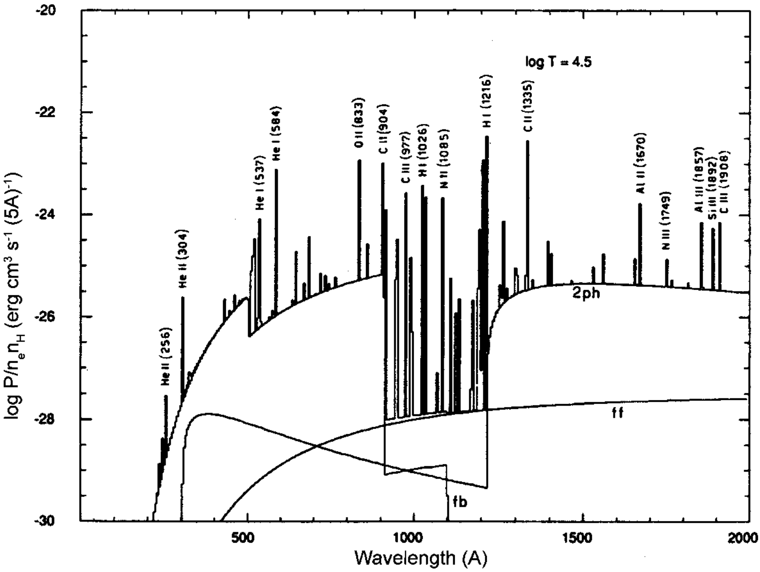

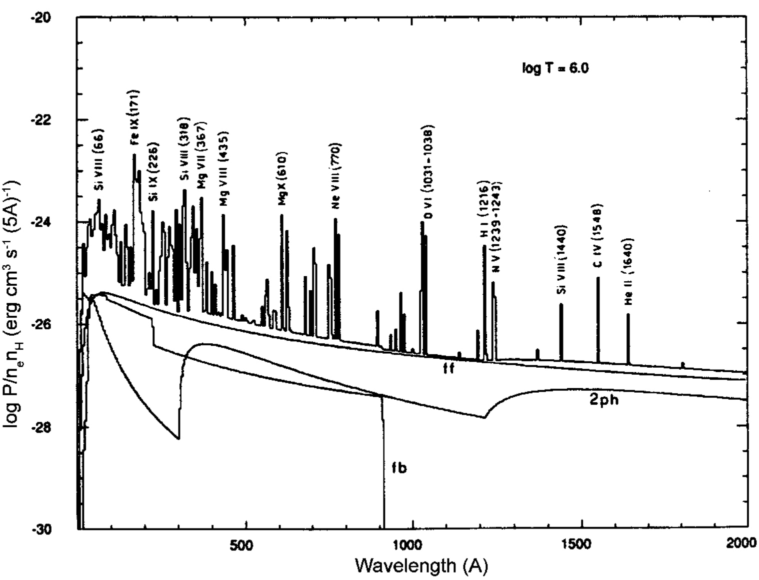

An incomplete list of astrophysically important ultraviolet spectral features

Identification	Wavelength (Å)†	Identification	Wavelength (Å)†
[Ne III]	3869	H I, D I	973
[O II]	3727	H I, D I	950
[Ne V]	3426	N II	917
Mg II	2798	H I, D I Ly edge	912
V II	2326	N II	916
C III	1909	O II	834
O III	1663	O III	834
He II	1640	O II	833
C IV	1549	O III	833
O IV	1402	S IV	816
Si IV	1397	O V	760
C II	1335	S IV	745
O I	1302	O II	719
Si II	1264	O II	718
S II	1260	O III	704
N V	1240	S IV	657
H I, D I	1216	O V	630
S III	1207	O III	600
N I	1201	He I	584
N I	1200	O IV	555
Si II	1190	O IV	554
C III	1176	O IV	553
O III	1175	O II	539
Fe II	1145	He I	537
N I	1134	He I	522
N II	1085	O III	508
N II	1084	O III	507
Ar I	1067	He I cont. edge	504
Si IV	1067	Ne VII	465
H_2	1062	Mg IX	368
H_2	1050	O III	306
H_2	1049	He II	304
O VI	1038	Si XI	303
O II	1036	Fe XV	284
O VI	1032	He II	256
H I, D I	1026	Fe XXIV	255
N III	992	He II	243
N III	990	He II cont. edge	227
C III	977	O V	172

†$h\nu$ (ev) = $12399/\lambda$ (Å)
Brackets denote forbidden transitions.

Prominent UV emission lines

λ (Å)	Ion	λ (Å)	Ion	λ (Å)	Ion
538	O II	1561	C I	2511.96	He II
584.33	He I	1574.77	Ne V	2586–2632	Fe II
834	O III	1577	C III	2664.06	He I
916	N II	1602	Ne IV	2696.92	He I
933.4	S VI	1640	He II	2724.00	He I
977.02	C III	1641.31	O I	2734.14	He I
1033	O IV	1657	C I	2764.62	He I
1066.66	Ar I	1663	O III	2783.03	Mg V
1085	N II	1670.79	Al II	2786.81	Ar V
1175	C III	1710	Si II	2794	Mg II
1199	S III	1718.55	N IV	2800	Mg II
1215.67	H I	1728.94	S III	2829.91	He I
1240	N V	1750	N III	2838	C II
1247.38	C III	1760	C II	2852.96	Mg I
1256	S II	1815	Si II	2854.48	Ar IV
1279	C I	1814.63	Ne III	2869.00	Ar IV
1299	Si III	1860	Al III	2928.34	Mg V
1304	O I	1882.71	Si III	2933	Mg II
1309	Si II	1892.03	Si III	2945.97	He I
1335	C II	1900.29	S I	2950.07	Mn II
1342	O IV	1908.73	C III	2973.15	O I
1371.29	O V	1914.70	S I	2978	N III
1394	Si IV	1993.62	C I	3005.36	Ar III
1397-1407	O IV	2321.67	O III	3024.33	O III
1402.77	Si IV	2326	C II	3046	O III
1460	C I	2328–2414	Fe II	3068	N II
1473	S I	2329.23	Si II	3109	Ar III
1483.32	N IV	2335	Si II	3133.77	O III
1486	S I	2381.13	He II	3188.67	He I
1487	N IV	2424	Ne IV	3204.03	He II
1550	C IV	2471.04	O II		

A line with a wavelength given to two decimal places is a single line; otherwise the line is a blend and the wavelength given is that which would be seen in low-resolution spectra.

(From *Ultraviolet Astronomy,* Teays, T.J., in *Allen's Astrophysical Quantities,* Cox, A.N., ed., Springer-Verlag 2000.)

Important strong lines

Wavelengths of important spectral lines of abundant elements and molecular hydrogen (H_2). Also indicated are the typical element abundances on a logarithmic scale where hydrogen is 12.00, and the temperatures of maximum fractional amount of each ion assuming collisional ionization equilibrium. Regions of continuous absorption by photoionization are indicated for hydrogen and helium. (From *FUSE Science Working Group Report*, NASA, 1983.)

SPECIES	LOG N	LOG T
H I	12.00	4.0
D I	7.2	4.0
H_2	6.0–11.7	1.9
He I	11.00	4.3
He II	11.00	4.3
C III	8.57	4.9
C IV	8.57	5.1
N V	8.06	5.3
O V	8.83	5.5
O VI	8.83	5.5
Ne VII	7.45	5.8
Ne VIII	7.45	5.9
Mg VIII	7.54	6.1
Mg IX	7.54	6.1
Mg X	7.54	6.2
Si XII	7.55	6.5
Fe IX	7.40	< 6.0
Fe X		6.2
Fe XII		6.4
Fe XV		6.6
Fe XVI		6.8
Fe XVIII		7.1
Fe XIX		7.2
Fe XXI		7.2
Fe XXIV		7.5

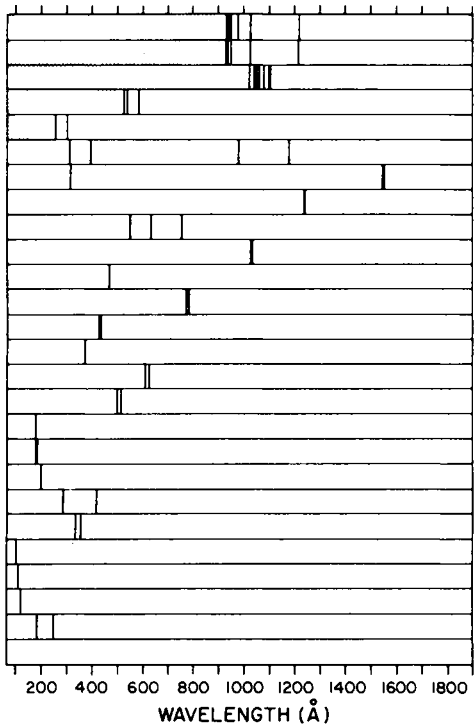

Ultraviolet absorption cross-sections

		Absorption cross-sections (10^{-18} cm^2)		
λ (Å)	Line identification	O	O_2	N_2
1215	Ly α	0	0.01	0.000 03
1176	C III	0	1.30	0
1085	N II	0	2.00	0
1038	O VI	0	0.78	0.0007
1032	O VI	0	1.04	0.0007
1026	Ly β	0	1.58	0.0001
977	C III	0	4.0	0.7
897	Ly cont	2.9	13.0	~ 11.0
870	Ly cont	2.9	13.0	~ 10.0
800	Ly cont	2.9	29.0	~ 10.0
791	O IV	3.2	28.0	25.0
703	O III	7.0	25.0	26.0
630	O V	12.0	30.0	24.0
625	Mg X	12.0	25.0	24.0
584	He I	13.0	23.0	23.0
554	O IV	13.0	26.0	25.0
537	He I	12.0	21.0	25.0
504	He I	12.0	25.0	~ 22.0
499	Si XII	12.0	25.0	~ 22.0
465	Ne VII	11.0	23.0	23.0
368	Mg IX	9.0	18.0	16.0
335	Fe XVI	8.8	17.0	14.0
304	He II	9.0	17.0	12.0
284	Fe XV	7.7	15.0	9.8

(Adapted from Sullivan, J. O. and Holland, A. C., NASA CR-371, 1964.)

Interstellar extinction in the UV

The UV extinction $X(x) = A_\lambda/E_{B-V}$ against $x = 1/\lambda$ in microns. A_λ is the extinction in magnitudes; $E_{B-V} = A_B - A_V$ where A_B and A_V are the extinctions at the wavelengths of the B and V filters. E_{B-V} is called the color excess. The curve is from the analytical fit of the table below. (Figure courtesy of M.J. Seaton, University College London.)

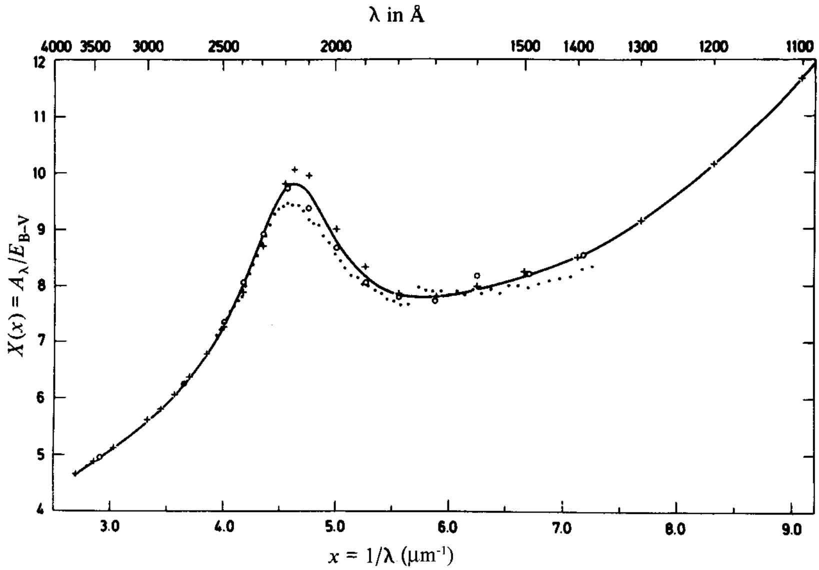

Analytical fit to the UV extinction (see figure above)

Range of $1/\lambda(\mu) = x$	$A_\lambda/E(B-V) = X$
$2.70 \leq 1/\lambda \leq 3.65$	$1.56 + 1.048/\lambda + 1.01/\{(1/\lambda - 4.60)^2 + 0.280\}$
$3.65 \leq 1/\lambda \leq 7.14$	$2.29 + 0.848/\lambda + 1.01/\{(1/\lambda - 4.60)^2 + 0.280\}$
$7.14 \leq 1/\lambda \leq 10.0$	$16.17 - 3.20/\lambda + 0.2975/\lambda^2$

(From Seaton, M.J., *M.N.R.A.S.*, **187**, 1979.)

Interstellar EUV attenuation

Distances (parsecs) corresponding to unit optical depth (1/e attenuation) as a function of neutral hydrogen density and wavelength

λ (Å)	$n_{HI} = 1$ (cm^{-3})	$n_{HI} = 0.1$ (cm^{-3})	$n_{HI} = 0.01$ (cm^{-3})	$n_{HI} = 0.001$ (cm^{-3})
912	0.05	0.5	5	50
500	0.2	2	20	200
200	1.5	15	150	1500
100	10	100	1000	10000

(From FUSE Science Working Group Report, NASA, 1983.)

Distance at which the attenuation of EUV radiation reaches 90%. An ionized interstellar medium of normal composition is assumed. (Adapted from Paresce, F. in. *Astrophysics from Spacelab*, P. L. Bernacca and R. Ruffini, eds., D. Reidel Pub. Co., 1980.)

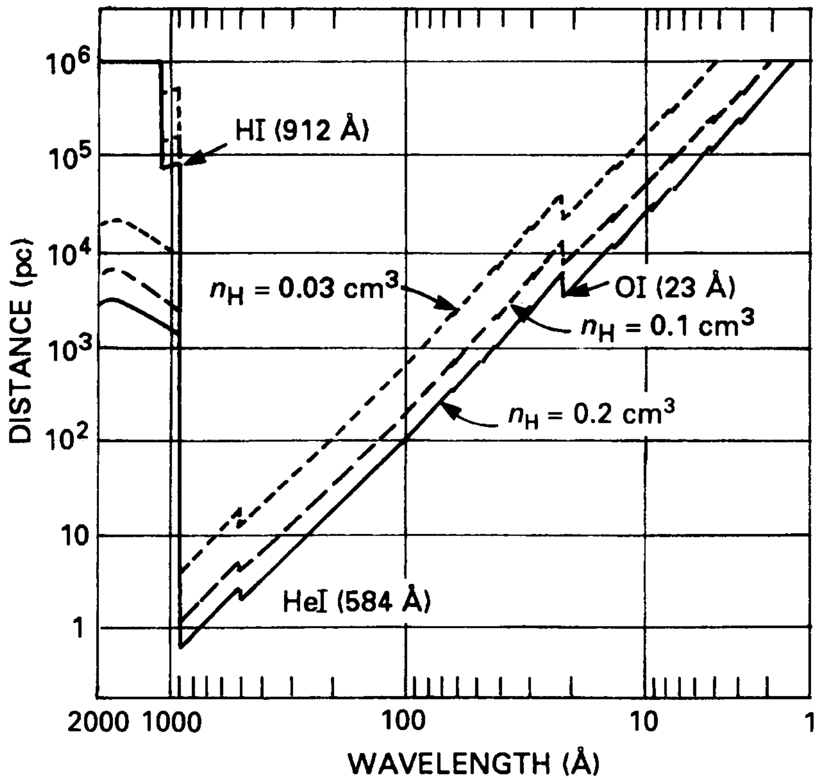

Average interstellar hydrogen densities within 100 pc

In the direction of	Distance (pc)	$n_{\rm HI}$ (cm^{-3})
Sun	–	0.05
α Cen	1.34	0.06–0.30
ϵ Eri	3.3	0.06–0.20
ϵ Ind	3.4	$\sim$ 0.1
ϵ CMi	3.5	0.09–0.13
β Gem	10.8	0.02–0.15
α Boo	11.1	0.02–0.15
α Aur	14	0.04–0.05
α Tau	21	0.02–0.15
α Leo	22	0.02
		0.01†
α Eri	28	0.07
α Gru	29	0.09–0.18
		0.18†
HR 1099	33	0.003–0.007
η UMa	42	0.005
G191–B2B	47	$>$ 0.03
σ Sgr	57	$<$ 0.17
HZ 43	62	$<$ 0.013
α Pav	63	$<$ 0.1
β Cen	81	0.13
β Lib	83	0.06–0.13
ζ Cen	83	$<$ 0.39
α Vir	87	0.037
Feige 24	90	0.02–0.05
λ Sco	100	$<$ 0.078

Mean hydrogen column density within 100 pc = 1.8×10^{17} cm^{-2} pc^{-1}.
† Multiple entries denote independent measurements.
(Adapted from Cash, W., Bowyer, S. & Lampton, M., *Astron. Astrophys.*, **80**, 67, 1979.)

Neutral hydrogen column density

Neutral hydrogen column density $N_{\rm HI}$ contours projected onto the plane of the galaxy ($b = 0°$). The Sun is at the center of this plot, distances out to 100 pc are indicated, and the direction towards the galactic center ($l = 0°$) is at the bottom. Line A is the contour of $N_{\rm HI} \sim 5 \times 10^{17}$ cm^{-2}, corresponding to $\tau_{500Å} = 1$, $\tau_{200Å} \approx 0.1$, and $\tau_{100Å} \approx 0.01$. Line B is the contour of $N_{\rm HI} = 25 \times 10^{17}$ cm^{-2}, corresponding to $\tau_{500Å} = 5$, $\tau_{200Å} \approx 0.5$, and $\tau_{100Å} \approx 0.05$. Line C is the contour of $N_{\rm HI} \sim 50 \times 10^{17}$ cm^{-2}, corresponding to $\tau_{500Å} = 10$, $\tau_{200Å} \approx 1$, and $\tau_{100Å} \approx 0.1$. All open circles are white dwarfs. Small circles represent stars with $N_{\rm HI} \leq 5 \times 10^{17}$ cm^{-2}, medium circles represent stars with $5 \times 10^{17} < N_{\rm HI} < 25 \times 10^{17}$ cm^{-2}, the large circles represent stars with $25 \times 10^{17} < N_{\rm HI} < 50 \times 10^{17}$ cm^{-2}, and the crosses represent stars with $N_{\rm HI} > 50 \times 10^{17}$ cm^{-2}. Stars with measured hydrogen column densities but which are located within 10 pc projected distance are not plotted. (From *FUSE Science Working Group Report*, NASA, 1983.)

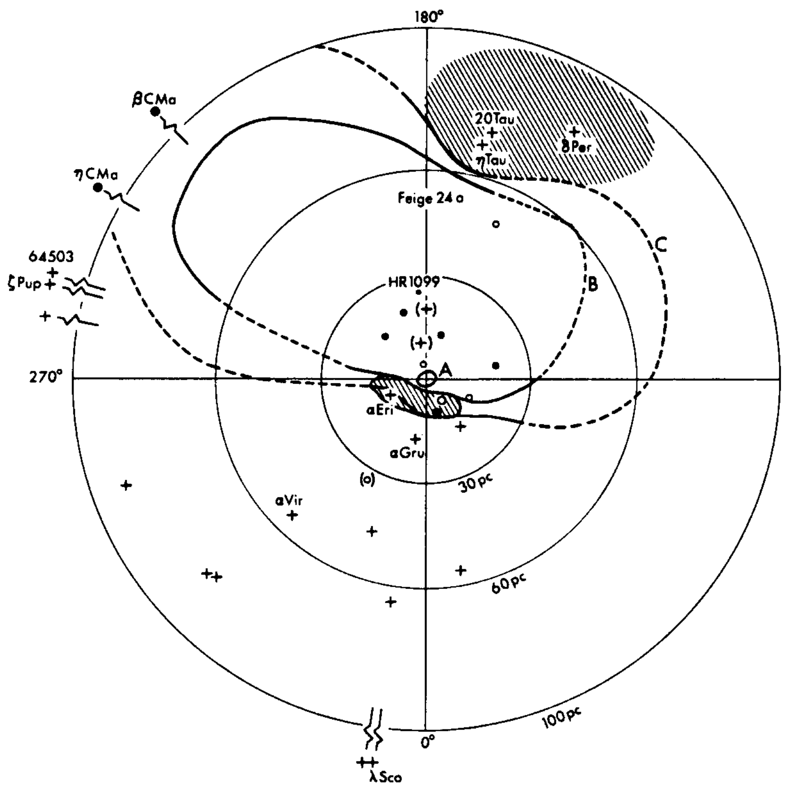

Neutral hydrogen column density *(cont.)*

Same as previous diagram but projected onto a plane intercepting the Galactic plane at Galactic longitudes $l = 0°$ and $180°$, and passing through the North Galactic Pole *(top)* and South Galactic Pole *(bottom)*. The symbols have the same meanings as before, and those stars with projected distances of less than 10 pc are generally not plotted. W symbols designate white dwarfs not yet observed. Many of these are within the cavity of low HI absorption and will be observable below 900 Å. (From *FUSE Science Working Group Report*, NASA, 1983.)

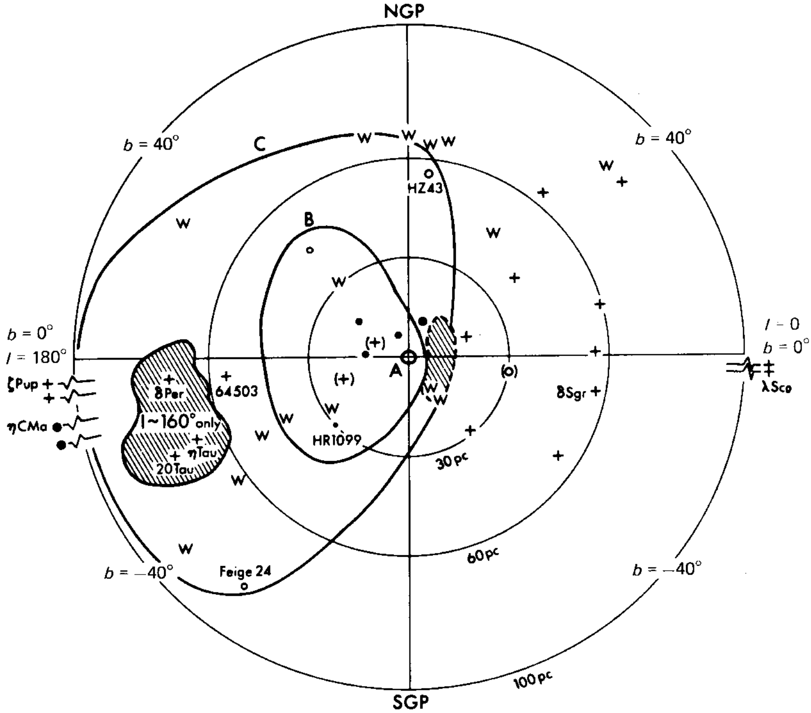

Bibliography

New Developments in X-ray and Ultraviolet Astronomy, Drew, J.E. ed., Adv. Space. Res., **16**, No. 3, 25, 1995.

Extreme Ultraviolet Astronomy, Malina, R.F. and Bowyer, S., ed., Pergamon Press, 1989.

Proceedings of the Fourth European IUE Conference, ESA SP-218, 1984.

The Universe at Ultraviolet Wavelengths, NASA Conference Publication 2171, 1980.

Note: Links to WWW resources which supplement the material in this chapter can be found at:

http://www.astrohandbook.com

Chapter 6

X-ray astronomy

The black holes of nature are the most perfect macroscopic objects there are in the Universe: the only elements in their construction are our concepts of space and time. - Subrahmanyan (Chandra) Chandrasekhar

The HEAO Al all sky map

Discrete X-ray sources observed by the NRL Sky Survey Experiment on HEAO-1 are displayed in galactic coordinates. The size of the dot representing a source is proportional to the logarithm of the intensity averaged over the time interval when the source was in the field of view. 700 sources are shown. (Courtesy of K. Wood, Naval Research Laboratory.)

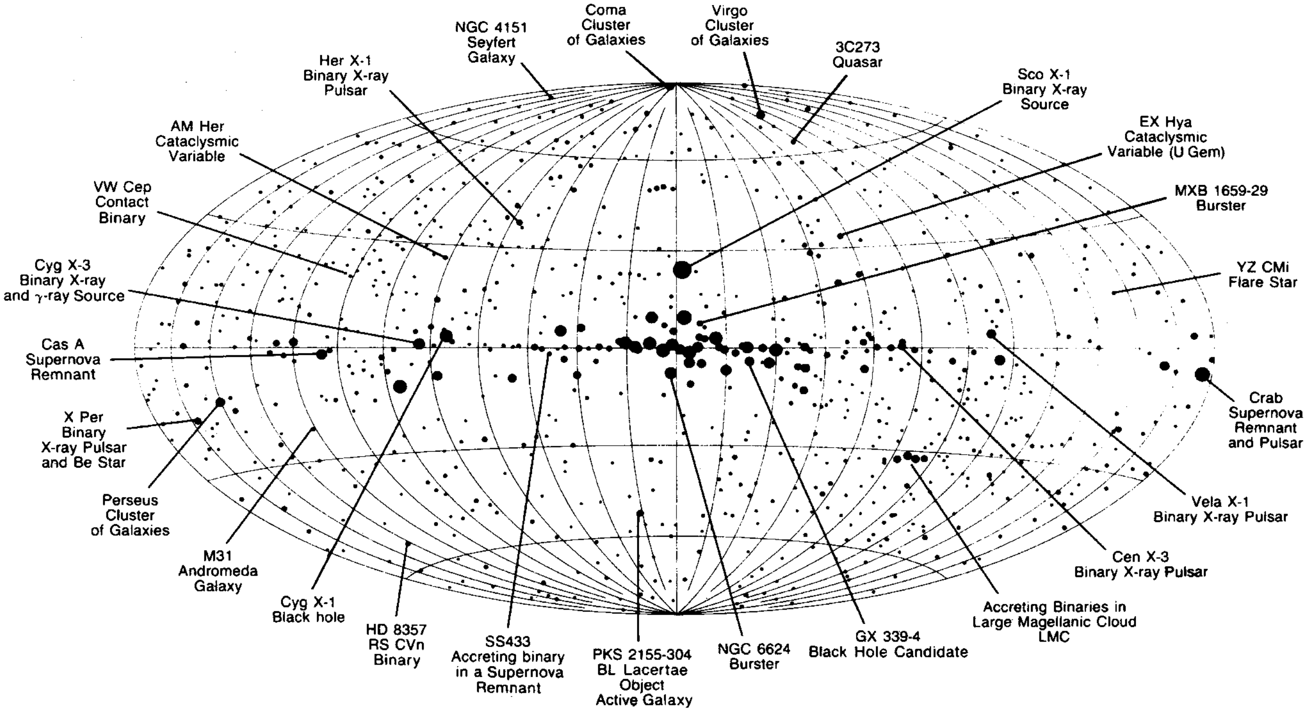

Representative galactic sources: binaries and stars

Source	α 1950 δ 1950	Flux density[(a)] (2–11 keV) max (μJy) min (μJy)	$L(X)$ max (2–11 keV) (erg s^{-1})	V magnitude	$\frac{L(X)}{L(O)}$	Spectral type	Periods	Distance	Remarks
SMC X−1	$01^h15^m45\overset{s}{.}6$ −73° 42′ 22″	57 2	6×10^{38}	13.3	1.2	B0 I	3.89^d 0.71^s	65 kpc	Sanduleak 160
β Per	03 04 54.3 40 45 52	9	2×10^{31}	2.2	5×10^{-5}	B8 V/K0 IV/ Am	2.9^d	32 pc	Algol
3U 0352+30	03 52 15.1 30 54 01	37 11	1.2×10^{34}	6.0–6.7	1×10^{-4}	O9.5 (III−V)e	581^d(?) 13.9^m	350 pc	X Per
A 0620−00	06 20 11.1 −00 19 11	~50000 $\lesssim 5$	3×10^{38}	10.4 (18.3)	85			1.5–2.5 kpc	X-ray Nova V616 Mon
Vela X−1	09 00 13.2 −40 21 25	280 < 28	1.4×10^{36}	6.9	3×10^{-3}	B0.5 Ib	8.97^d 283^s	1.4 kpc	HD 77581
Cen X−3	11 19 01.9 −60 20 57	224 < 21	4×10^{37}	13.4	0.05	O6.5 II–III	2.09^d 4.8^s	8 kpc	Krzeminski's star
Sco X−1	16 17 04.5 −15 31 15	19000 6900	2×10^{37}	12.2–13.3	600		0.787^d	0.7 kpc	V818 Sco
Her X−1	16 56 01.7 35 25 05	160 11	1.0×10^{37}	13.2	10	A09–F0	34.8^d 1.7^d 1.2^s	5 kpc	HZ Her
3U 1700−37	17 00 32.7 −37 46 29	110 < 11	3×10^{36}	6.6	5×10^{-4}	O6.5f	3.4^d	1.7 kpc	
4U 1813+50	18 14 58.6 49 50 55	7 2.5	8×10^{33}	13.1–12.3	0.6		0.129^d	300 kpc	AM Her

Representative galactic sources: binaries and stars (cont.)

Source	α 1950 δ 1950	Flux density[(a)] (2–11 keV) max (μJy) min (μJy)	$L(X)$ max (2–11 keV) (erg s^{-1})	V magnitude	$\frac{L(X)}{L(O)}$	Spectral type	Periods	Distance	Remarks
Cyg X−1	19 56 28.9 35 03 55.0	1320 260	2×10^{37}	8.9	2×10^{-2}	O9.7 Iab	5.6^d	2.5 kpc	Blackhole candidate HDE 226868
Cyg X−3	20 30 37.6 40 47 13	430 90	1.2×10^{38}				16.8^d(?) 4.8^h	10.5 kpc	IR/radio
SS Cygni	21 40 42.6 43 21 51	20 5	$1–5 \times 10^{32}$	12.1–8.1	1.3		6^h38^m	100 pc	Dwarf nova (U Gem)
Cyg X−2	21 42 36.9 38 05 28	740 220		15.5	450		11.2^d		Sub-dwarf
		X-ray intensity (> 0.2 keV) (erg cm^{-2} s^{-1})							
UV Cet	1 36 24 −18 13 00	7×10^{-11}		6.8–12.9	2×10^{-3}	dM5.5 e			Flare star
α Aur	5 12 59.5 45 56 58	3×10^{-10}		0.1	1×10^{-5}	G8 III+F	104^d	14 pc	Capella
α CMa	6 42 54 −16 39 00	9.5×10^{-12}		−1.5		A IV+D0	44.98^y	2.7 pc	Sirius
HZ 43	13 14 00 29 22 00	9×10^{-10}		12.9	6				White dwarf

[(a)] Flux density = (integrated 2 − 11 keV flux)/9keV; 1 μJy $= 0.242 \times 10^{-11}$ erg cm^{-2} s^{-1} keV^{-1} $= 1.51 \times 10^{-3}$ keV cm^{-2} s^{-1} keV^{-1}. (Adapted from Bradt, H. V., Doxsey, R. E. and Jernigan, J. G., *COSPAR Symposium on X-ray Astronomy*, Innsbruck, Austria, May 31, 1978).

Representative binary X-ray pulsars

Source	Optical counter-part	Pulse period (s)	$-\dot{P}/P$ (yr^{-1})	Orbital period (d)	$a_x \sin i$ (lt-s)	$f(M)$ ($M_\odot$)	Orbital eccen-tricity	$K_c^{(a)}$ (km $^{-1}$)	Eclipse half-angle (°)	$L_x^{(b)}$ (erg s^{-1})
A 0538–66	Identified	0.069	–	16.66	–	–	> 0.4	–	–	1.2×10^{39}
SMC X–1	Sk 160	0.714	7.1×10^{-4}	3.892	53.46(3)	10.8	< 0.0007	19(2)	26.5–29	6×10^{38}
Her X–1	HZ Her	1.24	2.9×10^{-6}	1.700	13.1831(3)	0.85	< 0.0003	20.2(3.5)	24.4–24.7	7×10^{36}
1E 2259+586	Identified	3.49	–	< 0.08	–	–	–	–	–	3×10^{34}
4U 0115+63	Identified	3.61	3.2×10^{-5}	24.31	140.13(10)	5.00	0.3402(2)	–	0	8×10^{36}
Cen X–3	V779 Cen	4.84	2.8×10^{-4}	2.087	39.792(5)	15.5	0.0008(1)	24(6)	35–40	8×10^{37}
4U 1626–67	KZ TrA	7.68	1.9×10^{-4}	0.0288	< 0.04	$< 8 \times 10^{-5}$	–	280(76)	0	–
2S 1553-54	–	9.26	–	30.7(2.8)	165(30)	5.1(2.9)	< 0.07	–	–	–
LMC X–4	Identified	13.5	$< 1.2 \times 10^{-3}$	1.408	30(5)	15(8)	< 0.2	37.9(2.4)	25.5–33	4×10^{38}
2S 1417–62	–	17.6	9×10^{-3}(?)	> 15	> 25	–	–	–	–	–
OAO 1653–40	–	38.2	5.4×10^{-3}	–	–	–	–	–	–	–
A 0535+26	HDE 245770	104	3.5×10^{-2}	111(?)	–	–	–	$\lesssim 20$	–	2×10^{37}
GX 1+4	V2116 Oph	122	2.1×10^{-2}	> 15	> 60	–	–	–	–	6×10^{37}
GX 304–1	Identified	272	–	132(?)	–	–	–	–	–	3×10^{36}
4U 0900–40	HD 77581	283	1.7×10^{-4}	8.965	113.0(8)	19.3	0.092(5)	21.8(1.2)	31–37	6×10^{36}
4U 1145–61	HEN 715	292	$< 10^{-4}$	187(?)	> 100	–	–	–	–	6×10^{36}
IE 1145.1–6141	Identified	297	$< 10^{-4}$	> 12	> 50	–	–	–	–	3×10^{36}
A 1118–61	HEN 3–640	405	–	–	–	–	–	–	–	5×10^{36}
4U 1538–52	QV Nor	529	$< 2 \times 10^{-3}$	3.730	55.2(3.7)	13	–	33(7)	25–33	4×10^{36}
GX 301–2	WRA 977	696	7×10^{-3}	41.4	367(3)	31	0.47(1)	–	0	1×10^{37}
4U 0352+30	X Per	835	1.8×10^{-4}	580(?)	–	–	–	< 20	–	1×10^{34}

[a] K_c = semiamplitude of the optical Doppler velocity curve.
[b] L_x = X-ray luminosity (2–11 keV) from Bradt, H. and McClintock. *Ann. Rev. Astron. Astrophys.*, **21**, 13, 1983.
(Adapted from Joss, P. C. and Rappaport, S. A., *Ann. Rev. Astron. Astrophys.*, **22**, 537, 1984.)

Sky map, in galactic coordinates, of 21 binary X-ray pulsars (•) and 27 X-ray burst sources (∘). (Reproduced, with permission, from the *Annual Review of Astronomy and Astrophysics*, Vol. 22, © 1984, by Annual Reviews Inc. Courtesy of Paul C. Joss, MIT.)

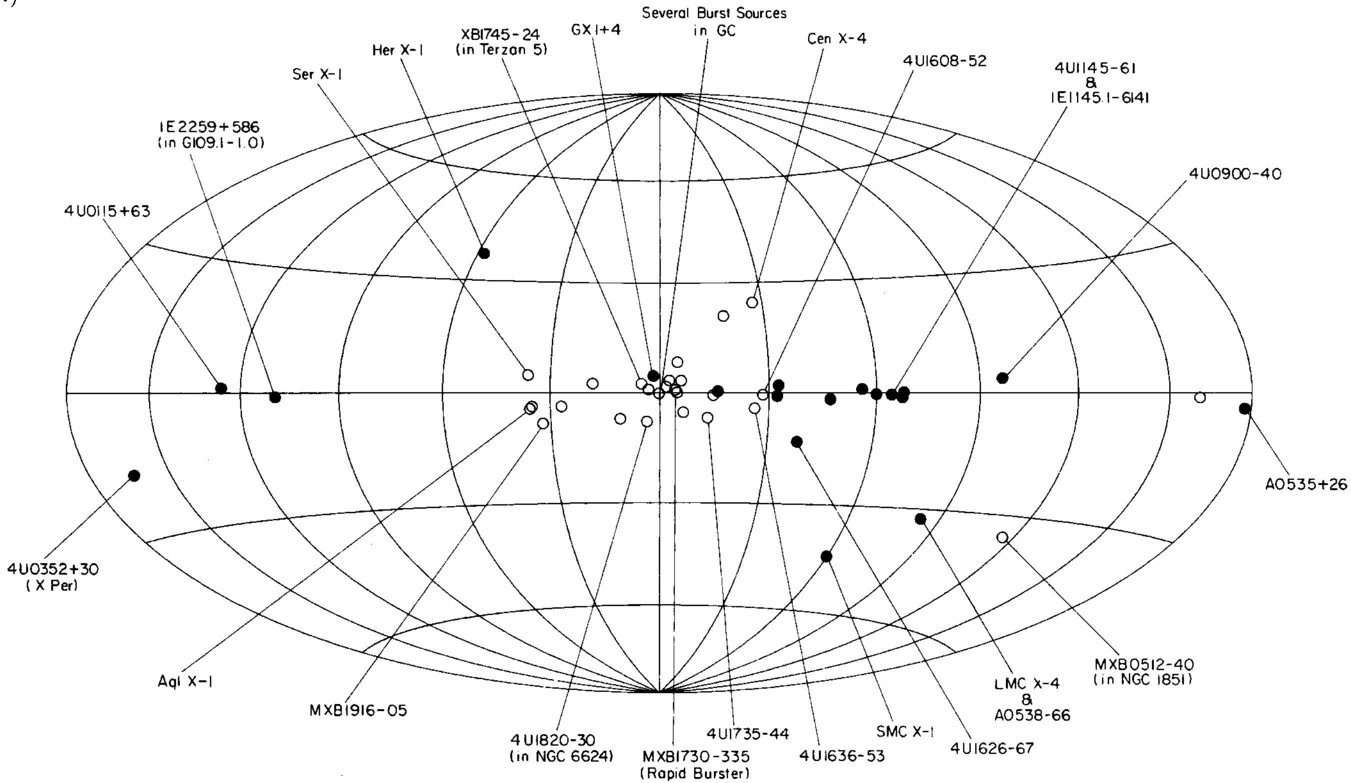

Orbits to scale for a selection of massive X-ray binaries and the masses of neutron stars that have been measured from optical, X-ray, and radio observations. (Charles, P.A. and Seward, F.D., *Exploring the X-ray Universe*, Cambridge University Press, 1995, with permission.)

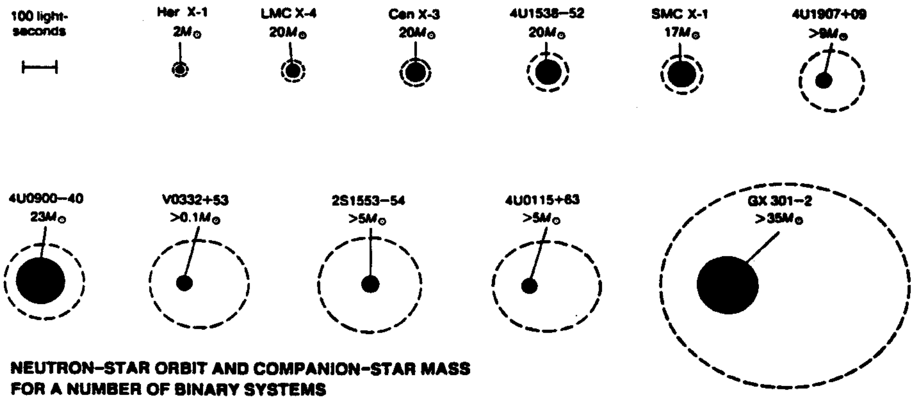

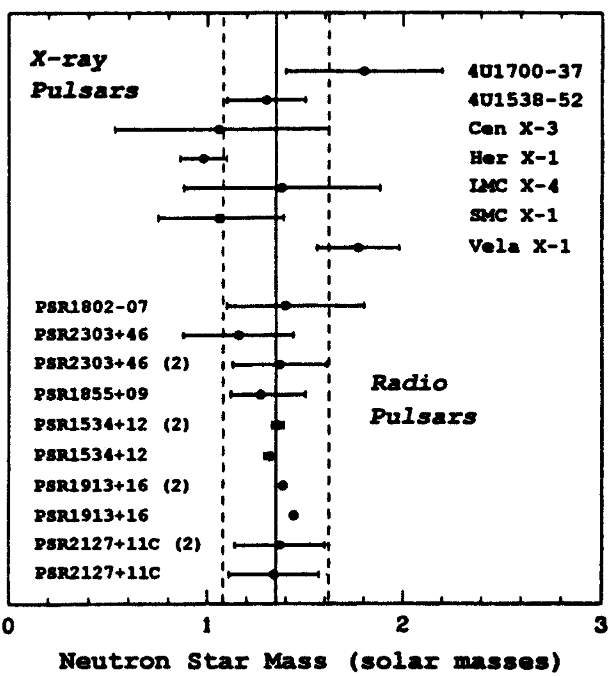

Galactic black-hole candidates in binary systems

Source	$P_{orb}(d)$	$K(km\ s^{-1})$	$f(M/M_0) = PK^3/2\pi G$
XTE J1859+226	0.382 ± 0.003	570 ± 27	7.4 ± 0.1
XTE J 1550–564	1.552 ± 0.010	349 ± 12	6.86 ± 0.71
V404 Cyg	6.4714 ± 0.0001	208.5 ± 0.7	6.08 ± 0.06
XTE J1118+480	0.17013 ± 0.00010	698 ± 14	6.00 ± 0.36
GS2000+25	0.3516 ± 0.0034	518.4 ± 3.5	4.97 ± 0.10
XN Oph 1977	0.5229 ± 0.0044	447.6 ± 3.9	4.86 ± 0.13
GRO J1655–40	2.62157 ± 0.00015	228.2 ± 2.2, 215.5 ± 2.4	3.24 ± 0.09, 2.73 ± 0.09
XN Mus 1991	0.4326058 ± 0.0000031	406 ± 7, 420.8 ± 6.3	3.01 ± 0.15, 3.34 ± 0.15
GRS 1009–45	0.286 ± 0.005	475.4 ± 5.9	3.17 ± 0.12
A0620–00	0.323014 ± 0.000001	443 ± 4, 433 ± 3	2.91 ± 0.08, 2.72 ± 0.06
SAX J1819.3–2525	2.81678 ± 0.00056	211.0 ± 3.1	2.74 ± 0.12
GRO J04222+32	0.21159 ± 0.00057	380.6 ± 6.5	1.21 ± 0.06
Cyg X–1	5.59974 ± 0.00008	74.6 ± 1.6	0.241 ± 0.013
4U1543–47	1.123 ± 0.008	124 ± 4	0.22 ± 0.02

(Courtesy of J. McClintock, Harvard-Smithsonian Center for Astrophysics, 2001)

The mass function

If only the period of a binary system and the radial velocity curve of one component are known, it is only possible to determine the mass ratio of the two stars. The mass function f is a useful expression for determining this ratio from observable quantities:

$$\begin{aligned} f_1\ (M_1, M_2, i) &\equiv (M_2 \sin i)^3/(M_1 + M_2)^2 = M_1(\sin i)^3/(1 + q)^2 q \\ &= PK_1^3/2\pi G \quad \text{(by Kepler's 3rd law)} \\ &= 1.0362 \times 10^{-7}\ PK_1^3 \end{aligned}$$

where f is in units of solar mass, i is the inclination of the binary's orbital plane with respect to the plane tangent to the celestial sphere, M_1 and M_2 are the stellar masses in units of solar mass, $q = M_1/M_2$, P is the binary period in days, and K_1 is the semi-amplitude of the radial velocity of star 1 in km s^{-1}.

Properties and X-ray characteristics for a selection of rotation-powered pulsars

Name[a]	P^b (s)	$\dot{P}^b$ (10^{-15} ss^{-1})	$\dot{E}$ (erg s^{-1})	τ_c^g (kyr)	d^b (kpc)	$\dot{E}/4\pi d^2$[f] (erg s^{-1} cm^{-2})	L_x^c pulsed (erg s^{-1})	L_x^d syn−neb (erg s^{-1})	nebular size[e] ang (θ)	nebular size[e] lin (pc)	DM[b] (pc cm^{-3})	$N_H(10^{21})$ (cm^2)	SNR[h]
B0531+21	0.033	421	4.5×10^{38}	1.3	2.5	6.0×10^{-7}	7.4×10^{35}	1.2×10^{37}	$\sim1.7'$	~1.0	57	3.0	Crab
B0833−45	0.089	124	6.9×10^{36}	11.4	0.5	2.3×10^{-7}	5.0×10^{31}	9.0×10^{31}	$2'$	0.3	68	3.0	Vela
J1617−5055	0.069	135	1.6×10^{37}	8.1	3.3	1.2×10^{-8}	6.4×10^{33}	3.4×10^{33}	$<1.5'$	<1.4	467	6.8	RCW 103
B1509−58	0.151	1537	1.8×10^{37}	1.6	4.2	8.3×10^{-9}	9.0×10^{34}	2.1×10^{35}	$\sim8'$	~10	253	13	G320.4−1.2
B1706−44	0.102	93.0	3.5×10^{36}	17.4	2.4	5.0×10^{-9}	…	6.6×10^{32}	$54''$	0.6	76	1.3	G343.1−2.3
B1951+32	0.040	5.8	3.7×10^{36}	107	2.5	5.0×10^{-9}	2.7×10^{33}	1.6×10^{33}	$70''$	0.8	45	3.0	CTB 80
B1046−58	0.124	95.9	2.0×10^{36}	20.4	3.0	1.8×10^{-9}	…	2.0×10^{32}	$<3'$	<2.6	129	5	…
J0537−6910	0.016	51.3	4.9×10^{38}	5.0	47	1.8×10^{-9}	1.7×10^{35}	1.2×10^{36}	$<7''$	<1.6	…	15	N157B
B1823−13	0.101	75.0	2.9×10^{36}	21.3	4.0	1.5×10^{-9}	…	4.7×10^{33}	$38''$	0.7	231	40	…
B1800−21	0.134	134	2.2×10^{36}	15.8	3.9	1.2×10^{-9}	…	5.8×10^{32}	$<3.0'$	<3.4	234	14	W30
B1757−24	0.125	128	2.6×10^{36}	15.4	4.6	1.0×10^{-9}	…	$<8.0\times10^{32}$	…	…	289	9	G5.4−1.2
B1727−33	0.139	85.0	1.3×10^{36}	25.9	4.2	5.9×10^{-10}	…	$<2.7\times10^{32}$	…	…	256	8	…
B0540−69	0.050	479	1.5×10^{38}	1.7	49	5.1×10^{-10}	3.0×10^{36}	8.5×10^{36}	$<10''$	<2.4	146	4.0	N158A
B1853+01	0.267	208	4.3×10^{35}	20.3	3.0	4.6×10^{-10}	…	1.3×10^{33}	$\sim3'$	~2	97	10	W44
J1105−6107	0.063	15.8	2.5×10^{36}	63.4	7.0	4.2×10^{-10}	…	3.8×10^{33}	$<3'$	<6.1	271	7	…
J1119−6127	0.408	4023	2.3×10^{36}	1.6	8.0	3.1×10^{-10}	…	2.0×10^{32}	$<3'$	<7.0	707	15	G292.2−0.5
B31610−50	0.232	495	1.6×10^{36}	7.4	7.3	2.5×10^{-10}	…	$<7.0\times10^{32}$	…	…	583	20	…
B1055−52	0.197	5.8	3.0×10^{34}	538	1.5	1.1×10^{-10}	2.1×10^{33}	2×10^{31}	$<3''$	<0.02	30	0.3	…
B1737−30	0.607	465	8.2×10^{34}	20.7	3.3	6.3×10^{-11}	…	$<1.2\times10^{32}$	…	…	153	7	…

[a] B1950 and J2000 names, where the first four digits are the right ascension of the object in hours and minutes and the last two, the declination in degrees.

[b] Period P, period derivative $\dot{\mathrm{P}}$, distance d, and dispersion measure DM (see chapter 2).

Properties and X-ray characteristics for a section of rotation-powered pulsars (cont.)

[c] Luminosities are for the 2-10 keV band and assume a power law spectrum, except for B0833−45 and B1055−52, where the values are bolometric blackbody luminosities.

[d] Luminosities are for the 2-10 keV band and assume a power law spectrum.

[e] Nebular dimensions are in either angular (θ) or linear (pc) diameter. Except for B0531+21 and B1509-58, which have definite elongations, most PSRs are roughly symmetric.

[f] Spin-down energy flux density

[g] The pulsar characteristic age, $\tau_c = \dfrac{P}{2\dot{\mathrm{P}}}$

[h] Associated supernova remnant.

A neutron star's surface magnetic field is taken to be approx. $3.2 \times 10^{19}\ (\mathrm{P}\dot{\mathrm{P}})^{1/2}$

(Adapted from Pivovaroff, M.J., *X-ray Astronomy with CCDS*, MIT Thesis, 2000.)

X-ray emission from a selection of stars

Name	Stellar Type	Distance (pc)	L_x 0.2–4 keV (erg s^{-1})
ζ Ori	09.5 I	490	3.5×10^{32}
ϵ Ori	BO I	460	2.0×10^{32}
HZ43	WD	64	4.0×10^{31}
Algol (β Per)	B8 V	31	5.0×10^{30}
Capella (α Aur)	G8 V+F V	13.5	2.0×10^{30}
24 UMa	G1 V	25	1.0×10^{30}
YY Gem	M V	15	4.0×10^{29}
α Tri	F2 V	18	3.2×10^{29}
Wolf 630	M4 V+M5 V	6.1	2.0×10^{29}
Sirius (α CMa B)	WD	2.6	6.0×10^{28}
EQ Peg	M V	6.1	6.0×10^{28}
ϵ Eri	K2 V	3.3	2.0×10^{28}
α Cen	K5 V + G2 V	1.4	3.2×10^{27}
Proxima Cen	M5 V	1.3	2.5×10^{27}
The Sun	G2 V	4.8×10^{-6}	$\sim 1.0 \times 10^{23}$ [a] $\sim 1.0 \times 10^{26}$ [b] $\sim 1.0 \times 10^{27}$ [c]

[a] Sunspot minimum, [b] sunspot maximum, [c] very large flare

Note: 1 pc = 3.262 light years = 3.086×10^{16} m.

(Adapted from *Cosmic X-ray Sources*, Seward, F., in *Allen's Astrophysical Quantities*, Cox, A.N., Ed., Springer, 2000.)

X-ray emitting supernova remnants (selection)

Source	α 1950 δ 1950	Distance (kpc)	Diameter (pc)	L_x (0.2–2 keV) (10^{35} erg s^{-1})	Age (yr)	1 GHz flux density (fu)	Angular size (arcmin)
Crab Nebula	$05^h\,31^m$ $21°\,59'$	2	3	160	900	1000	3.0 × 4.2
Cas A	23 21 58 33	3	3.5	30	300	3000	4.0 × 3.8
Cygnus Loop	20 49 30 30	0.8	40	8	20 000	180	200 × 160
Vela	08 32 −45 00	0.5	44	4	13 000	1800	220 × 180
IC 443	06 14 22 30	1.5	20	0.4	6 000	160	40 diameter
Tycho's SNR	00 22 63 52	6	13	40	400	58	6.0 × 7.0
SN 1006	15 00 −41 45	1.2	10	0.2	970	25	30 × 22
GKP SNR	19 31 31 10	1.2	70	0.8	300 000	50	240 × 200
Lupus Loop	15 09 −40 00	0.5	40	0.1	20 000	340	270 diameter
RCW 86	14 39 −62 15	2.5	28	2	1800	33	40 diameter
RCW 103	16 14 −50 56	3.3	9	1	1 000	22	7.0 × 7.9
PKS 1209−52	12 06 −52 10	2 0	40	0.7	20 000	49	86 × 75
Pup A	08 20 −42 50	1.2	17	6	10 000	145	55 diameter
65.6 + 6.5	19 31 31 10	1.2	60–80	0.7	$< 2 \times 10^4$		180 × 240

Crab Nebula

The observed electromagnetic spectrum of the Crab Nebula and the Crab Pulsar. Dashed lines show corrections made for absorption and scattering of interstellar material. (Adapted from Seward, F. O., *Journal of the British Interplanetary Society*, **31**, 83, 1978.)

X-ray spectrum (0.1 – 100 keV):

$$\frac{dN}{dE} = 10\ \mathrm{E(keV)}^{-2.05} \exp(-\sigma N_{\mathrm{H}})\ \text{photons cm}^{-2}\ \text{s}^{-1}\ \text{keV}^{-1},$$

$$N_{\mathrm{H}} = 3 \times 10^{21}\ \text{cm}^{-2}$$

$$\sigma = \text{absorption and scattering cross-section}$$

X-ray luminosity (0.1 – 100 keV):

$$L_{\mathrm{x}} = 4.9 \times 10^{37}\ \text{erg s}^{-1}$$

Distance:	2200 pc
Diameter:	3 pc (5 arcmin)
m_{v}:	8.6
A_{v} (absorption):	1.5
Coordinates:	$\alpha = 05^{\mathrm{h}}31^{\mathrm{m}}$, $\delta = +22°$
Total radiated energy:	1.8×10^{38} erg s^{-1}
Age:	950 years (AD or CE (politically correct) 1054)
Pulsar period, $P(1969)$:	0.0331 s
Rate of period increase, $\dot{P}$:	422.69×10^{-15} ss^{-1}.

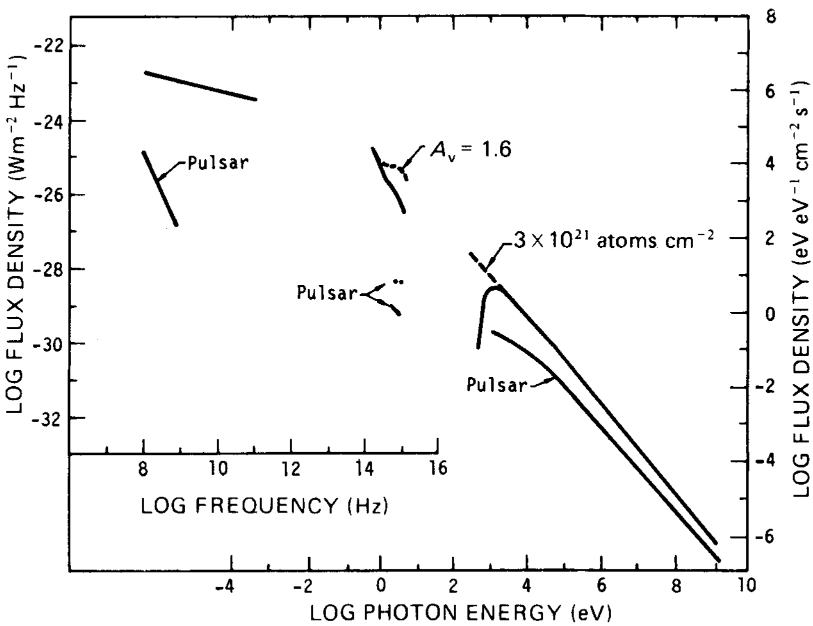

X-ray emission from a selection of low mass globular clusters

Cluster	Log L_x (erg s^{-1})	Distance (kpc)	$radius_{core}$ (arcsec)
NGC 6624	38.0	8.0	5
NGC 6441	36.8	11.7	8
Liller 1	36.8	10.0	4
Terzan 1	36.8	10.6	6
M15*	36.7	9.7	6
Terzan 2	36.7	10.0	6
NGC 6712	36.4	6.2	49
NGC 1851	36.1	12.0	6
NGC 6440	Transient	8.5	8
NGC 5824	34.3	23.5	4
M79	33.9	13.0	16
M3	33.6	10.4	29
NGC 6541	33.3	7.0	34
ω Cen	32.6-32.9	5.2	144
M22	32.0-32.6	3.1	114

*M15 (NGC 7078) consists of two sources.

Note: 1 kpc = 3.262×10^3 light years = 3.086×10^{19} m.

The core radius, $radius_{core}$, is defined to be the radius at which the surface brightness has dropped to half the central value.

(Adapted from *Exploring the X-ray Universe*, Charles, P.A. and Seward, F.D., Cambridge University Press, 1995.)

For a catalog of galactic globular clusters see Harris, W.E. 1996, AJ, **112**, 1487 or http://www.physics.mcmaster.ca/Globular.html

X-ray emission from a selection of normal galaxies

Galaxy	Type	Distance (Mpc)	L_x 0.2-4 keV (erg s^{-1})
NGC 507	S0	98	1.1×10^{43}
NGC 720	E	32	2.2×10^{41}
NGC 4382	S0	28	5.2×10^{40}
NGC 4472	E/S0	28	1.1×10^{42}
M31	Sb	0.68	3.6×10^{39}
NGC 253	Sc	3.1	7.4×10^{39}
M81	Sb	3.4	1.3×10^{40}
M82	Irr	3.4	3.5×10^{40}

Note: Distance calculated from redshift for
$H_0 = 50$ km s^{-1} Mpc^{-1}, $q_0 = 0.5$.
1 Mpc = 3.262×10^6 light years = 3.086×10^{22} m.
(Adapted from *Cosmic X-ray Sources,* Seward, F., in *Allen's Astrophysical Quantities*, Cox, A.N., Ed., Springer, 2000.)

The brightest X-ray emitting clusters of galaxies

Cluster	α, δ (2000)	Redshift z	Distance 2–10 keV (Mpc)	kT^*	L_x (erg^{-1})
A426 (Perseus)	03 18.6 +41 30	0.0183	110	6.3	1.4×10^{45}
Ophiuchus Cluster	17 12.4 −23 22	0.028	170	9–11	2.5×10^{45}
M87 (Virgo)	12 30.8 +12 23	0.0037	22	2.4	3×10^{43}
A1656 (Coma)	12 59.8 +27 58	0.0235	140	8.1	9×10^{44}
Centaurus Cluster	12 48.8 −41 19	0.0107	64	10	6×10^{43}
A2199	16 28.6 +39 31	0.0305	180	4.5	3×10^{44}
A496	04 33.6 −13 14	0.0316	190	3.9	3×10^{44}
A85	00 41.6 −09 20	0.0518	310	6.2	8×10^{44}

Note: Distance calculated from redshift for $H_0 = 50$ km s^{-1} Mpc^{-1}, $q_0 = 0.5$.

1 Mpc = 3.262×10^6 light years

= 3.086×10^{22} m.

$^*kT$ is the cluster gas temperature in keV (Jones, C. and Forman, W., Ap. J., **511**, 65, 1999.)

(Adapted from *Cosmic X-ray Sources*, Seward, F., in *Allen's Astrophysical Quantities*, Cox, A.N., Ed., Springer, 2000.)

X-ray properties of rich clusters (clusters with hundreds to thousands of galaxies)

L_x (2–10 keV) $\sim (10^{42.5}\text{–}10^{45})h^{-2}$ erg s^{-1},

k$T \sim$ 2–14 keV, cluster core radius

R_c(X-ray) $\sim (0.1\text{–}0.3)h^{-1}$ Mpc,

$n_e \sim 3 \times 10^{-3} h^{1/2}$ cm^{-3},

$M_{gas}(\leq 1.5h^{-1}$ Mpc$) \sim 10^{13.5} M_{\text{solar}}$ [range: $(10^{13}\text{–}10^{14})h^{-2.5} M_{\text{solar}}$]

X-ray emission from a selection of active galaxies

Name	Redshift z	Distance (Mpc)	L_x 0.2-4 keV (erg s^{-1})	Type
MRK348	0.014	83	1×10^{43}	Seyfert 2
NGC1068	0.0037	22	9×10^{41}	Seyfert 2
Q0420-388	3.12	24600	2×10^{46}	High redshift quasar
3C120	0.033	200	2×10^{44}	VLBI radio galaxy
M81	0.0006	3.6	5×10^{39}	Low luminosity AGN
NGC4151	0.0033	20	4×10^{42}	Seyfert 1.5
3C273	0.158	980	6×10^{45}	Radio loud quasar
M87	0.0037	22	3×10^{43}	Radio galaxy
3C279	0.538	3400	6×10^{45}	Blazar
Cen A	0.0008	4.8	5×10^{41}	Radio galaxy
NGC5548	0.0017	10	4×10^{41}	Seyfert 1
E1821+643	0.297	1900	7×10^{45}	Radio quiet quasar
NGC6814	0.005	30	4×10^{42}	Seyfert 1
PKS 2155-304	0.17	1100	2×10^{46}	BL Lac

Note: Distance calculated from redshift for
$H_0 = 50$ km s^{-1} Mpc^{-1}, $q_0 = 0.5$.

1 Mpc $= 3.262 \times 10^6$ light years

$= 3.086 \times 10^{22}$ m.

(Adapted from *Cosmic X-ray Sources*, Seward, F., in *Allen's Astrophysical Quantities*, Cox, A.N., Ed., Springer, 2000.)

3C 273

The observed electromagnetic spectrum of the quasar 3C273 (3C273 is variable). (From Worrall, D. M. *et. al.*, *Ap. J.*, **232**, 683, 1979.)

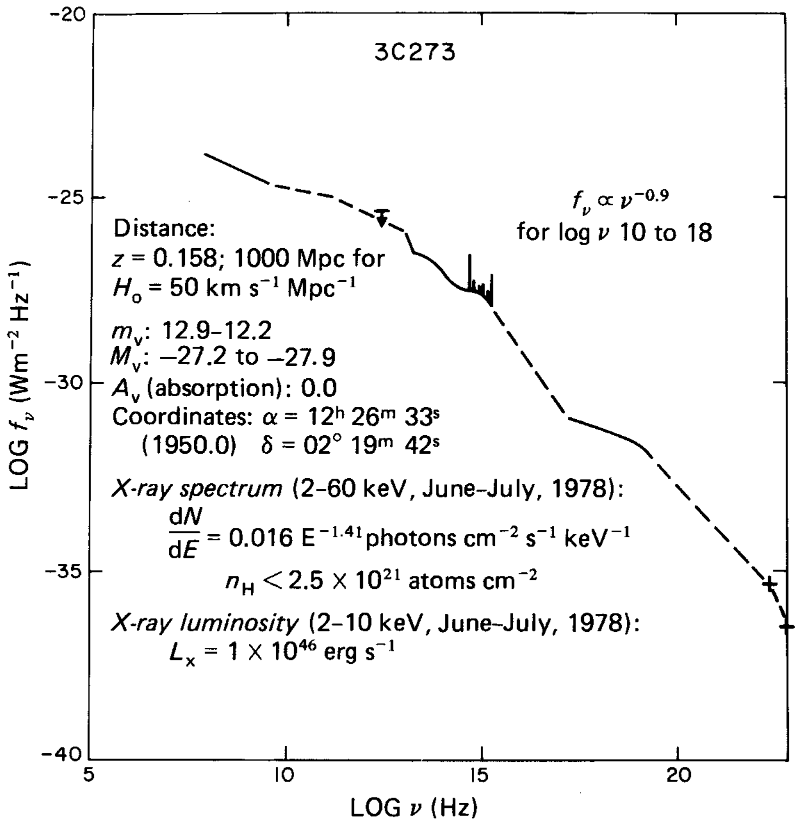

Quasar X-ray luminosity

Quasar X-ray luminosity (0.5-4.5 keV) versus redshift. (Courtesy H. Tananbaum, Harvard/Smithsonian Center for Astrophysics, 1982.)

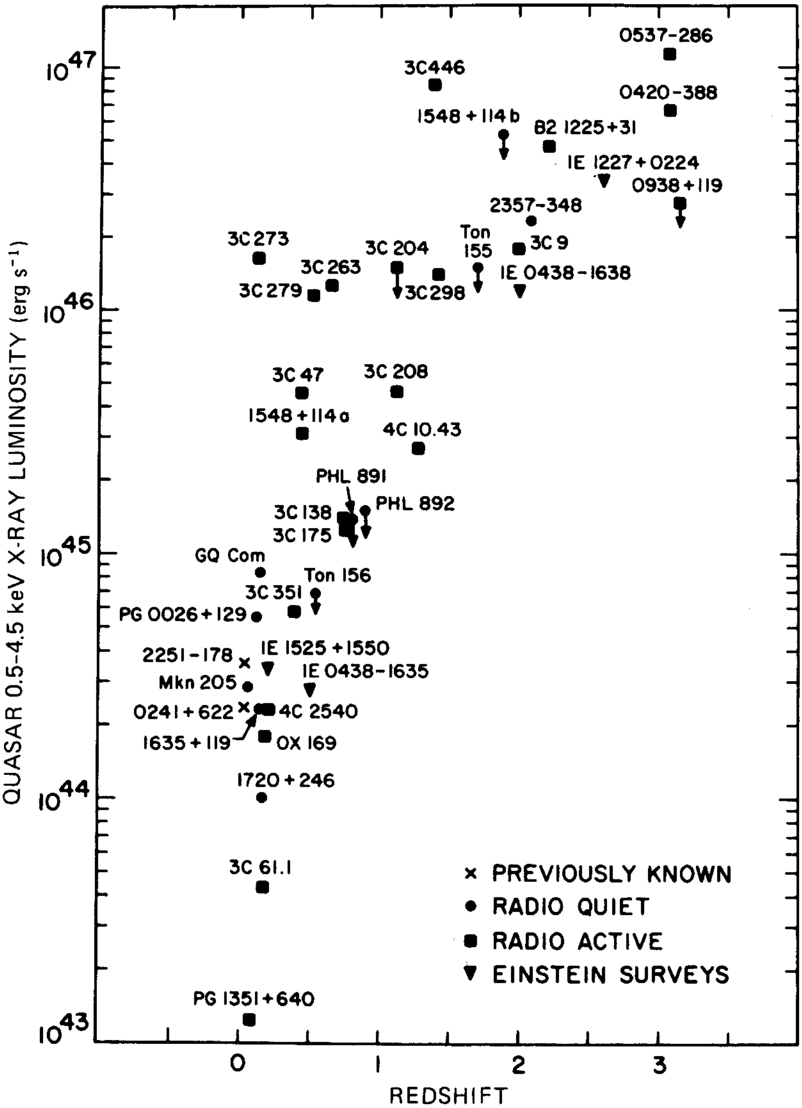

X-ray source nomogram

Nomogram to compute $\log(f_x/f_v)$ for X-ray sources, where f_x is the X-ray flux density in erg cm^{-2} s^{-1} in the 0.3 – 3.5 keV band and f_v is the flux density in the V band. For each object class indicated (stars: B–F, G, K, M; normal galaxies; active galactic nuclei; BL Lac objects) a continuous horizontal line indicates the range of $\log(f_x/f_v)$ comprising 70% of the known sources in the class and a dashed line indicates the range comprising the highest and lowest 15% of the sources. For example, for an X-ray source with a flux density of 2×10^{-13} erg cm^{-2} s^{-1} and a V magnitude of 20, $\log(f_x/f_v)$ is ~ 0.7 and the source is most likely a BL Lac object. (From Maccacaro, T. *et. al.*, *Ap. J.*, **326**, 680, 1988).

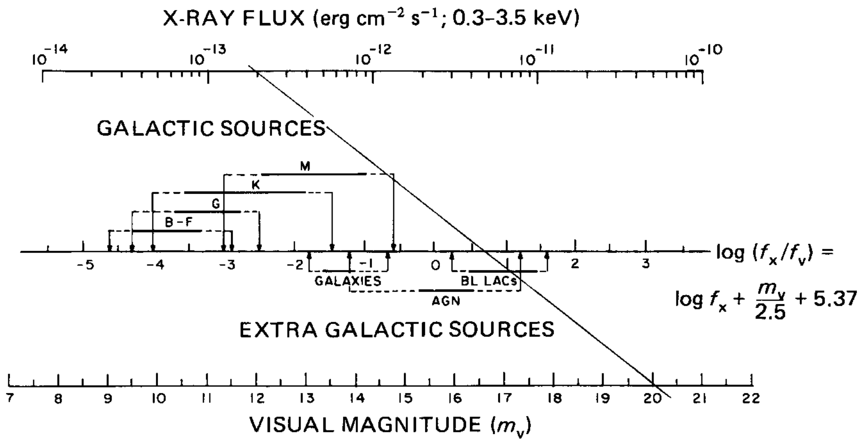

Diffuse X-ray background

Energy spectrum of the diffuse X-ray background. The solid line is an empirical fit; the fitting equations are given below. (Gruber, D.E., in *The X-ray Background*, Barcons, X. and Fabian, A.C., eds., Cambridge University Press, 1992, with permission.)

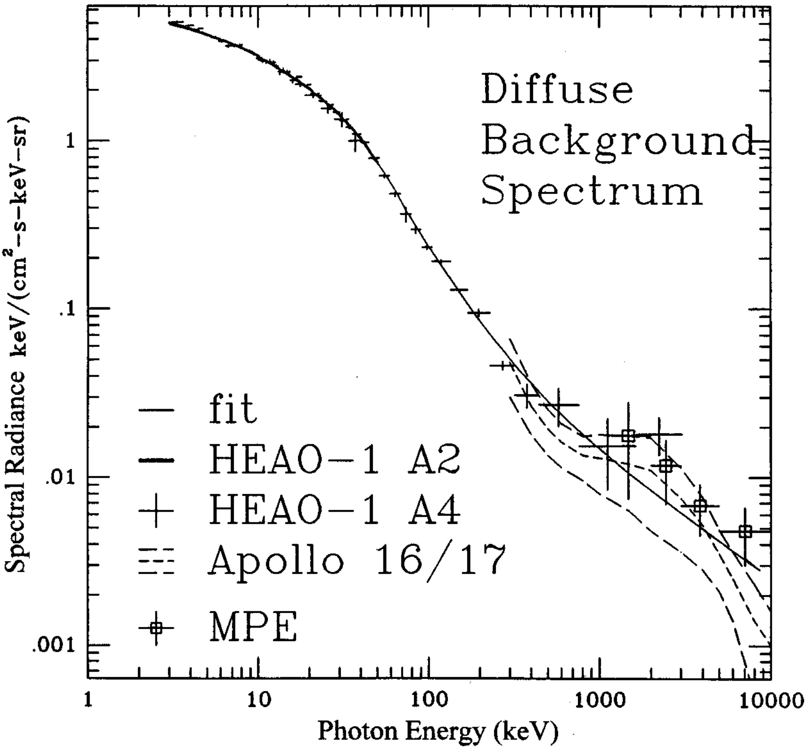

$$I(E) = 7.877E^{-0.29}e^{-E/41.13} \text{ keV cm}^{-2} \text{ s}^{-1} \text{ keV}^{-1}\text{sr}^{-1},$$

$$3 \text{ keV} < E < 60 \text{ keV}$$

$$I(E) = 1652E^{-2.00} + 1.754E^{-0.70} \text{ keV cm}^{-2} \text{ s}^{-1} \text{ keV}^{-1}\text{sr}^{-1},$$

$$60 \text{ keV} < E < 6000 \text{ keV}$$

Absorption of X-rays

Photoabsorption cross-sections (UV-X-ray) of abundant elements

Photoabsorption cross-sections of the abundant elements in the interstellar medium as a function of wavelength. (Adapted from Cruddace, R., Paresce, F., Bowyer, S. & Lampton, M., *Ap. J.*, **187**, 497, 1974.)

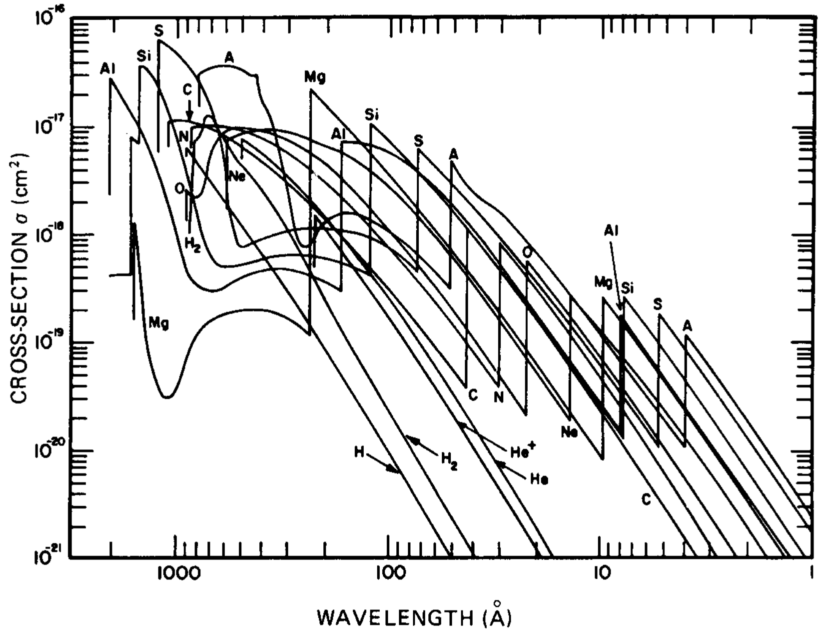

Effective cross-section of the interstellar medium

Effective cross-section (cross-section per hydrogen atom or proton) of the interstellar medium: — gaseous component with normal composition and temperature; –·– hydrogen, molecular form; – – HII region about a B star; – – – HII region about an O star; – – – – dust. (Adapted from Cruddace, R., Paresce, F., Bowyer, S. & Lampton, M., *Ap. J.*, **187**, 497, 1974.)

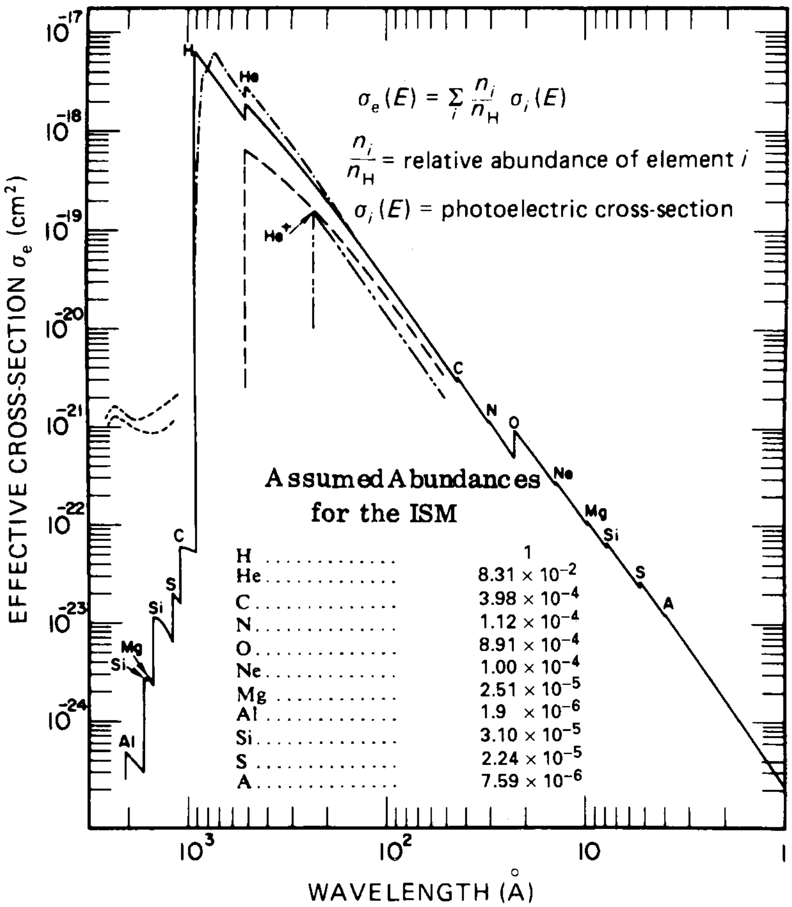

Total photoionization cross-section

Total photo-ionization cross-section per hydrogen atom $[x(E/1\ \text{keV})^3]$ in units 10^{-22} cm^2 as a function of incident photon energy for a gas having a cosmic elemental abundance. The elements responsible for the discontinuities due to their K edges are shown. (Adapted from Brown, R.L. & Gould, R.J., *Physical Review*, **D**, **1**, 2252, No. 8, 1970.)

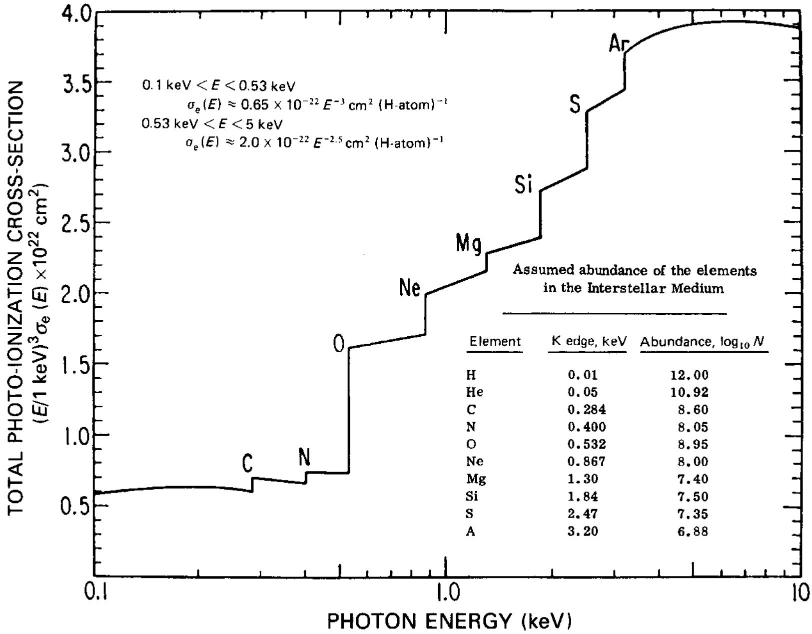

Photoelectric absorption cross-section

Net photoelectric absorption cross-section per hydrogen atom as a function of energy, scaled by $(E/1\ \mathrm{keV})^3$. The solid line is for relative abundances given in the table of elemental abundances below, with all elements in the gas phase and in neutral atomic form. The dotted line shows the effect of condensing the fraction of each element indicated in the table into 0.3 μm grains. The contributions of hydrogen and hydrogen plus helium to the total cross-section are also shown. (From Morrison, R. & McCammon, D., *Ap. J.*, **270**, 119, 1983. Diagram courtesy of D. McCammon.)

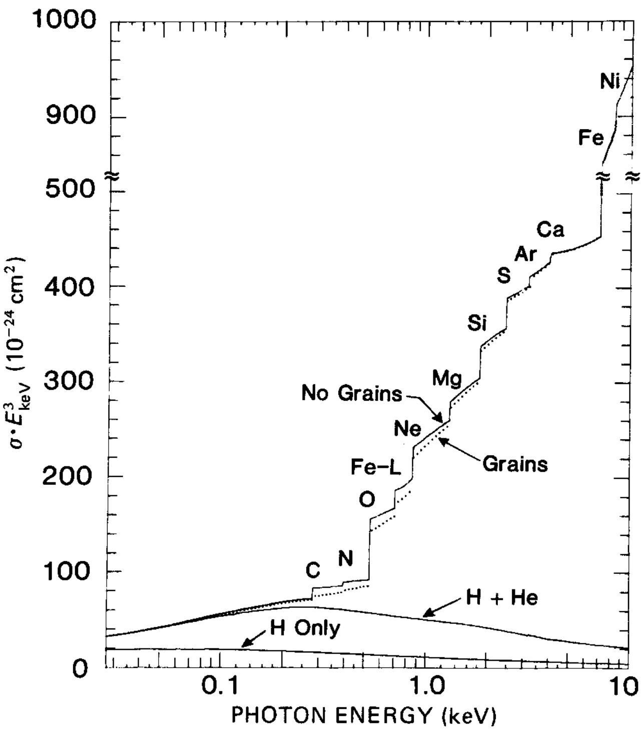

Elemental abundances

Element	Abundance[a]	Fraction in grains[b]
H	12.00	0
He	11.00	0
C	8.65	1
N	7.96	1
O	8.87	0.25
Ne	8.14	0
Na	6.32	1
Mg	7.60	1
Al	6.49	1
Si	7.57	1
S	7.28	1
Cl	5.28	1
Ar	6.58	0
Ca	6.35	1
Cr	5.69	1
Fe	7.52	1
Ni	6.26	1

[a] Log_{10} abundance relative to hydrogen = 12.00. All values except helium are from Anders and Ebihara, 1982.

[b] Fraction of atoms of each element assumed depleted from gas phase and condensed into grains of average thickness 2.1×10^{18} atoms cm^{-2} for case shown as dotted line in the diagram.

Coefficients of analytic fit to cross-section

Energy range (keV)	c_0	c_1	c_2
0.030 – 0.100[a]	17.3	608.1	−2150
0.100 – 0.284	34.6	267.9	−476.1
0.284 – 0.400	78.1	18.8	4.3
0.400 – 0.532	71.4	66.8	−51.4
0.532 – 0.707	95.5	145.8	−61.1
0.707 – 0.867	308.9	−380.6	294.0
0.867 – 1.303	120.6	169.3	−47.7
1.303 – 1.840	141.3	146.8	−31.5
1.840 – 2.471	202.7	104.7	−17.0
2.471 – 3.210	342.7	18.7	0.0
3.210 – 4.038	352.2	18.7	0.0
4.038 – 7.111	433.9	−2.4	0.75
7.111 – 8.331	629.0	30.9	0.0
8.331 – 10.000	701.2	25.2	0.0

Note: cross-section per hydrogen atom $= (c_0 + c_1 E + c_2 E^2) E^{-3} \times 10^{-24}$ cm^2 (E in keV).

[a] Break introduced to allow adequate fit with quadratic: no absorption edge at 0.1 keV.

(From Morrison, R. & McCammon, D., *op. cit.*)

Attenuation of photons in the atmosphere

Attenuation of photons in the 1972 COSPAR International Reference Atmosphere with 1/e absorption length plotted as a function of energy and altitude or atmospheric depth.

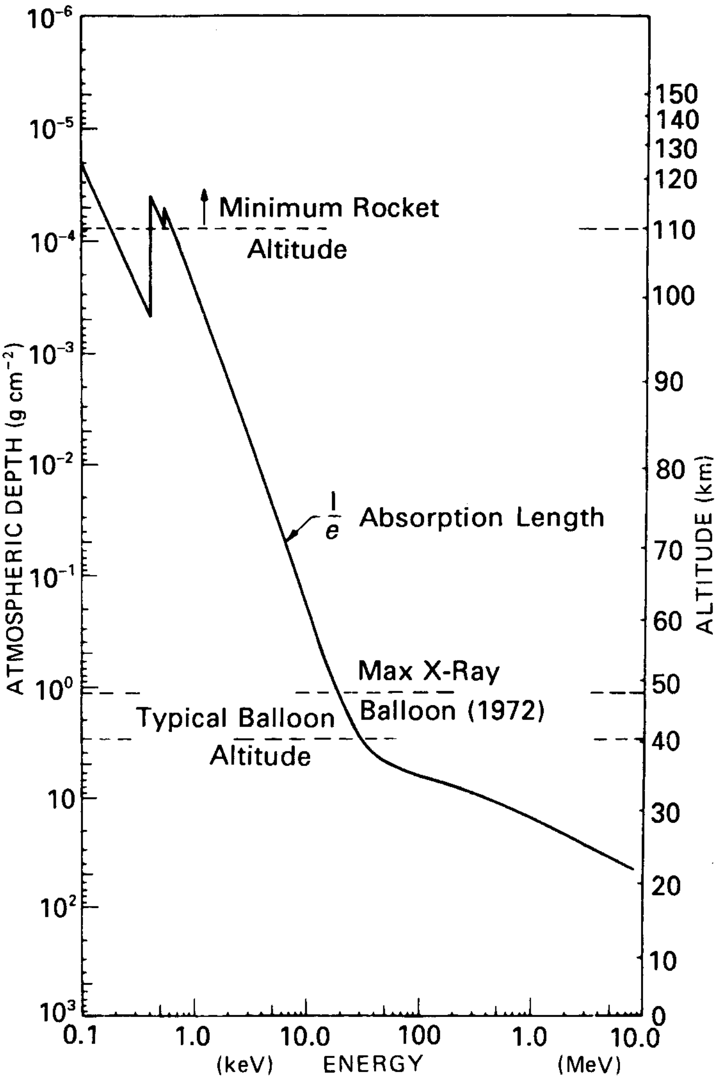

Photoelectric absorption in the interstellar medium

The vertical axis gives the column density in units of hydrogen atoms cm^{-2} at which the transmission of the interstellar medium is 1/e at the photon energy E, *i.e.* for $N_H\sigma(E) = 1$. (For a hydrogen atom number density of 1 per cm^3, 1 kpc is equivalent to a column density of 3.1×10^{21} hydrogen atoms cm^{-2}.) The cross-section $\sigma(E)$ is from Morrison, R. and McCammon, D., *op.cit.*.

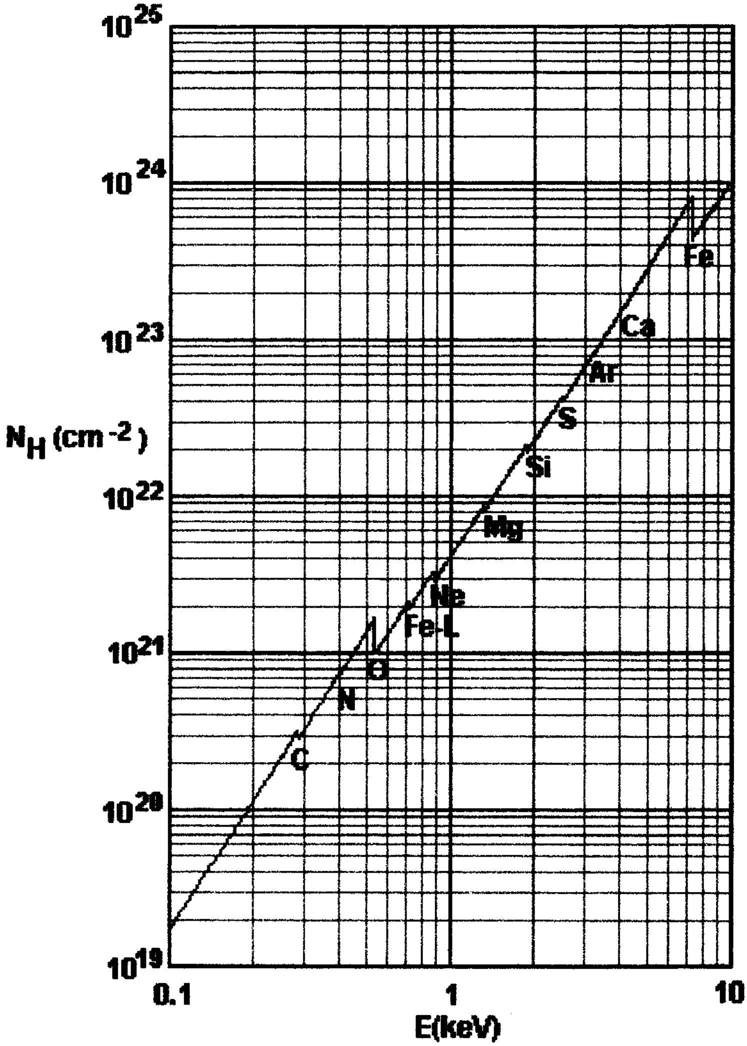

An incomplete list of astrophysically important X-ray spectral features

Identification	Energy (keV)†	Identification	Energy (keV)†
Ne VII	0.127	N VII	0.500
Si XI	0.283	O I K edge	0.532
C I K edge	0.284	O VII	0.569
Si XII	0.303	O VII	0.574
C V	0.308	O VIII	0.654
N I K edge	0.402	O VII	0.666
N VI	0.431	O VII	0.698
Fe I LIII edge	0.707	Si XIII	1.86
Fe I LII edge	0.721	S I K edge	2.472
Fe XVII	0.826	Ar I K edge	3.203
Ne I K edge	0.867	Fe I Kα_2	6.391
Ne IX	0.915	Fe I Kα_1	6.404
Ne IX	0.922	Fe XXV	6.64
Fe XX	0.996	Fe XXV	6.68
Ne X	1.022	Fe XXV	6.70
Mg I K edge	1.305	Fe XXVI	6.93
Mg XI	1.340	Fe I Kβ	7.058
Mg XI	1.352	Fe I K edge	7.111
Si K edge	1.839		

† $\lambda(\text{Å}) = 12.399/E$ (keV).

Model X-ray spectral distributions for non-dispersive spectroscopy

$$f(E) = C\ \mathrm{e}^{-\sigma_\mathrm{e}(E)N_\mathrm{H}} f(\mathrm{S,E}) \quad \text{photons cm}^{-2}\ \text{s}^{-1}\ \text{keV}^{-1},$$

where

C = normalization constant,

N_H = hydrogen column density to source,

$\sigma_\mathrm{e}(E)$ = photoelectric cross-section perhydrogen atom for absorption of photons of energy E by interstellar medium. For $E > 3$ keV: $\sigma_\mathrm{e}(E)N_\mathrm{H} \approx (E_\mathrm{a}/E)^{8/3}$, where E_a is a low energy cutoff parameter.

S is a parameter in the intrinsic spectral shape:

Thermal bremsstrahlung:

$$S = T, \quad f(S,E) = \overline{g(T,E)}\ \mathrm{e}^{-E/kT}/E(kT)^{1/2},$$

where $\overline{g(T,E)}$ is the temperature-averaged Gaunt factor.

Power law:

$$S = n, \quad f(S,E) = E^{-n}.$$

Blackbody:

$$S = T, \quad f(S,E) = E^2/(\mathrm{e}^{E/kT} - 1).$$

Hydrogen column density from optical extinction

For optically identified sources the relation between X-ray absorption and optical extinction is given by

$N_H = 1.9 \times 10^{21}\ A_V$ hydrogen atoms cm^{-2}

$N_H = (5.9 \pm 1.6) \times 10^{21}\ E_{B-V}$ hydrogen atoms cm^{-2}

where A_v is the optical extinction in magnitudes and E_{B-V} is the color excess in magnitudes.

Copernicus observations yield

$N(HI + H_2) = 5.8 \times 10^{21} E_{B-V}$ atoms cm^{-2}

ROSAT (P. Predehl and J.H.M.M. Schmitt, Astron. Astrophys., **293**, 889, 1995) observations yield

$N_H = (1.79 \pm 0.03) \times 10^{21} A_V$ hydrogen atoms cm^{-2}

(Adapted from F. Seward in *Allen's Astrophysical Quantities*, Cox, A.N., ed., Springer, 2000.)

X-ray plasma spectrum

Calculated X-ray spectrum of an optically thin collisionally ionized equilibrium plasma at 1 keV. Upper curve with spectral lines): Astrophysical Plasma Emission Code (APEC, http://hea-www.harvard.edu/APEC/) calculation; lower curve with spectral lines): Raymond-Smith (Raymond, J. C., & Smith, B. W. 1977, ApJS, **35**, 419; 1993 update) calculation (divided by 100); dotted curve: bremsstrahlung;dashed curve: blackbody. Abundances are solar (Anders, E., & Grevesse, N. 1989, Geochim. Cosmochim. Acta, 53, 197.)

(Courtesy of Randall Smith, Harvard-Smithsonian Center for Astrophysics, 2001)

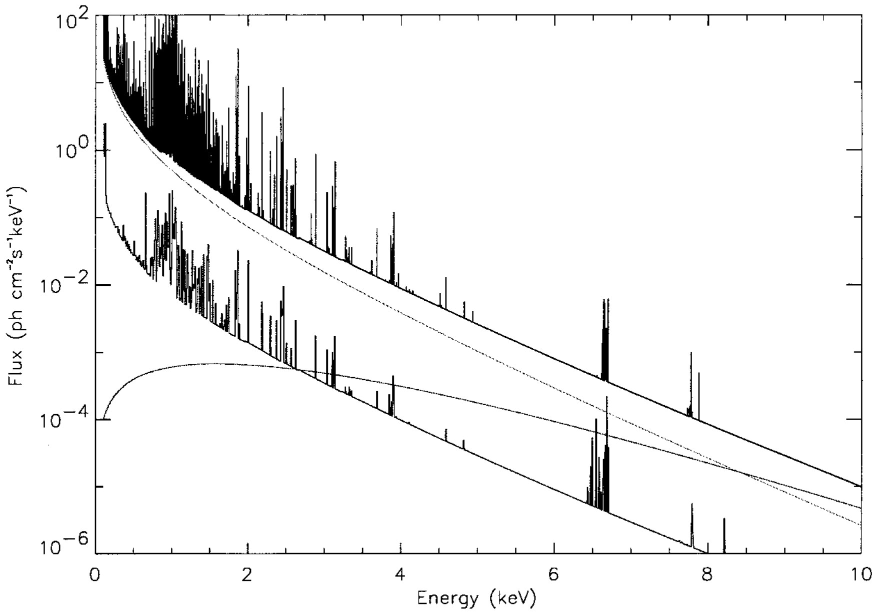

X-ray emission lines from an optically thin plasma

Power per unit emission measure for the most prominent emission lines in the X-ray band for an optically thin plasma as a function of temperature. The calculations are based on the Raymond-Smith model (Raymond, J. C., & Smith, B. W. 1977, ApJS, **35**, 419; 1993 update). Abundances are solar (Anders, E., & Grevesse, N. 1989, Geochim. Cosmochim. Acta, 53, 197.) The plots are for Fe lines for Fe XIII - Fe XIV; He-like ions for C, N, O, Ne, Mg, Si, S, and Fe; H-like ions for C, N, O, Ne, Mg, Si, S, and Fe.

(Courtesy of Randall Smith, Harvard-Smithsonian Center for Astrophysics, 2001)

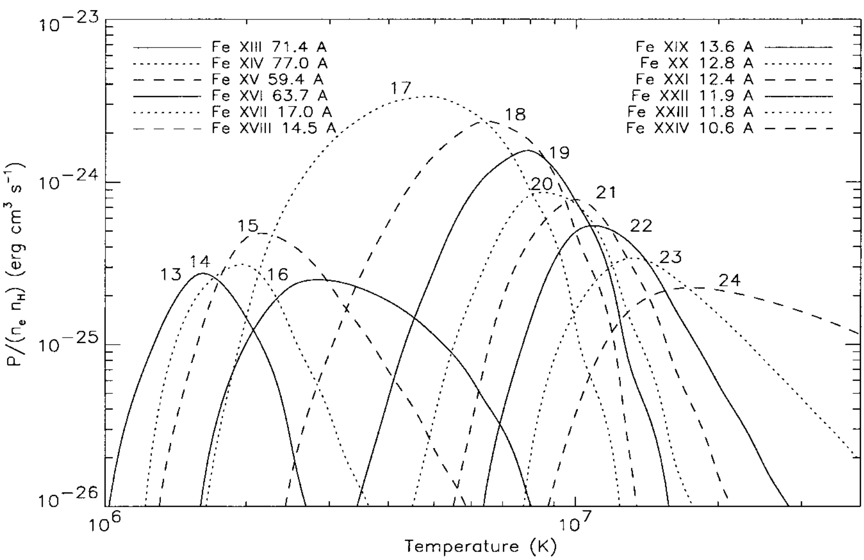

X-ray emission lines from an optically thin plasma (cont.)

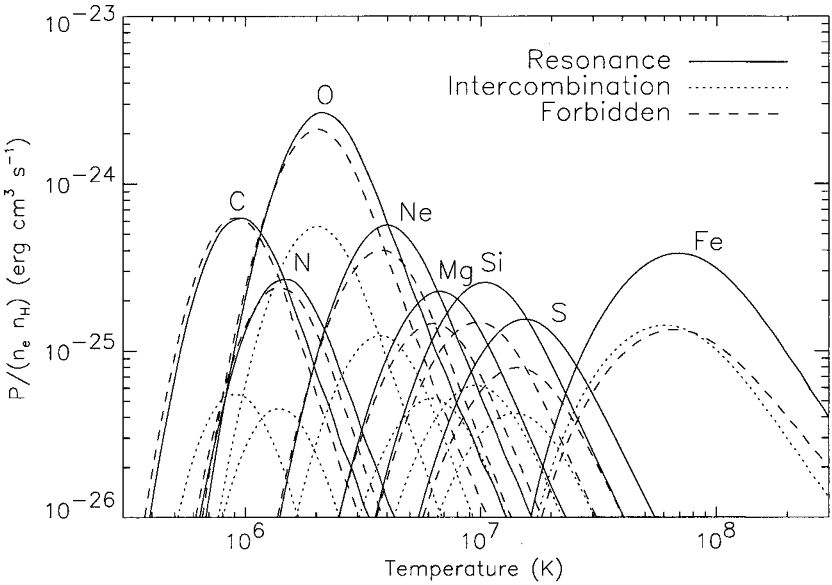

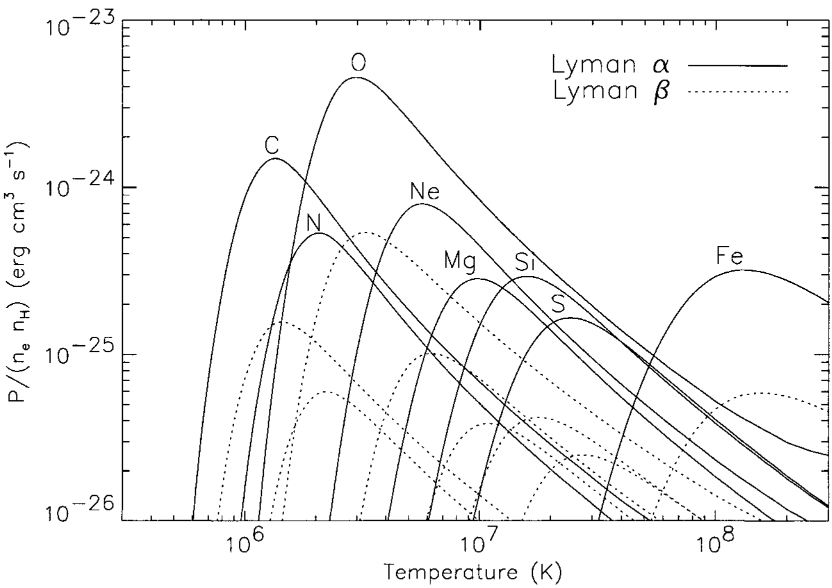

X-ray emission lines from an optically thin plasma (cont.)

X-ray wavelengths (A) of He-like lines.

Element	Z	Resonance	Intercombination	Intercombination	Forbidden
C	6	40.2673645	40.7279816	40.7302322	41.4715347
N	7	28.7869663	29.0818634	29.0843220	29.5346870
O	8	21.6015053	21.8010178	21.8036385	22.0977230
Ne	10	13.4473066	13.5502510	13.5531101	13.6989765
Mg	12	9.1687498	9.2281675	9.2312088	9.3143387
Si	14	6.6479473	6.6849880	6.6881871	6.7402945
S	16	5.0387268	5.0631452	5.0664926	5.1015010
Fe	26	1.8503995	1.8554125	1.8595167	1.8681941

(Kelly, R.L., J. Phys. Chem. Ref. Data, 16, Supp 1, 1987)

X-ray wavelengths (A) of H-like lines.

Element	Z	Lyman α	Lyman α	Lyman β	Lyman β
C	6	33.7398	33.7344	28.4665	28.4654
N	7	24.7848	24.7794	20.9107	20.9096
O	8	18.9726	18.9672	16.0068	16.0056
Ne	10	12.1376	12.1322	10.2396	10.2386
Mg	12	8.4247	8.4193	7.1070	7.1058
Si	14	6.1859	6.1805	5.2180	5.2169
S	16	4.7328	4.7274	3.9920	3.9908
Fe	26	1.7835	1.7781	1.5035	1.5024

(G. W. Ericsson 1977, J. Phys. Chem. Ref. Data, Vol 6, No. 3, "Energy Levels of One Electron Atoms")

Power radiated from an optically thin plasma

Total power radiated per unit emission measure for an optically thin plasma as a function of temperature. Models: Astrophysical Plasma Emission Code (APEC, http://hea-www.harvard.edu/APEC/), Raymond-Smith (Raymond, J. C., & Smith, B. W. 1977, ApJS, **35**, 419; 1993 update). Abundances are solar (Anders, E., & Grevesse, N. 1989, Geochim. Cosmochim. Acta, 53, 197.)

(Courtesy of Randall Smith, Harvard-Smithsonian Center for Astrophysics, 2001)

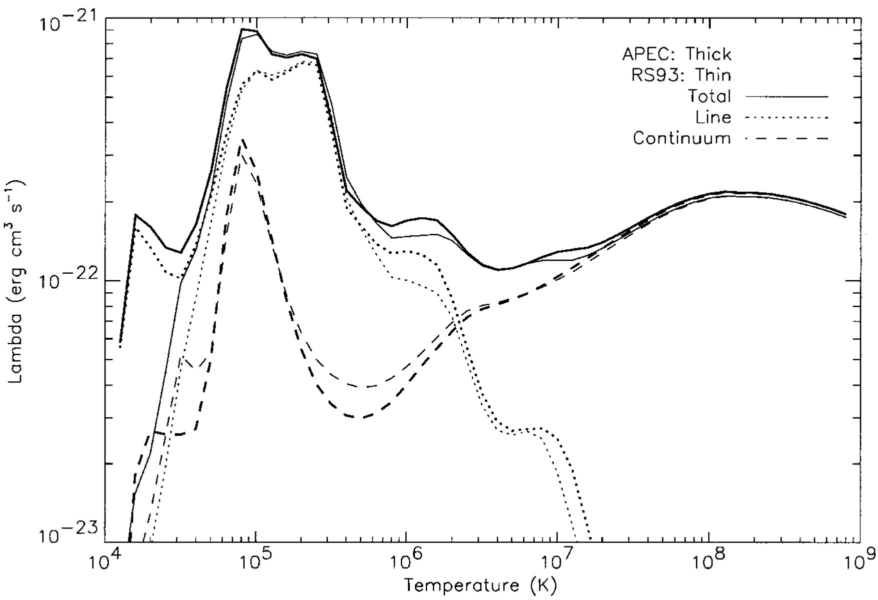

Chandra X-ray Observatory (AXAF)

Sketch of the Chandra X-ray Observatory (CXO). The High Resolution Mirror Assembly (HRMA) consists of four pairs of nested reflecting surfaces arranged in the Wolter type I (paraboloid-hyperboloid) geometry. The diameter of the outer mirror pair is 1.2 m and the focal length of the HRMA is 10 m. At 1.5 keV the 50% encircled energy radius is 0.3 arc sec. There are two focal plane instruments, the High Resolution Camera (HRC) and the Advanced CCD Imaging Spectrometer (ACIS), and two transmission grating assemblies, the Low Energy Transmission Grating Spectrometer (LETG) and the High Energy Transmission Grating assembly (HETG), the latter having two sets of transmission gratings, High Energy Gratings (HEG) and Medium Energy Gratings (MEG). The HRC is comprised of two microchannel plate (MCP) imaging detectors: the HRC-I (imaging) is designed for wide-field imaging and the HRC-S (spectroscopy) is designed to serve as a readout for the LETG. ACIS is comprised of two CCD arrays, a 4-chip array, ACIS-I (imaging) and a 6-chip array, ACIS-S (spectroscopy), to read out the HETG.

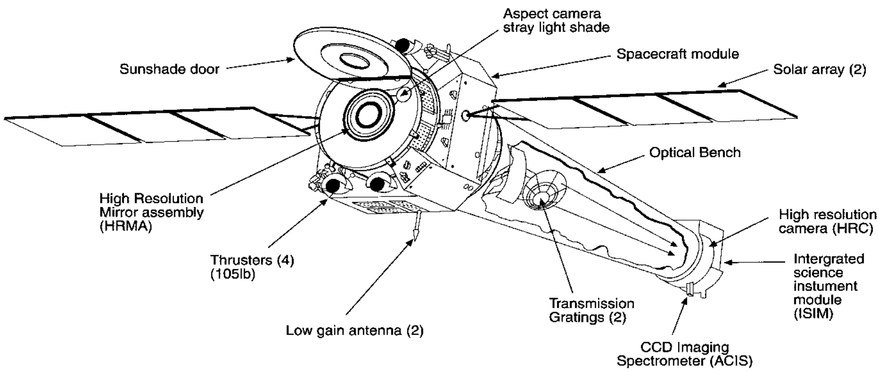

Aperture Diameter (m)	Geometric Area (cm^2)	Focal Length (m)	Spatial Resolution (FWHM) (arcsec)	FOV (arcmin)	Energy Range (keV)	Spectral Resolution (Å)
1.2	1100	10.0	0.3	30	0.1-10	0.01-0.05

Chandra X-ray Observatory characteristics—an overview

Instrument	**ACIS-I**	**HRC-I**	**ACIS-S(1)**	**HRC-S(2)**
Bandpass (keV)	0.15–10	0.08–10	0.4–10	0.070–10
$E/\Delta E$	~ 50	1 @ 1 keV	65–1070	> 1000
Field of View arc min	16.9×16.9	30×30	8.3×50.6	6×99
Effective Area cm^2	600 @ 1.5 keV	227 @ 1.5 keV	200 @ 1.5 keV	1–25
Time Res.	2.85 ms	16 μs	2.85 ms	16 μs
Sensitivity(4)	$4 \times 10^{-15(5)}$	$1 \times 10^{-15(6)}$	–	–

(1)with the HEG and MEG, (2)with the LETG, (3)for 0.070–0.2 keV, (4)in erg cm^{-2} s^{-1}, (5) in 10^4 s, (6)in 3×10^5 s.

(From the Chandra X-ray Center's (CXC) Users' Guide, 2004.)

XMM-Newton X-ray Observatory

Sketch of the XMM-Newton payload. The mirror modules, two of which are equipped with Reflection Grating Arrays, are visible at the lower left. At the right end of the assembly, the focal X-ray instruments are shown: The EPIC MOS cameras with their radiators "horns"), the radiator of the EPIC pn camera and those of the RGS detectors. The OM telescope is obscured by the lower mirror module.

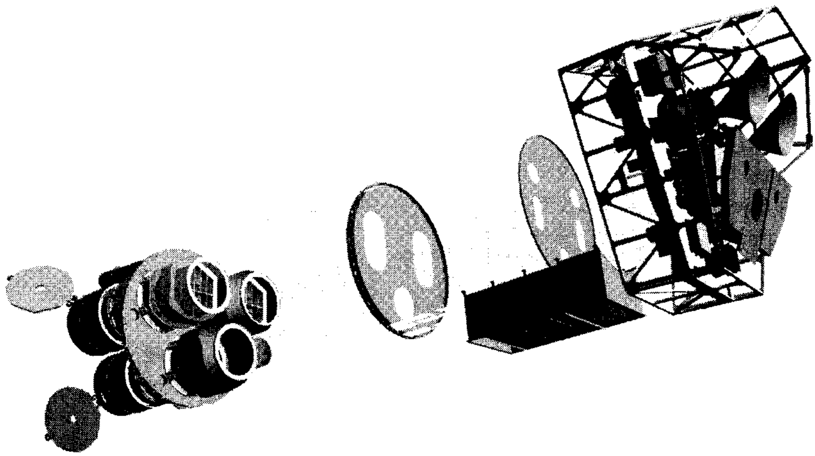

XMM-Newton *characteristics – an overview*

Instrument	EPIC MOS	EPIC pn	RGS	OM
Bandpass	0.15–12 keV	0.15–15 keV	0.35–2.5 keV	180–600 nm
Orbital target vis.	5–135 ks	5–135 ks	5–145 ks	5–145 ks
Sensitivity	$\sim 10^{-14}$	$\sim 10^{-14}$	$\sim 8\times 10^{-5}$	20.7 mag
Field of view (FOV)	30'	30'	~5'	17'
PSF (*FWHM/HEW*)	5"/14"	6"/15"	N/A	1.4"–1.9"
Pixel size	40 μm (1.1")	150 μm (4.1")	81 μm (9×10^{-3} Å)	0.476513"
Timing resolution	1.5 ms	0.03 ms	16 ms	0.5 s
Spectral resolution	~70 eV	~80 eV	0.04/0.025 Å	350

EPIC – European Photon Imaging Camera
(pn - pn CCDs, MOS - MOS (Metal Oxide Semi-conductor) CCD arrays)

RGS – Reflection Grating Spectrometer

OM – Optical Monitor

(From the XMM-Newton Users' Handbook, 2004)

Conversions and equivalencies

1 keV: $hc/E = 12.39854 \times 10^{-8}$ cm
1 keV: $E/h = 2.417965 \times 10^{17}$ Hz
1 keV: $E/k = 11.6048 \times 10^{6}$ K
1 Ehz: $h\nu = 4.13571$ keV
1 keV $= 1.602177 \times 10^{-9}$ erg $= 1.602177 \times 10^{-16}$ joule
1 μJy $= 10^{-11}$ erg cm^{-2} s^{-1} EHz^{-1}
$= 0.242 \times 10^{-11}$ erg cm^{-2} s^{-1} keV^{-1}
$= 1.509 \times 10^{-3}$ keV cm^{-2} s^{-1} keV^{-1}
1 Uhuru ct s^{-1}: 1.7×10^{-11} erg cm^{-2} s^{-1} (2-6 keV)
: 2.4×10^{-11} erg cm^{-2} s^{-1} (2-10 keV)

X-ray source intensity in millicrabs

$$= 10^3 \int_{E_1}^{E_2} E(dN/dE)dE / \int_{E_1}^{E_2} E(dN/dE)_{Crab} dE$$

dN/dE and $(dN/dE)_{Crab}$ is the source and Crab Nebula photon spectral flux density, respectively.

For $E_2 = 10$ keV and $E_1 = 2$ keV,

$$\int_{E}^{E_2} E(dN/dE)_{Crab} dE = 2.3 \times 10^{-8} \text{ erg cm}^{-2} \text{ s}^{-1}$$

Crab spectrum is from Chapter 6.

Spectral irradiance conversions:

I_v(erg cm^{-2} s^{-1} Hz^{-1}) $= 3.336 \times 10^{-19} \lambda^2$(Å)$I_\lambda$(erg cm^{-2} s^{-1} Å^{-1})
I_v(erg cm^{-2} s^{-1} Hz^{-1}) $= 6.626 \times 10^{-27} I_E$(keV cm^{-2} s^{-1} keV^{-1})
I_λ(erg cm^{-2} s^{-1} Å^{-1}) $= 3.336 \times 10^{-19} \nu^2$(Hz) I_ν(erg cm^{-2} s^{-1} Hz^{-1})
I_λ(erg cm^{-2} s^{-1} Å^{-1}) $= 1.292 \times 10^{-10}$
E^2(keV) I_E(keV cm^{-2} s^{-1} keV^{-1})
I_E(keV cm^{-2} s^{-1} keV^{-1}) $= 1.509 \times 10^{26} I_\nu$(erg cm^{-2} s^{-1} Hz^{-1})
I_E(keV cm^{-2} s^{-1} keV^{-1}) $= 5.034 \times 10^{7} \lambda^2$(Å)$I_\lambda$(erg cm^{-2} s^{-1} Å^{-1})
N_p(photons cm^{-2} s^{-1} keV^{-1}) $= I_E$(keV cm^{-2} s^{-1} keV^{-1})E^{-1} (keV)

Bibliography

Astrophysical Formulae, Lang, K.R., Springer, 1999.

Cosmic X-ray Sources, Seward, F., in *Allen's Astrophysical Quantities*, Cox, A.N., Ed., Springer, 2000.

Exploring the X-ray Universe, Charles, P.A. and Seward, F.D., Cambridge University Press, 1995.

High Energy Astrophysics, Longair, M.S., Cambridge University Press, 1992.

Note: Links to WWW resources which supplement the material in this chapter can be found at:

http://www.astrohandbook.com

Chapter 7

Gamma-ray astronomy

The Universe: a device contrived for the perpetual astonishment of astronomers. - Arthur C. Clarke

Gamma-ray burst map

2704 BATSE (Burst and Transient Source Experiment of the Compton Observatory) gamma-ray bursts (as of 2000), in galactic coordinates.

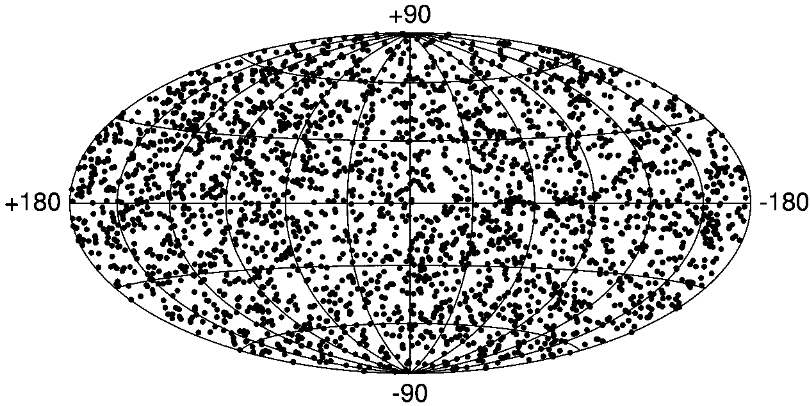

High-energy gamma-ray sources

The third EGRET (Energetic Gamma-ray Experiment of the Compton Observatory) high-energy gamma-ray source catalog.

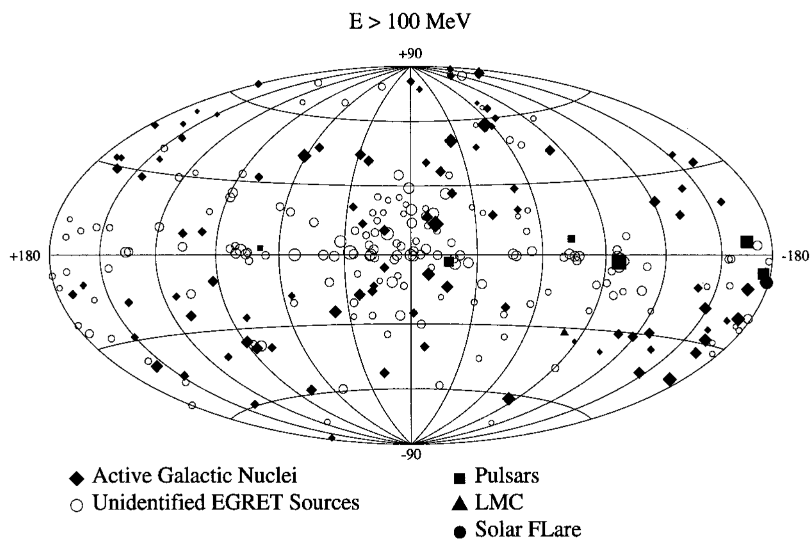

Intensities of X- and gamma-ray sources

Compilation of the intensities of a variety of X- and gamma-ray sources. The ordinate, the number of photons cm^{-2} s^{-1} MeV^{-1}, is multiplied by E^2. (Adapted from Schönfelder, V. in *Non-Solar Gamma-Rays*, R. Cowsik & R. Wills, eds., Pergamon Press, 1980.)

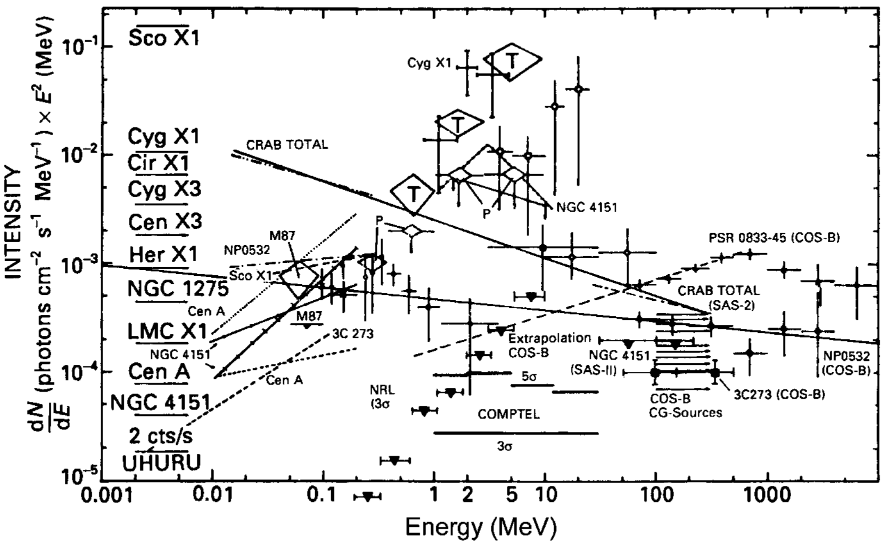

Crab Nebula spectra

Photon number spectrum of the total Crab emission. (Adapted from Schönfelder, V., *op. cit.*, see reference for explanation of symbols.)

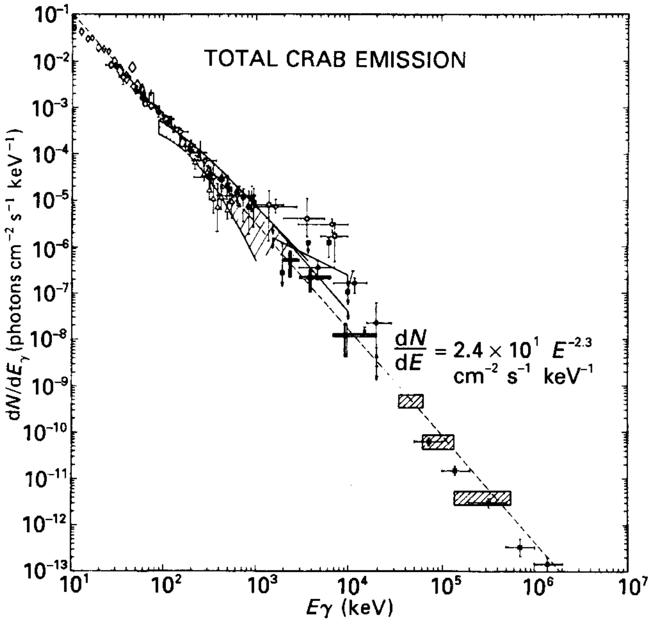

Photon number spectrum of the Crab pulsar. (Adapted from Schönfelder, V., *op. cit.*, see reference for explanation of symbols.)

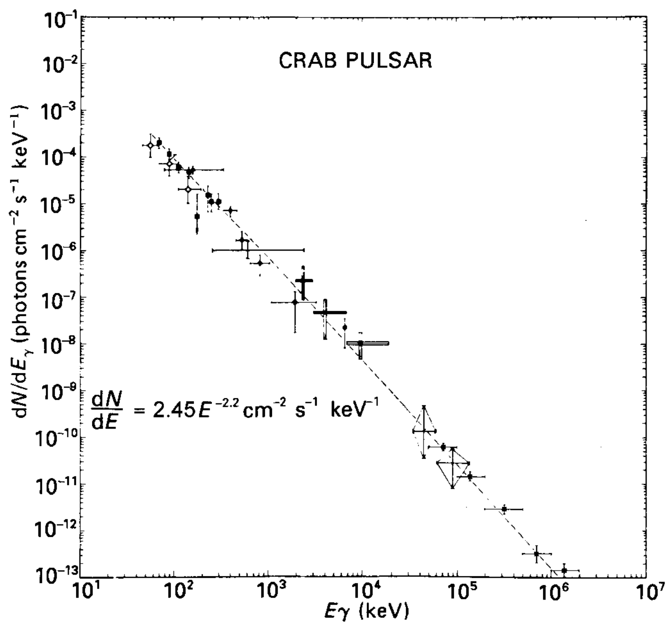

Diffuse gamma-ray background

Spectrum of diffuse gamma-ray background. (Adapted from Fichtel, C.E., Simpson, G.A. & Thompson, D.J., *Ap. J.*, **22**, 833, 1978.)

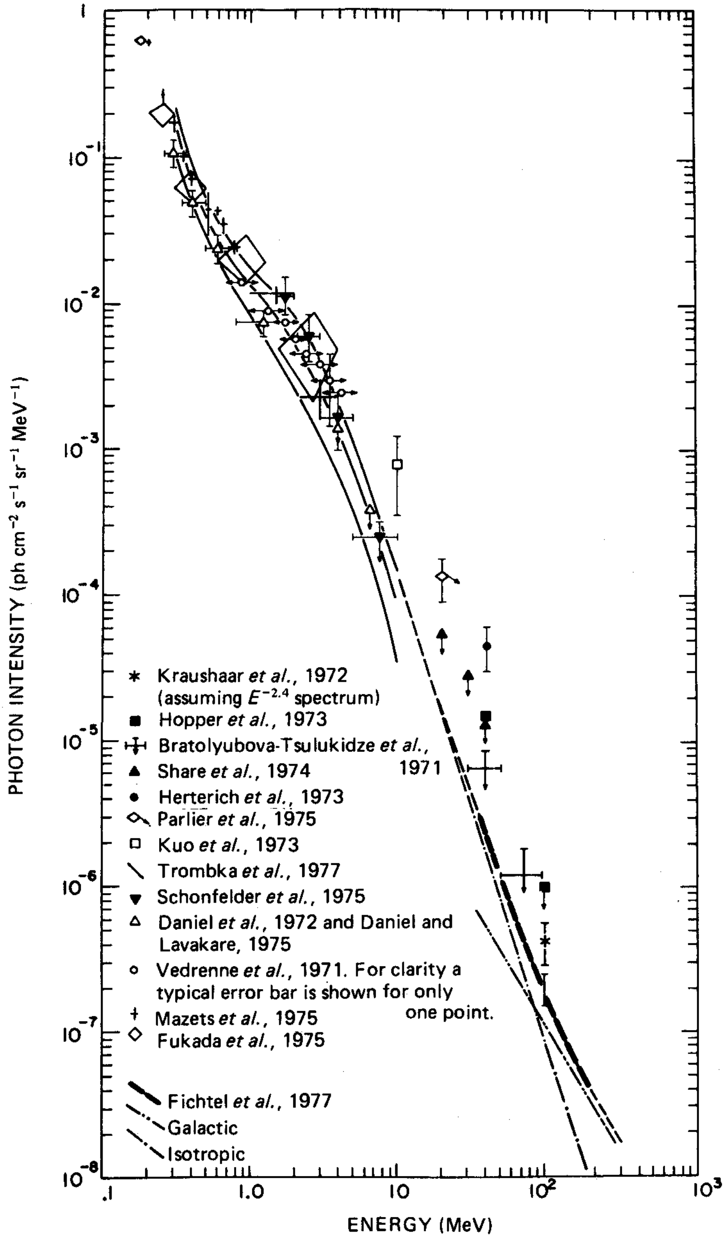

Gamma-ray production mechanisms

Continuum radiation

Bremsstrahlung (free-free emission)

See Ch. 12

Magnetobremsstrahlung (synchrotron radiation)

See Ch. 12

Inverse Compton effect

See Ch. 12

Line radiation

Annihilation radiation

Direct electron-positron annihilation ($e^+ + e^- \longrightarrow 2\gamma$) leads to line emission with a mean energy of

$$h\nu = m_e c^2 \begin{cases} +kT_e/2, & T_e \ll 10^7 \text{ K}, \\ +3kT_e/4, & 10^7 < T_e < 10^{10} \text{ K}, \\ +kT_e, & T_e > 10^{10} \text{ K}, \end{cases}$$

where $m_e c^2 = 510.9991$ keV and T_e is the temperature of the electrons and positrons.

Nuclear de-excitation and radioactive decay

See next page

Gamma-ray lines

Nucleosynthetic radioactive decay gamma-ray lines.

Process	Half-life	Line Energy (keV)
${}^{56}_{28}\mathrm{Ni} + \mathrm{e}^- \longrightarrow {}^{56}_{27}\mathrm{Co} + \nu$	6.1 d	158.4
		811.9
${}^{56}_{27}\mathrm{Co} \longrightarrow {}^{56}_{26}\mathrm{Fe} + \mathrm{e}^+ + \nu$	77 d	846.8
${}^{56}_{27}\mathrm{Co} + \mathrm{e}^- \longrightarrow {}^{56}_{26}\mathrm{Fe} + \nu$		1238.8
${}^{57}_{27}\mathrm{Co} + \mathrm{e}^- \longrightarrow {}^{57}_{26}\mathrm{Fe} + \nu$	272 d	122.1
${}^{22}_{11}\mathrm{Na} \longrightarrow {}^{22}_{10}\mathrm{Ne} + \mathrm{e}^+ + \nu$	2.6 y	1274.5
${}^{22}_{11}\mathrm{Na} + \mathrm{e}^- \longrightarrow {}^{22}_{10}\mathrm{Ne} + \nu$		511.0
${}^{44}_{22}\mathrm{Ti} + \mathrm{e}^- \longrightarrow {}^{44}_{21}\mathrm{Sc} + \nu$	~ 60 y	67.9
		78.4
${}^{26}_{13}\mathrm{Al} \longrightarrow {}^{26}_{12}\mathrm{Mg} + \mathrm{e}^+ + \nu$	7.1×10^5 y	1808.7
${}^{26}_{13}\mathrm{Al} + \mathrm{e}^- \longrightarrow {}^{26}_{12}\mathrm{Mg} + \nu$		511.0
${}^{60}_{26}\mathrm{Fe} \longrightarrow {}^{60}_{27}\mathrm{Co} + \mathrm{e}^- + \overline{\nu}$	1.5×10^6 y	–
${}^{60}_{27}\mathrm{Co} \longrightarrow {}^{60}_{28}\mathrm{Ni} + \mathrm{e}^- + \overline{\nu}$	5.3 y	1332.5
		1173.2

(From Gehrels, N. and Paul, J., *The New Gamma-ray Astronomy*, in Physics Today, February, 1998.)

Gamma-ray line features

Observed gamma-ray line features. (From von Ballmoos, P. in *TEV Gamma-ray Astrophysics*, Voelk, H.J. and Aharonian, F.A., eds., Kluwer Academic Publishers, 1996.)

Physical Process	**Energy** [keV]	**Source**	**Flux** ph cm^{-2} s^{-1}
Nuclear de-excitation			
^{56}Fe (p, p′, γ)	847	Solar flares	≤ 0.05
^{24}Mg (p, p′, γ)	1369	Solar flares	≤ 0.08
^{20}Ne (p, p′, γ)	1634	Solar flares	≤ 0.1
^{28}Si (p, p′, γ)	1779	Solar flares	≤ 0.08
^{12}C (p, p′, γ)	4439	Solar flares	≤ 0.1
	4439	Orion Comp.	$\leq 5 \cdot 10^{-5}$
^{16}O (p, p′, γ)	6129	Solar flares	≤ 0.1
	6129	Orion Comp.	$\leq 5 \cdot 10^{-5}$
Radioactive decay			
^{56}Co(EC,γ)^{56}Fe	847, 1238 2598	SN 1987A	$\approx 10^{-3}$ **
	847, 1238	SN 1991T	$5 \cdot 10^{-5}$ **
^{57}Co(EC,γ)^{57}Fe	122, 136	SN 1987A	$\approx 10^{-4}$
^{44}Ti(EC)^{44}Sc($\beta^+\gamma$)	1157	Cas A SNR	$7 \cdot 10^{-5}$
^{26}Al($\beta^+\gamma$)^{26}Mg	1809	gal. plane	$4 \cdot 10^{-4}$
	1809	Vela SNR	1-6 $\cdot 10^{-5}$
e^-e^+ Annihilation			
	511	Gal. bulge	$1.7 \cdot 10^{-3}$
	511	Gal. disk	$4.5 \cdot 10^{-4}$
	480 ± 120*	1E 1740-29***	$1.3 \cdot 10^{-2}$
	511	Solar Flares	≤ 0.1
	479 ± 18*	Nova Muscae	$6.3 \cdot 10^{-3}$
	400–500*	Bursts ?c)	≤ 70
	440 ± 10*	Crab PSR ?***	$3 \cdot 10^{-4}$
Neutron Capture			
^{1}H(n,γ)^{2}H	2223	Solar flares	≤ 1
^{56}Fe(n,γ)^{57}Fe	5947*	6/10/1974 tr.	1.5 10^{-2}
Cyclotron Lines			
	20-58	Hercules X-1	$\leq 3 \cdot 10^{-3}$

* Redshifted line ** Maximum emission *** Detection uncertain

An incomplete list of astrophysically important gamma-ray spectral features

Identification	Energy (MeV)	Identification	Energy (MeV)
Cf-249	0.34	N-14	2.313
Cf-249	0.39	Ne-20	2.613
Annihil. rad.	0.511	O-16	2.741
Ni-56	0.812	Mg-24	2.754
Fe-56	0.847	Ne-20	3.34
Co-56	0.847	C-12	4.438
Fe-56	1.238	N-14	5.105
Mg-24	1.369	O-16	6.129
Ne-20	1.634	Si-28	6.878
Si-28	1.779	O-16	6.917
Al-26	1.81	O-16	7.117
Neutron capture	2.23		

Absorption and scattering processes

Photoelectric absorption *(see also Ch. 14)*

The cross-section for photoelectric absorption of a photon of energy $h\nu$ by the ejection of a K-shell electron from an atom of atomic number Z is, in the relativistic case

$$\sigma_K = \frac{3\sigma_T Z^5 \alpha^4}{2}\left(\frac{mc^2}{h\nu}\right)^5 \left(\gamma^2-1\right)^{3/2}$$
$$\times\left\{\frac{4}{3}+\frac{\gamma(\gamma-2)}{\gamma+1}\left[1-\frac{1}{2\gamma\sqrt{\gamma^2-1}}\ln\left(\frac{\gamma+\sqrt{\gamma^2-1}}{\gamma-\sqrt{\gamma^2-1}}\right)\right]\right\}$$
$$\approx \frac{3\sigma_T Z^5 \alpha^4}{2}\left(\frac{mc^2}{h\nu}\right) \quad \text{for } h\nu \gg mc^2,$$

where

$$\gamma = \left[1-\left(\frac{v}{c}\right)^2\right]^{-1/2} = \frac{h\nu+mc^2}{mc^2},$$

$\alpha = 2\pi e^2/hc = 1/137.036$, the fine structure constant

$mc^2 = 510.9991$ keV, the rest mass of the electron

$\sigma_T = (8\pi/3)(e^2/mc^2)^2 = 6.65 \times 10^{-25}$ cm^2, the Thomson cross-section

Pair production *(see also Ch. 14)*

The cross-section for electron-positron pair production (pp) by a photon in the presence of a nucleus of charge Z is

$$\sigma(h\nu)_{\rm pp} = \frac{3\alpha Z^2 \sigma_T}{2\pi}\left[\frac{7}{9}\ln\left(\frac{2h\nu}{mc^2}\right)-\frac{109}{54}\right]$$

for no screening when $1 \ll h\nu/mc^2 \ll 1/\alpha Z^{1/3}$, and

$$\sigma(h\nu)_{\rm pp} = \frac{3\alpha Z^2 \sigma_T}{2\pi}\left[\frac{7}{9}\ln\left(\frac{183}{Z^{1/3}}\right)-\frac{1}{54}\right]$$

for complete screening when $h\nu/mc^2 \gg 1/\alpha Z^{1/3}$.

Compton scattering

See Ch. 12 and Ch. 14

Cyclotron absorption

In a magnetic field, the cross-section for absorption of photons by scattering from the ground state to higher Landau levels is

$$\sigma^n_{\rm abs}(\theta) = \frac{\alpha\pi^2\hbar^2c^2}{E_n}\delta(h\nu - h\nu_n)\frac{e^{-Z}Z^{n-1}}{(n-1)!}\left((1+\cos^2\theta) + \frac{Z}{n}\sin^2\theta\right),$$

where

$$Z = h^2\nu^2\sin^2\theta/2mc^2B^*,$$

$$E_n = (m^2c^4 + h^2\nu^2\cos^2\theta + 2nB^*m^2c^4)^{1/2},$$

$$B^* = B/4.414\times10^{13}\ \mathrm{G}$$

$\delta =$ the delta function

The photons are absorbed at the resonant energies

$$h\nu_n = mc^2[(1+2nB^*\sin^2\theta)^{1/2} - 1]/\sin^2\theta.$$

In the nonrelativistic limit, $nB^* = nB/4.414\times10^{13}\ \mathrm{G} \ll 1$, the absorption cross section is

$$\sigma^n_{\rm abs}(\theta) \approx \frac{\alpha\pi^2\hbar^2c^2}{m}\left(\frac{n^2}{2}B^*\sin^2\theta\right)^{n-1}\frac{1+\cos^2\theta}{(n-1)!},$$

where photons are absorbed at harmonics $h\nu_n = nehB/2\pi mc$.

$$h\nu_n = 11.6nB_{12}\ \mathrm{keV},$$

where B_{12} is the magnetic field strength in units of 10^{12} G.

(From γ-Ray and Neutrino Astronomy, Lingenfelter, R.E. and Rothschild, R.E., in *Allen's Astrophysical Quantities*, Cox, A.N., ed., Springer-Verlag, 2000.)

Very high energy (VHE) gamma-rays

Crab Nebula

The Crab Nebula unpulsed spectrum (E^2 times the differential energy spectrum dN/dE for the energy range 100 keV to 300 TeV. (From De Jager, O.C., Ap.J. **457**, 253, 1996.)

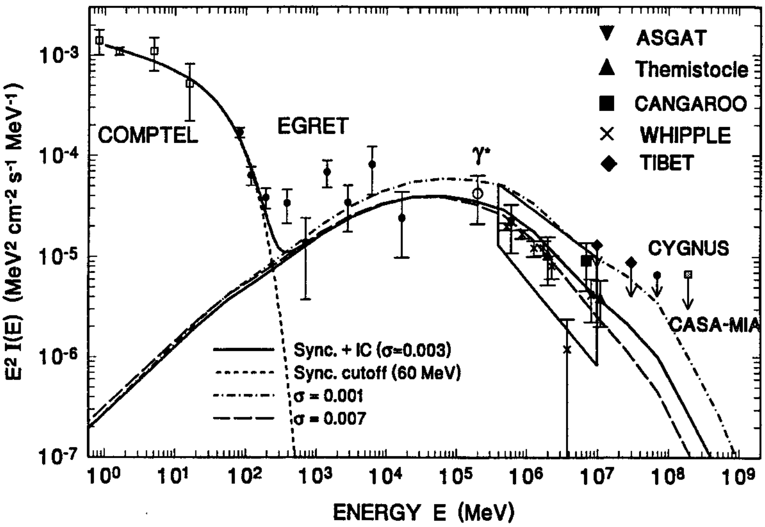

Integral flux from the Crab Nebula

Group	Integral Flux (10^{-11} photons cm^{-2} s^{-1})	E_{th} (TeV)
Whipple (1998)	$(3.2 \pm 0.7)(E/\text{TeV})^{-2.49 \pm 0.06_{stat} \pm 0.05_{syst}}$	0.3
HEGRA (1999)	$(2.7 \pm 0.2 \pm 0.8)(E/\text{TeV})^{-2.61 \pm 0.06_{stat} \pm 0.10_{syst}}$	0.5
CAT (1998)	$(2.7 \pm 0.17 \pm 0.40)(E/\text{TeV})^{-2.57 \pm 0.14_{stat} \pm 0.08_{syst}}$	0.25

Operating atmospheric Cerenkov imaging telescopes (1999)

Group	Countries	Location	Threshold (TeV)
Whipple	USA-UK-Ireland	Arizona, USA	0.25
Crimea	Ukraine	Crimea	1
SHALON	Russia	Tien Shen, Russia	1.0
CANGAROO	Japan-Australia	Woomera, Australia	0.5
HEGRA	Germany-Armenia-Spain	La Palma, Spain	0.5
CAT	France	Pyrenées	0.25
Durham	UK	Narrabri, Australia	0.25
TACTIC	India	Mount Abu, India	0.3
Seven Telescope Array	Japan	Utah, USA	0.5

Observations of shell-type supernova remnants

Object Name	Observation Time (minutes)	Energy (TeV)	Integral Flux (10^{-11} cm^{-2} s^{-1})
Tycho	867.2	> 0.3	< 0.8
IC 443	1076.7	> 0.3	< 2.1
	678.0	> 0.5	< 1.9
W44	360.1	> 0.3	< 3.0
W51	468.0	> 0.3	< 3.6
γ Cygni	560.0	> 0.3	< 2.2
	2820.0	> 0.5	< 1.1
W 63	140.0	> 0.3	< 6.4
SN 1006	2040.0	> 1.7	$0.46 \pm 0.6_{stat} \pm 1.4_{sys}$

Properties of the VHE BL LAC objects

Object	z	EGRET Flux ($E > 100$ MeV) (10^{-7} cm^{-2} s^{-1})	Average Integral Flux ($E > 300$ GeV) (10^{-12} cm^{-2} s^{-1})	M_v	$\mathcal{F}_X$ (2 keV) (μJy)	$\mathcal{F}_R$ (5 GHz) (mJy)
Mrk 421	0.031	1.4 ± 0.2	40	14.4	3.9	720
Mrk 501	0.034	3.2 ± 1.3	≥ 8.1	14.4	3.7	1370
1ES 2344 + 514	0.044	< 0.7	$\lesssim 8.2$	15.5	1.1	220
PKS 2155 − 304	0.116	3.2 ± 0.8	42	13.5	5.7	310
3C 66A	0.444	2.0 ± 0.3	30	15.5	0.6	806

TeV observations of plerions

Source	Energy (GeV)	Flux/Upper Limit (10^{-11} cm^{-2} s^{-1})
Crab Nebula ..	400	7.0
PSR 1706–44 ..	1000	0.8
Vela	2500	0.29
SS 433	550	< 1.8
3C 58	550	< 1.1
PSR 0656 + 14	1000	< 3.4

(Tables are adapted from Catanese, M. and Weekes, T.C., ASP, **111**, 1193, 1999.)

Downward gamma-ray flux

Measurements of the total downward gamma-ray flux at 5 g cm^{-2} over Palestine, Texas. See original work for references. (From Gehrels, N., Instrumental background in balloon-borne gamma-ray spectrometers and techniques for its reduction, *NASA Technical Memorandum 86162*, 1985.)

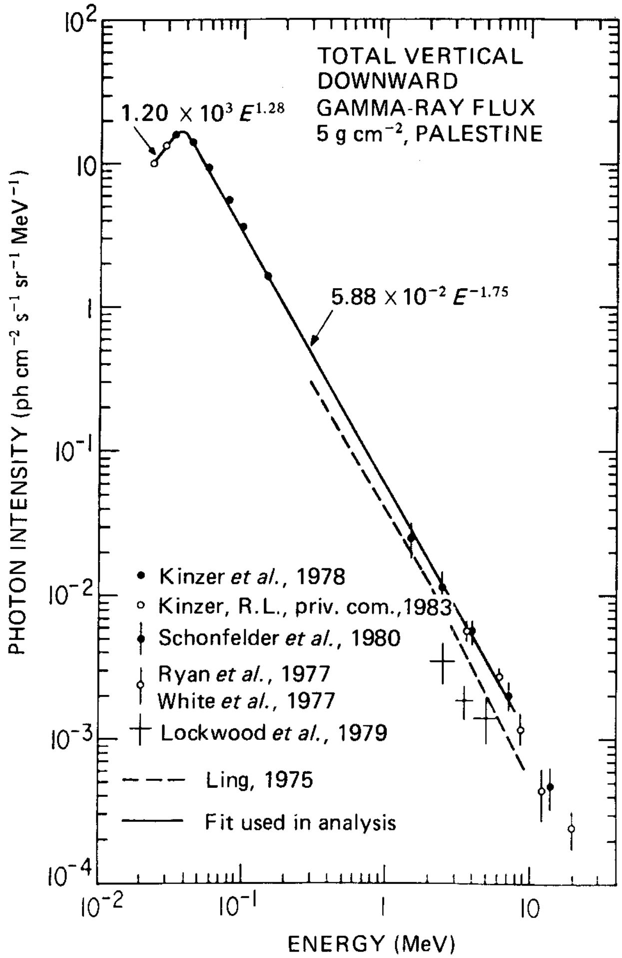

Bibliography

Very High Energy Gamma-ray Astronomy, Catanese, M. and Weekes, T.C., ASP, **111**, 1193–1222, 1999 October.

Gamma-ray Astronomy, Chupp, E.L., D. Reidel Publishing Co., 1976.

Gamma-ray and Neutrino Astronomy, Lingenfelter, R.E. and Rothschild, R.E., in Allen's Astrophysical Quantities, Cox, Arthur N., ed., Springer-Verlag, 1999.

Astrophysical Formulae, Volume 1, Lang, K.R., Springer-Verlag, 1999.

High Energy Astrophysics, Longair, M.S., Cambridge University Press, 1997.

Gamma-ray Astronomy, Murthy, Poola V. Ramana and Wolfendale, Arnold, W., Cambridge University Press, 1986.

Cosmic Gamma Rays, Stecker, F.W., NASA SP-249, 1971.

TEV Gamma-ray Astrophysics, Voelk, H.J. and Aharonian, F.A., eds. Kluwer Academic Publishers, 1996.

Note: Links to WWW resources which supplement the material in this chapter can be found at:

http://www.astrohandbook.com

Chapter 8

Cosmic rays

If I could remember the names of all these particles, I'd be a botanist. - Enrico Fermi

Cosmic ray source abundances compared with the local Galactic abundances, both normalized to [Si] = 100.

Element	Cosmic ray source abundance (1990 update)	Local Galactic abundance
H	$8.9 \pm 2.2 \times 10^4$	$2.7 \pm 0.3 \times 10^6$
He	2.4×10^4	$2.6 \pm 0.7 \times 10^5$
C	431 ± 34	1260 ± 330
N	19 ± 9	225 ± 90
O	511 ± 20	2250 ± 560
F	< 2.5	0.09 ± 0.06
Ne	64 ± 8	325 ± 160
Na	6 ± 4	5.5 ± 1.0
Mg	106 ± 6	105 ± 3
Al	10 ± 4	8.4 ± 0.4
Si	100	100
P	< 2.5	0.9 ± 0.2
S	12.6 ± 2.0	43 ± 15
Cl	< 1.6	0.5 ± 0.3
Ar	1.8 ± 0.6	11 ± 5
K	< 1.9	0.3 ± 0.1
Ca	5.1 ± 0.9	6.2 ± 0.9
Sc	< 0.8	$3.5 \pm 0.5 \times 10^{-3}$
Ti	< 2.4	0.27 ± 0.04
V	< 1.1	0.026 ± 0.005
Cr	2.2 ± 0.6	1.3 ± 0.1
Mn	1.7 ± 1.7	0.8 ± 0.2
Fe	93 ± 6	88 ± 6
Co	0.32 ± 0.12	0.21 ± 0.03
Ni	5.1 ± 0.5	4.8 ± 0.6
Cu	0.06 ± 0.01	0.06 ± 0.03
Zn	0.07 ± 0.01	0.10 ± 0.02
Ga	$5.6 \pm 2.8 \times 10^{-3}$	$\sim 3.7 \times 10^{-3}$
Ge	$7.4 \pm 1.0 \times 10^{-3}$	$\sim 11.4 \times 10^{-3}$

(From Longair, M.S., High Energy Astrophysics, 2nd edition, Cambridge University Press, 1997)

Abundances in the galactic cosmic rays

Comparison of the abundances of the elements in the galactic cosmic rays with the solar abundances (normalized to C). (Courtesy of C. Meyer, University of Chicago.)

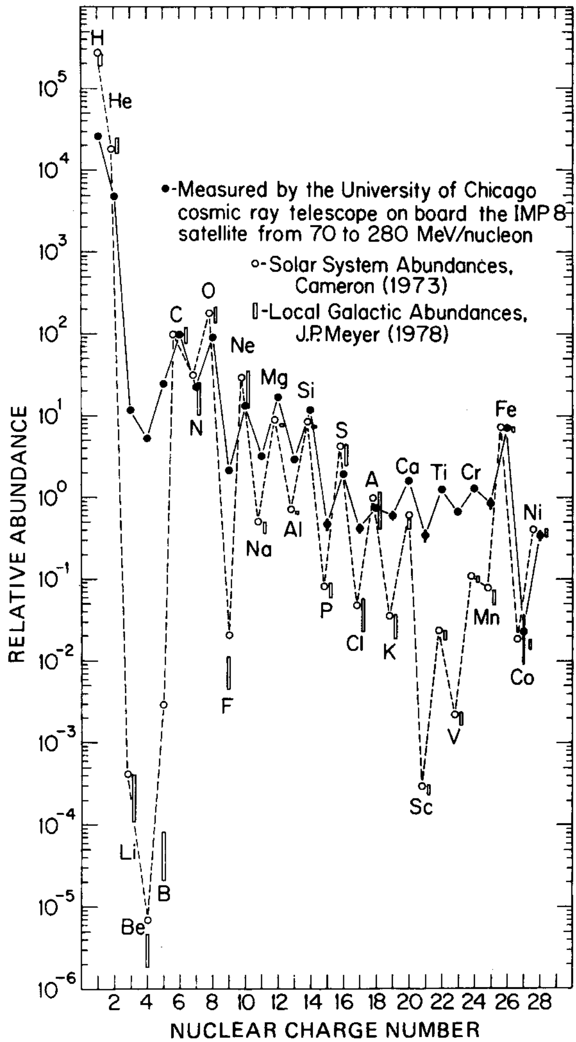

Relative abundances of nuclei normalized to oxygen

Element	Solar flare cosmic rays	Sun	Galactic cosmic rays
^{1}H	700	1000	350
^{2}He	107 ± 14	~ 100	50
^{3}Li	...	$<< 0.001$	0.3
^{4}Be ^{5}B	< 0.02	$<< 0.001$	0.8
^{6}C	0.59 ± 0.07	0.6	1.8
^{7}N	0.19 ± 0.04	0.1	≤ 0.8
^{8}O	1.0	1.0	1.0
^{9}F	< 0.03	$<< 0.001$	≤ 0.1
^{10}Ne	0.13 ± 0.02	?	0.30
^{11}Na	...	0.002	0.19
^{12}Mg	0.043 ± 0.011	0.027	0.32
^{13}Al	...	0.002	0.06
^{14}Si	0.033 ± 0.011	0.035	0.12
^{15}P–^{21}Sc	0.057 ± 0.017	0.032	0.13
^{22}Ti–^{28}Ni	≤ 0.02	0.006	0.28

(Adapted from Johnson, F. S., ed., *Satellite Environment Handbook*, Stanford University Press, 1965.)

Cosmic ray spectra

Cosmic-ray energy spectra of the more abundant nuclear species as measured near Earth. Below a few GeV/nucleon, these spectra are strongly influenced by modulation within the solar system. The different curves for the same species at those energies represent measurements at various levels of general solar activity, the lowest intensity being observed at the highest activity level. (From Meyer, P., Ramaty, R., & Webber, W.R., *Cosmic rays-Astronomy with Energetic Particles*, in Physics Today, October 1974.)

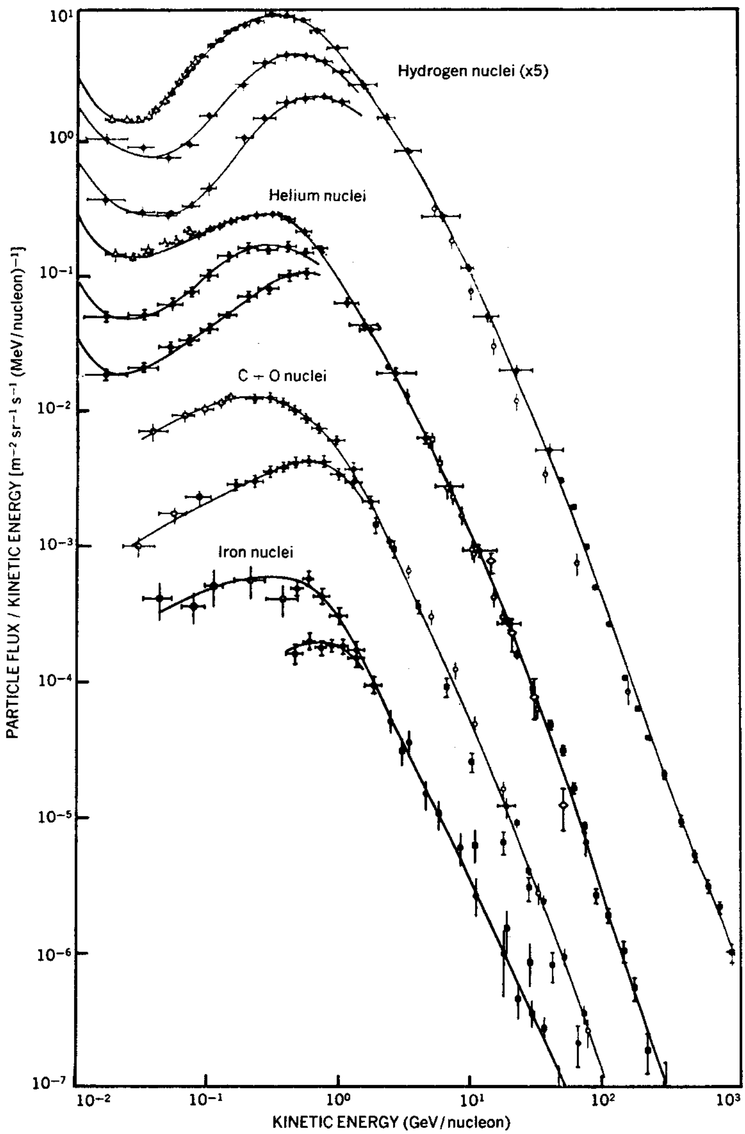

The energy spectra of cosmic-ray protons (solid line) and electrons (data points) as measured near the Earth. Below a few GeV, interstellar spectra are strongly influenced by the Sun. (From Meyer, P., Ramaty, R., & Webber, W.R., *Cosmic rays-Astronomy with Energetic Particles*, in Physics Today, October 1974.)

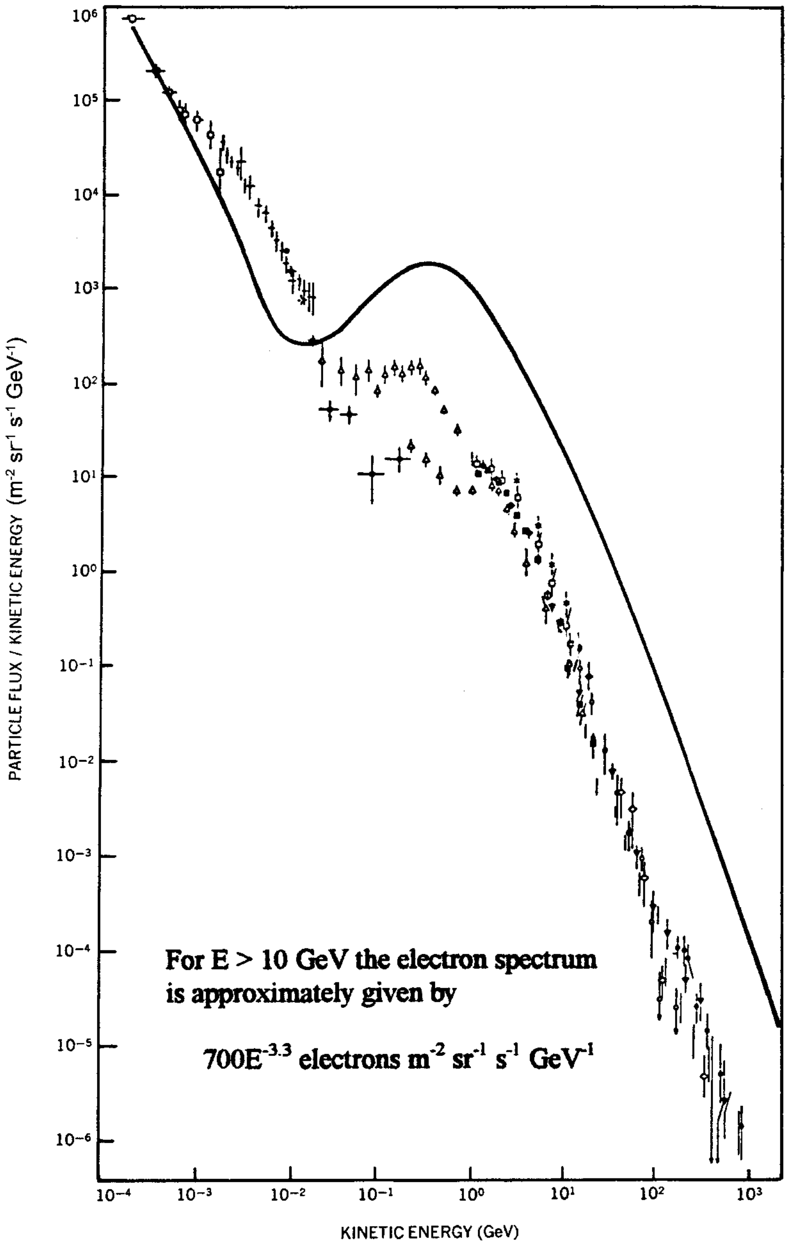

Observed energy spectrum of high-energy cosmic rays. The straight line shows an E_0^{-3} falloff for comparison. (From Physics Today, January 1998)

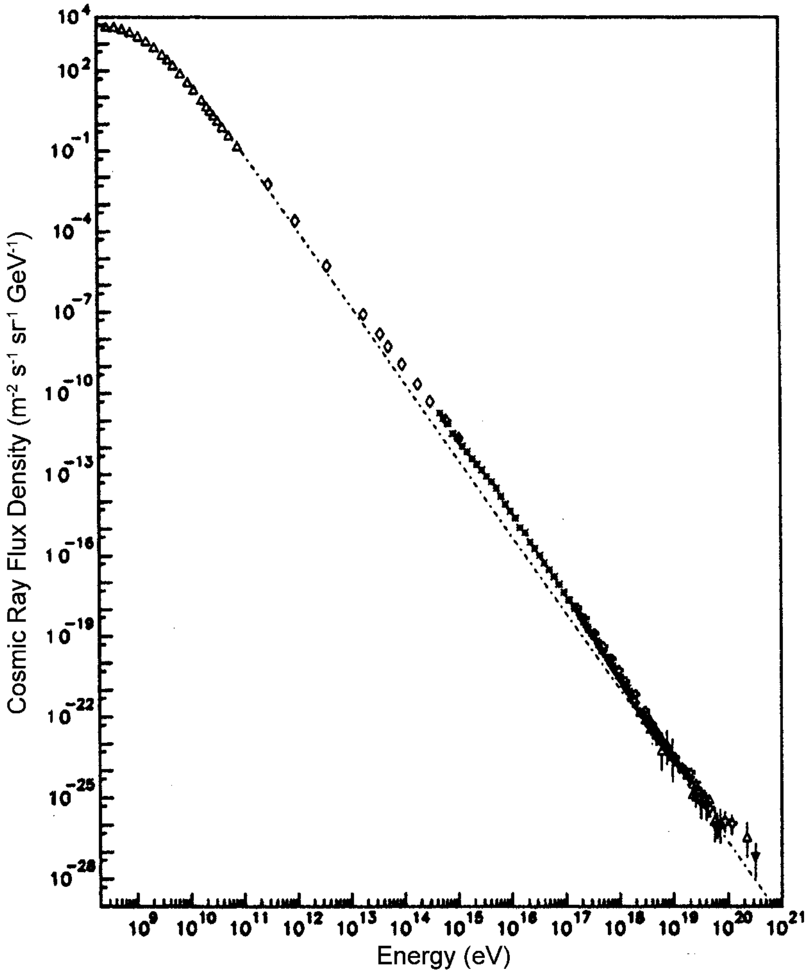

Vertical fluxes

The vertical fluxes of different components of cosmic rays in the atmosphere. (From Hillas, A.M., *Cosmic Rays*, Pergamon Press, 1972.)

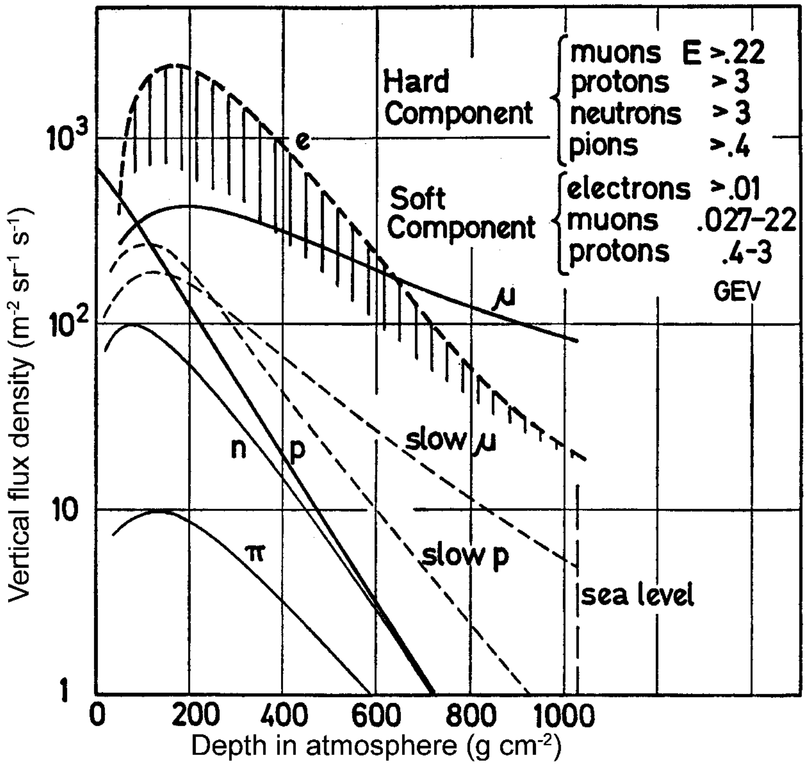

Cutoff rigidity

The Earth's magnetic field affects the penetration of charged particles in the vicinity of the Earth. The minimum rigidity (cutoff rigidity) necessary to reach some geomagnetic latitude λ and geocentric radius R is given by:

$$\frac{pc}{ze} = \frac{M}{R^2} \frac{\cos^4 \lambda}{[(1 + \cos\theta \cos^3 \lambda)^{1/2} + 1]^2},$$

where

M is the Earth's dipole moment,

$\left(\frac{pc}{ze}\right)$ is the magnetic rigidity of the particle; for charge $z = 1$ it is numerically equal, when expressed in volts, to the momentum in units of ev/c,

$\left(\frac{M}{R_0^2}\right) \approx 60 \times 10^9$ volts, where R_0 is the radius of the Earth,

θ is the angle between the direction of arrival of the particle and the tangent to the circle of latitude. ($\theta = 0$ corresponds to arrival from the *west* for *positive* particles; $\theta = 0$ corresponds to arrival from the *east* for *negative* particles.)

Conversion from magnetic rigidity to kinetic energy per nucleon for electrons, protons and alpha particles. (From Smart, D.F. & Shea, M.A., in *Handbook of Geophysics and the Space Environment*, Jursa, A.S., ed., Air Force Geophysics Laboratory, 1985.)

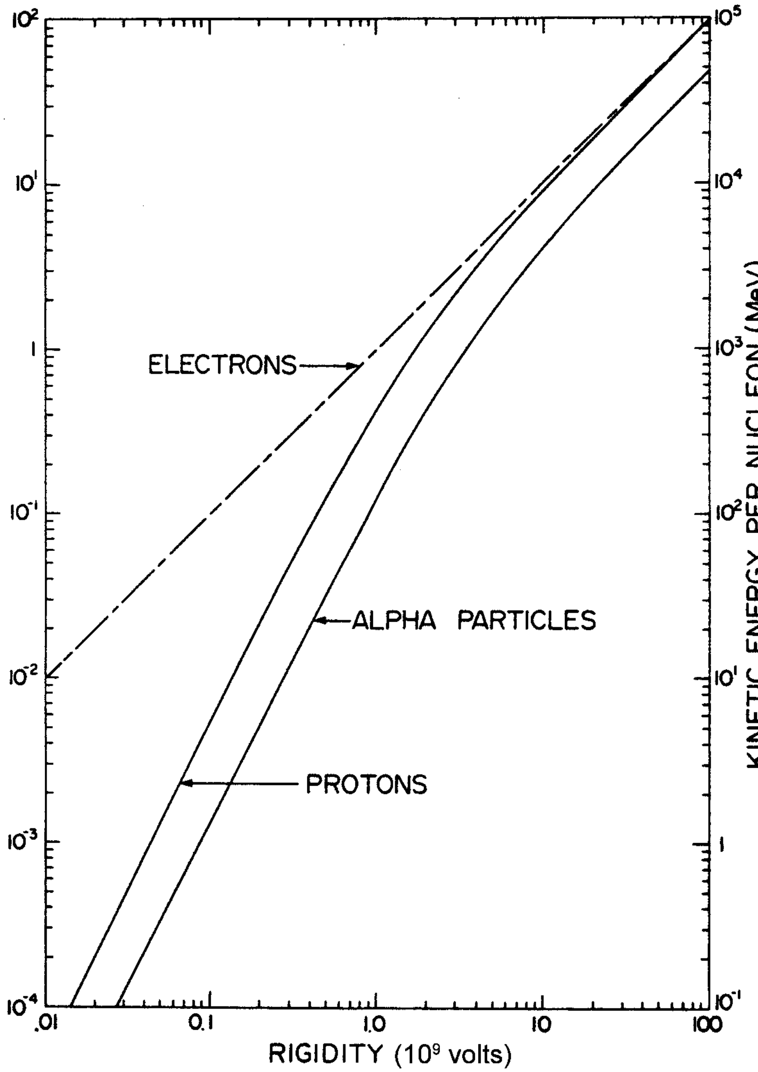

Particle production in the atmosphere

Schematic representation of the development of particle production in the atmosphere. (Adapted from Simpson *et al.*, *Phys. Rev.*, **90**, 934, 1953.)

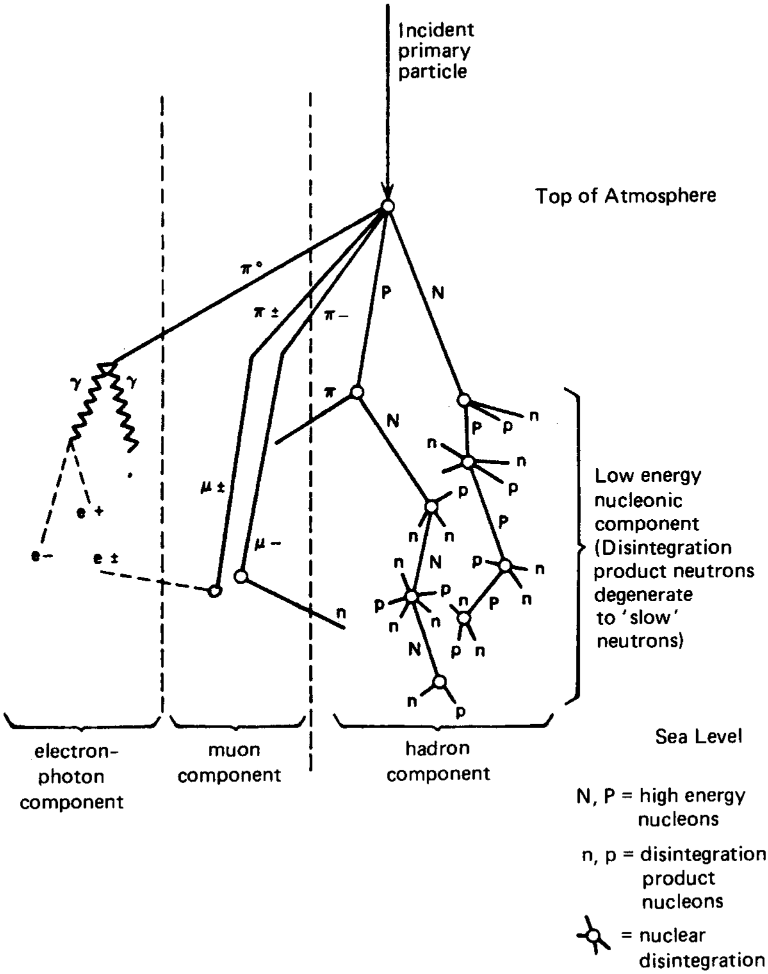

Gamma-ray production in the atmosphere

Schematic diagram of gamma-ray production processes in the atmosphere. Neutrinos are ignored. (From Allkofer, O. C. & Grieder, P. K. F., *Cosmic Rays on Earth*, Physik Daten, ISSN 0344–8401, 1984.)

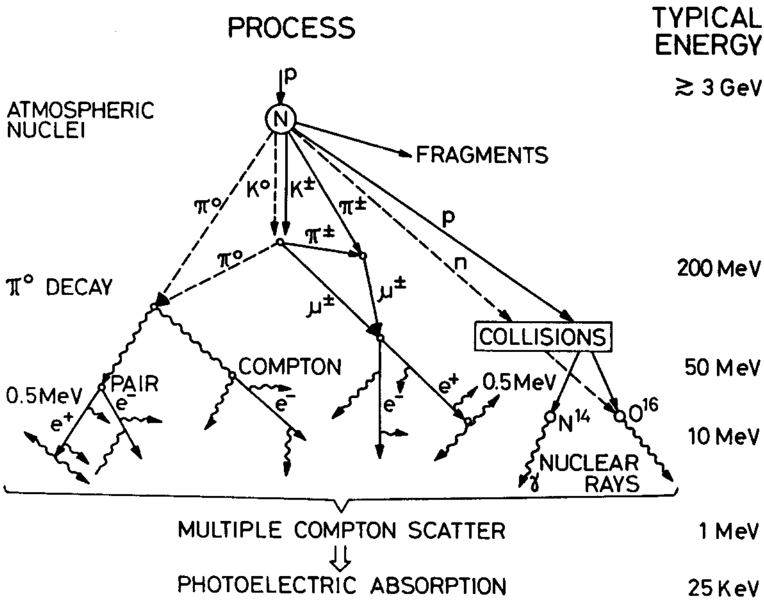

Atmospheric depth

Relation between atmospheric depth and altitude for an isothermal atmosphere. (From Allkofer, O. C. & Grieder, P. K. F., *Cosmic Rays on Earth*, Physik Daten, ISSN 0344–8401, 1984.)

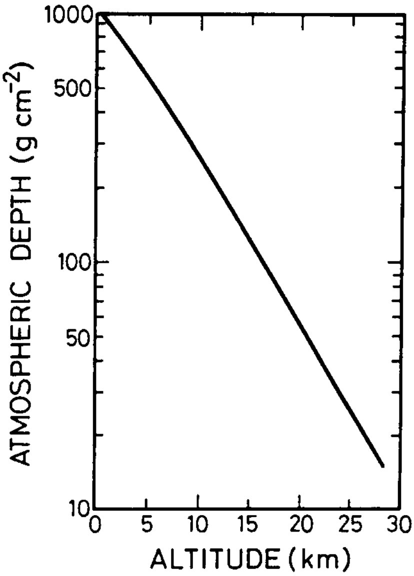

Relation between zenith angle and atmospheric depth at sea level in an isothermal atmosphere. (From Allkofer, O. C. & Grieder, P. K. F. *Cosmic Rays on Earth*, Physik Daten, ISSN 0344–8401, 1984.)

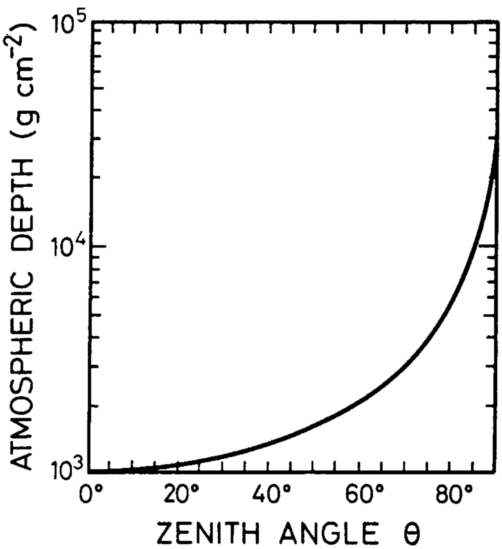

Pressure and atmospheric thickness

Relations between altitude and pressure, and altitude and depth in the real atmosphere. (After Cole, A. E. & Kantor, A. J., Air Force Reference Atmosphere, AFGL-TR-78-0051, 1978.)

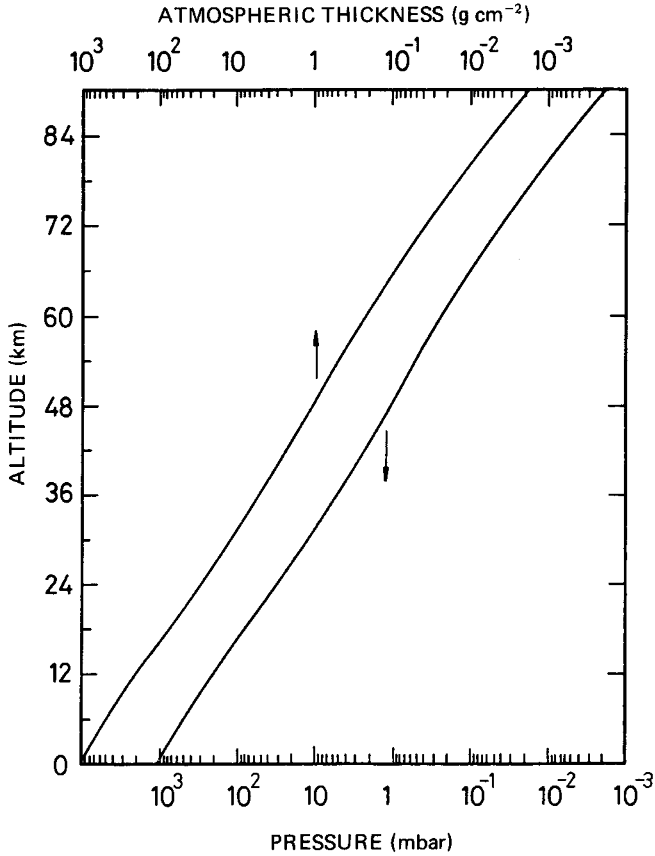

Bibliography

'Cosmic rays on Earth', Allkofer, O. C. & Grieder, P. K. F. in *Physics Data*, ISSN 0344–8401, 1984, nr. 25-1, Fachinformationszentrum, Karlsruhe.

Note: Links to WWW resources which supplement the material in this chapter can be found at:

http://www.astrohandbook.com

Chapter 9

Earth's atmosphere and environment

Space isn't remote at all. It's only an hour's drive away, if your car could go straight upwards. - Sir Fred Hoyle

Atmospheric radiance in the ultraviolet

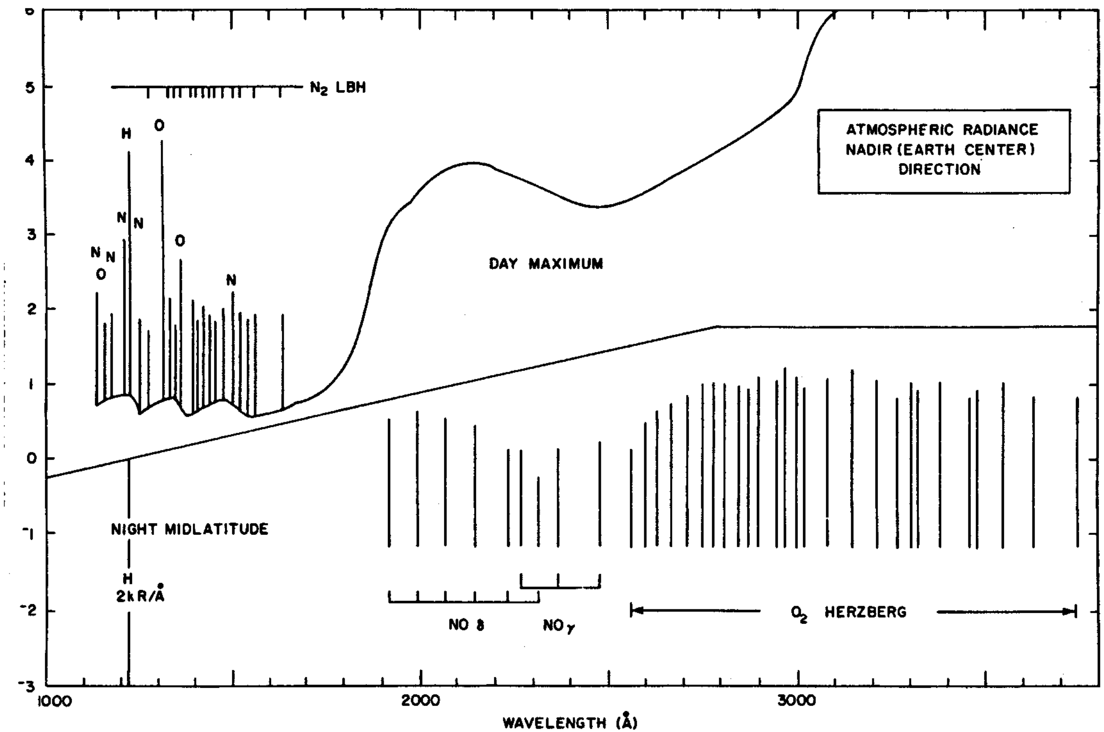

(Huffman, R.E. in *Handbook of Geophysics and the Space Environment*, A.S. Jura, ed., Air Force Geophysics Laboratory, 1985.)

Earth's magnetic field

The largest contribution to the Earth's field at low altitudes comes from its main field. The main field is produced in the Earth's fluid core. The main field is distorted at the surface by crustal anomalies and at higher altitudes, by magnetic fields from current sources external to the Earth (ionospheric currents, plasmas in the magnetosphere, solar wind). Models of the geomagnetic field are required for trapped particle, solar event, and cosmic-ray environment modeling.

At low altitude, the Earth's main field can be described approximately by the field of a magnetic dipole placed at the Earth's center (geocentric dipole) with its axis tilted to intersect the Earth at 78.5°N, 291.0°E, the geomagnetic north pole, and 78.5°S, 111.0°E, the geomagnetic south pole. In spherical coordinates, r, θ, and ϕ, with r measured from the center of the Earth and θ measured from the dipole axis (geomagnetic colatitude), the dipole field has the vector components:

$$\begin{aligned} B_r &= -\frac{M}{r^3} 2\cos\theta \\ B_\theta &= -\frac{M}{r^3}\sin\theta \\ B_\phi &= 0. \end{aligned}$$

The total intensity is then

$$B = -\frac{M}{r^3}[3\cos\theta + 1]^{1/2}$$

where M is the dipole moment of the Earth (about 8×10^{15} Tm^3). B is measured in teslas (1 T = 10^4 gauss; 1 nT (nanotesla) = 1 gamma).

The centered dipole is a poor approximation to the field, producing errors as large as 25% at the equator. If the dipole is considered to be eccentric, 10% discrepancies remain.

The geomagnetic field (including the external field) is more accurately modeled by a spherical harmonic expansion of the magnetic scalar potential:

$$V = a \sum_{n=1}^{\infty} \sum_{m=0}^{n} P_n^m(\cos\theta) \times \left[\left(\frac{a}{r}\right)^{n+1} (g_n^m \cos m\phi + h_n^m \sin m\phi) + \left(\frac{a}{r}\right)^{-n} (A_n^m \cos m\phi + B_n^m \sin m\phi) \right],$$

where r, θ, and ϕ are the geographical polar coordinates of radial distance, colatitude, and east longitude, and a is the radius of the earth.

Earth's magnetic field *(cont.)*

The functions $P_n^m(\cos\theta)$ are the Schmidt functions:

$$P_n^m(\cos\theta) = \left[\frac{\epsilon_m (n-m)!}{(n+m)!}\right]^{1/2} \times \left[\frac{(1-\cos^2\theta)^{m/2}}{2^n n!} \frac{d^{n+m}}{d(\cos\theta)^{n+m}}(\cos^2\theta - 1)^n\right]$$

$$\epsilon_m = 2 \quad \text{if } m > 0$$

$$\epsilon_m = 1 \quad \text{if } m = 0.$$

The second quantity in brackets is the associated Legendre function $P_{n,m}(\cos\theta)$.

In the potential, those terms containing g_n^m and h_n^m arise from sources internal to the earth, while those containing A_n^m and B_n^m arise from external currents; the potential function is valid in the space above the surface and below the external current system. The field is given by

$$\mathbf{B} = -\nabla V.$$

The northward, eastward, and downward components of the field are thus

$$X = \frac{1}{r}\frac{\partial V}{\partial \theta}$$

$$Y = -\frac{1}{r\sin\theta}\frac{\partial V}{\partial \phi}$$

$$Z = \frac{\partial V}{\partial r}.$$

The spherical-harmonic expansion model specifies the magnetic field to an accuracy of about 10 nT for low earth orbiting satellites (eg. 500 km).

(Adapted from Knecht, D.J. & B.M. Shuman, in *Handbook of Geophysics and the Space Environment*, A.S. Jursa, ed., Air Force Geophysics Laboratory, 1985)

Earth's magnetosphere

Schematic views of the Earth's magnetosphere.

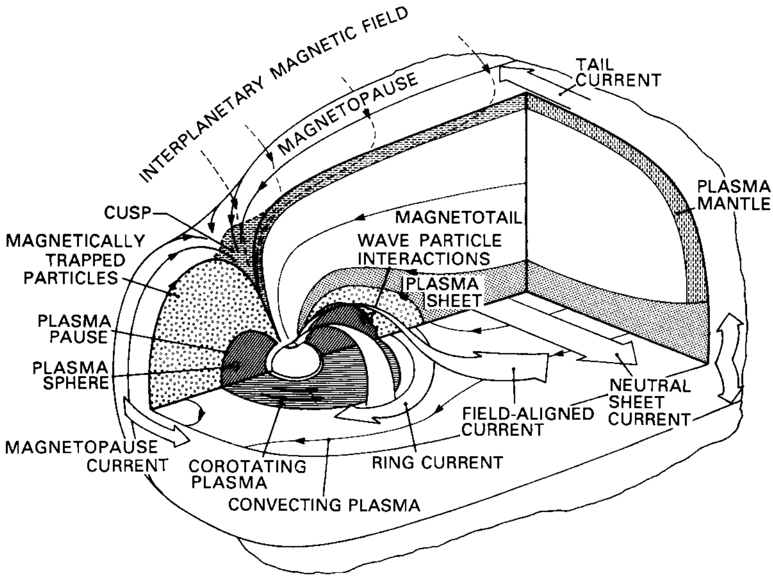

(From NASA)

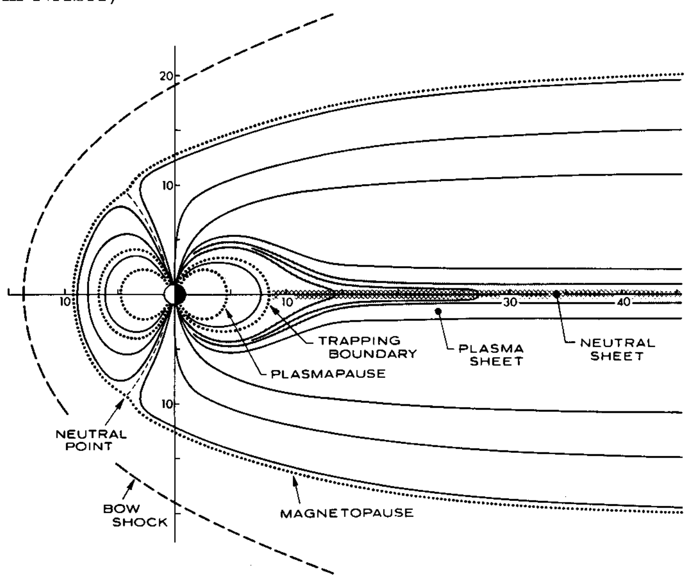

(From Knecht, D.J. & B.M. Shuman, in *Handbook of Geophysics and the Space Environment*, A.S. Jura, ed., Air Force Geophysics Laboratory, 1985.)

Solar wind

Observed properties of the solar wind near the orbit of the Earth.

Proton density	6.6 cm^{-3}
Electron density	7.1 cm^{-3}
He^{2+} density	0.25 cm^{-3}
Flow speed (nearly radial)	450 $km\,s^{-1}$
Proton temperature	1.2×10^5K
Electron temperature	1.4×10^5K
Magnetic field (induction)	7×10^{-9} tesla (T)

Solar wind flux densities and fluxes near the orbit of the Earth.

	Flux Density	**Flux Through Sphere at 1 AU**
Protons	3.0×10^8 $cm^{-2}\,s^{-1}$	8.4×10^{35} s^{-1}
Mass	5.8×10^{-16} $g\,cm^{-2}\,s^{-1}$	1.6×10^{12} $g\,s^{-1}$
Radial momentum	2.6×10^{-9} pascal (Pa)	7.3×10^{14} newton (N)
Kinetic energy	0.6 $erg\,cm^{-2}\,s^{-1}$	1.7×10^{27} $erg\,s^{-1}$
Thermal energy	0.02 $erg\,cm^{-2}\,s^{-1}$	0.05×10^{27} $erg\,s^{-1}$
Magnetic energy	0.01 $erg\,cm^{-2}\,s^{-1}$	0.025×10^{27} $erg\,s^{-1}$
Radial magnetic flux	5×10^{-9} T	1.4×10^{15} weber (Wb)

(Hundhausen A.J., in *Introduction to Space Physics*, Kivelson, M.G. & C.T. Russell, eds., Cambridge University Press, 1995, with permission.)

Solar irradiance (1 AU)

Visible and infrared radiation

Radiant energy distribution:

approximated by that from a 5800 K blackbody

Fraction of solar radiation:

Above 7000Å = 53.12%

Above 4000Å ~ 91.28%

3000Å–30 000Å = 96.62%

Ultraviolet and X-ray radiation

Fraction of solar radiation:

Below 4000Å = 8.72%

Below 3000Å = 1.21%

Below 2000Å = 0.008% (variable)

Below 1000Å = 10^{-4}% (variable)

Principal line emission fluxes at 1.0 AU:

Lyman Alpha H I (1215.67Å): 51.0×10^{-4} W m^{-2}

He II (303.8Å): 2.5×10^{-4} W m^{-2}

H I (1025.72Å): 0.60×10^{-4} W m^{-2}

C III (977Å): 0.50×10^{-4} W m^{-2}

X-ray flux (W m^{-2}):

	1–8Å	8–20Å	20–200Å
Sunspot min	1×10^{-8}	1×10^{-7}	$\sim 1 \times 10^{-4}$
Sunspot max	3×10^{-6}	2×10^{-5}	$\sim 1 \times 10^{-3}$
Flare activity (large flares)	1×10^{-4}	5×10^{-4}	$\sim 1 \times 10^{-2}$

Solar irradiance *(cont.)*

Solar variation

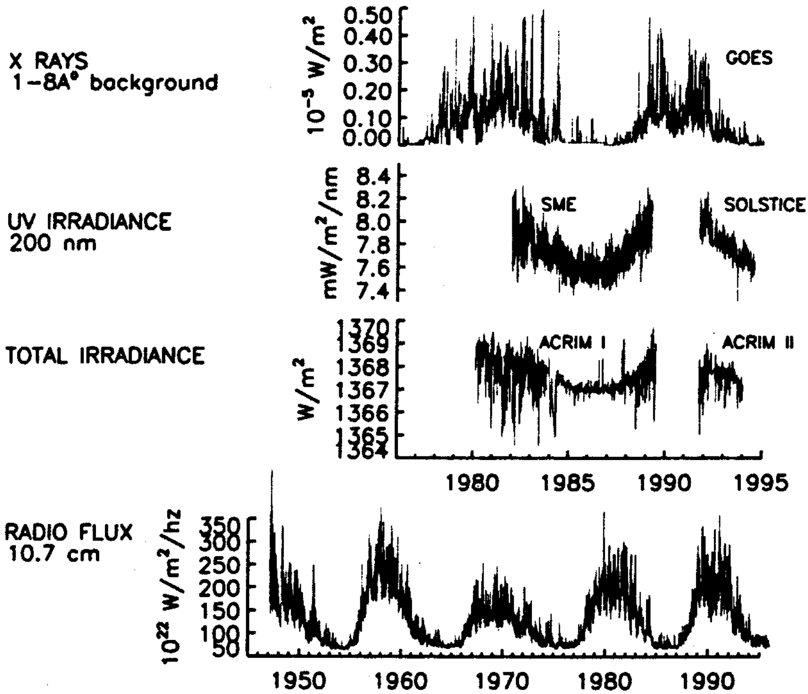

(From Lean, J., *Annual Review of Astronomy and Astrophysics*, v. 35, 33, 1997, Annual Reviews, Inc.)

Solar Flare Classification

The ranking of a solar flare is based on its x-ray output. Flares are classified according to the order of magnitude of the peak burst intensity I measured at the Earth in the 1 to 8Å wavelength band as follows:

Class	Peak, 1 to 8Å band ($W\,m^{-2}$)
B	$I < 10^{-6}$
C	$10^{-6} < I < 10^{-5}$
M	$10^{-5} < I < 10^{-4}$
X	$I > 10^{-4}$

A multiplier is used to indicate the level within each class.
For example:

M6: $I = 6 \times 10^{-5}\ W\,m^{-2}$.

The solar spectrum

The solar spectral irradiance from radio waves to gamma-rays. (Courtesy H. Malitson and the National Space Science Data Center.)

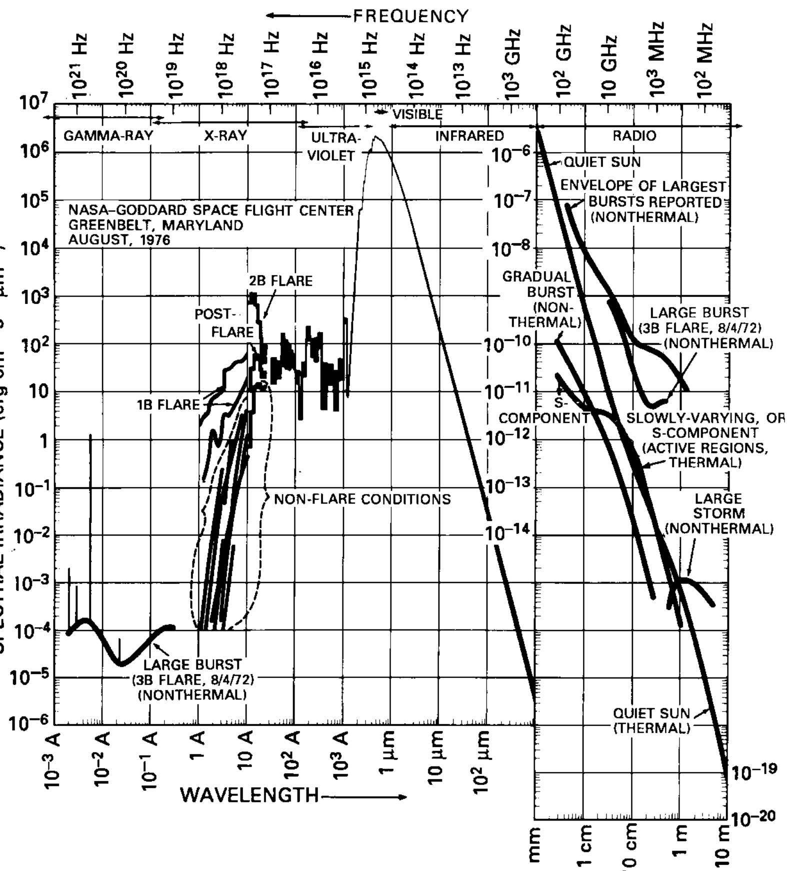

Radiation environment

Galactic cosmic radiation

Flux at sunspot minimum:	~ 4 protons $\mathrm{cm^{-2}\,s^{-1}}$ (isotropic)
Integrated yearly rate:	$\sim 1.3 \times 10^8$ protons $\mathrm{cm^{-2}}$
Flux at sunspot maximum:	2.0 protons $\mathrm{cm^{-2}\,s^{-1}}$ (isotropic)
Integrated yearly rate:	$\sim 7 \times 10^7$ protons $\mathrm{cm^{-2}}$
Energy range:	40 MeV–10^{13} MeV; predominantly 10^3–10^7 MeV
Integrated dose (without shielding):	$\sim$ 4–10 rad $\mathrm{yr^{-1}}$

Solar high energy particle radiation

Composition: predominantly protons (H^+) and alpha particles (He^{++}).
Integrated yearly flux at 1 AU:

Energy > 30 MeV,	$N \approx 8 \times 10^9$ protons $\mathrm{cm^{-2}}$ near solar maximum
	$N \approx 5 \times 10^5$ protons $\mathrm{cm^{-2}}$ near solar minimum
Energy > 100 MeV,	$N \approx 6 \times 10^8$ protons $\mathrm{cm^{-2}}$ near solar maximum
	$N \approx 5 \times 10^4$ protons $\mathrm{cm^{-2}}$ near solar minimum

Maximum dosage with shielding of 5 $\mathrm{g\,cm^{-2}}$ (equivalent thickness): $\sim$ 200 rad per week (3 flares), skin dose at a point detector.

Solar radiation storms

The NOAA space weather scale for solar radiation storms:

Scale	Descriptor	Flux level*	Number of Events**
S4	Extreme	10^5	< 1 per cycle
S4	Severe	10^4	3 per cycle
S3	Strong	10^3	10 per cycle
S2	Moderate	10^2	25 per cycle
S1	Minor	10	50 per cycle

* Flux levels are 5 minute averages. Flux in > 10 MeV particles (ions) $\mathrm{s^{-1}\,sr^{-1}\,cm^{-2}}$.

** These events can last more than one day.

B, L coordinates

Trapped radiation environment models give energetic particle fluxes as functions of energy and of the geomagnetic coordinates B and L. Surfaces of constant B (magnetic field intensity) are concentric, roughly ellipsoidal shells encircling the Earth, while surfaces of constant L approximate the concentric shells generated by dipole field lines rotating with the Earth.

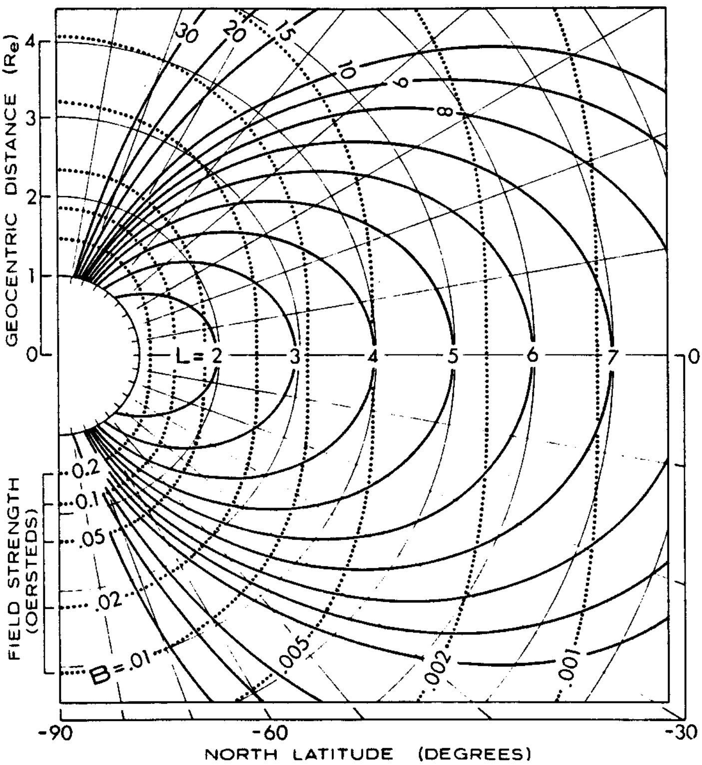

B and L can be approximately mapped into polar coordinates by means of the following transformation:

$$B = \frac{M}{R^3}\left(4 - \frac{3R}{L}\right)^{1/2}; \quad R = L\cos^2\lambda$$

(where M is the magnetic dipole moment of the earth). Thus a radial distance R and a "latitude" λ may be computed.

(Adapted from Knecht, D.J. & B.M. Shuman, in *Handbook of Geophysics and the Space Environment*, A.S. Jursa, ed., Air Force Geophysics Laboratory, 1985)

Trapped radiation

Electron distribution in the Earth's field. (Published by Vette in August 1964.)

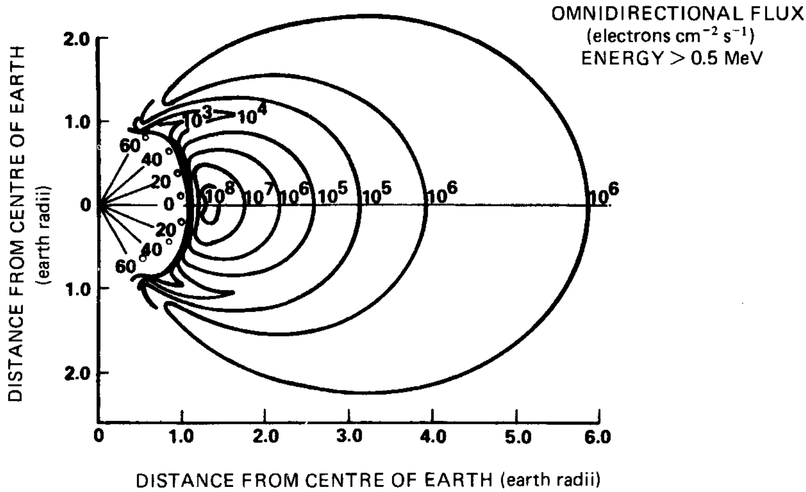

Proton distribution in the Earth's field. (Published by Vette in September 1963).

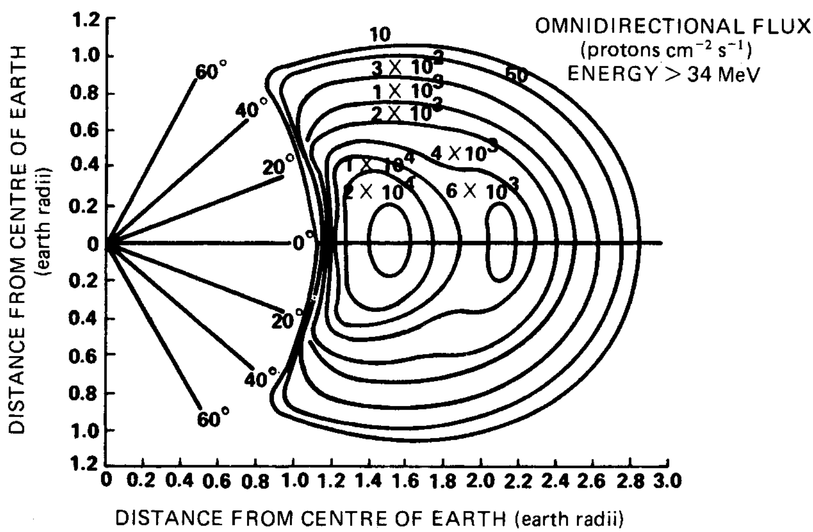

Trapped radiation *(cont.)*

Omni-directional flux in protons $cm^{-2}\,s^{-1}$. (Adapted from Stassinopoulos, E.G., *World Maps of Constant B, L, and Flux Contours* NASA SP-3054, 1970.)

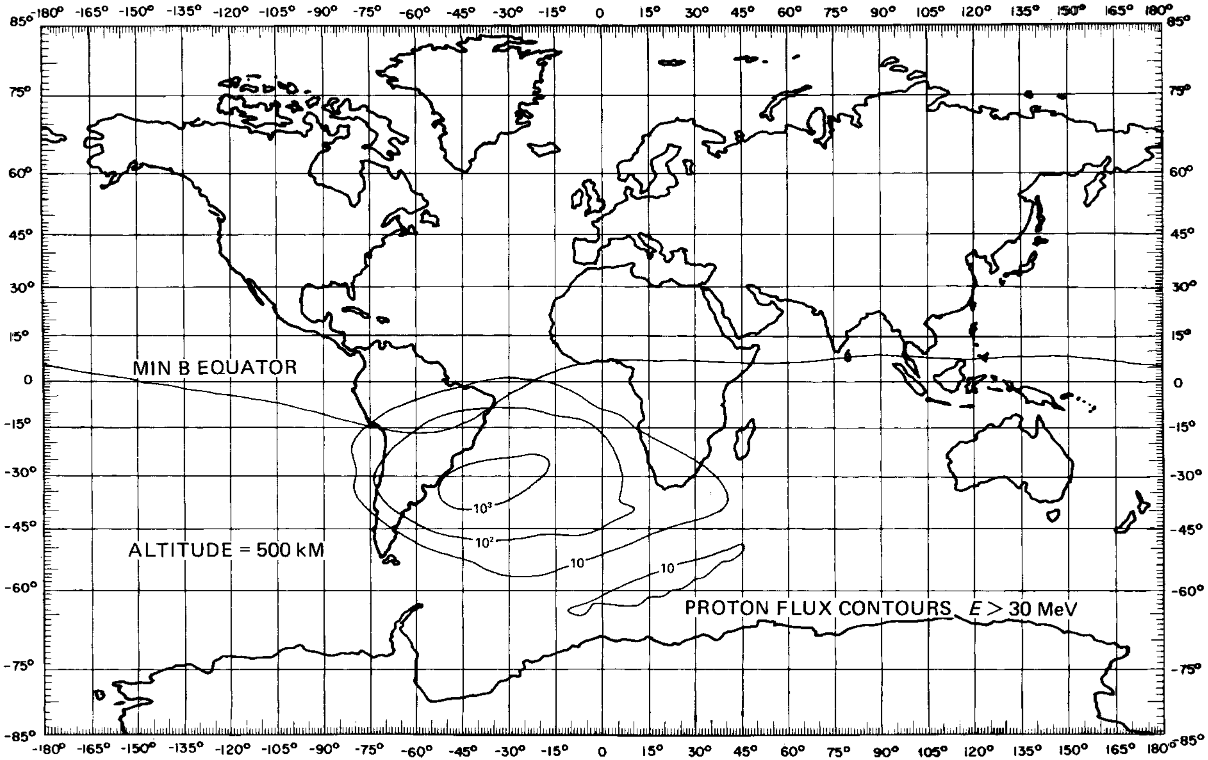

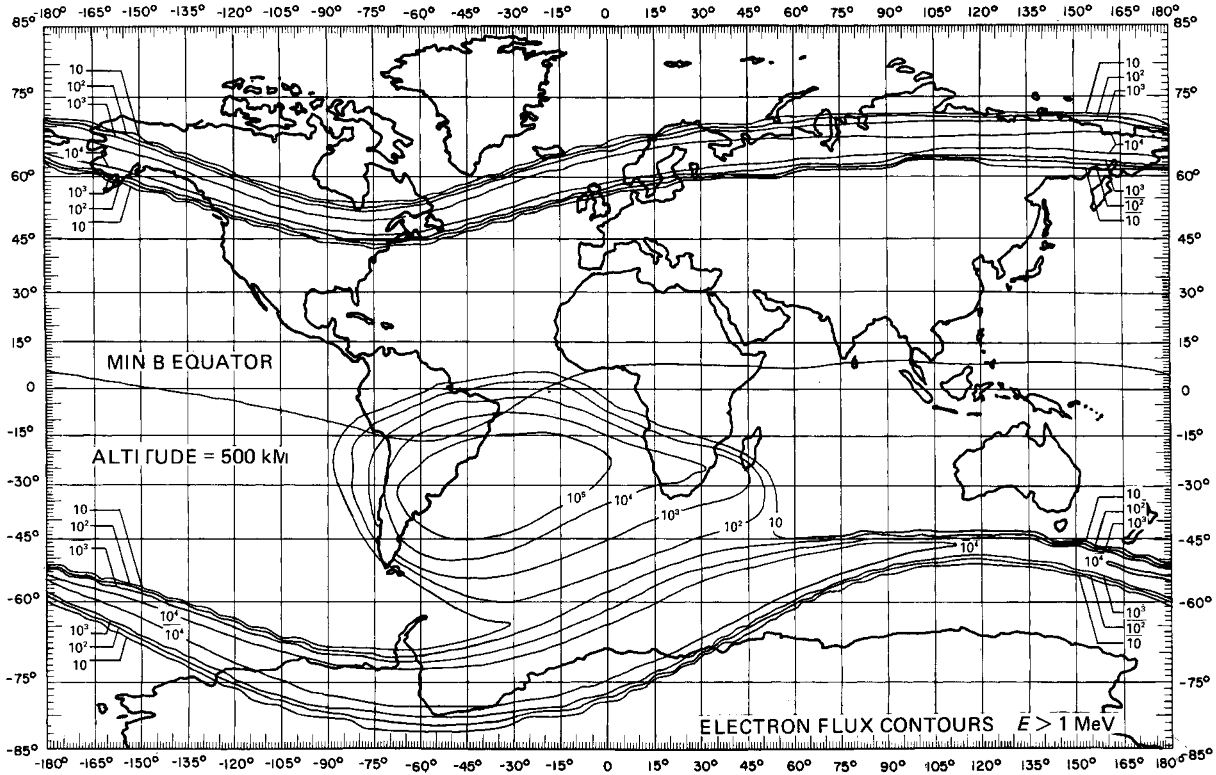

Omni-directional flux in electrons cm^{-2} s^{-1}. (Adapted from Stassinopoulos, E.G., *World Maps of Constant B, L, and Flux Contours*, NASA SP-3054, 1970.)

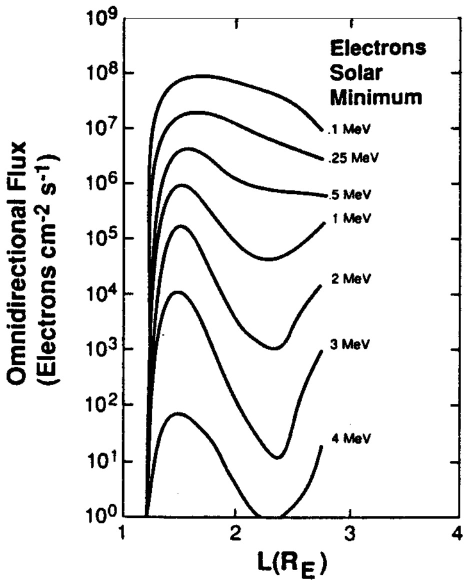

Equatorial omnidirectional electron flux versus L shell for the AE5 solar-minimum radiation-belt model. The flux curves are labeled by threshold energy. Each curve gives the total electron flux above the specified threshold.

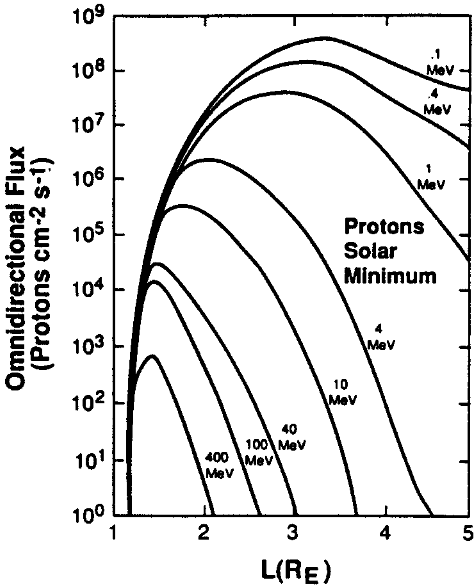

Radial distribution of proton omnidirectional fluxes in the equatorial plane, according to the AP8 solar-minimum radiation model. The curves give total fluxes above various threshold energies from 0.1 to 400 MeV.

(Wolf, R.A. in "*Introduction to Space Physics*", M.G. Kivelson & C.T. Russell, eds., Cambridge University Press, 1995, with permission.)

International reference atmosphere

(COSPAR International Reference Atmosphere, 1961.)

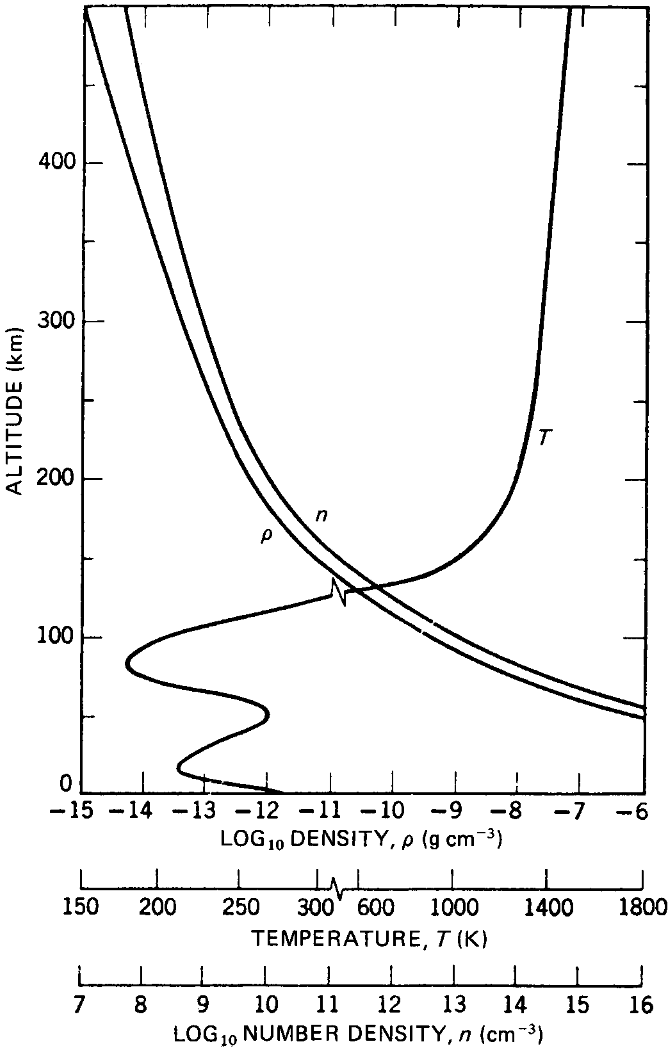

Altitude variation of atmospheric constituents

Variation with altitude of the various constituents of the atmosphere. The horizontal scale is the logarithm of the particle density n in particles cm^{-3}. (Adapted from Pecker, J., *Space Observatories*, D. Reidel Publishing Company, Dordrecht, 1970.)

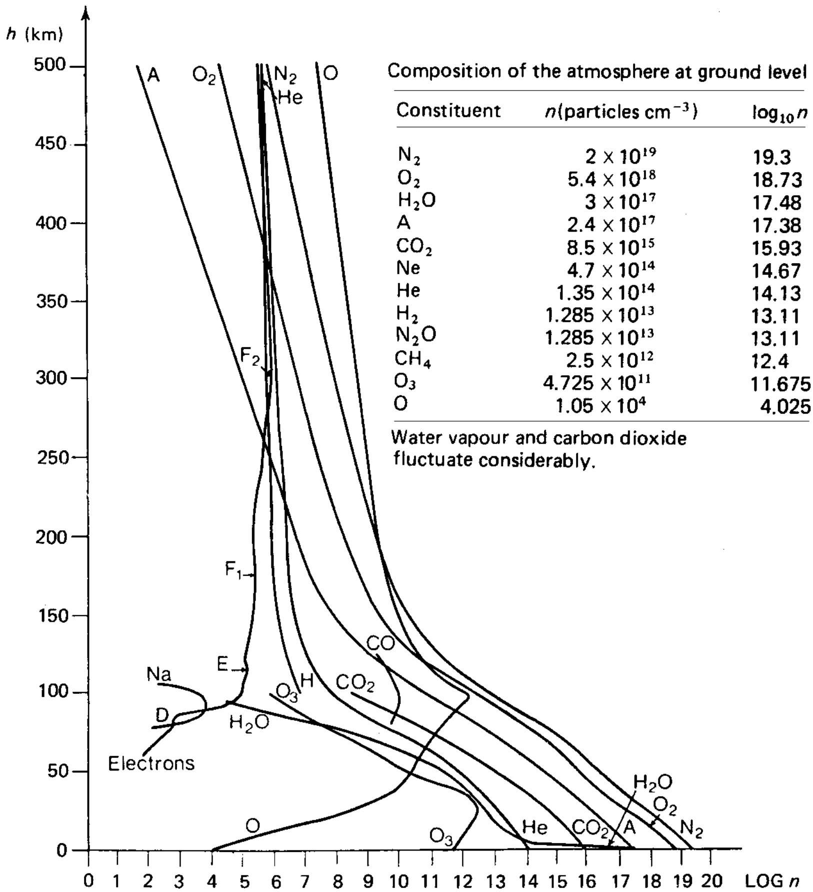

Composition of the atmosphere at ground level

Constituent	n(particles cm^{-3})	$\log_{10} n$
N_2	2×10^{19}	19.3
O_2	5.4×10^{18}	18.73
H_2O	3×10^{17}	17.48
A	2.4×10^{17}	17.38
CO_2	8.5×10^{15}	15.93
Ne	4.7×10^{14}	14.67
He	1.35×10^{14}	14.13
H_2	1.285×10^{13}	13.11
N_2O	1.285×10^{13}	13.11
CH_4	2.5×10^{12}	12.4
O_3	4.725×10^{11}	11.675
O	1.05×10^{4}	4.025

Water vapour and carbon dioxide fluctuate considerably.

Opacity of the atmosphere

Attenuation of photons as a function of wavelength for various constituents of the atmosphere. The ordinate is the mass attenuation coefficient in $cm^2\ g^{-1}$. (a) X-ray and EUV region; (b) UV, visible, and infrared region; (c) radio region. (Adapted from Pecker, J., *Space Observatories*, D. Reidel Publishing Company, Dordrecht, 1970.)

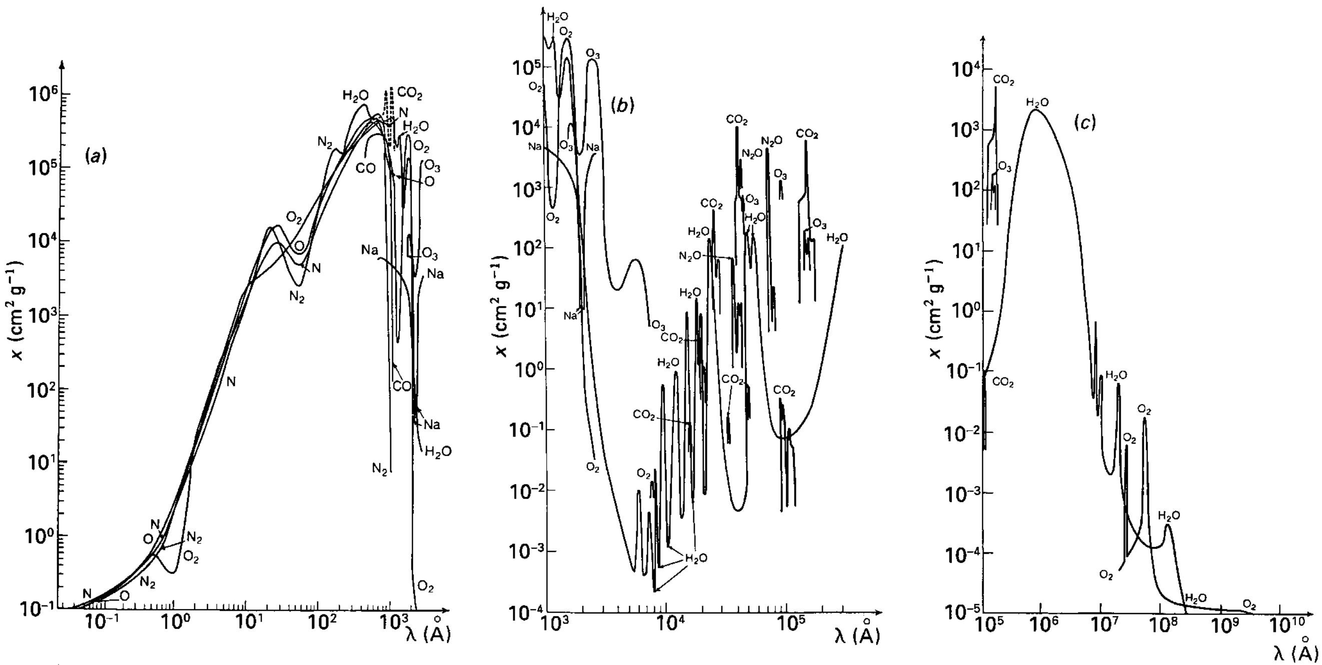

US standard atmosphere, 1976

(a) Mean free path as a function of geometric altitude. (b) Speed of sound as a function of geometric altitude. (c) Mean molecular weight as a function of geometric altitude. (d) Total pressure and mass density as a function of geometric altitude.

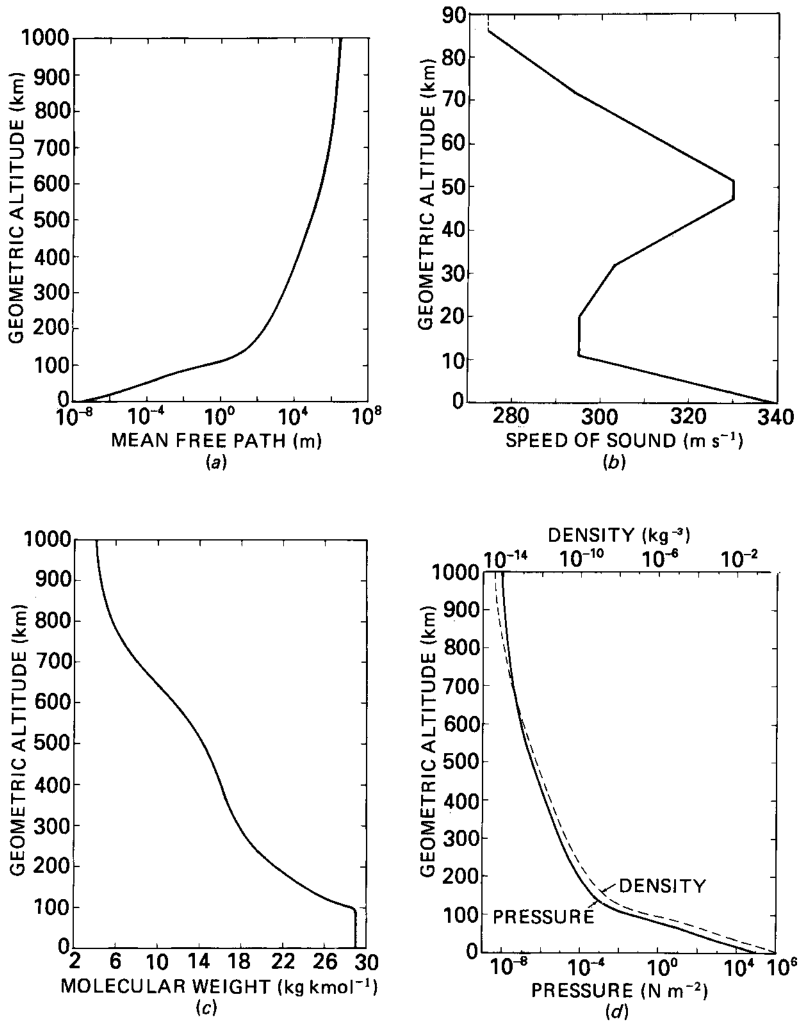

US standard atmosphere, 1976 *(cont.)*

(e) Dynamic viscosity as a function of geometric altitude. (f) Coefficient of thermal conductivity as a function of geometric altitude. (g) Kinetic temperature as a function of geometric altitude. (h) Mean air-particle speed as a function of geometric altitude.

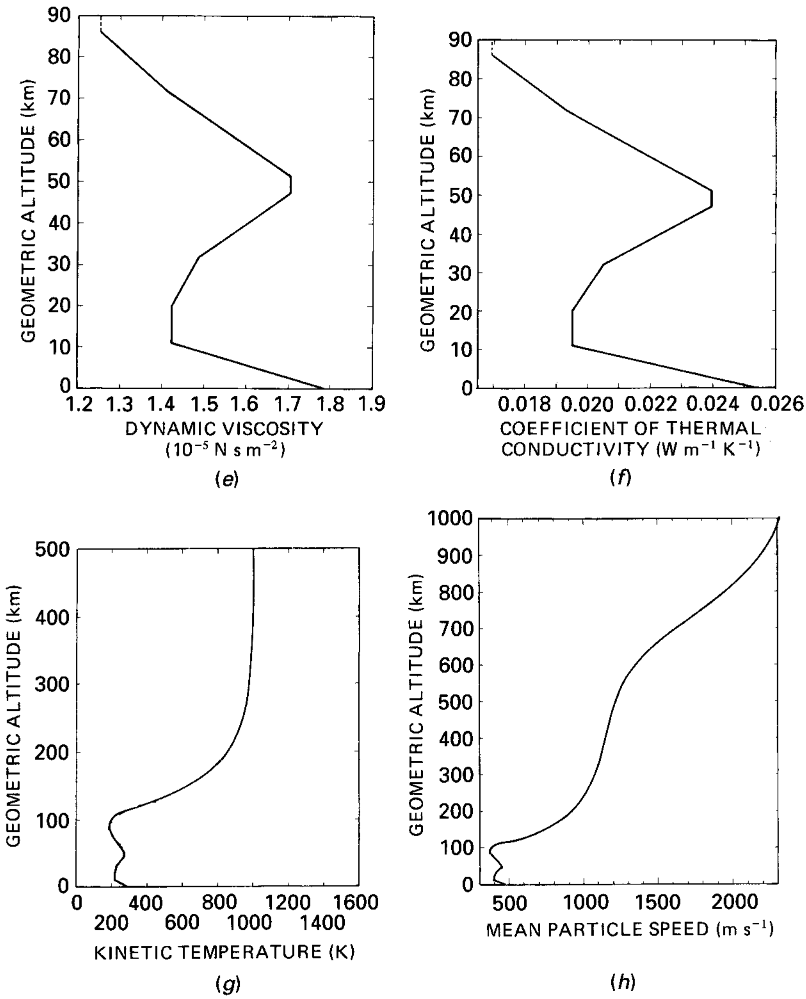

Structure of the upper atmosphere

(Adapted from Harris, M.F. in *American Institute of Physics Handbook*, D.E. Gray, ed., McGraw-Hill Book Company, 1972.)

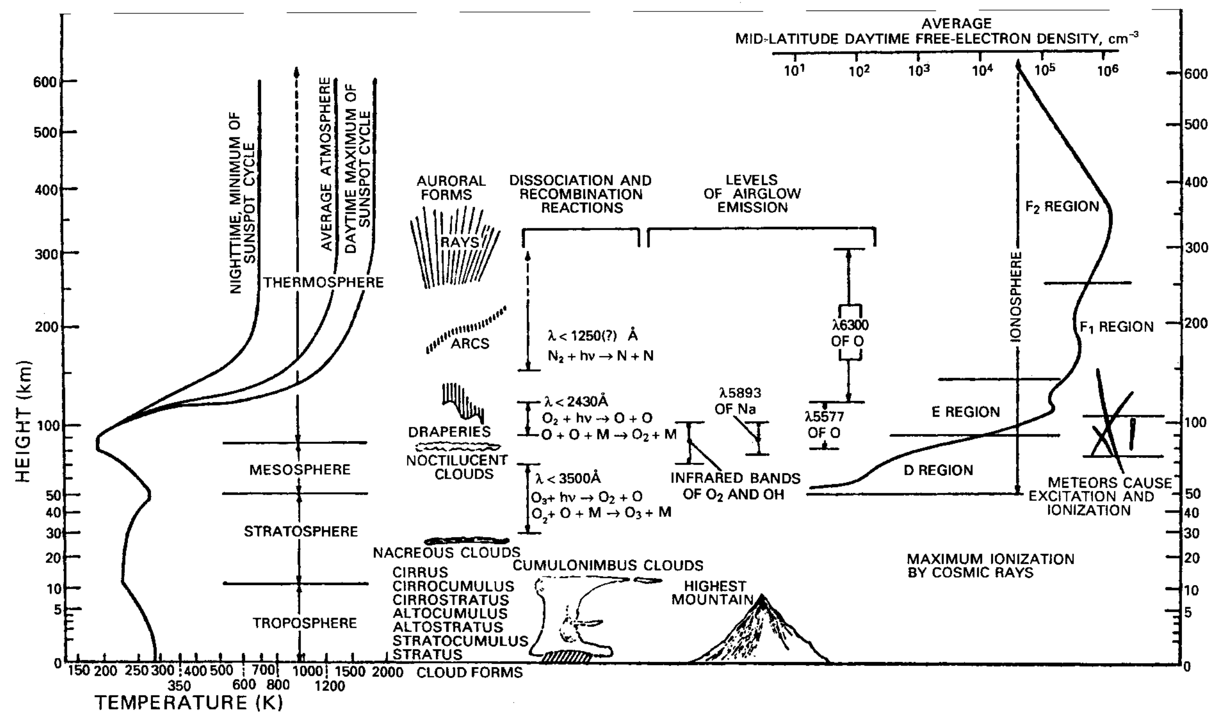

Earth's ionosphere

The international quiet solar year (IQSY) daytime ionospheric and atmospheric composition based on mass spectrometer measurements.

(Luhmann, J.G., in *Introduction to Space Physics*, Kivelson, M.G. & C.T. Russell, eds., Cambridge University Press, 1995, with permission.)

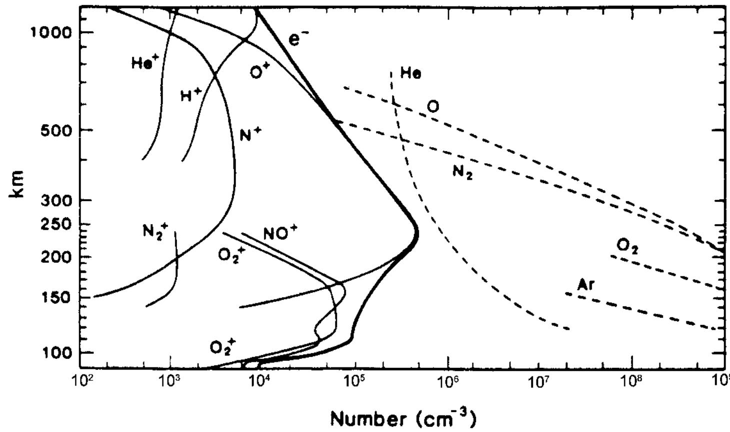

The concentration of electrons in the Earth's ionosphere. The D-layer disappears at night, and the F1- and F2-layers coalesce in the absence of sunlight. These data apply at midlatitudes.

(Haymes, R.C., Introduction to Space Science, John Wiley & Sons, Inc., 1971, with permission.)

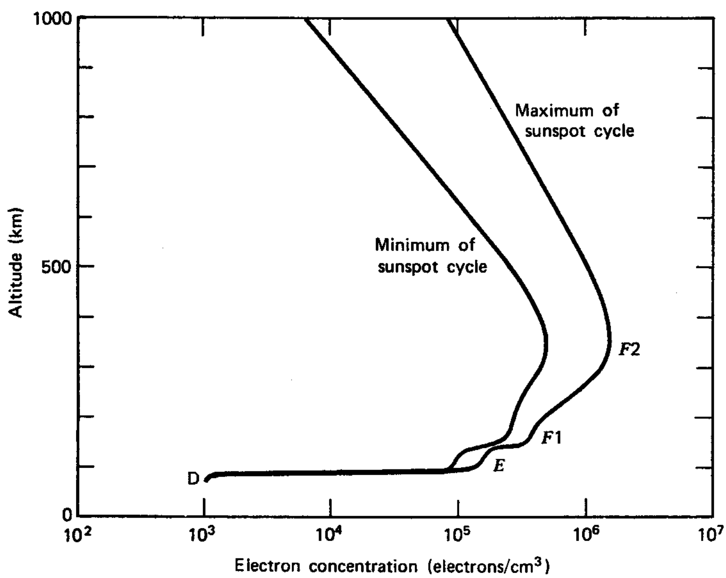

Bibliography

World Maps of Constant B, L, and Flux Contours,
Stassinopoulos, E.G., NASA SP-3054, 1970.

US Standard Atmosphere, 1976, 1976-0-588-256, US Government Printing Office.

Satellite Environment Handbook, F.S. Johnson, ed., Stanford University Press, 1965.

A.S. Jura, ed., *Handbook of Geophysics and the Space Environment*, Air Force Geophysics Laboratory, 1985.

Kivelson, M.G. & C.T. Russell, eds., *Introduction to Space Physics*, Cambridge University Press, 1995.

Haymes, R.C., Introduction to Space Science, John Wiley & Sons, Inc., 1971.

Note: Links to WWW resources which supplement the material in this chapter can be found at:

http://www.astrohandbook.com

Chapter 10

Relativity and cosmology

Cosmologists are often in error, but never in doubt. - Yakov Zel'dovich

Special relativity

Fundamental kinematical relations for a particle of rest mass m_0 and velocity v:

$p = m_0 v/(1 - v^2/c^2)^{1/2}$	momentum
$E = m_0 c^2/(1 - v^2/c^2)^{1/2}$	total energy
$T = E - m_0 c^2$	kinetic energy
$m = m_0/(1 - v^2/c^2)^{1/2}$	relativistic mass
$E_0 = m_0 c^2$	rest energy

From the above, the following relations can be derived:

$$E = mc^2 = (m_0^2 c^4 + c^2 p^2)^{1/2}$$

$$p = [(E/c)^2 - m_0^2 c^2]^{1/2}$$

$$v = c^2 p/E = c[1 - (m_0 c^2/E)^2]^{1/2} = p/[m_0 c^2 + (p/c)^2]^{1/2}$$

$$m = E/c^2 = [m_0^2 + (p/c)^2]^{1/2}$$

Relativistic Doppler effect:

$$1 + z = \frac{1 + (v/c)\cos\theta}{(1 - v^2/c^2)^{1/2}},$$

where

$\theta =$ angle between direction of observation and direction of motion,

$\theta = 0$ for motion directly away from observer,

$z = (\lambda_{\text{obs}} - \lambda)/\lambda$.

$z \approx (v/c)\cos\theta$ for $v << c$.

Lorentz transformation (Gaussian units)

4-Vector transformation

$$B'_\mu = \sum_{\nu=1}^{4} a_{\mu\nu} B_\nu \equiv a_{\mu\nu} B_\nu.$$

For a Lorentz transformation from system k to a system k' moving with a velocity v parallel to the z-axis, the transformation coefficients are given by:

$$(a_{\mu\nu}) = \begin{bmatrix} 1 & 0 & 0 & 0 \\ 0 & 1 & 0 & 0 \\ 0 & 0 & \gamma & i\gamma\beta \\ 0 & 0 & -i\gamma\beta & \gamma \end{bmatrix}, \quad \beta = v/c, \ \gamma = (1 - v^2/c^2)^{-1/2}.$$

Examples of 4-vectors

$$x_\mu = (\mathbf{x}, \mathrm{i}ct),$$

where $\mathbf{x} = x_1\hat{i} + x_2\hat{j} + x_3\hat{k}$.

$$A_\mu = (\mathbf{A}, \mathrm{i}\phi),$$

where $\mathbf{A}$ and ϕ are the electromagnetic vector and scalar potential.

$$J_\mu = (\mathbf{J}, \mathrm{i}c\rho),$$

where $\mathbf{J}$ and ρ are the current density and charge density.

$$k_\mu = (\mathbf{k}, \mathrm{i}\omega/c),$$

where $\mathbf{k}$ and ω are the wave vector and frequency of a plane electromagnetic wave.

$$p_\mu = (\mathbf{p}, \mathrm{i}E/c),$$

where $\mathbf{p}$ and E are the momentum and energy of a particle.

2nd rank tensor transformation

$$S'_{\mu\nu} = \sum_{\lambda,\sigma=1}^{4} a_{\mu\lambda}a_{\nu\sigma}S_{\lambda\sigma} \equiv a_{\mu\lambda}a_{\nu\sigma}S_{\lambda\sigma}.$$

Electromagnetic field strength tensor

$$F_{\mu\nu} = \frac{\partial A_\nu}{\partial x_\mu} - \frac{\partial A_\mu}{\partial x_\nu} = \begin{bmatrix} 0 & B_3 & -B_2 & -\mathrm{i}E_1 \\ -B_3 & 0 & B_1 & -\mathrm{i}E_2 \\ B_2 & -B_1 & 0 & -\mathrm{i}E_3 \\ \mathrm{i}E_1 & \mathrm{i}E_2 & \mathrm{i}E_3 & 0 \end{bmatrix}.$$

Covariant formulation of Maxwell's equations

$$\frac{\partial F_{\mu\nu}}{\partial x_\nu} = \frac{4\pi}{c}J_\mu; \quad \frac{\partial F_{\mu\nu}}{\partial x_\lambda} + \frac{\partial F_{\lambda\mu}}{\partial x_\nu} + \frac{\partial F_{\nu\lambda}}{\partial x_\mu} = 0,$$

where λ, μ and ν are any three of the integers $1, 2, 3, 4$.

Lorentz force

$$\mathbf{f} = \rho\mathbf{E} + \frac{1}{c}(\mathbf{J} \times \mathbf{B}).$$

$$f_\mu = \frac{1}{c}F_{\mu\nu}J_\nu = \frac{1}{4\pi}F_{\mu\nu}\frac{\partial F_{\nu\lambda}}{\partial x_\lambda} = \frac{\partial T_{\mu\nu}}{\partial x_\nu} = \left(\mathbf{f}, \frac{\mathrm{i}}{c}\mathbf{E}\cdot\mathbf{J}\right),$$

where $T_{\mu\nu}$ is the electromagnetic stress-energy-momentum tensor:

$$T_{\mu\nu} = \frac{1}{4\pi}\left[F_{\mu\lambda}F_{\lambda\nu} + \frac{1}{4}\delta_{\mu\nu}F_{\lambda\sigma}F_{\lambda\sigma}\right].$$

Cosmology

Robertson-Walker line element (homogeneous and isotropic universe)

The Minkowski space-time interval of special relativity is a valid metric for a homogeneous, isotropic space of constant curvature:

$$ds^2 = c^2dt^2 - R(t)du^2$$

The spatial part of the metric is non-Euclidean with the form in polar coordinates:

$$du^2 = \frac{dr^2}{1-kr^2} + r^2d\theta^2 + r^2\sin^2\theta d\phi^2,$$

where

$R(t)$ = cosmic scale factor
r, θ, ϕ = co-moving spherical coordinates (a co-moving observer is an observer at rest with respect to matter in his vicinity),
k = curvature index $= 0, \pm 1$ ($k = 1$, elliptical closed space; $k = 0$, Euclidean flat space; $k = -1$, hyperbolic open space).

r is a co-moving coordinate "distance". It is not the distance measured by an astronomer. R is constant in time for any given galaxy.

The interval distance, the distance that can be measured by an astronomer is

$$d = R(t)u = R(t)\int_0^r \frac{dr}{\sqrt{1-kr^2}}.$$

This integrates to

$$\begin{aligned} d &= R(t)\sin^{-1} r && \text{for } k = 1 \\ d &= R(t)r && \text{for } k = 0 \\ d &= R(t)\sinh^{-1} r && \text{for } k = -1. \end{aligned}$$

The volume enclosed within r is

$$\begin{aligned} V(r) &= R^3 \int_0^r \frac{r^2dr}{\sqrt{1-kr^2}} \int_0^\pi \sin\theta d\theta \int_0^{2\pi} d\phi \\ &= 4\pi R^3 \int_0^r \frac{r^2dr}{\sqrt{1-kr^2}} \\ &= 2\pi(Rr)^3\left[\frac{\sin^{-1} r}{r^3} - \frac{\sqrt{1-r^2}}{r^2}\right], \text{ for } k = 1. \end{aligned}$$

and

$$V(\infty) = 2\pi^2R^3$$

Einstein field equations

$$\frac{3\dot{R}^2}{R^2} + \frac{3kc^2}{R^2} = 8\pi G\rho + \Lambda c^2,$$

$$\frac{2\ddot{R}}{R} + \frac{\dot{R}^2}{R^2} + \frac{kc^2}{R^2} = -\frac{8\pi GP}{c^2} + \Lambda c^2,$$

$$\frac{\ddot{R}}{R} = \frac{\Lambda c^2}{3} - \frac{4\pi G}{3}\left[\rho + \frac{3P}{c^2}\right],$$

where

ρ = mean density of matter and energy,

Λ = cosmological constant,

P = hydrodynamic pressure of matter and radiation,

G = gravitational constant, and

$H_0 \equiv \dot{R}_0/R_0$, Hubble constant,

$q_0 \equiv -\ddot{R}_0/R_0H_0^2$, deceleration constant, where the subscript zero denotes the present value.

Friedmann universes $(\Lambda, P = 0)$

We obtain from the above

$$\rho_0 = 3H_0^2 q_0/4\pi G$$

$$kc^2/R_0^2 = H_0^2(2q_0 - 1) = (4\pi G\rho_0/3q_0)(2q_0 - 1)$$

Curvature	Space	q_0	Ω_0[a]	Density ρ_0	Expansion
$k = +1$	Closed	$> 1/2$	> 1	$> \dfrac{3H_0^2}{8\pi G}$	Turns eventually into contraction
$k = 0$	Flat (Euclidean)	$1/2$	1	$\rho_c = \dfrac{3H_0^2}{8\pi G}$[b]	Stops in infinite future
$k = -1$	Open	$0 \le q_0 < 1/2$	$0 \le \Omega_0 < 1$	$< \dfrac{3H_0^2}{8\pi G}$	Forever

[a] The 'density parameter' $\Omega \equiv \rho/\rho_c$, where ρ_c is the critical closure density (i.e., for the case $q_0 = 1/2$).

[b] With $H_0 = 50$ km s^{-1} Mpc^{-1}, the present critical density becomes $\rho_c = 4.7 \times 10^{-30}$ g cm^{-3}.

The relation between the co-moving coordinate r and z (light source redshift), H_0, and q_0 is given by the solution of

$$\frac{\dot{R}^2}{R^2} + \frac{2\ddot{R}}{R} = -\frac{kc^2}{R^2}$$

Using the Lemaitre equation relating the scale factor to the redshift

$1 + z = R_0/R_1$

where R_1 is the scale factor when light left the source with redshift z and R_0 is the scale factor at the time of light detection (now), the Mattig equation can be derived (see Sandage, A.R. in the *The Deep Universe*, Binggeli, B. and Buser, R., ed., Springer-Verlag, 1995.):

$$R_0 r = \frac{c}{H_0 q_0^2 (1+z)} \left\{ q_0 z + (q_0 - 1)\left[-1 + \sqrt{1 + 2q_0 z}\right]\right\}$$

Useful relationship and quantities (Friedmann universe)

Differential volume:

$$dV = \frac{R_{\mathrm{H}}^3}{(1+z)^3} \frac{\{q_0 z + (q_0 - 1)[(1 + 2q_0 z)^{1/2} - 1]\}^2}{q_0^4 (1 + 2q_0 z)^{1/2}} d\Omega\, dz,$$

where

$$R_{\mathrm{H}} = \frac{c}{H_0}, \text{ the Hubble radius.}$$

Time differential:

$$dt = -dz/[(1+z)^2 H_0 (1 + 2q_0 z)^{1/2}].$$

Look-back time:

$$\tau = -\int_0^z dt.$$

$q_0 = 0$,

$$\tau = \frac{1}{H_0}(1 - 1/(1+z)); \quad \lim_{z\to\infty} \tau = 1/H_0,$$

$q_0 = 1/2$,

$$\tau = \frac{2}{3H_0}(1 - 1/(1+z)^{3/2}); \quad \lim_{z\to\infty} \tau = 2/3(1/H_0),$$

$q_0 = 1$,

$$\tau = \frac{1}{H_0}[(2z+1)^{1/2}/(z+1) + 2\tan^{-1}(2z+1)^{1/2} - 1 - \pi/2];$$

$$\lim_{z\to\infty} \tau = 0.57(1/H_0),$$

Redshift-magnitude relationship (Friedmann universe):

$$m_{\rm bol} = 5\log\left\{\frac{c}{H_0 q_0^2}[1 - q_0 + q_0 z + (q_0 - 1)(2q_0 z + 1)^{1/2}]\right\} + M_{\rm bol} + 25 = 5\log D_{\rm L} + M_{\rm bol} + 25.$$

where $m_{\rm bol}$ is the apparent bolometric magnitude of a source with absolute bolometric magnitude $M_{\rm bol}$ and redshift z.

Expanded in powers of z:

$$m_{\rm bol} = 5\log\left(\frac{zc}{H_0}\right) + 1.086(1 - q_0)z + \cdots + M_{\rm bol} + 25,$$

where H_0 is in km s^{-1} Mpc^{-1}; zc is in km s^{-1}, and z is the observed redshift.

$$\begin{aligned} D_{\rm L} &= \frac{c}{H_0 q_0^2}[1 - q_0 + q_0 z + (q_0 - 1)(2q_0 z + 1)^{1/2}] \\ &\approx \frac{cz}{H_0}[1 + 0.5z(1 - q_0)], \quad q_0 z << 1. \end{aligned}$$

$m_{\rm bol} - M_{\rm bol} = m - M - K - A$, $m - M$ = observed distance modulus, for heterochromatic magnitudes, where K = redshift correction, A = interstellar absorption.

$$K = 2.5\log(1 + z) + 2.5\log\frac{\displaystyle\int_0^\infty I(\lambda)S(\lambda)d\lambda}{\displaystyle\int_0^\infty I\left(\frac{\lambda}{1+z}\right)S(\lambda)d\lambda}\ [\text{mag}],$$

where $I(\lambda)$ is the incident energy flux per unit wavelength and $S(\lambda)$ is the photometer response function.

Angular diameter-redshift relationship (Friedmann universe)

$$\theta = \frac{l(1+z)^2}{D_{\rm L}},$$

where

θ = apparent angular diameter of source,

l = linear diameter of spherical source,

$D_{\rm L}$ = luminosity distance.

Observed energy flux density (Friedmann universe)

$$S_0(E_0) = \frac{P_e((1+z)E_0)}{4\pi D_L^2},$$

where P_e is the monochromatic power emitted at the energy $(1+z)E_0$, and S_0 is the observed monochromatic energy flux density at the energy E_0. The observed energy flux density integrated from E_1 to E_2 is:

$$F_0(E_1, E_2) = \frac{1}{4\pi D_L^2} \int_{(1+z)E_1}^{(1+z)E_2} p_e(E)\, dE,$$

where $p_e(E)$ is the differential power emitted per unit energy in the emitted rest frame.

Redshift functions

Angular size vs. redshift

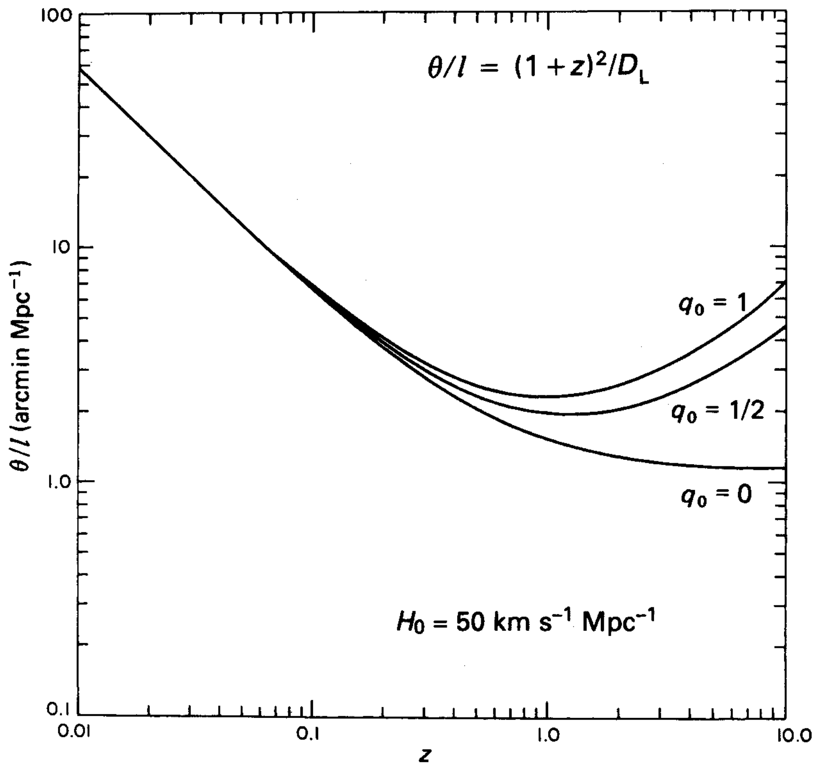

Redshift functions (cont.)

Luminosity distance vs. redshift

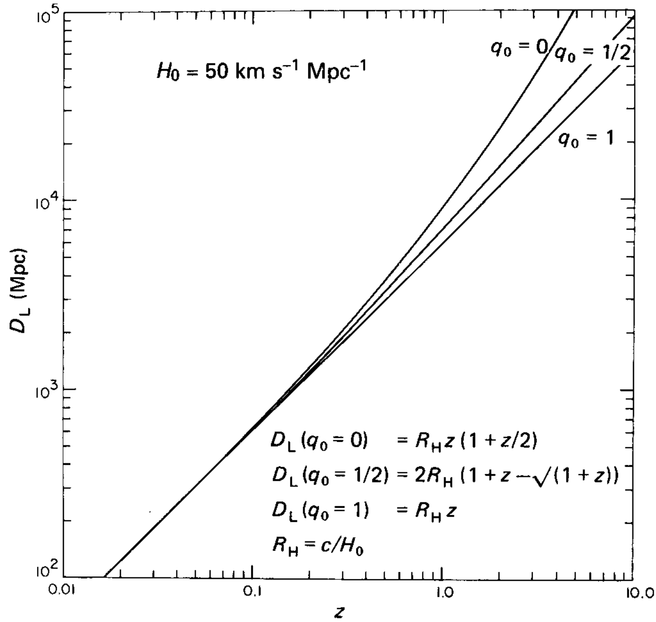

Look-back time

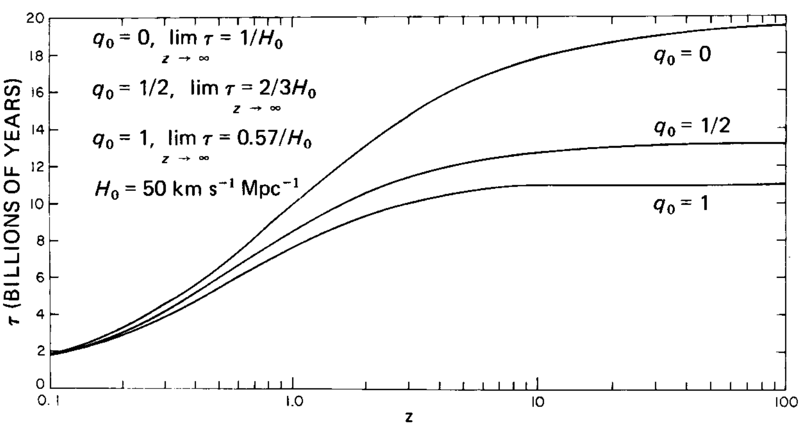

Redshift functions (cont.)

Angular density of sources per unit z vs. redshift

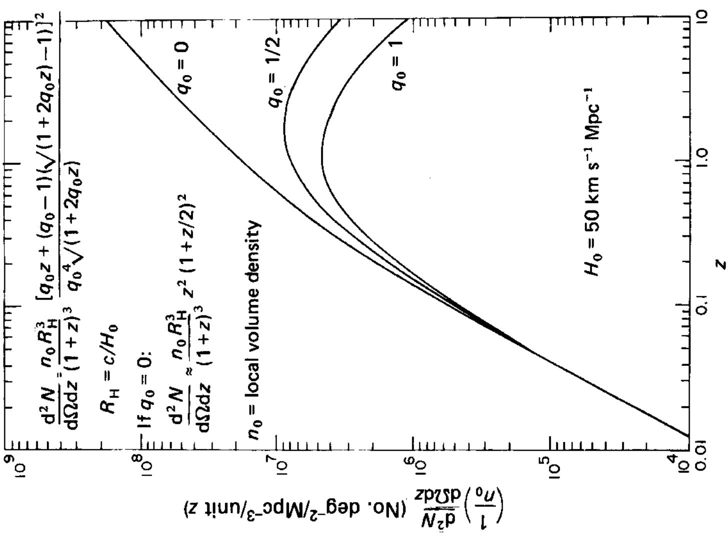

Integrated angular density vs. redshift

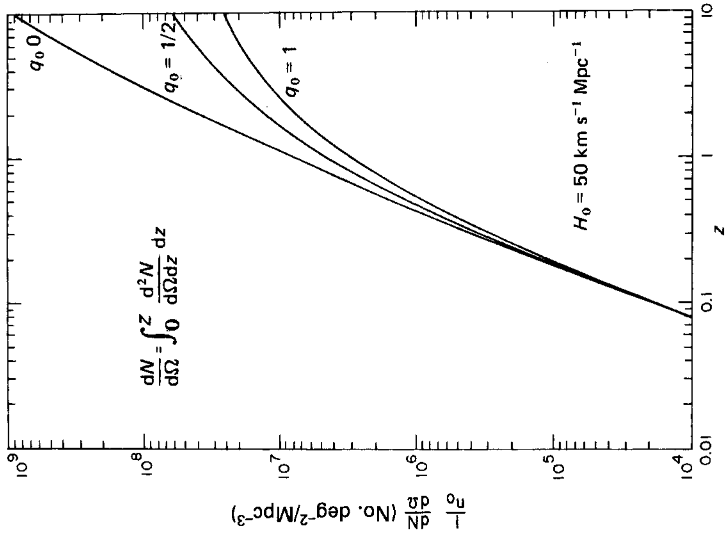

Other world models ($\Lambda \neq 0, P = 0$)

This section is based upon Carroll, S.M., Press, W.H., and Turner, E.L., *The Cosmological Constant*, Annu. Rev. Astron. Astrophys., 1992.

The first of Einstein's field equations (see the beginning of this section) provides a definition of the Hubble constant H (the present value is designated as H_0):

$$H^2 \equiv \left(\frac{\dot{R}}{R}\right) = \frac{8\pi G}{3}\rho_M + \frac{\Lambda c^2}{3} - \frac{kc^2}{R^2}$$

where

$R(t)$ = cosmic scale factor
G = gravitational constant
ρ_M = mass density of matter and energy
Λ = cosmological constant
k = curvature index $= 0, \pm 1$ ($k = 1$, elliptical closed space; $k = 0$, Euclidean flat space; $k = -1$, hyperbolic open space).

The fractional contributions to the universal expansion at the present epoch can be defined as:

$$\Omega_M \equiv \frac{8\pi G}{3H_0^2}\rho_{M0}, \quad \Omega_\Lambda \equiv \frac{\Lambda c^2}{3H_0^2}, \quad \Omega_k \equiv -\frac{kc^2}{R_0^2 H_0^2},$$

$$\Omega_M + \Omega_\Lambda + \Omega_k = 1.$$

Defining an Ω_{tot}

$$\Omega_{\text{tot}} \equiv \Omega_M + \Omega_\Lambda = 1 - \Omega_k$$

A deceleration parameter can be specified from the third of Einstein's field equations:

$$q_0 = \frac{-\ddot{R}_0}{R_0 H_0^2} = \frac{1}{2}\Omega_M - \Omega_\Lambda.$$

H_0 is often written as:

$$H_0 = 100 \text{ h km s}^{-1} \text{ Mpc}^{-1}$$

where h is a dimensionless constant between 0.5 and 1.0.

The Hubble time is defined by:

$$1/H_0 = 9.78 \times 10^9/\text{h yr}$$

The Hubble distance is defined by:

$$R_H = c/H_0 = 3025/\text{h Mpc}$$

Note: The term dark energy is often used interchangeably for Λ. Alternatively, dark energy might arise from the particle-like excitations in a dynamical field, referred to as "quintessence". Quintessence differs from the cosmological constant in that it can vary in space and time.

See *The Cosmological Constant and Dark Energy*, Peebles, P.J.E. and Ratra, B., Rev. Mod. Phys., **75**, 559, 2003 and Padmanabhan, T., e-print, arXiv:hep-th/0212290 v2, 26, Feb 2003 for extensive (and intensive) treatments of Λ.

Useful relationships

Look-back time:

$$\tau = H_0^{-1} \int_0^z (1+z)^{-1}[(1+z)^2(1+\Omega_M z) - z(2+z)\Omega_\Lambda]^{-1/2} dz.$$

Look-back time (in units of the Hubble time) for five cosmological models.

Model	Ω_{tot}	Ω_M	Ω_Λ
A	1	1	0
B	0.1	0.1	0
C	1	0.1	0.9
D	0.01	0.01	0
E	1	0.01	0.99

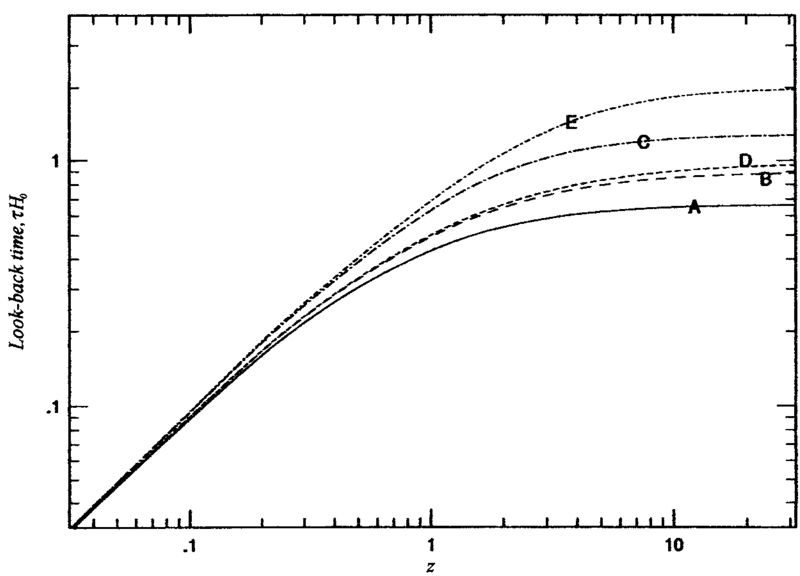

Distance

angular diameter distance:

$d_A = D/\theta$

where D is the proper size of the object and θ is its apparent angular size.

proper motion distance:

$d_M = u/\dot{\theta}$

where u is the object's transverse proper velocity and $\dot{\theta}$ is an apparent angular motion.

luminosity distance:

$d_L = (L/4\pi\Phi)^{1/2}$

where L is the rest-frame luminosity of the object and Φ is its apparent flux density.

d_M is given by

$$\frac{d_M}{R_H} = \frac{1}{|\Omega_k|^{1/2}} \sinh \left\{ |\Omega_k|^{1/2} \int_0^z [(1+z)^2(1+\Omega_M z) - z(2+z)\Omega_\Lambda]^{-1/2} dz \right\}$$

where $\sinh(x) = \sinh(x)$ for $\Omega_k > 0$.

$\sinh(x) = \sin(x)$ for $\Omega_k < 0$.

For $\Omega_k = 0$, only the integral is evaluated.

The three distances are related by:

$d_L = (1+z)^2 d_A = (1+z) d_M$

The angular diameter distance (in units of the Hubble distance) for five cosmological models.

Model	Ω_{tot}	Ω_M	Ω_Λ
A	1	1	0
B	0.1	0.1	0
C	1	0.1	0.9
D	0.01	0.01	0
E	1	0.01	0.99

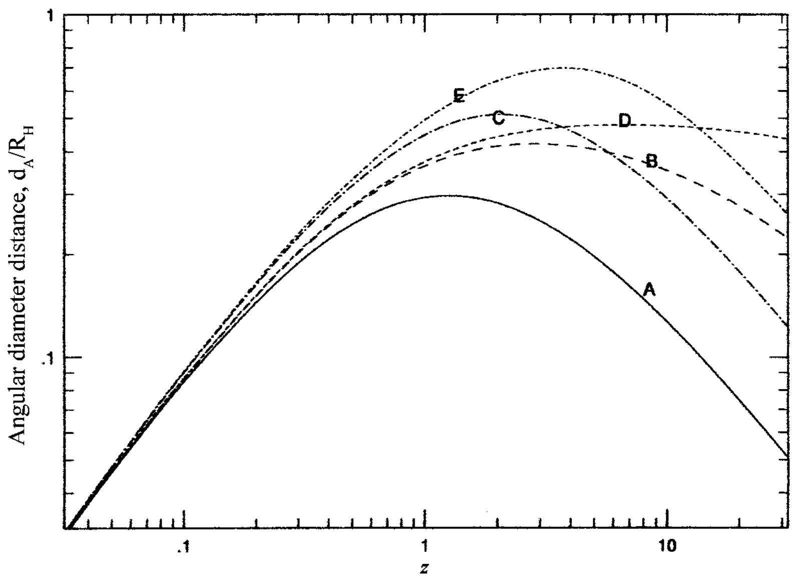

Measurements of the Hubble constant H_0

H_0 in km s^{-1} Mpc^{-1}	Reference
100	Baade, W. and Swope, H.H., Astron. J., **60**, 151, 1955
50	Sandage, A., in *Nuclei of Galaxies,* North Holland, 1971
57 ± 3	Sandage, A. and Tammann, G.A., Ap. J., **196**, 313, 1975
100 ± 10	De Vaucouleurs, G. and Bollinger, G., Ap. J., **233**, 433, 1979
95 ± 4	Aaronson, M., *et al.*, Ap. J., **239**, 12, 1980
95 ± 1	De Vaucouleurs, G., Nature, **299**, 303, 1982
50 ± 7	Sandage, A. and Tammann, G.A., Nature, **307**, 326, 1984
85 ± 10	Pierce, M.J. and Tully, R.B., Ap. J., **330**, 579, 1988
57 ± 1	Kraan-Kortweg, *et al.*, Ap. J., **331**, 620, 1988
67 ± 8	Van den Bergh, S., Astron. Ap. Rev., **1**, 111, 1989
87 ± 10	Tully, R.B., *Astrophys. Ages and dating methods*, Editiones Frontieres, 1990
76 ± 9	Van den Bergh, S., P.A.S.P., **104**, 861, 1992
47 ± 7	Sandage, A. and Tammann, G.A., Ap. J., **415**, 1, 1993
86 ± 1	De Vaucouleurs, G., Ap. J., **415**, 10, 1993
90 ± 10	Tully, R.B., Proc. Nat. Acad. Sci., **90**, 4806, 1993
87 ± 7	Pierce, M.J., *et al.*, Nature, **371**, 385, 1994
69 ± 8	Tanvir, N.R., *et al.*, Nature, **377**, 27, 1995
55 ± 7	Sandage, A. and Tammann, G.A., Ap. J., **446**, 1, 1995
67 ± 7	Riess, A.G., Press, W.H., and Kirshner, R.P., Ap. J. (L), **438**, L17, 1995
58 ± 4	Sandage, A. *et al.*, Ap. J. (L), **460**, L15, 1996
70 ± 7	Freedman, W., American Astronomical Society Meeting 194, #39.0, 1999
$64 + 8 - 6$	Jha, S., Ap. J. Supp., **125**, 73, 1999

(List to 1996 taken from Lang, K.R., Astrophysical Formulae, v. II, Springer-Verlag, 1999.)

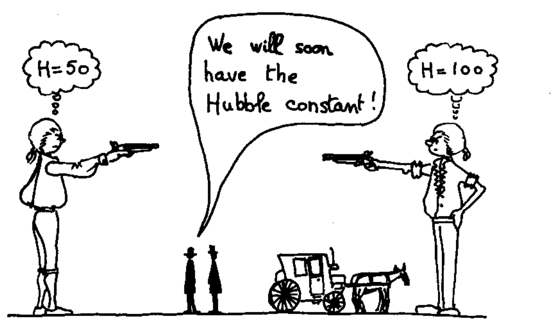

An old way to derive the Hubble constant

(Courtesy of G. Paturel, Observatoire de Lyon)

Gravitational lensing (point-mass or Schwarzschild lens)

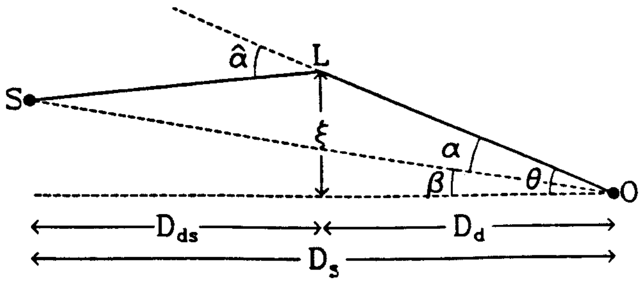

Basic ray geometry of gravitational lensing. A light ray from a *source* S at redshift z_s, is incident on a *deflector* or *lens* L at redshift z_d with impact parameter ξ relative to some fiducial lens "center." Assuming the lens is thin compared to the total path length, its influence can be described by a deflection angle $\hat{\alpha}(\xi)$ (a two-vector) suffered by the ray on crossing the "lens plane." The deflected ray reaches the observer O, who sees the image of the source apparently at position θ on the sky. The true direction of the source, i.e., its position on the sky in the absence of the lens, is indicated by β. Also shown are the angular diameter distances $D_{\rm d}, D_{\rm s}, D_{\rm ds}$, separating the source, deflector, and observer. (Blandford, R.D. and Narayan, R., Annu. Rev. Astron. Astrophys. **30**, 311, 1992, with permission.)

The deflection angle for impact parameter ξ relative to a point mass M is given by $\hat{\alpha}(\xi) = 4GM\xi/c^2\xi^2$. A source on the optic axis will form an *Einstein ring* of angular radius

$$\theta_E = \left(\frac{4GM}{c^2 D}\right)^{1/2} = 3\left(\frac{M}{M_\odot}\right)^{1/2}\left(\frac{D}{1\text{Gpc}}\right)^{-1/2} \mu\text{arcsec}, \quad D \equiv \frac{D_{\rm d} D_{\rm s}}{D_{\rm ds}},$$

For comprehensive treatments of gravitational lensing see R.D. Blandford and R. Narayan (*op. cit.*) or P. Schneider, J. Ehlers, and E.E. Falco, *Gravitational Lenses*, Springer-Verlag, 1992.

Gravitationally lensed systems (mid 1994)

Name	θ_{max}	Images	z_{source}	z_{lens}	O/R
$B0957 + 561$	$6''.1$	2	1.41	0.36	R(adio)
$MGB2016 + 112$	$3''.8$	3	3.27	1.01	R
$B1115 + 080$	$2''.3$	4	1.72	0.29	O(ptical)
$B0142 - 100$	$2''.2$	2	2.72	0.49	O
$MG0414 + 0534$	$2''.1$	4	2.63		R
$MG1131 + 0456$	$2''.1$	Ring			R
$MG1654 + 1346$	$2''.0$	Ring	1.75	0.25	R
$B2237 + 031$	$1''.8$	4	1.69	0.039	O
$MG1549 + 304$	$1''.7$	Ring		0.111	R
$B1413 + 117$	$1''.4$	4	2.55		O
$B1422 + 231$	$1''.3$	4	3.62	0.64	R
$0751 + 271$	$1''$	4			R
$PKS1830 - 211$	$0''.98$	Ring			R
$B1938 + 666$	$0''.92$	4			R
$B0218 + 356$	$0''.33$	Ring		0.685	R

(From *An Introduction to Radio Astronomy*, Burke, B.F. & Graham-Smith, Cambridge University Press, 1997.)

The Sunyaev-Zeldovich Effect

Cosmic microwave background photons are scattered via the inverse Compton effect by the energetic electrons of the gas in a galactic cluster. The microwave spectrum is distorted in the direction of the cluster with the low energy side suffering a decrement in intensity and the high energy side an increment in intensity. The magnitude of the distortion is given by the following line-of-sight integral:

$\Delta T_{SZ}/T = \left(2kT_e\sigma_T/m_ec^2\right)\int n_e dl$, where T is the microwave radiation temperature, T_e is the electron temperature (obtained from X-ray observations), n_e is the electron density, σ_T is the Thompson scattering cross-section, and the other symbols have their usual meaning. The expected magnitude of the distortion is on the order of a millikelvin. X-ray surface brightness measurements of the cluster can be used to determine the electron density in terms of the Hubble constant and the Hubble constant can then be obtained from the equation above.

Thermal history of the standard Hot Big Bang

The radiation temperature decreases as $T_r \propto R^{-1}$ except for abrupt jumps as different particle-antiparticle pairs annihilate at $kT \approx mc^2$. Various important epochs in the standard model are indicated. An approximate time scale is indicated along the top of the diagram. The neutrino and photon barriers are indicated. In the standard model, the Universe is optically thick to neutrinos and photons prior to these epochs.

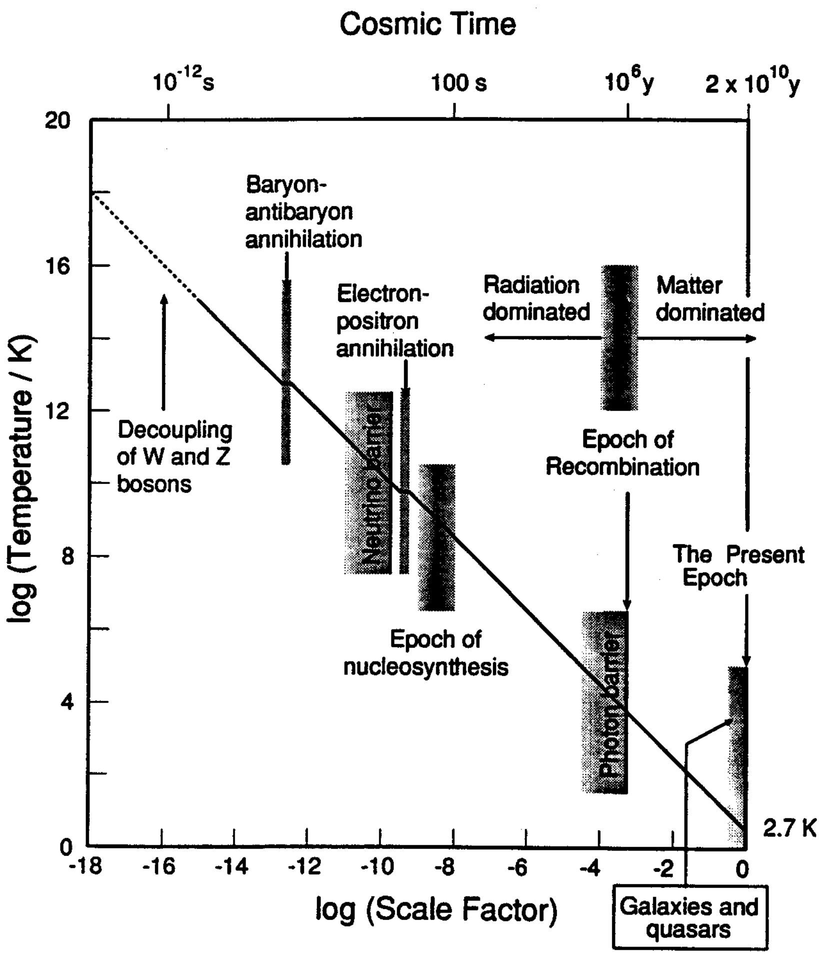

(Longair, M.S., in *The Deep Universe*, Sandage, A.R., Kron, R.G., Longair, M.S., Springer-Verlag, 1995, with permission.)

Cosmological parameters

Quantity	Value	Conf. Level	Ref.
H_0	70 ± 5	2σ	[1]
$\Omega_B h^2$	0.02 ± 0.004	2σ	[1]
Ω_B (baryons)	0.045 ± 0.015	2σ	[1]
Ω_M (matter)	0.3 ± 0.05	2σ	[1]
Ω_Λ (cosmol. const.)	0.7 ± 0.1	2σ	[1]
$\Omega_{tot} = \Omega_M + \Omega_\Lambda$	1.03 ± 0.1	2σ	[1]
t_0	$11.2 \leq t_0 \leq 20$ Gyr	2σ	[1]
ω	≤ -0.7	2σ	[1]
T_0	2.728 ± 0.002	2σ	[2]
$\Delta T/T$	$\leq 3 \times 10^{-5}$ on most scales		
Primordial ^{4}He	$0.221 \leq Y \leq 0.243$	2σ	[3]
Primordial D/H	$3.3 \pm 0.5\ 10^{-5}$	2σ	[4]
Primordial ^{7}Li	$0.7 \times 10^{-10} \leq {}^7\text{Li/H} \leq 3.5 \times 10^{-10}$	2σ	[3]
Largest Structures	approx. $150h^{-1}$ Mpc		[2]

$h = H_0/100$, a dimensionless constant.

t_0, the age of the Universe based upon stellar models.

$\omega = P/\rho$, where P is the hydrodynamic pressure of matter and radiation and ρ is the mean density of matter and energy.

[1] Krauss, L.M., *The State of the Universe: Cosmological Parameters 2002*, Proceedings, ESO-CERN-ESA Symposium on Astronomy, Cosmology and Fundamental Physics, March 2002.

[2] *Cosmology*, Scott, D., Silk, J., Kolb, E.W., and Turner, M.S., in *Allen's Astrophysical Quantities*, Cox, A.N., ed., Springer-Verlag, 2000.

[3] Copi, C.J., Schramm, D.N., and Turner, M.S., Science, **267**, 192, 1995.

[4] Burles, S. and Tytler, D., Ap. J., **499**, 699, 1998.

See http://pdg.lbl.gov/ for current values.

Bibliography

Astrophysical Formulae, Lang, K.R., Springer-Verlag, 1999.

Cosmology, Scott, D., Silk, J., Kolb, E.W., and Turner, M.S., in *Allen's Astrophysical Quantities*, Cox, A.N., ed., Springer-Verlag, 2000.

The Deep Universe, Sandage, A.R., Kron, R.G., Longair, M.S., lecturers, Binggeli, B. and Buser, R., ed., Springer-Verlag, 1995.

Encyclopedia of Cosmology, Hetherington, N.S., ed. Garland Publishing Co., 1993.

General Relativity and Cosmology, 2nd ed., McVittie, G.C., University of Illinois Press, 1965.

Gravitation and Cosmology, Weinberg, S., John Wiley and Sons, 1971.

Principles of Physical Cosmology, Peebles, P.J.E., Princeton University Press, 1993.

Note: Links to WWW resources which supplement the material in this chapter can be found at:

http://www.astrohandbook.com

Chapter 11

Atomic physics

We can say that the Universe consists of a substance, and this substance we call "atoms" or else we call it "monads". Democritus called it atoms. Leibniz called it monads. Fortunately, the two never met or there would have been a very dull argument. - Woody Allen

Electronic structure of the elements

		Element	Electron configuration ($3d^5$ = five $3d$ electrons, etc.)	Ground state $^{2S+1}L_J$	Ionization energy (eV)
1	H	Hydrogen	$1s$	$^2S_{1/2}$	13.5984
2	He	Helium	$1s^2$	$^1S_0$	24.5874
3	Li	Lithium	(He)$2s$	$^2S_{1/2}$	5.3917
4	Be	Beryllium	(He)$2s^2$	$^1S_0$	9.3227
5	B	Boron	(He)$2s^2\ 2p$	$^2P_{1/2}$	8.2980
6	C	Carbon	(He)$2s^2\ 2p^2$	$^3P_0$	11.2603
7	N	Nitrogen	(He)$2s^2\ 2p^3$	$^4S_{3/2}$	14.5341
8	O	Oxygen	(He)$2s^2\ 2p^4$	$^3P_2$	13.6181
9	F	Fluorine	(He)$2s^2\ 2p^5$	$^2P_{3/2}$	17.4228
10	Ne	Neon	(He)$2s^2\ 2p^6$	$^1S_0$	21.5646
11	Na	Sodium	(Ne)$3s$	$^2S_{1/2}$	5.1391
12	Mg	Magnesium	(Ne)$3s^2$	$^1S_0$	7.6462
13	Al	Aluminum	(Ne)$3s^2\ 3p$	$^2P_{1/2}$	5.9858
14	Si	Silicon	(Ne)$3s^2\ 3p^2$	$^3P_0$	8.1517
15	P	Phosphorus	(Ne)$3s^2\ 3p^3$	$^4S_{3/2}$	10.4867
16	S	Sulfur	(Ne)$3s^2\ 3p^4$	$^3P_2$	10.3600
17	Cl	Chlorine	(Ne)$3s^2\ 3p^5$	$^2P_{3/2}$	12.9676
18	Ar	Argon	(Ne)$3s^2\ 3p^6$	$^1S_0$	15.7596
19	K	Potassium	(Ar) $4s$	$^2S_{1/2}$	4.3407
20	Ca	Calcium	(Ar) $4s^2$	$^1S_0$	6.1132
21	Sc	Scandium	(Ar)$3d\ 4s^2$	$^2D_{3/2}$	6.5615
22	Ti	Titanium	(Ar)$3d^2\ 4s^2$	$^3F_2$	6.8281
23	V	Vanadium	(Ar)$3d^3\ 4s^2$	$^4F_{3/2}$	6.7463
24	Cr	Chromium	(Ar)$3d^5\ 4s$	$^7S_3$	6.7665
25	Mn	Manganese	(Ar)$3d^5\ 4s^2$	$^6S_{5/2}$	7.4340
26	Fe	Iron	(Ar)$3d^6\ 4s^2$	$^5D_4$	7.9024
27	Co	Cobalt	(Ar)$3d^7\ 4s^2$	$^4F_{9/2}$	7.8810
28	Ni	Nickel	(Ar)$3d^8\ 4s^2$	$^3F_4$	7.6398
29	Cu	Copper	(Ar)$3d^{10}4s$	$^2S_{1/2}$	7.7264
30	Zn	Zinc	(Ar)$3d^{10}4s^2$	$^1S_0$	9.3942
31	Ga	Gallium	(Ar)$3d^{10}4s^2 4p$	$^2P_{1/2}$	5.9993
32	Ge	Germanium	(Ar)$3d^{10}4s^2 4p^2$	$^3P_0$	7.8994
33	As	Arsenic	(Ar)$3d^{10}4s^2 4p^3$	$^4S_{3/2}$	9.7886
34	Se	Selenium	(Ar)$3d^{10}4s^2 4p^4$	$^3P_2$	9.7524
35	Br	Bromine	(Ar)$3d^{10}4s^2 4p^5$	$^2P_{3/2}$	11.8138
36	Kr	Krypton	(Ar)$3d^{10}4s^2 4p^6$	$^1S_0$	13.9996

Electronic structure of the elements (*cont.*)

37	Rb	Rubidium	(Kr) $5s$	$^2S_{1/2}$	4.1771
38	Sr	Strontium	(Kr) $5s^2$	$^1S_0$	5.6949
39	Y	Yttrium	(Kr)$4d\ 5s^2$	$^2D_{3/2}$	6.2171
40	Zr	Zirconium	(Kr)$4d^2\ 5s^2$	$^3F_2$	6.6339
41	Nb	Niobium	(Kr)$4d^4\ 5s$	$^6D_{1/2}$	6.7589
42	Mo	Molybdenum	(Kr)$4d^5\ 5s$	$^7S_3$	7.0924
43	Tc	Technetium	(Kr)$4d^5\ 5s^2$	$^6S_{5/2}$	7.28
44	Ru	Ruthenium	(Kr)$4d^7\ 5s$	$^5F_5$	7.3605
45	Rh	Rhodium	(Kr)$4d^8\ 5s$	$^4F_{9/2}$	7.4589
46	Pd	Palladium	(Kr)$4d^{10}$	$^1S_0$	8.3369
47	Ag	Silver	(Kr)$4d^{10}\,5s$	$^2S_{1/2}$	7.5763
48	Cd	Cadmium	(Kr)$4d^{10}\,5s^2$	$^1S_0$	8.9938
49	In	Indium	(Kr)$4d^{10}\,5s^2\,5p$	$^2P_{1/2}$	5.7864
50	Sn	Tin	(Kr)$4d^{10}\,5s^2\,5p^2$	$^3P_0$	7.3439
51	Sb	Antimony	(Kr)$4d^{10}\,5s^2\,5p^3$	$^4S_{3/2}$	8.6084
52	Te	Tellurium	(Kr)$4d^{10}\,5s^2\,5p^4$	$^3P_2$	9.0096
53	I	Iodine	(Kr)$4d^{10}\,5s^2\,5p^5$	$^2P_{3/2}$	10.4513
54	Xe	Xenon	(Kr)$4d^{10}\,5s^2\,5p^6$	$^1S_0$	12.1298
55	Cs	Cesium	(Xe) $6s$	$^2S_{1/2}$	3.8939
56	Ba	Barium	(Xe) $6s^2$	$^1S_0$	5.2117
57	La	Lanthanum	(Xe) $5d\ 6s^2$	$^2D_{3/2}$	5.5770
58	Ce	Cerium	(Xe)$4f\ 5d\ 6s^2$	$^1G_4$	5.5387
59	Pr	Praseodymium	(Xe)$4f^3\ 6s^2$	$^4I_{9/2}$	5.464
60	Nd	Neodymium	(Xe)$4f^4\ 6s^2$	$^5I_4$	5.5250
61	Pm	Promethium	(Xe)$4f^5\ 6s^2$	$^6H_{5/2}$	5.58
62	Sm	Samarium	(Xe)$4f^6\ 6s^2$	$^7F_0$	5.6436
63	Eu	Europium	(Xe)$4f^7\ 6s^2$	$^8S_{7/2}$	5.6704
64	Gd	Gadolinium	(Xe)$4f^7\ 5d\ 6s^2$	$^9D_2$	6.1501
65	Tb	Terbium	(Xe)$4f^9\ 6s^2$	$^6H_{15/2}$	5.8638
66	Dy	Dysprosium	(Xe)$4f^{10}\ 6s^2$	$^5I_8$	5.9389
67	Ho	Holmium	(Xe)$4f^{11}\ 6s^2$	$^4I_{15/2}$	6.0215
68	Er	Erbium	(Xe)$4f^{12}\ 6s^2$	$^3H_6$	6.1077
69	Tm	Thulium	(Xe)$4f^{13}\ 6s^2$	$^2F_{7/2}$	6.1843
70	Yb	Ytterbium	(Xe)$4f^{14}\ 6s^2$	$^1S_0$	6.2542
71	Lu	Lutetium	(Xe)$4f^{14}5d\ 6s^2$	$^2D_{3/2}$	5.4259
72	Hf	Hafnium	(Xe)$4f^{14}5d^2 6s^2$	$^3F_2$	6.8251
73	Ta	Tantalum	(Xe)$4f^{14}5d^3 6s^2$	$^4F_{3/2}$	7.5496
74	W	Tungsten	(Xe)$4f^{14}5d^4 6s^2$	$^5D_0$	7.8640
75	Re	Rhenium	(Xe)$4f^{14}5d^5 6s^2$	$^6S_{5/2}$	7.8335
76	Os	Osmium	(Xe)$4f^{14}5d^6 6s^2$	$^5D_4$	8.4382
77	Ir	Iridium	(Xe)$4f^{14}5d^7 6s^2$	$^4F_{9/2}$	8.9670
78	Pt	Platinum	(Xe)$4f^{14}5d^9 6s$	$^3D_3$	8.9587

Electronic structure of the elements (*cont.*)

79	Au	Gold	(Xe)$4f^{14}5d^{10}6s$	$^2S_{1/2}$	9.2255
80	Hg	Mercury	(Xe)$4f^{14}5d^{10}6s^2$	$^1S_0$	10.4375
81	Tl	Thallium	(Xe)$4f^{14}5d^{10}6s^2\ 6p$	$^2P_{1/2}$	6.1082
82	Pb	Lead	(Xe)$4f^{14}5d^{10}6s^2\ 6p^2$	$^3P_0$	7.4167
83	Bi	Bismuth	(Xe)$4f^{14}5d^{10}6s^2\ 6p^3$	$^4S_{3/2}$	7.2856
84	Po	Polonium	(Xe)$4f^{14}5d^{10}6s^2\ 6p^4$	$^3P_2$	8.4167
85	At	Astatine	(Xe)$4f^{14}5d^{10}6s^2\ 6p^5$	$^2P_{3/2}$	
86	Rn	Radon	(Xe)$4f^{14}5d^{10}6s^2\ 6p^6$	$^1S_0$	10.7485
87	Fr	Francium	(Rn) $7s$	$^2S_{1/2}$	4.0727
88	Ra	Radium	(Rn) $7s^2$	$^1S_0$	5.2784
89	Ac	Actinium	(Rn) $6d\ 7s^2$	$^2D_{3/2}$	5.17
90	Th	Thorium	(Rn) $6d^2\ 7s^2$	$^3F_2$	6.3027
91	Pa	Protactinium	(Rn)$5f^2\ 6d\ 7s^2$	$^4K_{11/2}$	5.89
92	U	Uranium	(Rn)$5f^3\ 6d\ 7s^2$	$^5L_6$	6.1941
93	Np	Neptunium	(Rn)$5f^4\ 6d\ 7s^2$	$^6L_{11/2}$	6.2657
94	Pu	Plutonium	(Rn)$5f^6\ 7s^2$	$^7F_0$	6.0262
95	Am	Americium	(Rn)$5f^7\ 7s^2$	$^8S_{7/2}$	5.9738
96	Cm	Curium	(Rn)$5f^7\ 6d\ 7s^2$	$^9D_2$	5.9915
97	Bk	Berklium	(Rn)$5f^9\ 7s^2$	$^6H_{15/2}$	6.1979
98	Cf	Californium	(Rn)$5f^{10}\ 7s^2$	$^5I_8$	6.2817
99	Es	Einsteinium	(Rn)$5f^{11}\ 7s^2$	$^4I_{15/2}$	6.42
100	Fm	Fermium	(Rn)$5f^{12}\ 7s^2$	$^3H_6$	6.50
101	Md	Mendelevium	(Rn)$5f^{13}\ 7s^2$	$^2F_{7/2}$	6.58
102	No	Nobelium	(Rn)$5f^{14}\ 7s^2$	$^1S_0$	6.65
103	Lr	Lawrencium	(Rn)$5f^{14}\ 7s^2\ 7p$?	$^2P_{1/2}$?	
104	Rf	Rutherfordium	(Rn)$5f^{14}6d^2\ 7s^2$?	$^3F_2$?	6.0?

(From Martin, W.C. and Wiese, W.L. in *Atomic, Molecular, & Optical Physics Handbook*, Drake, G.W.F., ed., American Institute of Physics, 1996, with permission.)

Ionization energies of neutral atoms

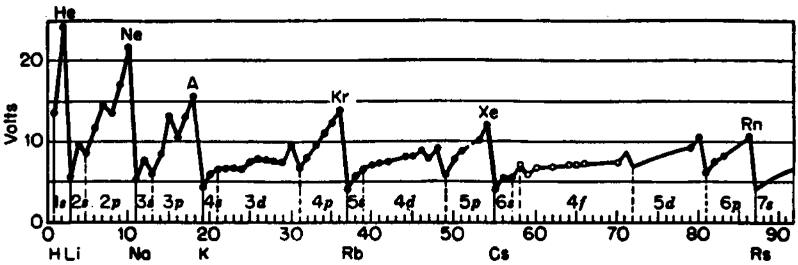

Atomic radiation

Spectroscopic terminology

Orbital angular momentum L or l	0	1	2	3	4	5	6	7	8
L	S	P	D	F	G	H	I	K	L
l	s	p	d	f	g	h	i	k	l

$L = \sum l$ (individual electrons), orbital angular momentum,
$S = \sum s$ (individual electrons), spin angular momentum,
$J = L + S$ (LS coupling), total angular momentum,
$J = \sum j;\ \ j = l + s$ (jj coupling),
M = magnetic quantum number; components of J in magnetic field.

n(total quantum number)	1	2	3	4	5	6	7
Shell	K	L	M	N	O	P	Q

The quantities n, l, S, L, J, M define a Zeeman *state.*

The quantities n, l, S, L, J define a *level* which includes $2J + 1$ *states*, e.g., the atomic level $2p^3\,{}^4S^0_{3/2}$.

Interpretation:

- 2: outer electrons, $n = 2$ (L shell).
- p^3: 3 outer electrons, $l = 1$.
- 4: multiplicity $= 4$ ($2S + 1 = 4, S = 3/2$, the spin).
- S: orbital momentum $L = 0$.
- 3/2: $J = 3/2$.
- 0: the level has odd parity.

The quantities n, l, S, L define an atomic *term*, the set of $(2S + 1) \times (2L + 1)$ states characterized by given values of L and S.

A transition between two *levels* is called a spectral *line.*

The totality of transitions between two *terms* is a *multiplet.*

Atomic radiation (*cont.*)

Emission and absorption of radiation (cgs units)

N_k — W_k $g_k = 2J_k + 1$, statistical weight of level k

absorption: $N_i B_{ik} I_v$ (transitions cm^{-3} s^{-1})

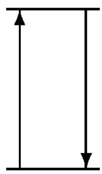

$N_k(A_{ki} + B_{ki}I_v)$: *spontaneous emission and induced emission* (transitions cm^{-3} s^{-1})

N_i — W_i $g_i = 2J_i + 1$

where

A_{ki} = Einstein coefficient of spontaneous emission,

N_k = number of atoms per unit volume in level k,

B_{ik} = induced transition probability from level i to level k,

I_ν = specific intensity of radiation field at frequency ν,

$h\nu = W_k - W_i$, transition energy,

$$g_k B_{ki} = g_i B_{ik},$$

$$\frac{g_k}{g_i} A_{ki} = \frac{2h\nu^3}{c^2} B_{ik} = \frac{8\pi^2 e^2 \nu^2}{m_e c^3} f_{ik},$$

where f_{ik} = absorption oscillator strength.

$$\sigma_i = \int \sigma_\nu d\nu = \frac{\pi e^2}{m_e c} f_{ik} N_i,$$

is the integrated atomic scattering cross-section for a spectrum line.
σ_ν = atomic scattering cross-section near an absorption line.

Local thermodynamic equilibrium

Saha distribution

This connects equilibrium densities $\tilde{n}_i, \tilde{n}_e$ and N^+ of bound levels i, of free electrons at temperature T_e and of ions by

$$\frac{\tilde{n}_i}{\tilde{n}_e \tilde{N}^+} = \left[\frac{g(i)}{g_e g_A^+}\right] \frac{h^3}{(2\pi m_e k T_e)^{3/2}} \exp\left(\frac{I_i}{k_B T_e}\right),$$

where the electronic statistical weights of the free electron, the ion of charge $Z + 1$ and the recombined $e^- - A^+$ species of net charge Z and ionization potential I_i are $g_e = 2$, g_A^+ and $g(i)$, respectively.

Boltzmann distribution

This connects the equilibrium populations of bound levels i of energy E_i by

$$\frac{\tilde{n}_i}{\tilde{n}_j} = \left[\frac{g(i)}{g(j)}\right] \exp\left[-\frac{(E_i - E_j)}{k_B T_e}\right].$$

Atomic radiation (*cont.*)

Doppler shift

$$\frac{\Delta\lambda}{\lambda} \approx \frac{v}{c} \quad (v = \text{velocity of source}).$$

Doppler width of spectral line (FWHM, Maxwellian distribution)

$$\frac{\Delta\lambda_D}{\lambda} = \frac{2[(2\ln 2)kT/M]^{1/2}}{c} = 7.162 \times 10^{-7}\sqrt{\left[\frac{T(K)}{\text{at. wt.}}\right]},$$

where M is the mass of the radiating atom, and T is the temperature.

Electron-ion recombination

This proceeds via the following four processes:

(1) radiative recombination

$$e^- + A^+(i) \longrightarrow A(nl) + h\nu,$$

(2) three-body collisional-radiative recombination

$$e^- + A^+ + e^- \longrightarrow A + e^-,$$

$$e^- + A^+ + M \longrightarrow A + M,$$

(3) dielectronic recombination in which an electron collides with an ion to give a doubly excited ion followed by a radiative transition to a singly excited state

$$e^- + A^{Z+}(i) \rightleftharpoons \left[A^{Z+}(k) - e^-\right]_{nl} \longrightarrow A^{(Z-1)+}_{n'l'}(f) + h\nu,$$

(4) dissociative recombination for molecular ions

$$e^- + AB^+ \longrightarrow A + B^*.$$

Selection rules for discrete atomic transitions

	Electric dipole (E1) ("allowed")	Magnetic dipole (M1) ("forbidden")	Electric quadrupole (E2) ("forbidden")
Rigorous rules	1. $\Delta J = 0, \pm 1$ (except $0 \not\leftrightarrow 0$)	$\Delta J = 0, \pm 1$ (except $0 \not\leftrightarrow 0$)	$\Delta J = 0, \pm 1, \pm 2$ (except $0 \not\leftrightarrow 0$, $1/2 \not\leftrightarrow 1/2$, $0 \not\leftrightarrow 1$)
	2. $\Delta M = 0, \pm 1$ (except $0 \not\leftrightarrow 0$ when $\Delta J = 0$)	$\Delta M = 0, \pm 1$ (except $0 \not\leftrightarrow 0$ when $\Delta J = 0$)	$\Delta M = 0, \pm 1, \pm 2$
	3. Parity change	No parity change	No parity change
With negligible configuration interaction	4. One electron jumping, with $\Delta l = \pm 1$, Δn arbitrary	No change in electron configuration; i.e., for all electrons, $\Delta l = 0$, $\Delta n = 0$	No change in electron configuration; *or* one electron jumping with $\Delta l = 0, \pm 2, \Delta n$ arbitrary
For LS coupling only	5. $\Delta S = 0$	$\Delta S = 0$	$\Delta S = 0$
	6. $\Delta L = 0, \pm 1$ (except $0 \not\leftrightarrow 0$)	$\Delta L = 0$ $\Delta J = \pm 1$	$\Delta L = 0, \pm 1, \pm 2$ (except $0 \not\leftrightarrow 0, 0 \not\leftrightarrow 1$)

(From Martin, W.C. and Wiese, W.L. in *Atomic, Molecular, & Optical Physics Handbook*, Drake, G.W.F., ed., American Institute of Physics, 1996, with permission.)

X-ray atomic energy levels (eV)

Z	element	K	L_{I}	$L_{\mathrm{II,III}}$
1	H	13.598		
2	He	24.587		
3	Li	54.75		
4	Be	111.0		
5	B	188.0		4.7
6	C	283.8		6.4
7	N	401.6		9.2
8	O	532.0	23.7	7.1
9	F	685.4	31	8.6
10	Ne	866.9	45	18.3
11	Na	1072.1	63.3	31.1
12	Mg	1305.0	89.4	51.4
13	Al	1559.6	117.7	73.1
14	Si	1838.9	148.7	99.2
15	P	2145.5	189.3	132.2
16	S	2472.0	229.2	164.8

Permitted transitions

K series	L series
$K\alpha_1 = K - L_{\mathrm{III}}$	$L\alpha_1 = L_{\mathrm{III}} - M_{\mathrm{V}}$
$K\alpha_2 = K - L_{\mathrm{II}}$	$L\alpha_2 = L_{\mathrm{III}} - M_{\mathrm{IV}}$
$K\beta_1 = K - M_{\mathrm{III}}$	$L\beta_1 = L_{\mathrm{II}} - M_{\mathrm{IV}}$
$K\beta_3 = K - M_{\mathrm{II}}$	
$K\beta_2 = K - N_{\mathrm{II,III}}$	

X-ray atomic energy levels (eV) (*cont.*)

Z element	K	L_{I}	L_{II}	L_{III}	M_{I}	$M_{II,III}$	$M_{IV,V}$	
17 Cl	2822.4	270.2	201.6	200.0	17.5	6.8		
18 Ar	3202.9	320	247.3	245.2	25.3	12.4		
19 K	3607.4	377.1	296.3	293.6	33.9	17.8		
20 Ca	4038.1	437.8	350.0	346.4	43.7	25.4		
21 Sc	4492.8	500.4	406.7	402.2	53.8	32.3	6.6	
22 Ti	4966.4	563.7	461.5	455.5	60.3	34.6	3.7	
23 V	5465.1	628.2	520.5	512.9	66.5	37.8	2.2	
24 Cr	5989.2	694.6	583.7	574.5	74.1	42.5	2.3	
25 Mn	6539.0	769.0	651.4	640.3	83.9	48.6	3.3	
26 Fe	7112.0	846.1	721.1	708.1	92.9	54.0	3.6	
27 Co	7708.9	925.6	793.6	778.6	100.7	59.5	2.9	
28 Ni	8332.8	1008.1	871.9	854.7	111.8	68.1	3.6	
29 Cu	8978.9	1096.6	951.0	931.1	119.8	73.6	1.6	
30 Zn	9658.6	1193.6	1042.8	1019.7	135.9	86.6	8.1	
31 Ga	10367.1	1297.7	1142.3	1115.4	158.1	106.8	102.9	17.4
32 Ge	11103.1	1414.3	1247.8	1216.7	180.0	127.9	120.8	28.7

X-ray atomic energy levels (eV) (*cont.*)

Z	element	K	L_{I}	L_{II}	L_{III}	M_{I}	M_{II}	M_{III}	M_{IV}	M_{V}	N_{I}	N_{II}	N_{III}
47	Ag	25514.0	3805.8	3523.7	3351.1	717.5	602.4	571.4	372.8	366.7	95.2	62.6	55.9
53	I	33169.4	5188.1	4852.1	4557.1	1072.1	930.5	874.6	631.3	619.4	186.4	122.7	
54	Xe	34561.4	5452.8	5103.7	4782.2		999.0	937.0		672.3		146.7	
55	Ca	35984.6	5714.3	5359.4	5011.9	1217.1	1065.0	997.6	739.5	725.5	230.8	172.3	161.6
74	W	69525.0	12099.8	11544.0	10206.8	2819.6	2574.9	2281.0	1871.6	1809.2	595.0	491.6	425.3
78	Pt	78394.8	13879.9	13272.6	11563.7	3296.0	3026.5	2645.4	2201.9	2121.6	722.0	609.2	519.0
79	Au	80724.9	14352.8	13733.6	11918.7	3424.9	3147.8	2743.0	2291.1	2205.7	758.8	643.7	545.4
82	Pb	88004.5	15860.8	15220.0	13035.2	3850.7	3554.2	3066.4	2585.6	2484.0	893.6	763.9	644.5
92	U	115606.1	21757.4	20947.6	17166.3	5548.0	5182.2	4303.4	3727.6	3551.7	1440.8	1272.6	1044.9

Z	element	N_{IV}	N_{V}	N_{VI}	N_{VII}	O_{I}	O_{II}	O_{III}	O_{IV}	O_{V}	P_{I}	P_{II}	P_{III}
47	Ag	3.3											
53	I	49.6				13.6							
54	Xe						3.3						
55	Ca	78.8	76.5			22.7	13.1	11.4					
74	W	258.8	245.4	36.5	33.6	77.1	46.8	35.6	6.1				
78	Pt	330.8	313.3	74.3	71.1	101.7	65.3	51.7	2.2				
79	Au	352.0	333.9	86.4	82.8	107.8	71.7	53.7	2.5				
82	Pb	435.2	412.9	142.9	138.1	147.3	104.8	86.0	21.8	19.2	3.1	0.7	
92	U	780.4	737.7	391.3	380.9	323.7	259.3	195.1	105	96.3	70.7	42.3	32.3

(List from Bearden, J. A. and Burr, A. F., *Rev. Mod. Phys.*, **39**, 125, 1967.)

X-ray atomic energy levels (eV) (*cont.*)

Notation for X-ray lines

Siegbahn notation	Transition	Siegbahn notation	Transition	Siegbahn notation	Transition	Siegbahn notation	Transition
$K\alpha_1$	KL_{III}	$L\gamma_2$	$L_{\mathrm{I}}N_{\mathrm{II}}$	LV	$L_{\mathrm{II}}N_{\mathrm{VI}}$	$L\beta_2$	$L_{\mathrm{III}}N_{\mathrm{V}}$
$K\alpha_2$	KL_{II}	$L\gamma_3$	$L_{\mathrm{I}}N_{\mathrm{III}}$	$L\gamma_8$	$L_{\mathrm{II}}O_{\mathrm{I}}$	Lu	$L_{\mathrm{III}}N_{\mathrm{VI,\,VII}}$
$K\beta_3$	KM_{II}	$L\gamma_{11}$	$L_{\mathrm{I}}N_{\mathrm{V}}$	$L\gamma_6$	$L_{\mathrm{II}}O_{\mathrm{IV}}$	$L\beta_7$	$L_{\mathrm{III}}O_{\mathrm{I}}$
$K\beta_1$	KM_{III}	$L\gamma_4$	$L_{\mathrm{I}}O_{\mathrm{III}}$	Ll	$L_{\mathrm{III}}M_{\mathrm{I}}$	$L\beta_3$	$L_{\mathrm{III}}O_{\mathrm{IV,\,V}}$
$K\beta_5$	$KM_{\mathrm{IV,\,V}}$	$L\gamma_{13}$	$L_{\mathrm{I}}P_{\mathrm{II,\,III}}$	Lt	$L_{\mathrm{III}}M_{\mathrm{II}}$	$M\gamma$	$M_{\mathrm{III}}N_{\mathrm{V}}$
$K\beta_2$	$KN_{\mathrm{II,\,III}}$	$L\eta$	$L_{\mathrm{II}}M_{\mathrm{I}}$	Ls	$L_{\mathrm{III}}M_{\mathrm{III}}$	$M\beta$	$M_{\mathrm{IV}}N_{\mathrm{VI}}$
$K\beta_4$	$KN_{\mathrm{IV,\,V}}$	$L\beta_{17}$	$L_{\mathrm{II}}M_{\mathrm{III}}$	$L\alpha_2$	$L_{\mathrm{III}}M_{\mathrm{IV}}$	$M\zeta_2$	$M_{\mathrm{IV}}N_{\mathrm{II}}$
$L\beta_4$	L_IM_{II}	$L\beta_1$	$L_{\mathrm{II}}M_{\mathrm{IV}}$	$L\alpha_1$	$L_{\mathrm{III}}M_{\mathrm{V}}$	$M\zeta_1$	$M_{\mathrm{IV}}N_{\mathrm{III}}$
$L\beta_3$	$L_{\mathrm{I}}M_{\mathrm{III}}$	$L\gamma_5$	$L_{\mathrm{II}}N_{\mathrm{I}}$	$L\beta_6$	$L_{\mathrm{III}}N_{\mathrm{I}}$	$M\alpha_2$	$M_{\mathrm{V}}N_{\mathrm{VII}}$
$L\beta_{10}$	$L_{\mathrm{I}}M_{\mathrm{IV}}$	$L\gamma_1$	$L_{\mathrm{II}}N_{\mathrm{IV}}$	$L\beta_{13}$	$L_{\mathrm{III}}N_{\mathrm{IV}}$	$M\alpha_1$	$M_{\mathrm{V}}N_{\mathrm{VII}}$
$L\beta_9$	$L_{\mathrm{I}}M_{\mathrm{V}}$						

X-ray energy level diagram

X-ray energy-level diagram for ^{92}U, showing the transitions permitted by the selection rules $\Delta l = \pm 1$; $\Delta j = \pm 1, 0$. (Adapted from Richtmyer, F. K., Kennard, E. H. & Lauritsen, T., *Introduction to Modern Physics*, McGraw-Hill Book Company, 1955.)

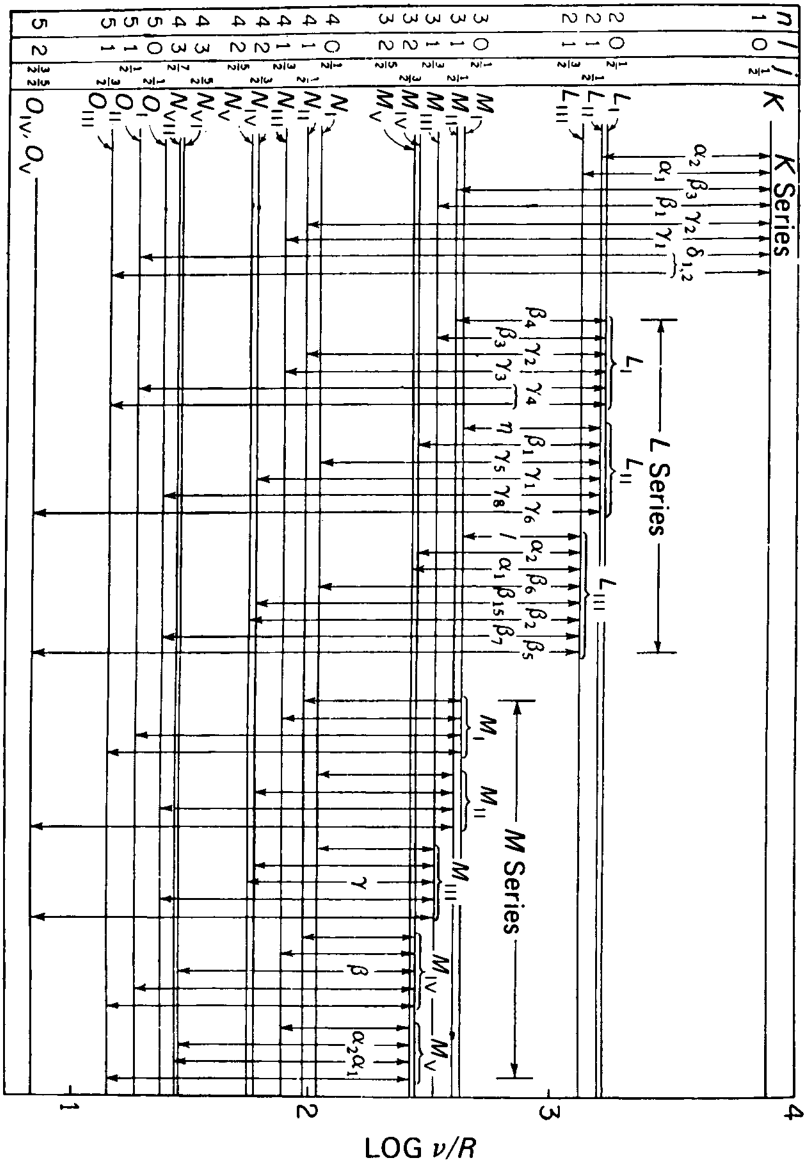

X-ray wavelengths

Wavelengths of K series lines representing transitions in the ordinary X-ray energy-level diagram allowed by the selection principles (Ångstrom)

Siegbahn		$K\alpha_2$	$K\alpha_1$	$K\beta$	$K\beta_1$	$K\beta_2$
Sommerfeld		$K\alpha'$	$K\alpha$	$K\beta_2$	$K\beta$	$K\gamma$
transition		$K - L_{II}$	$K - L_{III}$	$K - M_{II}$	$K - M_{III}$	$K - L_{II}N_{III}$
4	Be	115.7				
5	B	67.71				
6	C	44.54				
7	N	31.557				
8	O	23.567				
9	F	18.275				
11	Na	11.885		11.594		
12	Mg	9.869		9.539		
13	Al	8.3205		7.965		
14	Si	7.11106		6.7545		
15	P	6.1425		5.7921		
16	S	5.3637	5.3613	5.0211		
17	Cl	4.7212	4.7182	4.3942		
19	K	3.73707	3.73368	3.4468		
20	Ca	3.35495	3.35169	3.0834		
21	Sc	3.02840	3.02503	2.7739		
22	Ti	2.74681	2.74317	2.5090		
23	V	2.50213	2.49835	2.2797		
24	Cr	2.28891	2.28503	2.0806		
25	Mn	2.10149	2.09751	1.90620		
26	Fe	1.936012	1.932076	1.753013		
27	Co	1.78919	1.78529	1.61744		
28	Ni	1.65835	1.65450	1.47905		1.48561
29	Cu	1.541232	1.537395	1.38935		1.37824
30	Zn	1.43603	1.43217	1.29255		1.28107
31	Ga	1.34087	1.33715	1.20520		1.1938
32	Ge	1.25521	1.25130	1.12671		1.11459
33	As	1.17743	1.17344	1.05510		1.04281
34	Se	1.10652	1.10248	0.99013		0.97791
35	Br	1.04166	1.03759	0.93087		0.91853
36	Kr	0.9821	0.9781	0.8767		0.8643
37	Rb	0.92776	0.92364	0.82749	0.82696	0.81476
38	Sr	0.87761	0.87345	0.78183	0.78130	0.76921
39	Y	0.83132	0.82712	0.73972	0.73919	0.72713
40	Zr	0.78851	0.78430	0.70083	0.70028	0.68850
41	Nb	0.74889	0.74465	0.66496	0.66438	0.65280
42	Mo	0.712105	0.707831	0.631543	0.630978	0.619698
43	Te	0.675	0.672	0.610		
44	Ru	0.64606	0.64174	0.57193	0.57131	0.56051

Wavelengths of K series lines representing transitions in the ordinary X-ray energy-level diagram allowed by the selection principles *(cont.)*

Siegbahn		$K\alpha_2$	$K\alpha_1$	$K\beta$	$K\beta_1$	$K\beta_2$
Sommerfeld		$K\alpha'$	$K\alpha$	$K\beta_2$	$K\beta$	$K\gamma$
transition		$K-L_{II}$	$K-L_{III}$	$K-M_{II}$	$K-M_{III}$	$K-L_{II}N_{III}$
45	Rh	0.61637	0.61202	0.54509	0.54449	0.53396
46	Pd	0.58863	0.58427	0.52009	0.51947	0.50918
47	Ag	0.56267	0.55828	0.49665	0.49601	0.48603
48	Cd	0.53832	0.53390	0.47471	0.47408	0.46420
49	In	0.51548	0.51106	0.45423	0.45358	0.44408
50	Sn	0.49402	0.48957	0.43495	0.43430	0.42499
51	Sb	0.47387	0.46931	0.41623		0.40710
52	Te	0.45491	0.45037	0.39926		0.39037
53	I	0.43703	0.43249	0.38292	0.38315	0.37471
54	Xe	0.417		0.360		
55	Cs	0.40411	0.39959	0.35436	0.35360	0.34516
56	Ba	0.38899	0.38443	0.34089	0.34022	0.33222
57	La	0.37466	0.37004	0.32809	0.32726	0.31966
58	Ce	0.36110	0.35647	0.31572	0.31501	0.30770
59	Pr	0.34805	0.34340	0.30439	0.30360	0.29625
60	Nd	0.33595	0.33125	0.29351	0.29275	0.28573
62	Sm	0.31302	0.30833	0.27325	0.27250	0.26575
63	Eu	0.30265	0.29790	0.26386	0.26307	0.25645
64	Gd	0.29261	0.28782	0.25471	0.25394	0.24762
65	Tb	0.28286	0.27820	0.24629	0.24551	0.23912
66	Dy	0.27375	0.26903	0.23787	0.23710	0.23128
67	Ho	0.26499	0.26030			
68	Er	0.25664	0.25197	0.22300	0.22215	0.21671
69	Tm	0.24861	0.24387	0.21558	0.21487	
70	Yb	0.24098	0.23028	0.20916	0.20834	0.20322
71	Lu	0.23358	0.2282	0.20252	0.20171	0.19649
72	Hf	0.22653	0.22173	0.19583	0.19515	0.19042
73	Ta	0.21973	0.21488	0.18991		0.18452
74	W	0.21337	0.20856	0.18475	0.18397	0.17906
76	Os	0.20131	0.19645	0.17361		0.16875
77	Ir	0.19550	0.19065	0.16850		0.16376
78	Pt	0.19004	0.18223	0.16370		0.15887
79	Au	0.18483	0.17996	0.15902		0.15426
81	Tl	0.17466	0.16980	0.15011		0.14539
82	Pb	0.17004	0.16516	0.14606		0.14125
83	Bi	0.16525	0.16041	0.14205		0.13621
92	U	0.13095	0.12640	0.11187		0.10842

(From *Smithsonian Physical Tables.*)

Wavelength of the more prominent L group lines (Ångstrom)

Siegbahn		α_2	α_1	β_1	l	η
Sommerfeld		α'	α	β	ε	η
transition		$L_{III}-M_{IV}$	$L_{III}-M_V$	$L_{II}-M_V$	$L_{III}-M_I$	$L_{II}-M_I$
16	S	...		...	83.75	
20	Ca	36.27		...	40.90	
21	Sc	31.37		...	35.71	
22	Ti	27.37		...	31.33	
23	V	24.31		...	27.70	
24	Cr	21.53		21.19	23.84	23.28
25	Mn	19.40		19.04	22.34	
26	Fe	17.57		17.23	20.09	19.76
27	Co	15.93		15.63	18.25	17.86
28	Ni	14.53		14.25	16.66	16.28
29	Cu	13.306		13.027	15.26	14.87
30	Zn	12.229		11.960	13.97	13.61
31	Ga	11.27		11.01	12.89	12.56
32	Ge	10.415		10.153	11.922	11.587
33	As	9.652		9.395	11.048	10.711
34	Se	8.972		8.718	10.272	9.939
35	Br	8.358		8.109	9.564	9.235
37	Rb	7.3027				
38	Sr	6.8486		6.610	7.822	7.506
39	Y	6.4357		6.2039	...	7.0310
					β_2	γ
					γ	δ
					$L_{III}-N_V$	$L_{III}-N_V$
40	Zr	6.057		5.8236	5.5742	5.3738
41	Nb	5.718	5.7120	5.4803	5.2260	5.0248
42	Mo	5.401	5.3950	5.1665	4.9100	
44	Ru	4.8437	4.8357	4.6110	4.3619	4.1728
45	Rh	4.5956	4.5878	4.3640	4.1221	3.9357
46	Pd	4.3666	4.3585	4.1373	3.9007	3.7164
47	Ag	4.1538	4.1456	3.9266	3.6938	3.5149
48	Cd	3.9564	3.9478	3.7301	3.5064	3.3280
49	In	3.7724	3.7637	3.5478	3.3312	3.1553
50	Sn	3.60151	3.59257	3.3779	3.16861	2.99494
51	Sb	3.4408	3.4318	3.2184	3.0166	2.8451
52	Te	3.2910	3.2820	3.0700	2.8761	2.7065
53	I	3.1509	3.1417	2.9309	2.7461	2.5775
55	Cs	2.8956	2.8861	2.6778	2.5064	2.3425
56	Ba	2.7790	2.7696	2.5622	2.3993	2.2366
57	La	2.6689	2.6597	2.4533	2.2980	2.1372
58	Ce	2.5651	2.5560	2.3510	2.2041	2.0443
59	Pr	2.4676	2.4577	2.2539	2.1148	1.9568
60	Nd	2.3756	2.3653	2.1622	2.0314	1.8738
62	Sm	2.2057	2.1950	1.9936	1.8781	1.7231
63	Eu	2.1273	2.1163	1.9163	1.8082	1.6543

Wavelength of the more prominent L group lines (*cont.*)

Siegbahn Sommerfeld transition	α_2 α' $L_{III} - M_{IV}$	α_1 α $L_{III} - M_V$	β_1 β $L_{II} - M_V$	l ε $L_{III} - M_I$	η η $L_{II} - M_I$
64 Gd	2.0526	2.0419	1.8425	1.7419	1.5886
65 Tb	1.9823	1.9715	1.7727	1.6790	1.5266
66 Dy	1.9156	1.9046	1.7066	1.6198	1.4697
67 Ho	1.8521	1.8410	1.6435	1.5637	1.4142
68 Er	1.79202	1.78068	1.58409	1.51094	1.3611
69 Tm	1.7339	1.7228	1.5268	1.4602	1.3127
70 Yb	1.67942	1.66844	1.4725	1.41261	1.26512
71 Lu	1.6270	1.61617	1.42067	1.36731	1.21974
72 Hf	1.57704	1.56607	1.3711	1.3235	1.1765
73 Ta	1.52978	1.51885	1.32423	1.28190	1.13558
74 W	1.48438	1.47336	1.27917	1.24203	1.09630
75 Re	1.4410	1.42997	1.23603	1.2041	1.0587
76 Os	1.39866	1.38859	1.19490	1.16884	1.02296
77 Ir	1.3598	1.34847	1.15540	1.13297	0.98876
78 Pt	1.32155	1.31033	1.11758	1.09974	0.95599
79 Au	1.28502	1.27377	1.08128	1.06801	0.92461
80 Hg	1.24951	1.23863	1.04652	1.03770	0.8946
81 Tl	1.21626	1.20493	1.01299	1.00822	0.86571
82 Pb	1.18408	1.17258	0.98083	0.98083	0.83801
83 Bi	1.15301	1.14150	0.95002	0.95324	0.81143
90 Th	0.96585	0.95405	0.76356	0.79192	0.65176
91 Pa	0.9427	0.9309	0.7407	0.7721	0.6325
92 U	0.92062	0.90874	0.71851	0.75307	0.61359

(From *Smithsonian Physical Tables*)

Main bound-bound electromagnetic transitions

Transitions	Energy [eV]	Spectral region	Example
Hyperfine structure	10^{-5}	Radiofrequencies	21 cm hydrogen line
Spin-orbit coupling	10^{-5}	Radiofrequencies	1666 MHz transitions of OH molecule
Molecular rotation	10^{-2}–10^{-4}	Millimetric, infrared	1-0 transition of CO molecule at 2.6 mm
Molecular rotation-vibration	1–10^{-1}	Infrared	H_2 lines near 2μm
Atomic fine structure	1–10^{-3}	Infrared	Ne II line at 12.8 μm
Electronic transitions of atoms, molecules and ions	10^{-2}–10	Ultraviolet, visible, infrared	Lyman, Balmer, etc. series of H, resonance lines of CI, HeI
	10–10^4	Ultraviolet, X-ray	K,L shell electron lines

(Adapted from Lena, P., *Observational Astrophysics*, Springer-Verlag, 1986.)

Bibliography

Atomic, Molecular, & Optical Physics Handbook, Drake, G.W.F., ed., American Institute of Physics, 1996.

Atomic Energy Levels, Moore, C.E., NBS Circular 467, US Government Printing Office.

An Ultraviolet Multiplet Table, Moore, C.E., NBS Circular 488, US Government Printing Office.

Note: Links to WWW resources which supplement the material in this chapter can be found at:

http://www.astrohandbook.com

Chapter 12

Electromagnetic radiation

And God said:

$$\nabla \cdot \mathbf{D} = 4\pi\rho \qquad \nabla \times \mathbf{H} = \frac{4\pi\mathbf{J}}{c} + \frac{1}{c}\frac{\partial \mathbf{D}}{\partial t}$$

$$\nabla \cdot \mathbf{B} = 0 \qquad \nabla \times \mathbf{E} + \frac{1}{c}\frac{\partial \mathbf{B}}{\partial t} = 0$$

And there was light. - Unknown

Radiation by a point charge (cgs units)

The Liénard-Wiechert potentials for a point charge e:

$$\left.\begin{aligned}\Phi(\mathbf{x},t) &= e\left[\frac{1}{\kappa R}\right]_{\mathrm{ret}}\\ \mathbf{A}(\mathbf{x},t) &= e\left[\frac{\boldsymbol{\beta}}{\kappa R}\right]_{\mathrm{ret}}\end{aligned}\right\}$$

The square bracket with subscript ret means that the quantity in brackets is to be evaluated at the retarded time, $t' = t - [R(t')/c]$.

$\kappa = 1 - \mathbf{n}\cdot\boldsymbol{\beta}$, where $c\boldsymbol{\beta}$ is the instantaneous velocity of the particle, and $\mathbf{n} = \mathbf{R}/R$ is a unit vector directed from the position of the charge to the observation point.

The electric field and magnetic fields:

$$\mathbf{E}(\mathbf{x},t) = e\left[\frac{(\mathbf{n}-\boldsymbol{\beta})(1-\beta^2)}{\kappa^3 R^2}\right]_{\mathrm{ret}} + \frac{e}{c}\left[\frac{\mathbf{n}}{\kappa^3 R}\times\{(\mathbf{n}-\boldsymbol{\beta})\times\dot{\boldsymbol{\beta}}\}\right]_{\mathrm{ret}}$$

$$\mathbf{B} = \mathbf{n}\times\mathbf{E}$$

Total power radiated:

$$P = \frac{2}{3}\frac{e^2}{c}\gamma^6[(\dot{\beta})^2 - (\boldsymbol{\beta}\times\dot{\boldsymbol{\beta}})^2]$$

where $\gamma = (1-\beta^2)^{-1/2}$, the Lorentz factor.

If the charge is observed in a reference frame where its velocity is small compared to that of light,

$$P = \frac{2}{3}e^2\,\frac{\dot{\beta}^2}{c}$$

Blackbody radiation (cgs units)

Planck functions (brightness of a blackbody)

$$B_\nu(T) = \frac{2h\nu^3}{c^2}\frac{1}{\left(\exp\left(\frac{h\nu}{kT}\right)-1\right)} \text{ erg cm}^{-2}\text{ s}^{-1}\text{ Hz}^{-1}\text{ sr}^{-1}$$

$$B_\lambda(T) = \frac{2hc^2}{\lambda^5}\frac{1}{\left(\exp\left(\frac{hc}{\lambda kT}\right)-1\right)} \text{ erg cm}^{-2}\text{ s}^{-1}\text{ cm}^{-1}\text{ sr}^{-1}$$

$$B_{\tilde\nu}(T) = \frac{2hc^2\tilde\nu^3}{\left(\exp\left(\frac{hc\tilde\nu}{kT}\right)-1\right)} \text{ erg cm}^{-2}\text{ s}^{-1}\text{ (cm}^{-1})^{-1}\text{ sr}^{-1}$$

$$B_\nu(T)d\nu = B_\lambda(T)d\lambda = B_{\tilde\nu}(T)d\tilde\nu$$

Rayleigh-Jeans law

$h\nu/kT << 1$

$$B_\nu(T) = 2\left(\frac{\nu}{c}\right)^2 kT$$

Wien's law

$h\nu/kT >> 1$

$$B_\nu(T) = \frac{2h\nu^3}{c^2}\exp\left(-\frac{h\nu}{kT}\right)$$

Stefan-Boltzmann law

$$\text{total emittance} = \pi\int_0^\infty B_\nu(T)d\nu = \sigma T^4 \text{ erg cm}^{-2}\text{ s}^{-1}$$

$$\text{where } \sigma = \frac{2\pi^5 k^4}{15c^2h^3} = 5.67\times10^{-5}\text{ erg cm}^{-2}\text{ deg}^{-4}\text{ s}^{-1}$$

Wien displacement law

Maximizing B_ν:	Maximizing B_λ:
$\nu_\mathrm{m} = 5.9\times10^{10}T$ Hz	$\nu_\mathrm{m} = 10.3\times10^{10}T$ Hz
$\lambda_\mathrm{m} = 0.51T^{-1}$ cm	$\lambda_\mathrm{m} = 0.29T^{-1}$ cm

Mean photon energy

$$\langle h\nu \rangle = \frac{\int_0^\infty B_\nu(T)d\nu}{\int_0^\infty (B_\nu(T)/h\nu)d\nu} = \left(\frac{\zeta(4)}{\zeta(3)}\right)\left(\frac{\Gamma(4)}{\Gamma(3)}\right) kT = 2.7012kT.$$

where $\zeta(n)$ = Riemann zeta function; $\Gamma(n)$ = gamma function.

Radiation curves

Planck-law radiation curves. (Adapted from Kraus, J.D., *Radio Astronomy*, McGraw-Hill Book Company, 1966.)

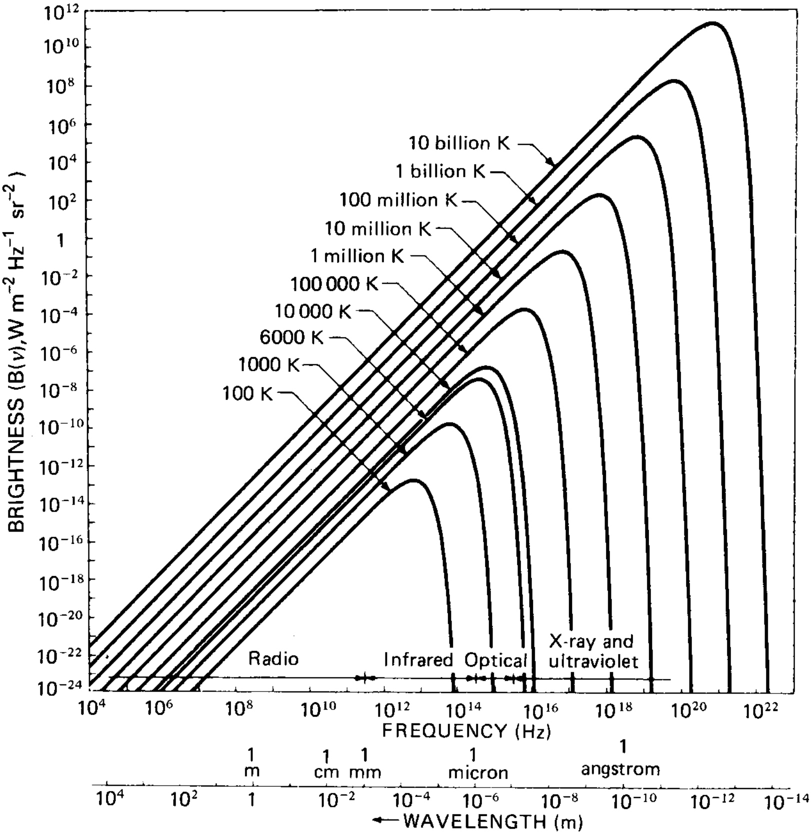

Synchrotron radiation (cgs units)

Single electron in a magnetic field

Total radiated power:

$$P = 1.6 \times 10^{-15}\gamma^2 B^2 \beta^2 \sin^2\alpha \quad \text{erg s}^{-1},$$

where

$\gamma = (1-\beta^2)^{-1/2} = E/mc^2$,

E = total energy of particle,

$\beta = \nu/c$,

B = magnetic induction in Gauss,

α = pitch angle, angle between B and velocity vector.

Synchrotron lifetime:

$$t_s = \frac{3 \times 10^8}{\gamma B^2 \beta^2 \sin^2\alpha} \text{ s.}$$

Spectrum:

$P(\nu) = 2.3 \times 10^{-22} B \sin\alpha F(\nu/\nu_c)$ erg s^{-1} Hz^{-1} ($\alpha \gg 1/\gamma$).

$\nu_c = 4.3 \times 10^6 B\gamma^2 \sin\alpha$ Hz (critical frequency).

$$F(x) = x \int_x^\infty d\xi\, K_{5/3}(\xi), \quad x = \nu/\nu_c.$$

$K_{5/3}(\xi)$ is the modified Bessel function of fractional order 5/3.

A plot of the function $F(x)$ or, equivalently, the dimensionless synchrotron spectrum. $F(\nu/\nu_c)$ reaches its maximum value of 0.918 at $\nu_m = 0.29\nu_c$. (Adapted from Blumenthal, G.R. & Tucker, W. H. in *X-ray Astronomy*, R. Giacconi & H. Gursky, eds., D. Reidel Publishing Company, Dordrecht, 1974.)

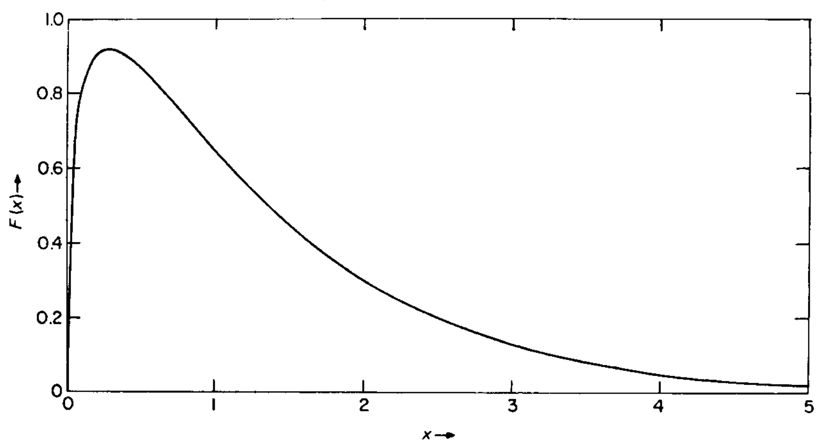

General distribution of electrons

$$\frac{dP}{dV\,d\nu} = \iint d\gamma\, d\Omega_\alpha\, n(\gamma, \alpha) P(\nu),$$ the spectral emission per unit volume,

where $n(\gamma, \alpha)\, d\gamma\, d\Omega_\alpha$ = density of electrons with Lorentz factor between γ and $\gamma + d\gamma$ and pitch angle between α and $\alpha + d\alpha$; $d\Omega_\alpha = 2\pi \sin\alpha\, d\alpha$; $P(\nu)$ = single electron spectrum.

Power law distribution of electrons

$$n(\gamma, \alpha) = N\gamma^{-s} g(\alpha)/4\pi,$$

and for local isotropy $g(\alpha) = 1$,

$$\frac{dP}{dV\,d\nu} = 1.7 \times 10^{-21} N a(s) B (4.3 \times 10^6 B/\nu)^{(s-1)/2} \text{ erg s}^{-1} \text{ cm}^{-3} \text{ Hz}^{-1}.$$

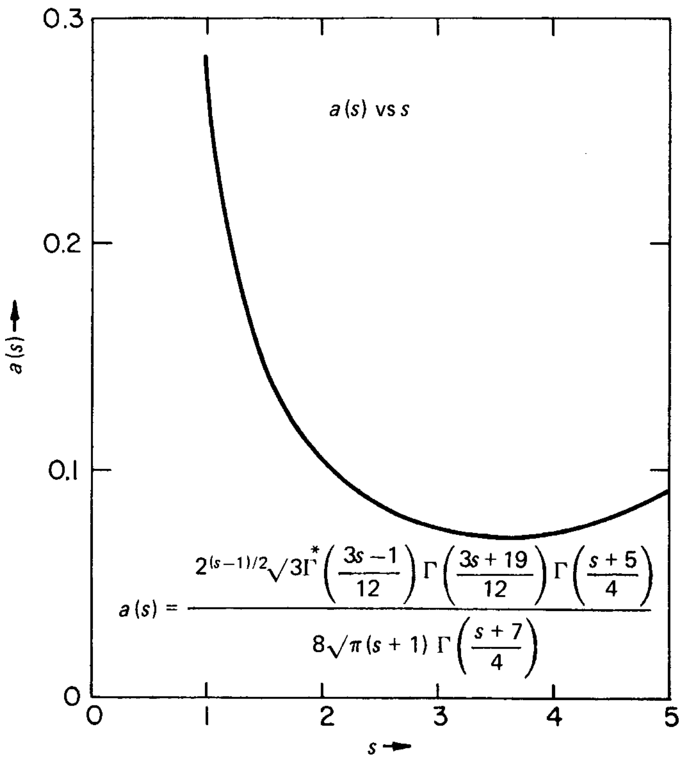

* note: $\Gamma(x)$ is the gamma function.

(Blumenthal, G.R., & Tucker, W.H., *op. cit.*)

Cerenkov radiation (cgs units)

Cerenkov radiation is the electromagnetic shock wave that arises from a charged particle moving through a transparent medium at a speed greater than that of light within the medium. Thus only if the particle

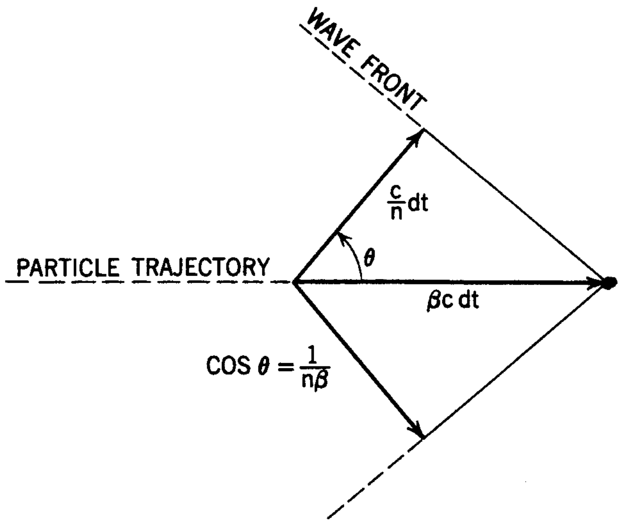

relative velocity $\beta = v/c$ and the refractive index n of the medium are such that $n\beta > 1$ will the radiation exist. When this condition is fulfilled, the Cerenkov light is emitted at the angle given by

$$\cos\theta = \frac{1}{n\beta}$$

where θ is the angle between the velocity for the particle and the propagation vector for any portion of the conical radiation wavefront, as illustrated above.

The spectral intensity of the radiation from a particle of charge ze is

$$\frac{d^2W}{dx\,d\nu} = \frac{4\pi z^2 e^2 \nu}{c^2}\left(1 - \frac{1}{1}n^2\beta^2\right) \text{ erg cm}^{-1}\text{Hz}^{-1}$$

In terms of photon emission, this becomes

$$\frac{d^2N}{dx\,d\nu} = 2\pi\left(\frac{e^2}{\hbar c}\right)\frac{z^2}{c}\left(1 - \frac{1}{n^2\beta^2}\right) = \frac{2\pi}{137}\cdot\frac{z^2}{c}\sin^2\theta \text{ photons cm}^{-1}\text{Hz}^{-1}$$

Compton scattering (cgs units)

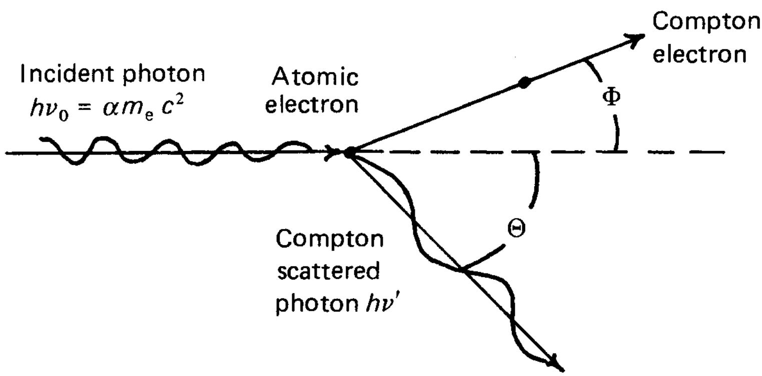

Compton shift

$$\frac{c}{\nu'} - \frac{c}{\nu_0} = \lambda' - \lambda_0 = \frac{h}{m_e c}(1 - \cos\theta).$$

Energy of scattered photon

$$h\nu' = \frac{m_e c^2}{1 - \cos\theta + (1/\alpha)}, \quad \alpha = h\nu_0/m_e c^2.$$

Energy of struck electron

$$T = h\nu' - h\nu_0,$$

$$T = h\nu_0 \frac{\alpha(1 - \cos\theta)}{1 + \alpha(1 - \cos\theta)},$$

$$T_{\max} = \frac{h\nu_0}{1 + (1/2\alpha)}.$$

Relation between the scattering angles, ϕ and θ

$$\cot\phi = (1 + \alpha)\frac{1 - \cos\theta}{\sin\theta} = (1 + \alpha)\tan\frac{\theta}{2}.$$

Klein-Nishina cross-sections for unpolarized incident radiation

Differential collision cross-section:

$$\frac{d\sigma}{d\Omega}=r_0^2\left[\frac{1}{1+\alpha(1-\cos\theta)}\right]^2\left(\frac{1+\cos^2\theta}{2}\right)\left[1+\frac{\alpha^2(1-\cos\theta)^2}{(1+\cos^2\theta)[1+\alpha(1-\cos\theta)]}\right]$$

$$\text{cm}^2\ \text{electron}^{-1}\ \text{sr}^{-1}.$$

where $r_0 = \dfrac{e^2}{m_e c^2}$, classical electron radius $= 2.82 \times 10^{-13}$ cm.

Total collision cross-section:

$$\int \frac{d\sigma}{d\Omega}d\Omega = 2\pi r_0^2 \left\{ \frac{1+\alpha}{\alpha^2}\left[\frac{2(1+\alpha)}{1+2\alpha} - \frac{1}{\alpha}\ln(1+2\alpha)\right] + \frac{1}{2\alpha}\ln(1+2\alpha) - \frac{1+3\alpha}{(1+2\alpha)^2}\right\} \text{cm}^2\ \text{electron}^{-1}$$

or, for small values of α,

$$\int \frac{d\sigma}{d\Omega}d\Omega = \frac{8\pi}{3} r_0^2 (1 - 2\alpha + 5.2\alpha^2 - 13.3\alpha^3 + \cdots)\ \text{cm}^2\ \text{electron}^{-1}$$

The differential cross-section for the electromagnetic energy scattered is obtained from the collision cross-section by multiplying by the fraction of the original energy carried off by the scattered photon, $1/[1+\alpha(1-\cos\theta)]$

$$\frac{d\sigma_s}{d\Omega}=r_0^2\left[\frac{1}{1+\alpha(1-\cos\theta)}\right]^3\left(\frac{1+\cos^2\theta}{2}\right)\left[1+\frac{\alpha^2(1-\cos\theta)^2}{(1+\cos^2\theta)[1+\alpha(1-\cos\theta)]}\right]$$

$$\text{cm}^2\ \text{electron}^{-1}\ \text{sr}^{-1}.$$

Klein-Nishina differential cross-sections (*cont.*)

Differential cross-sections, $d\sigma(\theta)/d\Omega$, for the production of secondary photons from Compton scattering. Curves are shown for six different values of primary photon energy. (From Davisson & Evans, *Rev. Mod. Phys.*, **34**, 79, 1953.)

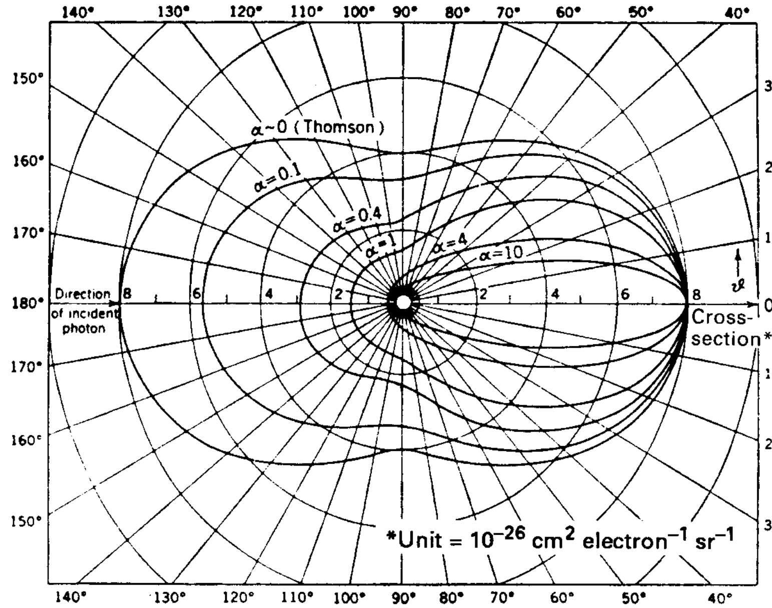

Differential cross-sections, $d\sigma(\theta)/d\theta$, for the production of secondary photons from Compton scattering. (From Davisson & Evans, *Rev. Mod. Phys.*, **34**, 79, 1953.)

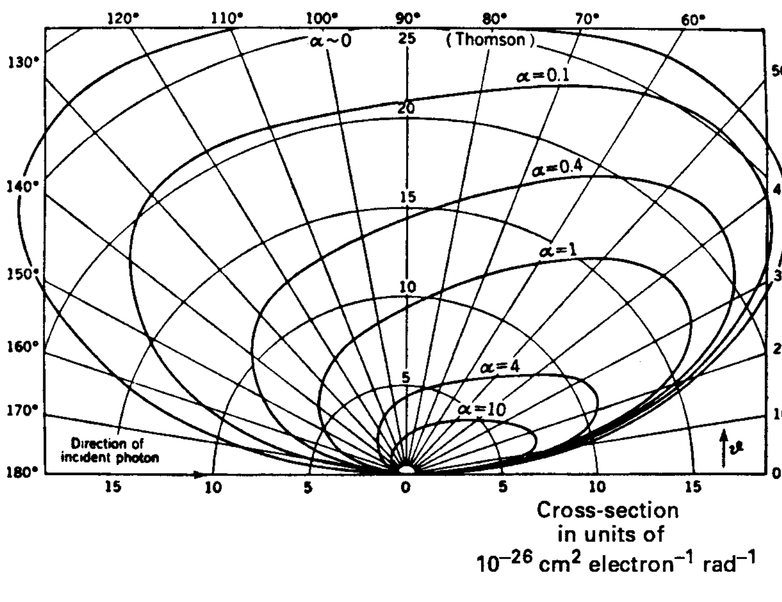

Klein-Nishina differential cross-sections (*cont.*)

Differential cross-sections, $d\sigma_e(\phi)/d\phi$, for the production of secondary electrons from Compton scattering. (From Davisson & Evans, *Rev. Mod. Phys.*, **34**, 79, 1953.)

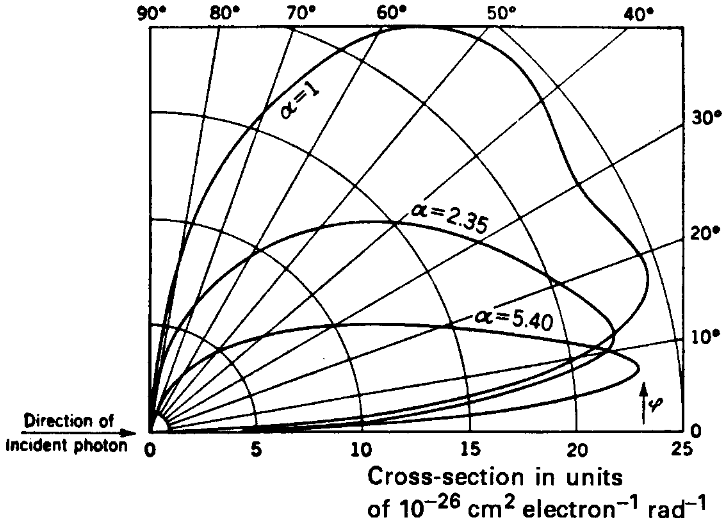

Inverse Compton scattering (cgs units)

Compton collisions between relativistic electrons and low frequency photons.

Thomson limit

$$\gamma h\nu_0 << m_e c^2,$$

where γ is the Lorentz factor for the relativistic electrons.

Total energy loss rate (Thomson limit)

$$-\frac{dE}{dt} = \frac{4}{3}\sigma_T c\gamma^2 u = 2.6 \times 10^{-14}\gamma^2 u \text{ erg s}^{-1} \text{ electron}^{-1},$$

where

$$u = \text{radiation energy density},$$

$$\sigma_T = \frac{8\pi}{3} r_0^2, \text{ the Thomson cross-section},$$

$$r_0 = \frac{e^2}{m_e c^2}.$$

Spectra

Thomson limit-power law electron distribution function and blackbody radiation: when the initial radiation field is given by a blackbody distribution and the density of electrons is given by a power law, viz., $N(\gamma)d\gamma = N\gamma^{-s}d\gamma$ (the density of electrons with a Lorentz factor between γ and $(\gamma + \mathrm{d}\gamma)$, the spectral power density is:

$$\frac{dP}{dV\,d\nu} = 4.2 \times 10^{-40} N b(s) T^3 (2.1 \times 10^{10} T/\nu)^{(s-1)/2} \quad \text{erg cm}^{-3}\ \text{s}^{-1}\ \text{Hz}^{-1},$$

with T in degrees Kelvin.

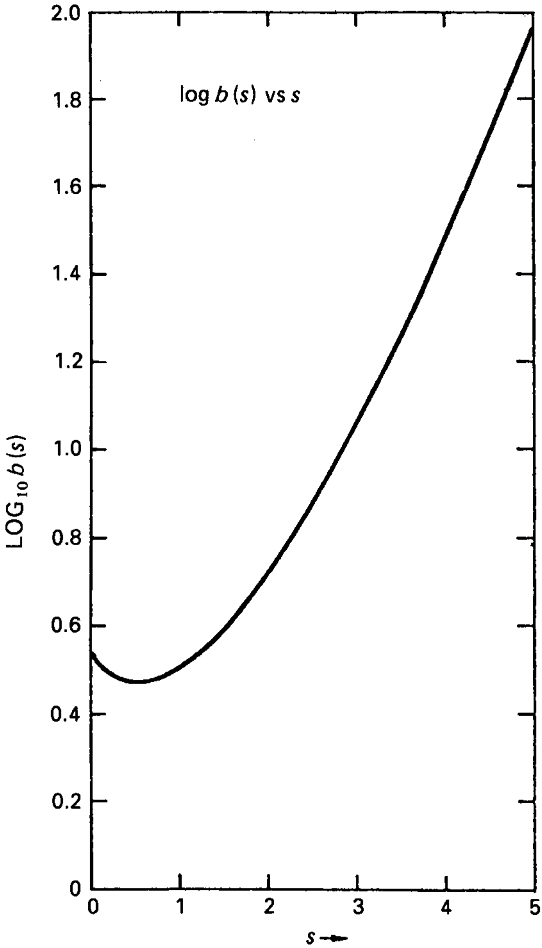

(Blumenthal G.R. & Tucker, W. H., *op. cit.*)

Hot plasma emission (cgs units)

Bremsstrahlung from a hot plasma

For a Maxwellian distribution of electron velocities, the spectral emission per unit volume:

$$\frac{dP_B(T)}{dV\,d\nu} = 6.8 \times 10^{-38} T^{-1/2} e^{-E/kT} N_e N_Z Z^2 \overline{g_B(T,E)} \quad \text{erg cm}^{-3}\ \text{s}^{-1}\ \text{Hz}^{-1},$$

where

N_e = electron density,

N_Z = ion density (charge z),

$E = h\nu$ = photon energy, and

g_B is the Gaunt factor.

$$\overline{g_B(T,E)} \approx \frac{\sqrt{3}}{\pi} \ln\left(\frac{4kT}{\Gamma E}\right), \text{ for } E \ll kT \quad (\ln\Gamma = 0.577)$$

$$\approx (E/kT)^{-0.4}, \quad \text{for } E \sim kT.$$

The total bremsstrahlung emission:

$$\frac{dP_B}{dV} = 1.4 \times 10^{-27} T^{1/2} N_e N_Z Z^2 g_B(T) \text{ erg cm}^{-3}\ \text{s}^{-1},$$

where $g_B(T) \approx 1.2$.

$$\frac{dP_B}{dV} = 2.4 \times 10^{-27} T^{1/2} N_e^2 \text{ erg cm}^{-3}\ \text{s}^{-1}$$

for a plasma with cosmic abundances, since the contribution from all ions

$$\sum N_e N_Z Z^2 \approx 1.4 N_e^2.$$

Non-thermal bremsstrahlung

For a flux density $J(E) = J_0 E^{-s}$ erg cm^{-2} s^{-1} erg^{-1} of non-thermal electrons, the spectral emission per unit volume:

$$\frac{dP_B}{dV\,d\nu} = 1.2 \times 10^{-6} Z^2 N_Z J_0 \frac{E^{-s-1}}{s} \text{ erg cm}^{-3}\ \text{s}^{-1}\ \text{Hz}^{-1}.$$

X-ray line emission from a hot plasma (electron collisional excitation)

For a Maxwellian distribution of electron velocities, the power emitted per unit volume due to excitations of level n' of ion Z in the ground state n is:

$$\frac{dP_L}{dV} = 2.7 \times 10^{-15} T^{-1/2} e^{E_{nn'}/kT} f_{nn'} \overline{g_{nn'}} N_e N_Z \text{ erg cm}^{-3}\ \text{s}^{-1},$$

where

$E_{nn'}$ = energy of excitation,

$f_{nn'}$ = oscillator strength for the transition,

$\overline{g_{nn'}}$ = mean Gaunt factor ≈ 0.2 for $kT/E_{nn'} < 1$.

In some cases, a line is produced by a transition to a state other than the ground state. In this case, the emitted power above is not equal to the power in the line and the branching ratio to the state of interest must be taken into account. For 1s–2p transitions in hydrogen and helium-like ions, this branching is not significant.

Radiative recombination radiation

$$\frac{dP_{RR,\,Z,\,n}}{dV\,dE} = \frac{2.8\times 10^{-6}T^{-3/2}e^{(I_{Z-1,\,n}-E)/kT}}{n^3}N_eN_ZZ^4 \quad \text{erg cm}^{-3}\ \text{s}^{-1}\ \text{erg}^{-1},$$

where

$E = W_i + I_{Z-1,\,n}$,

E = energy of emitted photon,

W_i = energy of free electron,

$I_{Z,\,n}$ = ionization energy of level n for ion Z.

(Adapted from Blumenthal, G. R. & Tucker, W.H., in *X-ray Astronomy*, R. Giacconi & H. Gursky, eds., D. Reidel Publishing Company, Dorderecht, 1974.)

Maxwell's equations (Gaussian units)

$$\nabla\cdot\mathbf{D} = 4\pi\rho, \qquad \nabla\times\mathbf{H} = \frac{4\pi\mathbf{J}}{c} + \frac{1}{c}\frac{\partial D}{\partial t},$$

$$\nabla\cdot\mathbf{B} = 0, \qquad \nabla\times\mathbf{E} + \frac{1}{c}\frac{\partial\mathbf{B}}{\partial t} = 0.$$

Constitutive relations for an isotropic, permeable, conducting dielectric:

$$\mathbf{D} = \epsilon\mathbf{E}, \qquad \mathbf{J} = \sigma\mathbf{E}, \qquad \mathbf{B} = \mu\mathbf{H}.$$

Macroscopic media:

polarization: $\mathbf{P} = \frac{1}{4\pi}(\mathbf{D}-\mathbf{E})$,

magnetization: $\mathbf{M} = \frac{1}{4\pi}(\mathbf{B}-\mathbf{H})$.

Vector and scalar potentials:

$$\mathbf{B} = \nabla\times\mathbf{A}, \qquad \mathbf{E} = -\nabla\phi - \frac{1}{c}\frac{\partial\mathbf{A}}{\partial t}.$$

For homogeneous, isotropic media, Maxwell's equations become:

$$\nabla^2\phi = \frac{\epsilon\mu}{c^2}\frac{\partial^2\phi}{\partial t^2} - \frac{1}{c}\frac{\partial}{\partial t}\left(\nabla\cdot\mathbf{A} + \frac{\epsilon\mu}{c}\frac{\partial\phi}{\partial t}\right) - \frac{4\pi\rho}{\epsilon}.$$

$$\nabla^2 \mathbf{A} = \frac{\mu\epsilon}{c^2}\frac{\partial^2}{\partial t^2}\mathbf{A} + \nabla\left(\boldsymbol{\nabla}\cdot\mathbf{A} + \frac{\epsilon\mu}{c}\frac{\partial\phi}{\partial t}\right) - \frac{4\pi\mu}{c}\mathbf{J}.$$

Lorentz gauge:

$$\left(\boldsymbol{\nabla}\cdot\mathbf{A} + \frac{\epsilon\mu}{c}\frac{\partial\phi}{\partial t}\right) = 0.$$

Coulomb gauge:

$$\boldsymbol{\nabla}\cdot\mathbf{A} = 0.$$

Conversion table for given amount of physical quantity

Physical quantity	Symbol	Rationalized mks	Gaussian
Charge	q	1 coulomb	3×10^9 statcoulombs
Charge density	ρ	1 coul m^{-3}	3×10^3 statcoulombs cm^{-3}
Current	I	1 ampere	3×10^9 statamperes
Current density	J	1 amp m^{-2}	3×10^5 statamperes cm^{-2}
Electric field	E	1 volt m^{-1}	$1/3 \times 10^{-4}$ statvolt cm^{-1}
Potential	ϕ, V	1 volt	1/300 statvolt
Polarization	P	1 coul m^{-2}	3×10^5 statcoulombs cm^{-2}
Displacement	D	1 coul m^{-2}	$12\pi \times 10^5$ statvolt cm^{-1}
Conductivity	σ	1 mho m^{-1}	9×10^9 s^{-1}
Magnetic induction	B	1 weber m^{-2}	10^4 gauss
Magnetic field	H	1 ampere-turn m^{-1}	$4\pi \times 10^{-3}$ oersted
Magnetization	M	1 weber m^{-2}	$1/4\pi \times 10^4$ gauss

(Adapted from *Classical Electrodynamics*, Jackson, J. D., John Wiley and Sons, 1962.)

Standard definitions in radiative transport theory

Quantity	Symbol	Units (cgs)
Specific intensity or radiance	I_ν	erg cm^{-2} s^{-1} Hz^{-1} sr^{-1}
Brightness	$B_\nu = -I_\nu$	erg cm^{-2} s^{-1} Hz^{-1} sr^{-1}
Flux density	$F_\nu = \int I_\nu \cos\theta \mathrm{d}\Omega$	erg cm^{-2} s^{-1} Hz^{-1}
Mean intensity	$J_\nu = \frac{1}{4\pi}\int I_\nu \mathrm{d}\Omega$	erg cm^{-2} s^{-1} Hz^{-1}
Radiation density	$u_\nu = \frac{1}{c}\int I_\nu \mathrm{d}\Omega = \frac{4\pi}{c} J_\nu$	erg cm^{-3} Hz^{-1}
Emission coefficient	j_ν	erg cm^{-3} s^{-1} Hz^{-1} sr^{-1}
Emissivity	$\epsilon_\nu = \frac{4\pi}{\rho} j_\nu$ (isotropic emission, $\rho =$ density)	erg gm^{-1} s^{-1} Hz^{-1}
Linear absorption coefficient	$\alpha_\nu = n\sigma_\nu$ ($n =$ number density, $\sigma_\nu =$ cross-section)	cm^{-1}
Mean free path	$l_\nu = \frac{1}{\alpha_\nu}$	cm
Optical depth	$\tau_\nu = \int \alpha_\nu \mathrm{d}s$	dimensionless

Electromagnetic relations

Quantity	Gaussian cgs	Rationalized mks (SI)
Conversion factors:		
Charge:	2.99792458×10^9 esu	$= 1$ C $= 1$ A s
Potential:	(1/299.792458) statvolt (ergs/esu)	$= 1$ V $= 1$ J C^{-1}
Magnetic field:	10^4 gauss $= 10^4$ dyne/esu	$= 1$ T $= 1$ N A^{-1} m^{-1}
Lorentz force:	$\mathbf{F} = q\left(\mathbf{E} + \frac{\mathbf{v}}{c} \times \mathbf{B}\right)$	$\mathbf{F} = q(\mathbf{E} + \mathbf{v} \times \mathbf{B})$
Maxwell equations:	$\nabla \cdot \mathbf{D} = 4\pi\rho$	$\nabla \cdot \mathbf{D} = \rho$
	$\nabla \times \mathbf{H} - \frac{1}{c}\frac{\partial \mathbf{D}}{\partial t} = \frac{4\pi}{c}\mathbf{J}$	$\nabla \times \mathbf{H} - \frac{\partial \mathbf{D}}{\partial t} = \mathbf{J}$
	$\nabla \cdot \mathbf{B} = 0$	$\nabla \cdot \mathbf{B} = 0$
	$\nabla \times \mathbf{E} + \frac{1}{c}\frac{\partial \mathbf{B}}{\partial t} = 0$	$\nabla \times \mathbf{E} + \frac{\partial \mathbf{B}}{\partial t} = 0$
Constitutive relations:	$\mathbf{D} = \mathbf{E} + 4\pi\mathbf{P}$, $\mathbf{H} = \mathbf{B} - 4\pi\mathbf{M}$	$\mathbf{D} = \epsilon_0\mathbf{E} + \mathbf{P}$, $\mathbf{H} = \mathbf{B}/\mu_0 - \mathbf{M}$
Linear media:	$\mathbf{D} = \epsilon\mathbf{E}$, $\mathbf{H} = \mathbf{B}/\mu$	$\mathbf{D} = \epsilon\mathbf{E}$, $\mathbf{H} = \mathbf{B}/\mu$
Permitivity of free space:	1	$\epsilon_0 = 8.854\ 187\ldots \times 10^{-12}$ F m^{-1}
Permeability of free space:	1	$\mu_0 = 4\pi \times 10^{-7}$ N A^{-2}
Fields from potentials:	$\mathbf{E} = -\nabla V - \frac{1}{c}\frac{\partial \mathbf{A}}{\partial t}$	$\mathbf{E} = -\nabla V - \frac{\partial \mathbf{A}}{\partial t}$
	$\mathbf{B} = \nabla \times \mathbf{A}$	$\mathbf{B} = \nabla \times \mathbf{A}$
Static potentials: (Coulomb gauge)	$V = \sum_{\text{charges}} \frac{q_i}{r_i}$	$V = \frac{1}{4\pi\epsilon_0} \sum_{\text{charges}} \frac{q_i}{r_i}$
	$= \int \frac{\rho(\mathbf{r}')}{\lvert\mathbf{r} - \mathbf{r}'\rvert} d^3x'$	$= \frac{1}{4\pi\epsilon_0} \int \frac{\rho(\mathbf{r}')}{\lvert\mathbf{r} - \mathbf{r}'\rvert} d^3x'$
	$\mathbf{A} = \frac{1}{c} \oint \frac{I\,\mathrm{d}\mathbf{l}}{\lvert\mathbf{r} - \mathbf{r}'\rvert}$	$\mathbf{A} = \frac{\mu_0}{4\pi} \oint \frac{I\,\mathrm{d}\mathbf{l}}{\mathbf{r} - \mathbf{r}'}$
	$= \frac{1}{c} \int \frac{\mathbf{J}(\mathbf{r}')}{\lvert\mathbf{r} - \mathbf{r}'\rvert} d^3x'$	$= \frac{\mu_0}{4\pi} \frac{\mathbf{J}(\mathbf{r}')}{\lvert\mathbf{r} - \mathbf{r}'\rvert} d^3x'$
Relativistic transformations:	$\mathbf{E}'_{\parallel} = \mathbf{E}_{\parallel}$	$\mathbf{E}'_{\parallel} = \mathbf{E}_{\parallel}$
(v is the velocity of the primed frame as seen in the unprimed frame)	$\mathbf{E}'_{\perp} = \gamma\left(\mathbf{E}_{\perp} + \frac{1}{c}\mathbf{v} \times \mathbf{B}\right)$	$\mathbf{E}'_{\perp} = \gamma(\mathbf{E}_{\perp} + \mathbf{v} \times \mathbf{B})$
	$\mathbf{B}'_{\parallel} = \mathbf{B}_{\parallel}$	$\mathbf{B}'_{\parallel} = \mathbf{B}_{\parallel}$
	$\mathbf{B}'_{\perp} = \gamma\left(\mathbf{B}_{\perp} - \frac{1}{c}\mathbf{v} \times \mathbf{E}\right)$	$\mathbf{B}'_{\perp} = \gamma\left(\mathbf{B}_{\perp} - \frac{1}{c^2}\mathbf{v} \times \mathbf{E}\right)$

$$\frac{1}{4\pi\epsilon_0} = c^2 \times 10^{-7}\ \text{N A}^{-2} = 8.987\ 55\ldots \times 10^9\ \text{m F}^{-1};$$

$$\frac{\mu_0}{4\pi} = 10^{-7}\ \text{N A}^{-2};\ c = \frac{1}{\sqrt{\mu_0\epsilon_0}} = 2.997\ 924\ 58 \times 10^8\ \text{m s}^{-1}$$

(From Caso, C., et al., European Physical Journal, C3, 1, 1998)

Maxwell's equations in various system of units (ϵ_0, μ_0, **D**, **H**, macroscopic Maxwell's equations, and Lorentz force equation in various system of units)

System	ϵ_0	μ_0	$\mathbf{D}, \mathbf{H}$	Macroscopic Maxwell's equations				Lorentz force per unit charge
Electrostatic (esu)	1	c^{-2}	$\mathbf{D} = \mathbf{E} + 4\pi\mathbf{P}$ $\mathbf{H} = c^2\mathbf{B} - 4\pi\mathbf{M}$	$\nabla \cdot \mathbf{D} = 4\pi\rho$	$\nabla \times \mathbf{H} = 4\pi\mathbf{J} + \frac{\partial \mathbf{D}}{\partial t}$	$\nabla \times \mathbf{E} + \frac{\partial \mathbf{B}}{\partial t} = 0$	$\nabla \cdot \mathbf{B} = 0$	$\mathbf{E} + \mathbf{v} \times \mathbf{B}$
Electro-magnetic (emu)	c^{-2}	1	$\mathbf{D} = (1/c^2)\mathbf{E} + 4\pi\mathbf{P}$ $\mathbf{H} = \mathbf{B} - 4\pi\mathbf{M}$	$\nabla \cdot \mathbf{D} = 4\pi\rho$	$\nabla \times \mathbf{H} = 4\pi\mathbf{J} + \frac{\partial \mathbf{D}}{\partial t}$	$\nabla \times \mathbf{E} + \frac{\partial \mathbf{B}}{\partial t} = 0$	$\nabla \cdot \mathbf{B} = 0$	$\mathbf{E} + \mathbf{v} \times \mathbf{B}$
Gaussian	1	1	$\mathbf{D} = \mathbf{E} + 4\pi\mathbf{P}$ $\mathbf{H} = \mathbf{B} - 4\pi\mathbf{M}$	$\nabla \cdot \mathbf{D} = 4\pi\rho$	$\nabla \times \mathbf{H} = \frac{4\pi}{c}\mathbf{J} + \frac{1}{c}\frac{\partial \mathbf{D}}{\partial t}$	$\nabla \times \mathbf{E} + \frac{1}{c}\frac{\partial \mathbf{B}}{\partial t} = 0$	$\nabla \cdot \mathbf{B} = 0$	$\mathbf{E} + \frac{\mathbf{v}}{c} \times \mathbf{B}$
Heaviside-Lorentz	1	1	$\mathbf{D} = \mathbf{E} + \mathbf{P}$ $\mathbf{H} = \mathbf{B} - \mathbf{M}$	$\nabla \cdot \mathbf{D} = \rho$	$\nabla \times \mathbf{H} = \frac{1}{c}\left(\mathbf{J} + \frac{\partial \mathbf{D}}{\partial t}\right)$	$\nabla \times \mathbf{E} + \frac{1}{c}\frac{\partial \mathbf{B}}{\partial t} = 0$	$\nabla \cdot \mathbf{B} = 0$	$\mathbf{E} + \frac{\mathbf{v}}{c} \times \mathbf{B}$
Rationalized mks (SI)	$\frac{10^7}{4\pi c^2}$	$4\pi \times 10^{-7}$	$\mathbf{D} = \epsilon_0\mathbf{E} + \mathbf{P}$ $\mathbf{H} = (1/\mu_0)\mathbf{B} - \mathbf{M}$	$\nabla \cdot \mathbf{D} = \rho$	$\nabla \times \mathbf{H} = \mathbf{J} + \frac{\partial \mathbf{D}}{\partial t}$	$\nabla \times \mathbf{E} + \frac{\partial \mathbf{B}}{\partial t} = 0$	$\nabla \cdot \mathbf{B} = 0$	$\mathbf{E} + \mathbf{v} \times \mathbf{B}$

(Adapted from Jackson, J.D., *Classical Electrodynamics*, John Wiley and Sons, 1962.)

Spectrum nomogram

Electromagnetic spectrum nomogram.

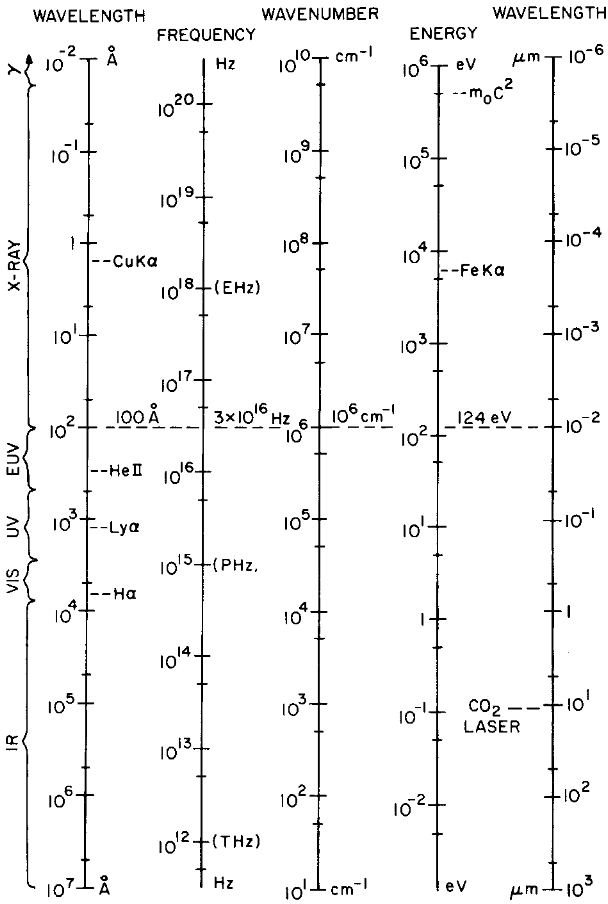

Bibliography

Radiation Processes in Astrophysics, Tucker, W., The MIT Press, 1975.

Radiative Processes in Astrophysics, Rybicki, G. B. & Lightman, A. P., John Wiley and Sons, 1979.

Classical Electrodynamics, Jackson, J. D., John Wiley and Sons, 1999.

Astrophysical Formulae, Lang, K. R., Springer-Verlag, 1999.

Note: Links to WWW resources which supplement the material in this chapter can be found at:

http://www.astrohandbook.com

Chapter 13

Plasma physics

We have learned that matter is weird stuff. - Freeman J. Dyson

Fundamental plasma physics parameters

All quantities are in Gaussian cgs units except temperature (T, T_e, T_i) expressed in eV and ion mass (m_i) expressed in units of the proton mass, $\mu = m_i/m_p$; Z is charge state; k is Boltzmann's constant; K is wavenumber; γ is the adiabatic index; $\ln\Lambda$ is the Coulomb logarithm.

Frequencies

electron gyrofrequency	$f_{ce} = \omega_{ce}/2\pi = 2.80 \times 10^6 B$ Hz $\omega_{ce} = eB/m_e c = 1.76 \times 10^7 B$ rad/s
ion gyrofrequency	$f_{ci} = \omega_{ci}/2\pi = 1.52 \times 10^3 Z\mu^{-1} B$ Hz $\omega_{ci} = ZeB/m_i c = 9.58 \times 10^3 Z\mu^{-1} B$ rad/s
electron plasma frequency	$f_{pe} = \omega_{pe}/2\pi = 8.98 \times 10^3 n_e^{\frac{1}{2}}$ Hz $\omega_{pe} = (4\pi n_e e^2/m_e)^{\frac{1}{2}} = 5.64 \times 10^4 n_e^{\frac{1}{2}}$ rad/s
ion plasma frequency	$f_{pi} = \omega_{pi}/2\pi$ $= 2.10 \times 10^2 Z\mu^{-\frac{1}{2}} n_i^{\frac{1}{2}}$ Hz $\omega_{pi} = (4\pi n_i Z^2 e^2/m_i)^{\frac{1}{2}}$ $= 1.32 \times 10^3 Z\mu^{-\frac{1}{2}} n_i^{\frac{1}{2}}$ rad/s
electron trapping rate	$\nu_{Te} = (eKE/m_e)^{\frac{1}{2}}$ $= 7.26 \times 10^8 K^{\frac{1}{2}} E^{\frac{1}{2}}$ s^{-1}
ion trapping rate	$\nu_{Ti} = (ZeKE/m_i)^{\frac{1}{2}}$ $= 1.69 \times 10^7 Z^{\frac{1}{2}} K^{\frac{1}{2}} E^{\frac{1}{2}} \mu^{-\frac{1}{2}}$ s^{-1}
electron collision rate	$\nu_e = 2.91 \times 10^{-6} n_e \ln\Lambda T_e^{-3/2}$ s^{-1}
ion collision rate	$\nu_i = 4.80 \times 10^{-8} Z^4 \mu^{-\frac{1}{2}} n_i \ln\Lambda T_i^{-3/2}$ s^{-1}

Lengths

electron deBroglie length	$\lambda\!\!\!^{-} = \hbar/(m_e k T_e)^{\frac{1}{2}} = 2.76 \times 10^{-8} T_e^{-\frac{1}{2}}$ cm
classical distance of minimum approach	$e^2/kT = 1.44 \times 10^{-7} T^{-1}$ cm
electron gyroradius	$r_e = v_{Te}/\omega_{ce} = 2.38 T_e^{\frac{1}{2}} B^{-1}$ cm
ion gyroradius	$r_i = v_{T_i}/\omega_{ci}$ $= 1.02 \times 10^2 \mu^{\frac{1}{2}} Z^{-1} T_i^{\frac{1}{2}} B^{-1}$ cm
plasma skin depth	$c/\omega_{pe} = 5.31 \times 10^5 n_e^{-\frac{1}{2}}$ cm
Debye length	$\lambda_D = (kT/4\pi n e^2)^{\frac{1}{2}}$ $= 7.43 \times 10^2 T^{\frac{1}{2}} n^{-\frac{1}{2}}$ cm

Fundamental plasma physics parameters (cont.)

Velocities	
electron thermal velocity	$v_{Te} = (kT_e/m_e)^{\frac{1}{2}}$ $= 4.19 \times 10^7 T_e^{\frac{1}{2}}$ cm s^{-1}
ion thermal velocity	$v_{Ti} = (kT_i/m_i)^{\frac{1}{2}}$ $= 9.79 \times 10^5 \mu^{-\frac{1}{2}} T_i^{\frac{1}{2}}$ cm s^{-1}
ion sound velocity	$C_s = (\gamma Z k T_e/m_i)^{\frac{1}{2}}$ $= 9.79 \times 10^5 (\gamma Z T_e/\mu)^{\frac{1}{2}}$ cm s^{-1}
Alfvén velocity	$v_A = B/(4\pi n_i m_i)^{\frac{1}{2}}$ $= 2.18 \times 10^{11} \mu^{-\frac{1}{2}} n_i^{-\frac{1}{2}} B$ cm s^{-1}
Dimensionless	
(electron/proton mass ratio)$^{\frac{1}{2}}$	$(m_e/m_p)^{\frac{1}{2}} = 2.33 \times 10^{-2} = 1/42.9$
number of particles in Debye sphere	$(4\pi/3) n \lambda_D^3 = 1.72 \times 10^9 T^{3/2} n^{-\frac{1}{2}}$
Alfvén velocity/speed of light	$v_A/c = 7.28 \mu^{-\frac{1}{2}} n_i^{-\frac{1}{2}} B$
electron plasma/gyrofrequency ratio	$\omega_{pe}/\omega_{ce} = 3.21 \times 10^{-3} n_e^{\frac{1}{2}} B^{-1}$
ion plasma/gyrofrequency ratio	$\omega_{pi}/\omega_{ci} = 0.137 \mu^{\frac{1}{2}} n_i^{\frac{1}{2}} B^{-1}$
thermal/magnetic energy ratio	$\beta = \dfrac{8\pi n k T}{B^2} = 4.03 \times 10^{-11} n T B^{-2}$
magnetic/ion rest energy ratio	$B^2/8\pi n_i m_i c^2 = 26.5 \mu^{-1} n_i^{-1} B^2$

Miscellaneous (note: T is in °K)

electrical resistivity $\quad \eta \approx 3.80 \times 10^3 \dfrac{Z \ln \Lambda}{\gamma_E T^{3/2}}$ ohm-cm

with

Ionic Charge Z	1	2	4	16	∞
γ_E	0.582	0.683	0.785	0.923	1.000

In a strong magnetic field, the resistivity transverse to the field is

$$\eta = 1.29 \times 10^4 \frac{Z \ln \Lambda}{T^{3/2}} \text{ ohm-cm}$$

Fundamental plasma physics parameters (cont.)

Coulomb logarithm $\ln\Lambda = \dfrac{3}{2ZZ_1e^3}\left(\dfrac{k^3T^3}{\pi n_e}\right)^{1/2}$

$\ln\Lambda$ for an electron-proton gas

	Electron Density n_e cm^{-3}								
T°K	1	10^3	10^6	10^9	10^{12}	10^{15}	10^{18}	10^{21}	10^{24}
10^2	16.3	12.8	9.43	5.97					
10^3	19.7	16.3	12.8	9.43	5.97				
10^4	23.2	19.7	16.3	12.8	9.43	5.97			
10^5	26.7	23.2	19.7	16.3	12.8	9.43	5.97		
10^6	29.7	26.3	22.8	19.3	15.9	12.4	8.96	5.54	
10^7	32.0	28.5	25.1	21.6	18.1	14.7	11.2	7.85	4.39
10^8	34.3	30.9	27.4	24.0	20.5	17.0	13.6	10.1	6.69

(From Spitzer, L., *Physics of Fully Ionized Gases*, Interscience Publishers, 1956.)

life of magnetic field in a plasma:

$$\tau = 4\pi L^2/\eta c^2$$
$$= 1.5 \times 10^{-12} L^2 (\ln\Lambda)^{-1}\ \mathrm{T}^{3/2}\ \mathrm{s}$$

(L is the characteristic scale of the field).

Maxwellian velocity distribution:

$$f(v)dv = 4\pi\left(\frac{m}{2\pi kT}\right)^{3/2} e^{-mv^2/(2kT)} v^2 dv,$$

$$\int_0^\infty f(v)dv = 1,$$

$$\overline{v} = (8kT/\pi m)^{1/2}\ \mathrm{cm\ s^{-1}},$$

$$v_{\mathrm{rms}} = (3kT/m)^{1/2}$$
$$= 6.7 \times 10^5 T^{1/2} \quad \text{for electrons}$$
$$= 1.57 \times 10^4 T^{1/2} \quad \text{for protons},$$

$$\frac{1}{2} m_e v_{\mathrm{rms}}^2 = 3kT/2 = 2.1 \times 10^{-16} T\ \mathrm{erg}.$$

magnetic pressure is given by

$$P_{\mathrm{mag}} = B^2/8\pi = 3.98 \times 10^6 (B/B_0)^2\ \mathrm{dynes/cm^2} = 3.93(B/B_0)^2\ \mathrm{atm},$$

where $B_0 = 10$ kG $= 1$ T.

(From Huba, J.D., *NRL Plasma Formulary*, U.S. Naval Research Laboratory, 2000 and Spitzer, L., *Physics of Fully Ionized Gases*, Interscience Publishers, 1962.)

Approximate magnitudes in some typical plasmas

Plasma Type	n cm^{-3}	T eV	ω_{pe} s^{-1}	λ_D cm	$n\lambda_D^3$	ν_{ei} s^{-1}
Interstellar gas	1	1	6×10^4	7×10^2	4×10^8	7×10^{-5}
Gaseous nebula	10^3	1	2×10^6	20	10^7	6×10^{-2}
Solar Corona	10^9	10^2	2×10^9	2×10^{-1}	8×10^6	60
Diffuse hot plasma	10^{12}	10^2	6×10^{10}	7×10^{-3}	4×10^5	40
Solar atmosphere, gas discharge	10^{14}	1	6×10^{11}	7×10^{-5}	40	2×10^9
Warm plasma	10^{14}	10	6×10^{11}	2×10^{-4}	10^3	10^7
Hot plasma	10^{14}	10^2	6×10^{11}	7×10^{-4}	4×10^4	4×10^6
Thermonuclear plasma	10^{15}	10^4	2×10^{12}	2×10^{-3}	10^7	5×10^4
Theta pinch	10^{16}	10^2	6×10^{12}	7×10^{-5}	4×10^3	3×10^8
Dense hot plasma	10^{18}	10^2	6×10^{13}	7×10^{-6}	4×10^2	2×10^{10}
Laser Plasma	10^{20}	10^2	6×10^{14}	7×10^{-7}	40	2×10^{12}

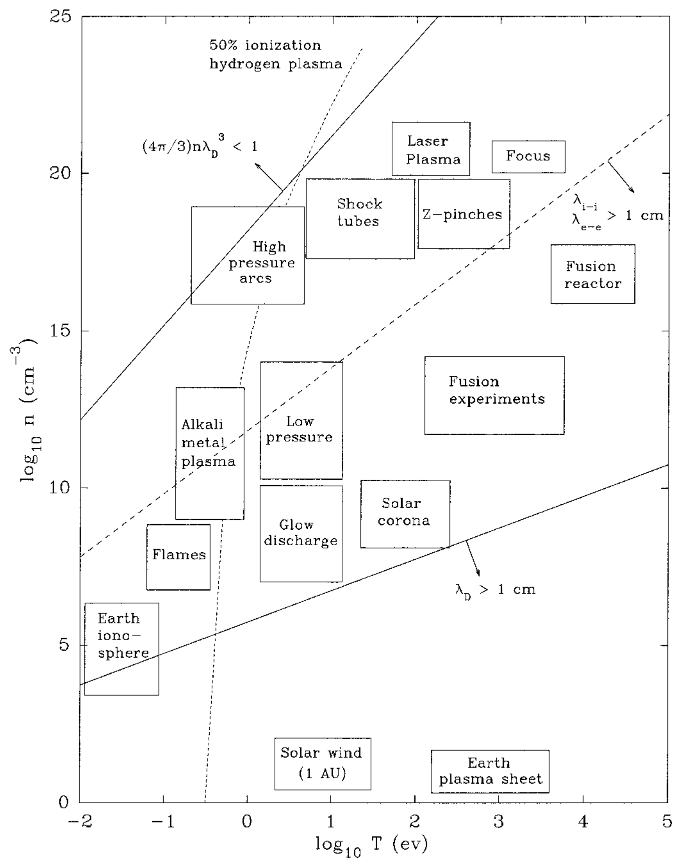

(From Huba, J.D., *NRL Plasma Formulary*, U.S. Naval Research Laboratory, 2000.)

Approximate magnitudes for some astrophysical plasmas

Plasma	N_e (cm^{-3})	T_e(K)	B (gauss)	$\nu_{\rm pe}$ (Hz)	$\lambda_{\rm D}$ (cm)
Ionosphere	$10^3 - 10^6$	$10^2 - 10^3$	10^{-1}	$3 \times 10^5 - 10^7$	$7 \times 10^{-2} - 7$
Interplanetary space	$1 - 10^4$	$10^2 - 10^3$	$10^{-6} - 10^{-5}$	$10^4 - 10^6$	$7 \times 10^{-1} - 2 \times 10^2$
Solar corona	$10^8 - 10^{12}$(flare)	$10^6 - 10^7$(flare)	$10^{-5} - 1$	$10^8 - 10^{10}$	$10^{-2} - 2$
Solar chromosphere	10^{12}	$2 - 3 \times 10^4$	10^3	10^{10}	10^{-3}
Stellar interiors	10^{27}	$10^{7.5}$	–	3×10^{17}	10^{-9}
Planetary nebulae	$10^3 - 10^5$	$10^3 - 10^4$	$10^{-4} - 10^{-3}$	$3 \times 10^5 - 3 \times 10^6$	$7 \times 10^{-1} - 2 \times 10^1$
H II regions	$10^2 - 10^3$	$10^3 - 10^4$	10^{-6}	$10^5 - 3 \times 10^5$	$7 - 7 \times 10^1$
H I regions	10^{-3}	10^2	–	3×10^2	2×10^3
White dwarfs	10^{32}	10^7	10^6(surface)	10^{20}	2×10^{-12}
Pulsars	10^{42}(center)	–	10^{12}(surface)	10^{25}	–
	10^{12}(surface)	–	–	10^{10}	–
Interstellar space	$10^{-3} - 10$	10^2	10^{-6}	$3 \times 10^2 - 3 \times 10^4$	$2 \times 10^1 - 2 \times 10^3$
Intergalactic space	$\lesssim 10^{-5}$	$10^5 - 10^6$	$\lesssim 10^{-8}$	< 30	2×10^6

$N_{\rm e}$ = electron density; $T_{\rm e}$ = electron temperature; B = magnetic field; $\nu_{\rm pe}$ = plasma frequency; $\lambda_{\rm D}$ = Debye length.

Ionospheric parameters

The following tables give average nighttime values. Where two numbers are entered, the first refers to the lower and the second to the upper portion of the layer.

Quantity	E Region	F Region
Altitude(km)	$90 - 160$	$160 - 500$
Number density(m^{-3})	$1.5 \times 10^{10} - 3.0 \times 10^{10}$	$5 \times 10^{10} - 2 \times 10^{11}$
Height-integrated number density (m^{-2})	9×10^{14}	4.5×10^{15}
Ion-neutral collision frequency (s^{-1})	$2 \times 10^{3} - 10^{2}$	$0.5 - 0.05$
Ion gyro-/collision frequency ratio κ_i	$0.09 - 2.0$	$4.6 \times 10^{2} - 5.0 \times 10^{3}$
Ion Pederson factor $\kappa_i/(1+\kappa_i^2)$	$0.09 - 0.5$	$2.2 \times 10^{-3} - 2 \times 10^{-4}$
Ion Hall factor $\kappa_i^2/(1+\kappa_i^2)$	$8 \times 10^{-4} - 0.8$	1.0
Electron-neutral collision frequency	$1.5 \times 10^{4} - 9.0 \times 10^{2}$	$80 - 10$
Electron gyro-/collision frequency ratio κ_e	$4.1 \times 10^{2} - 6.9 \times 10^{3}$	$7.8 \times 10^{4} - 6.2 \times 10^{5}$
Electron Pedersen factor $\kappa_e/(1+\kappa_e^2)$	$2.7 \times 10^{-3} - 1.5 \times 10^{-4}$	$10^{-5} - 1.5 \times 10^{-6}$
Electron Hall factor $\kappa_e^2/(1+\kappa_e^2)$	1.0	1.0
Mean molecular weight	$28 - 26$	$22 - 16$
Ion gyrofrequency (s^{-1})	$180 - 190$	$230 - 300$
Neutral diffusion coefficient (m^2s^{-1})	$30 - 5 \times 10^{3}$	10^{5}

The terrestrial magnetic field in the lower ionosphere at equatorial latitudes is approximately $B_0 = 0.35 \times 10^{-4}$ tesla. The earth's radius is $R_E = 6371$ km.

(From Huba, J.D., *NRL Plasma Formulary*, U.S. Naval Research Laboratory, 2000.)

Bibliography

NRL Plasma Formulary, Huba, J.D., Naval Research Laboratory, 2000.

Physics of Fully Ionized Gases, Spitzer, L., Interscience Publishers, 1962.

Note: Links to WWW resources which supplement the material in this chapter can be found at:

http://www.astrohandbook.com

Chapter 14

Experimental astronomy and astrophysics

...no one believes an hypothesis except its originator but everyone believes an experiment except the experimenter. - W. I. B. Beveridge

Attenuation of electromagnetic radiation

$I = I_0 e^{-(\mu/\rho)\rho t}$,

I_0 = initial intensity of a collimated photon beam,

I = intensity of beam after traversing a thickness t of material density ρ,

(μ/ρ) = total mass attenuation coefficient

$= \sigma/\rho + \tau/\rho + k/\rho$,

σ/ρ = total Compton mass attenuation coefficient,

τ/ρ = photoelectric mass absorption coefficient

$(\sim \frac{Z^4}{A} E^{-8/3}$ between absorption edges),

k/ρ = pair production mass attenuation coefficient.

Mixtures of materials:

$$\mu/\rho = \sum_i (\mu_i/\rho_i)\omega_i,$$

where

μ_i/ρ_i = mass attenuation coefficient of element i,

ω_i = fraction by weight of element i.

Photon mean free path = $[(\mu/\rho)\rho]^{-1}$.

Relative importance of the three major types of electromagnetic interactions. The lines show the values of Z and $h\nu$ for which the two neighboring effects are just equal. (Evans, R.D., *The Atomic Nucleus*, McGraw-Hill, 1955, with permission.)

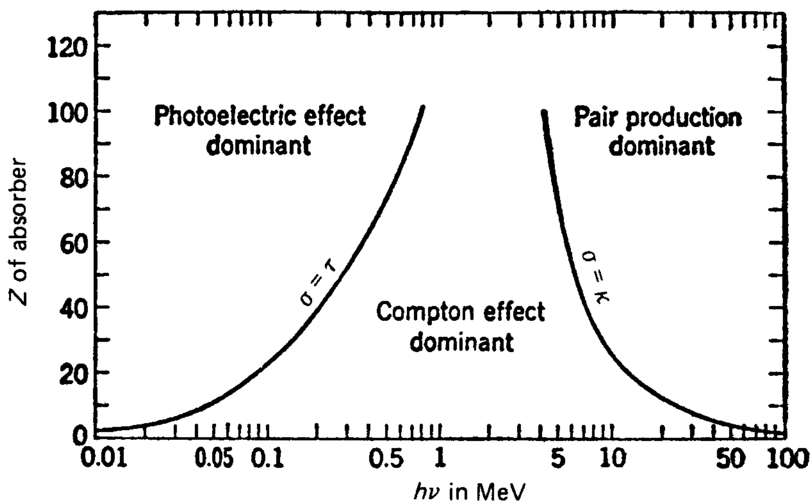

Extrapolated absorption and absorption-jump ratios (r) at the K-edge

Z	element	Atomic weight	Density (g cm^{-3})	λ_k (Å)	E_k (keV)	Fluor. yield ω_k	$(\mu/\rho)^-$ (cm^{2}g^{-1})	$(\mu/\rho)^+$ (cm^{2}g^{-1})	r
4	Be	9.01	1.85	112	0.111		179000	(5000)	(35)
5	B	10.81	2.34	66.0	0.188		88400	3130	28.3
6	C	12.01	2.26	43.7	0.284		53900	2230	24.2
7	N	14.01	0.00125	30.9	0.402		32800	1540	21.4
8	O	16.00	0.00143	23.3	0.532		22400	1160	19.3
9	F	19.00	0.00170	18.1	0.685		14800	846	17.5
10	Ne	20.18	0.00090	14.3	0.867		10950	687	15.94
11	Na	22.99	0.97	11.56	1.072		7760	525	14.78
12	Mg	24.31	1.74	9.50	1.305		6000	440	13.63
13	Al	26.98	2.70	7.95	1.560	0.036	4500	355	12.68
14	Si	28.09	2.33	6.74	1.839	0.047	3640	307	11.89
15	P	30.97	1.82	5.77	2.146	0.060	2800	251	11.18
16	S	32.06	2.07	5.01	2.472	0.076	2340	222	10.52
17	Cl	35.45	0.00317	4.38	2.822	0.094	1840	185	9.92
18	Ar	39.95	0.00178	3.87	3.203	0.115	1440	154	9.34
19	K	39.10	0.86	3.44	3.607	0.138	1300	148	8.79
20	Ca	40.08	1.55	3.07	4.038	0.163	1120	135	8.28

(After Henke, B.L. & Elgin, R.L. in *Advances in X-ray Analysis*, Vol. 13. Plenum Press, New York, 1970.)

Absorption-edge jump ratios and differences

(From Bertin, P., *Principles and Practice of X-ray Spectrometric Analysis*, Plenum Press, 1975, with permission.)

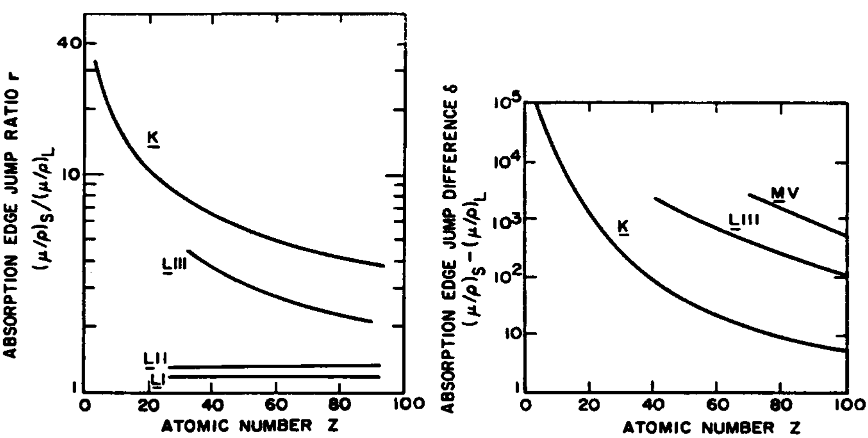

Wavelengths of K absorption edges

(Adapted from Bertin, P., *Principles and Practice of X-ray Spectrometric Analysis*, Plenum Press, 1975.)

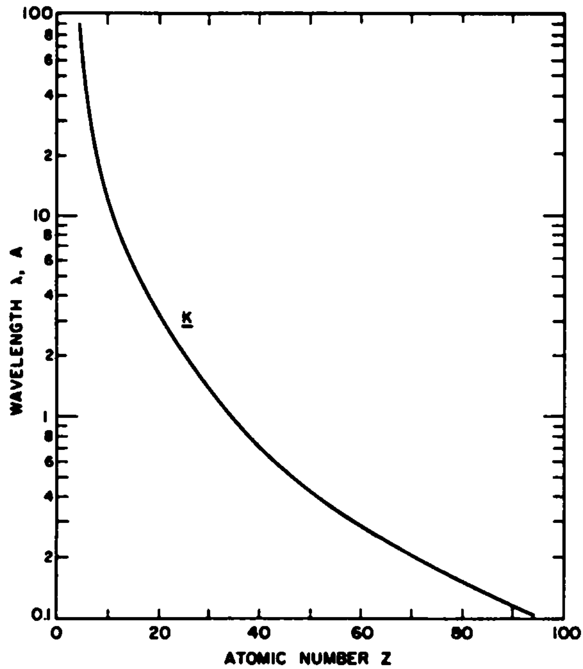

Binding (absorption edge) energies of the elements

(From Feldman, L.C. and Mayer, J.W, *Fundamentals of Surface and Thin Film Analysis*, Elsevier Science Publishing Co., Inc., 1986.)

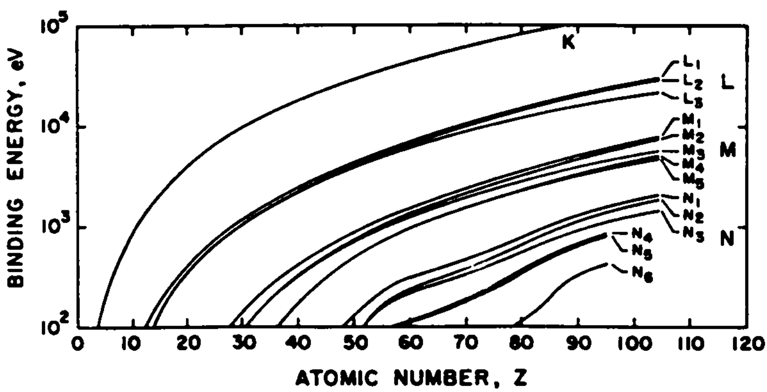

Mass attenuation coefficients (cm^2 g^{-1})

Wave-length (Å)	Poly-propylene (CH_2)	Mylar ($C_{10}H_8O_4$)	Teflon (CF_2)	Air O = 21% N = 78% Ar = 1%	P 10 CH_4 = 10% Ar = 90%	Methane (CH_4)	Energy (eV)
2.0	8	14	28	21	230	7	6199.0
4.0	69	116	220	148	162	60	3099.5
6.0	234	384	700	481	467	205	2066.3
8.0	550	870	1540	1090	1020	479	1549.8
10.0	1040	1630	2800	2020	1850	910	1239.8
12.0	1740	2680	4250	3310	3010	1520	1033.2
14.0	2660	4040	6700	4980	4500	2330	885.6
16.0	3830	5800	9400	7100	6400	3350	774.9
18.0	5200	7800	12600	9500	8400	4570	688.8
20.0	6900	10200	2780	12400	10900	6100	619.9
22.0	8800	12900	3540	15700	13500	7700	563.5
24.0	11000	8500	4430	14100	16400	9700	516.6
26.0	13500	10400	5400	17100	19600	11800	476.8
28.0	16200	12400	6500	20400	22800	14100	442.8
30.0	19200	14700	7800	24000	26300	16800	413.3
32.0	22400	17200	9100	2290	29700	19600	387.4
34.0	25900	19900	10600	2650	33300	22700	364.6
36.0	29600	22800	12100	3040	36900	25900	344.4
38.0	33600	25800	13800	3460	40500	29300	326.3
40.0	37800	29100	15600	3810	37600	33000	309.9
42.0	42200	32500	17500	4270	40900	36900	295.2
44.0	1940	3350	6900	4780	42600	1700	281.8
46.0	2180	3760	7800	5300	45600	1910	269.5
48.0	2430	4170	8600	5900	48900	2130	258.3
50.0	2690	4590	9500	6400	52000	2350	248.0
52.0	2960	5100	10500	6300		2590	238.4
54.0	3240	5600	11500	7000		2840	229.6
56.0	3540	6100	12500	7600		3100	221.4
58.0	3860	6600	13600	8200		3380	213.8
60.0	4190	7200	14800	8900		3660	206.6
62.0	4540	7800	16000	9700		3970	200.0
64.0	4880	8400	17300	10400		4270	193.7
66.0	5200	9000	18600	11200		4570	187.8
68.0	5700	9700	19900	12100		4940	182.3
70.0	6000	10300	21300	12900		5200	177.1
72.0	6400	11100	22700	13800		5600	172.2
74.0	6800	11800	24200	14700		6000	167.5
76.0	7300	12500	25700	15600		6400	163.1

Mass attenuation coefficients (cont.)

Wave-length (Å)	Poly-propylene (CH_2)	Mylar ($C_{10}H_8O_4$)	Teflon (CF_2)	Air O = 21% N = 78% Ar = 1%	P 10 CH_4 = 10% Ar = 90%	Methane (CH_4)	Energy (eV)
78.0	7700	13300	27200	16600		6700	158.9
80.0	8100	14100	28800	17600		7100	155.0
82.0	8600	14900	30500	18600		7600	151.2
84.0	9100	15800	32100	19700		7900	147.6
86.0	9600	16600	33800	20800		8400	144.2
88.0	10100	17500	35500	21900		8800	140.9
90.0	10600	18400	37300	23100		9300	137.8
92.0	11100	19400	39100	24200		9700	134.8
94.0	11700	20300	40900	25400		10300	131.9
96.0	12200	21300	43000	26700		10700	129.1
98.0	12800	22300	44600	28000		11200	126.5
100.0	13400	23300	46300	29200		11800	124.0
105.0	15000	26000	51000	32700		13100	118.1
110.0	16600	28800	56000	36200		14500	112.7
115.0	18200	31600	61000	39900		15900	107.8
120.0	20000	34600	67000	43800		17500	103.3
125.0	21900	38000	72000	48000		19200	99.2
130.0	23900	41100	78000	52000		20900	95.4
135.0	25900	44600	83000	57000		22700	91.8
140.0	28100	48200	89000	61000		24600	88.6
145.0	30300	52000	95000	65000		26500	85.5
150.0	32600	55000	101000	71000		28500	82.7

(Adapted from *The Handbook of Chemistry and Physics*, CRC Press, Cleveland, 1976.)

Mass attenuation coefficients (cont.)

Total mass-attenuation coefficients for gamma-rays in all elements from Be to U. Energy range 1.8 keV–10 MeV. (From *Nucleonics*, **19**, 62, 1961.)

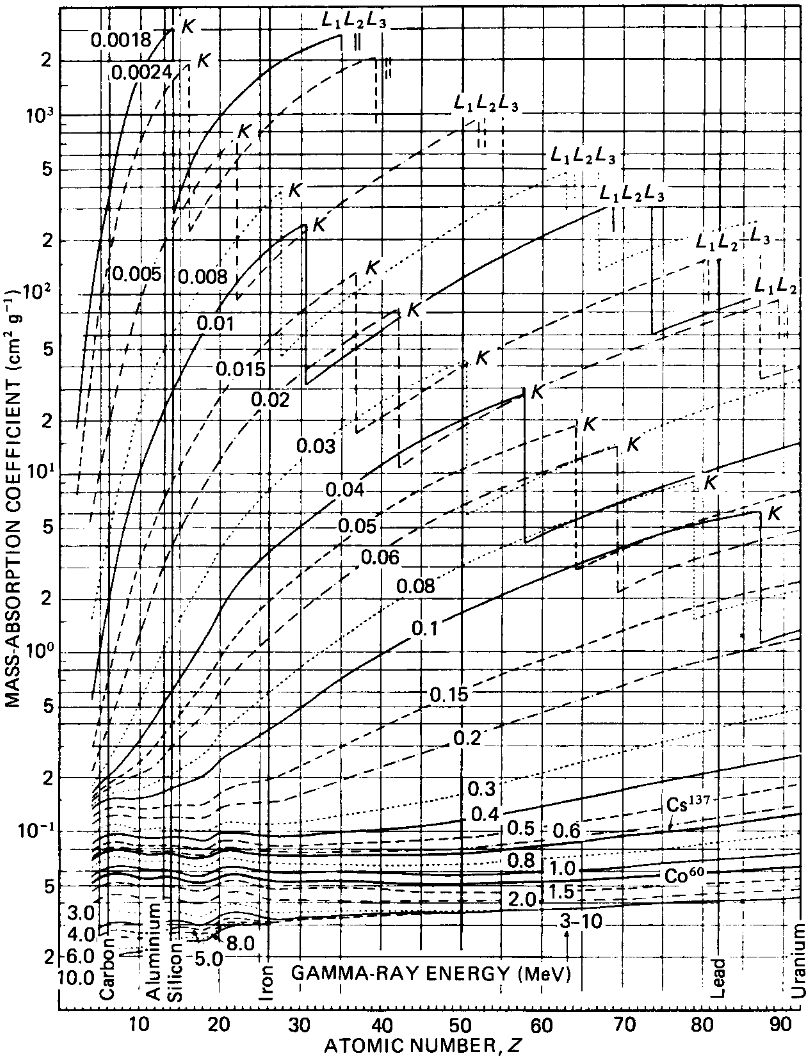

The curves are labeled with the incident energy in Mev. For example, for tin (Z = 50), at 0.2 Mev, the mass-attenuation coefficient is 0.3 $cm^2\ g^{-1}$.

Mass attenuation coefficients (cont.)

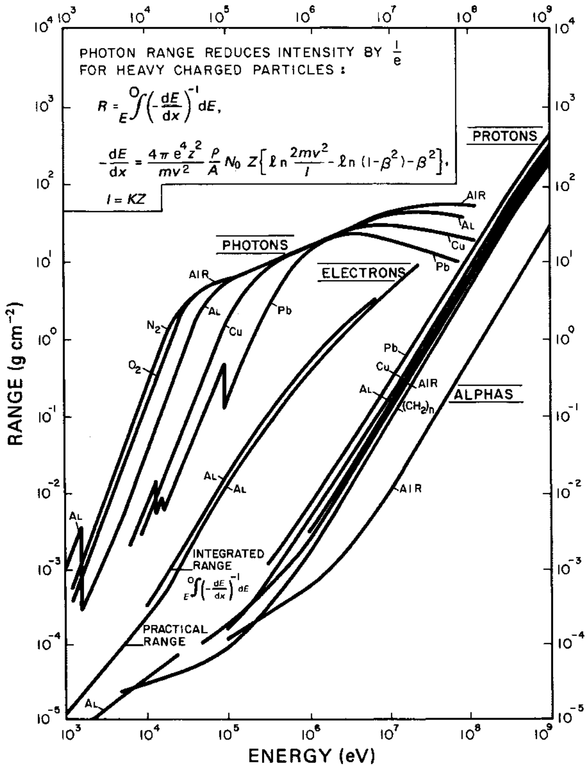

RANGE-ENERGY CURVES FOR PENETRATING RADIATION

(Adapted from Filius, R., *Satellite Instruments Using Solid State Detectors*, Ph.D. thesis, State University of Iowa, Iowa City, 1963.)

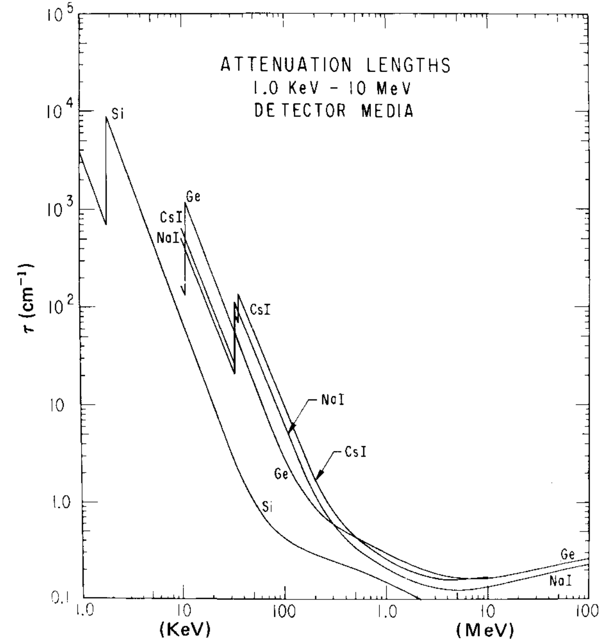

PHOTON ENERGY

(Adapted from Peterson, L. in *Annual Review of Astronomy and Astrophysics*, Annual Review Inc., Palo Alto, California, 1975.)

Mass attenuation coefficients (cont.)

Photoelectric mass absorption coefficients for various window or filter materials.

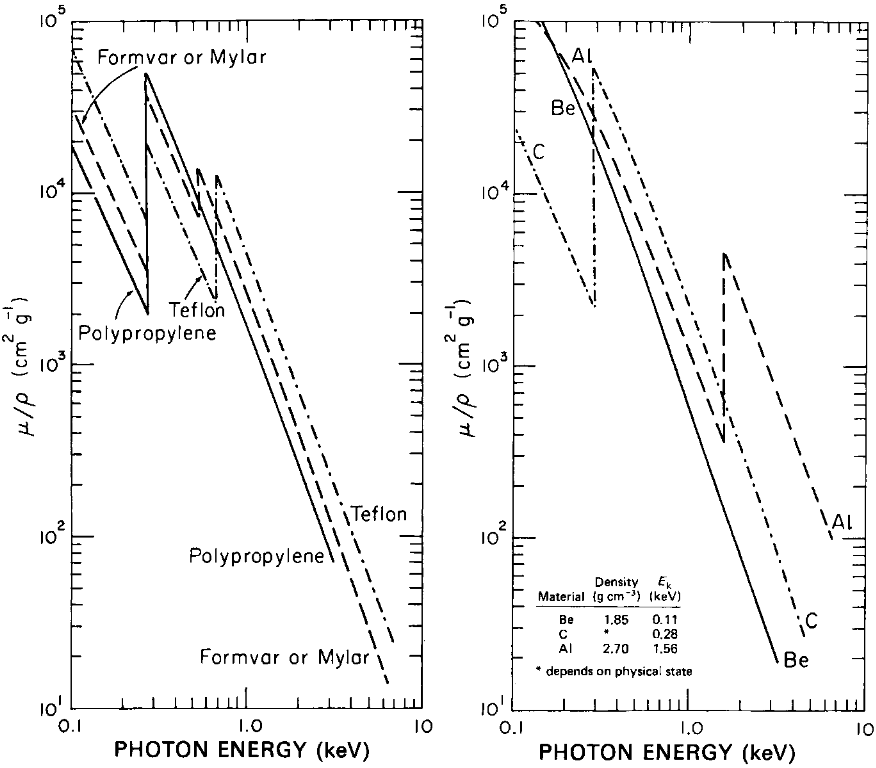

Mass attenuation coefficients (cont.)

Photoelectric mass absorption coefficients for various gases.

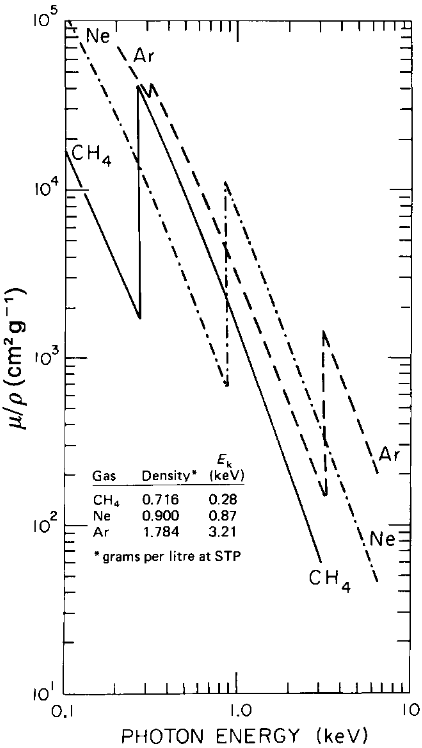

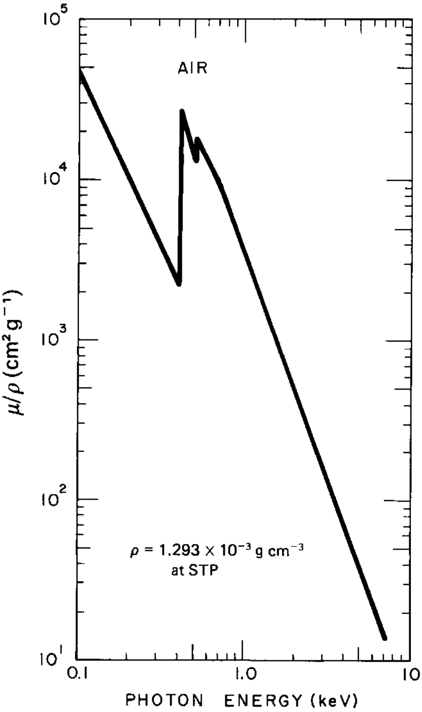

Mass attenuation coefficients (cont.)

Photoelectric cross-section of xenon and argon as a function of photon energy. (Adapted from Anderson, F.D., *A high Resolution Large Area Gas Scintillation Proportional Counter for Use in X-ray Astronomy*, Ph.D. thesis, Columbia University, 1978.)

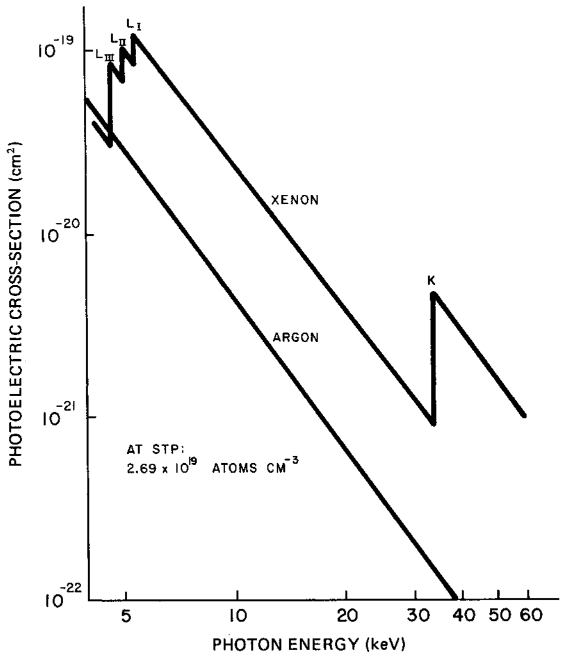

Photon mean free path versus energy for various gases at STP.

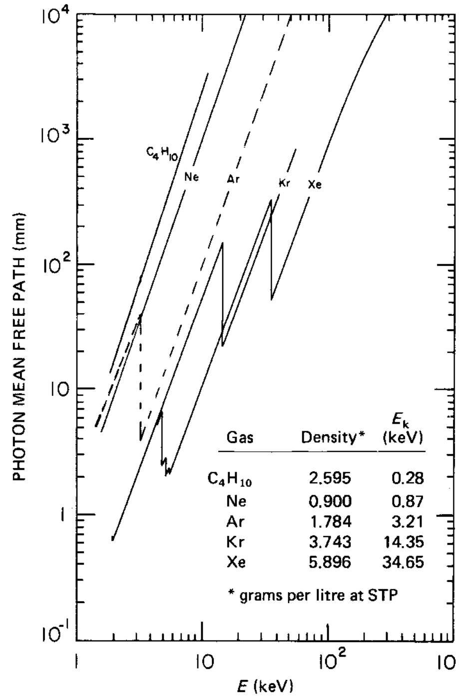

Gas	Density*	E_k (keV)
C_4H_{10}	2.595	0.28
Ne	0.900	0.87
Ar	1.784	3.21
Kr	3.743	14.35
Xe	5.896	34.65

* grams per litre at STP

Mass attenuation coefficients for photons in air. The curve marked 'total absorption' is $(\mu_a/\rho) = (\sigma_a/\rho) + (\tau/\rho) + (\kappa/\rho)$, where σ_a, τ, and κ are the corresponding linear coefficients for Compton absorption, photoelectric absorption, and pair production. When the Compton scattering coefficient σ_s is added to μ_a, we obtain the curve marked 'total attenuation' which is $(\mu_0/\rho) = (\mu_a/\rho) + (\sigma_s/\rho)$. The total Rayleigh scattering cross-section (σ_r/ρ) is shown separately. Because the Rayleigh scattering is elastic and is confined to small angles, it has not been included in μ_0/ρ. In computing these curves, the composition of 'air' was taken as 78.04 volume per cent nitrogen, 21.02 volume per cent oxygen, and 0.94 volume per cent argon. At 0°C and 760 mm Hg pressure, the density of air is $\rho = 0.001293$ g cm^{-3}. (Adapted from Evans, R.D., *The Atomic Nucleus*, McGraw-Hill, 1955, with permission.)

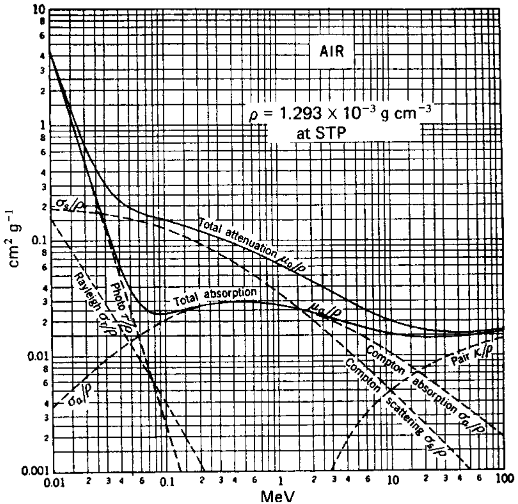

Mass attenuation coefficients for photons in water. (From Evans, R.D., *op. cit.*)

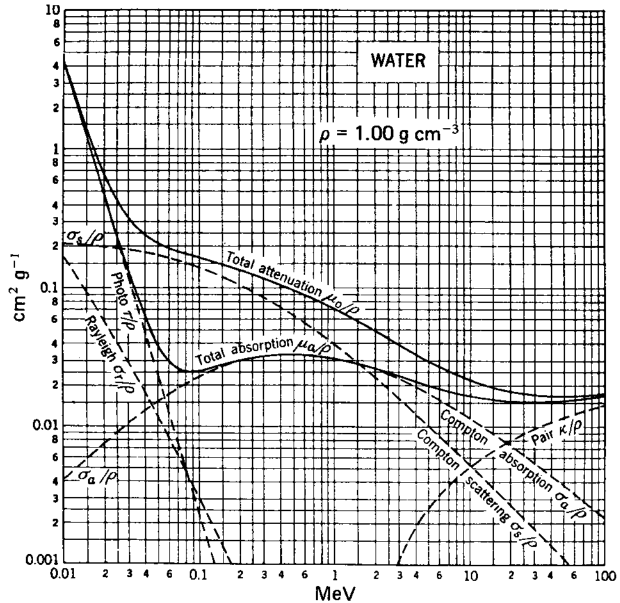

Mass attenuation coefficients (cont.)

Mass attenuation coefficients for photons in lead. (From Evans, R.D., *op. cit.*)

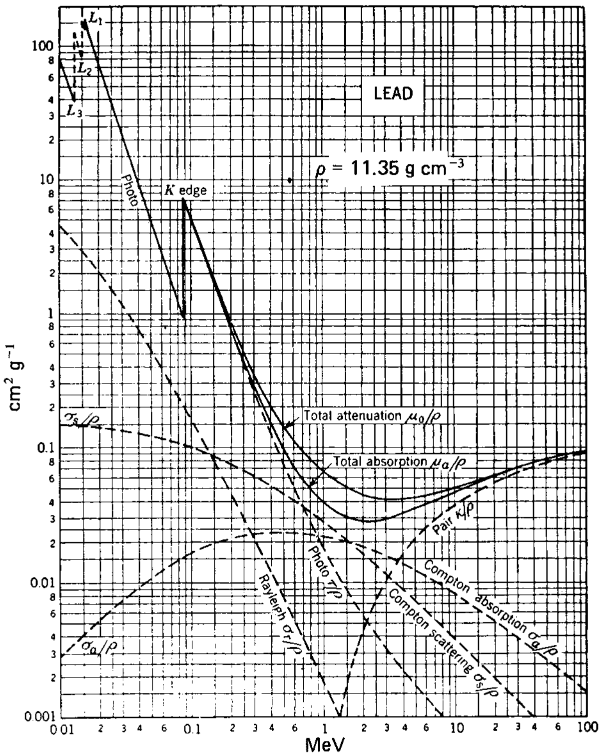

Mass attenuation coefficients for photons in aluminium. (From Evans, R.D., *op. cit.*,)

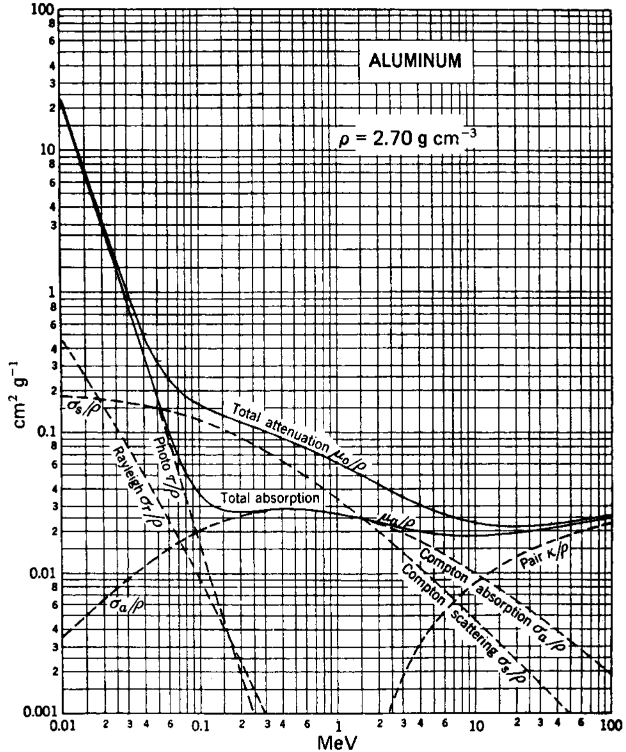

Mass attenuation coefficients for sodium iodide. The 'Compton total' attenuation coefficient $\sigma/\rho = \sigma_a/\rho + \sigma_s/\rho$ is shown explicity. (From Evans, R.D., *op. cit.*)

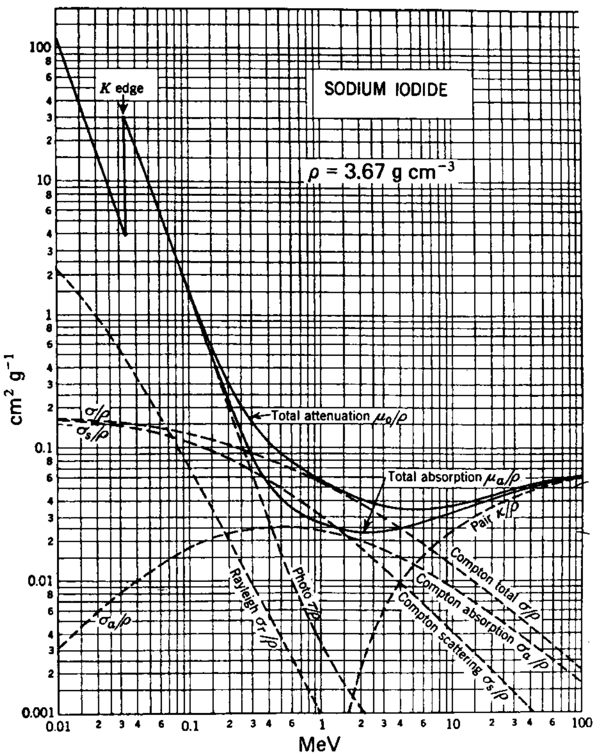

Mass attenuation coefficient for photons in xenon. (Adapted from Chupp, E.L., *Gamma-Ray Astronomy*, D. Reidel Publishing Co., Dordrecht, 1976, with permission.)

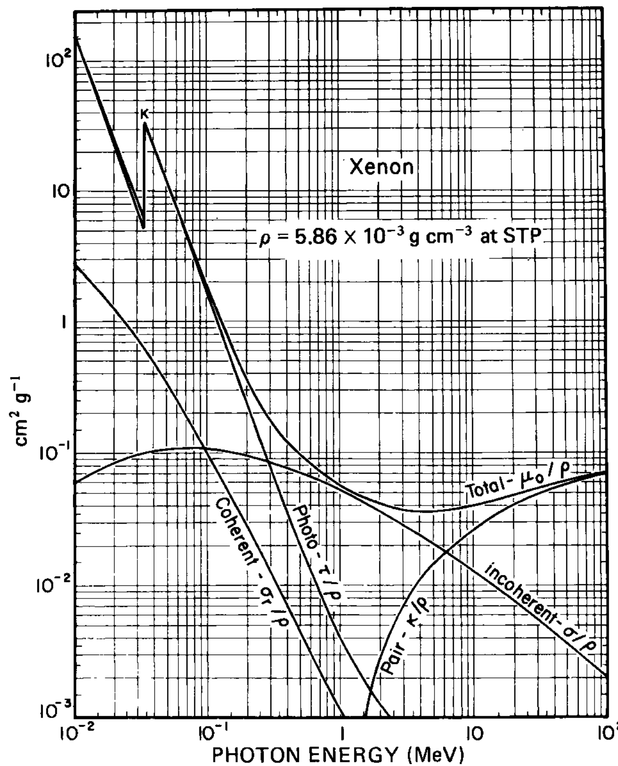

Mass attenuation coefficients (cont.)

Mass attenuation coefficients for photons in hydrogen. (From Chupp, E.L., *op. cit.*)

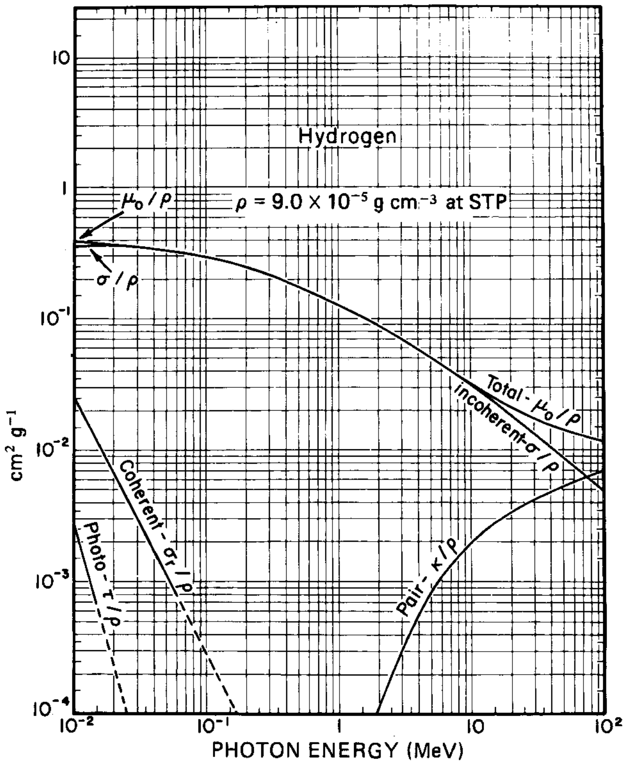

Mass attenuation coefficients for photons in polystyrene. (From Chupp, E.L., *op. cit.*,)

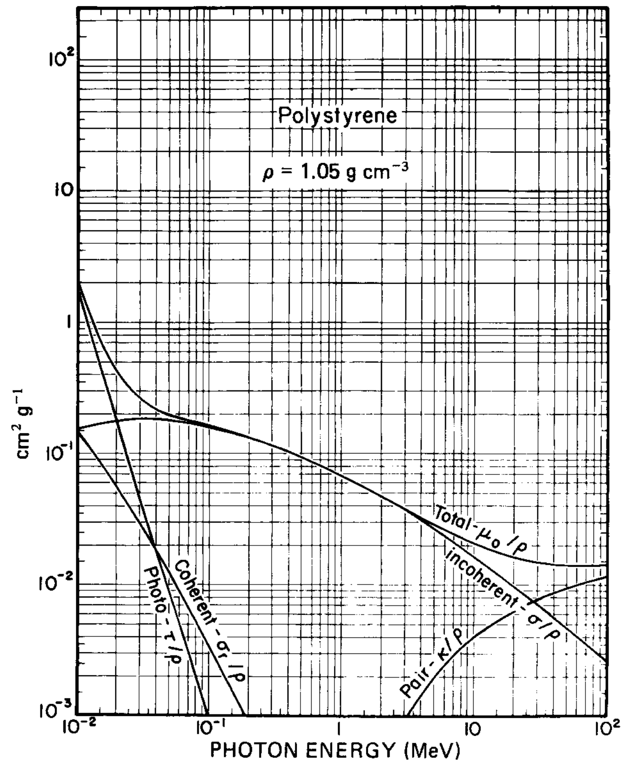

Mass attenuation coefficient for photons in cesium iodide. (From Chupp, E.L., *op. cit.*)

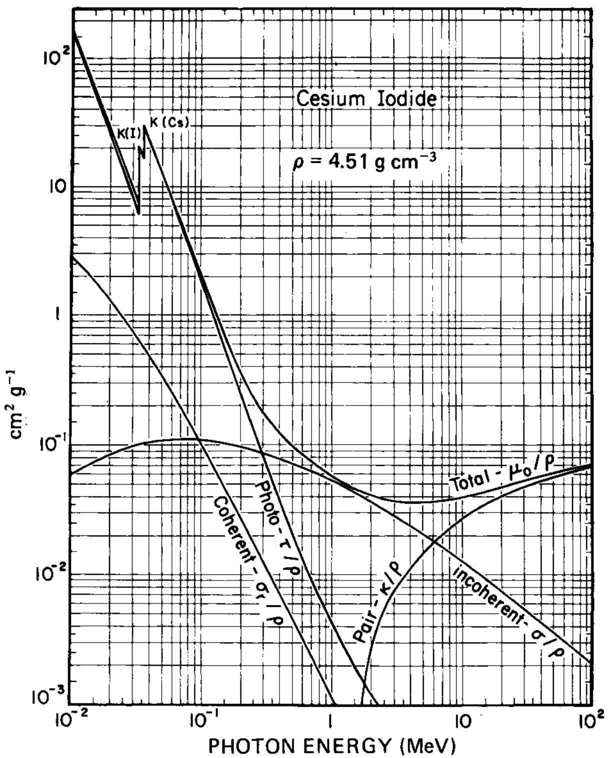

Mass attenuation coefficient for photons in germanium. (From Chupp, E.L., *op. cit.*,)

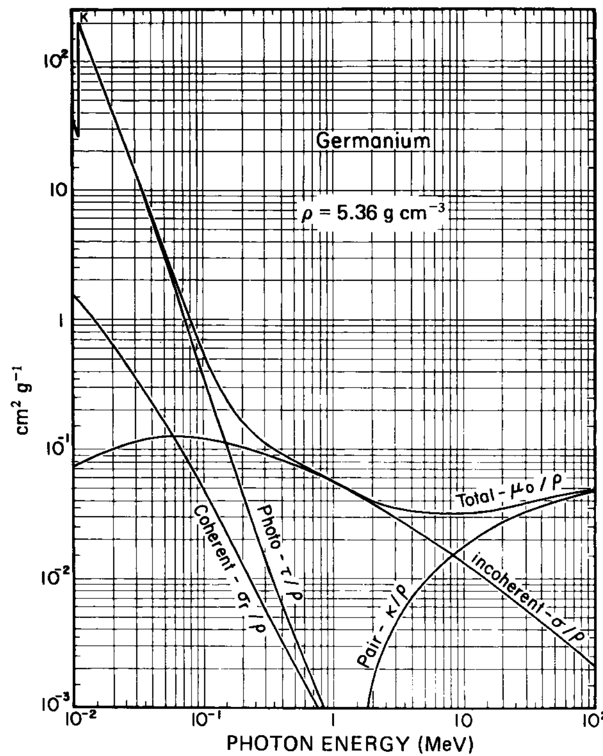

Photon attenuation length

The photon mass attenuation length (or mean free path) $\lambda = 1/(\mu/\rho)$ for various elemental absorbers as a function of photon energy. The mass attenuation coefficient is μ/ρ, where ρ is the density. The intensity I remaining after traversal of thickness t (in mass/unit area) is given by $I = I_0 \exp(-t/\lambda)$. The accuracy is a few percent. For a chemical compound or mixture, $1/\lambda_{\text{eff}} \approx \Sigma_{\text{elements}} w_Z/\lambda_Z$, where w_Z is the proportion by weight of the element with atomic number Z.

(From Caso, C., *et al.* European journal, C3, 1, 1998)

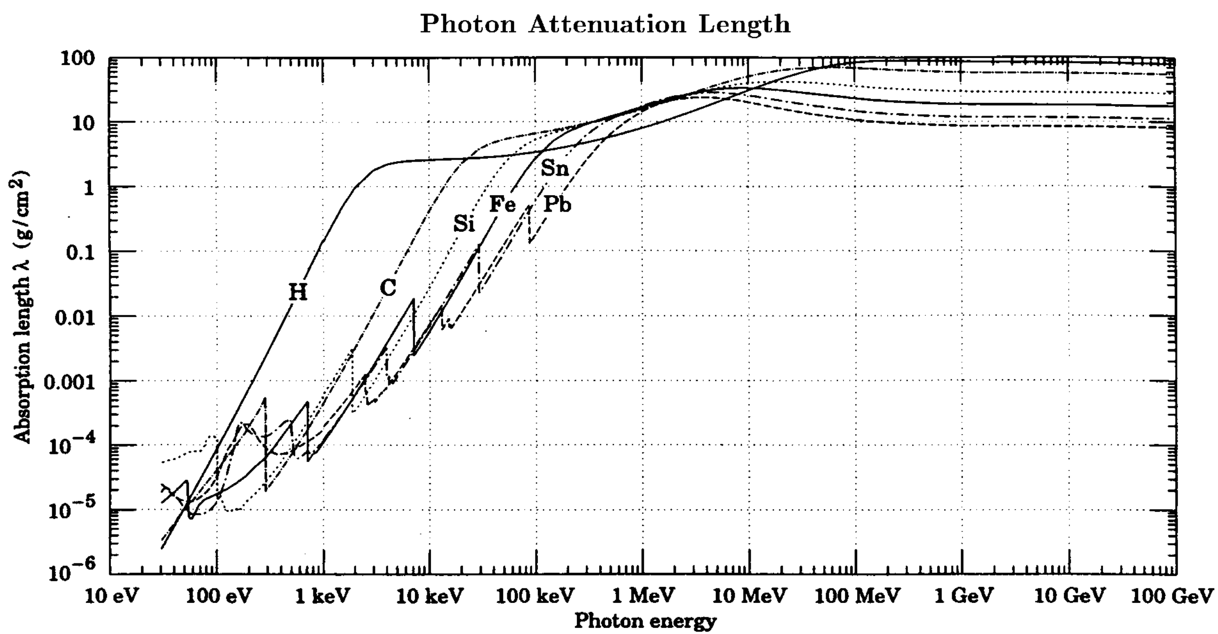

K fluorescence yields

Element	$\omega_K{}^{(a)}$	$\omega_K{}^{(b)}$	$\omega_K{}^{(c)}$	Element	$\omega_K{}^{(a)}$	$\omega_K{}^{(b)}$	$\omega_K{}^{(c)}$
B		0.0007		Ru		0.812	0.793
C		0.0025		Rh		0.828	0.807
N		0.0054		Pd		0.841	0.819
O		0.0086		Ag	0.834	0.849	0.830
F		0.0124		Cd		0.863	0.840
Ne		0.0183		In		0.873	0.850
Na		0.0241		Sn		0.878	0.859
Mg		0.0303		Sb		0.897	0.867
Al	0.0380	0.0381	0.0357	Te	0.857	0.897	0.875
Si	0.043	0.052	0.0470	I		0.911	0.882
P	0.060	0.066	0.0604	Xe	0.894	0.908	0.902
S	0.082	0.081	0.0761	Cs	0.889		0.895
Cl	0.0955	0.1000	0.0942	Ba		0.916	0.901
Ar	0.122	0.120	0.115	La			0.906
K		0.142	0.138	Ce		0.926	0.911
Ca		0.168	0.163	Pr			0.915
Sc	0.190	0.196	0.190	Nd		0.935	0.920
Ti	0.221	0.224	0.219	Pm			0.924
V	0.253	0.252	0.250	Sm			0.928
Cr	0.283	0.284	0.282	Eu	0.925		0.931
Mn	0.313	0.319	0.314	Gd			0.934
Fe	0.342	0.357	0.347	Tb		0.952	0.937
Co	0.366	0.388	0.381	Dy	0.943		0.940
Ni		0.423	0.414	Ho			0.943
Cu	0.443	0.458	0.445	Er			0.945
Zn		0.492	0.479	Tm			0.948
Ga	0.528	0.524	0.510	Yb		0.963	0.950
Ge	0.554	0.556	0.540	In			0.952
As	0.588	0.584	0.567	Hf			0.954
Se		0.612	0.596	Ta			0.956
Br		0.639	0.622	W			0.957
Kr	0.660	0.663	0.646	Re			0.959
Rb	0.669	0.689	0.669	Os			0.961
Sr	0.702	0.712	0.691	Ir			0.962
Y		0.732	0.711	Pt	0.967		0.963
Zr		0.747	0.730	Au			0.964
Nb		0.769	0.748	Hg	0.958		0.966
Mo		0.786	0.764	Pb	0.972		0.968
Tc		0.801	0.779	U	0.970		0.976

(Data from Bambynek, W., *et al.*, Rev. Mod. Phys., **44**, 716, 1972)

[(a)] "Most reliable" experimental values.

[(b)] Unweighted means of theoretical values. See Bambynek, W., *op. cit.* for authors.

[(c)] Fitted values.

Fitting function: $[\omega_K/(1-\omega_K)]^{1/4} = B_0 + B_1 Z + B_3 Z^3$ where Z is the atomic number and $B_0 = 0.015 \pm 0.010$, $B_1 = 0.327 \pm 0.0005$, $B_3 = -(0.64 \pm 0.07) \times 10^{-6}$

An atom can de-excite by either emitting radiation (fluorescence) or an electron (Auger effect). The K fluorescence yield is defined as the probability of the excited atom (K shell vacancy) emitting a characteristic K X-ray when it de-excites.

K, L and M fluorescent yields

Fluorescence yields for K, L and M shells.
(Data from Bambynek, W., *et al.*, Mod. Phys., **44**, 716, 1972)

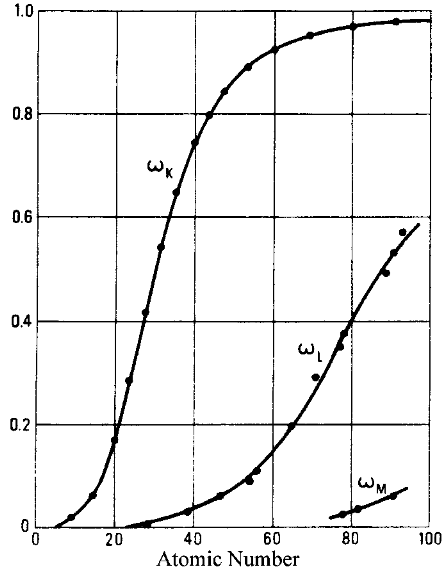

Passage of charged particles through matter

Total ionization loss by electrons or positrons (valid for all cases except extremely relativistic electrons)

$$-\left(\frac{dT}{ds}\right)_{\text{ion}} = \frac{2\pi e^4}{m_0 v^2} NZ \left\{ \ln\left[\frac{m_0 v^2 T}{I^2(1-\beta^2)}\right] - \beta^2 \right\} \quad \text{erg cm}^{-1}$$

(all quantities in cgs units).

For numerical calculations:

$$-\left(\frac{dT}{ds}\right)_{\text{ion}} = 4\pi r_0^2 \frac{m_0 c^2}{\beta^2} NZ \left[\ln\left[\beta\left(\frac{T + m_0 c^2}{I}\right)\left(\frac{T}{m_0 c^2}\right)^{1/2}\right] - \frac{1}{2}\beta^2 \right] \text{ MeV cm}^{-1}.$$

where

$\beta^2 = (v/c)^2 = 1 - [(T/m_0c^2) + 1]^{-2}$,

v = velocity of particle,

$m_0c^2 = 0.51$ MeV,

$4\pi r_0^2 = 1.00 \times 10^{-24}$ cm^2,

$r_0 = e^2/m_0c^2$ = classical electron radius,

NZ = electrons cm^{-3},

$Z =$ atomic number,
$I =$ mean excitation potential (MeV),
$I \simeq (13 \times 10^{-6})Z$ (MeV),
$T =$ kinetic energy (MeV),
$N =$ atoms cm^{-3}
(e.g., 0.1 MeV electron: 4.7 keV per cm of air).

Mean excitation potential I			
	Z	I (eV)	I/Z
H_2	1	19	19
He	2	44	22
Be	4	64	16
Air	7.2	94	13.1
Al	13	166	12.7
Ar	18	230	12.8
Cu	29	371	12.8
Ag	47	586	12.5
Xe	54	660	12.2
Au	79	1017	12.8
Pb	82	1070	13.1

(List from Sternheimer, R.M., *Methods of Experimental Physics*, L. Marton, ed., Vol. 5, part A, Academic Press, New York, 1961.)

For $I \ll T \ll m_0c^2$:

$$-\left(\frac{dT}{ds}\right)_{\text{ion}} = \frac{2\pi e^4}{T} NZ \ln\left(\frac{T\sqrt{2}}{I}\right) \text{ erg cm}^{-1}.$$

In the range 0 – 10 MeV:

$$-\left(\frac{dT}{ds}\right)_{\text{ion}} \approx \frac{45}{\beta^2} \text{ ion pairs (air-cm)}^{-1}.$$

Radiative loss for non-relativistic electrons

$$-\left(\frac{dT}{ds}\right)_{\text{rad}} = 3.09 \times 10^{-27} NZ^2(T + m_0c^2) \text{ MeV cm}^{-1},$$

where
$T + m_0c^2 =$ total energy of electron in MeV,
$N =$ atoms $\text{cm}^{-3} = (\rho/A) \times 6.022 \times 10^{23}$,
$Z =$ atomic number of absorber,
$A =$ atomic weight of absorber,
$\rho =$ density of absorber.

Ionization and radiative loss for highly relativistic electrons ($T \gg m_0c^2$)

$$-\left(\frac{dT}{ds}\right)_{\text{ion}} = \frac{2\pi e^4 NZ}{m_0 v^2}\left[\ln\frac{m_0 v^2 T}{2I^2(1-\beta^2)} - (2\surd(1-\beta^2) - 1 + \beta^2)\ln 2 + 1 - \beta^2 + \frac{1}{8}(1-\surd(1-\beta^2))^2\right] \text{erg cm}^{-1}.$$

(Bethe, H.A., *Handbuch der Physik*, Vol. 24, p. 273, Julius Springer, Berlin, 1933)

$$-\left(\frac{dE}{ds}\right)_{\text{rad}} = N\frac{Z^2}{137}r_0^2 E\left[4\ln\left(\frac{2E}{mc^2}\right) - \frac{4}{3}\right] \text{erg cm}^{-1}$$

(for $mc^2 \ll E \ll 137mc^2Z^{-1/3}$).

$$-\left(\frac{dE}{ds}\right)_{\text{rad}} = N\frac{Z^2 r_0^2}{137}E\left[4\ln(183Z^{-1/3}) + \frac{2}{9}\right] \text{erg cm}^{-1}$$

(for $E \gg 137mc^2Z^{-1/3}$).

$$E = T + m_o c^2$$

(Bethe, H.A. & Heitler, W., *Proc. Roy. Soc.* (*London*), **A146**, 83, 1934.)

$$-\left(\frac{dT}{d\xi}\right)_{\text{rad}} = \frac{T}{X_0}, \quad T = T_0 e^{-\xi/X_0},$$

where

ξ is the distance travelled measured in g cm^{-2}, T_0, the initial energy,

X_0, the radiation length $= \dfrac{716M_{\text{A}}}{Z(Z+1.3)[\ln(183Z^{-1/3}) + \frac{1}{8}]}$ g cm^{-2}

(M_{A} = atomic weight).

Radiation lengths X_0 and critical energy T_c for various susbstances

Absorber	Z	M_{A}	X_0 (gm cm^{-2})	T_c (MeV)
Hydrogen	1	1	58	340
Helium	2	4	85	220
Carbon	6	12	42.5	103
Nitrogen	7	14	38	87
Oxygen	8	16	34.2	77
Aluminium	13	27	23.9	47
Argon	18	39.9	19.4	34.5
Iron	26	55.8	13.8	24
Copper	29	63.6	12.8	21.5
Lead	82	207.2	5.8	6.9
Air			36.5	83
Water			35.0	93

(List from Bethe, H.A. & Ashkin, J., *Experimental Nuclear Physics*, E. Segrè, ed., Vol. I, John Wiley and Sons, New York, 1953.)

$T_c \simeq \dfrac{1600 m_0 c^2}{Z}$, the energy at which ionization losses equal radiation losses.

$$\frac{(dT/dx)_{\text{rad}}}{(dT/dx)_{\text{ion}}} \simeq \frac{TZ}{1600mc^2}.$$

Total ionization loss by heavy charged particles (kinetic energy $\leq$ rest mass)

$$-\left(\frac{dT}{ds}\right)_{\text{ion}} = \frac{4\pi z^2 e^4}{m_0 V^2} NZ \left[\ln \frac{2m_0 V^2}{I} - \ln(1-\beta^2) - \beta^2\right] \text{ erg cm}^{-1}$$

(all quantities in cgs units).

For numerical calculations:

$$-\left(\frac{dT}{ds}\right)_{\text{ion}} = 4.58 \times 10^{-4} \frac{z^2 NZ}{V^2} \left[\ln\left(\frac{1.14 \times 10^{-15} V^2}{I}\right) - \ln(1-\beta^2) - \beta^2\right] \text{ MeV cm}^{-1},$$

where

z = particle charge,
Z = absorber atomic number,
V = velocity of particle in cm $\text{s}^{-1} = 3 \times 10^{10}\beta$,
N = absorber atomic density $= \rho/A \times 6.022 \times 10^{23}$,
I = mean excitation potential (in eV),
$I \approx 13Z$ (eV),
$(1-\beta^2) = (1+T/M)^{-2}$,
T = kinetic energy in MeV,
M = mass of particle in MeV
(e.g., 2 MeV α particle in Si: 0.27 MeV μm^{-1}).

Approximate range–energy relationships

Range–energy for monoenergetic electrons

20 eV $\leq E \leq$ 10 keV:

$$\ln((Z/A)R_{\text{ex}}) = -4.5467 + 0.31104 \ln E + 0.07773(\ln E)^2$$

where

R_{ex} = extrapolated range in $\mu\text{g cm}^{-2}$ (25% precision),
Z/A = charge to mass ratio for absorbing medium,
E = energy in eV.

(Iskef, H. *et al.*, *Phys. Med. Biol.*, **28**, 535, 1983.)

Approximate range–energy relationships (cont.)

$10\ \text{keV} \lesssim E \lesssim 3\ \text{MeV}$:

$$R_{\text{ex}}\ (\text{mg cm}^{-2}) = 412E\ (\text{MeV})^n, \text{ where}$$
$$n = 1.265 - 0.0954 \ln E\ (\text{MeV}).$$

$1\ \text{MeV} \lesssim E \lesssim 20\ \text{MeV}$:

$$R_{\text{ex}}\ (\text{mg cm}^{-2}) = 530E\ (\text{MeV}) - 106.$$

Continuous β-ray spectra

β-ray spectra are exponentially attenuated with a mass-absorption coefficient nearly independent of the absorbing material:

$$\mu/\rho\ (\text{cm}^2\text{gm}^{-1}) = 17E_{\text{m}}^{-1.14},$$

where E_{m} (in MeV) is the maximum energy of the β-ray spectrum.

The thickness of absorber required to reduce the β-ray intensity to one-half its original value:

$$t_{1/2}(\text{mg cm}^{-2}) = 0.693/(\mu/\rho) = 41E_{\text{m}}^{1.14}.$$

Range-energy relationships for heavy particles

Alpha particles in air at 15°C, 760 mm, 4 – 15 MeV,

$$R(\text{cm}) = (0.005E(\text{MeV}) + 0.285)E(\text{MeV})^{1.5}.$$

Protons in air at 15°C, 760 mm, 10 – 200 MeV,

$$R(\text{cm}) = 100\left(\frac{E(\text{MeV})}{9.3}\right)^{1.8}.$$

Range of heavy particles in other materials

Bragg-Kleeman rule:

$$\frac{R_1}{R_0} = \frac{\rho_0}{\rho_1}\sqrt{\left(\frac{A_1}{A_0}\right)} \quad (\pm 15\%),$$

where

$$\rho = \text{density}$$
$$A = \text{atomic weight}.$$

For mixtures:

$$\sqrt{A} = \sum_i n_i \sqrt{A_i},$$

where n_i = atomic fraction of element i.

For air, $\sqrt{A_0} = 3.81$, $\rho_0 = 1.226 \times 10^{-3}$ gm cm^{-3} at 15°C, 760 mm, and therefore:

$$R_1 = 3.2 \times 10^{-4}\frac{\sqrt{A_1}}{\rho_1}R_{\text{air}}.$$

Energy units for high-energy particles

When dealing with high-energy particles from accelerators, nuclear reactions, and cosmic rays, it is convenient to use a special system of units for measurement of mass, energy, and momentum. In this system the quantities E (total energy), T (kinetic energy), M_0c^2 (rest energy), and pc (momentum $\times$ speed of light) are all measured in units of 10^9 eV, abbreviated GeV. The symbols M and P are used to represent M_0c^2 and pc.

The "momentum" P and energy E of a particle of speed $u = \beta c$:

$$P = \gamma\beta M \quad \text{with } \gamma = (1 - \beta^2)^{-1/2}$$

$$E = \gamma M \quad \text{or } \gamma = E/M$$

$$P = \beta E \quad \text{or } \beta = P/E$$

Relations between E, P, and E:

$$E^2 = P^2 + M^2$$

$$E^2 = M + T$$

$$P^2 = 2MT + T^2$$

For example, a $K+$ menson ($M_0c^2 = 0.494$ GeV) with kinetic energy $T = 0.363$ GeV would have the following values for P, E, $\gamma\beta$, β, and γ:

$$P = 0.700 \text{ GeV } (p = 700 \text{ MeV/c})$$

$$E = 0.857 \text{ GeV}$$

$$\gamma\beta = 1.42$$

$$\beta = 0.82$$

$$\gamma = 1.73$$

Energy loss rate

Energy loss rate in liquid hydrogen, gaseous helium, carbon, aluminium, tin, and lead. (From Caso, C., *et al.*, European Physical Journal, **C3**, 1, 1998)

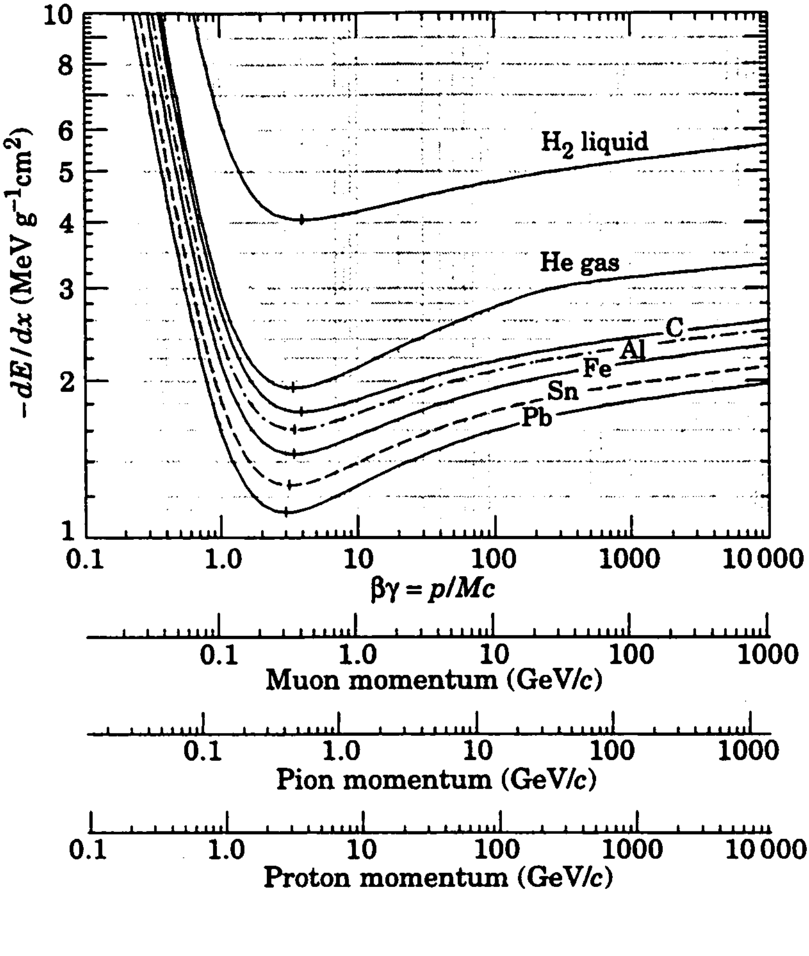

Range of heavy charged particles

Range of heavy charged particles in liquid hydrogen, gaseous helium, carbon, aluminum, tin, and lead. For example: for a $K^+(M = 0.4937$ GeV) whose momentum is 700 MeV/c ($T = 0.363$ GeV), $\beta\gamma = 1.42$. For lead we read R/M = 396, and so the range is $R = 196$ g cm^{-2}.
(From Caso, C., *et al.*, European Physical Journal, **C3**, 1. 1998)

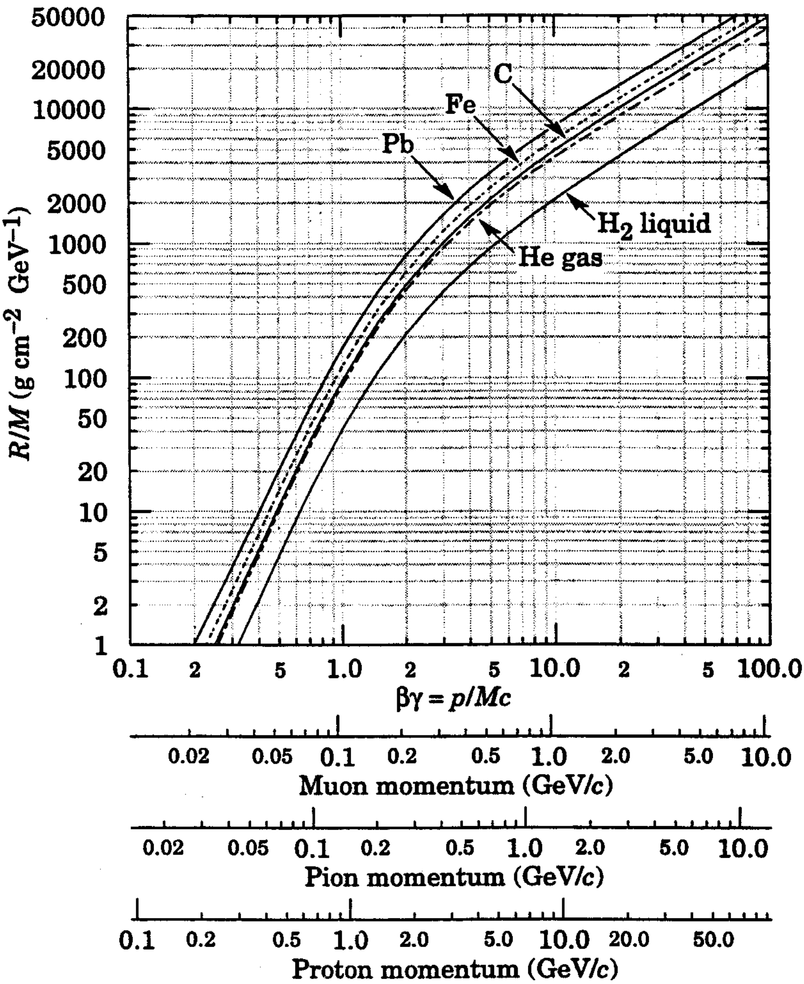

Charged particles in silicon

Range–energy curves for charged particles in silicon. Channeling of ions between crystal planes can result in significant variations from the data shown here. (Adapted from *ORTEC Manual on Surface Barrier Detectors.*)

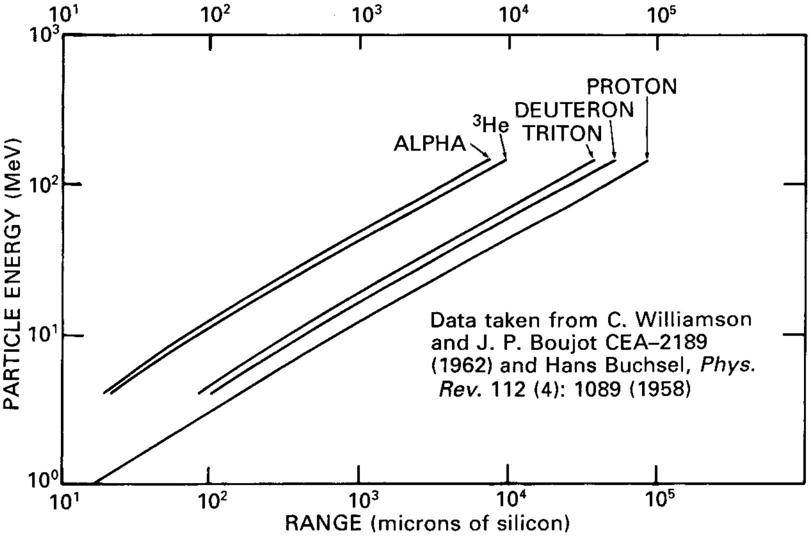

Specific energy loss for charged particles in silicon. Channeling of ions between crystal planes can result in significant variations from the data shown here. (Adapted from *ORTEC Manual on Surface Barrier Detectors.*)

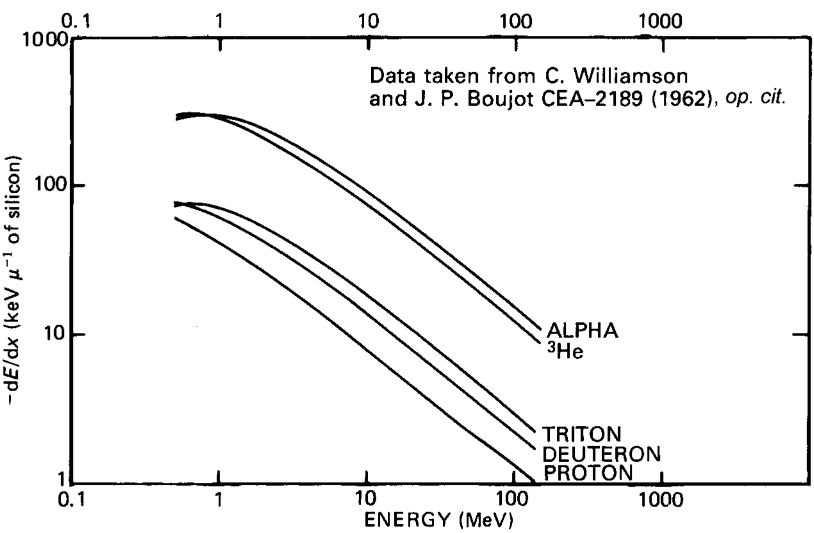

Charged particles in silicon (cont.)

Specific energy loss for electrons in silicon. Channeling between crystal planes can result in significant variations from the data shown here. (Adapted from *ORTEC Manual on Surface Barrier Detectors.*)

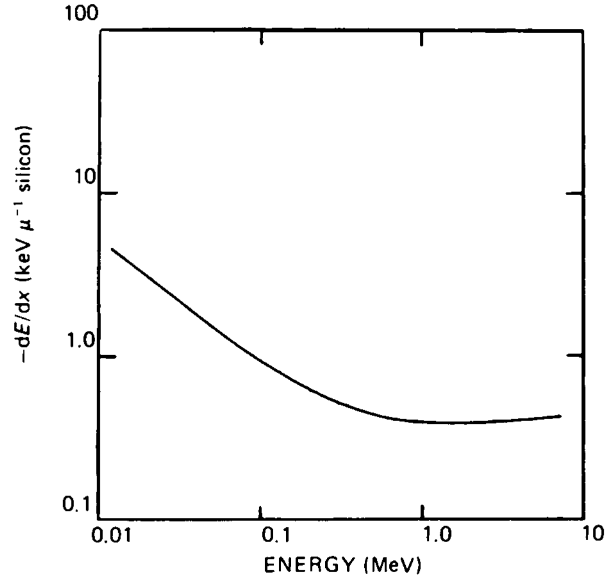

Specific energy loss for protons in silicon. Channeling of ions between crystal planes can result in significant variations from the data shown here. (Adapted from *ORTEC Manual on Surface Barrier Detectors.*)

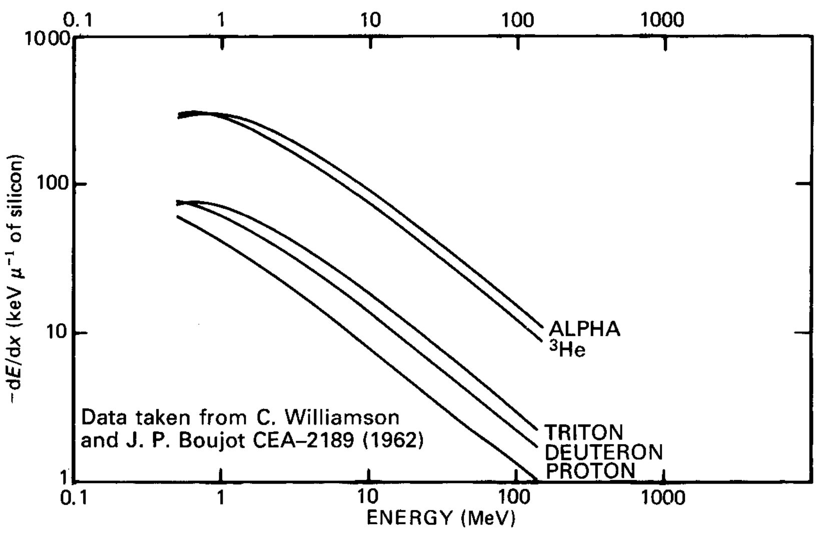

Charged particles in silicon (cont.)

Beta-ray range energy curve in silicon. Channeling between crystal planes can result in significant variations from the data shown here. (Adapted from *ORTEC Manual on Surface Barrier Detectors.*)

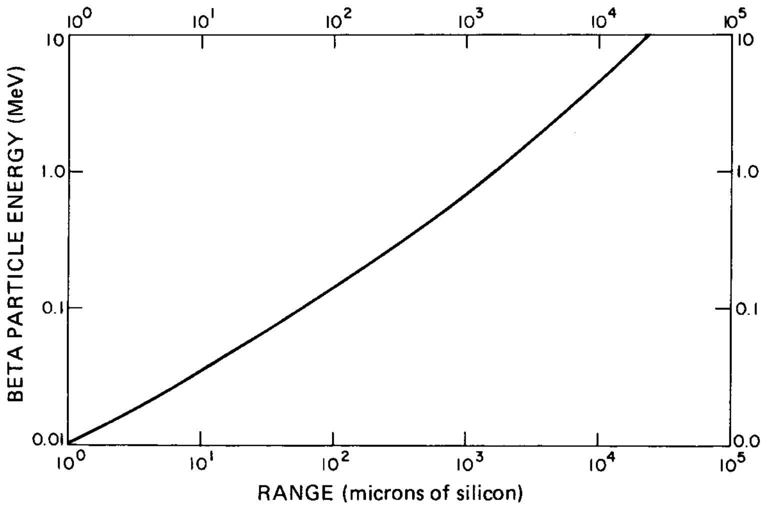

X-ray, gamma-ray, electron, neutron, and alpha radioactive sources (Adapted from Lederer, C. M. *et al.*, *Table of Isotopes*, John Wiley & Sons, 1968.)

X-ray sources

Source	X-ray energy (keV)	Half-life
^{37}Ar	Ar X-rays: 3.0, 3.2	35.1 d
^{41}Ca	Ca X-rays: 3.7, 4.0	8×10^4 yr
^{44}Ti	Ti X-rays: 4.5, 4.9	48 yr
^{49}V	Ti X-rays: 4.5, 4.9	330 d
^{55}Fe	Mn X-rays: 5.9, 6.5	2.6 yr
^{59}Ni	Co X-rays: 6.9, 7.7	8×10^4 yr
^{109}Cd	Ag X-rays: 22, 25	453 d
^{207}Bi	Pb X-rays: 73, 75, 85, 87	30 yr

Gamma-ray energy standards

Source	γ-ray energy (keV)	Half-life	Source	γ-ray energy (keV)	Half-life
^{57}Co	14.359	268 d	^{95}Nb	765.83	35 d
^{241}Am	26.350	458 yr	^{54}Mn	834.861	314 d
^{241}Am	59.554	458 yr	^{46}Sc	899.25	84.2 d
^{203}Hg	70.830	47 d	^{88}Y	898.033	108 d
^{203}Hg	72.871	47 d	^{207}Bi	1063.578	30 yr
^{131}I	80.164	8.05 d	^{65}Zn	1115.522	246 d
^{203}Hg	82.572	47 d	^{46}Sc	1120.50	84.2 d
^{203}Hg	84.916	47 d	^{60}Co	1173.231	5.26 yr
^{109}Cd	88.034	453 d	^{22}Na	1274.552	2.58 yr
^{57}Co	121.969	268 d	^{41}Ar	1293.641	1.85 hr
^{57}Co	136.328	268 d	^{60}Co	1332.518	5.26 yr
^{141}Ce	145.433	32.5 d	^{24}Na	1368.526	15.0 hr
^{139}Ce	165.85	140 d	^{52}V	1434.19	3.77 min
^{203}Hg	279.150	47 d	^{124}Sb	1691.24	60.9 d
^{131}I	284.307	8.05 d	^{28}Al	1778.77	2.31 min
^{51}Cr	320.102	27.8 d	^{88}Y	1836.111	108 d
^{131}I	364.493	8.05 d	Th C$''$	2614.47	1.91 yr
^{198}Au	411.795	2.70 d	^{24}Na	2753.92	15.0 hr
^{7}Be	477.556	53 d	^{12}B $(\beta^-)^{12}$C	4438.41	–
m_0c^2	511.003	–	^{14}C(d,p,β^+)^{15}N	5298.53	–
^{85}Sr	513.95	64 d	^{16}O(^{3}He, α)^{15}O	5240.03	–
^{207}Bi	569.62	30 yr	^{14}N(d,p)^{15}N	5270.10	–
Th C$'$	583.139	1.91 yr	^{16}O*	6127.8	–
^{137}Cs	661.632	30 yr	^{13}C(p,γ)^{14}N	9169.0	–

Electron energy standards

Source	Conversion-electron energy (keV)	Half-life
Cd^{109}	62.19	453 d
Cd^{109}	84.2	453 d
Ce^{141}	103.44	33 d
Ce^{139}	126.91	140 d
Ce^{141}	138.63	33 d
Ce^{139}	159.61	140 d
Hg^{203}	193.64	46.9 d
Hg^{203}	264.49	46.9 d
Au^{198}	328.69	2.698 d
Sn^{113}	363.8	115 d
Sn^{113}	387.6	115 d
Au^{198}	397.68	2.698 d
Bi^{207}	481.61	30 yr
Bi^{207}	554.37	30 yr
Cs^{137}	624.15	30.0 yr
Cs^{137}	655.88	30.0 yr
Co^{58}	803.35	71.3 d
Co^{58}	809.62	71.3 d
Mn^{54}	828.86	303 d
Mn^{54}	834.17	303 d
Y^{88}	881.86	108 d
Y^{88}	895.76	108 d
Bi^{207}	975.57	30 yr
Bi^{207}	1048.1	30 yr
Zn^{65}	1106.46	345 d
Zn^{65}	1114.35	245 d

Characteristic of Be(α,n) Neutron Sources

		E_α	Neutron Yield per 10^6 Primary Alpha Particles		Percent Yield with $E_n < 1.5$ MeV	
Source	Half-Life	(MeV)	Calculated	Experimental	Calculated	Experimetal
^{239}Pu/Be	24000 y	5.14	65	57	11	9–33
^{210}Po/Be	138 d	5.30	73	69	13	12
^{238}Pu/Be	87.4 y	5.48	79	–	–	–
^{241}Am/Be	433 y	5.48	82	70	14	15–23
^{244}Cm/Be	18 y	5.79	100	–	18	29
^{242}Cm/Be	162 d	6.10	118	106	22	26
^{226}Ra/Be + daughters	1602 y	Multiple	502	–	26	33–38
^{227}Ac/Be + daughters	21.6 y	Multiple	702	–	28	38

(From Knoll, G.F., *Radiation Detection and Measurement*, John Wiley & Sons, 1989 with permission.)

Common Alpha-Emitting Radioisotope Sources

Source	Half-Life	Alpha Particle Kinetic Energy (with Uncertainty) in MeV		Percent Branching
^{148}Gd	93 y	3.182787	±0.000024	100
^{232}Th	1.4×10^{10} y	4.012	±0.005	77
		3.953	±0.008	23
^{238}U	4.5×10^{9} y	4.196	±0.004	77
		4.149	±0.005	23
^{235}U	7.1×10^{8} y	4.598	±0.002	4.6
		4.401	±0.002	56
		4.374	±0.002	6
		4.365	±0.002	12
		4.219	±0.002	6
^{236}U	2.4×10^{7} y	4.494	±0.003	74
		4.445	±0.005	26
^{230}Th	7.7×10^{4} y	4.6875	±0.0015	76.3
		4.6210	±0.0015	23.4
^{234}U	2.5×10^{5} y	4.7739	±0.0009	72
		4.7220	±0.0009	28
^{231}Pa	3.2×10^{4} y	5.0590	±0.0008	11
		5.0297	±0.0008	20
		5.0141	±0.0008	25.4
		4.9517	±0.0008	22.8
^{239}Pu	2.4×10^{4} y	5.1554	±0.0007	73.3
		5.1429	±0.0008	15.1
		5.1046	±0.0008	11.5
^{240}Pu	6.5×10^{3} y	5.16830	±0.00015	76
		5.12382	±0.00023	24
^{243}Am	7.4×10^{3} y	5.2754	±0.0010	87.4
		5.2335	±0.0010	11
^{210}Po	138 d	5.30451	±0.00007	100
^{241}Am	433 d	5.48574	±0.00012	85.2
		5.44298	±0.00013	12.8
^{238}Pu	88 y	5.49921	±0.00020	71.1
		5.4565	±0.0004	28.7
^{244}Cm	18 y	5.80496	±0.00005	76.4
		5.762835	±0.000030	23.6
^{243}Cm	30 y	6.067	±0.003	1.5
		5.992	±0.002	5.7
		5.7847	±0.0009	73.2
		5.7415	±0.0009	11.5
^{242}Cm	163 d	6.11292	±0.00008	74
		6.06963	±0.00012	26
^{254m}Es	276 d	6.4288	±0.0015	93
^{253}Es	20.5 d	6.63273	±0.00005	90
		6.5916	±0.0002	6.6

(From Knoll, G.F., *Radiation Detection and Measurement,* John Wiley & Sons, 1989 with permission.)

Atomic and nuclear properties of materials

Material	Z	A	$\langle Z/A \rangle$	Nuclear[a] collision length λ_T {g/cm^2}	Nuclear[a] interaction length λ_I {g/cm^2}	$dE/dx\vert_{\min}^{b}$ $\left\{\frac{\text{MeV}}{\text{g/cm}^2}\right\}$	Radiation length[c] X_0 {g/cm^2}	Radiation length[c] X_0 {cm}	Density {g/cm^3} ({g/l} for gas)	Liquid boiling point at 1 atm (K)	Refractive index n ($(n-1) \times 10^6$ for gas)
H_2 gas	1	1.00794	0.99212	43.3	50.8	(4.103)	61.28[d]	(731000)	(0.088)[0.0899]		[139.2]
H_2	1	1.00794	0.99212	43.3	50.8	4.045[e]	61.28[d]	866	0.0708	20.39	1.112
D_2	1	2.0140	0.49652	45.7	54.7	(2.052)	122.4	724	0.169[0.179]	23.65	1.128[138]
He	2	4.002602	0.49968	49.9	65.1	(1.937)	94.32	756	0.1249[0.1786]	4.224	1.024[34.9]
Li	3	6.941	0.43221	54.6	73.4	1.639	82.76	155	0.534		–
Be	4	9.012182	0.44384	55.8	75.2	1.594	56.19	35.28	1.848		–
C	6	12.011	0.49954	60.2	86.3	1.745	42.70	18.8	2.265[f]		–
N_2	7	14.00674	0.49976	61.4	87.8	(1.825)	37.99	47.1	0.8073[1.250]	77.36	1.205[298]
O_2	8	15.9994	0.50002	63.2	91.0	(1.801)	34.24	30.0	1.141[10428]	90.18	1.22[296]
F_2	9	18.9984032	0.47372	65.5	95.3	(1.675)	32.93	21.85	1.507[1.696]	85.24	[195]
Ne	10	20.1797	0.49555	66.1	96.6	(1.724)	28.94	24.0	1.204[0.9005]	27.09	1.092[67.1]
Al	13	26.981539	0.48181	70.6	106.4	1.615	24.01	8.9	2.70		–
Si	14	28.0855	0.49848	70.6	106.0	1.664	21.82	9.36	2.33		3.95
Ar	18	39.948	0.45059	76.4	117.2	(1.519)	19.55	14.0	1.396[1.782]	87.28	1.233[283]
Ti	22	47.867	0.45948	79.9	124.9	1.476	16.17	3.56	4.54		–
Fe	26	55.845	0.46556	82.8	131.9	1.451	13.84	1.76	7.87		–
Cu	29	63.546	0.45636	85.6	134.9	1.403	12.86	1.43	8.96		–
Ge	32	72.61	0.44071	88.3	140.5	1.371	12.25	2.30	5.323		–
Sn	50	118.710	0.42120	100.2	163	1.264	8.82	1.21	7.31		–
Xe	54	131.29	0.41130	102.8	169	(1.255)	8.48	2.40	2.593[5.858]	165.0	[701]
W	74	183.84	0.40250	110.3	185	1.145	6.76	0.35	19.3		–
Pt	78	195.08	0.39984	113.3	189.7	1.129	6.54	0.305	21.45		–
Pb	82	207.2	0.39575	116.2	194	1.123	6.37	0.56	11.35		–
U	92	238.0289	0.38651	117.0	199	1.082	6.00	$\approx$ 0.32	$\approx$ 18.95		–

Atomic and nuclear properties of materials (cont.)

Material Z A	$\langle Z/A\rangle$	Nuclear[a] collision length λ_T {g/cm^2}	Nuclear[a] interaction length λ_I {g/cm^2}	$dE/dx\vert^{b}_{\min}$ $\left\{\frac{\mathrm{MeV}}{\mathrm{g/cm^2}}\right\}$	Radiation length[c] X_0 {g/cm^2}	Radiation length[c] X_0 {cm}	Density {g/cm^3} ({g/l} for gas)	Liquid boiling point at 1 atm (K)	Refractive index n ($(n-1)\times 10^6$ for gas)
Air, (20°C, 1 atm.), [STP]	0.49919	62.0	90.0	(1.825)	36.66	[30420]	(1.205)[1.2931]	78.8	(273)[293]
H_2O	0.55509	60.1	83.6	1.991	36.08	36.1	1.00	373.15	1.33
CO_2	0.49989	62.4	89.7	(1.819)	36.2	[18310]	[1.977]		[410]
Shielding concrete[g]	0.50274	67.4	99.9	1.711	26.7	10.7	2.5		–
Borosilicate glass (Pyrex)[h]	0.49707	66.2	97.6	1.695	28.3	12.7	2.23		1.474
SiO_2 (fused quartz)	0.49926	66.5	97.4	1.70[i]	27.05	12.3	2.20[j]		1.458
Dimethyl ether, $(CH_3)_2O$	0.54778	59.4	82.9	–	38.89	–	–	248.7	–
Methane, CH_4	0.62333	54.8	73.4	(2.417)	46.22	[64850]	0.4224[0.717]	111.7	[444]
Ethane, C_2H_6	0.59861	55.8	75.7	(2.304)	45.47	[34035]	0.509(1.356)[k]	184.5	(1.038)[k]
Propane, C_3H_8	0.58962	56.2	76.5	(2.262)	45.20	–	(1.879)	231.1	–
Isobutane, $(CH_3)_2$ $CHCH_3$	0.58496	56.4	77.0	(2.239)	45.07	[16930]	[2.67]	261.42	[1900]
Octane, liquid, $CH_3(CH_2)_6CH_3$	0.57778	56.7	77.7	2.123	44.86	63.8	0.703	398.8	1.397
Paraffin wax, $CH_3(CH_2)_{n\approx 23}CH_3$	0.57275	56.9	78.2	2.087	44.71	48.1	0.93		–
Nylon, type 6[l]	0.54790	58.5	81.5	1.974	41.84	36.7	1.14		–
Polycarbonate (Lexan)[m]	0.52697	59.5	83.9	1.886	41.46	34.6	1.20		–
Polyethylene teraphthlate (Mylar)[n]	0.52037	60.2	85.7	1.848	39.95	28.7	1.39		–
Polyethylene[o]	0.57034	57.0	78.4	2.076	44.64	≈ 47.9	0.92–0.95		–
Polyimide film (Kapton)[p]	0.51364	60.3	85.8	1.820	40.56	28.6	1.42		–
Lucite, Plexiglas[q]	0.53937	59.3	83.0	1.929	40.49	≈ 34.4	1.16–1.20		≈ 1.49
Polystyrene, scintillator[r]	0.53768	58.5	81.9	1.936	43.72	42.4	1.032		1.581
Polytetrafluoroethylene (Teflon)[s]	0.47992	64.2	93.0	1.671	34.84	15.8	2.20		–
Polyvinyltolulene, scintillator[t]	0.54155	58.3	81.5	1.956	43.83	42.5	1.032		–

Atomic and nuclear properties of materials (cont.)

Material	Z	A	$\langle Z/A \rangle$	Nuclear[a] collision length λ_T {g/cm^2}	Nuclear[a] interaction length λ_I {g/cm^2}	$dE/dx\|^b_{min}$ $\left\{\frac{\text{MeV}}{\text{g/cm}^2}\right\}$	Radiation length[c] X_0 {g/cm^2}	X_0 {cm}	Density {g/cm^3} ({g/l} for gas)	Liquid boiling point at 1 atm (K)	Refractive index n (($(n-1)\times 10^6$ for gas)
Barium fluoride (BaF_2)			0.42207	92.0	145	1.303	9.91	2.05	4.89		1.56
Bismuth germanate (BGO)[u]			0.42065	98.2	175	1.251	7.97	1.12	7.1		2.15
Cesium iodide (CsI)			0.41569	102	167	1.243	8.39	1.85	4.53		1.80
Lithium fluoride (LiF)			0.46262	62.2	88.2	1.614	39.25	14.91	2.632		1.392
Sodium fluoride (NaF)			0.47632	66.6	98.3	1.69	29.87	11.68	2.558		1.336
Sodium iodide (NaI)			0.42697	94.6	151	1.305	9.49	2.59	3.67		1.775
Silica Aerogel[v]			0.52019	64	92	1.83	29.83	≈ 150	0.1–0.3		$1.0 + 0.25\rho$
NEMA G10 plate[w]				62.6	90.2	1.87	33.0	19.4	1.7		–

Revised April 1998 by D.E. Groom (LBNL). Gases are evaluated at 20°C and 1 atm (in parentheses) or at STP [square brackets]. Densities and refractive indices without parthentheses or brackets are for solids or liquids, or are for cryogenic liquids indicated boiling point (BP) at 1 atm. Refractive indices are evaluated at the sodium D line. Data for compounds and mixtures are from Refs. 1 and 2.

Atomic and nuclear properties of materials (cont.)

Material	Dielectric constant ($\kappa = \epsilon/\epsilon_0$) () is $(\kappa - 1)\times 10^6$ for gas	Young's modulus [10^6 psi]	Coeff. of thermal expansion [10^{-6} cm/cm-°C]	Specific heat [cal/g-°C]	Electrical resistivity [$\mu\Omega$cm(@°C)]	Thermal conductivity [cal/cm-°C-sec]
H_2	(253.9)	–	–	–	–	–
He	(64)	–	–	–	–	–
Li	–	–	56	0.86	8.55(0°)	0.17
Be	–	37	12.4	0.436	5.885(0°)	0.38
C	–	0.7	0.6–4.3	0.165	1375(0°)	0.057
N_2	(584.5)	–	–	–	–	–
O_2	(495)	–	–	–	–	–
Ne	(127)	–	–	–	–	–
Al	–	10	23.9	0.215	2.65(20°)	0.53
Si	11.9	16	2.8–7.3	0.162	–	0.20
Ar	(517)	–	–	–	–	–
Ti	–	16.8	8.5	0.126	50(0°)	–
Fe	–	28.5	11.7	0.11	9.71(20°)	0.18
Cu	–	16	16.5	0.092	1.67(20°)	0.94
Ge	16.0	–	5.75	0.073	–	0.14
Sn	–	6	20	0.052	11.5(20°)	0.16
Xe	–	–	–	–	–	–
W	–	50	4.4	0.032	5.5(20°)	0.48
Pt	–	21	8.9	0.032	9.83(0°)	0.17
Pb	–	2.6	29.3	0.038	20.65(20°)	0.083
U	–	–	36.1	0.028	29(20°)	0.064

1. R.M. Sternheimer, M.J. Berger, and S.M. Seltzer, Atomic Data and Nuclear Data Tables **30**, 261–271 (1984).
2. S.M. Seltzer and M.J. Berger, Int. J. Appl. Radiat. **33**, 1189-1218 (1982).
3. S.M. Seltzer and M.J. Berger, Int. J. Appl. Radiat. **35**, 665–676 (1984).

Atomic and nuclear properties of materials (cont.)

[a] σ_T, λ_T and λ_I are energy dependent. Values quoted apply to high energy range, where energy dependence is weak. Mean free path between collisions (λ_T) or inelastic interactions (λ_I), calculated from $\lambda^{-1} = N_A \sum w_j \sigma_j / A_j$, where N is Avogadro's number and w_j is the weight fraction of the jth element in the element, compound, or mixture. σ_{total} at 80–240 GeV for neutrons ($\approx$ σ for protons) from Murthy *et al.*, Nucl. Phys. **B92**, 269 (1975). This scales approximately as $A^{0.77}$. $\sigma_{\text{inelastic}} = \sigma_{\text{total}} - \sigma_{\text{elastic}} - \sigma_{\text{quasielastic}}$; for neutrons at 60–375 GeV from Roberts *et al.*, Nucl. Phys. **B159**, 56 (1979). For protons and other particles, see Carroll *et al.*, Phys. Lett. **80B**, 319 (1979); note that $\sigma_I(p) \approx \sigma_I(n)$. σ_I scales approximately as $A^{0.71}$

[b] For minimum-ionizing pions (results are very slightly different for other particles). Minimum dE/dx calculated in 1994, using density effect correction coefficients from Ref. 1. For electrons and positrons see Ref. 3. Ionization energy loss is discussed in Sec. 23.

[c] From Y.S. Tsai, Rev. Mod. Phys. **46**, 815 (1974); X_0 data for all elements up to uranium are given. Corrections for molecular binding applied for H_2 and D_2. For atomic H, $X_0 = 63.05$ g/cm^2.

[e] Density effect constants evaluated for $\rho = 0.0600$ g/cm^3 (H_2 bubble chamber?).

[d] For molecular hydrogen (deuterium). For atomic H, $X_0 = 63.047$ g cm^{-2}.

[f] For pure graphite; industrial graphite density may vary 2.1–2.3 g/cm^3.

[g] Standard shielding blocks, typical composition O_2 52%, Si 32.5%, Ca 6%, Na 1.5%, Fe 2%, Al 4%, plus reinforcing iron bars. The attenuation length, $l = 115 \pm 5$ g/cm^2, is also valid for earth (typical $\rho = 2.15$), from CERN-LRL-RHEL Shielding exp., UCRL-17841 (1968).

[h] Main components: 80% SiO_2 + 12% B_2O_3 + 5% Na_2O.

[i] Calculated using Sternheimer's density effect parameterization for $\rho = 2.32$ g cm^{-3}. Actual value may be slightly lower.

[j] For typical fused quartz. The specific gravity of crystalline quartz is 2.64.

Atomic and nuclear properties of materials (cont.)

[k] Solid ethane density at $-60°$C; gaseous refractive index at $0°$C, 546 mm pressure.

[l] Nylon, Type 6, $(NH(CH_2)_5CO)_n$

[m] Polycarbonate (Lexan), $(C_{16}H_{14}O_3)_n$

[n] Polyethylene terephthlate, monomer, $C_5H_4O_2$

[o] Polyethylene, monomer $CH_2{=}CH_2$

[p] Polymide film (Kapton), $(C_{22}H_{10}N_2O_5)_n$

[q] Polymethylmethacralate, monomer $CH_2{=}C(CH_3)CO_2CH_3$

[r] Polystyrene, monomer $C_6H_5CH{=}CH_2$

[s] Teflon, monomer $CF_2{=}CF_2$

[t] Polyvinyltolulene, monomer 2-$CH_3C_6H_4CH{=}CH_2$

[u] Bismuth germanate (BGO), $(Bi_2O_3)_2(GeO_2)_3$

[v] $n(SiO_2) + 2n(H_2O)$ used in Čerenkov counters, ρ = density in g/cm^3. From M. Cantin *et al.*, Nucl. Instrum. Methods **118**, 177 (1974).

[w] G10-plate, typical 60% SiO_2 and 40% epoxy.

(From Caso, C., *et al.*, European Physical Journal, **C3**, 1, 1998)

Characteristics of synchrotron radiation

The angular and spectral distribution of radiation emitted by a relativistic electron in instantaneously circular motion is, according to Schwinger (*Phys. Rev.*, **75**, 1912, 1949), given by (cgs units):

$$\frac{\partial^2 P}{\partial\lambda\partial\psi} = \frac{27}{32\pi^3}\frac{e^2 c}{R^3}\left(\frac{\lambda_c}{\lambda}\right)^4 \gamma^8(1+(\gamma\psi)^2)^2\left[K^2_{2/3}(\xi) + \frac{(\gamma\psi)^2}{1+(\gamma\psi)^2}K^2_{1/3}(\xi)\right]$$

erg s^{-1} rad^{-1} cm^{-1},

where

e = electron charge,
c = velocity of light,
R = radius of curvature,
λ = wavelength,
$\lambda_c = \frac{4}{3}\pi R\gamma^{-3}$, the 'critical wavelength',
$\gamma = E/m_0c^2$,
where E = total electron energy and m_0 = electron mass,
ψ = vertical angle measured from the plane of the orbit,
$K_{1/2}(\xi)$, $K_{2/3}(\xi)$ are modified Bessel functions of the second kind, where $\xi \equiv (\lambda_c/2\lambda)(1+(\gamma\psi)^2)^{3/2}$.

The first term within the brackets correspond to radiation polarized in the plane of the orbit, the second to radiation polarized perpendicular to the orbital plane.

The universal synchrotron radiation function $G(y)$ for monoenergetic electrons as a function of $1/y$.

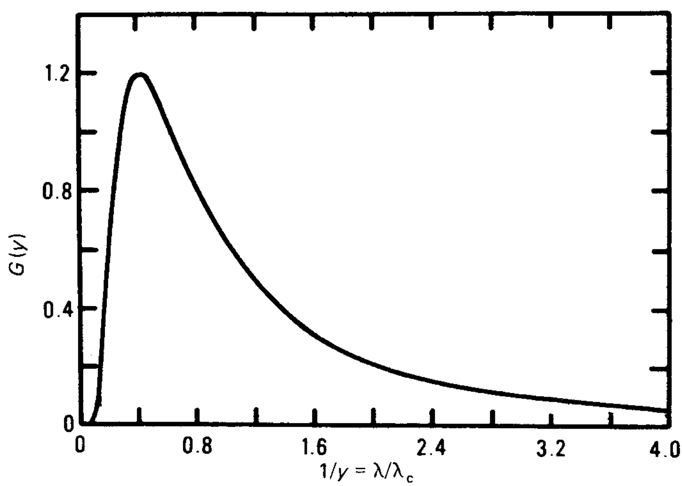

The spectral distribution of power is obtained by integrating the above equation over the angle ψ:

$$\frac{dP}{d\lambda} = \frac{3^{5/2}}{16\pi^2}\frac{e^2c}{R^3}\left(\frac{E}{mc^2}\right)^7 G(y),$$

where

$$G(y) = y^3\int_y^\infty K_{5/3}(\eta)d\eta, \quad y = \lambda_c/\lambda.$$

The total power radiated,

$$P = \int \frac{dP}{d\lambda}d\lambda = \frac{2}{3}\frac{e^2c}{R^2}\left(\frac{E}{mc^2}\right)^4.$$

The photon flux distribution is obtained by dividing the power distribution function by the photon energy:

$$\frac{\partial^3 N}{\partial\lambda\partial\psi\partial t} = \frac{\lambda}{hc}\frac{\partial^2 P}{\partial\lambda\partial\psi} \quad \text{photons s}^{-1}\text{ rad}^{-1}\text{ cm}^{-1}.$$

The radiation emitted by the electron in the plane of its orbit is 100% polarized. Above and below this plane, the radiation is elliptically polarized.

Polarization:

$$(I_{\|} - I_{\perp})(I_{\|} + I_{\perp}) = \frac{K_{2/3}^2(\xi) - [(\gamma\psi)^2/(1+(\gamma\psi)^2)]K_{1/3}^2(\xi)}{K_{2/3}^2(\xi) + [(\gamma\psi)^2/(1+(\gamma\psi)^2)]K_{1/3}^2(\xi)}.$$

Fraction of radiation, integrated over vertical angle ψ, that is parallel polarized (From Krinsky, S. *et al.* in *Handbook of Synchrotron Radiation*, E. Koch, ed., North-Holland Publishing Co., 1983, with permission.)

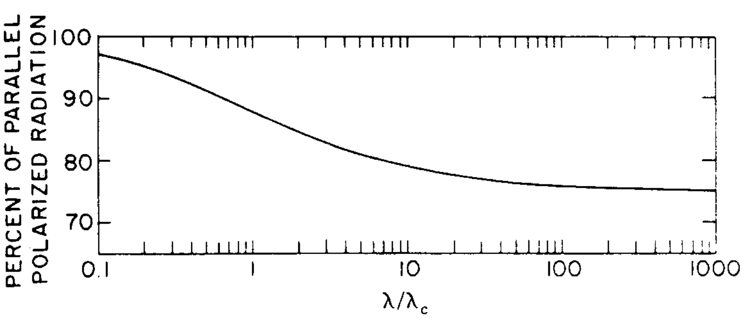

Dependence on the vertical angle ψ of the intensities of the parallel (solid line) and perpendicular (dashed line) polarization components of the photon flux. The individual curves, plotted for $\lambda/\lambda_c = \frac{1}{3}$, 1, 10, and 100, are individually normalized to the intensity in the orbital plane ($\psi = 0$) at the respective λ/λ_c value. Note that the abscissa, ψ multiplied by the electron energy γ, makes these curves universal. (From Krinsky, S. *et al.* in *Handbook of Synchrotron Radiation*, E. Koch, ed., North-Holland Publishing Co., 1983, with permission.)

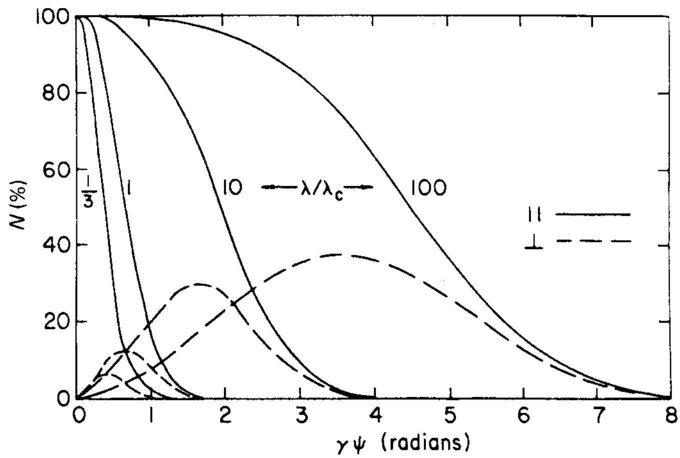

Practical formulae for electron storage rings

E: electron energy R: radius of ring J: electron current.

Energy loss per turn, per electron:

$$\delta E \text{ (keV)} = 88.5 \frac{E^4(\text{GeV})}{R(\text{m})}.$$

Critical wavelength:

$$\lambda_c \text{ (Å)} = 5.59 \frac{R(\text{m})}{E^3(\text{GeV})}.$$

Characteristic energy:

$$\varepsilon_c \text{ (eV)} = 2218 \frac{E^3(\text{GeV})}{R(\text{m})} = 2.96 \times 10^{-7} \frac{\gamma^3}{R(\text{m})}.$$

Emission angle:

$$\approx \frac{1}{\gamma} = \frac{m_0 c^2}{E},$$

with

$$\gamma = \frac{E}{m_0 c^2} = 1957 E(\text{GeV}).$$

Energy of a photon:

$$\varepsilon(\text{KeV}) = \frac{12.40}{\lambda(\text{Å})}.$$

Photon flux angular distribution:

$$\frac{\partial^4 N}{\partial\lambda\,\partial\psi\,\partial\theta\,\partial t} = 8.267\times 10^{-5}\left(\frac{\lambda_c}{\lambda}\right)\frac{3\gamma^5}{R}F\left(\frac{\lambda_c}{\lambda},\ \gamma\psi\right)J$$

photons s^{-1} mrad^{-1} Å^{-1},

where

$$F\left(\frac{\lambda_c}{\lambda},\gamma\psi\right) = (1+\gamma^2\psi^2)^2\left[K^2_{2/3}(\xi) + \frac{\gamma^2\psi^2}{1+\gamma^2\psi^2}K^2_{1/3}(\xi)\right],$$

$$\xi = \frac{1}{2}\frac{\lambda_c}{\lambda}(1+\gamma^2\psi^2)^{3/2},$$

where

θ = horizontal angle,

ψ = vertical angle,

J = current (mA),

R = radius of ring (m).

Photon flux integrated over all vertical angles

$$\frac{\partial^3 N}{\partial\lambda\,\partial\theta\,\partial t} = 7.9\times 10^{11} G(y) J(\text{mA})\frac{[E(\text{GeV})]^7}{[R(\text{m})]^2}\lambda(\text{Å})$$

photons s^{-1} mrad^{-1} Å^{-1},

$$\frac{\partial^3 N}{\partial\varepsilon\,\partial\theta\,\partial t} = 5.56\times 10^{7} G(y) J(\text{mA})\frac{[E(\text{GeV})]^7}{[R(\text{m})]^2}\lambda^3(\text{Å})$$

photons s^{-1} mrad^{-1} eV^{-1},

for $\lambda \gg \lambda_c$

$$\frac{\partial^3 N}{\partial\lambda\,\partial\theta\,\partial t} = 9.35\times 10^{13} J(\text{mA})\frac{[R(\text{m})]^{1/3}}{[\lambda(\text{Å})]^{4/3}}$$

photons s^{-1} mrad^{-1} Å^{-1}.

V. Kostroun (*Nuc. Inst. Meth.*, **172**, 371, 1980) provides series expressions for the modified Bessel functions of fractional order which are suitable for evaluation with programmable calculators or desktop computers.

X-ray spectroscopy

Crystal spectroscopy

Collimated single crystal Bragg spectrometer. Bragg condition: $n\lambda = 2d\sin\theta$, where d is the effective spacing of the crystal planes that participate in the reflection. (Adapted from Burek, A., *Space Sci. Inst.*, **2**, 53, 1976.)

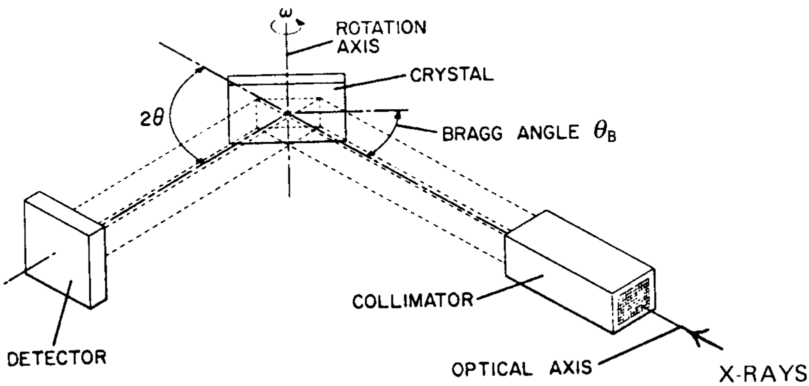

Single crystal rocking curve $C_\lambda \cdot \theta_B + \Delta = \sin^{-1}(n\lambda/2d_\infty)$, where Δ = refraction correction, d_∞ = physical spacing of reflection planes, and θ_B = Bragg angle ignoring refraction. (Adapted from Burek, A., *Space Sci. Inst.*, **2**, 53, 1976.)

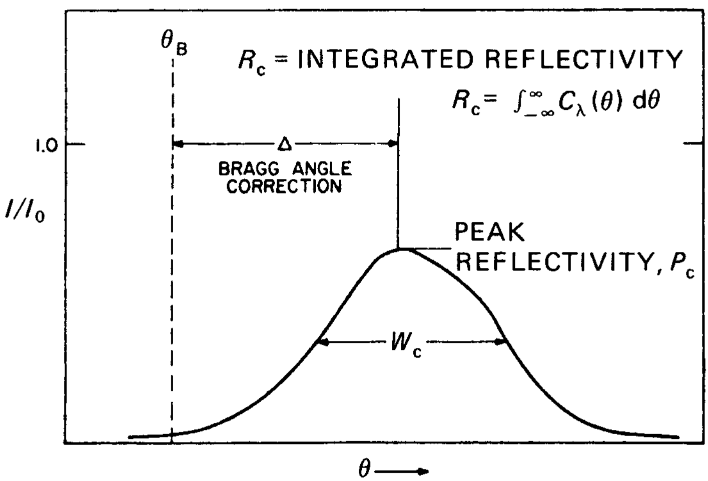

Crystal properties

Crystal	Density (g cm^{-3})	Plane	$2d$ (Å)	Integrated reflectivity ($\theta = 60°$)
Quartz	2.66	$10\bar{1}0$	8.350	6.25×10^{-5}(D)
		$10\bar{1}\bar{1}$	6.592	1.23×10^{-4}(D)
		$20\bar{2}\bar{3}$	2.750	$\approx 1.5 \times 10^{-5}$(D)
		$22\bar{4}\bar{3}$	2.028	$\approx 6 \times 10^{-6}$(D)
Topaz	3.49–3.57	303	2.712	(40°) 6×10^{-5}(D)
		040	4.40	
		400	2.3246	(43°) 1×10^{-5}(D)
		200	4.64	
Calcite	2.710	211	6.083	1.62×10^{-4}(D)
Silicon	2.33	111	6.284	1.2×10^{-4}(D)
		220	3.840	8×10^{-5}(D)
		200	5.44169	
Germanium	5.33	111	6.545	
		220	4.000	2.3×10^{-4}(D)
		200	5.66897	
Beryl (golden)	2.66	$10\bar{1}0$	15.9549	$\approx 6 \times 10^{-5}$(D)
Sylvite	1.99	200	6.292	
Halite	2.164	200	5.641	
KBr	2.756	200	6.584	
Fluorite	3.18	111	6.306	
		200	5.4744	
Aluminum	2.699	200	4.057	
		111	4.676	
LiF	2.64	420	1.80	
		200	4.027	10^{-4}–3×10^{-4}(D)
		220	2.848	
Graphite	2.21	002	6.708	1.52×10^{-3}(S)
Mica	2.77–2.88	002	19.84	$\approx 2 \times 10^{-5}$(S)
Clinochlore	2.6–3.3	001	28.392	
ADP	1.803	101	10.648	9.0×10^{-5}(S)
		220	5.305	1.4×10^{-5}(S)
		200	7.50	
EDDT	1.538	020	8.808	1.15×10^{-4}(S)
PET	1.39	002	8.742	2.2×10^{-4}(S)
SHA	1.3	110	13.98	
KAP	1.636	001	26.5790	5×10^{-5}(S)
RAP	1.94	001	26.121	1.5×10^{-4}(S)
TlAP	2.7	001	25.7567	7.0×10^{-4}(S)
CsAP	2.178	001	25.68	
NH_4AP	1.415	002	26.14	1.5×10^{-4}(S)
NaAP	1.504	002	26.42	

D = double crystal; S = single crystal.
(Adapted from Burek, A., *Space Sci. Inst.*, **2**, 53, 1976.)

Useful characteristic lines for X-ray spectroscopy

Wavelength(Å)	Energy(keV)	Element	Designation
1.54	8.04	Cu	$K\alpha_{1,2}$
1.66	7.47	Ni	$K\alpha_{1,2}$
1.94	6.40	Fe	$K\alpha_{1,2}$
2.29	5.41	Cr	$K\alpha_{1,2}$
2.75	4.51	Ti	$K\alpha_{1,2}$
3.60	3.44	Sn	$L\alpha_{1,2}$
4.15	2.98	Ag	$L\alpha_{1,2}$
5.41	2.29	Mo	$L\alpha_{1,2}$
6.86	1.80	Sr	$L\alpha_{1,2}$
7.13	1.74	Si	$K\alpha_{1,2}$
8.34	1.49	Al	$K\alpha_{1,2}$
8.99	1.38	Se	$L\alpha_{1,2}$
9.89	1.25	Mg	$K\alpha_{1,2}$
10.44	1.19	Ge	$L\alpha_{1,2}$
12.25	1.01	Zn	$L\alpha_{1,2}$
13.34	0.930	Cu	$L\alpha_{1,2}$
14.56	0.852	Ni	$L\alpha_{1,2}$
15.97	0.776	Co	$L\alpha_{1,2}$
17.59	0.705	Fe	$L\alpha_{1,2}$
18.32	0.677	F	$K\alpha$
19.45	0.637	Mn	$L\alpha_{1,2}$
21.64	0.573	Cr	$L\alpha_{1,2}$
23.62	0.525	O	$K\alpha$
27.42	0.452	Ti	$L\alpha_{1,2}$
31.36	0.395	Ti	Ll
31.60	0.392	N	$K\alpha$
44.7	0.277	C	$K\alpha$
58.4	0.212	W	$N_{\rm V}N_{\rm VII}$
64.38	0.193	Mo	$M\zeta$
67.6	0.183	B	$K\alpha$
82.1	0.151	Zr	$M\zeta$
114	0.109	Be	$K\alpha$

Concave grating spectroscopy

Concave grating equation:

$$\pm m\lambda = d(\sin\alpha + \sin\beta),$$

where m is the spectral order, d is the groove separation, α is the angle of incidence, and β is the angle of diffraction. The negative sign applies when the spectrum lies between the central image ($\alpha = \beta$) and the tangent to the grating (sometimes referred to as the 'outside order'). When the spectrum lies between the incident beam and the central image, the positive sign must be used, and the spectrum is referred to as the 'inside order'. The signs of α and β are opposite when they lie on different sides of the grating normal.

Angular dispersion (α fixed):

$$\frac{d\beta}{d\lambda} = \frac{m}{d\cos\beta}.$$

Plate factor:

$$\frac{d\lambda}{dl} = \frac{d\cos\beta}{mR}, \quad \frac{d\lambda}{dl} = \frac{\cos\beta}{mR(1/d)} \times 10^4 \text{ Å mm}^{-1},$$

where R is in meters, $1/d$ is the number of lines mm^{-1}, and l is the distance along the Rowland circle.

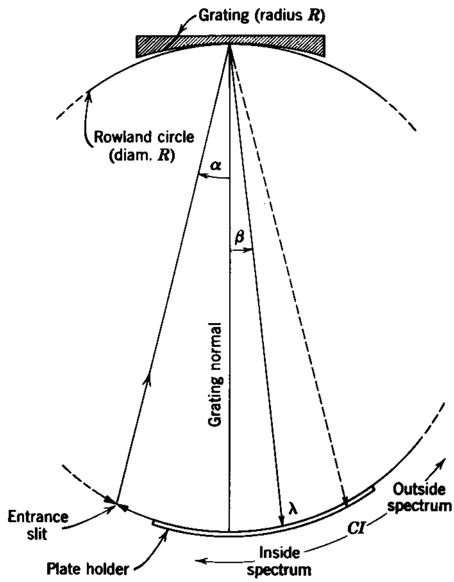

Optical layout of basic spectograph.

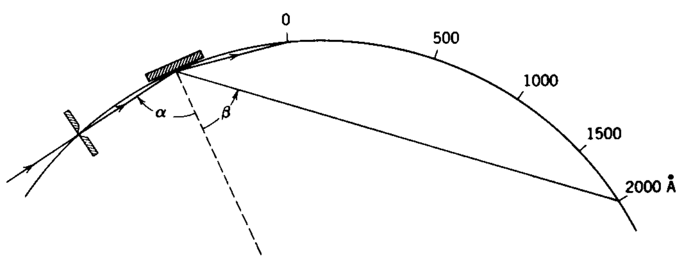

Grazing incidence spectrograph.

(Adapted from Samson, J., *Techniques of Vacuum Ultraviolet Spectroscopy*; John Wiley and Sons, 1967.)

Transmission grating spectroscopy

Principle of the X-ray transmission grating. **m** is the diffraction order.

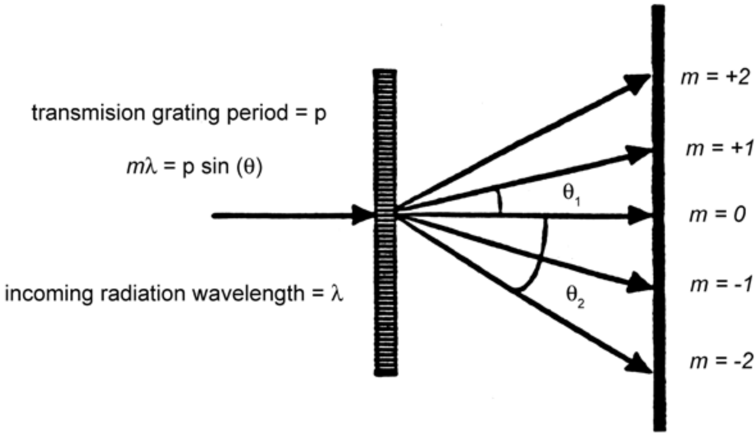

An example partial spectrum (binary star Capella) produced by the Chandra X-ray Observatory's Low Energy Transmission Grating Spectrometer (LETGS). The spectral resolving power is > 1000 in the wavelength range 50–160 Å.

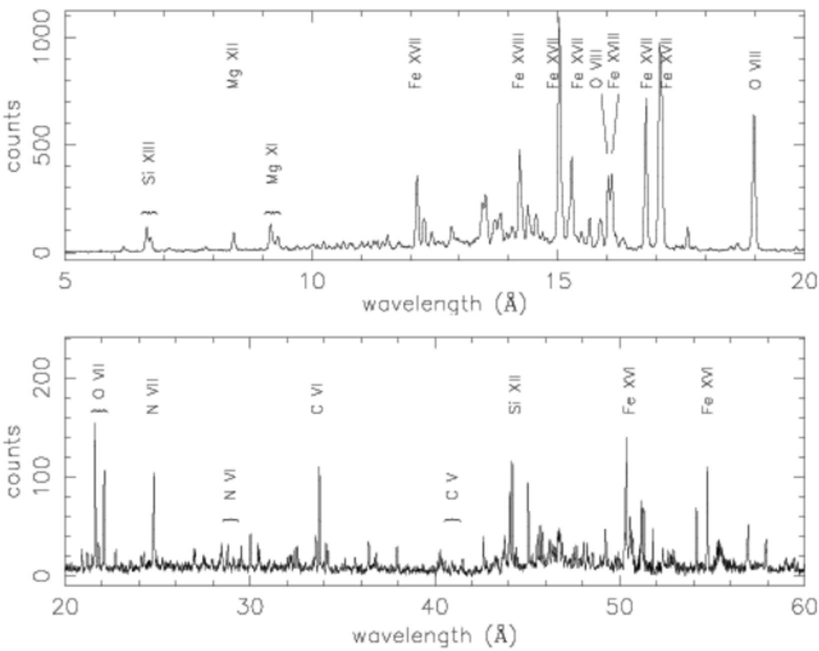

(From Brinkman *et al.*, 2000, ApJ, **530**, L111)

Reflection of X-rays

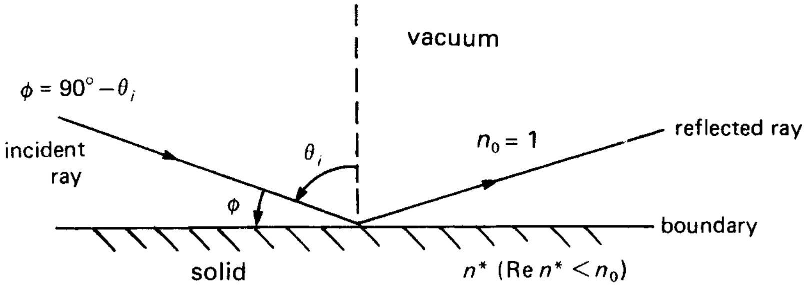

In the X-ray band the complex refractive index n^* is usually expressed as:

$$n^* = (1 - \delta) - i\beta,$$

with

$$\delta = \frac{1}{2\pi}\left(\frac{e^2}{m_e c^2}\right)\left(\frac{N_0 \rho}{A}\right) f_1 \lambda^2$$

and

$$\beta = \frac{1}{2\pi}\left(\frac{e^2}{m_e c^2}\right)\left(\frac{N_0 \rho}{A}\right) f_2 \lambda^2,$$

where

$\frac{e^2}{m_e c^2} = r_e =$ the classical electron radius,
$N_0 =$ Avogadro's number,
$\rho =$ density,
$A =$ atomic weight,
$\lambda =$ wavelength of the incident radiation,
$f_1 =$ real part of the atomic scattering factor, and
$f_2 =$ imaginary part of the atomic scattering factor, and

$$f_1 = (\pi r_e h c)^{-1} \int_0^\infty \frac{E'^2 \mu_a(E') dE'}{E^2 - E'^2} + Z,$$

$$f_2 = \frac{\pi}{2}(\pi r_e h c)^{-1} E \mu_a,$$

where

$Z =$ atomic number,
$h =$ Planck's constant,
$c =$ velocity of light,
$E =$ incident photon energy, and
$\mu_a =$ atomic photoabsorption cross-section.

The atomic photoabsorption cross-section μ_a is related to the mass absorption coefficient (μ/ρ) or to the linear absorption coefficient μ by:

$$\mu_a = \left(\frac{A}{N_0}\right)\left(\frac{\mu}{\rho}\right) = \left(\frac{A}{N_0\rho}\right)\mu.$$

Numerically,

$$\delta = 2.701 \times 10^{-6}\frac{\rho(\text{g cm}^{-3})}{A}\lambda^2(\text{Å})f_1,$$

$$\beta = 2.701 \times 10^{-6}\frac{\rho(\text{g cm}^{-3})}{A}\lambda^2(\text{Å})f_2.$$

The reflection of X-rays by a perfectly smooth surface for an angle of incidence θ_i is given by the Fresnel equations:

$$R_s = \frac{a^2 + b^2 - 2a\cos\theta_i + \cos^2\theta_i}{a^2 + b^2 + 2a\cos\theta_i + \cos^2\theta_i}$$

for perpendicular polarization, and

$$R_p = R_s\frac{a^2 + b^2 - 2a\sin\theta_i\tan\theta_i + \sin^2\theta_i\tan^2\theta_i}{a^2 + b^2 + 2a\sin\theta_i\tan\theta_i + \sin^2\theta_i\tan^2\theta_i}$$

for parallel polarization, where

$$2a^2 = \left[(n^2 - \beta^2 - \sin^2\theta_i)^2 + 4n^2\beta^2\right]^{1/2} + (n^2 - \beta^2 - \sin^2\theta_i),$$

and

$$2b^2 = \left[(n^2 - \beta^2 - \sin^2\theta_i)^2 + 4n^2\beta^2\right]^{1/2} - (n^2 - \beta^2 - \sin^2\theta_i),$$

with $n = 1 - \delta$.

Since the real part of the index of refraction is less than 1, near total external reflection occurs at a grazing angle ϕ_c given by Snell's law:

$$\cos\phi_c = 1 - \delta,$$

$$\phi_c \approx \sqrt{(2\delta)} \quad \text{for} \quad \delta \ll 1.$$

Since $\beta \neq 0$, reflection is not total for $\phi < \phi_c$ but is less than 1.

Away from an absorption edge,

$$\delta \approx 2.70 \times 10^{-6}\left(\frac{Z_c}{A}\right)\rho \quad (\text{g cm}^{-3})\lambda^2(\text{Å})$$

where Z_e is the number of electrons associated with wavelengths greater than λ. $Z_e = Z$ for $\lambda < \lambda_k$ (K edge).

Calculated spectral reflectivity of an ideal surface as a function of normalized grazing angle ϕ/ϕ_c for various values of β/δ. (After Hendrick, *JOSA*, **47**, 165, 1957.)

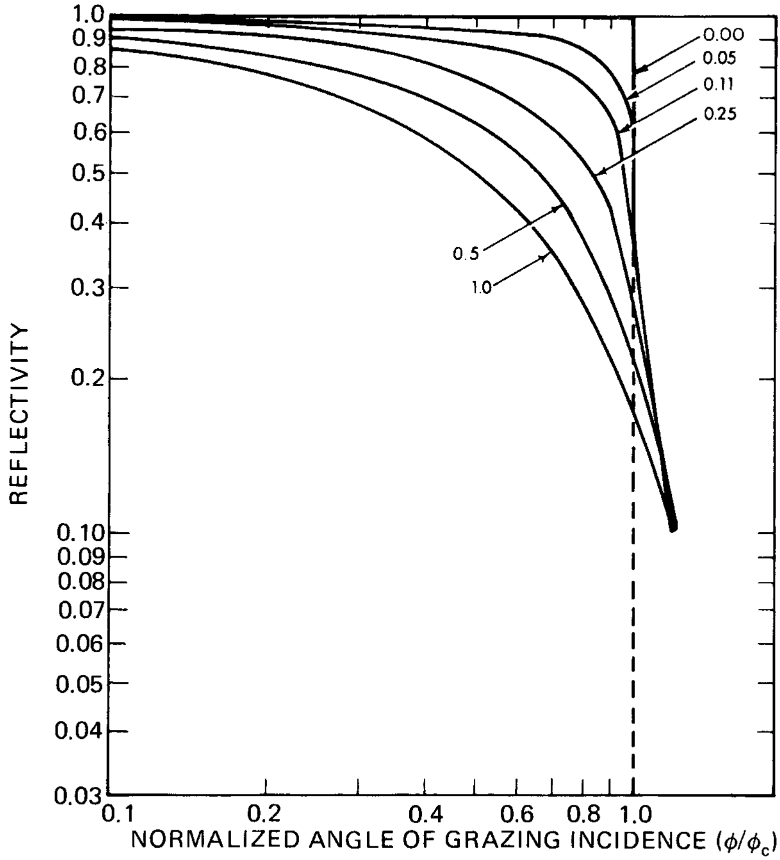

Reflectivity vs. wavelength (energy) for various grazing angles and materials

(Courtesy of M. Hettrick, Lawrence Berkeley Laboratory, Berkeley, CA.) Whenever possible, direct measurements should be made of grazing incidence reflectivity in the X-ray region because of uncertainties in the optical constants and the density of the material.

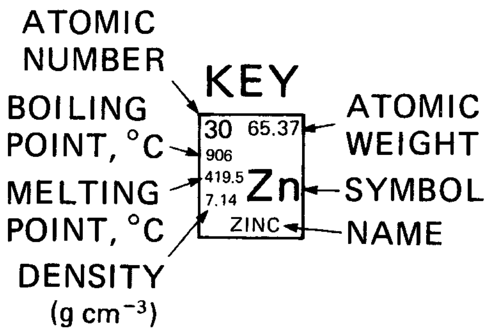

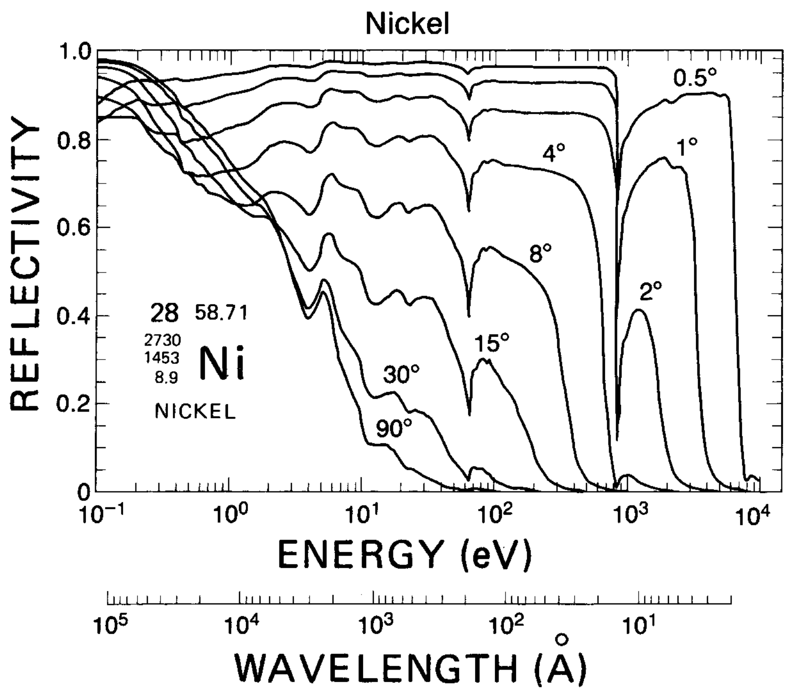

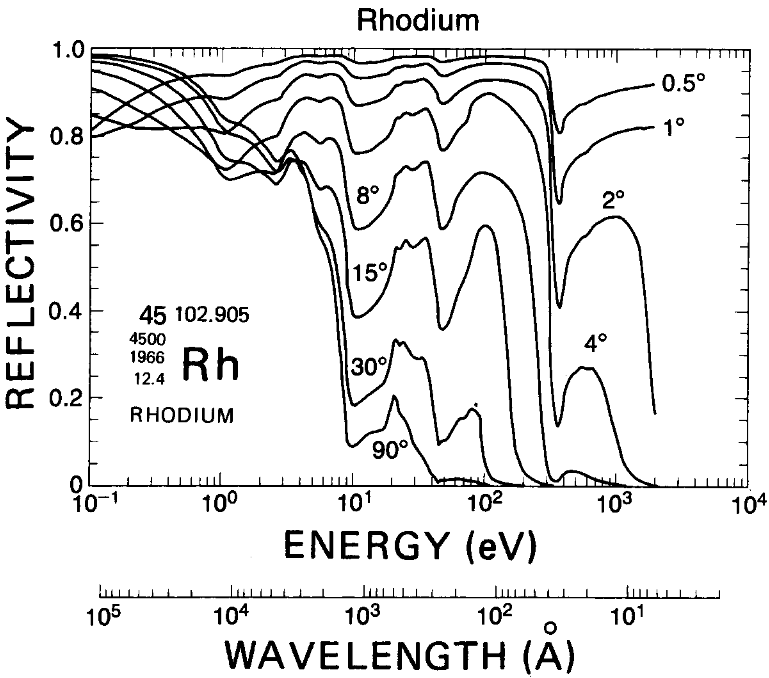
Rhodium
1.0
0.8
0.6
0.4
0.2
0
REFLECTIVITY
0.5°
1°
2°
4°
8°
15°
30°
90°
45 102.905
4500
1966
12.4
Rh
RHODIUM
10^{-1}
10^0
10^1
10^2
10^3
10^4
ENERGY (eV)
10^5
10^4
10^3
10^2
10^1
WAVELENGTH (Å)

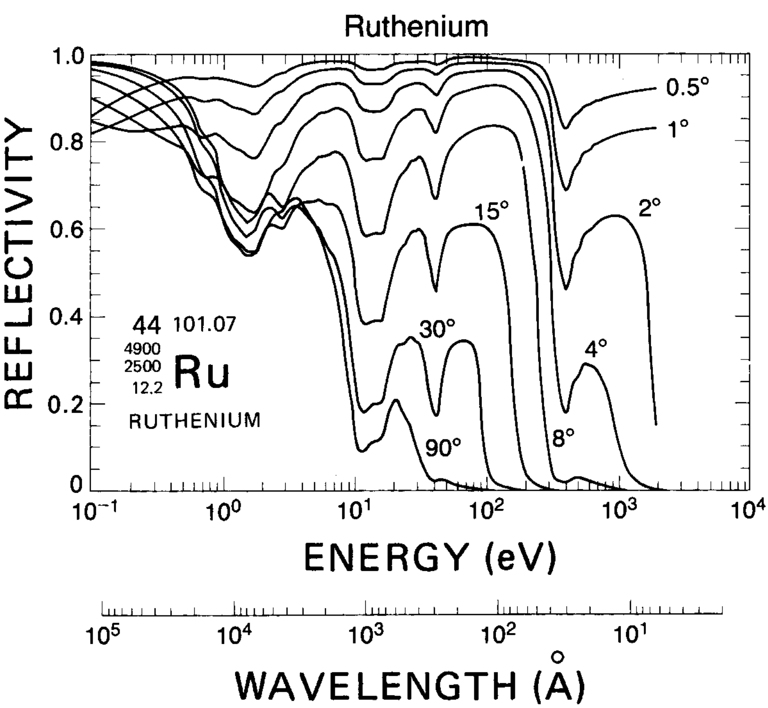
Ruthenium
1.0
0.8
0.6
0.4
0.2
0
REFLECTIVITY
0.5°
1°
2°
4°
8°
15°
30°
90°
44 101.07
4900
2500
12.2
Ru
RUTHENIUM
10^{-1}
10^0
10^1
10^2
10^3
10^4
ENERGY (eV)
10^5
10^4
10^3
10^2
10^1
WAVELENGTH (Å)

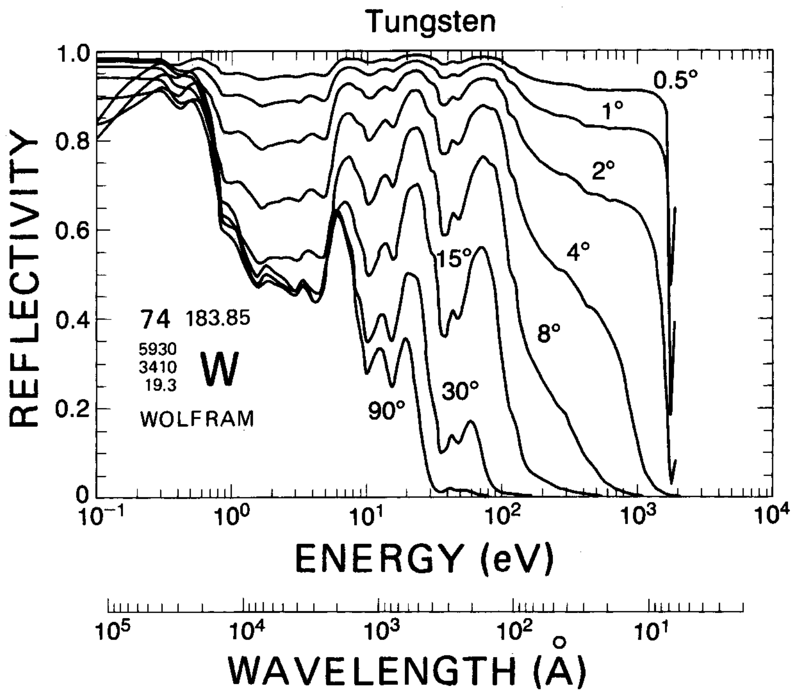
Tungsten
REFLECTIVITY
1.0
0.8
0.6
0.4
0.2
0
0.5°
1°
2°
4°
8°
15°
30°
90°
74 183.85
5930
3410
19.3
W
WOLFRAM
10−1
10^0
10^1
10^2
10^3
10^4
ENERGY (eV)
10^5
10^4
10^3
10^2
10^1
WAVELENGTH (Å)

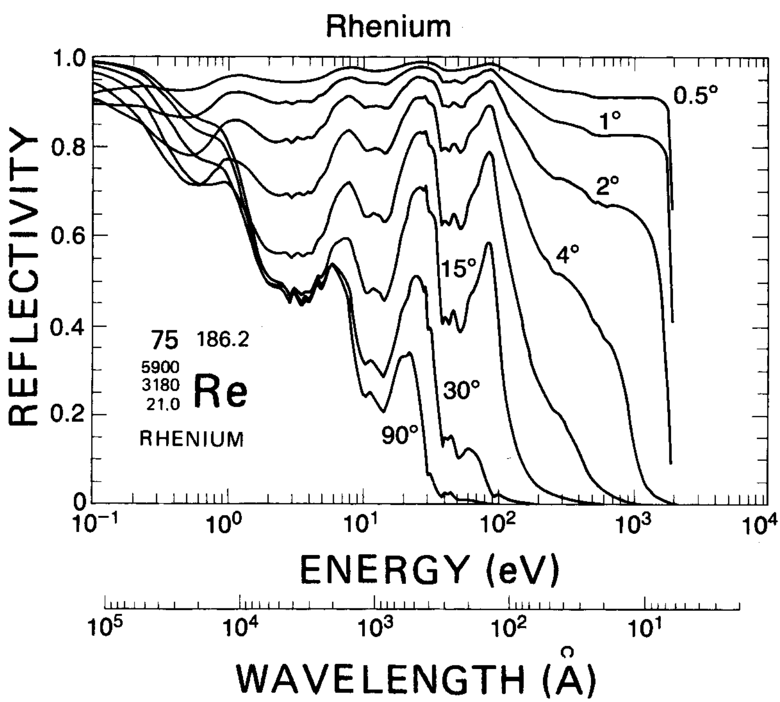
Rhenium
REFLECTIVITY
1.0
0.8
0.6
0.4
0.2
0
0.5°
1°
2°
4°
15°
30°
90°
75 186.2
5900
3180
21.0
Re
RHENIUM
10−1
10^0
10^1
10^2
10^3
10^4
ENERGY (eV)
10^5
10^4
10^3
10^2
10^1
WAVELENGTH (Å)

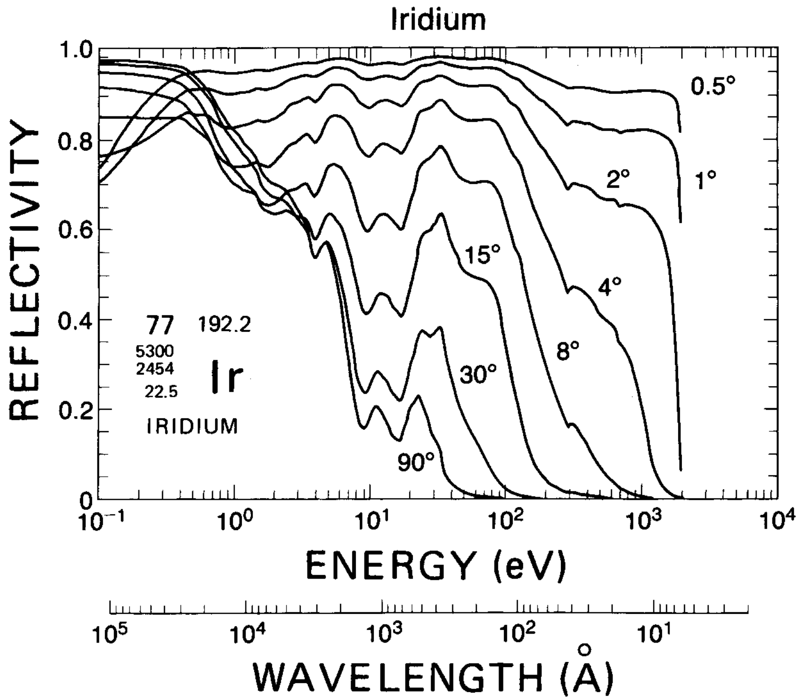
Iridium
REFLECTIVITY
1.0
0.8
0.6
0.4
0.2
0
0.5°
1°
2°
4°
8°
15°
30°
90°
77 192.2
5300
2454
22.5
Ir
IRIDIUM
10^{-1} 10^{0} 10^{1} 10^{2} 10^{3} 10^{4}
ENERGY (eV)
10^{5} 10^{4} 10^{3} 10^{2} 10^{1}
WAVELENGTH (Å)

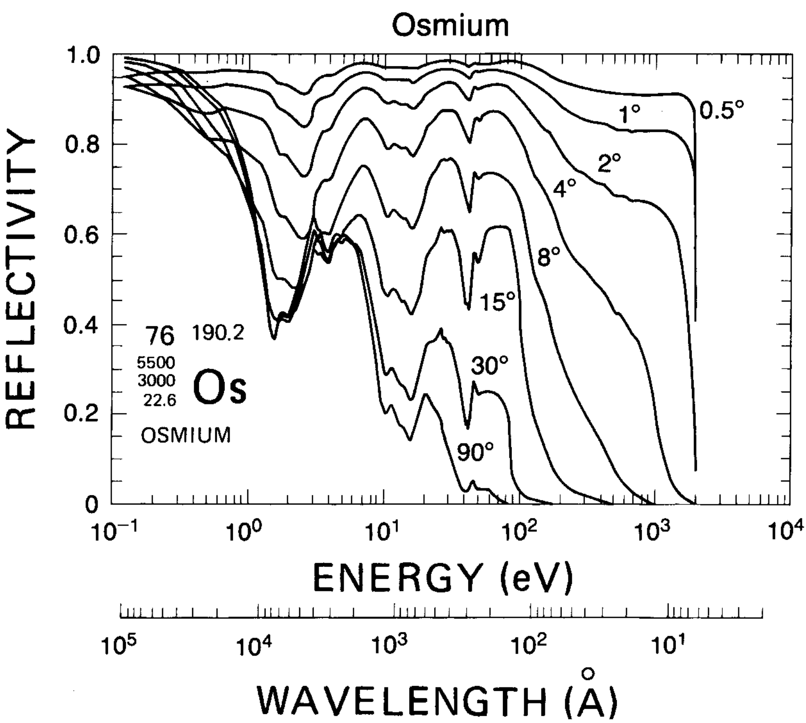
Osmium
REFLECTIVITY
1.0
0.8
0.6
0.4
0.2
0
0.5°
1°
2°
4°
8°
15°
30°
90°
76 190.2
5500
3000
22.6
Os
OSMIUM
10^{-1} 10^{0} 10^{1} 10^{2} 10^{3} 10^{4}
ENERGY (eV)
10^{5} 10^{4} 10^{3} 10^{2} 10^{1}
WAVELENGTH (Å)

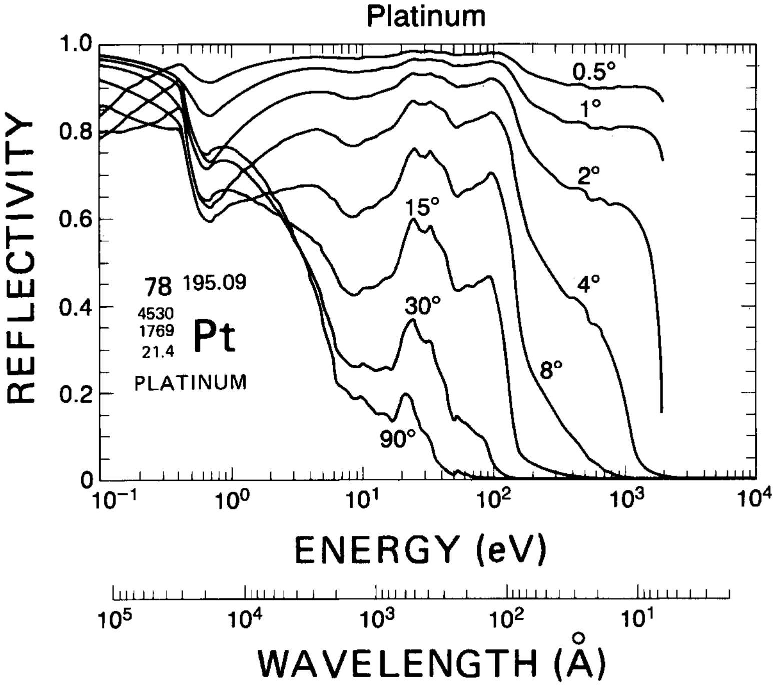
Platinum
REFLECTIVITY
ENERGY (eV)
WAVELENGTH (Å)
0.5°
1°
2°
4°
8°
15°
30°
90°
78 195.09
4530
1769
21.4
Pt
PLATINUM

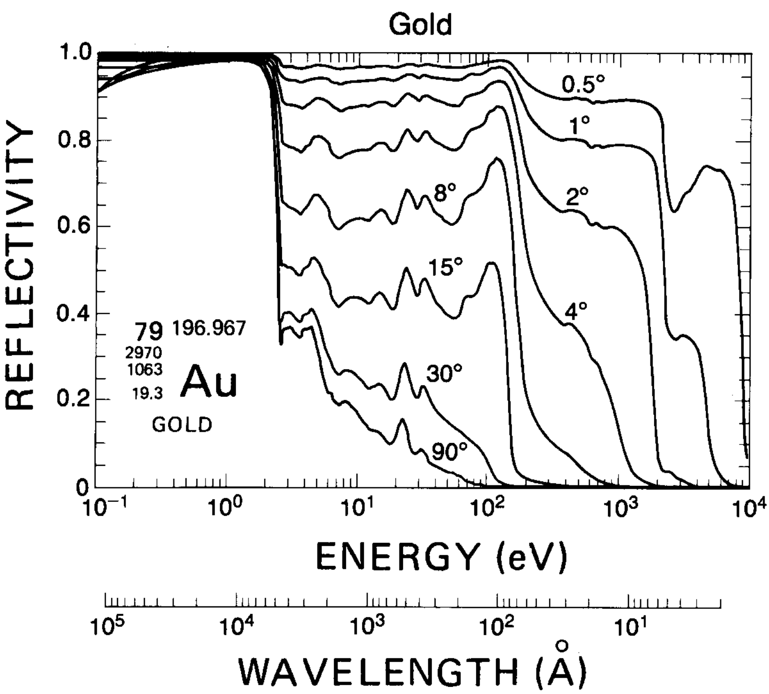
Gold
REFLECTIVITY
ENERGY (eV)
WAVELENGTH (Å)
0.5°
1°
2°
4°
8°
15°
30°
90°
79 196.967
2970
1063
19.3
Au
GOLD

Reflectivity versus wavelength for various materials and grazing angles. (Adapted from Giacconi, R. *et al.*, *Space Science Review*, **9**, 3, 1969.)

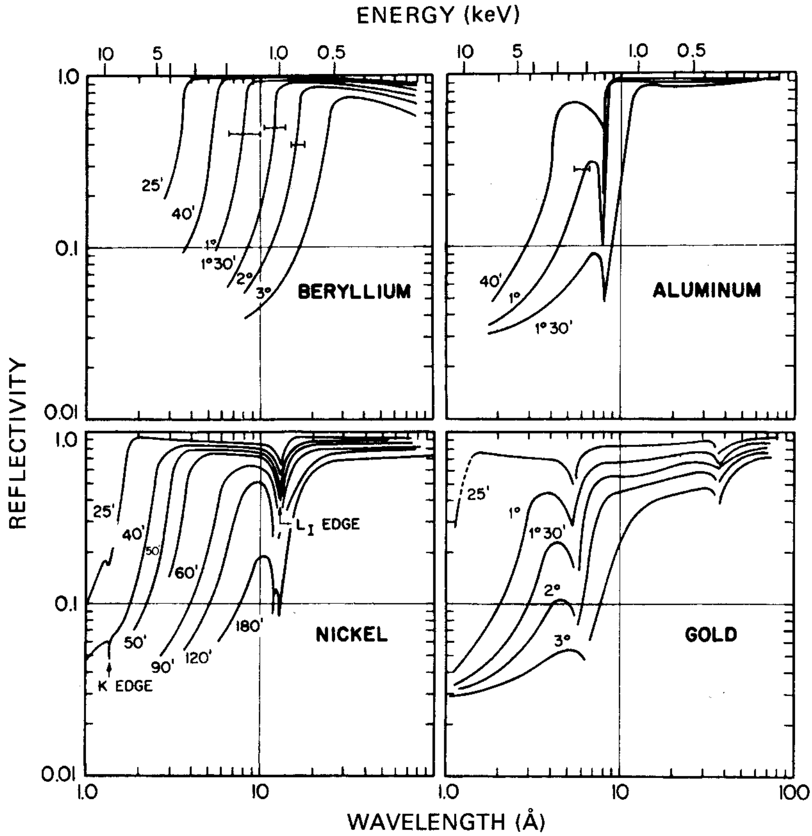

Photoabsorption cross sections and atomic scattering factors–nickel

Nickel (Ni)
$Z = 28$
Atomic Weight = 58.693
μ_a(barns/atom) = μ(cm^2/gm) × 97.46
E(keV)μ(cm^2/gm) = f_2 × 716.92

Edge Energies

K	8332.8 eV	L_I	1008.6 eV	M_I	110.8 eV
		L_{II}	870.0 eV	M_{II}	68.0 eV
		L_{III}	852.7 eV	M_{III}	66.2 eV

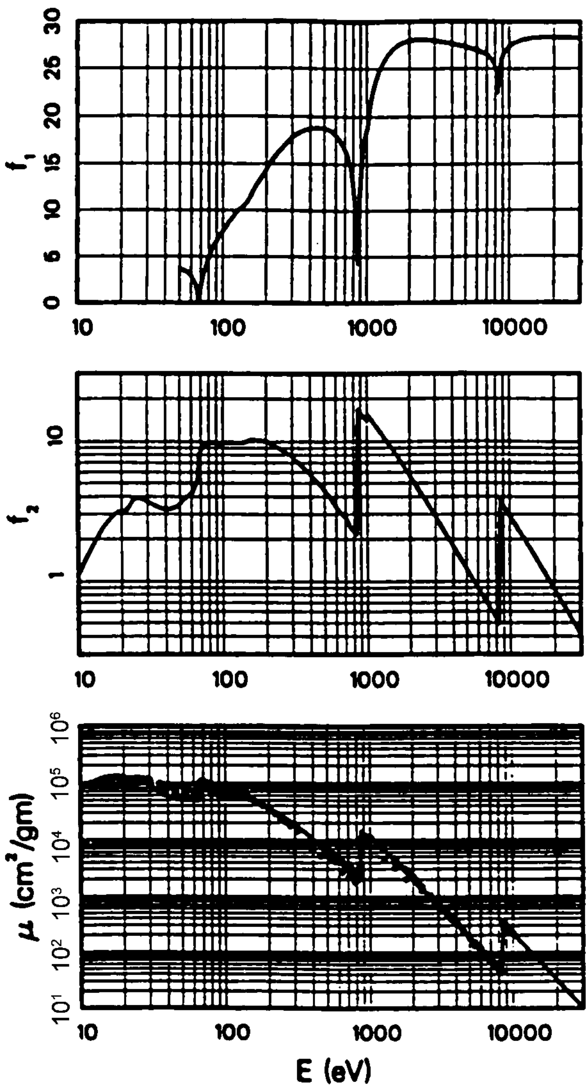

(From Henke, B.L., Gullikson, E.M., Davis, J.C., *Atomic Data and Nuclear Data Tables*, **54**, 240, 1993, with permission.)

Photoabsorption cross sections and atomic scattering factors–gold

Gold (Au)				Edge Energies				
Z = 79	L_I	14352.8 eV	M_I	3424.9 eV	N_I	762.1 eV	O_I	107.2 eV
Atomic = 196.967	L_{II}	13733.6 eV	M_{II}	3147.8 eV	N_{II}	642.7 eV	O_{II}	74.2 eV
weight	L_{III}	11918.7 eV	M_{III}	2743.0 eV	N_{III}	546.3 eV	O_{III}	57.2 eV
			M_{IV}	2291.1 eV	N_{IV}	353.2 eV		
			M_V	2205.7 eV	N_V	335.1 eV		
					N_{VI}	87.6 eV		
					N_{VII}	83.9 eV		

μ_a(barns/atom) = μ(cm^2/gm) $\times$ 327.08

E(keV)μ(cm^2/gm) = $f_2 \times$ 213.63

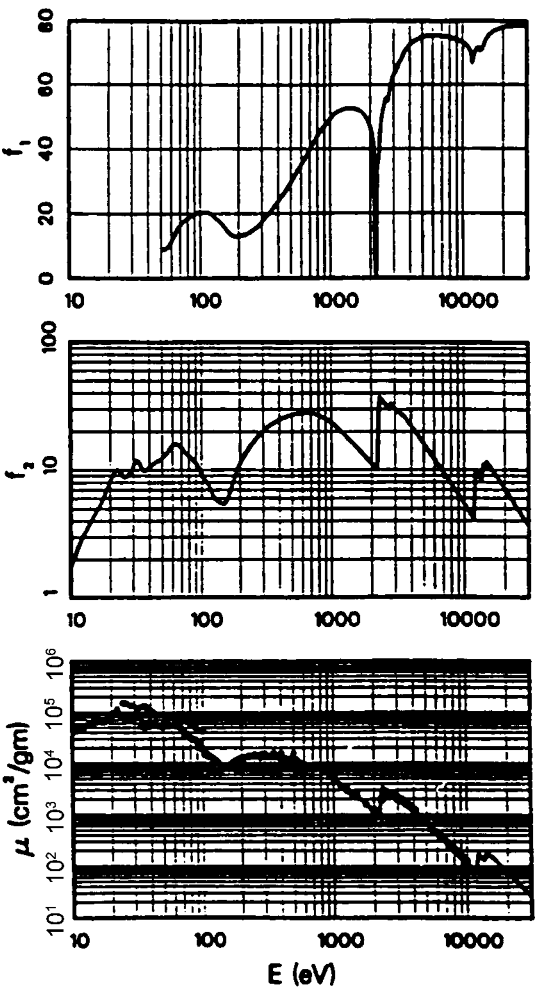

(From Henke, B.L., Gullikson, E.M., Davis, J.C., *Atomic Data and Nuclear Data Tables*, **54**, 291, 1993, with permission.)

Wolter type I mirror system

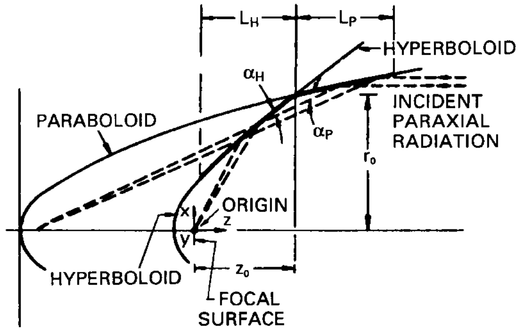

The equations for a paraboloid and hyperboloid which are concentric and confocal can be written as:

$$r_\mathrm{p}^2 = P^2 + 2PZ + [4e^2Pd/(e^2-1)] \quad \text{(paraboloid)},$$
$$r_\mathrm{h}^2 = e^2(d+Z)^2 - Z^2 \quad \text{(hyperboloid)},$$

where d is the distance from the system focus to the generating hyperbola's directrix, e is the eccentricity of this hyperbola, and P is the distance from the focus of the generating parabola to its directrix.

The origin is at the focus for axial rays, Z is the coordinate along the axis of symmetry, and r is the radius of the surface at Z.

RMS blur circle radius:

$$\sigma = \frac{(\xi+1)}{10}\frac{\tan^2\theta}{\tan\alpha}\left(\frac{L_\mathrm{p}}{Z_0}\right) + 4\tan\theta\tan^2\alpha \quad \text{radians}$$

and

$$\xi = \alpha_\mathrm{p}^*/\alpha_\mathrm{h}^*$$

(α_p^* and α_h^* are the grazing angles between the two surfaces and the path of an axial ray that strikes at an infinitesimal distance from the intersection).

For most telescope designs: $\xi = 1$.

$$\alpha = \frac{1}{4}\tan^{-1}(r_0/Z_0) = \frac{1}{2}(\alpha_\mathrm{p}^* + \alpha_\mathrm{h}^*),$$

θ = angle between incident rays and optical axis.

Geometrical collecting area:

$$A \approx 2\pi r_0 L_\mathrm{p}\tan\alpha.$$

Effective collecting area:

$$A_\mathrm{e}(\alpha, E) \approx AR^2(\alpha, E) \approx 8\pi Z_0 L_\mathrm{p} R^2(\alpha, E)\alpha^2,$$

where R is the Fresnel reflectivity at energy E and mean grazing angle α.

(Adapted from Van Speybroeck, L. & Chase, R., *AP. Opt.*, **11**, 440, 1972.)

Vacuum technology

Vacuum nomograph. (Adapted from Roth, A., *Vacuum Technology*, North-Holland Pub. Co., 1976.)

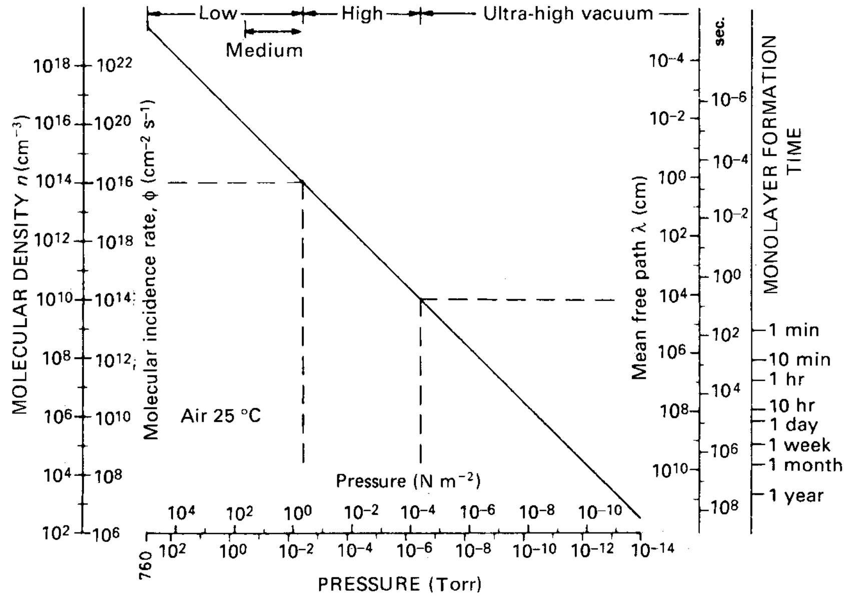

Pumping speed of an aperture of area A:

$$\frac{dV}{dt} = A(\mathrm{cm}^2)\sqrt{[1.32 \times 10^7 T\ (\mathrm{K})/\mathrm{mol.wt}]}\ \mathrm{cm}^3\ \mathrm{s}^{-1}.$$

Kinetic theory of gases

Mean free path, $\lambda = 1/\sqrt{2}\pi n\sigma^2$
viscosity, $\eta = \rho\bar{v}\lambda/3$
heat conductivity, $K = \eta c_{\mathrm{v}}\varepsilon$,
mean speed, $\bar{v} = \sqrt{[2.1 \times 10^8 T\ (\mathrm{K})/\mathrm{mol.wt}]}\ \mathrm{cm\ s}^{-1}$,
where

n = number of molecules cm^{-3},
ρ = gas density in g cm^{-3},
σ = mol. diameter,
c_{v} = specific heat capacity at constant volume,
ε = 2.5 and 1.9 for monoatomic and diatomic gas, respectively.

Rate at which molecules strike a surface:

$$\nu = n v_a / 4$$

where

n = the number density of molecules
v_a = the average molecular velocity

$$\nu = 3.513 \times 10^{22} P(MT)^{-1/2}\ \text{cm}^{-2}\ \text{s}^{-1}$$

where

P = pressure in Torr
M = molecular weight
T = temperature in K

Mass of gas incident on unit area per unit time

$$G = 5.833 \times 10^{-2} P(MT)^{1/2}\ \text{g cm}^{-2}\ \text{s}^{-1}$$

where P, M and T are defined above.

Time to form a monolayer:

On the assumption that the molecular spacing is that of a close-packed (face-centered) lattice, the number of molecules per unit area to form a monomolecular layer is given by

$$N_s = 1.154\sigma^2$$

where σ is the molecular diameter. If we assume that the accomodation coefficient is 1, that is, the molecule sticks to the surface on first impact, the time to form a monolayer is

$$\tau = 1/\nu N_s$$

For example, at a pressure of 10^{-6} Torr and at a temperature of 20°C, the time to form a monolayer of nitrogen molecules ($\sigma = 3.7 \times 10^{-8}$ cm) would be about 2 seconds.

See Dushman, S., *Scientific Foundations of Vacuum Technique*, John Wiley & Sons, Inc., 1949, for a comprehensive treatment of the application of kinetic theory to vacuum systems.

Physical properties of gases and vapors

Gas	Chemical Formula	Molecular Weight M	Molecular Diameter (10^{-8} cm)
Hydrogen	H_2	2.016	2.74
Deuterium	D_2	4.028	2.74
Helium	He	4.002	2.18
Methane	CH_4	16.04	4.14
Ammonia	NH_3	17.03	4.43
Water vapor	H_2O	18.02	4.60
Neon	Ne	20.18	2.59
Nitrogen	N_2	28.01	3.75
Oxygen	O_2	31.99	3.61
Argon	Ar	39.94	3.64
Carbon dioxide	CO_2	44.01	4.59
Krypton	Kr	83.80	4.11
Xenon	Xe	131.30	4.85
Mercury	Hg	200.59	4.26

Units of gas quantity

1 Molar Volume	=	22.41 Liters (at standard conditions–STP)
1 Mole	=	6.023×10^{23} Molecules
1 Liter-Atmos	=	2.68×10^{22} Molecules
1 Std. cc	=	2.68×10^{19} Molecules
1 Torr-Liter	=	3.52×10^{19} Molecules
1 Std. cc	=	.76 Torr-Liter
1 Std. cc	=	1 Atmos cm^3
1 Cubic Foot	=	7.6×10^{23} Molecules (at standard conditions–STP)

(Standard Conditions are 1 Atmosphere at 273°K)

Permeability of gases

(Permeation constant K for various polymer seal materials and for various gases in the range 20–30°C)

	K (std. cm^3 s^{-1} cm^{-2} $Torr^{-1}$ $\times 10^{10}$)			
Polymer	He	N_2	CO_2	H_2O
Nitrile (Buna-N)	1.0	0.024	0.75	100
Butyl	0.86	0.032	0.52	4–20
Ethylene propylene	2.6–3.9	0.44	0.92	7–70
Polyurethane	0.47	0.049	1.4–4.0	35–1,250
Fluoroelastomer(Viton)	1.2–2.3	0.03–0.07	0.3–0.8	5.2
Perfluoroelastomer				
Kalrez	11.2	0.30	2.5	—
Chemraz	14.3	0.88	—	—
Silicone	31–33	10–16	60–300	400–1,000
PTFE (Teflon)	6.8	0.14–0.32	1.2	3.6
PCTFE (Kel-F)	0.22	0.0005	0.014	0.01
Polyimide (Kapton)	0.25	0.0039	0.26	–

$Q = \Delta PKA/d$ where Q is the quantity of gas per unit time permeating the material of area A and thickness d, and ΔP is the pressure difference across the material. (Adapted from Peacock, R.N. in, *Handbook of Vacuum Science and Technology*, Hoffman, D.M., Singh, B., and Thomas, J.H., eds., Academic Press 1998.)

Outgassing rates for polymers

Outgassing rates at room temperature for some polymers commonly used in vacuum sealing. The samples were originally outgassed in vacuum, then exposed to room air. (From Peacock, R.N. in, *Handbook of Vacuum Science and Technology*, Hoffman, D.M., Singh, B., and Thomas, J.H., eds., Academic Press, 1998, with permission.)

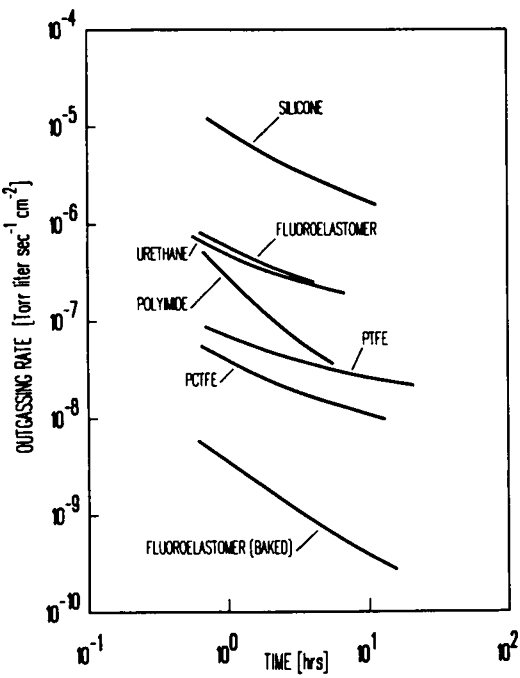

Physical and thermodynamic properties of cryogenic fluids

Property	Units	Air	N_2	O_2	H_2	He	Ne	Ar	Kr	Xe	CH_4
M	g/mol	28.96	28.014	31.999	2.0159	4.0026	20.180	39.948	83.800	131.290	16.043
T_t	K	59.75	63.15	54.3584	13.8		24.5561	83.8058	115.8	161.4	90.694
P_t	kPa		12.463	0.14633	7.042		50.00	68.95	72.92	81.59	11.696
ρ_t(l)	g/mL	0.959	0.870	1.306	0.0770		1.251	1.417	2.449	2.978	0.4515
T_b	K	78.67	77.35	90.188	20.28	4.2221	27.07	87.293	119.92	165.10	111.668
$\rho(l)@T_b$	g/mL	0.8754	0.807	1.141	0.0708	0.124901	1.204	1.396	2.418	2.953	0.4224
$\rho(g)@T_b$	g/L	3.199	4.622	4.467	1.3390	16.89	9.51	5.79	8.94		1.816
T_c	K	132.5	126.20	154.581	32.98	5.1953	44.40	150.663	209.40	289.73	190.56
P_c	MPa	3.766	3.390	5.043	1.293	0.227460	2.760	4.860	5.500	5.840	4.592
ρ_c	g/mL	0.316	0.313	0.436	0.031	0.06964	0.484	0.531	0.919	1.110	0.1627

M	Molar mass in grams per mole	$\rho(l)@T_b$	Liquid density at the normal boiling point in grams per milliliter
T_t	Triple point temperature in kelvins	$\rho(g)@T_b$	Vapor density at the normal boiling point in grams per liter
P_t	Triple point pressure in kilopascals	T_c	Critical temperature in kelvins
$\rho_t(l)$	Liquid density at the triple point in grams per milliliter	P_c	Critical pressure in megapascals
T_b	Normal boiling point in kelvins at a pressure of 101325 pascals (760 mm Hg)	ρ_c	Critical density in grams per milliliter

The triple point is the point in the pressure-temperature diagram of a substance in which all three phases can exist simultaneously.

The critical temperature is the temperature above which it is no longer possible to liquefy a gas by increasing the pressure. The pressure that is needed to cause the gas or vapor to condense at the critical temperature is the critical pressure. The critical density is the density of the substance at the critical temperature and pressure.

1 Mpa = 9.8692 atmos = 7500.6 Torr = 145.0377 psi

(From *Handbook of Chemistry and Physics*, *CRC Press*, 1995.)

Equivalents for various cryogenic fluids

Fluid	Boiling point at 1 atm	Weight in pounds	Ft^3 at 70°F and 1 atm	Liquid liters at b.p.	Liquid gallons at b.p.	Heat of vapor. (Btu)
Nitrogen	−320.4 F	1	13.81	0.5618	0.1484	85.2
	−195.8 C	0.0724	1	0.0407	0.0108	6.168
	77.3 K	1.780	24.58	1	0.2642	151.7
		6.738	92.94	3.785	1	574.1
Helium	−452.1 F	1	96.8	3.628	0.9585	8.8
	−268.9 C	0.0103	1	0.375	0.0099	0.0906
	4.2 K	0.2756	26.68	1	0.2642	2.425
		1.043	101.0	3.785	1	9.178
Oxygen	−297.4 F	1	12.09	0.3973	0.1050	91.7
	−183.0 C	0.827	1	0.0329	0.0087	7.584
	90.1 K	2.517	30.43	1	0.2642	230.8
		9.527	115.2	3.785	1	873.6
Hydrogen	−423.2 F	1	192.3	6.481	1.712	193
	−252.9 C	0.0052	1	0.0337	0.0089	1.004
	20.2 K	0.1543	29.67	1	0.2642	29.78
		0.5841	112.3	3.785	1	112.7
Argon	−302.6 F	1	9.680	0.3235	0.0855	70.2
	−185.9 C	0.1033	1	0.0334	0.0088	7.251
	87.2 K	3.091	29.92	1	0.2642	217.0
		11.70	113.3	3.785	1	821.3

Paschen curves for various gases

Static breakdown voltages for various gases as a function of the product of the pressure (Torr) and gap distance (mm). (From Knoll, M., Ollendorf, F., and Rompe, R., *Gasentladungstabellen,* Springer-Verlag, 1935.)

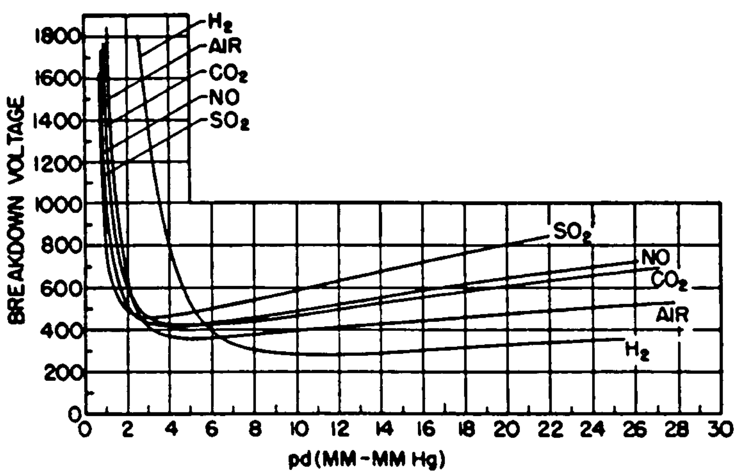

Optical point spread function

The irradiance distribution of the monochromatic image of a point object, $h_\lambda(x, y; \alpha, \beta)$ is called the point spread function (PSF) of an optical system. x and y are the coordinates of the image points and α and β are the coordinates of the ideal image of the object (a point). If $f_\lambda(x, y)$ is the ideal image of an extended monochromatic object, the image produced by the optical system is given by:

$$g_\lambda(x, y) = \int\int_{-\infty}^{\infty} h_\lambda(x, y; \alpha, \beta) f_\lambda(\alpha, \beta) d\alpha\, d\beta.$$

In some cases, the optical system is *shift-invariant* (at least, over a restricted field):

$$h_\lambda(x, y; \alpha, \beta) = K_\lambda(x - \alpha, y - \beta),$$

and the above integral can be written as a convolution:

$$g_\lambda(x, y) = \int\int_{-\infty}^{\infty} K_\lambda(x_\lambda - \alpha, y - \beta) f_\lambda(\alpha, \beta) d\alpha\, d\beta.$$

In general, for optical systems, the PSF is wavelength dependent, *shift-varying*, and asymmetric. Over a restricted field, say within a few arc minutes of the optical axis, it is approximately shift-invariant and symmetric and it is possible to simplify the deconvolution of an image and use Fourier transforms.

In the following discussion we will consider the PSF to be shift invariant and symmetric and will drop the λ subscript.

The PSF is the function that completely characterizes the imaging properties of an optical system. Several useful functions and quantities can be derived from it:

The line spread function

$$A(x) = \int_{-\infty}^{\infty} K(x, y) dy \quad (K(x, y) \text{ is the PSF})$$

represents the intensity distribution for a line object.

The edge trace

$$I(x_o) = \int_{-\infty}^{x_o} A(x) dx$$

represents the intensity distribution for a knife edge object.

***The modulation transfer function* (MTF)**

This represents the response of an optical system to an object with a sinusoidally varying radiance G of spatial frequency ν:

$$\text{MTF}(\nu) = \frac{M_\text{i}(\nu)}{M_\text{o}(\nu)},$$

where M_{i} and M_{o} are the modulation of the image and object, respectively. The modulation is given by:

$$M_{\text{i or o}}(\nu) = \left(\frac{\max - \min}{\max + \min}\right) \text{ image or object.}$$

Since the radiance of the object (image) varies sinusoidally, we can write:

$$G_{\text{o}}(x) = a_{\text{o}} + b_{\text{o}} \sin 2\pi\nu x,$$

$$G_{\text{i}}(x) = a_{\text{i}} + b_{\text{i}} \sin 2\pi\nu s.$$

Then

$$M_{\text{o}} = \frac{(a_{\text{o}} + b_{\text{o}}) - (a_{\text{o}} - b_{\text{o}})}{(a_{\text{o}} + b_{\text{o}}) + (a_{\text{o}} - b_{\text{o}})} = \frac{b_{\text{o}}}{a_{\text{o}}},$$

$$M_{\text{i}} = \frac{(a_{\text{i}} + b_{\text{i}}) - (a_{\text{i}} - b_{\text{i}})}{(a_{\text{i}} + b_{\text{i}}) + (a_{\text{i}} - b_{\text{i}})} = \frac{b_{\text{i}}}{a_{\text{i}}},$$

and the modulation transfer function,

$$\text{MTF} = \frac{(b_{\text{i}}/a_{\text{i}})}{(b_{\text{o}}/a_{\text{o}})}.$$

The MTF is also given by the absolute value of the Fourier transform of the line spread function:

$$\text{MTF}(\nu) = \int_{-\infty}^{\infty} A(x) e^{-2\pi i \nu x} dx.$$

***The full-width half-maximum* (FWHM)** of a rotationally symmetric PSF is the width of the function at half its peak value. If $K(x, y) = K(r)$ where r the radial coordinate in the image plane, and the radius r_0 is such that:

$$K(r_0) = \frac{1}{2} K(0) \quad \text{(half the peak value of the PSF),}$$

then

$$\text{FWHM} = 2r_0; \ r_0 = \textit{half-width},$$

or half-width-half-maximum (HWHM).

The root mean square (rms) radius $\langle r \rangle$ is defined by:

$$\langle r \rangle^2 = \frac{\displaystyle\int_0^{\infty} r^2 K(r) r\, dr}{\displaystyle\int_0^{\infty} K(r) r\, dr}.$$

The encircled energy function $E(r)$, the fraction of the total imaged photons that are within a circle of radius r, is given by:

$$E(r) = \frac{\displaystyle\int_0^{r} K(r) r\, dr}{\displaystyle\int_0^{\infty} K(r) r\, dr}.$$

The radius of the circle which contains 50% of the imaged photons, the ***half-power radius***, $r_{1/2}$ defined by:

$$E(r_{1/2}) \equiv 0.50 = \frac{\int_0^{r_{1/2}} K(r) r\, dr}{\int_0^{\infty} K(r) r\, dr}.$$

In order to complete the discussion of the point spread function, we give here the various functions and parameters derived from a Gaussian point spread since this can be a useful description of the inner core of the PSF.

The form of the radial symmetric Gaussian is given as:

$$\mathrm{PSF} = Ce^{-r^2/2\sigma^2},$$

where C and σ are arbitrary constants. We have derived the following functions and quantities:

the line spread function,

$$A(x) = C\sigma\sqrt{(2\pi)}e^{-x^2/2\sigma^2},$$

the edge trace,

$$I(x_0) = C\sigma\frac{\sqrt{(2\pi)}}{2}(1 + \mathrm{erf}(x_0/\sigma\sqrt{2}))$$

where $\mathrm{erf}(z)$ is the error function,

the modulation transfer function,

$$M(\nu) = Ce^{-2(\pi\nu\sigma)^2}, \text{ and}$$

the encircled energy,

$$E(r) = 1 - e^{-r^2/2\sigma^2}.$$

The table below gives the relations between the FWHM, the rms radius, and the half-power radius for the Gaussian spread function.

PARAMETERS FOR THE GAUSSIAN SPREAD FUNCTION

Spread function	rms radius $\langle r \rangle$	Full width half maximum (FWHM)	Half power radius $r_{1/2}$
$Ce^{-r^2/2\sigma^2}$	$\sigma\sqrt{2}$	2.36σ	1.18σ

Point spread function for a circular aperture (diffraction by a circular aperture)

If the transmission of the system is uniform over the (circular) aperture and the system is aberration-free, the illuminance distribution in the image becomes:

$$P(y,z) = \pi \left(\frac{\mathrm{NA}}{\lambda}\right)^2 P_t \left[\frac{2J_1(m)}{m}\right]^2,$$

where NA is the numerical aperture of the system, J_1 is the first-order Bessel function:

$$J_1(x) = \frac{x}{2} - \frac{(x/2)^3}{1^2 2} + \frac{(x/2)^5}{1^2 2^2 3} - \cdots,$$

P_t is the total power in the point image, and m is the normalized radial coordinate:

$$m = \frac{2\pi}{\lambda}\mathrm{NA}(y^2 + z^2)^{1/2} = \frac{2\pi}{\lambda}\mathrm{NA} \cdot r.$$

The fraction of the total power falling within a radial distance r_0 of the center of the pattern is given by $1 - J_0^2(m_0) - J_1^2(m_0)$, where J_0 is the zero-order Bessel function:

$$J_0(x) = 1 - \left(\frac{x}{2}\right)^2 + \frac{(x/2)^4}{1^2 2^2} - \frac{(x/2)^6}{1^2 2^2 3^2} + \cdots$$

Fraunhofer diffraction at a rectangular aperture (a) and at a circular aperture (b). (Adapted from Born, M. & Wolf, E., *Principles of Optics*, Pergamon Press 1984.)

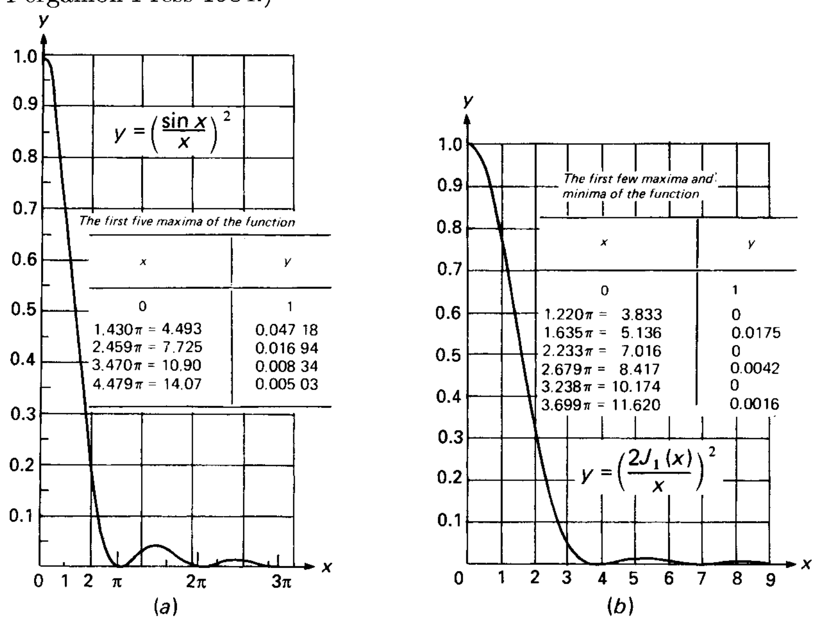

Optical telescopes

Configurations of optical telescopes. (Adapted from the Encyclopedia of Astronomy and Astrophysics, 2001.)

TYPE	PRIMARY	SECONDARY	CONFIGURATION
KEPLERIAN GALILEAN (if refractive)	SPHERE or PARABOLA	NONE	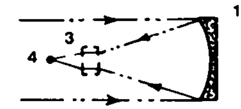
HERSCHELIAN	OFF-AXIS PARABOLA	NONE	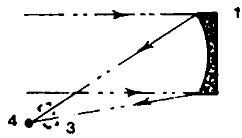
NEWTONIAN	PARABOLA	DIAGONAL FLAT	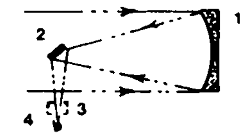
GREGORIAN	PARABOLA	ELLIPSE	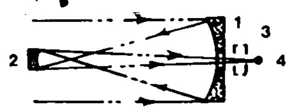
MERSENNE	PARABOLA	PARABOLA	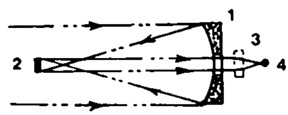
CASSEGRAIN RITCHEY- CHRÉTIEN DALL-KIRKHAM	PARABOLA MODIFIED PARABOLA ELLIPSE	HYPERBOLA MODIFIED HYPERBOLA SPHERE	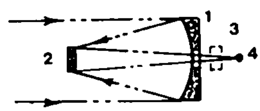
SCHMIDT	ASPHERIC REFRACTOR	SPHERE	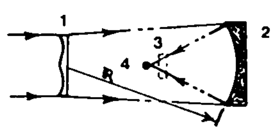
BOUWERS- MAKSUTOV	REFRACTIVE MENISCUS	SPHERE	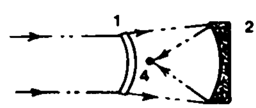

1-PRIMARY
2-SECONDARY
3-EYEPIECES/CORRECTORS
4-FOCUS

Optical telescopes (cont.)

Focus configurations for optical telescopes. (Adapted from *Survey of Catadioptric Optical Systems*, J.B. Galligan, ed., Itek Corporation, 1966.)

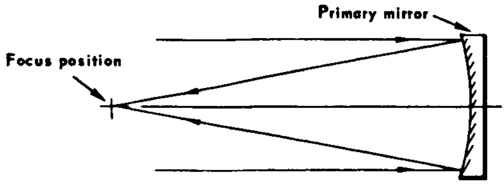

Prime Focus

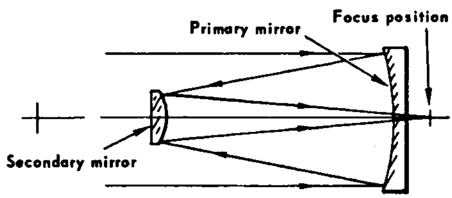

Cassegrain Focus

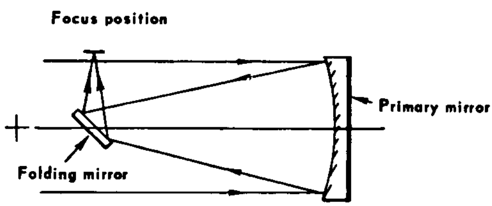

Newtonian Focus

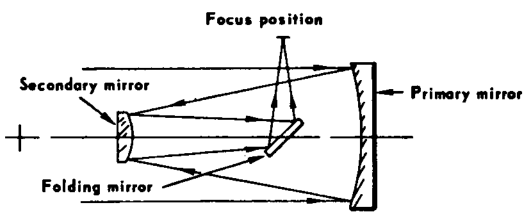

Coudé Focus

Photometry

Spectral luminous efficiency. Relative luminosity values for photopic and scotopic vision

Wavelength (nm)	Photopic $V(\lambda)$ ($B > 3$ cd m^{-2})	Scotopic $V(\lambda)$ ($B < 3 \times 10^{-5}$ cd m^{-2})
350	—	0.0003
360	—	0.0008
370	—	0.0022
380	0.00004	0.0055
390	0.00012	0.0127
400	0.0004	0.0270
410	0.0012	0.0530
420	0.0040	0.0950
430	0.0116	0.157
440	0.023	0.239
450	0.038	0.339
460	0.060	0.456
470	0.091	0.576
480	0.139	0.713
490	0.208	0.842
500	0.323	0.948
510	0.503	0.999
520	0.710	0.953
530	0.862	0.849
540	0.954	0.697
550	0.995	0.531
560	0.995	0.365
570	0.952	0.243
580	0.870	0.155
590	0.757	0.0942
600	0.631	0.0561
610	0.503	0.0324
620	0.381	0.0188
630	0.265	0.0105
640	0.175	0.0058
650	0.107	0.0032
660	0.061	0.0017
670	0.032	0.0009
680	0.017	0.0005
690	0.0082	0.0002
700	0.0041	0.0001
710	0.0021	—
720	0.00105	—
730	0.00052	—
740	0.00025	—
750	0.00012	—
760	0.00006	—
770	0.00003	—

$K(\lambda)$, spectral luminous efficacy for scotopic and photopic vision.
Scotopic:
max $K = K$ (511 nm) = 1746 lm W^{-1}.
Photopic:
max $K = K$ (555 nm) = 680 ln W^{-1}

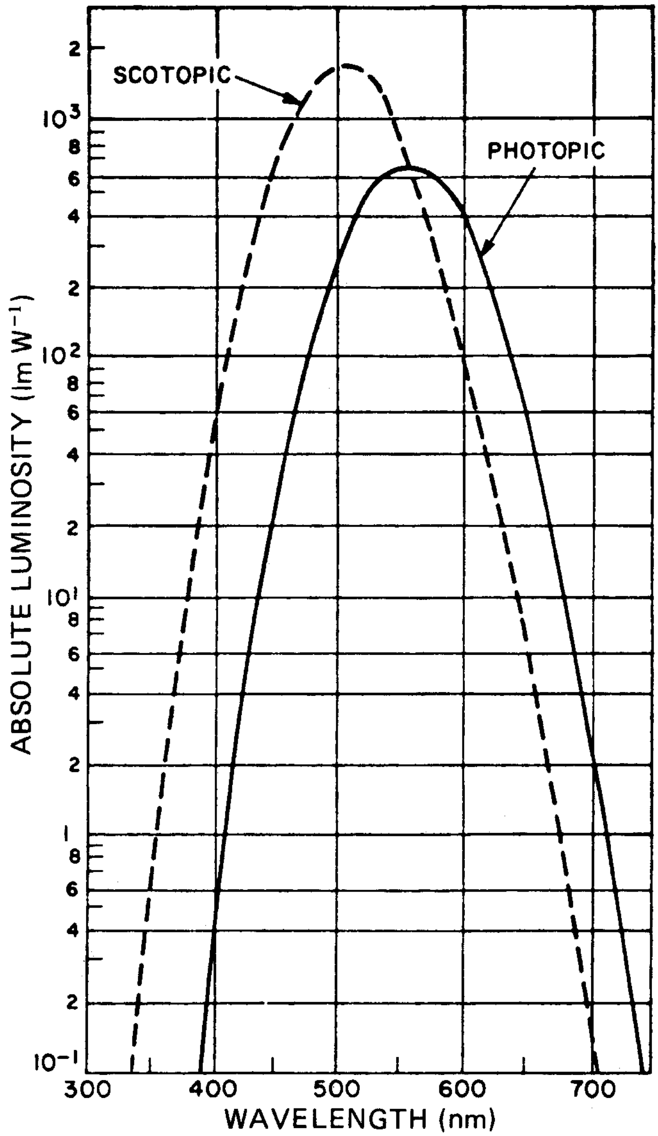

Summary of typical sources/parameters for the most commonly used radiant energy sources

Lamp type	DC input power (watts)	Arc dimensions (mm)	Luminous flux (lm)†	Luminous efficiency (lm W^{-1})	Average luminance (cd mm^{-2})
Mercury short arc(high pressure)	200	2.5×1.8	9500	47.5	250
Xenon short arc	150	1.3×1.0	3200	21	300
Xenon short arc	20 000	12.5×6	1 150 000	57	3000 (in 3 mm $\times 6$ mm)
Zirconium arc	100	1.5 (diam.)	250	2.5	100
Vortex-stabilized argon arc	24 800	3×10	422 000	17	1400
Tungsten light bulbs	10	–	79	7.9	10 to 25
	100	–	1630	16.3	
	1000	–	21500	21.5	
Fluorescent lamp standard warm white	40	–	2560	64	–
Carbon arc, non-rotating	2000	$\approx 5 \times 5$	36 800	18.4	175 to 800
rotating	15 800	$\approx 8 \times 8$	350 000	22.2	
Deuterium lamp	40	1.0 (diam.)	(Nominal irradiance at 250 nm at 30 cm = 0.2μ W cm^{-2} nm^{-1})		

†Luminous flux Φ in lumens from a source of total radiant power $W(\lambda)$ watts per unit wavelength:

$$\Phi = 680 \int_0^\infty W(\lambda)V(\lambda)d\lambda.$$

where $V(\lambda)$ represents the spectral luminous efficiency.

Conversion table for various photometric units

Luminous intensity (I)

1 candela (cd) = 1 lumen/steradian (lm sr^{-1})

Luminous flux (Φ) [lumen (lm)]

4π lumens = total flux from uniform point source of 1 candela

Illuminance (E)

1 footcandle (fc) = 1 lumen $foot^{-2}$

1 lux (lx) = 1 lumen m^{-2} = 0.0929 footcandle

Luminance (L)
1 footlambert (fL) = $1/\pi$ candela foot^{-2}.
1 nit (nt) = 1 candela m^{-2} = 0.2919 footlambert

Luminance values for various sources

Source	Luminance (fL)	Luminance (cd m^{-2})
Sun, as observed from Earth's surface at meridian	4.7×10^8	1.6×10^9
Moon, bright spot, as observed from Earth's surface	730	2500
Clear blue sky	2300	7900
Lightning flash	2×10^{10}	7×10^{10}
Atomic fission bomb, 0.1 ms after firing, 90-ft diameter ball	6×10^{11}	2×10^{12}
Tungsten filament lamp, gas-filled, 16 lm W^{-1}	2.6×10^6	9×10^6
Plain carbon arc, positive crater	4.7×10^6	1.6×10^7
Fluorescent lamp, T-12 bulb, cool white, 430 mA, medium loading	2000	7000
Colour television screen, average brightness	50	170

Typical values of natural scene illuminance

Sky condition	Approximate levels of illuminance (lux)
Direct sunlight	$1\text{–}1.3 \times 10^5$
Full daylight (not direct sunlight)	$1\text{–}2 \times 10^4$
Overcast day	10^3
Very dark day	10^2
Twilight	10
Deep twilight	1
Full moon	10^{-1}
Quarter moon	10^{-2}
Moonless, clear night sky	10^{-3}
Moonless, overcast night sky	10^{-4}

Natural illuminance on the Earth for the hours immediately before and after sunset with a clear sky and no moon

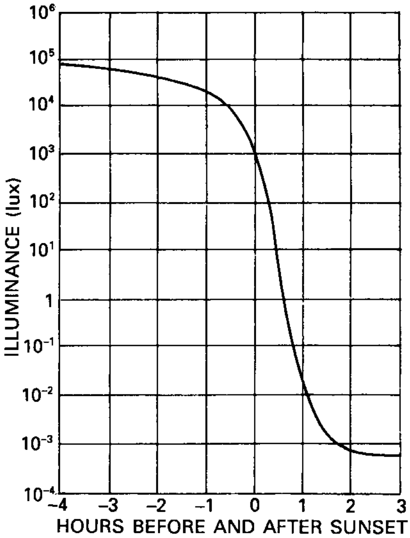

Radiant responsivity

Calculation of radiant responsivity from lumminous responsivity for photocathodes:

The response of a photocathode (in amperes) to the total radiation $W(\lambda)$ watts per unit wavelength is:

$$\int \sigma R(\lambda)W(\lambda)d\lambda,$$

where the relative spectral response of the photocathode is $R(\lambda)$ ($R_{\text{max}} = 1$) and σ is the absolute radiant response at the peak of the response curve (amperes per watt). The light flus (in lumens) is given by:

$$680 \int V(\lambda)W(\lambda)d\lambda.$$

where $V(\lambda)$ is the spectral luminous efficiency. The luminous responsivity of the photocathode in amperes per lumen is then given by:

$$S = \frac{\sigma \int R(\lambda)W(\lambda)d\lambda}{680 \int V(\lambda)W(\lambda)d\lambda}$$

and, therefore,

$$\sigma = \frac{680S \int V(\lambda)W(\lambda)d\lambda}{\int R(\lambda)W(\lambda)d\lambda}.$$

(The material in the preceding sections was adapted from Engstrom, R. W., *Photomultiplier Handbook*, RCA Corporation, 1980.)

Standard units, symbols, and defining equations for fundamental photometric and radiometric quantities

Quantity$^{(a)}$	Symbol$^{(a)}$	Defining equation$^{(b)}$	Commonly used units$^{(c)}$	Symbol
RADIOMETRIC				
Radiant energy	Q (Q_e)	–	erg	
			†joule	J
			kilowatt-hour	kWh
Radiant density	w (w_e)	$w = dQ/dV$	†joule per cubic meter	$J\,m^{-3}$
			erg per cubic centimeter	$erg\ cm^{-3}$
Radiant flux	Φ (Φ_e)	$\Phi = dQ/dt$	erg per second	$erg\,s^{-1}$
			†watt	W
Radiant flux density at a surface				
Radiant exitance (radiant emittance)$^{(d)}$	M (M_e)	$M = d\Phi/dA$	watt per square centimeter	$W\,cm^{-2}$
Irradiance	E (E_e)	$E = d\Phi/dA$	†watt per square meter, etc.	$W\,m^{-2}$
Radiant intensity	I (I_e)	$I = d\Phi/d\omega^{(i)}$	†watt per steradian	$W\,sr^{-1}$
Radiance	L (L_e)	$L = d^2\Phi/d\omega(dA\cos\theta)$	watt per steradian and square centimeter	$W\,sr^{-1}\ cm^{-2}$
		$= dl/(dA\cos\theta)^{(e)}$	†watt per steradian and square meter	$W\,sr^{-1}\ m^{-2}$
Emissivity	ε	$\varepsilon = M/M_{blackbody}{}^{(f)}$	one (numeric)	–
PHOTOMETRIC				
Absorptance	α (α_ν, α_e)	$\alpha = \Phi_a/\Phi_i{}^{(g)}$	one (numeric)	–
Reflectance	ρ (ρ_ν, ρ_e)	$\rho = \Phi_r/\Phi_i{}^{(g)}$	one (numeric)	–
Transmittance	τ (τ_ν, τ_e)	$\tau = \Phi_t/\Phi_i{}^{(g)}$	one (numeric)	–
			lumen-hour	lm-h
Luminous energy (quantity of light)	Q (Q_ν)	$Q_\nu = \int_{380}^{760} K(\lambda) Q_e \lambda d\lambda$	†lumen-second (talbot)	lm-s
Luminous density	w (w_ν)	$w = dQ/dV$	†lumen-second per cubic meter	$lm\text{-}s\,m^{-3}$
Luminous flux	Φ (Φ_ν)	$\Phi = dQ/dt$	†lumen	lm

Standard units, symbols, and defining equations for fundamental photometric and radiometric quantities *(cont.)*

Quantity[(a)]	Symbol[(a)]	Defining equation[(b)]	Commonly used units[(c)]	Symbol
Luminous flux density at a surface				
Luminous exitance (luminous emittance)[(d)]	M (M_ν)	$M = d\Phi/dA$	lumen per square foot	lm ft^{-2}
Illumination (illuminance)	E (E_ν)	$E = d\Phi/dA$	footcandle (lumen per square foot)	fc
			†lux (lm m^{-2})	lx
			phot (lm cm^{-2})	ph
Luminous intensity (candlepower)	I (I_ν)	$I = d\Phi/d\omega^{(i)}$	†candela (lumen per steradian)	cd
Luminance (photometric brightness)	L (L_ν)	$L = d^2\Phi/d\omega(dA\cos\theta)$	candela per unit area	cd in^{-2}, etc.
		$= dl/(dA\cos\theta)^{(e)}$	stilb (cd cm^{-2})	sb
			nit (†cd m^{-2})	nt
			footlambert (cd per π ft^2)	fL
			lambert (cd per π cm^2)	L
			apostilb (cd per π m^2)	asb
Luminous efficacy	K	$K = \Phi_\nu/\Phi_e$	†lumen watt^{-1}	lm W^{-1}
Luminous efficiency	V	$V = K/K_{max}{}^{(h)}$	one (numeric)	–

[(a)] The symbols for photometric quantities are the same as those for the corresponding radiometric quantities. When it is necessary to differentiate them, the subscripts ν and e, respectively should be used, e.g., Q_ν and Q_e. Quantities may be restricted to a narrow wavelength band by adding the word spectral and indicating the wavelength. The corresponding symbols are changed by adding a subscript λ, e.g., Q_λ for a spectral concentration or a λ in parentheses, e.g., $K(\lambda)$, for a function of wavelength.

[(b)] The equations in this column are given merely for identification.

[(c)] International System (SI) unit indicated by dagger (†)

[(d)] To be deprecated.

[(e)] θ is the angle between line of sight and normal to surface considered.

[(f)] M and $M_{\mathrm{blackbody}}$ are respectively, radiant exitance of a measured specimen and of a blackbody at the same temperature as the specimen.

[(g)] Φ_i is the incident flux, Φ_a is absorbed flux, Φ_r is reflected flux, Φ_t is transmitted flux.

[(h)] $K_{\max}$ is the maximum value of the $K(\lambda)$ function.

[(i)] ω is the solid angle through which flux from point source is radiated.

(*Photoelectronic Imaging Devices*, Vol. 1, L.M. Biberman & S. Nudelman, eds., Plenum Press, 1971, with permission.)

Commercial lasers

Wavelength (μm)	Type	Wavelength (μm)	Type
0.152	Molecular fluorine (F_2)	0.635–0.66	InGaAlP diode
0.192	ArF excimer	0.647	Krypton ion
0.2–0.35	Doubled dye	0.67	GaInP diode
0.235–0.3	Tripled Ti-sapphire	0.68–1.13	Ti-sapphire
0.248	KrF excimer	0.694	Ruby
0.266	Quadrupled Nd	0.72–0.8	Alexandrite
0.275–0.306	Argon-ion	0.75–0.9	GaAlAs diode
0.308	XeCl excimer	0.98	InGaAs diode
0.32–1.0	Pulsed dye	1.047 or 1.053	Nd-YLF
0.325	He-Cd	1.061	Nd-glass
0.33–0.38	Neon	1.064	Nd-YAG
0.337	Nitrogen	1.15	He-Ne
0.35–0.47	Doubled Ti-sapphire	1.2–1.6	InGaAsP diode
0.351	XeF excimer	1.313	Nd-YLF
0.355	Tripled Nd	1.32	Nd-YAG
0.36–0.4	Doubled alexandrite	1.4–1.6	Color center
0.37–1.0	CW dye	1.523	He-Ne
0.442	He-Cd	1.54	Erbium-glass (bulk)
0.45–0.52	Ar-ion	1.54	Erbium-fiber (amplifier)
0.51	Copper vapor	1.75–2.5	Cobalt-MgF_2
0.523	Doubled Nd-YLF	2.3–3.3	Color center
0.532	Doubled Nd-YAG	2.6–3.0	HF chemical
0.5435	He-Ne	3.3–29	Lead-salt diode
0.578	Copper vapor	3.39	He-Ne
0.594	He-Ne	3.6–4.0	DF chemical
0.612	He-Ne	5–6	Carbon monoxide
0.628	Gold vapor	9–11	Carbon dioxide
0.6328	He-Ne	40-100	Far-infrared gas

(From *The Laser Guidebook*, 2nd ed., Hecht, J., McGraw-Hill, 1991.)

Index of refraction of air

The following formula gives the index of refraction of dry air at 15°C and a pressure of 101.325 kPa (1 atmos.; 760 Torr) and containing 0.03% by volume of carbon dioxide ("standard air"). The index of refraction is defined as $n = \lambda_{\text{vac}}/\lambda_{\text{air}}$, where λ is the wavelength of the radiation.

$$(n-1)\times 10^8 = 8342.13 + 2406030(130-\sigma^2)^{-1} + 15997(38.9-\sigma^2)^{-1}$$

where $\sigma = 1/\lambda_{\text{vac}}$ and λ_{vac} has unit of μm. The equation is valid for λ_{vac} from 200 nm to 2 μm.

If the air is at a temperature t in °C and a pressure p in pascals, a value of $(n-1)$ should be multiplied by

$$\frac{p[1+p(61.3-t)\times 10^{-10}]}{96095.4(1+0.003661t)}.$$

Properties of optical materials

Material	*Useful Transmission Range* ($\gtrsim$10% *transmission*) *in* 2-mm *Thickness*	*Index of Refraction* [*wavelength* (μm) *in parentheses*]
LiF	0.104–7	1.60(0.125), 1.34(4.3)
MgF_2	0.1216–9.7	n_o = 1.3777, n_e = 1.38950(0.589)[(f)]
CaF_2	0.125–12	1.47635(0.2288), 1.30756(9.724)
BaF_2	0.1345–15	1.51217(0.3652), 1.39636(10.346)
Sapphire (Al_2O_3)	0.15–6.3	n_o = 1.8336(0.26520), n_o = 1.5864(5.577)[(f)], n_e slightly less than n_o
Fused silica (SiO_2)	0.165–4[(d)]	1.54715(0.20254), 1.40601(3.5)
Pyrex 7740	0.3–2.7	1.474(0.589), $\simeq$ 1.5(2.2)
Vycor 7913	0.26–2.7	1.458(0.589)
As_2S_3	0.6–0.13	2.84(1.0), 2.4(8)
RIR 2	$\simeq$ 0.4–4.7	1.75(2.2)
RIR 20	$\simeq$ 0.4–5.5	1.82(2.2)
NaF	0.13–12	1.393(0.185), 0.24(24)
RIR 12	$\simeq$ 0.4–5.7	1.62(2.2)
MgO	0.25–8.5	1.71(2.0)
Acrylic	0.340–1.6	1.5066(0.4101), 1.4892(0.6563)
Silver chloride (AgCl)	0.4–32	2.134(0.43), 1.90149(20.5)
Silver bromide (AgBr)	0.45–42	2.313(0.496), 2.2318(0.671)
Kel-F	0.34–3.8	–
Diamond (Type IIA)	0.23–200	2.7151(0.2265), 2.4237(0.5461)
NaCl	0.21–25	1.89332(0.185), 1.3403(22.3)
KBr	0.205–25	1.55995(0.538), 1.46324(25.14)
KCl	0.18–30	1.78373(0.19), 1.3632(23)
CsCl	0.19–$\simeq$ 30	1.8226(0.226), 1.6440(0.538)
CsBr	0.21–50	1.75118(0.365), 2.55990(39.22)
KI	0.25–40	2.0548(0.248), 1.6381(1.083)
CsI	0.235–60	1.98704(0.297), 1.61925(53.12)
$SrTiO_3$	0.4–7.4	2.23(2.2), 2.19(4.3)
SrF_2	0.13–14	1.438(0.538)
Rutile (TiO_2)	0.4–7	n_o = 2.5(1.0), n_e = 2.7(1.0)[(f)]
Thallium bromide (TlBr)	0.45–45	2.652(0.436), 2.3(0.75)
Thallium bromoiodide (KRS-5)	0.56–60	2.62758(0.577), 2.21721(39.38)
Thalliun chlorobromide (KRS-6)	0.4–32	2.3367(0.589), 2.0752(24)
ZnSe	0.5–22	2.4(10.6)
Irtran 2(ZnS)	0.6–15.6	2.26(2.2), 2.25(4.3)
Si	1.1–15[(e)]	3.42(5.0)
Ge	1.85–30[(e)]	4.025(4.0), 4.002(12.0)
GaAs	1–15	3.5(1.0), 3.135(10.6)
CdTe	0.9–16	2.83(1.0), 2.67(10.6)
Te	3.8–8	n_o = 6.37(4.3), n_e = 4.93(4.3)[(f)]
$CaCO_3$	0.25–3	n_o = 1.90284(0.200), n_e = 1.57796(0.198)[(f)] n_o = 1.62099(2.172), n_e = 1.47392(3.324)

Properties of optical materials (cont.)

Material	*Thermal-Expansion Coefficient* (10^{-6}/°C)	*Knoop Hardness*	*Melting Point* (°C)
LiF	9	100	870
MgF_2	16	415	1396
CaF_2	25	158	1360
BaF_2	26	65	1280
Al_2O_3	$6.66^{(a)}$, $5.0^{(b)}$	$1525–2000^{(c)}$	2040±10
SiO_2	0.55	615	1600
Pyrex	3.25	≃ 600	$820^{(g)}$
Vycor	0.8	–	1200
As_2S_3	26	109	300
RIR 2	8.3	≃ 600	≃ 900
RIR 20	9.6	542	760
NaF	36	60	980
RIR 12	8.3	594	≃ 900
MgO	43	692	2800
Acrylic	110–140	–	Distorts at 72
AgCl	30	9.5	455
AgBr	–	≳ 9.5	432
Kel-F	–	–	–
Diamond	0.8	$5700–10{,}400^{(c)}$	–
NaCl	44	18	803
KBr	–	7	730
KCl	–	–	776
CsCl	–	–	646
CsBr	48	19.5	636
KI	–	5	723
CsI	50	–	621
$SrTiO_3$	9.4	620	2080
SrF_2	–	130	1450
TiO_2	9	880	1825
TlBr	–	12	460
KRS-5	51	40	414.5
KRS-6	60	39	423.5
ZnSe	8.5	150	–
ZnS	–	354	800
Si	4.2	1150	1420
Ge	5.5	692	936
GaAs	5.7	750	1238
CdTe	4.5	45	1045
Te	16.8	–	450
$CaCO_3$	–	–	–
	–	135	$894.4^{(h)}$

$^{(a)}$ Parallel to c-axis. $^{(b)}$ Perpendicular to c-axis.
$^{(c)}$ Depends on crystal orientation. $^{(d)}$ Depends on grade.
$^{(e)}$ Long-wavelength limit depends on purity of material. $^{(f)}$ Birefringent
$^{(g)}$ Softening temperature. $^{(h)}$ Decomposition temperature.

(From *Building Scientific Apparatus*, Moore, J.H., Davis, C.C., and Coplan, M.A., Addison-Wesley Publishing Company, Inc., 1989.)

Theory of lenses

Thin lens

If a lens can be characterized by a single focal length F measured from a single plane then the lens is "thin." Various relations hold among the quantities shown in the figure.

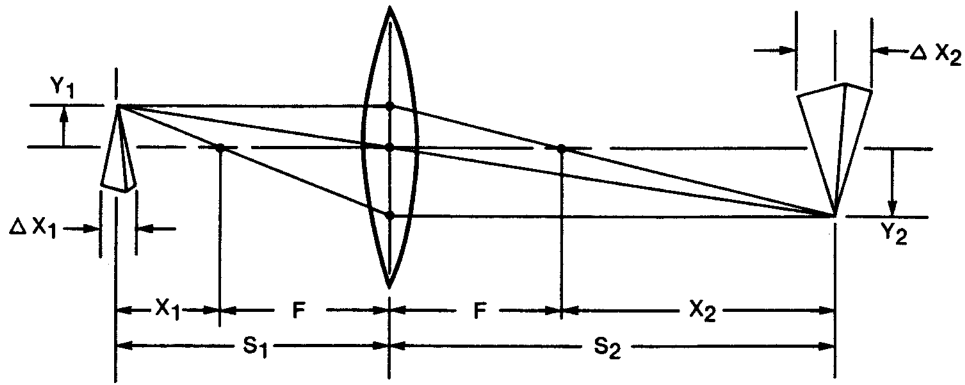

Gaussian: $1/s_1 + 1/s_2 = 1/F$

Newtonian: $x_1 x_2 = -F^2$

Magnification:

Transverse: $M_T = y_2/y_1 = -s_2/s_1$

$M_T < 0$–Image inverted

Longitudinal: $M_L = \Delta x_2/\Delta x_1 = -M_T^2$

$M_L < 0$–No front to back inversion

Thick lens

A **thick lens** cannot be characterized by a single focal length measured from a single plane. A single focal length F may be retained if it is measured from two planes, H_1, H_2, at distances P_1, P_2 from the vertices of the lens, V_1, V_2. The two back focal lengths, BFL_1 and BFL_2, are measured from the vertices. The thin lens equations may be used, provided all quantities are measured from the principal planes.

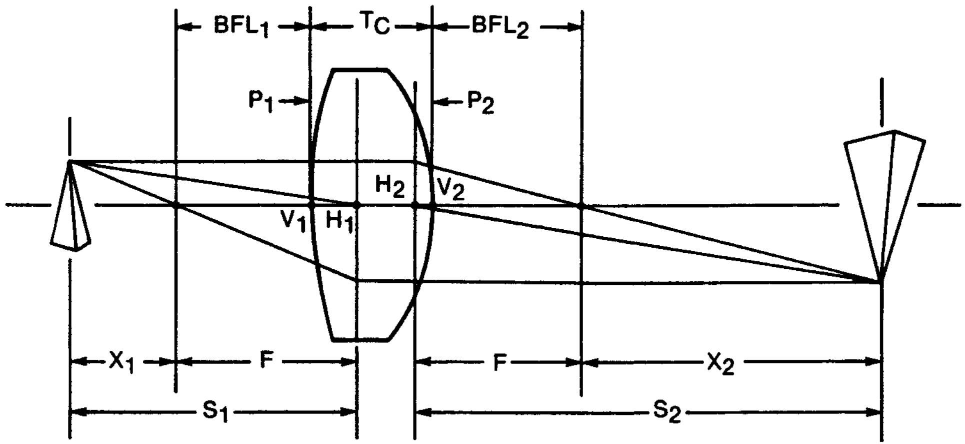

The lensmaker's equation

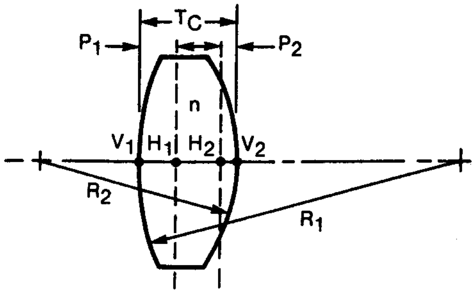

$$\frac{1}{F} = (n-1)\left[\frac{1}{R_1} - \frac{1}{R_2} + \frac{(n-1)T_c}{nR_1R_2}\right]$$

$$P_1 = -\frac{F(n-1)T_c}{nR_2}$$

$$P_2 = -\frac{F(n-1)T_c}{nR_1}$$

Convex surfaces facing left have positive radii. In the above $R_1 > 0$, $R_2 < 0$. Principal plane offsets are positive to right. As illustrated, $P_1 > 0$, $P_2 < 0$. The **thin lens focal length** is given when $T_c = 0$.

Numerical aperture

$\mathrm{NA} = n_0 \sin(\phi_{\mathrm{MAX}}/2)$

ϕ_{MAX} is the full angle of the cone of light rays that can pass through the system.

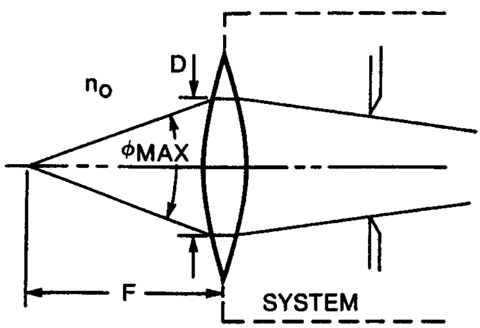

For small ϕ:

$$f/\#(\text{f-number}) = F/D \approx 2\ \mathrm{NA}$$

Both f-number and NA refer to the *system* and not the exit lens.

Visible and ultraviolet light detectors

Photodiode

Schematics of photodiodes (a) sealed with semi-transparent photocathode, (b) open (or sealed) with opaque photocathode. (From Timothy, J.G. & Madden, R.P. in *Handbook on Synchrotron Radiation*, E. Koch, ed., North-Holland Publishing Co., 1983, with permission.)

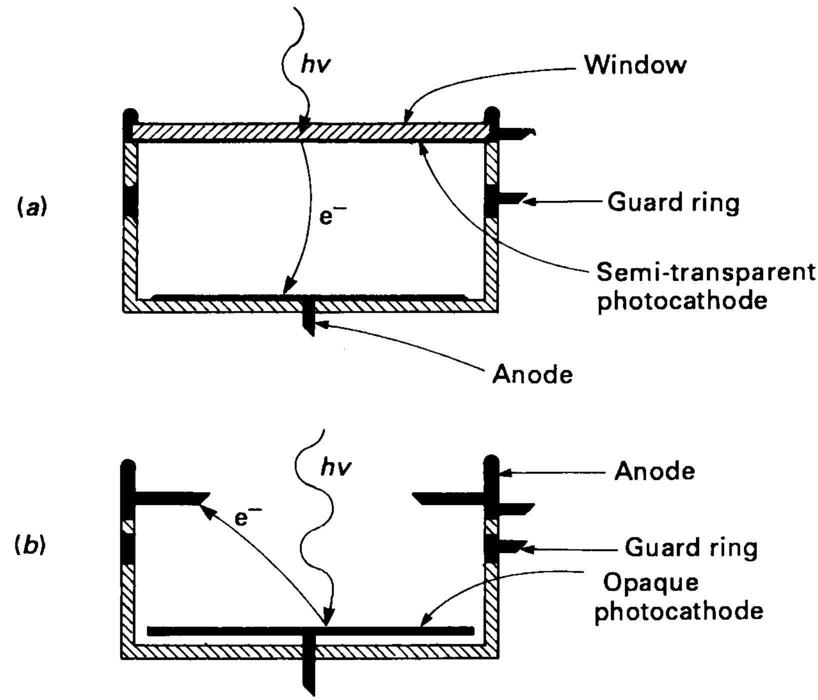

(a) (116–254 nm) Incident UV photons cause the photocathode (usually semi-transparent cesium telluride deposited on a magnesium fluoride window) to emit low energy electrons, which are accelerated away by the electric field established by the anode potential (150 V). A calibrated picoammeter measures photocurrent. Quantum energy range (typ): 0.02–0.2 electrons per photon.

(b) (5–122 nm) Incident UV photons cause the photocathode (usually aluminum with a 15 nm aluminum oxide layer) to emit low energy electrons, which are accelerated away by the electric field established by the anode potential (60–100 V). A calibrated picoammeter measures photocurrent. The useable range of photocurrents is approximately 10^{-9} to 10^{-15} amp. Quantum efficiency range (typ): 0.01–0.15 electrons per photon.

Quantum efficiencies of opaque Cs_2Te and CsI photocathodes. (From Timothy, J.G. & Madden, R.P., *op. cit.*)

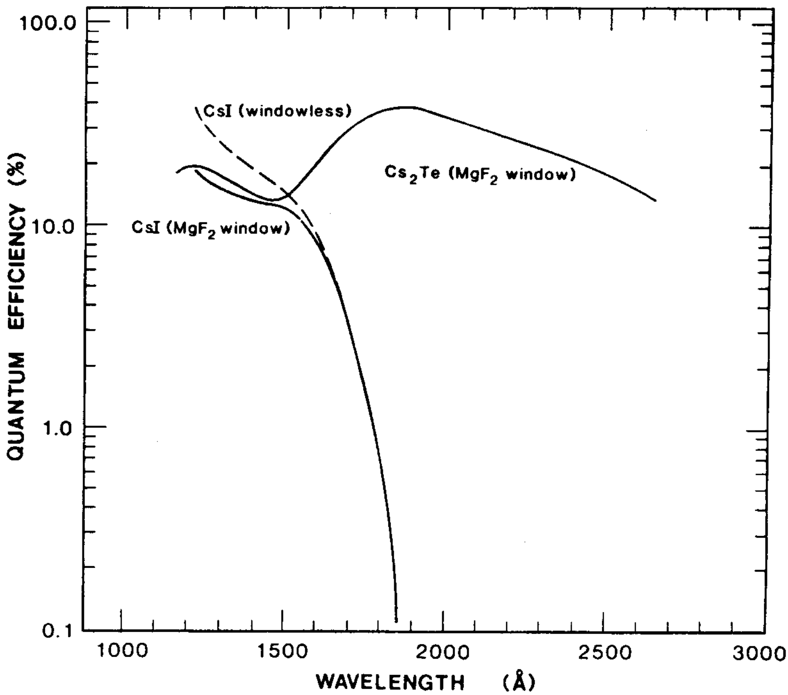

Quantum efficiencies of transfer standard detectors available from NBS. (From Timothy, J.G. & Madden, R.P., *op. cit.*)

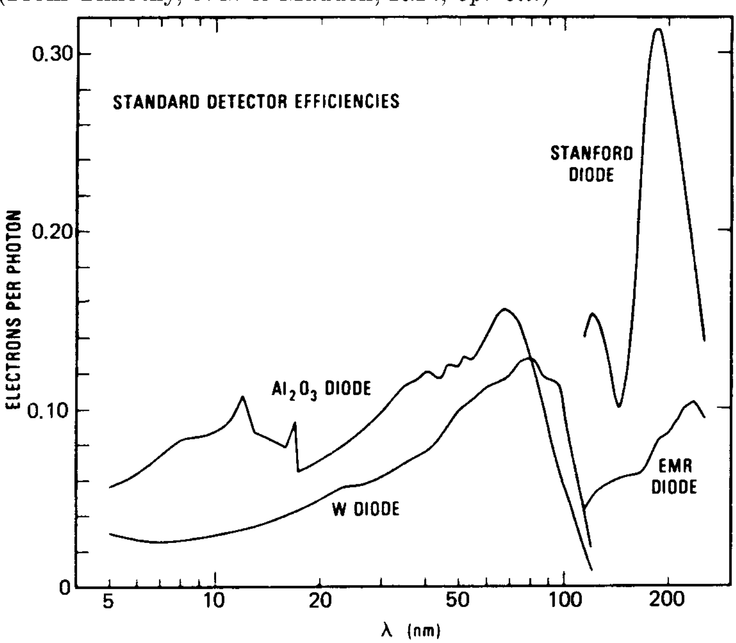

Image intensifiers

Generation I electrostatically focused image intensifier. (Reproduced with permission of the publisher, Howard W. Sams & Co., Indianapolis, *Image Tubes*, by Illes P. Csorba, ©1985.)

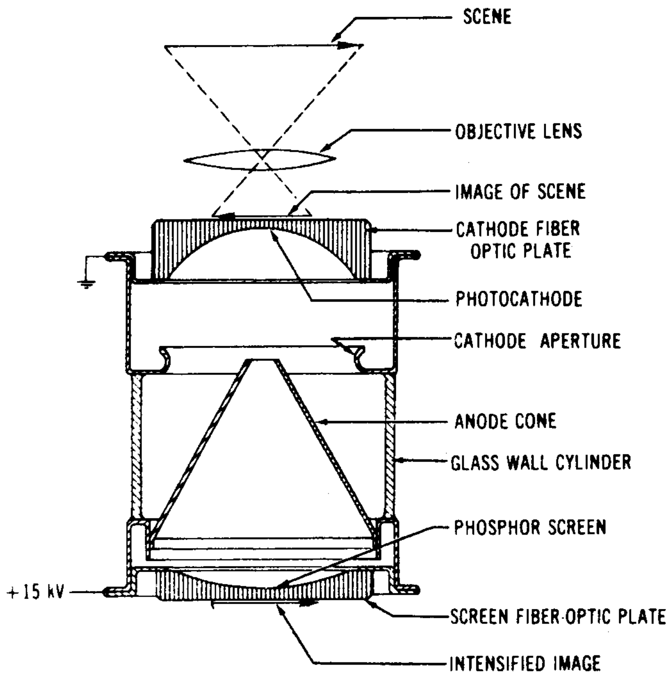

The electrostatic image-inverting generation II image intensifier employs a microchannel plate (MCP). (From Csorba, I.P., *op. cit.*)

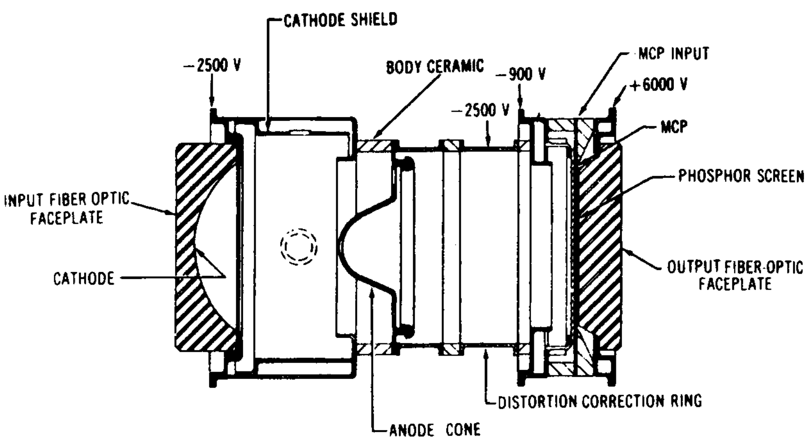

Charge-coupled devices (CCD's)

Schematic voltage operation of a typical three-phase CCD. The clock voltages are shown at three times during the readout process, indicating their clock cycle of 0, 10, and 5 volts. One clock cycle causes the stored charge within a pixel to be transfered to its neighboring pixel. CCD readout continues until all the pixels have had their charge transfered completely out of the array and through the A/D converter. (From *Handbook of CCD Astronomy*, S.B. Howell, Cambridge University Press, 2000)

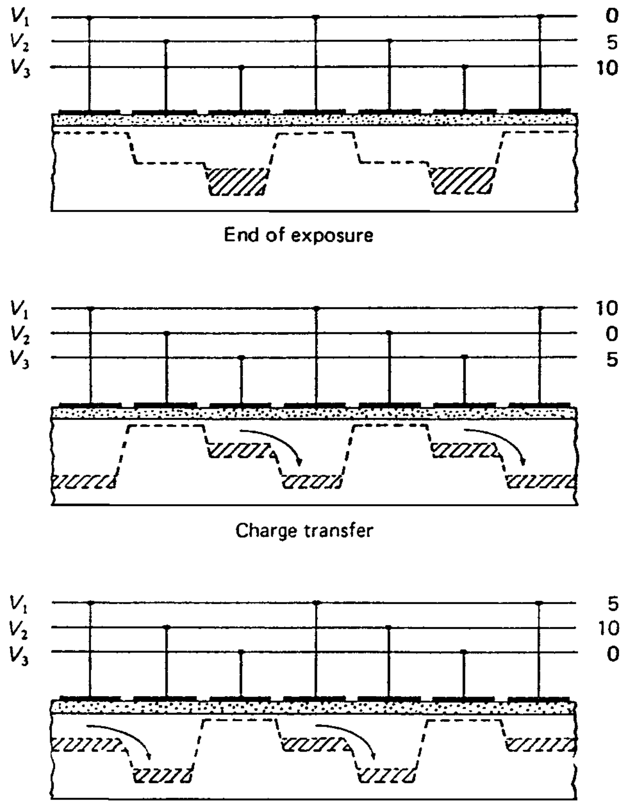

Various typical CCD properties

	RCA	Fairchild	TI	EEV	Thomsom	Kodak	Lorel (Ford)	Tektronix (SITe)
Pixel Format	320×512	380×488	800×800	2048×4096	1024×1024	765×510	3072×1024	1024×1024
Pixel Size (μ)	30	18×30	15	13.5	19	9	15	24
Detector size (mm)	10×15	7×15	12×12	28×55	20×20	7×4.5	46×15	25×25
Full Well Capacity (e^-)	350,000	$> 200,000$	50,000	180,000	500,000	85,000	$> 140,000$	$> 170,000$
Dark Current (e^-/pixel/hr)	40	> 1000	16	< 2	22	1800	11	< 5
Illumination	Front	Front	Back	Back	Front	Front	Back	Back
Peak QE (%)	70	12	70	85	40	40	90	75
Read Noise (e^-)	80	> 150	15	7	5	12	9	6
CTE	0.99995	0.99975	0.999985	0.99999	0.99996	0.99997	0.99997	0.999999
Operating Temp. (°C)	−100	−100	−120	−120	−110	−35	−120	−111
Gain (e^-/ADU)	13.5	50	5	1.1	5	2.3	1.2	1.3
Readout Time (s)	45	65	70	185	45	45	142	300

(From *Handbook of CCD Astronomy*, S.B.Howell, Cambridge University Press, 2000)

A comparison of the quantum efficiency for various optical detectors.

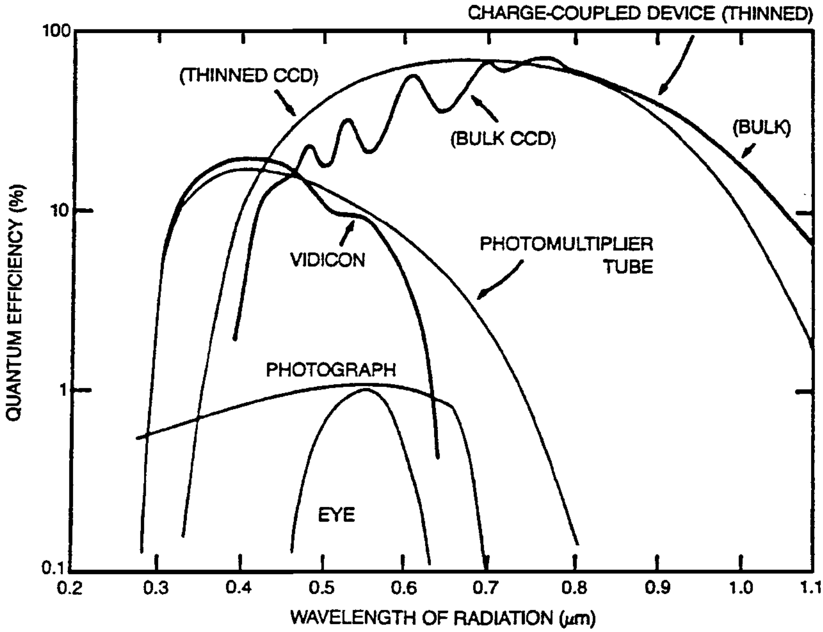

(From *Handbook of CCD Astronomy*, S.B. Howell, Cambridge University Press, 2000)

Photomultipliers

Schematic of typical photomultiplier showing some electron trajectories (RCA).

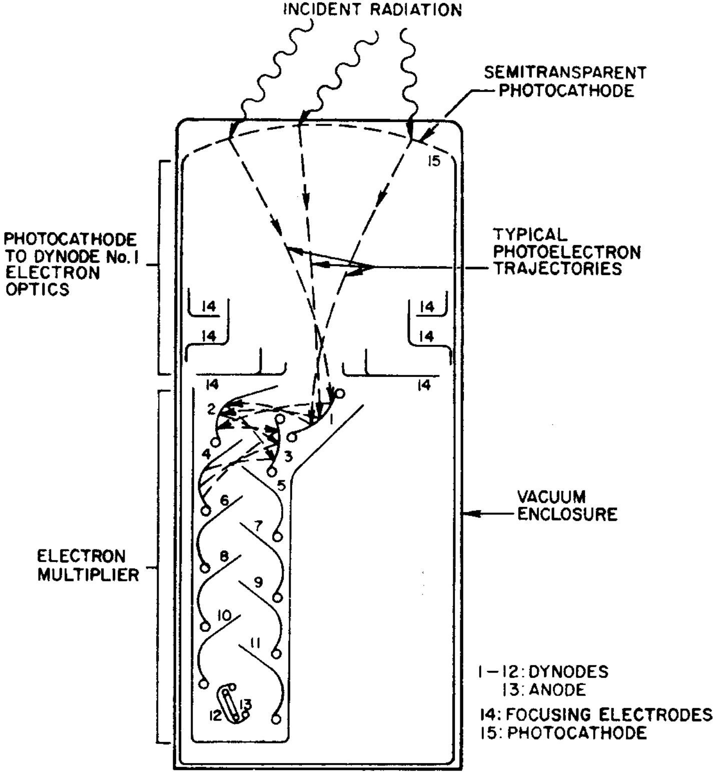

Typical anode sensitivity and amplification characteristics of a 9-dynode photomultiplier tube as a function of applied voltage (RCA).

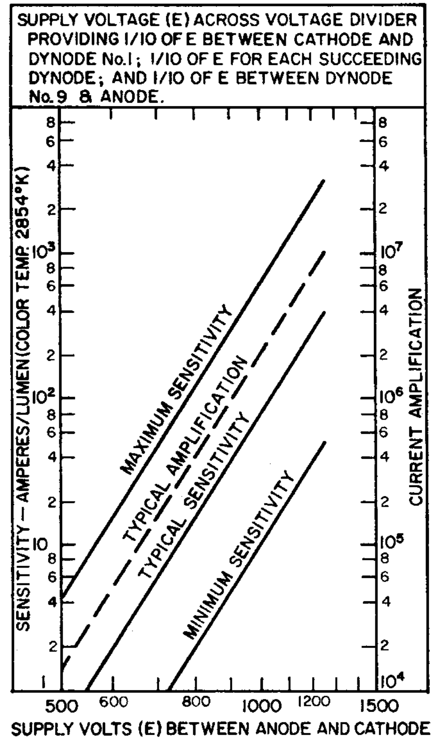

Typical voltage-divider arrangement for fast pulse response and high peak current systems.

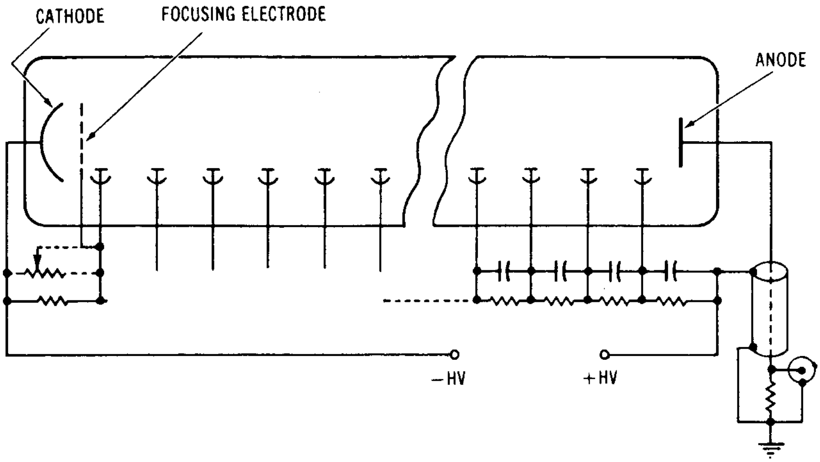

Source and detector matching

The average power radiating from a light source is given by:

$$P = P_0 \int_0^\infty W(\lambda)d\lambda,$$

where P_0 is the incident power in watts per unit wavelength at the peak of the relative spectral radiation characteristic, $W(\lambda)$, which is normalized to unity.

The resulting photocathode current I, when the light is incident on the detector, is given by:

$$I_k = \sigma P_0 \int_0^\infty W(\lambda)R(\lambda)d\lambda,$$

where σ is the radiant sensitivity of the photocathode in amperes per watt at the peak of the relative curve, and $R(\lambda)$ represents the relative photocathode spectral response as a function of wavelength normalized to unity at the peak.

$$I_k = \sigma P \frac{\int_0^\infty W(\lambda)R(\lambda)d\lambda}{\int_0^\infty W(\lambda)d\lambda}.$$

The ratio of the dimensionless integrals can be defined as the *matching factor*, M.

$$M = \frac{\int_0^\infty W(\lambda)R(\lambda)d\lambda}{\int_0^\infty W(\lambda)d\lambda}.$$

Spectral matching factors

Source	Photocathodes							Photopic eye	Scotopic eye
	S1	S4	S10	S11	S17	S20	S25		
PHOSPHORS									
P1	0.278	0.498	0.807	0.687	0.892	0.700	0.853	0.768	0.743
P4	0.310	0.549	0.767	0.661	0.734	0.724	0.861	0.402	0.452
P7	0.312	0.611	0.805	0.709	0.773	0.771	0.882	0.411	0.388
P11	0.217	0.816	0.949	0.914	0.954	0.877	0.953	0.201	0.601
P15	0.385	0.701	0.855	0.787	0.871	0.802	0.904	0.376	0.495
P16	0.830	0.970	0.853	0.880	0.855	0.902	0.922	0.003	0.042
P20	0.395	0.284	0.612	0.427	0.563	0.583	0.782	0.707	0.354
P22B	0.217	0.893	0.974	0.960	0.948	0.927	0.979	0.808	0.477
P22G	0.278	0.495	0.807	0.686	0.896	0.699	0.855	0.784	0.747
P22R	0.632	0.036	0.264	0.055	0.077	0.368	0.623	0.225	0.008
P24	0.279	0.545	0.806	0.696	0.827	0.725	0.869	0.540	0.621
P31	0.276	0.533	0.811	0.698	0.853	0.722	0.868	0.626	0.651
NaI	0.534	0.923	0.885	0.889	0.889	0.900	0.933	0.046	0.224

Spectral matching factors (cont.)

	Photocathodes								
Source	S1	S4	S10	S11	S17	S20	S25	Photopic eye	Scotopic eye
LAMPS									
2870/2856 std	0.516†	0.046†	0.095†	0.060†	0.072†	0.112†	0.227†	0.071†	0.040†
Fluorescent	0.395	0.390	0.650	0.496	0.575	0.635	0.805	0.502	0.314
SUN									
In space	0.535†	0.308†	0.388†	0.328†	0.380†	0.406†	0.547†	0.179†	0.172†
+ 2 air masses	0.536†	0.236†	0.348†	0.277†	0.315†	0.360†	0.513†	0.197†	0.175†
Day sky	0.537†	0.520†	0.556†	0.508†	0.589†	0.581†	0.700†	0.170†	0.218†
BLACK BODIES									
6000K	0.533†	0.308†	0.376†	0.320†	0.375†	0.397†	0.521†	0.167†	0.159†
3000K	0.512†	0.053†	0.102†	0.067†	0.080†	0.120†	0.232†	0.075†	0.044†
2870K	0.504†	0.044†	0.090†	0.057†	0.069†	0.106†	0.216†	0.067†	0.038†
2856K	0.500†	0.042†	0.088†	0.055†	0.068†	0.103†	0.211†	0.065†	0.037†
2810K	0.493†	0.039†	0.081†	0.051†	0.062†	0.097†	0.150†	0.061†	0.034†
2042K	0.401†	0.008†	0.023†	0.011†	0.014†	0.033†	0.090†	0.018†	0.007†

† Entry valid only for 300–1200 nm wavelength interval.

Nominal composition and characteristics of various photocathodes

Nominal composition	JETEC response designation	Conversion factor[a] (lumen watt^{-1} at λ_{max})	Luminous responsivity (μA lumen^{-1})	Wavelength of maximum response, λ_{max}(nm)	Responsivity at λ_{max} (mA watt^{-1})	Quantum efficiency at λ_{max} (%)	Dark emission at 25°C (fA cm^{-2})
Ag-O-Cs	S-1	92.7	25	800	2.3	0.36	900
Ag-O-Rb	S-3	285	6.5	420	1.8	0.55	–
Cs_3Sb	S-19	1603	40	330	64	24	0.3
Cs_3Sb	S-4	1044	40	400	42	13	0.2
Cs_3Sb	S-5	1262	40	340	50	18	0.3
Cs_3Bi	S-8	757	3	365	2.3	0.77	0.13
Ag-Bi-O-Cs	S-10	509	40	450	20	5.6	70
Cs_3Sb	S-13	799	60	440	48	14	4
Cs_3Sb	S-9	683	30	480	20	5.3	–
Cs_3Sb	S-11	808	60	440	48	14	3
Cs_3Sb	S-21	783	30	440	23	6.7	–
Cs_3Sb	S-17	667	125	490	83	21	1.2
Na_2KSb	S-24	758	85	420	64	19	0.0003

Nominal composition and characteristics of various photocathodes (cont'd)

Nominal composition	JETEC response designation	Conversion factor[a] (lumen watt^{-1} at λ_{max})	Luminous responsivity (μA lumen^{-1})	Wavelength of maximum response, λ_{max}(nm)	Responsivity at λ_{max} (mA watt^{-1})	Quantum efficiency at λ_{max} (%)	Dark emission at 25°C (fA cm^{-2})
K_2CsSb	–	1117	85	400	95	29	0.02
Rb-Cs-Sb	–	767	120	450	92	25	1
Na_2KSb:Cs	–	429	150	420	64	19	0.4
Na_2KSb:Cs	S-20	428	150	420	64	19	0.3
Na_2KSb:Cs	S-25	276	160	420	44	13	–
Na_2KSb:Cs	ERMA II	220	200	530	44	10.3	2.1
Na_2KSb:Cs	ERMA III	160	230	575	37	8	0.2
GaAs:Cs-O	–	116	1025	850	119	17	92
GaAsP:Cs-O	–	310	200	450	61	17	0.01
$In_{0.06}Ga_{0.94}As$:Cs-O	–	200	250	400	50	15.5	220
$In_{0.12}Ga_{0.88}As$:Cs-O	–	255	270	400	69	21	40
$In_{0.18}Ga_{0.82}As$:Cs-O	–	280	150	400	42	13	75
Cs_2Te	–			250	25	12.4	0.0006
CsI	–			120	24	20	Very low
CuI	–			150	13	10.7	Very low
K-Cs-Rb-Sb	–	672	125	440	84	24	Very low

[a] These conversion factors are the ratio of the radiant responsivity at the peak of the spectral response characteristic in amperes per watt to the luminous responsivity in amperes per lumen for a tungsten lamp operated at a color temperature of 2856 K.

Typical photocathode spectral response characteristics (from RCA Corp.)

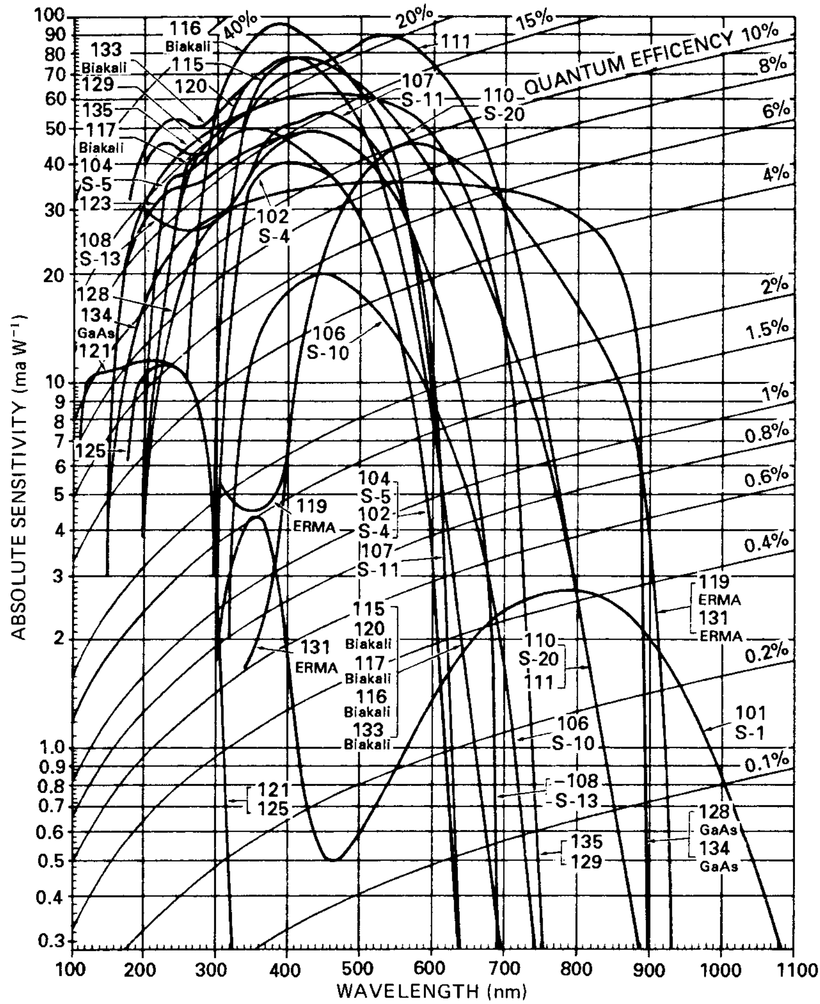

Short wavelength transmission limits of some UV window materials

Material	Approximate limit (10%, 2 mm thick)
LiF	1040 Å
MgF_2	1120
CaF_2	1220
SrF_2	1280
BaF_2	1340
Al_2O_3 (sapphire)	1410
SiO_2 (fused quartz)	1600

UV fluorescent converters (wavelength shifters)

Sodium salicylate	Diphenylstilbene
Tetraphenyl butadiene	*p*-Terphenyl
Coronene	Dimethyl POPOP
p-Quaterphenyl	POPOP

X-ray and gamma-ray detectors

Detection principles – quantum efficiency

In general, the quantum efficiency, $\varepsilon(E)$, for an incident photon of energy E is determined by the transmission of the detector window or any 'dead layer' and by the absorption of the detector medium:

$$\varepsilon(E) = e^{-(\mu/\rho)_w \rho_w t_w}(1 - e^{-(\mu/\rho)_d \rho_d t_d}),$$

where $(\mu/\rho)_w$ and $(\mu/\rho)_d$ are the mass absorption coefficients of the detector window (or 'dead layer') and detector medium, respectively, ρ_w and ρ_d are the densities of the detector window (or 'dead layer') and detector medium, respectively, and t_w and t_d are the thicknesses of the detector window (or 'dead layer') and detector medium, respectively.

Detection principles – point source detection with X-ray telescopes

The fluctuation δN_s in the number of counts from a point source of flux density F photons cm^{-2} s^{-1} keV^{-1} is given by:

$$\delta N_s = (A_{\text{eff}} \Delta E F t + f^2 \omega B_{\text{i}} \Delta E t + A_{\text{eff}} \omega j_{\text{D}} \Delta E t)^{1/2},$$

where

A_{eff} = effective area (cm^2) of telescope including detector,

ΔE = energy interval (keV),

t = observing time (s),

f = focal length (cm) of telescope,

ω = solid angle (sr) of picture element,

B_{i} = internal background (ct cm^{-2} s^{-1} keV^{-1}) of detector,

j_{D} = diffuse X-ray background (photons cm^{-2} s^{-1} keV^{-1} sr^{-1}).

The background, both internal and from diffuse X-rays, is assumed to be steady and well known. For a strong source, the signal-to-noise ratio $N_{\text{s}}/\delta N_{\text{s}} = (A_{\text{eff}} \Delta E F t)^{1/2}$ is given by the fluctuations in the source only.

For a weak source, fluctuations in the background determine the signal-to-noise ratio:

$$\frac{N_{\text{s}}}{\delta N_{\text{s}}} = \frac{(A_{\text{eff}} \Delta E F t)^{1/2}}{\omega^{1/2}(f^2 B_{\text{i}}/A_{\text{eff}} + j_{\text{D}})^{1/2}}.$$

Scintillation detector

Illustration representing a NaI scintillation detector showing sequence of events producing output from electron multiplier and various processes which contribute to response of detector to a gamma-ray source. (Adapted from Heath, R.L., *Scintillation Spectrometry, USAEC Report*, IDO-16880, 1964.)

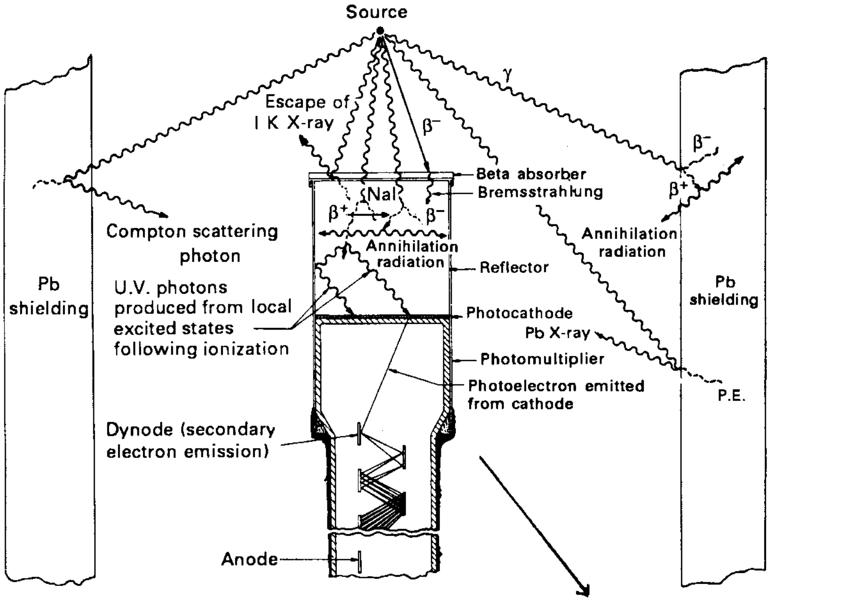

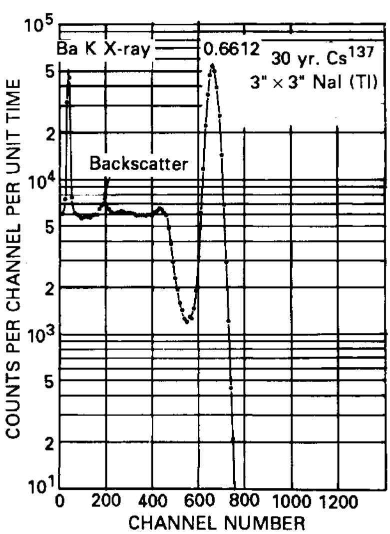

A typical pulse-height spectrum obtained with a NaI(Tl) spectrometer, illustrating the energy response of inorganic scintillators. The scale of the abscissa is 1 keV per channel.

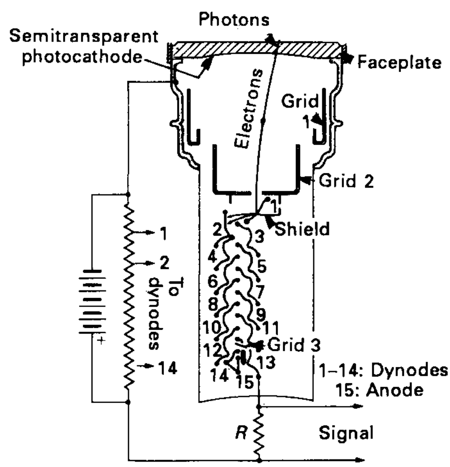

Gas proportional counter

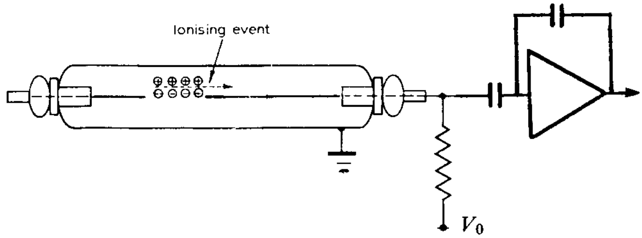

Since a proportional counter has internal gain, the system noise can be neglected and the energy resolution is:

$$(\Delta E)_{\mathrm{FWHM}} = 2.35[(F + f)WE]^{1/2} \text{ eV},$$

where

E = energy deposited in counter (eV),
F = Fano factor,
f = a factor to account for variance in the gas gain,
W = mean energy to form an ion pair (eV).

As an example, for methane gas:

$F = 0.26$
$f = 0.75$
$W = 27$ eV,

so that for a proportional counter:

$$\frac{E}{(\Delta E)_{\mathrm{FWHM}}} = 2.6E^{1/2} \quad \text{(with } E \text{ in keV).}$$

Relative number of ion pairs collected in a gas-filled chamber as a function of the voltage across electrodes of the chamber.

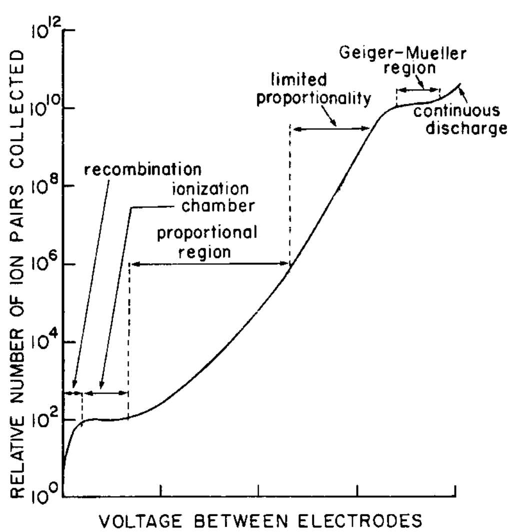

Position sensitive gas proportional detector

Readout system of detector. Incident photon is absorbed at point a; electrons drift toward anode-cathode planes. An avalanche at the anode (A) gives rise to pulse distributions at the cathodes ($K_{\parallel}$ and $K_{\perp}$). The position (X, Y) is obtained by analog summation and division. (Adapted from Bade, E. *et al.*, *Nucl. Inst. and Meth.*, **201**, 193, 1982.)

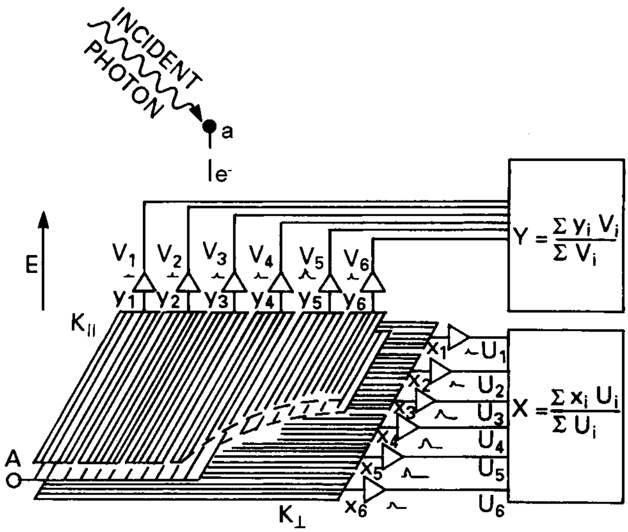

Typical performance

Spatial resolution:

0.25 mm (FWHM) at 1 keV.

Energy resolution:

$$\frac{E}{(\Delta E)_{\mathrm{FWHM}}} = 2.2E^{1/2} \quad \text{(with } E \text{ in keV)}.$$

Format:

10 cm × 10 cm.

The solid-state detector

$$(\Delta E)_{\mathrm{FWHM}} = 2.35[(\eta\sigma)^2 + (F\eta E)]^{1/2} \text{ eV}.$$

where

η = conversion factor (Si: 3.6 eV per electron-hole pair: Ge: 2.9 eV per electron-hole pair),

σ = detector rms noise (electrons),

F = Fano factor (Si: 0.14; Ge: 0.13),

E = photon or particle energy (eV).

Electron drift velocities

Electron drift velocities in various gases. From Knoll, G.F., *Radiation Detection and Measurement*, John Wiley & Sons, 1989, with permission.)

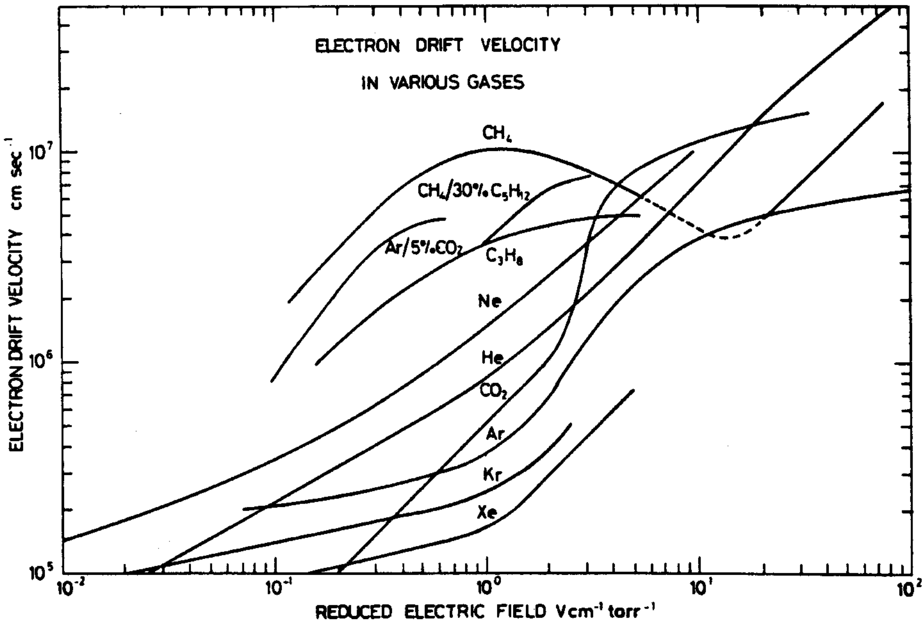

Ionization and excitation data for a number of gases

Gas	Atomic number	First ionization potential (eV)	Second ionization potential (eV)	First excited state (eV)	Principal emission wavelengths Å
He	2	24.48	54.40	20.9	584
				19.8 meta	3888
					5875
Ne	10	21.56	41.07	16.68	734
				16.53 meta	743
				16.62 meta	5400
					5832
					5852
					6402
Ar	18	15.76	27.62	11.56	1048
				11.49 meta	1066
				11.66 meta	6965
					7067
					7503
					8115
Kr	36	14.00	24.56	9.98	1236
				9.86 meta	5570
				10.51 meta	5870
Xe	54	12.13	21.2	8.39	1296
				8.28 meta	1470
				9.4 meta	4501
					4624
					4671
H	1	13.60		10.2	1215
					4861
					6562
N	7	14.53	29.59	6.3	1200
					4110
O	8	13.61	35.11	9.1	1302
					7771
H_2		15.4		11.2	
N_2		15.8		6.1	
O_2		12.5			
I_2		9.0		1.9	1782
					2062

(Adapted from Rice-Evans, P., *Spark, Streamer, Proportional and Drift Chambers*, The Richelieu Press, London, 1974.)

Schematic diagram of a ***solid state detector***. (Adapted from Enge, H., *Introduction to Nuclear Physics*, Addison-Wesley, 1966.)

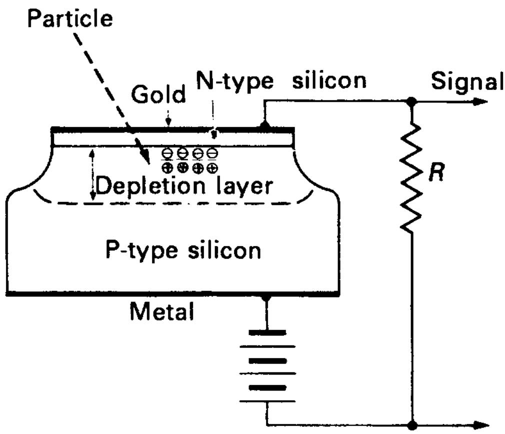

Charge-coupled device **(CCD)**

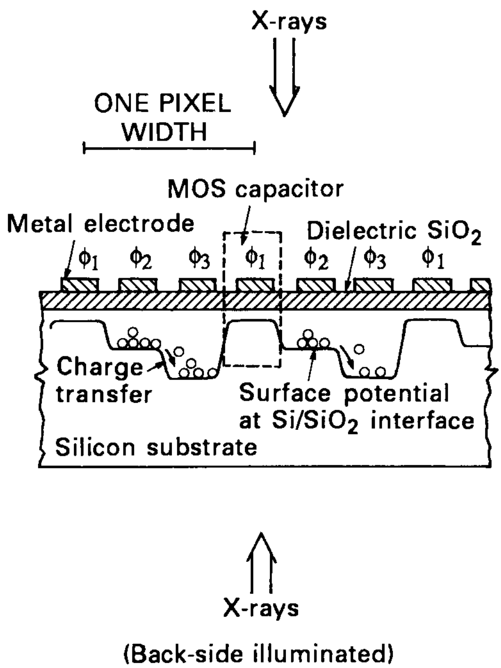

$$(\Delta E)_{\mathrm{FWHM}} = 2.35[(\eta\sigma)^2 + (\eta i_{\mathrm{d}} t)^2 + \eta F E]^{1/2} \quad \mathrm{keV},$$

where

i_{d} = dark current (electrons s^{-1}),
σ = rms readout noise (electrons),

η = mean energy required to produce one electron-hole pair (0.0036 keV for silicon),
t = integration time (s),
F = Fano factor ($\sim$ 0.15),
E = energy of incident photon (keV).

Expected quantum efficiency (defined as the probablity that an incident X-ray photon is detected as an 'event') vs. energy. The calculations consider only the interactions of X-rays in Si, for two hypothetical CCD's whose dead-layer and substrate thicknesses are separately within the range spanned by real devices. There will be a low energy cutoff (not shown) depending on the minimum signal which can be discriminated against the system noise.

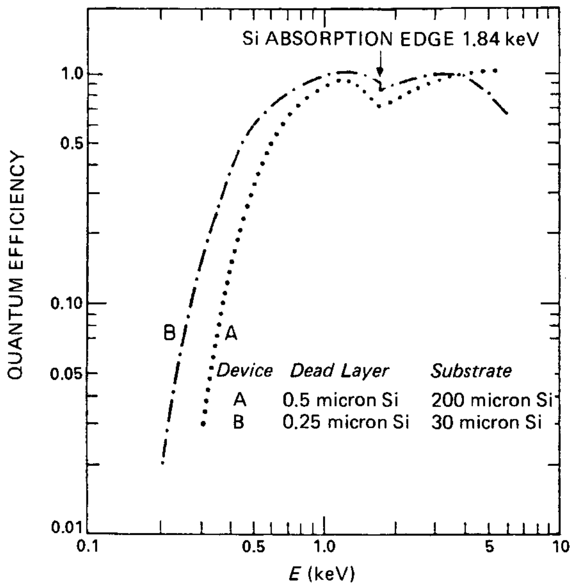

Microchannel plate detector

Typical performance

Spatial resolution:

20–30 μm (FWHM).

Quantum efficiency:

25% at 1.5 keV (CsI photocathode).

Format:

25–100 mm in diameter.

Schematic diagram of a microchannel plate detector. (Adapted from Behr, A. in Landolt-Bornstein, subvol. 2a, Springer-Verlag, 1981.)

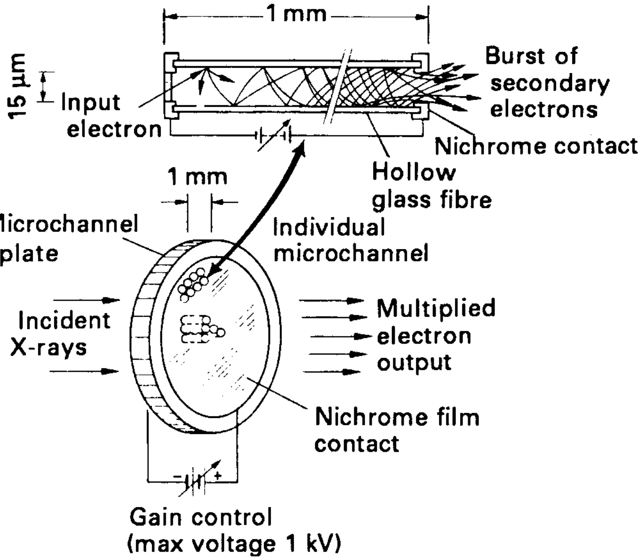

Properties of common X-ray detectors

Detector	Energy range (keV)	$\Delta E/E^{(a)}$ at 5.9 keV (%)	Dead time/event (μs)	Maximum count rate (s^{-1})
Geiger counter	3–50	none	200	10^4
Gas ionization in current mode	0.2–50	n/a	n/a	10^{11} [b]
Gas proportional	0.2–50	15	0.2	10^5
Multiwire proportional chamber	3–50	20	0.2	10^5/anode wire
Scintillation [NaI(Tl)]	3–10 000	40	0.25	10^6
Semiconductor [Si(Li)]	1–60	3.0	4–30	5×10^4
Semiconductor (Ge)	1–10 000	3.0	4–40	5×10^4

[a] FWHM.

[b] Maximum count rate density is limited by space-charge effects to around 10^{11} photons s^{-1} cm^{-3}.

(From Thompson, A.C. in *X-ray Data Booklet*, Lawrence Berkely Laboratory, University of California, 1986.)

Properties of intrinsic silicon and germanium

	Si	Ge
Atomic number	14	32
Atomic weight	28.09	72.60
Stable isotope mass numbers	28-29-30	70-72-73-74-76
Density (300 K); $g\,cm^{-3}$	2.33	5.32
Atoms cm^{-3}	4.96×10^{22}	4.41×10^{22}
Dielectric constant	12	16
Forbidden energy gap (300 K); eV	1.115	0.665
Forbidden energy gap (0 K); eV	1.165	0.746
Intrinsic carrier density (300 K); cm^{-3}	1.5×10^{10}	2.4×10^{13}
Intrinsic resistivity (300 K); $\Omega\cdot$ cm	2.3×10^{5}	47
Electron mobility (300 K); $cm^2\,V^{-1}\,s^{-1}$	1350	3900
Hole mobility (300 K); $cm^2\,V^{-1}\,s^{-1}$	480	1900
Electron mobility (77 K); $cm^2\,V^{-1}\,s^{-1}$	2.1×10^{4}	3.6×10^{4}
Hole mobility (77 K); $cm^2\,V^{-1}\,s^{-1}$	1.1×10^{4}	4.2×10^{4}
Energy per electron-hole pair (300 K); eV	3.62	
Energy per electron-hole pair (77 K); eV	3.76	2.96
Fano factor (77 K)	0.085–0.16	0.057–0.129
Best gamma-ray energy resolution (77 K) (FWHM)	–	420 eV at 100 keV 920 eV at 661 keV 1300 eV at 1330 keV

(Adapted from Knoll, G.F., *Radiation Detection and Measurement*, John Wiley & Sons, 1989.)

Properties of scintillation and solid-state detector materials

Material	Density (g cm^{-3})	Band gap (eV)	λ of max. emission (Å)	Decay time$^{(a)}$ (μs)	Index of refraction$^{(b)}$	Energy$^{(c)}$ (eV)	K-edge (keV)	Scintillation conversion$^{(d)}$ efficiency (%)	Notes
SCINTILLATORS									
NaI(Tl)	3.67	5.38	4100	0.23	1.85	–	1.07, 33.2	100	Hygroscopic
CaF_2 (Eu)	3.18	–	4350	0.94	1.47	–	0.68, 4.04	50	Non-hygroscopic
CsI(Na)	4.51	5.67	4200	0.63	1.84	–	33.2, 36.0	80	Hygroscopic
CsI(Tl)	4.51	5.67	5650	1.0	1.80	–	33.2, 36.0	45	Non-hygroscopic
Plastics	1.06	–	3500–4500	0.002–0.020	Varies	–	0.284	20–30	Non-hygroscopic
Liquids	0.86	–	3500–4500	0.002–0.008	Varies	–	0.284	20–30	Non-hygroscopic
SOLID-STATE									
Si(Li)	2.35	1.21	–	–	–	3.6	1.84	–	LN_2 required during operation
Ge(Li)	5.36	0.785	–	–	–	2.9	11.1	–	LN_2 required during operation
CdTe	5.85	1.44	–	–	–	4.43	26.7, 31.8	–	LN_2 required during operation
CdZnTe (CZT)	5.81	1.6	–	–	–	4.6	26.7, 9.7, 31.8	–	LN_2 required during operation

$^{(a)}$Room temperature, exponential decay constant.
$^{(b)}$At emission maximum.
$^{(c)}$Per electron-hole pair.
$^{(d)}$Referred to NaI(Tl) with S-11 photocathode.
(Adapted from *Harshaw Scintillation Phosphors*, The Harshaw Chemical Company.)

Properties of materials used in X-ray detector systems

	Atomic number, Z	Density (STP) (g cm^{-3})	Shell energy[a] (keV)	X-ray lines[b] (keV)	Fluorescence yield[c]	Energy at which photoelectric equals Compton cross-section (keV)
PROPORTIONAL COUNTER GASES						
Methane (CH_4)	6	0.713×10^{-3}	0.284	0.277		20
Ne	10	0.901×10^{-3}	0.867	0.849, 0.858	0.01	38
Ar	18	1.78×10^{-3}	3.203	2.96	0.105	72
			(0.285,0.246, 0.244)			
Kr	36	3.74×10^{-3}	14.32	12.64, 14.12	0.625	170
			(1.92, 1.73, 1.67)		(0.04)	
Xe	54	5.85×10^{-3}	34.56	29.67, 33.78	0.875	300
			(5.46, 5.10, 4.78)	(4.10, 4.49, 5.30)	(0.14)	
CRYSTALS						
NaI	53	3.61	33.16	28.47, 32.30	0.865	260
			(5.19, 4.86, 4.56)	(3.93, 4.22, 4.80)	(0.13)	
CsI	55	4.54	35.97	30.81, 34.99	0.885	300
				(4.28, 4.62, 5.28)	(0.15)	
Si	14	2.33	1.84	1.74, 1.83	0.04	53
Ge	32	5.36	11.10	9.88, 10.98	0.49	145
			(1.42, 1.41, 1.21	(1.19, 1.22)	(0.01)	

Properties of materials used in X-ray detector system (cont.)

	Atomic number, Z	Density (STP) (g cm^{-3})	Shell energy[a] (keV)	X-ray lines[b] (keV)	Fluorescence yield[c]	Energy at which photoelectric equals Compton cross-section (keV)
WINDOWS, FILTERS						
Be	4	1.82	0.111	0.109		14
Mylar	8	1.4	0.532	0.525		
$(C_{10}H_8O_4)n$	6		0.284	0.277		
Formvar	8	1.2[d]	0.532	0.525		
$(C_5H_7O_2)n$	6		0.284	0.277		
Polypropylene						
$(CH_2)n$	6	0.95[d]	0.284	0.277		22
Air (1.3% Ar,	18	1.29×10^{-3}	3.20	2.96	0.105	27
23.2% O,	8		0.532	0.525		
75.5% N)	7		0.400	0.392		
Mg	12	1.74	1.30	1.25, 1.30	0.02	46
Al	13	2.7	1.56	1.49, 1.55	0.03	50
Fe	26	7.87	7.11	6.40, 7.06	0.31	135
			(0.849, 0.722, 0.709)			
Ni	28	8.9	8.33	7.47, 8.27	0.38	140
			(1.01, 0.877, 0.858)			
Cu	29	8.96	8.99	8.04, 8.91	0.40	145
			(1.10, 0.954, 0.935)			

[a] The first line is the K-shell energy. The three L-shell energies are listed in the parentheses.

[b] The first line for each material gives $K\alpha$ and $K\beta$ energies. $L\alpha$, $L\beta$ and $L\gamma$ are listed in the parentheses.

[c] The first line is the K fluorescence yield. The L fluorescence yield is listed in the parentheses. If the fluorescence yield is less than 1% the space is left blank.

[d] Variable depending on the detailed preparation of a batch of film.

Quantum calorimeter

Schematic diagram of a quantum calorimeter or microcalorimeter. (Courtesy of Brian Ramsey, Marshall Space Flight Center)

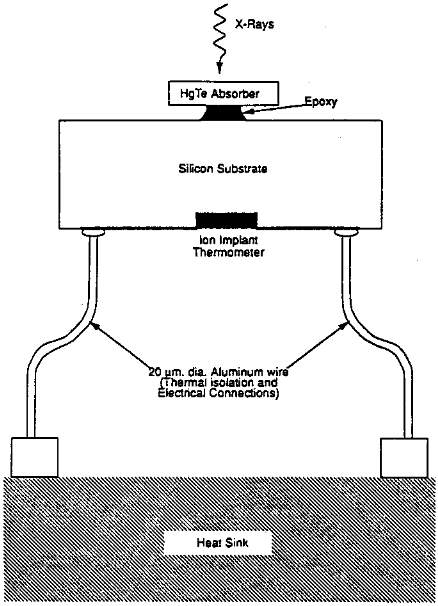

The energy resolution of a quantum calorimeter is limited by fluctuations in its thermal energy content:

$$\Delta = 2.35\sqrt{kT^2C} \quad \text{(FWHM)}$$

where k is Boltzmann's constant, T is the heat sink temperature, and C is the heat capacity of the detector. In principle, energy resolution as good as 1 eV (FWHM) is possible.

Schematic diagram of a biasing circuit for a semiconductor thermistor, a resistive thermometer extensively used in quantum calorimeters.

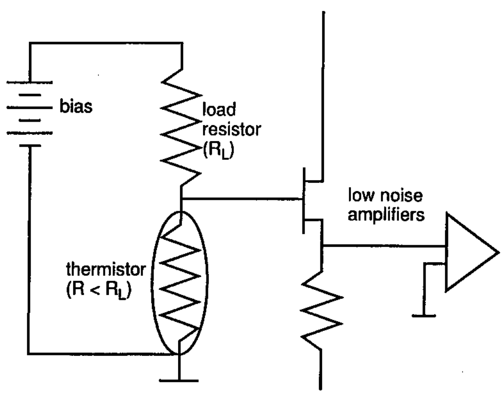

Compton telescope for high energy gamma-rays

a) Configuration of a Compton telescope which relies on the detection of scattered photons: S, scatterer; C, collector; A_1, A_2, anticoincidence detectors. b) Basic configuration of a Compton telescope which relies on the detection of secondary electrons. (Adapted from Hillier, R., *Gamma Ray Astronomy*, Clarendon Press, 1984.)

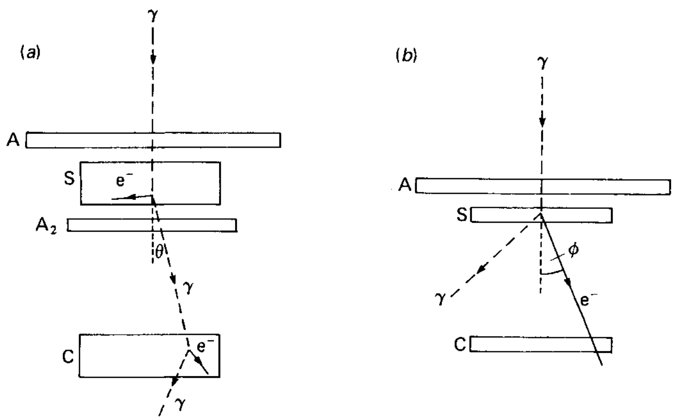

Spark chamber telescope for high energy gamma rays

Diagram showing the basic design of a spark chamber with plates (S), anticoincidence shield (A), and triggering detectors (C_1 and C_2). (Adapted from Hillier, R., *Gamma Ray Astronomy*, Clarendon Press, 1984.)

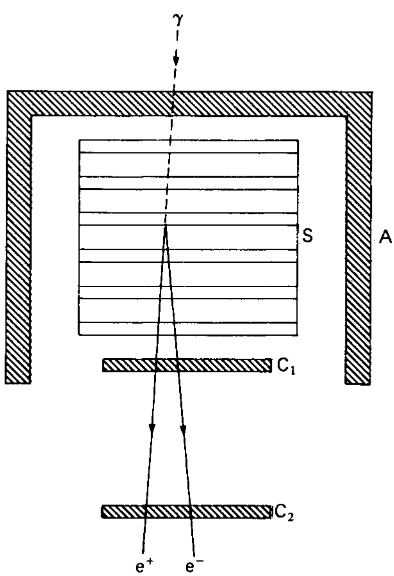

Level of activity for common materials

Level of activity for common materials used in the construction of detector systems.

Material	Disintegrations/min per gram of Material		
	^{232}Th(583 keV)	^{238}U	^{40}K
Aluminium (6061 from Harshaw)	0.42	0.04	$<$ 0.05
Aluminium (1100 from Harshaw)	0.24	$<$ 0.017	$<$ 0.06
Aluminium (1100 from ALCOA)	0.08	$<$ 0.026	$<$ 0.11
Aluminium (3003 from ALCOA)	0.10	$<$ 0.026	0.56
Stainless steel (304)	$<$ 0.006	$<$ 0.007	$<$ 0.06
Stainless steel (304-L)	$<$ 0.005	$<$ 0.005	$<$ 0.02
Magnesium (rod)	0.06	$<$ 0.04	0.1
Magnesium (ingot)	$<$ 0.01	$<$ 0.002	$<$ 0.02
Magnesium (4 in. × 4 in. from Dow)	$<$ 0.005	$<$ 0.002	$<$ 0.02
Magnesium (from PGT)	$<$ 0.05	$<$ 0.03	$<$ 0.05
Beryllium copper alloy	$<$ 0.02	$<$ 0.06	$<$ 0.2
Copper (sheet)	$<$ 0.05	$<$ 0.06	$<$ 0.2
Pyrex window	0.45	0.27	3.8
Quartz window	$<$ 0.018	$<$ 0.018	$<$ 0.07
Molecular sieve	4.4	3.0	9.0
Neoprene	$<$ 0.008	$<$ 0.01	$<$ 0.36
Rubber	0.12	1.0	2.0
Apiezon Q	4.5	4.5	2.7
Electrical tape–3M	$<$ 0.04	$<$ 0.06	$<$ 0.1
Cement (Portland)	0.25	1.3	4.5
Epoxy	0.006	0.01	0.19
Lacquer	0.002	0.005	0.04

(From Camp, *et al.*, Nuc. Inst. Meth., 117, 189, 1974.)

Properties of coaxial cables

	Insulating Material	Cable Diameter (cm)	Characteristic Impedance (ohms)	Signal[a] Propagation	HV Rating	Cable Capacitance (pF/m)	Signal Attenuation per Meter[b]	
							MHz	dB
RG-8/U	Polyethylene	1.03	52	0.659	5000	96.8	100	0.066
							400	0.154
RG-11/U	Polyethylene	1.03	75	0.659	5000	67.3	100	0.066
							400	0.138
RG-58/U	Polyethylene	0.50	53.5	0.659	1900	93.5	100	0.135
							400	0.312
RG-58C/U	Polyethylene	0.50	50	0.659	1900	100.1	100	0.174
							400	0.413
RG-59/U	Polyethylene	0.61	73	0.659	2300	68.9	100	0.112
							400	0.233
RG-62/U	Semisolid polyethylene	0.61	93	0.840	750	44.3	100	0.102
							400	0.207
RG-174/U	Polyethylene	0.25	50	0.659	1500	101.0	100	0.289
							400	0.656
RG-178/U	TFE teflon	0.18	50	0.694	1500	95.1	400	0.951
DOUBLE SHIELDED COAXIAL CABLES								
RG-9/U	Polyethylene	1.07	51	0.659	5000	98.4	100	0.062
							400	0.135
RG-223/U	Polyethylene	0.52	50	0.659	1900	101.0	100	0.157
							400	0.328

[a]Fraction of speed of light in a vacuum (3.00×10^8 m s^{-1})

[b]The ratio of two signals, in decibels, is $dB = 20 \log_{10}(A_2/A_1)$, where A_1 and A_2 are the two signal amplitudes.

(From *The Art of Electronics*, Horowitz, P. and Hill, W., Cambridge University Press, 1980, with permission.)

Resistor color code

Resistance values are coded by 4 colored bands around the resistor as shown below

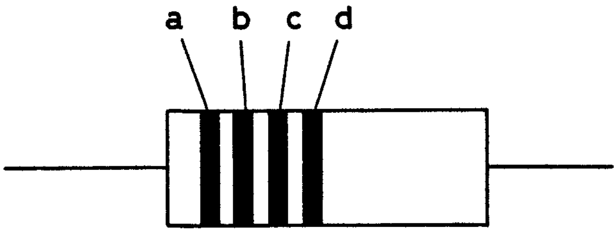

The value of the resistance is then

$$R = ab \times 10^c \pm d,$$

where the colors have the following number values:

0	Black
1	Brown
2	Red
3	Orange
4	Yellow
5	Green
6	Blue
7	Violet
8	Gray
9	White
5%	Gold
10%	Silver
20%	No band

If the resistor has the band colors

a	green
b	orange
c	orange
d	gold

then the resistance is $R = 53 \times 10^3\ \Omega$ with a tolerance of 5%

(From *Techniques for Nuclear and Particle Physics Experiments*, Leo, W.R., Springer-Verlag, 1987, with permission.)

Bibliography

Building Scientific Apparatus, Moore, J.H., Davis, C.C., and Coplan, M.A., Addison-Wesley Publishing Company, Inc.

Electro-Optics Handbook, RCA Corporation, 1974.

Handbook of Chemistry and Physics, CRC Press, 1995.

Handbook of Vacuum Science and Technology, Hoffinan, D.M., Singh, B., Thomas, J.H. 111, Academic Press, 1998.

Matter and Methods at Law Temperatures, Pobell, F., Springer, 1996.

Measurement and Detection of radiation, Tsoulfanidis, N., Hemisphere Publishing Corporation, 1983.

Optical System Design, Kingslake, R., Academic Press, 1983.

Radiation Detection and Measurement, Knoll, G.F., John Wiley & Sons, 1989.

Scientific Foundations of Vacuum Techniques, Dushnivi, S., John Wiley & Sons, 1949.

Table of Isotopes, Lederer, C.M. & Shirley, V.S., eds., John Wiley and Sons,1978.

Techniques for Nuclear antiparticle Physics Experiments, Leo, W.R., Springer-Verlag, 1992.

Techniques of Vacuum Ultraviolet Spectroscopy, Samson, J. A. R., John Wiley and Sons, 1967.

The 1998 Review of Particle Physics, Caso, C., et al., Euro. Phys. Jour., **C3**, 1, 1998.

The Art of Electronics, Horowitz, P. and Hill, W., Cambridge University Press, 1980.

The Atomic Nucleus, Evans, R. B., McGraw-Hill Book Company, 1955. Vacuum Technology, Roth, A., Elsevier Science Publishers, 1990.

Vacuum Technology and Space Simulation, NASA SP- 1 05, US Government Printing Office, 1966.

X-ray Detectors in Astronomy, Fraser, G., Cambridge University Press, 1989.

X-ray interactions: photoabsorption, scattering, transmission, and reflection at E = 50–30000 eV, Z = 1-92, Henke, B.L., Guilikson, E.M, and Davis, J.C., Atomic Data and Nuclear Data Tables, **54**, 181-342, 1993.

X-ray Science and Technology, Mehette, A.G., Buckley, C.J., eds., Institute of Physics Publishing, 1993.

X-*ray Wavelengths*, Bearden, J. A., Rev. Mod. Phys., **39**, 78, 1967.

Note: Links to WWW resources which supplement the material in this chapter can be found at:

http://www.astrohandbook.com

Chapter 15

Astronautics

Having probes in space was like having a cataract removed. - Hannes Alfvén

Satellite orbits

The position and velocity of an orbiting satellite can be calculated from six quantities, the orbital elements:

Orbit **inclination**, i, the angle between the orbit plane and the equatorial plane of the Earth.

Right ascension of the ascending node, Ω, the angle between vernal equinox and the point where the orbit crosses the equatorial plane (going north)

Argument of perigee, ω, the angle between the ascending node and the orbit's point of closest approach to the Earth (perigee)

Semi-major axis, a, of the orbital ellipse

True anomaly, v, the angle between perigee and the satellite (in the orbit plane)

Orbit **eccentricity**, e, ($e = (a^2 - b^2)^{1/2}/a$, where b is the semi-minor axis of the orbital ellipse)

The elements above are specified for a given reference time or *epoch.*

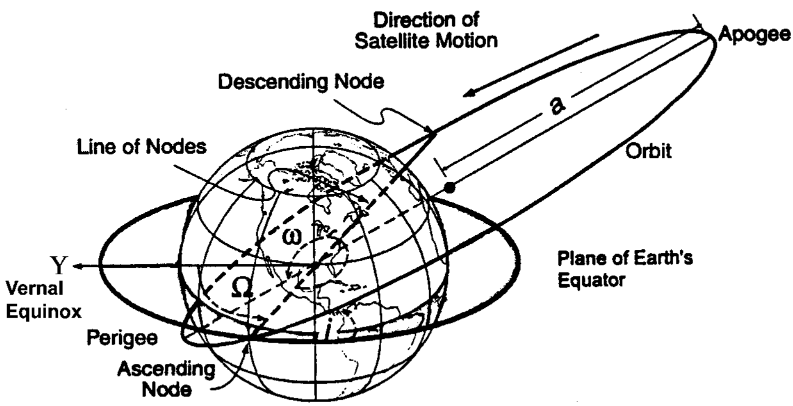

Υ marks the direction of the Vernal Equinox. Ω is measured in the plane of the Earth's equator, and ω is measured in the orbit plane.

(Diagram courtesy of J.R. Wertz, Microcosm, Inc.)

Often the mean anomaly M is given instead of the true anomaly. The mean anomaly is 360(t/P) deg, where P is the period of the orbit and t is the time since perigee passage of the satellite. $M = v$ for a circular orbit. If the mean anomaly is given, the true anomaly must be calculated. An intermediate variable, the eccentric anomaly, E, is introduced. E and M are related by Kepler's equation:

$M = E - e \sin E$, which can be solved using Newton's false root method.

E is related to v by Gauss' equation:

$$\tan(v/2) = [(1 + e)/(1 - e)]^{1/2} \tan(E/2)$$

The orbit period is given by

$P = 2\pi a^{\frac{3}{2}}/(GM_E)^{\frac{1}{2}} = 1.6585\times10^{-4} a(\mathrm{km})^{\frac{3}{2}}$ min (Kepler's Third Law),

where

G $= 6.670 \times 10^{-11}$ N m^2 kg^{-2}, the gravitational constant

M_E $= 5.977 \times 10^{24}$ kg, the mass of the Earth

a $= RE + (h_P + h_A)/2$, where R_E is the Earth's radius (6378 km) and h_P and h_A are the satellite's perigee height and apogee height, respectively.

Perturbations by the Earth's gravitational field cause the right ascension of the ascending node and the argument of perigee to vary with time:

$$\frac{\Delta\Omega}{\text{day}} = -\frac{9.^\circ 964}{(a/R_\mathrm{e})^{7/2}(1 - e^2)^2} \cos i,$$

where R_e is the equatorial radius of the Earth (6378 km)

$$\frac{\Delta\omega}{\text{day}} = \frac{4.^\circ 982}{(a/R_\mathrm{e})^{7/2}(1 - e^2)^2} (5\cos^2 i - 1).$$

Earth satellite parameters

Altitude (km)	Period* (min)	Velocity* (km/s)	Angular Velocity* (deg/min)	Maximum Eclipse** (min)
0	84.49	7.905	4.261	42.2
100	86.48	7.844	4.163	38.4
150	87.49	7.814	4.115	37.8
200	88.49	7.784	4.068	37.3
250	89.50	7.755	4.022	36.9
300	90.52	7.726	3.977	36.6
350	91.54	7.697	3.933	36.3
400	92.56	7.669	3.889	36.1
450	93.59	7.640	3.847	35.9
500	94.62	7.613	3.805	35.8
600	96.69	7.558	3.723	35.5
700	98.77	7.504	3.645	35.3
800	100.87	7.452	3.569	35.1
900	102.99	7.400	3.496	35.0
1,000	105.12	7.350	3.425	34.9
1,500	115.98	7.113	3.104	34.8
2,000	127.20	6.898	2.830	35.0
2,500	138.75	6.701	2.595	35.4
3,000	150.64	6.519	2.390	35.9
3,500	162.84	6.352	2.211	36.4
4,000	175.36	6.197	2.053	36.9
4,500	188.19	6.053	1.913	37.5
5,000	201.31	5.919	1.788	38.1
6,000	228.42	5.675	1.576	39.4
7,000	256.66	5.458	1.403	40.6
8,000	285.97	5.265	1.259	41.8
9,000	316.31	5.091	1.138	43.1
10,000	347.66	4.933	1.035	44.3
15,000	518.46	4.318	0.694	50.0
20,000	710.60	3.887	0.507	55.2
25,000	921.94	3.564	0.390	60.1
30,000	1150.85	3.310	0.313	64.6
35,786	1,436.07	3.075	0.251	69.4

*For circular orbit

**Longest eclipse for circular orbit. Eclipse in eccentric orbits can be longer.

(Adapted from Wertz, J.R. and Larson, W.J., eds., *Space Mission Analysis and Design,* Kluwer Academic Publishers, 1991.)

Perturbations of a satellite orbit

Order of magnitude perturbations of a satellite orbit. The acceleration due to gravitational forces is independent of the satellite's mass and area; drag and other surfaces forces (e.g. radiation pressure) are not. The area-mass ratio assumed for non-gravitational forces is 0.01 m^2 kg^{-1}.

(Adapted from *Satellite Orbits,* Montenbruck, O. and Gill, E., Springer, 2000.)

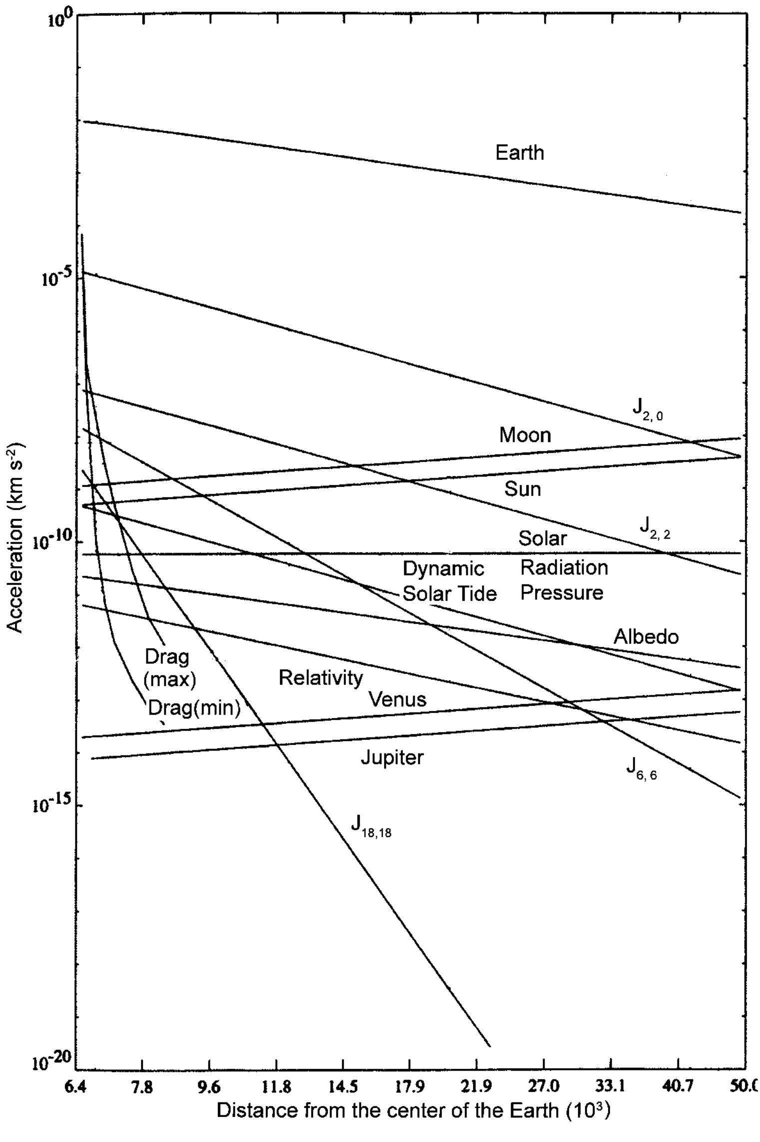

Satellite drag pressure as a function of altitude and temperature

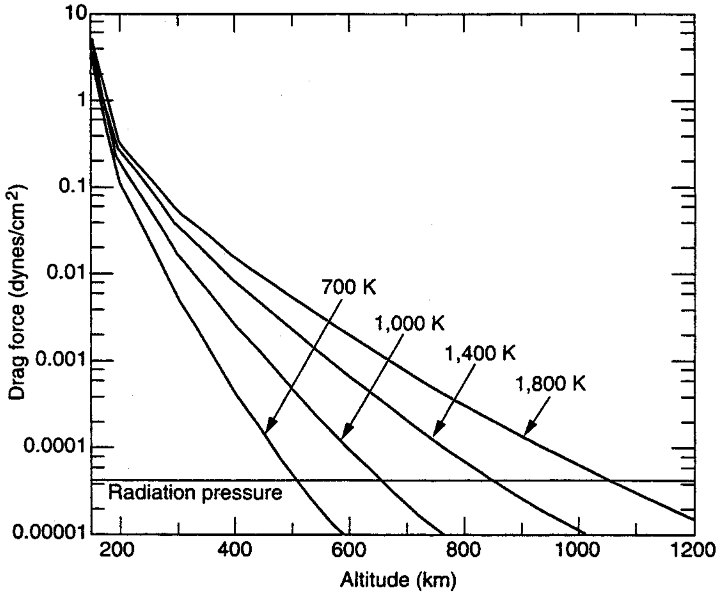

A temperature of 700 K corresponds to quiet solar conditions and 1700 K to active solar conditions.

(From the Italian Aerospace Research Center, CIRA, 1972)

Approximate lifetimes for Earth satellites

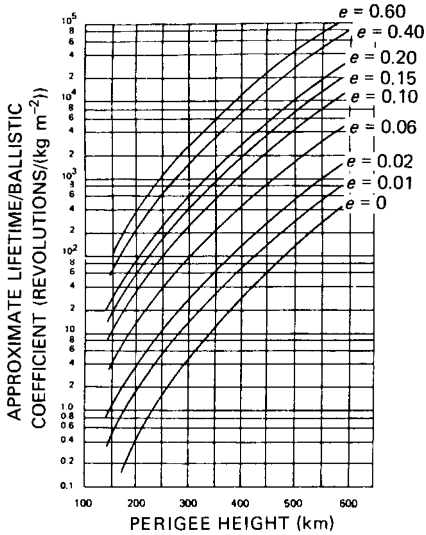

$$\text{Lifetime} = NP = N\left[\frac{4\pi^2}{GM_\mathrm{E}}\left(\frac{h_\mathrm{P}+R_\mathrm{E}}{1-e}\right)^3\right]^{1/2},$$

where

N = number of orbit revolutions in the satellite lifetime from the above diagram.

Ballistic coefficient $= m/(C_\mathrm{D}A)$ (typically, $25 - 100$ kg m^{-2}),
m = mass of the satellite,
C_D = the drag coefficient ($\approx 1 - 2$),
A = satellite cross-sectional area perpendicular to the velocity vector,

G = gravitational constant,

h_p = perigee height,

e = eccentricity of the orbit,

P = satellite period,

M_E = mass of the Earth,

R_E = radius of the Earth.

$$\text{Lifetime (d)} \approx 1.15\times 10^{-7}\times N\times\left(\frac{6378.14+h_\mathrm{p}(\mathrm{km})}{1-e}\right)^{3/2}.$$

Satellite period (hr) $= 1.41(a/R_\mathrm{E})^{3/2}$,
where a = semi-major axis.

(Adapted from Wertz, J., ed., *Spacecraft Attitude Determination and Control*, D. Reidel Publ. Co., 1980.)

Lagrange (libration) points

In the circular restricted three body problem—two co-orbiting bodies with nearly circular orbits of masses m_1 and m_2 (with $m_1 > m_2$) and a third small body having the same period of revolution as the other two - there are five points where the gravitational forces of the two large bodies exactly balance the "centrifugal force" "felt" by the small body. These are known as Lagrange or libration points. Two of these points, L_4 and L_5 form equilateral triangles with the primary masses. The other three points (L_1, L_2, L_3) are colinear with the primary masses. L_4 and L_5 are stable. L_1, L_2 and L_3 are unstable. There are, however, orbits (halo orbits) around the latter three points in planes skew to the plane of the orbit of the two major bodies which are almost stable, requiring only small occasional corrections.

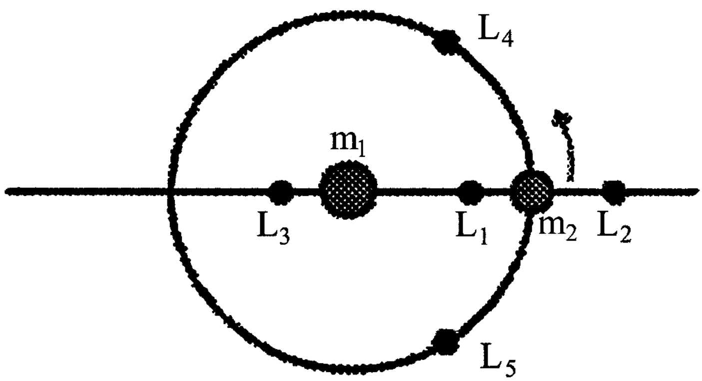

Assuming that $m_1 >> m_2$, setting the origin of a rectangular coordinate system at the center of m_1 and the $+x$-axis in the direction of m_2, with $\alpha = m_2/m_1$, approximate solutions to the first three Lagrange points can be found:

$L1 : (R[1 - (\alpha/3)^{1/3}], 0),$

$L2 : (R[1 + (\alpha/3)^{1/3}], 0),$

$L3 : (-R[1 + 5\alpha/12], 0),$

where R is the distance between $m_1 + m_2$.

For the Earth-Sun system $\alpha \approx 3 \times 10^{-6}$, $R = 1$ AU $\approx 1.5 \times 10^8$ km, and the first and second Lagrange points are located approximately 1.5×10^6 kilometers from the Earth, $L2$ occurring on the "night" side of the Earth. $L3$ orbits the Sun just a fraction further out than the Earth and is not visible from the Earth.

The fourth and fifth Lagrange points (stable if $m_1/m_2 > 25$) have coordinates

$L4 : (R/2[(m_1 - m_2)/(m_1 + m_2)], R\sqrt{3}/2),$

$L4 : (R/2[(m_1 - m_2)/(m_1 + m_2)], -R\sqrt{3}/2).$

Space transportation system (Space Shuttle)

Orbiter coordinate system and cargo bay envelope. The dynamic clearance allowed between the vehicle and the payload at each end is also illustrated.

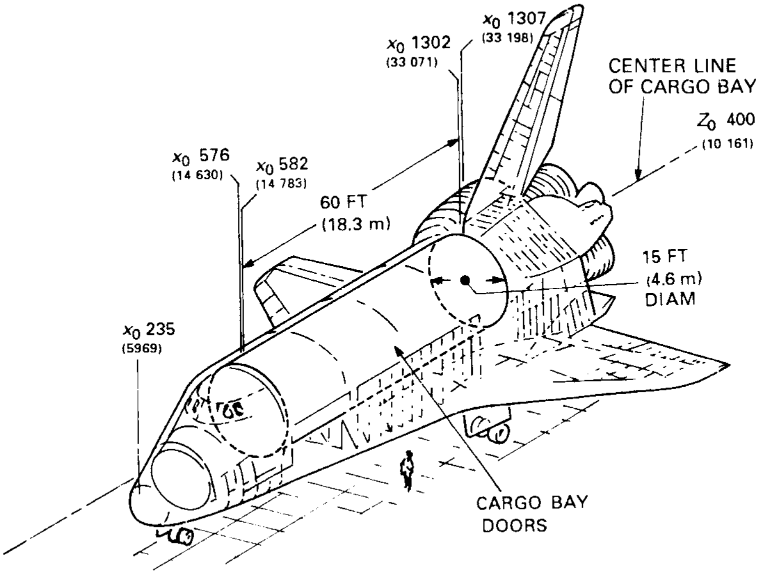

Principal Orbiter interfaces with payloads.

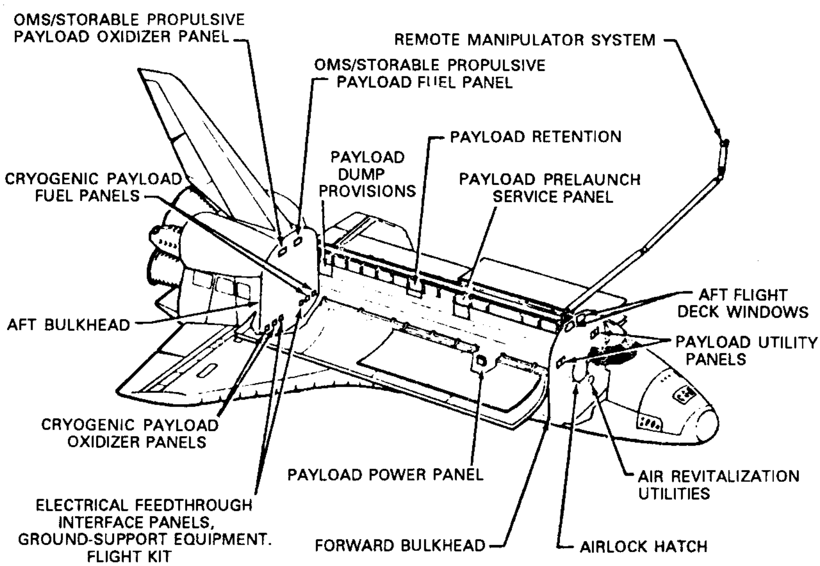

Shuttle performance capability

Launch azimuth and inclination limits from KSC in Florida. The inset globe illustrates the extent of coverage possible when launches are made from KSC.

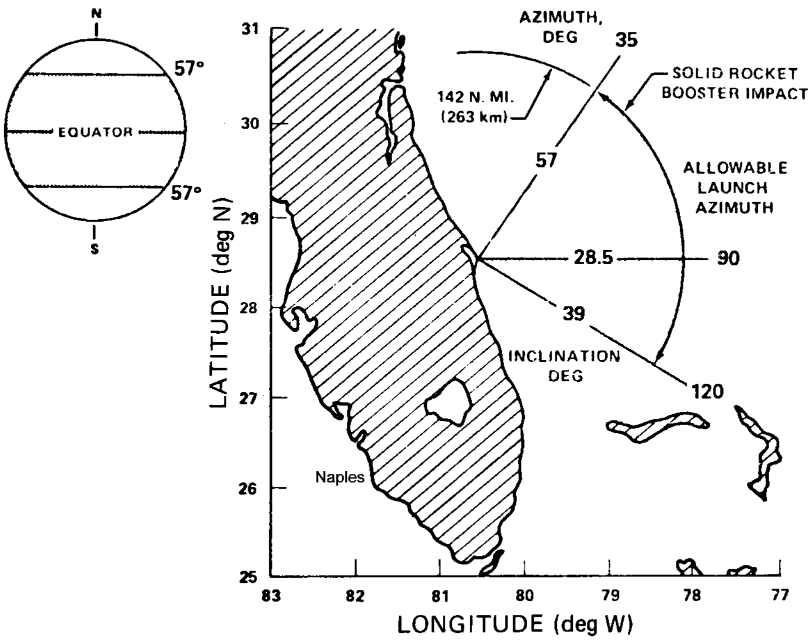

Cargo capability for a KSC (28.45 degree inclination) launch.

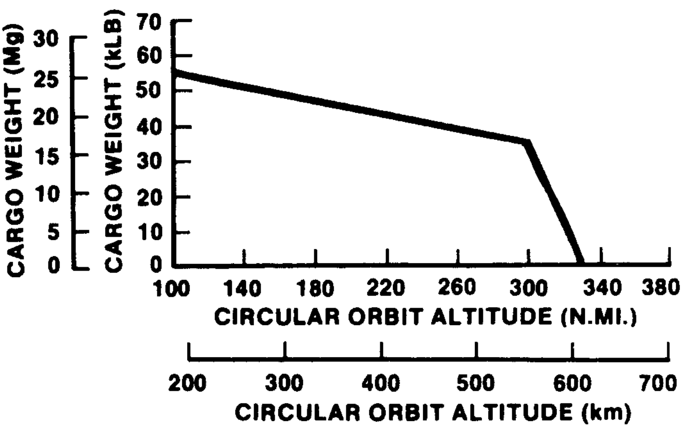

Space Launch Sites

Country	Launch Site	Latitude	Longitude
Australia	Woomera	31.1° S	136.8° E
Brazil	Alcantara Launch Center	2.3° S	44.4° W
Canada	Fort Churchill, Manitoba	58.759°	265.912° E
China	Jiuquan Space Launch Center–Shuang Cheng Tzu	40.6° N	99.9° E
China	Xichang Space Launch Center	28.25° N	102.0° E
China	Taiyuan Space Launch Center–Wuzhai	37.5° N	112.6° E
Europe	Kourou, French Guiana	5.2° N	52.8° W
France	Hammaguir, Algeria	31.0° N	8.0° W
France	Kourou, French Guiana	5.2° N	52.8° W
India	Sriharikota Island	13.9° N	80.4° E
Iraq	Al-Anbar	33.5° N	43.0° E
Israel	Palmachim Air Base in the Negev Desert	31.5° N	34.5° E
Italy	San Marco Range off the Kenya coast	2.9° S	40.3° E
Japan	Kagoshiuma on Kyushu Island	31.2° N	131.1° E
Japan	Tanegashima Island	30.4° N	131.0° E
Pakistan	SUPARCO	40.5° N	3.5° W
Russia	Kapustin Yar Cosmodrome – Volgograd Station	48.4° N	45.8° E
Russia	Baikonur Cosmodrome – Tyuratam	45.6° N	63.4° E
Russia	Plesetsk Cosmodrome	62.8° N	40.1° E
Russia	Svobodny Cosmodrome	51.4° N	128.3° E
South Africa	South of Cape Town	33.56° S	18.29° E
United Kingdom	Woomera	31.1° S	136.8° E
United States	Cape Canaveral Air Station, Florida	28.5° N	81.0° W
United States	Kennedy Space Center, Merrit Island, Florida	28.5° N	81.0° W
United States	Wallops Island, Virginia	37.8° N	75.5° W
United States	Vandenberg Air Force Base, California	34.4° N	120.35° W
United States	Poker Flat Research Range, Alaska	65.1° N	147.4° W
United States	Alaska Spaceport	57.5° N	153° W
United States	White Sands Space Harbor, Las Cruces, New Mexico		

(Adapted from *Space Today,* 2000.)

Deep Space Network facilities (DSN)

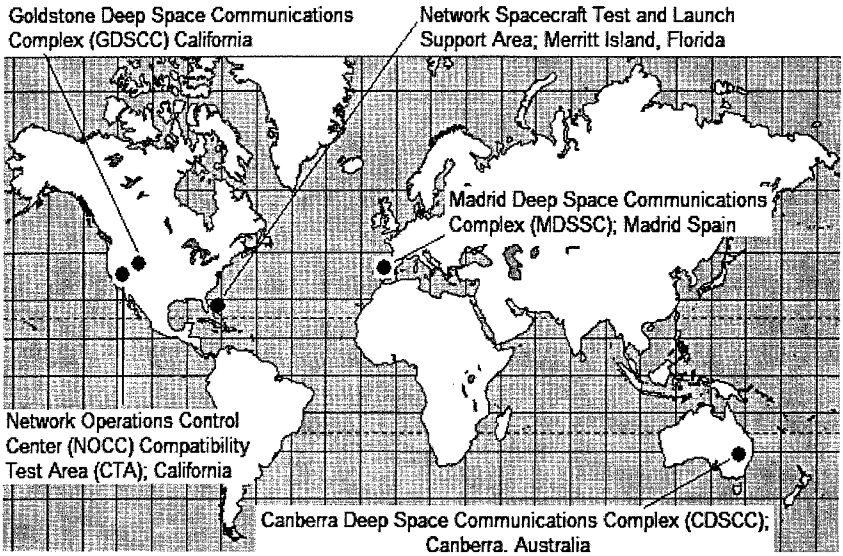

Spacecraft Tracking and Data Network facilities (STDN)

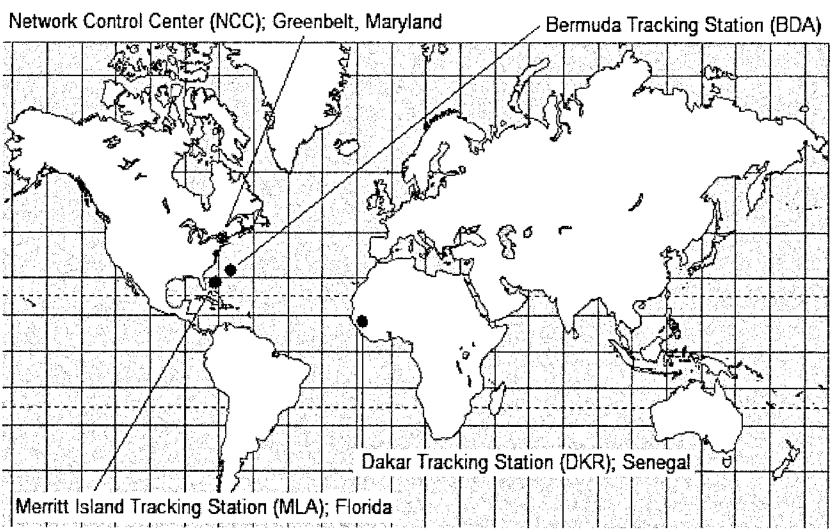

Aeronautics, balloons, and sounding rocket facilities

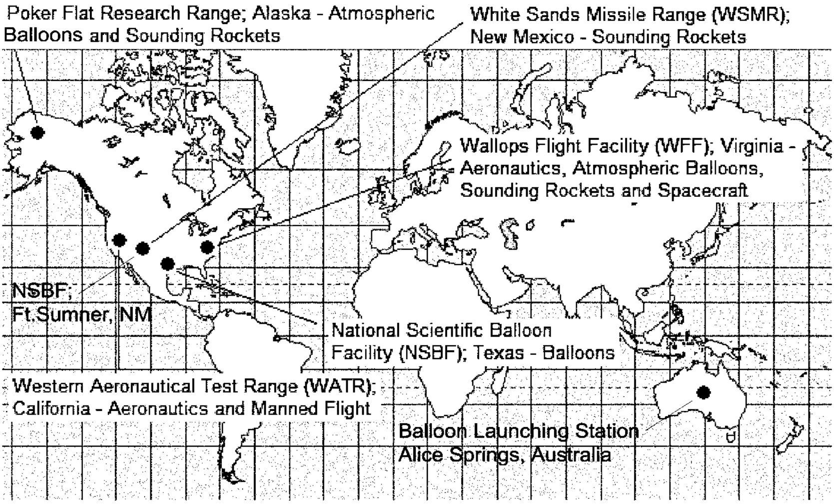

Astrodynamical constants

Quantity	Value	Remarks
Time		
MJD (J2000)	51544.5	Modified Julian Date, 2000 January 1, 12^{h}
TT – TAI	32.184 s	Terrestrial Time – International Atomic Time
GPS – TAI	−19 s	Global Positioning System Time –International Atomic Time
Universal		
c	299 792 458 m s^{-1}	Speed of light in a vacuum
G	6.673×10^{-20} km^3 kg^{-1} s^{-2}	Gravitational constant
Earth		
GM	398 600.4415 km^3 s^{-2}	Gravitational coefficient
J_2	0.00108263	Geopotential coefficient
R	6378.137 km	Equatorial radius
f	1/298.257223563	Flattening factor
ω	0.7292115×10^{-4} rad s^{-1}	Mean angular velocity
Sun		
GM	$1.32712440018 \times 10^{11}$ km^3 s^{-2}	Gravitational coefficient
AU	149 597 870.691 km	Astronomical unit
R	6.955×10^5 km	Radius
P	4.560×10^{-6} N m^{-2}	Radiation pressure at 1 AU
ϕ	1367 W m^{-2}	Solar constant
Moon		
GM	4 902.801 km^3 s^{-2}	Gravitational coefficient
a	384 400 km	Mean distance from Earth
R	1738.2 km	Mean radius
Artificial Satellites		
r_{GEO}	42 164 km	Geosynchronous orbit radius
v_{GEO}	3.075 km s^{-1}	Geosynchronous orbit velocity
P_{GEO}	$23^h 56^m 04^s$	Geosynchronous orbit period
r_{GPS}	26 561 km	Global Positioning System orbit radius
v_{GPS}	3.874 km s^{-1}	Global Positioning System orbit velocity
P_{GPS}	$11^h 58^m 02^s$	Global Positioning System orbit period
r_{LEO}	6678 – 7878 km	Low Earth orbit radius
v_{LEO}	7.726 – 7.113 km s^{-1}	Low Earth orbit velocity

(Adapted from Montenbruck, O. and Gill, E., *Satellite Orbits*, Springer, 2000)

Bibliography

AIAA, Aerospace Design Engineers Guide, American Institute of Aeronautics and Astronautics, Inc., 1998.

Aerospace Source Book, Aviation Week & Space Technology, McGraw-Hill, 2000.

International Reference Guide to Space Launch Systems, Isakowitz, S.J., AIAA, 1995.

Spacecraft Systems Engineering, Fortescue, P. and Stark, J., eds., John Wiley and Sons, 1995.

Space Transportation System User Handbook, National Aeronautics and Space Administration.

Fundamentals of Space Systems, Pisacane, V.L. and Moore, R.C., eds., Oxford University Press, 1994.

Introduction to Space Dynamics, Thomson, W.T., Dover Publications, Inc., 1986.

Satellite Orbits—Models, Methods, Applications, Montenbruck, O., Gill, E., Springer, 2000.

Spacecraft Attitude Determination and Control, Wertz, J.R, ed, Kluwer Academic Publishers, 1978.

Space Mission Analysis and Design, Wertz, J.R. and Larson, W.J., eds., Kluwer Academic Publishers, 1991.

Note: Links to WWW resources which supplement the material in this chapter can be found at:

http://www.astrohandbook.com

Chapter 16

Mathematics

The physicist in preparing for his work needs three things, mathematics, mathematics, mathematics. - Wilhelm Konrad Roentgen

Coordinate transformations

Components of a vector, $\mathbf{r}$, in Cartesian (x, y, z), spherical (r, θ, ϕ), and cylindrical (ρ, ϕ, z) coordinates.

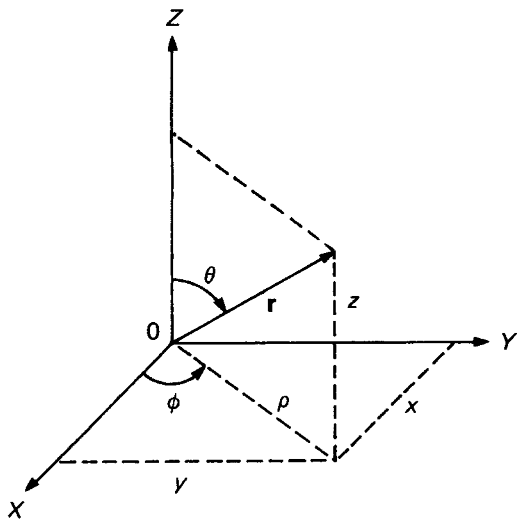

The following relationships exist between the Cartesian, Spherical, and Cylindrical systems:

$z = r\cos\theta$	$= z$	
$r = (x^2 + y^2 + z^2)^{1/2}$	$= (\rho^2 + z^2)^{1/2}$	
$\theta = \arccos\{z/(x^2 + y^2 + z^2)^{1/2}\}$	$= \arctan(\rho/z)$	$0 \leq \theta \leq \pi$
$\phi = \arctan(y/x)$	$= \phi$	$0 \leq \phi < 2\pi$
$\rho = (x^2 + y^2)^{1/2}$	$= r\sin\theta$	
$x = r\sin\theta\cos\phi$	$= \rho\cos\phi$	
$y = r\sin\theta\sin\phi$	$= \rho\sin\phi$	

Vector analysis

Vectors $\mathbf{a}$ and $\mathbf{b}$ defined in terms of the unit vectors $\mathbf{i}, \mathbf{j}, \mathbf{k}$ having the directions of the positive x, y, and z axes respectively:

$$\mathbf{a} = a_x\mathbf{i} + a_y\mathbf{j} + a_z\mathbf{k}$$

$$\mathbf{b} = b_x\mathbf{i} + b_y\mathbf{j} + b_z\mathbf{k}$$

The scalar product:

$$\mathbf{a} \cdot \mathbf{b} = a_x b_x + a_y b_y + a_z b_z$$

The vector product:

$$\mathbf{a} \times \mathbf{b} = (a_y b_z - a_z b_y)\mathbf{i} + (a_z b_x - a_x b_z)\mathbf{j} + (a_x b_y - a_y b_x)\mathbf{k}$$
$$= \begin{vmatrix} \mathbf{i} & \mathbf{j} & \mathbf{k} \\ a_x & a_y & a_z \\ b_x & b_y & b_z \end{vmatrix}.$$

Vector identities:

$$\mathbf{a} \cdot \mathbf{b} \times \mathbf{c} = (\mathbf{a} \times \mathbf{b}) \cdot \mathbf{c} = \mathbf{b} \cdot (\mathbf{c} \times \mathbf{a}) = (\mathbf{b} \times \mathbf{c}) \cdot \mathbf{a}$$
$$= \mathbf{c} \cdot (\mathbf{a} \times \mathbf{b}) = (\mathbf{c} \times \mathbf{a}) \cdot \mathbf{b},$$
$$\mathbf{a} \times (\mathbf{b} \times \mathbf{c}) = (\mathbf{a} \cdot \mathbf{c})\mathbf{b} - (\mathbf{b} \cdot \mathbf{a})\mathbf{c},$$
$$(\mathbf{a} \times \mathbf{b}) \cdot (\mathbf{c} \times \mathbf{d}) = (\mathbf{a} \cdot \mathbf{c})(\mathbf{b} \cdot \mathbf{d}) - (\mathbf{a} \cdot \mathbf{d})(\mathbf{b} \cdot \mathbf{c}),$$
$$(\mathbf{a} \times \mathbf{b}) \times (\mathbf{c} \times \mathbf{d}) = ((\mathbf{a} \times \mathbf{b}) \cdot \mathbf{d})\mathbf{c} - ((\mathbf{a} \times \mathbf{b}) \cdot \mathbf{c})\mathbf{d}.$$

Differentiation formulae:

$$\boldsymbol{\nabla} \cdot \phi\mathbf{u} = \phi\boldsymbol{\nabla} \cdot \mathbf{u} + \mathbf{u} \cdot \boldsymbol{\nabla}\phi,$$
$$\boldsymbol{\nabla} \times \phi\mathbf{u} = \phi\boldsymbol{\nabla} \times \mathbf{u} + \boldsymbol{\nabla}\phi \times \mathbf{u},$$
$$\boldsymbol{\nabla} \cdot (\mathbf{u} \times \mathbf{v}) = \mathbf{v} \cdot \boldsymbol{\nabla} \times \mathbf{u} - \mathbf{u} \cdot \boldsymbol{\nabla} \times \mathbf{v},$$
$$\boldsymbol{\nabla} \times (\mathbf{u} \times \mathbf{v}) = (\mathbf{v} \cdot \boldsymbol{\nabla})\mathbf{u} - (\mathbf{u} \cdot \boldsymbol{\nabla})\mathbf{v} + \mathbf{u}(\boldsymbol{\nabla} \cdot \mathbf{v}) - \mathbf{v}(\boldsymbol{\nabla} \cdot \mathbf{u}),$$
$$\boldsymbol{\nabla}(\mathbf{u} \cdot \mathbf{v}) = (\mathbf{u} \cdot \boldsymbol{\nabla})\mathbf{v} + (\mathbf{v} \cdot \boldsymbol{\nabla})\mathbf{u} + \mathbf{u} \times (\boldsymbol{\nabla} \times \mathbf{v}) + \mathbf{v} \times (\boldsymbol{\nabla} \times \mathbf{u}),$$
$$\boldsymbol{\nabla} \times (\boldsymbol{\nabla}\phi) = \text{curl grad } \phi = 0,$$
$$\boldsymbol{\nabla} \cdot (\boldsymbol{\nabla} \times \mathbf{u}) = \text{div curl } \mathbf{u} = 0,$$
$$\boldsymbol{\nabla} \times (\boldsymbol{\nabla} \times \mathbf{u}) = \text{curl curl } \mathbf{u} = \boldsymbol{\nabla}(\boldsymbol{\nabla} \cdot \mathbf{u}) - \boldsymbol{\nabla} \cdot \boldsymbol{\nabla}\mathbf{u}$$
$$= \text{grad div } \mathbf{u} - \nabla^2\mathbf{u}$$
$$\boldsymbol{\nabla} \cdot (\boldsymbol{\nabla}\phi_1 \times \boldsymbol{\nabla}\phi_2) = 0$$

In these formulas $\mathbf{u}$ and $\mathbf{v}$ are arbitrary vectors and ϕ, ϕ_1, and ϕ_2 are arbitrary scalars for which the indicated derivatives exist.

Surface integrals

Divergence theorem:

$$\iiint_v \boldsymbol{\nabla} \cdot \mathbf{V}\, dV = \iint \mathbf{V} \cdot \mathbf{n}\, dS$$

Stokes' theorem:

$$\iint_s \mathbf{n} \cdot (\boldsymbol{\nabla} \times \mathbf{V}) dS = \oint_C \mathbf{V} \cdot d\mathbf{r}$$

Green's theorem:

$$\iiint_v [\phi_1 \nabla^2 \phi_2 - \phi_2 \nabla^2 \phi_1] dV = \iint_s \mathbf{n} \cdot (\phi_1 \boldsymbol{\nabla} \phi_2 - \phi_2 \boldsymbol{\nabla} \phi_1) dS,$$

where $\mathbf{n}$ is the surface outward unit normal.

Differential elements

Cylindrical coordinates

Line element:

$$ds = \sqrt{(dr^2 + r^2 d\theta + dz^2)}$$

Area elements:

$$dS_r = r\, d\theta\, dz, \quad dS_\theta = dr\, dz, \quad dS_z = r\, d\theta\, dr$$

Volume element:

$$dV = r\, d\theta\, dr\, dz$$

Spherical coordinates

Line element:

$$ds = \sqrt{(dr^2 + r^2 d\theta + r^2 \sin^2\theta\, d\phi^2)}$$

Area elements:

$$dS_r = r^2 \sin\theta\, d\theta\, d\phi, \quad dS_\theta = r \sin\theta\, dr\, d\phi, \quad dS_\phi = r\, dr\, d\theta$$

Volume element:

$$dV = r^2 \sin\theta\, dr\, d\theta\, d\phi$$

Vector operations

Let $\mathbf{e_1}, \mathbf{e_2}, \mathbf{e_3}$ be orthogonal unit vectors associated with the coordinate systems specified and A_1, A_2, A_3 be the corresponding components of $\mathbf{A}$. Then

Cartesian $(x_1, x_2, x_3 = x, y, z)$

$$\boldsymbol{\nabla}\psi = \mathbf{e_1}\frac{\partial\psi}{\partial x_1} + \mathbf{e_2}\frac{\partial\psi}{\partial x_2} + \mathbf{e_3}\frac{\partial\psi}{\partial x_3}$$

$$\boldsymbol{\nabla}\cdot\mathbf{A} = \frac{\partial A_1}{\partial x_1} + \frac{\partial A_2}{\partial x_2} + \frac{\partial A_3}{\partial x_3}$$

$$\boldsymbol{\nabla}\times\mathbf{A} = \mathbf{e_1}\left(\frac{\partial A_3}{\partial x_2} - \frac{\partial A_2}{\partial x_3}\right) + \mathbf{e_2}\left(\frac{\partial A_1}{\partial x_3} - \frac{\partial A_3}{\partial x_1}\right) + \mathbf{e_3}\left(\frac{\partial A_2}{\partial x_1} - \frac{\partial A_1}{\partial x_2}\right)$$

$$\nabla^2\psi = \frac{\partial^2\psi}{\partial x_1^2} + \frac{\partial^2\psi}{\partial x_2^2} + \frac{\partial^2\psi}{\partial x_3^2}$$

Cylindrical (ρ, ϕ, z)

$$\boldsymbol{\nabla}\psi = \mathbf{e_1}\frac{\partial\psi}{\partial\rho} + \mathbf{e_2}\frac{1}{\rho}\frac{\partial\psi}{\partial\phi} + \mathbf{e_3}\frac{\partial\psi}{\partial z}$$

$$\boldsymbol{\nabla}\cdot\mathbf{A} = \frac{1}{\rho}\frac{\partial}{\partial\rho}(\rho A_1) + \frac{1}{\rho}\frac{\partial A_2}{\partial\phi} + \frac{\partial A_3}{\partial z}$$

$$\boldsymbol{\nabla}\times\mathbf{A} = \mathbf{e_1}\left(\frac{1}{\rho}\frac{\partial A_3}{\partial\phi} - \frac{\partial A_2}{\partial z}\right) + \mathbf{e_2}\left(\frac{\partial A_1}{\partial z} - \frac{\partial A_3}{\partial\rho}\right) + \mathbf{e_3}\frac{1}{\rho}\left(\frac{\partial}{\partial\rho}(\rho A_2) - \frac{\partial A_1}{\partial\phi}\right)$$

$$\nabla^2\psi = \frac{1}{\rho}\frac{\partial}{\partial\rho}\left(\rho\frac{\partial\psi}{\partial\rho}\right) + \frac{1}{\rho^2}\frac{\partial^2\psi}{\partial\phi^2} + \frac{\partial^2\psi}{\partial z^2}$$

Spherical (r, θ, ϕ)

$$\boldsymbol{\nabla}\psi = \mathbf{e_1}\frac{\partial\psi}{\partial r} + \mathbf{e_2}\frac{1}{r}\frac{\partial\psi}{\partial\theta} + \mathbf{e_3}\frac{1}{r\sin\theta}\frac{\partial\psi}{\partial\phi}$$

$$\boldsymbol{\nabla}\cdot\mathbf{A} = \frac{1}{r^2}\frac{\partial}{\partial r}(r^2 A_1) + \frac{1}{r\sin\theta}\frac{\partial}{\partial\theta}(\sin\theta A_2) + \frac{1}{r\sin\theta}\frac{\partial A_3}{\partial\phi}$$

$$\boldsymbol{\nabla}\times\mathbf{A} = \mathbf{e_1}\frac{1}{r\sin\theta}\left[\frac{\partial}{\partial\theta}(\sin\theta A_3) - \frac{\partial A_2}{\partial\phi}\right] + \mathbf{e_2}\left[\frac{1}{r\sin\theta}\frac{\partial A_1}{\partial\phi} - \frac{1}{r}\frac{\partial}{\partial r}(rA_3)\right] + \mathbf{e_3}\frac{1}{r}\left[\frac{\partial}{\partial r}(rA_2) - \frac{\partial A_1}{\partial\theta}\right]$$

$$\nabla^2\psi = \frac{1}{r^2}\frac{\partial}{\partial r}\left(r^2\frac{\partial\psi}{\partial r}\right) + \frac{1}{r^2\sin\theta}\frac{\partial}{\partial\theta}\left(\sin\theta\frac{\partial\psi}{\partial\theta}\right) + \frac{1}{r^2\sin^2\theta}\frac{\partial^2\psi}{\partial\phi^2}$$

$$\left[\text{Note that } \frac{1}{r^2}\frac{\partial}{\partial r}\left(r^2\frac{\partial\psi}{\partial r}\right) \equiv \frac{1}{r}\frac{\partial^2}{\partial r^2}(r\psi).\right]$$

Derivatives

$f(x)$	$f'(x)$	$f^{(r)}(x)$
x^a	ax^{a-1}	$a(a-1)(a-2)\cdots(a-r+1)x^{a-r}$
e^x	e^x	e^x
a^x	$a^x \log_e a$	$a^x(\log_e a)^r$
$\log_e x$	$\frac{1}{x}$	$(-1)^{r-1}(r-1)!\frac{1}{x^r}$
$\log_a x$	$\frac{1}{x}\log_a e$	$(-1)^{r-1}(r-1)!\frac{1}{x^r}\log_a e$
$\sin x$	$\cos x$	$\sin\left(x+\frac{\pi r}{2}\right)$
$\cos x$	$-\sin x$	$\cos\left(x+\frac{\pi r}{2}\right)$
$\tan x$	$1/\cos^2 x$	
$\cot x$	$-1/\sin^2 x$	
$\sec x$	$\sin x/\cos^2 x$	
$\operatorname{cosec} x$	$-\cos x/\sin^2 x$	
$\sinh x$	$\cosh x$	
$\cosh x$	$\sinh x$	
$\tanh x$	$1/\cosh^2 x$	
$\coth x$	$-1/\sinh^2 x$	
$\arcsin x$	$1/\sqrt{1-x^2}$	
$\arccos x$	$-1/\sqrt{1-x^2}$	
$\arctan x$	$1/1+x^2$	
$\operatorname{arccot} x$	$-1/1+x^2$	
$\sinh^{-1} x$	$1/\sqrt{x^2+1}$	
$\cosh^{-1} x$	$1/\sqrt{x^2-1}$	
$\tanh^{-1} x$	$1/1-x^2$	
$\coth^{-1} x$	$1/1-x^2$	
$f(x)g(x)$	$f'(x)g(x)+g'(x)f(x)$	
$f(x)/g(x)$	$(g(x)f'(x)-f(x)g'(x))/(g(x))^2$	

Indefinite integrals (Add a constant)

$$\int x^n dx = \frac{x^{n+1}}{n+1} \ (n \neq -1)$$

$$\int e^x dx = e^x$$

$$\int \frac{dx}{x} = \log_e |x| \ (x \neq 0)$$

$$\int a^x dx = \frac{a^x}{\log_e a} \ (a > 0,\ a \neq 1)$$

$$\int \sin x \, dx = -\cos x$$

$$\int \sinh x \, dx = \cosh x$$

$$\int \cos x \, dx = \sin x$$

$$\int \cosh x \, dx = \sinh x$$

$$\int \tan x \, dx = -\log_e |\cos x|$$

$$\int \tanh x \, dx = \log_e \cosh x$$

$$\int \cot x \, dx = \log_e |\sin x|$$

$$\int \coth x \, dx = \log_e |\sinh x|$$

$$\int \frac{dx}{\cos^2 x} = \tan x$$

$$\int \frac{dx}{\cosh^2 x} = \tanh x$$

$$\int \frac{dx}{\sin^2 x} = -\cot x$$

$$\int \frac{dx}{\sinh^2 x} = -\coth x$$

$$\int \frac{dx}{a^2 + x^2} = \frac{1}{a} \arctan \frac{x}{a} \ (a \neq 0)$$

$$\int \frac{dx}{a^2 - x^2} = \frac{1}{a} \tanh^{-1} \frac{x}{a} = \frac{1}{2a} \log_e \frac{a + x}{a - x} \ (|x| < a)$$

$$\int \frac{dx}{x^2 - a^2} = -\frac{1}{a} \coth^{-1} \frac{x}{a} = \frac{1}{2a} \log_e \frac{x - a}{x + a} \ (|x| > a)$$

$$\int \frac{dx}{\sqrt{a^2 - x^2}} = \arcsin \frac{x}{a} \ (a \neq 0)$$

$$\int \frac{dx}{\sqrt{a^2 + x^2}} = \log_e |x + \sqrt{a^2 + x^2}|$$

$$\int \frac{dx}{\sqrt{x^2 - a^2}} = \log_e |x + \sqrt{x^2 - a^2}|$$

Definite integrals

$$\int_0^\infty t^{2n+1}e^{-at^2}dt = \frac{n!}{2a^{n+1}} \ (n = 0, 1, 2, \ldots)$$

$$\int_0^\infty t^{2n}e^{-at^2}dt = \frac{1\cdot 3\cdots(2n-1)}{2^{n+1}a^n}\sqrt{\left(\frac{\pi}{a}\right)} \ (n = 0, 1, 2, \ldots)$$

$$\int_0^\infty t^n e^{-at}dt = \frac{n!}{a^{n+1}} \ (n = 1, 2, \ldots)$$

$$\int_{-\infty}^\infty e^{-\pi x^2}dx = 1 \qquad \int_{-\infty}^\infty e^{-Ax^2}dx = \left(\frac{\pi}{A}\right)^{1/2}$$

$$\int_0^\infty xe^{-x^2}dx = 1/2 \qquad \int_0^\infty \left(\frac{\sin x}{x}\right)^2 dx = \frac{\pi}{2}$$

$\operatorname{erf} x = \frac{2}{\sqrt{\pi}}\int_0^x e^{-t^2}dt$, error function

$C(x) = \int_0^x \cos\left(\frac{\pi}{2}t^2\right) dt$, $\quad S(x) = \int_0^x \sin\left(\frac{\pi}{2}t^2\right) dt$, Fresnel integrals

$Ei(x) = \int_{-\infty}^x \frac{e^t}{t}dt$, exponential integral

$\Gamma(x) = \int_0^\infty t^{x-1}e^{-t}dt$, gamma function

$L\{F(t)\}(s) = \int_0^\infty e^{-st}F(t)dt$, Laplace transform

The Fourier transform

The Fourier transform of $f(x)$ is:

$$F(s) = \int_{-\infty}^\infty f(x)e^{-i2\pi xs}dx$$

and

$$f(x) = \int_{-\infty}^\infty F(s)e^{i2\pi xs}ds.$$

There are two other equivalent versions:

$$F(s) = \int_{-\infty}^\infty f(x)e^{-ixs}dx,$$

$$f(x) = \frac{1}{2\pi}\int_{-\infty}^\infty F(s)e^{ixs}ds$$

and

$$F(s) = \frac{1}{(2\pi)^{1/2}} \int_{-\infty}^{\infty} f(x) e^{-ixs} dx,$$

$$f(x) = \frac{1}{(2\pi)^{1/2}} \int_{-\infty}^{\infty} F(s) e^{ixs} ds,$$

which are also used.

Useful definitions

The *convolution* of two functions $f(x)$ and $g(x)$ is:

$$\int_{-\infty}^{\infty} f(u) g(x-u) du = f * g = \int_{-\infty}^{\infty} g(u) f(x-u) du = g * f.$$

The *autocovariance* function of $f(x)$ is:

$$f(x) \otimes f(x) = \int_{-\infty}^{\infty} f^*(u) f(u+x) du$$

The *autocorrelation* function of $f(x)$ is:

$$\gamma(x) = \frac{\int_{-\infty}^{\infty} f^*(u) f(u+x) du}{\int_{-\infty}^{\infty} f(u) f^*(u) du},$$

$$\gamma(0) = 1.$$

The *cross-correlation* of two functions $g(x)$ and $h(x)$ is:

$$f(x) = \int_{-\infty}^{\infty} g(u-x) h(u) du$$

The *power spectrum* of a function $f(x)$ is:

$$\left| \int_{-\infty}^{\infty} f(x) e^{-i2\pi xs} dx \right|^2 = |F(s)|^2$$

The normalized *power spectrum* is the *power spectral density function*:

$$|\phi(s)|^2 = \frac{|F(s)|^2}{\int_{-\infty}^{\infty} |F(s)|^2 ds}$$

The *equivalent width* of a function $f(x)$ is:

$$W_f = \frac{\int_{-\infty}^{\infty} f(x) dx}{f(0)}$$

The *filtering* or *interpolation* function, $\operatorname{sinc} x$:

$$\operatorname{sinc} x = \frac{\sin \pi x}{\pi x}$$

Fourier transform theorems

Theorem	$f(x)$	$F(s) = \int_{-\infty}^{\infty} f(x)e^{-i2\pi xs}dx$
Similarity	$f(ax)$	$\frac{1}{\lvert a\rvert}F(s/a)$
Addition	$f(x) + g(x)$	$F(s) + G(s)$
Shift	$f(x - a)$	$e^{-i2\pi as}F(s)$
Convolution	$f(x) * g(x)$	$F(s)G(s)$
Autocovariance	$f(x) \otimes f(x)$	$\lvert F(s)\rvert^2$
Derivative	$f'(x)$	$i2\pi sF(s)$

Derivative of convolution:

$$\frac{d}{dx}[f(x) * g(x)] = f'(x) * g(x) = f(x) * g'(x)$$

Parseval:

$$\int_{-\infty}^{\infty} |f(x)|^2 dx = \int_{-\infty}^{\infty} |F(s)|^2 ds$$

Multiplication:

$$\int_{-\infty}^{\infty} f^*(x)g(x)dx = \int_{-\infty}^{\infty} F^*(s)G(s)ds$$

Sampling theorem:

A function whose Fourier transform is zero for $|s| > s_c$ is fully specified by values spaced at equal intervals not exceeding $\frac{1}{2}s_c^{-1}$ save for any harmonic term with zeros at the sampling points.

(Adapted from Bracewell, R. N. *The Fourier Transform and its Applications*, McGraw-Hill Book Company, 1978.)

Fourier transform pairs

	$f(t) = \int_{-\infty}^{\infty} F_F(i\omega) e^{-i\omega t}\frac{d\omega}{2\pi}$	$F_F(i\omega) = \int_{-\infty}^{\infty} f(t) e^{-i\omega t}\, dt$	
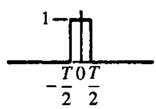	$\text{rect}\,\frac{t}{T} = \begin{cases}1 & (\lvert t\rvert < T/2)\\ 0 & (\lvert t\rvert > T/2)\end{cases}$	$T\,\text{sinc}\,\frac{\omega T}{2\pi} \equiv T\frac{\sin\frac{\omega T}{2}}{\frac{\omega T}{2}}$	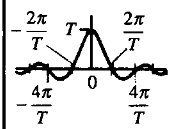
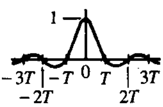	$\text{sinc}\,\frac{t}{T} \equiv \frac{\sin\frac{\pi t}{T}}{\frac{\pi t}{T}}$	$T\,\text{rect}\,\frac{\omega T}{2\pi} = \begin{cases}0 & (\lvert\omega\rvert < \frac{\pi}{T})\\ T & (\lvert\omega\rvert > \frac{\pi}{T})\end{cases}$	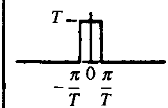
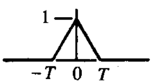	$\begin{cases}1-\frac{\lvert t\rvert}{T} & (\lvert t\rvert < T)\\ 0 & (\lvert t\rvert \ge T)\end{cases}$	$T\,\text{sinc}^2\,\frac{\omega T}{2\pi} \equiv T\left(\frac{\sin\frac{\omega T}{2}}{\frac{\omega T}{2}}\right)^2$	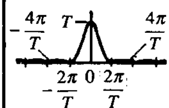
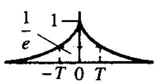	$e^{-\frac{\lvert t\rvert}{T}}$	$\frac{2T}{(\omega T)^2+1}$	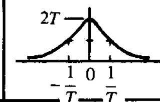
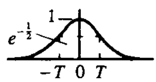	$e^{-\frac{1}{2}(\frac{t}{T})^2}$	$\sqrt{2\pi}\,T e^{-\frac{1}{2}(\omega T)^2}$	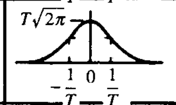
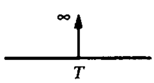	$\delta(t-T)$	$e^{-i\omega T}$	(Complex)
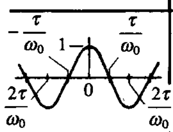	$\cos\omega_0 t$	$\pi[\delta(\omega-\omega_0)+\delta(\omega+\omega_0)]$	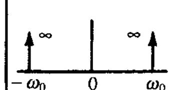
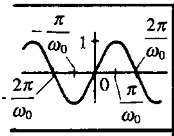	$\sin\omega_0 t$	$\frac{\pi}{i}[\delta(\omega-\omega_0)-\delta(\omega+\omega_0)]$	(Imaginary)
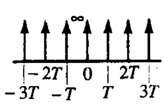	$\sum_{k=-\infty}^{\infty}\delta(t-kT) \equiv \frac{1}{T}\sum_{j=-\infty}^{\infty} e^{2\pi i j\frac{t}{T}}$	$\frac{2\pi}{T}\sum_{j=-\infty}^{\infty}\delta(\omega-\frac{2\pi j}{T}) \equiv \sum_{k=-\infty}^{\infty} e^{ik\omega T}\; T$	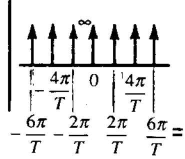

(From Korn, G. A., *Basic Tables in Electrical Engineering*, McGraw-Hill, New York, 1965, with permission.)

Special functions

Spherical harmonics, Legendre polynomials

$$Y_l^m(\theta,\phi) = \sqrt{\left[\frac{(2l+1)(l-m)!}{4\pi(l+m)!}\right]}\, P_l^m(\cos\theta)e^{im\phi}$$

$$P_l^m(\cos\theta) = (-1)^m \sin^m\theta \left[\left(\frac{d}{d(\cos\theta)}\right)^m P_l(\cos\theta)\right] \quad (m \le l)$$

$$P_l(\cos\theta) = \frac{1}{2^l l!}\left[\left(\frac{d}{d(\cos\theta)}\right)^l (-\sin^2\theta)^l\right]$$

$$Y_l^{-m}(\theta,\phi) = (-1)^m [Y_l^m(\theta,\phi)]^*$$

$$P_l^{-m}(\cos\theta) = (-1)^m \frac{(l-m)!}{(l+m)!} P_l^m(\cos\theta)$$

$l=0$ $$Y_0^0 = \frac{1}{\sqrt{(4\pi)}}$$

$l=1$ $$Y_1^0 = \sqrt{\left(\frac{3}{4\pi}\right)}\cos\theta$$

$$Y_1^1 = -\sqrt{\left(\frac{3}{8\pi}\right)}\sin\theta e^{i\phi}$$

$l=2$ $$Y_2^0 = \sqrt{\left(\frac{5}{16\pi}\right)}(3\cos^2\theta - 1)$$

$$Y_2^1 = -\sqrt{\left(\frac{15}{8\pi}\right)}\sin\theta\cos e^{i\phi}$$

$$Y_2^2 = \sqrt{\left(\frac{15}{32\pi}\right)}\sin^2\theta e^{2i\phi}$$

$l=3$ $$Y_3^0 = \sqrt{\left(\frac{7}{16\pi}\right)}(5\cos^3\theta - 3\cos\theta)$$

$$Y_3^1 = -\sqrt{\left(\frac{21}{64\pi}\right)}\sin\theta(5\cos^2\theta - 1)e^{i\phi}$$

$$Y_3^2 = \sqrt{\left(\frac{105}{32\pi}\right)}\sin^2\theta\cos\theta e^{2i\phi}$$

$$Y_3^3 = -\sqrt{\left(\frac{35}{64\pi}\right)}\sin^2\theta e^{3i\phi}.$$

Bessel functions

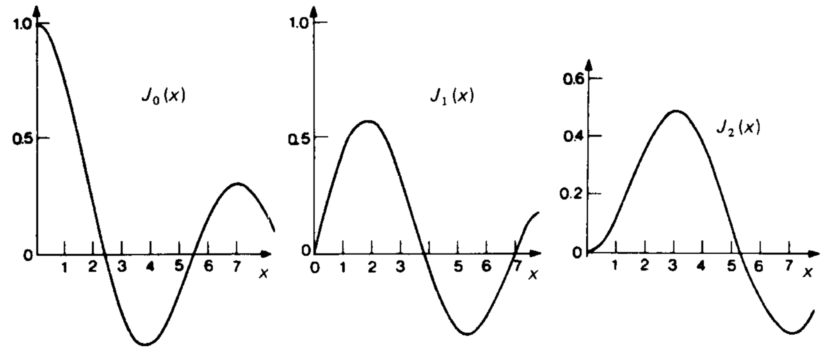

$$J_n(x) = \sum_{s=0}^{s=\infty} \frac{(-1)^s}{s!(n+s)!} \left(\frac{x}{2}\right)^{n+2s} \qquad J_{n-1}(x) + J_{n+1}(x) = (2n/x)J_n(x)$$

$$J_0(x) = (2/\pi x)^{\frac{1}{2}} \cos(x - \pi/4)$$

See Chapter 14 for an application of Bessel functions to astronomy.

(Adapted from Chantry, G.U.J., *Long-wave Optics*, Academic Press, New York, 1984.)

Function definitions and approximations

Function	Definition	Approximation	Range	Error
Error function		$\text{erf}(x) \simeq 1 - (a_1 t + a_2 t^2 + a_3 t^3) e^{-x^2}$		
$\text{erf}(x)$	$\text{erf}(x) = \frac{2}{\sqrt{\pi}} \int_0^x \exp(-t^2) dt$	$t = \frac{1}{1 + px}$	$0 \le x < \infty$	$\lvert\epsilon\rvert \le 2.5 \times 10^{-5}$
$(\text{erf}(-x) = -\text{erf}(x))$		$p = .47047 \quad a_1 = .3480242$		
		$a_2 = -.0958798 \quad a_3 = .7478556$		
$\text{erfc}(x)$	$\text{erfc}(x) = \frac{2}{\sqrt{\pi}} \int_x^\infty \exp(-t^2) dt$			
	$= 1 - \text{erf}(x)$			
$(\text{erfc}(-x) = 2 - \text{erfc}(x))$		$\text{erfc}(x) \simeq \frac{1.132x \exp(-x^2)}{2x^2 + 1}$	$x \ge 2.7$	$\lvert\epsilon_r\rvert \le 4 \times 10^{-3}$
Gaussian probability function	$P = \frac{1}{\sqrt{2\pi}} e^{-x^2/2}$	*not approximated*	$-\infty < x < \infty$	
Gamma function		*Stirling approximation :*		
$\Gamma(x)$	$\Gamma(x) = \int_0^\infty t^{x-1} \exp(-t) dt$	$\Gamma(x) \simeq \sqrt{\frac{2\pi}{x}} \exp(-x) x^x \left(1 + \frac{1}{12x}\right)$	$x \ge 0.4$	$\lvert\epsilon_r\rvert \le 4 \times 10^{-3}$
Factorial function		*Stirling approximation*		
$n!$	$n! = 1 \times 2 \times 3 \times \cdots \times (n-1) \times n$	$n! \simeq \sqrt{2\pi n} \exp(-n) n^n \left(1 + \frac{1}{12n}\right)$	$n \ge 2$	$\lvert\epsilon_r\rvert \le 4 \times 10^{-3}$
Exponential		$x e^x E_1 \simeq \frac{x^2 + a_1 x + a_2}{x^2 + b_1 x + b_2}$		
integral $E_1(x)$	$E_1(z) = \int_x^\infty \frac{e^{-t}}{t} dt$	$a_1 = 2.334733 \quad b_1 = 3.330657$	$1 \le x < \infty$	$\lvert\epsilon_r\rvert \le 5 \times 10^{-5}$
		$a_2 = .250621 \quad b_2 = 1.681534$		

The accuracy is specified as either relative or absolute. A relative error of ϵ_r implies $\left|\frac{f(x) - \hat{f}(x)}{f(x)}\right| \le \epsilon_r$ whereas an absolute error of ϵ implies $|f(x) - \hat{f}(x)| \le \epsilon$, where $\hat{f}(x)$ is the approximate value of the function $f(x)$.

Function definitions and approximations(cont.)

Function	Definition	Approximation	Range	Error
Complete Elliptic integral of the 1st kind $K(k)$	$K(k) = \int_0^{\pi/2} \frac{d\varphi}{\sqrt{1 - k^2 \sin^2 \varphi}}$	$\eta = 1 - k^2$ $K(k) \simeq (a_0 + a_1\eta + a_2\eta^2) + (b_0 + b_1\eta + b_2\eta^2) \ln \frac{1}{\eta}$ $a_0 = 1.3862944$ $b_0 = .5$ $a_1 = .1119723$ $b_1 = .1213478$ $a_2 = .0725296$ $b_2 = .0288729$	$0 \leq k < 1$	$\lvert\epsilon\rvert \leq 3 \times 10^{-5}$
Complete Elliptic integral of the 2nd kind $E(k)$	$E(k) = \int_0^{\pi/2} \sqrt{1 - k^2 \sin^2 \varphi}\, d\varphi$	$\eta = 1 - k^2$ $E(k) \simeq (1 + a_1\eta + a_2\eta^2) + (b_1\eta + b_2\eta^2) \ln \frac{1}{\eta}$ $a_1 = .4630151$ $b_1 = .2452727$ $a_2 = .1077812$ $b_2 = .0412496$	$0 \leq k < 1$	$\lvert\epsilon\rvert < 4 \times 10^{-5}$
0 order Bessel function of the first kind $J_0(x)$ $(J_0(-x) = J_0(x))$	$J_0(x) = \frac{1}{\pi} \int_0^{\pi} \cos(x \sin t) dt$	$J_0(x) = x^{-1/2} f_0 \cos\theta_0$	See aux. table	
1st order Bessel function of the second kind $J_1(x)$ $(J_1(-x) = -J_1(x))$	$J_1(x) = \frac{1}{\pi} \int_0^{\pi} \cos(x \sin -t) dt$	$J_1(x) = x^{-1/2} f_1 \cos\theta_1$	See aux. table	

Function definitions and approximations(cont.)

Function	Definition	Approximation	Range	Error
Fresnel sine integral $S(x)$ $(S(-x) = -S(x))$	$S(x) = \int_0^x \sin\left(\frac{\pi}{2}t^2\right) dt$	$S(x) = \frac{1}{2} - f_2(x)\cos\left(\frac{\pi}{2}x^2\right) - g_2(x)\sin\left(\frac{\pi}{2}x^2\right)$	See aux. table	
Fresnel cosine integral $C(x)$ $(C(-x) = -C(x))$	$C(x) = \int_0^x \cos\left(\frac{\pi}{2}t^2\right) dt$	$C(x) = \frac{1}{2} + f_2(x)\sin\left(\frac{\pi}{2}x^2\right) - g_2(x)\cos\left(\frac{\pi}{2}x^2\right)$	See aux. table	
Sine integral $Si(x)$	$Si(x) = \int_0^x \frac{\sin(t)}{t} dt$	$Si(z) = \frac{\pi}{2} - f_3(x)\cos x - g_3(x)\sin x$	See aux. table	
Cosine integral $Ci(x)$	$Ci(x) = -\int_x^\infty \frac{\cos(t)}{t} dt$	$Ci(x) = f(x)\sin x - g_3(x)\cos x$	See aux. table	
Hyperbolic tangent $\tanh(x)$	$\tanh(x) = \frac{\exp(x) - \exp(-x)}{\exp(x) + \exp(-x)}$	*not approximated*	$-\infty < x < \infty$	
Hyperbolic sine $\sinh(x)$	$\sinh(x) = \frac{\exp(x) - \exp(-x)}{2}$	*not approximated*	$-\infty < x < \infty$	
Hyperbolic cosine $\cosh(x)$	$\cosh(x) = \frac{\exp(x) + \exp(-x)}{2}$	*not approximated*	$-\infty < x < \infty$	
Legendre polynomial $P_n(x)$	$P_n(x) = \frac{1}{2^n n!} \frac{d^n (x^2-1)^n}{dx^n}$	*not approximated*	$0 \le n \le 9$ $-1 \le x \le \pm 1$	

Auxiliary table for function definitions and approximations

Function	Approximation	Range	Error
$f_0(x)$	$f_0 \simeq .79788\,456 - .00000\,077(3/x) - .00552\,740(3/x)^2 - .00009\,512(3/x)^3 + .00137\,237(3/x)^4 - .00072\,805(3/x)^5 + .00014\,476(3/x)^6$	$3 \leq x < \infty$	$\|\epsilon\| < 1.6 \times 10^{-8}$
$\theta_0(x)$	$\theta_0 \simeq x - .78539\,816 - .04166\,397(3/x) - .00003\,954(3/x)^2 + .00262\,573(3/x)^3 - .00054\,125(3/x)^4 - .00029\,333(3/x)^5 + .00013\,558(3/x)^6$	$3 \leq x < \infty$	$\|\epsilon\| < 7 \times 10^{-8}$
$f_1(x)$	$f_1 \simeq .79788\,456 + .00000\,156(3/x) + .01659\,667(3/x)^2 + .00017\,105(3/x)^3 - .00249\,511(3/x)^4 + .00113\,653(3/x)^5 - .00020\,033(3/x)^6$	$3 \leq x < \infty$	$\|\epsilon\| < 4 \times 10^{-8}$
$\theta_1(x)$	$\theta_1 \simeq 2.35619\,449 + .12499\,612(3/x) + .00005\,560(3/x)^2 - .00637\,879(3/x)^3 + .00074\,348(3/x)^4 + .00079\,824(3/x)^5 - .00029\,166(3/x)^6$	$3 \leq x < \infty$	$\|\epsilon\| < 9 \times 10^{-8}$
$f_2(x)$	$f_2(x) \simeq \dfrac{1 + .926x}{2 + 1.792x + 3.104x^2}$	$0 \leq x < \infty$	$\|\epsilon\| \leq 2 \times 10^{-3}$
$g_2(x)$	$g_2(x) \simeq \dfrac{1}{2 + 4.142x + 3.492x^2 + 6.670x^3}$	$0 \leq x < \infty$	$\|\epsilon\| \leq 2 \times 10^{-3}$
$f_3(x)$	$f_3(x) = \dfrac{1}{x}\left(\dfrac{x^4 + a_1x^2 + a_2}{x^4 + b_1x^2 + b_2}\right)$ $a_1 = 7.241163 \quad b_1 = 9.068580$ $a_2 = 2.463936 \quad b_2 = 7.157433$	$1 \leq x < \infty$	$\|\epsilon(x)\| < 2 \times 10^{-4}$
$g_3(x)$	$g_3(x) = \dfrac{1}{x^2}\left(\dfrac{x^4 + a_1x^2 + a_2}{x^4 + b_1x^2 + b_2}\right)$ $a_1 = 7.547478 \quad b_1 = 12.723684$ $a_2 = 1.564072 \quad b_2 = 15.723606$	$1 \leq x < \infty$	$\|\epsilon(x)\| < 10^{-4}$

(Adapted from Abramowitz, M. and Stegun, I.A., "Handbook of Mathematical Functions", Dover Publications, 1972, Hastings, C., "Approximations for Digitial Computers", Princeton University Press, 1955, and Spanier J. and Oldham, K.B., "An Atlas of Functions", Hemisphere Publishing Co., 1987.)

Named differential equations

Ordinary differential equations	Partial differential equations	
Airy equation: $y'' = xy$	Biharmonic equation:	$\nabla^4 u = 0$
Solution: $y = c_1 Ai(x) + c_2 Bi(x)$	Burgers' equation:	$u_t + uu_x = vu_{xx}$
Bernoulli equation: $y' = a(x)y^n + b(x)y$	Diffusion (or heat) equation:	$\nabla(c(x,t)\nabla_u) = u_t$
Bessel equation: $x^2y'' + xy' + (\lambda^2x^2 - n^2)y = 0$	Hamilton-Jacobi equation:	$V_t + H(t, x, V_{x_1}, \ldots, V_{x_n}) = 0$
Solution: $y = c_1 J_n(\lambda x) + c_2 Y_n(\lambda_x)$		
Bessel equation (transformed): $x^2y'' + (2p+1)xy' + (\lambda^2x^{2r} + \beta^2)y = 0$	Helmholtz equation:	$\nabla^2 u + k^2 u = 0$
Solution: $y = x^{-p}\left[c_1 J_{q/r}\left(\frac{\lambda}{r}x^r\right) + c_2 Y_{q/r}\left(\frac{\lambda}{r}x^r\right)\right]$ $q \equiv \sqrt{p^2 - \beta^2}$	Korteweg de Vries equation:	$u_t + u_{xxx} - 6uu_x = 0$
Duffing's equation: $y'' + y + \epsilon y^3 = 0$	Laplace's equation:	$\nabla^2 u = 0$
Emden-Fowler equation: $(x^p y')' \pm x^\sigma y^n = 0$	Navier-Stokes equations:	$u_t + (u \cdot \nabla)u = -\frac{\nabla P}{\rho} + \nu\nabla^2 u$
Legendre equation: $(1 - x^2)y'' - 2xy' + n(n+1)y = 0$	Poisson equation:	$\nabla^2 u = -4\pi\rho(x)$
Solution: $y = c_1 P_n(x) + c_2 Q_n(x)$	Schrödinger equation:	$-\frac{\hbar^2}{2m}\nabla^2 u + V(x)u = i\hbar u_t$
Mathieu equation: $y'' + (a - 2q\cos 2x)y = 0$	Sine-Gordon equation:	$u_{xx} - u_{yy} \pm \sin u = 0$
Painlevé transcendent (first equation): $y'' = 6y^2 + x$	Tricomi equation:	$u_{yy} = yu_{xx}$
Parabolic cylinder equation: $y'' + (ax^2 + bx + c)y = 0$	Wave equation:	$c^2\nabla^2 u = u_{tt}$
Riccati equation: $y' = a(x)y^2 + b(x)y + c(x)$	Telegraph equation:	$u_{xx} = au_{tt} + bu_t + cu$

(Adapted from *Standard Mathematical Tables and Formulae*, D. Zwillinger, ed. ch., CRC Press, 1996)

Complex analysis

Definitions

A complex number z has the form $z = x + iy$ where x and y are real numbers, and $i = \sqrt{-1}$.

Complex numbers can also be written in *polar form*, $z = re^{i\theta}$, where r, called the *modulus*, is given by $r = |z| = \sqrt{x^2 + y^2}$, and θ is called the *argument*: $\theta = \arg z = \tan^{-1}\left(\frac{y}{x}\right)$.

The *complex conjugate* of z, denoted $\overline{z}$, is defined as $\overline{z} = x - iy = re^{-i\theta}$. Note that $|z| = |\overline{z}|$, $\arg\overline{z} = -\arg z$, and $|z| = \sqrt{z\overline{z}}$. In addition, $\overline{\overline{z}} = z$, $\overline{z_1 + z_2} = \overline{z}_1 + \overline{z}_2$, and $\overline{z_1 z_2} = \overline{z}_1 \overline{z}_2$.

Operations

$$z_1 \pm z_2 = (x_1 + iy_1) \pm (x_2 + iy_2) = (x_1 \pm x_2) + i(y_1 \pm y_2)$$

$$\begin{aligned} z_1 z_2 &= (x_1 + iy_1)(x_2 + iy_2) = (x_1 x_2 - y_1 y_2) + i(x_1 y_2 + x_2 y_1) \\ &= r_1 r_2 e^{i(\theta_1 + \theta_2)} \end{aligned}$$

$$|z_1 z_2| = |z_1||z_2|$$

$$\arg(z_1 z_2) = \arg z_1 + \arg z_2 = \theta_1 + \theta_2$$

$$\frac{z_1}{z_2} = \frac{z_1 \overline{z}_2}{z_2 \overline{z}_2} = \frac{(x_1 x_2 + y_1 y_2) + i(x_2 y_1 - x_1 y_2)}{x_2^2 + y_2^2} = \frac{r_1}{r_2} e^{i(\theta_1 - \theta_2)}$$

$$\left|\frac{z_1}{z_2}\right| = \frac{|z_1|}{|z_2|}$$

$$\arg\left(\frac{z_1}{z_2}\right) = \arg z_1 - \arg z_2 = \theta_1 - \theta_2$$

Powers and roots

$z^n = r^n e^{in\theta} = r^n(\cos n\theta + i \sin n\theta)$ *(DeMoivre's Theorem).*

$$z^{1/n} = r^{1/n} e^{i\theta/n} = r^{1/n}\left(\cos\frac{\theta + 2k\pi}{n} + i\sin\frac{\theta + 2k\pi}{n}\right), \qquad k = 0, 1, 2, \ldots, n-1.$$

The principal root: $-\pi < \theta \leq \pi$ and $k = 0$.

Complex analysis (cont.)

Functions of a complex variable

A complex function

$$w = f(z) = u(x, y) + iv(x, y) = |w|e^{i\phi},$$

where $z = x+iy$, associates one or more values of the complex dependent variable w with each value of the complex independent variable z for those values of z in a given domain.

Cauchy-Riemann equations

A function $w = f(z)$ is said to be *analytic* at a point z_0 if it is differentiable in a neighborhood (i.e., at each point of a circle centered on z_0 with an arbitrarily small radius) of z_0. A function is called *analytic* in a connected domain if it is analytic at every point in that domain.

A necessary and sufficient condition for $f(z) = u(x, y) + iv(x, y)$ to be analytic is that $f(z)$ satisfy the Cauchy-Riemann equations,

$$\frac{\partial u}{\partial x} = \frac{\partial v}{\partial y}, \quad \text{and} \quad \frac{\partial u}{\partial y} = -\frac{\partial v}{\partial x}.$$

Cauchy integral theorem

If $f(z)$ is analytic at all points within and on a simple closed curve C, then

$$\int_C f(z)dz = 0.$$

Cauchy integral formula

If $f(z)$ is analytic inside and on a simple closed contour C and if z_0 is interior to C, then

$$f(z_0) = \frac{1}{2\pi i}\int_C \frac{f(z)}{z - z_0}dz.$$

If the derivatives $f'(z), f''(z), \ldots$ of all orders exist, then

$$f^{(n)}(z_0) = \frac{n!}{2\pi i}\int_C \frac{f(z)}{(z - z_0)^{n+1}}dz.$$

(Adapted from *Standard Mathematical Tables and Formulae*, D. Zwillinger, ed. ch., CRC Press, 1996)

Algebra

Quadratic equations

If $a \neq 0$, the roots of

$$ax^2 + bx + c = 0 \text{ are}$$

$$x_1 = \frac{-b + (b^2 - 4ac)^{1/2}}{2a} = \frac{-2c}{b - (b^2 - 4ac)^{1/2}}$$

$$x_2 = \frac{-b - (b^2 - 4ac)^{1/2}}{2a} = \frac{2c}{-b + (b^2 - 4ac)^{1/2}}$$

Binomial theorem

For n any positive integer,

$$(a+b)^n = a^n + na^{n-1}b + \frac{n(n-1)}{2!}a^{n-2}b^2 + \frac{n(n-1)(n-2)}{3!}a^{n-3}b^3 + \cdots + nab^{n-1} + b^n$$

or

$$(a+b)^n = \sum_{r=0}^{n} {}^nC_r a^{n-r}b^r = \sum_{r=0}^{n} \frac{n!}{r!(n-r)!}a^{n-r}b^r$$

Multinomial theorem

For n any positive integer, the general term in the expansion of $(a_1 + a_2 + \cdots + a_k)^n$ is

$$\frac{n!}{r_1!r_2!r_3!\ldots r_k!}a_1^{r_1}a_2^{r_2}a_3^{r_3}\ldots a_k^{r_k}$$

where $r_1, r_2, \ldots, r_k$ are positive integers such that $r_1 + r_2 + \cdots + r_k = n$.

Algebraic equations

The general equation of the nth degree

$$P(x) = a_0x^n + a_1x^{n-1} + a_2x^{n-2} + \cdots + a_{n-1}x + a_n = 0$$

has n roots. If the roots of $P(x) = 0$, or zeros of $P(x)$, are $r_1, r_2, \ldots, r_n$, then

$$P(x) = a_0(x - r_1)(x - r_2)\ldots(x - r_n)$$

and the symmetric functions of the roots

$$\sum r_i = -\frac{a_1}{a_0}, \ \sum r_i r_j = \frac{a_2}{a_0}, \ \sum r_i r_j r_k = -\frac{a_3}{a_0}, \ \ldots,$$

$$r_1 r_2 \ldots r_n = (-1)^n \frac{a_n}{a_0}$$

(Adapted from *Fundamental Formulas of Physics* D.H. Menzel, ed., Prentice-Hall, Inc., 1955)

Conics

Definition: the locus of a point which moves so that its distance from a fixed point (focus) bears a constant ratio e (eccentricity) to its distance from a fixed straight line (directrix). If $e = 1$, the conic is a parabola, $e > 1$, a hyperbola, and $e < 1$, an ellipse.

Parabola $(e = 1)$

$(y-k)^2 = 4a(x-h)$. Vertex at (h,k), axis parallel to x-axis.
$(x-h)^2 = 4a(y-k)$. Vertex at (h,k), axis parallel to y-axis.
Distance of vertex to focus $= a$. Distance of vertex to directrix $= a$.

Ellipse $(e < 1)$

$$\frac{(x-h)^2}{a^2} + \frac{(y-k)^2}{b^2} = 1.$$

Center at (h,k), major axis parallel to x-axis.

$$\frac{(y-k)^2}{a^2} + \frac{(x-h)^2}{b^2} = 1.$$

Center at (h,k), major axis parallel to y-axis.

Major axis $= 2a$. Minor axis $= 2b$.
Distance from center to either focus $= (a^2 - b^2)^{1/2}$.
Distance from center to either directrix $= a/e$
Eccentricity, $e = (a^2 - b^2)^{1/2}/a$

Hyperbola $(e > 1)$

$$\frac{(x-h)^2}{a^2} - \frac{(y-k)^2}{b^2} = 1.$$

Center at (h,k), transverse axis parallel to x-axis.
Slopes of asymptotes $= \pm b/a$

$$\frac{(y-k)^2}{a^2} - \frac{(x-h)^2}{b^2} = 1.$$

Center at (h,k), transverse axis parallel to y-axis.
Slopes of asymptotes $= \pm a/b$

Transverse axis $= 2a$. Conjugate axis $= 2b$.
Distance from center to either focus $= (a^2 - b^2)^{1/2}$.
Distance from center to either directrix $= a/e$
Eccentricity, $e = (a^2 + b^2)^{1/2}/a$

Examples of plane curves

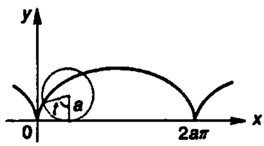

Cycloid

$\begin{cases} x=a(t-\sin t) \\ y=a(1-\cos t) \end{cases}$

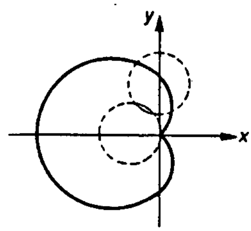

Cardioid

$r=2a(1-\cos t)$

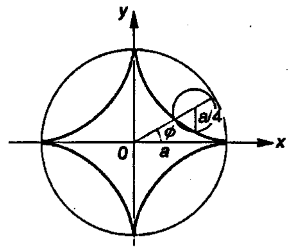

Astroid

$x^{2/3}+y^{2/3}=a^{2/3}$

$x=a\cos^3\phi$

$y=a\sin^3\phi$

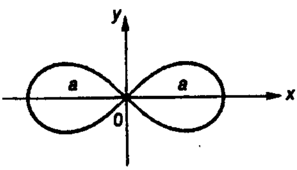

Lemniscate

$(x^2+y^2)^2=a^2(x^2-y^2)$

$r^2=a^2\cos 2\theta$

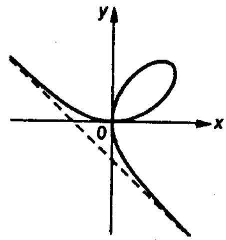

Folium of Descartes

$x^3+y^3-3axy=0$

$\begin{cases} x=3a\phi/(1+\phi^3) \\ y=3a\phi^2/(1+\phi^3) \end{cases}$

$r=\dfrac{3a\sin\theta\cos\theta}{\sin^3\theta+\cos^3\theta}$

[asymptote: $x+y+a=0$]

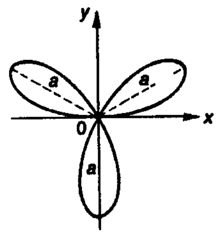

Three-leaved rose

$r=a\sin 3\phi$

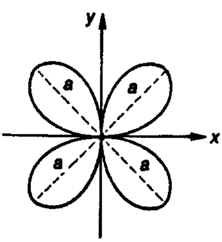

Four-leaved rose

$r=a\,|\sin 2\phi|$

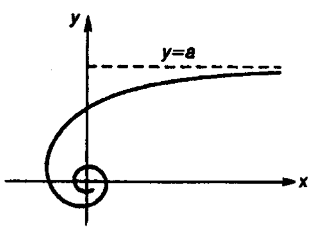

Hyperbolic spiral

$r=\dfrac{a}{\theta}$

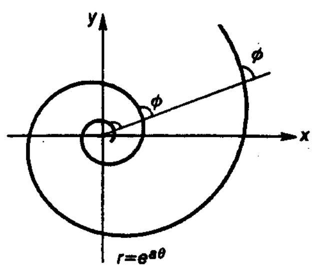

Logarithmic spiral

$\phi=\arctan\dfrac{1}{a}$

(From Rade, L. & B. Westergren, *Beta Mathematics Handbook*, CRC Press, 1992, with permission)

Numerical analysis

Taylor series

$$f(x) = f(x_0) + f'(x_0)(x - x_0) + f''(x_0)\frac{(x - x_0)^2}{2!} + \cdots + f^{(n)}(x_0)\frac{(x - x_0)^n}{n!} + R_n$$

$$R_n = f^{(n+1)}(\zeta)\frac{(x - x_0)^{n+1}}{(n+1)!} \quad (x_0 < \zeta < x)$$

Quadrature

Trapezoidal rule

$$\int_a^b f(x)dx = h\left(\frac{y_0}{2} + y_1 + y_2 + \cdots + y_{n-1} + \frac{y_n}{2}\right) - R_n$$

$$R_n = \frac{1}{12}(b - a)h^2 f''(x_1) \quad (a < x_1 < b)$$

$$h = (b - a)/n, \;\; y_k = f(a + kh), \;\; k = 0, 1, \ldots, n.$$

Simpson's rule (n even)

$$\int_a^b f(x)dx = \frac{h}{3}[y_0 + 4(y_1 + y_3 + \cdots + y_{n-1}) + 2(y_2 + y_4 + \cdots + y_{n-2}) + y_n] - R_n$$

$$R_n = \frac{1}{90}(b - a)h^4 f^{(4)}(x_1) \quad (a < x_1 < b), \;\; h = (b - a)/n.$$

Six-point Gauss-Legendre

$$\int_a^b f(x)dx \simeq \frac{b - a}{2}\sum_{i=1}^{6} w_i f\left(\frac{z_i(b - a) + b + a}{2}\right)$$

$$\int_a^\infty f(x)dx \simeq 2\sum_{i=1}^{6}\frac{w_i}{(1 + z_i)^2} f\left(\frac{2}{1 + z_i} + a - 1\right)$$

where

$$\begin{aligned}
z_1 &= -z_2 = 0.238\,619\,186\,1\\
z_3 &= -z_4 = 0.661\,209\,386\,5\\
z_5 &= -z_6 = 0.932\,469\,514\,2\\
w_1 &= w_2 = 0.467\,913\,934\,6\\
w_3 &= w_4 = 0.360\,761\,573\\
w_5 &= w_6 = 0.171\,324\,492\,4.
\end{aligned}$$

Linear interpolation

$$y = \frac{(x_{k+1} - x)y_k + (x - x_k)y_{k+1}}{x_{k+1} - x_k} \text{ for } x_k < x < x_{k+1}.$$

Approximations

$f(x)$	Approximation	Parameters	Maximum absolute error
$\log_{10} x$ $(1/\surd(10) \le x \le \surd(10))$	$a_1 t + a_3 t^3$ $t = (x-1)/(x+1)$	$a_1 = 0.863\,04$ $a_3 = 0.364\,15$	6×10^{-4}
$\arctan x$ $(-1 \le x \le 1)$	$\dfrac{x}{1 + 0.28x^2}$		5×10^{-3}
$\operatorname{erf} x$ $(0 \le x < \infty)$	$1 - (a_1 t + a_2 t^2 + a_3 t^3)e^{-x^2}$ $t = 1/(1 + px)$	$p = 0.470\,47$ $a_1 = 0.348\,024\,2$ $a_2 = -0.095\,879\,8$ $a_3 = 0.747\,855\,6$	2.5×10^{-5}

(Adapted from Hastings, C., *Approximations for Digital Computers*, Princeton, New Jersey, 1955.)

Curve fitting (linear least-squares)

$$y(x) = \sum_{j=0}^{n} a_j \phi_j(x), \text{ approximating function}$$

$$\chi^2 = \sum_{i=1}^{N} \frac{1}{\sigma_i^2}[y_i - y(x_i)]^2,$$

where

σ_i = standard deviation of the ith observation y_i,

N = number of observations.

Minimizing χ^2, $\dfrac{\partial}{\partial a_k}\chi^2 = 0$, yields the following set of normal equations:

$$\sum_{i=1}^{N}\left[\frac{1}{\sigma_i^2} y_i \phi_k(x_i)\right] = \sum_{j=0}^{n}\left(a_j \sum_{i=1}^{N}\left[\frac{1}{\sigma_i^2}\phi_j(x_i)\phi_k(x_i)\right]\right), \text{ for } k = 0 \text{ to } n.$$

(For the case of a least-squares fit to a straight line, see Chapter 17.)

Bibliography

A Table of Series and Products, Hansen, E. R., Prentice-Hall, Inc., New Jersey, 1975.

An Atlas of Functions, Spanie, J. & Oldham, K.B., Hemisphere Publishing Co., 1987.

Approximations for Digital Computers, Hastings, C., Princeton University Press, 1955.

Handbook of Mathematical Functions, Abramowitz, M. & Stegun, I. A., Dover Publications, Inc., New York, 1972.

Mathematical Handbook for Scientists and Engineers, Korn, G.A. & Korn, T.M., Mc-Graw Hill Book Company, 1968.

Mathematical Methods for Digital Computers, A. Ralston & H. S. Wilf, eds., John Wiley and Sons, New York, 1960.

Numerical Recipes: The Art of Scientific Computing, Press, W.H., Flannery, B., Teukolsky, S. & Vetterling, W., Cambridge University Press, 1985.

Tables of Higher Functions, Jahnke-Emde-Loesch, McGraw-Hill, New York, 1960.

Table of Integrals, Series, and Products, Gradshteyn, I. S. & Ryzhik, I. M., Academic Press, New York, 1980.

The Fast Fourier Transform, Brigham, E.O., Prentice-Hall, Inc., New Jersey, 1974.

The Fourier Transform and Its Applications, Bracewell, R. N., McGraw-Hill, New York, 1978.

Note: Links to WWW resources which supplement the material in this chapter can be found at:

http://www.astrohandbook.com

Chapter 17

Probability and statistics

There are three kinds of lies: lies, damned lies, and statistics. - Benjamin Disraeli

Fundamentals of probability theory

Probability theory is used to model experiments for which the outcomes occur randomly. The set of all possible outcomes is the sample space S. An event E is a subset of S.

Relative frequency definition of probability

If an experiment can occur in n mutually exclusive and equally likely ways, and if exactly m of these ways correspond to an event E, then the probability of E is given by

$$P(E) = m/n$$

Axioms of probability

Once a collection of events has been designated, each event E can be assigned a probability $P(E)$. P must satisfy the following properties:

1. If E is an event, then $0 \leq P(E) \leq 1$.
2. $P(S) = 1$.
3. If $\{E_1, E_2, E_3, \ldots\}$ is a countable collection of pairwise disjoint events, then
$$P\left(\bigcup_{i=1}^{\infty} E_i\right) = \sum_{i=1}^{\infty} P(E_i).$$

Probability theorems

If E is an event, then
$P(E^c) = 1 - P(E)$. E^c is the complement of E.

If A and B are events and $A \subset B$, then
$P(A) \leq P(B)$.

If A and B are events, then
$P(A \cup B) = P(A) + P(B) - P(A \cap B)$.

If A and B are mutually exclusive events (disjoint subsets of S), then
$P(A \cup B) = P(A) + P(B), \quad P(A \cap B) = 0$

If ϕ is the null set, then
$P(\phi) = 0$.

Conditional probability (definition)

If A and B are events, and $P(B) > 0$, then

$$P(A|B) = \frac{P(A \cap B)}{P(B)}.$$

Fundamentals of probability theory (cont.)

Bayes theorem

If $E_1, E_2, \ldots, E_n$ are n mutually exclusive events whose union is the sample space S and E is any arbitrary event of S such that $P(E) \neq 0$, then

$$P(E_k|E) = \frac{P(E_k) \cdot P(E|E_k)}{\sum_{j=1}^{n} [P(E_j) \cdot P(E|E_j)]}$$

Random variable

A function whose domain is a sample space S and whose range is some set of real numbers is a random variable, denoted by $\mathbf{X}$. The function $\mathbf{X}$ transforms sample points of S into points on the x-axis. $\mathbf{X}$ is a discrete random variable if it is a random variable that assumes only a finite or denumerable number of values on the x-axis. $\mathbf{X}$ is a continuous random variable if it assumes a continuum of values on the x-axis.

Set theory

Notation: $x \in A$, the element x belongs to the set A

$x \notin A$, the element x does not belong to the set A

The *union* of A and B is the set

$A \cup B = \{x \in S : x \in A \text{ or } x \in B\}$

and the *intersection* of A and B is the set

$A \cap B = \{x \in S : x \in A \text{ and } x \in B\}$.

The difference of A and B is the set

$A - B = \{x \in S : x \in A \text{ and } x \notin B\}$.

The set A is a subset of B, written $A \subset B$, if every element of A is also an element of B.

The complement of A is the set

$A^c = \{x \in S : x \notin A\}$

Venn diagrams

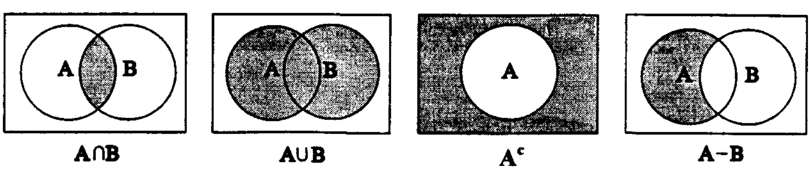

Fundamentals of probability theory (cont.)

Commutative laws

$A \cup B = B \cup A \quad A \cap B = B \cap A$

Associative laws

$(A \cup B) \cup C = A \cup (B \cup C) \quad (A \cap B) \cap C = A \cap (B \cap C)$

Distributive laws

$A \cup (B \cap C) = (A \cup B) \cap (A \cup C) \quad A \cap (B \cup C) = (A \cap B) \cup (A \cap C)$

Complementation

$\phi^c = S \qquad S^c = \phi \qquad (A^c)^c = A$

$A \cup A^c = S \qquad A \cap A^c = \phi$

De Morgan laws

$(A \cup B)^c = A^c \cap B^c \qquad (A \cap B)^c = A^c \cup B^c$

Probability density function (p.d.f.)

If X is a continuous real-valued random variable, a probability density function (p.d.f.) for X is a real-valued function f which satisfies

$$P(a \leq X \leq b) = \int_a^b f(x)\,dx$$

for all $a, b \in R$.

Cumulative distribution function (c.d.f.)

The cumulative distribution function (c.d.f.) of the random variable X is defined by

$$F_X(x) = P(X \leq x)$$

$$F(x) = \int_{-\infty}^{x} f(t)dt$$

with f the p.d.f. for X.

Fundamentals of probability theory (cont.)

Expectation value and moments

The *expectation value* of any function $u(x)$ is

$$E[u(x)] = \int_{-\infty}^{\infty} u(x) f(x)\, dx.$$

The nth moment of a distribution is

$$\alpha_n \equiv E(x^n) = \int_{-\infty}^{\infty} x^n f(x) dx,$$

and the nth moment about the mean of x, α_1, is

$$m_n \equiv E[(x - \alpha_1)^n] = \int_{-\infty}^{\infty} (x - \alpha_1)^n f(x)\, dx.$$

The most commonly used moments are the mean μ and variance σ^2:

$$\mu \equiv \alpha_1$$
$$\sigma^2 \equiv \text{Var}(x) \equiv m_2 = \alpha_2 - \mu^2.$$

Characteristic function

The characteristic function $\phi(u)$ associated with the p.d.f. $f(x)$ is essentially its (inverse) Fourier transform, or the expectation value of $\exp(iux)$:

$$\phi(u) = E(e^{iux}) = \int_{-\infty}^{\infty} e^{iux} f(x) dx.$$

The nth moment of the distribution $f(x)$ is given by

$$i^{-n} \frac{d^n \phi}{du^n}\bigg|_{u\,=\,0} = \int_{-\infty}^{\infty} x^n f(x) dx = \alpha_n.$$

(This section was based upon material from *Introduction to Probability*, Grinstead, C.M. and Snell, J.L., http//www.dartmouth.edu/~chance/teaching_aids/books_articles/probability_book/book.html and *An Introduction to Statistical Inference and Data Analysis*, Michael W. Trosset, College of William & Mary, Williamsburg, VA, 2001.)

Probability distributions

Gaussian distribution

$$P_G(x, \mu, \sigma) = (\sigma\sqrt{(2\pi)})^{-1} \exp\left[-\frac{1}{2}\left(\frac{x-\mu}{\sigma}\right)^2\right],$$

where

x = value of random observation,

μ = mean value of parent distribution,

σ = standard deviation of parent distribution,

σ^2 = variance.

FWHM:

$$\Gamma = 2.354\sigma.$$

Probable error:

$$\text{PE} = 0.6745\sigma.$$

Gaussian probability distribution $P_G(x, \mu, \sigma)$ vs. $x - \mu; \Gamma = 2.354\sigma$ probable error (PE)= $0.6745\ \sigma$. (Adapted from Bevington, P. R.,; *Data Reduction and Error Analysis for the Physical Sciences*, McGraw-Hill Book Company, 1969.)

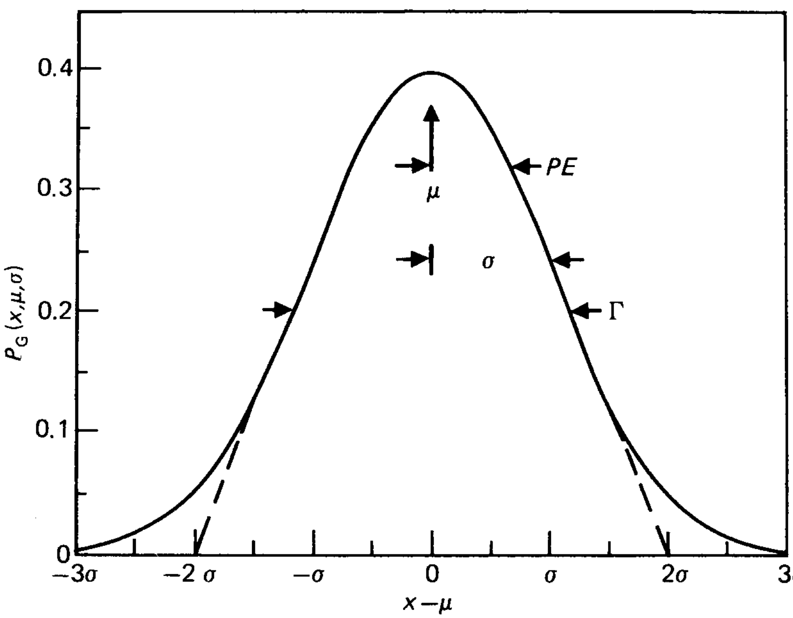

The Gaussian probability distribution $P_{\mathrm{G}}(x, \mu, \sigma)$ vs. $z = |x - \mu|/\sigma$.

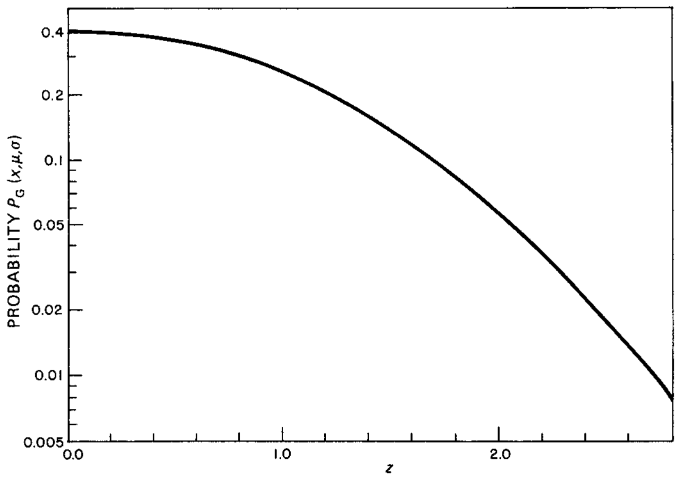

The integral of the Gaussian probability distribution

$A_{\mathrm{G}}(x, \mu, \sigma)$ vs. $z = |x - \mu|/\sigma$, where

$$A_{\mathrm{G}}(x, \mu, \sigma) = \int_{\mu - z\sigma}^{\mu + z\sigma} P_{\mathrm{G}}(x, \mu, \sigma) \mathrm{d}x$$

(Adapted from Bevington, P. R., *Data Reduction and Error Analysis for the Physical Sciences*, McGraw-Hill Book Company, 1969.)

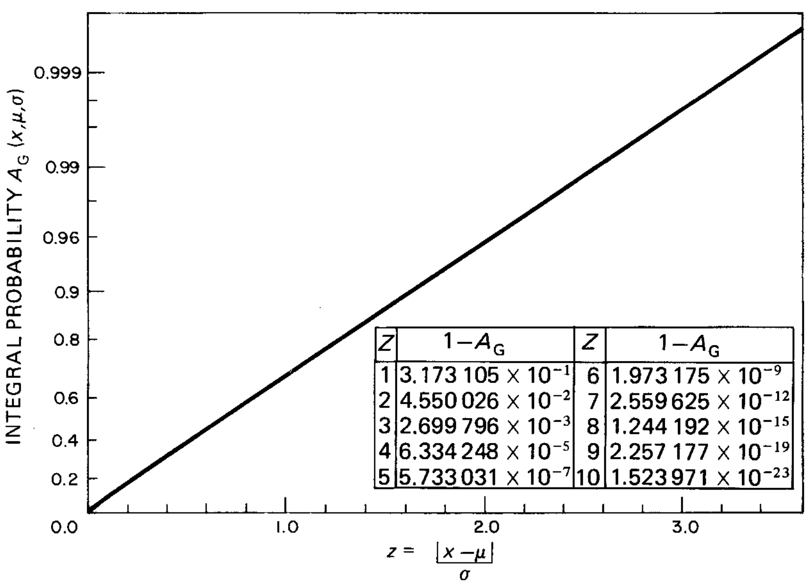

Z	$1 - A_G$	Z	$1 - A_G$
1	3.173105×10^{-1}	6	1.973175×10^{-9}
2	4.550026×10^{-2}	7	2.559625×10^{-12}
3	2.699796×10^{-3}	8	1.244192×10^{-15}
4	6.334248×10^{-5}	9	2.257177×10^{-19}
5	5.733031×10^{-7}	10	1.523971×10^{-23}

Binomial distribution

$$P_{\mathrm{B}}(x,n,p)=\frac{n!}{x!(n-x)!}p^x(1-p)^{n-x}$$

If p is the probability that an event will occur, then in a random group of n independent trials, P_{B} is the probability that the event will occur x times.

$$\mu=\text{mean}=np$$
$$\sigma^2=\text{variance}=np(1-p)$$

Poisson distribution

$$P_{\mathrm{P}}(x,\mu)=\frac{\mu^x}{x!}e^{-\mu}$$

P_p is the probability of observing x events when the average for a large number of trials is μ events.

$$\sigma^2=\text{variance}=\mu=\text{mean}$$

The probability of observing at least s events is:

$$P_p(x\geq s,\mu)=\sum_{x=s}^{\infty}\frac{\mu^x}{x!}e^{-\mu}$$

Confidence limits for Poisson statistics when the number of events is small

The customary estimate for the standard deviation of a Poisson distribution, $\sigma=\sqrt{n}$, where n is the number of events, is inadequate when n is small.

If n events are observed, the single-sided upper limit, λ_u, and lower limit, λ_l, for a confidence level CL are given by

$$\sum_{x=0}^{n}\lambda_u^x e^{-\lambda_u}/x!=1-\mathrm{CL},\ \sum_{x=0}^{n-1}\lambda_l^x e^{-\lambda_l}/x!=\mathrm{CL}\ (n\neq 0)$$

Gehrels (Gehrels, N., ApJ, **303**, 336, 1986) has provided tables and approximations for upper and lower limits for $n=0$ to 100 for various confidence levels. For a confidence level of 0.8413 the upper limit is given by the following simple expression

$\lambda_u\approx n+(n+3/4)^{1/2}+1$, and is accurate to 1.5% for all n.

Probability of n_t or more random events with Poisson distribution when the expected or mean number of events is $\overline{n}$ as a function of the threshold number n_t. (From RCA Electro-Optics Handbook, 1974.)

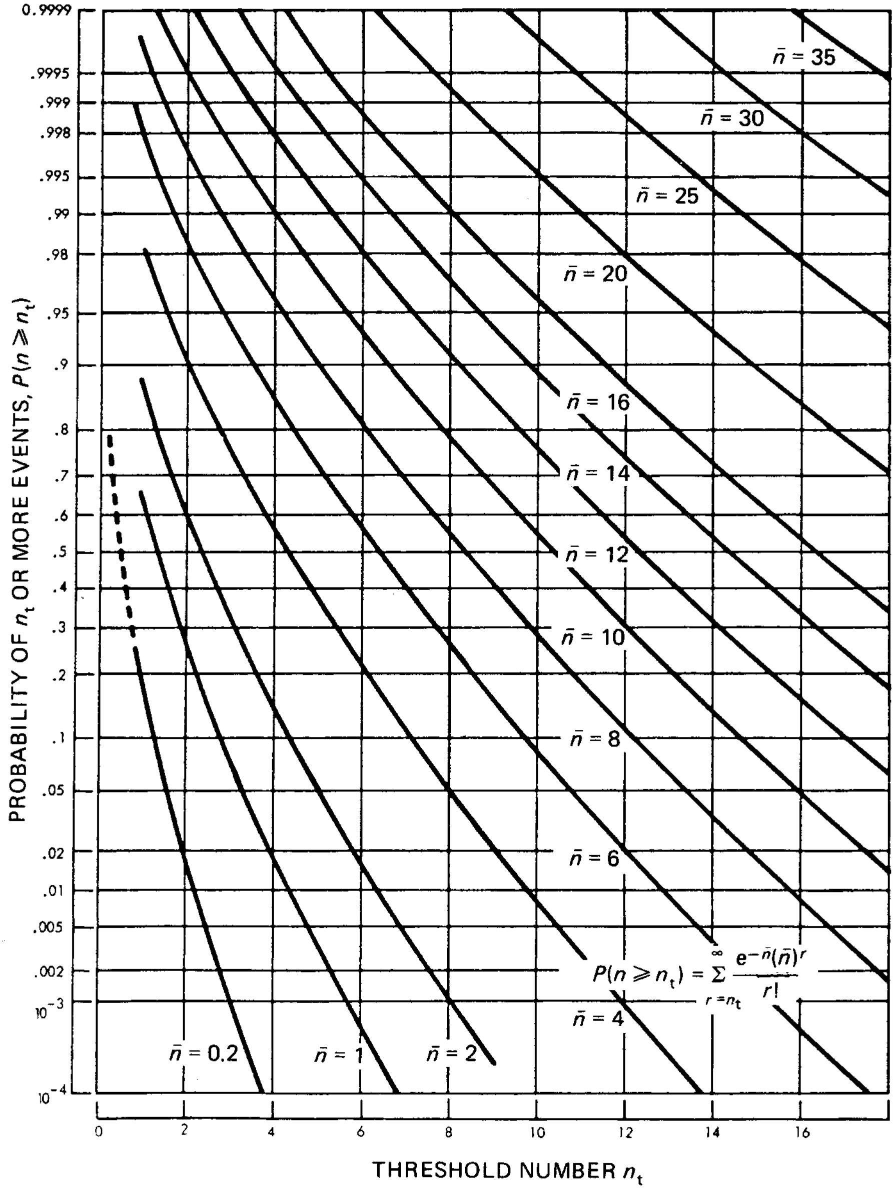

Poisson distribution (cont.)

Probability of n_t or more random events with Poisson distribution when the expected or mean number of events is $\overline{n}$ as a function of the threshold number n_t. Curves for $10^{-7} < \overline{n} < 10^{-4}$ are approximate. (From *RCA Electro-Optics Handbook*, 1974.)

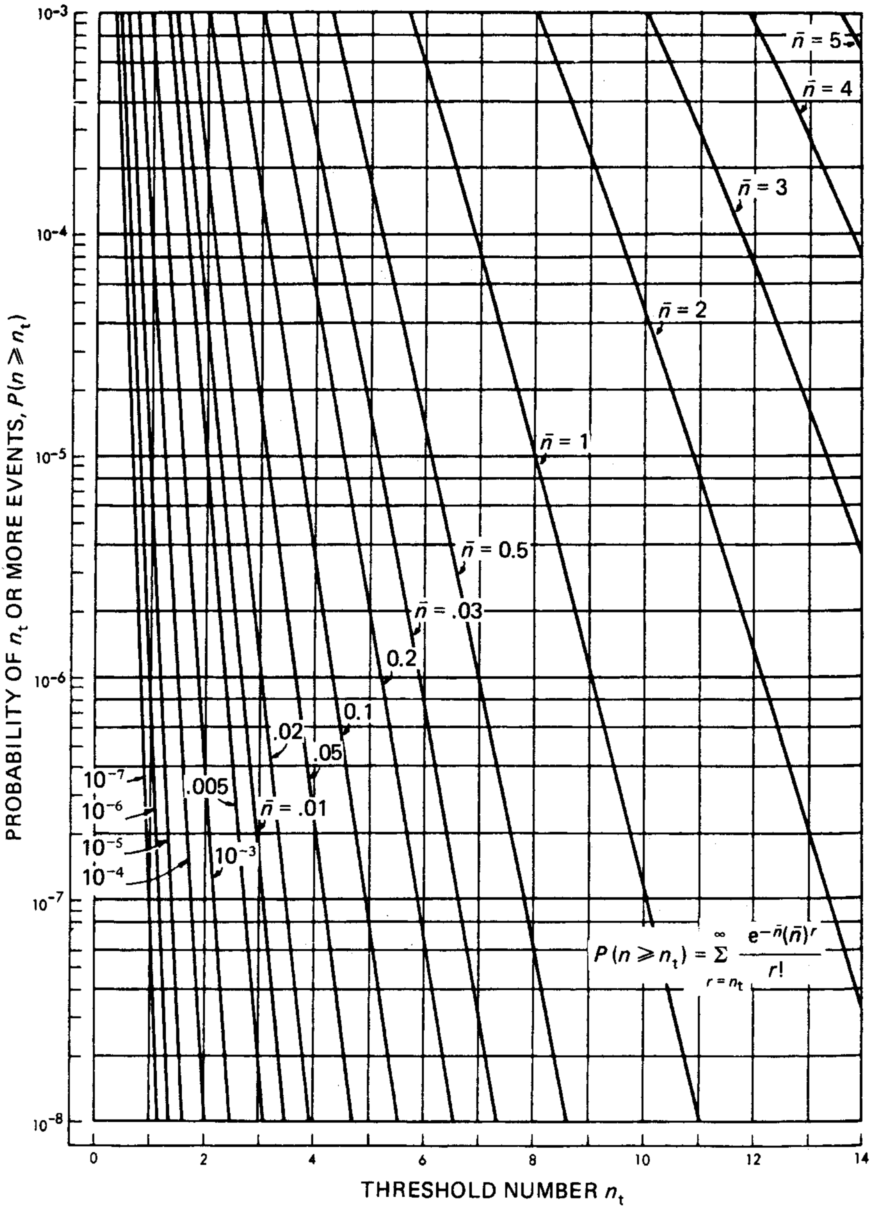

Chi-square distribution, confidence levels

The chi-square distribution for n_D degrees of freedom is given by:

$$P_{n_D}(\chi^2)d\chi^2 = \frac{1}{2^h\Gamma(h)}(\chi^2)^{h-1}e^{-\chi^2/2}d\chi^2$$

where h (for 'half') $= n_D/2$.

The confidence level CL associated with a given value of n_D and an observed χ^2 is the probability of χ^2 exceeding the observed value:

$$CL = \int_{\chi^2}^{\infty} d\chi^2 P_{n_D}(\chi^2)$$

χ^2 confidence level vs. χ^2 for n_D degrees of freedom. (From *Review of Particle Properties*, Lawrence Berkeley Laboratory, University of California, Berkeley, CA, 1982.)

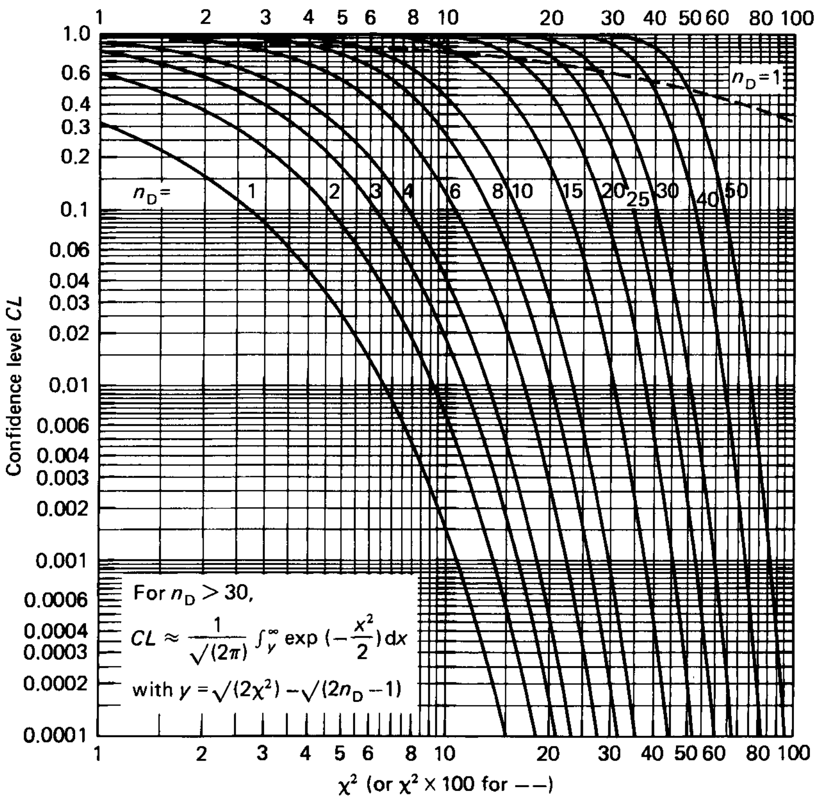

Table of common probability distributions

Distribution	$f(x)$	**Expectation** μ	**Variance** σ^2
Binomial $B(n,p)$	$\binom{n}{x}p^x(1-p)^{n-x}$ $x=0,1,\ldots,n$	np	$np(1-p)$
Geometric $G(p)$	$(1-p)^{x-1}p$ $x=1,2,3,\ldots$	$\frac{1}{p}$	$\frac{1-p}{p^2}$
Poisson $P(\lambda)$	$e^{-\lambda}\lambda^x/x!$ $x=0,1,2,\ldots$	λ	λ
Hypergeometric $H(N,n,p)$	$\frac{\binom{Np}{x}\binom{N-Np}{n-x}}{\binom{N}{n}}$	np	$np(1-p)\frac{N-n}{N-1}$
Negative binomial or Pascal $NB(r,p)$	$\binom{x-1}{r-1}p^r(1-p)^{x-r}$ $x=r,\ r+1,\ \ldots$	$\frac{r}{p}$	$\frac{r(1-p)}{p^2}$
Beta $\beta(p,q)$	$a_{p,q}x^{p-1}(1-x)^{q-1}$ $0\le x\le 1$ $a_{p,q}=\frac{\Gamma(p+q)}{\Gamma(p)\Gamma(q)}$ $p>0, q>0$	$\frac{p}{p+q}$	$\frac{pq}{(p+q)^2(p+q+1)}$
Weibull $W(\lambda,\beta)$	$\lambda^\beta\beta x^{\beta-1}e^{-(\lambda x)^\beta}$ $x\ge 0$ $F(x)=1-e^{-(\lambda x)^\beta}$	$\frac{1}{\lambda}\Gamma\left(1+\frac{1}{\beta}\right)$	$\frac{1}{\lambda^2}(A-B)$ $A=\Gamma\left(1+\frac{2}{\beta}\right)$ $B=\Gamma^2\left(1+\frac{1}{\beta}\right)$
Rayleigh $R(\sigma)$	$\frac{x}{\sigma^2}e^{-x^2/2\sigma^2}$ $x\ge 0$	$\sigma\sqrt{\frac{\pi}{2}}$	$2\sigma^2\left(1-\frac{\pi}{4}\right)$
Cauchy $C(a)$	$\frac{a}{\pi(a^2+x^2)}$	Does not exist	Does not exist

Table of common probability distributions (cont.)

Distribution	$f(x)$	**Expectation** μ	**Variance** σ^2
Uniform $U(a,b)$	$\frac{1}{b-a}$ $a \le x \le b$	$\frac{a+b}{2}$	$\frac{(b-a)^2}{12}$
Exponential $E(\lambda)$	$\lambda e^{-\lambda x}$ $x \ge 0$	$1/\lambda$	$1/\lambda^2$
Normed normal distribution $N(0,1)$	$\phi(x) = \frac{1}{\sqrt{2\pi}} e^{-x^2/2}$	0	1
General normal distribution $N(\mu,\sigma)$	$\frac{1}{\sigma}\phi\left(\frac{x-\mu}{\sigma}\right)$	μ	σ^2
Gamma $\Gamma(n,\lambda)$	$\frac{\lambda^n}{\Gamma(n)} x^{n-1} e^{-\lambda x}$	$\frac{n}{\lambda}$	$\frac{n}{\lambda^2}$
χ^2 $\chi^2(r)$	$\frac{1}{2^{r/2}\Gamma\left(\frac{r}{2}\right)} x^{\frac{r}{2}-1} e^{-\frac{x}{2}}$ $x \ge 0$ The parameter r is called the "number of degrees of freedom"	r	$2r$
t $t(r)$	$\frac{a_r}{b_r}\left(1+\frac{x^2}{r}\right)^{-\frac{r+1}{2}}$ $a_r = \Gamma\left(\frac{r+1}{2}\right)$ $b_r = \sqrt{r\pi}\,\Gamma\left(\frac{r}{2}\right)$	$0,\ r>1$	$\frac{r}{r-2},\ r>2$
F $F(r_1,r_2)$	$\frac{a_r x^{(r_1/r_2)-1}}{b_r(r_2+r_1x)^{\frac{r_1+r_2}{2}}}$ $x \ge 0$ $a_r = \Gamma\left(\frac{r_1+r_2}{2}\right) r_1^{r_1/2} r_2^{r_2/2}$ $b_r = \Gamma\left(\frac{r_1}{2}\right)\Gamma\left(\frac{r_2}{2}\right)$	$\frac{r_2}{r_2-2}$ $r_2 > 2$	$\frac{2r_2^2(r_1+r_2-2)}{r_1(r_2-2)^2(r_2-4)}$ $r_2 > 4$

(Adapted from Rade, L. and Westergren, B., *Beta Mathematics Handbook*, CRC Press, 1990)

Pearson's χ^2 test of distributions

$$\chi^2 = \sum_{j=1}^{n} \frac{[f(x_j) - NP(x_j)]^2}{NP(x_j)},$$

where

$f(x_j)$ = observed frequency distribution of possible observation x_j,
n = number of different values of x_j observed,
N = total number of measurements,
$P(x_j)$ = theoretical probability distribution.
$\chi_\nu^2 = \chi^2/\nu$ (for χ^2 tests, χ_ν^2 should be $\cong 1$),
ν = degrees of freedom = n − number of parameters calculated from the data to describe the distribution.

The probability $P_\chi(\chi^2, \nu)$ of exceeding χ^2 vs. the reduced chi-square $\chi_\nu^2 = \chi^2/\nu$ and the number of degrees of freedom ν.

$$P_\chi(\chi^2, \nu) = \frac{1}{2^{\nu/2}\Gamma(\nu/2)} \int_{\chi^2}^{\infty} (x^2)^{1/2(\nu-2)} e^{-x^2/2} dx^2$$

(Adapted from Bevington, P. R., *Data Reduction and Error Analysis for the Physical Sciences*, McGraw-Hill Book Company, 1969.)

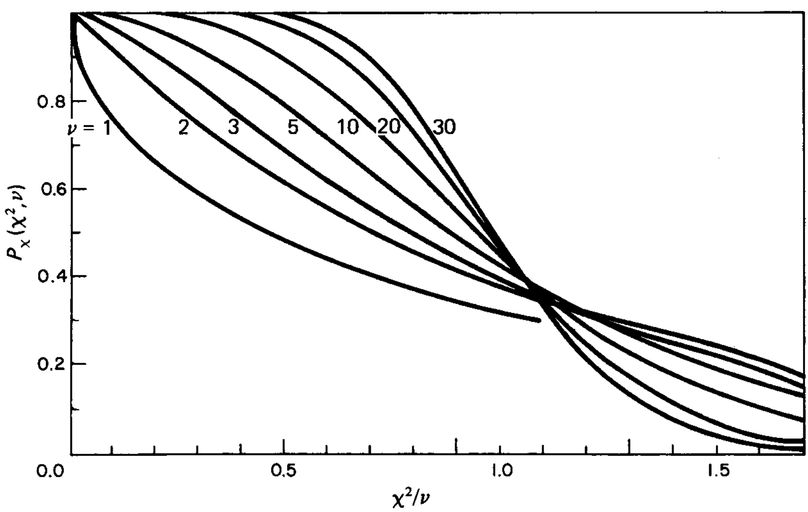

Propagation of errors

Sample mean:

$$\bar{x} = \frac{1}{N}\sum x_i \simeq \mu, \quad \text{parent mean.}$$

Sample variance:

$$s^2 = \frac{1}{N-1}\sum (x_i - \bar{x})^2 \simeq \sigma^2, \quad \text{parent variance.}$$

For $x = f(u, v, \ldots)$

$$\bar{x} = f(\bar{u}, \bar{v}, \ldots), \quad \text{the most probable value for } x\text{, and}$$

$$\sigma_x^2 \simeq \sigma_u^2 \left(\frac{\partial x}{\partial u}\right)^2 + \sigma_v^2 \left(\frac{\partial x}{\partial v}\right)^2 + 2\sigma_{uv}^2 \left(\frac{\partial x}{\partial u}\right)\left(\frac{\partial x}{\partial v}\right) + \cdots,$$

where

$$\sigma_u^2 = \lim_{N\to\infty} \frac{1}{N}\sum (u_i - \bar{u})^2, \quad \sigma_v^2 = \lim_{N\to\infty} \frac{1}{N}\sum (v_i - \bar{v})^2$$

and

$$\sigma_{uv}^2 = \lim_{N\to\infty} \frac{1}{N}\sum [(u_i - \bar{u})(v_i - \bar{v})], \quad \text{the covariance.}$$

For u and v uncorrelated, $\sigma_{uv}^2 = 0$.

Least-squares fit to a straight line

Linear function:

$$y(x) = a + bx.$$

Chi-square:

$$\chi^2 = \sum \left[\frac{1}{\sigma_i^2} (y_i - a - bx_i)^2 \right],$$

σ_i = standard deviation of the observation y_i

Least-squares fitting procedure:

minimize χ^2 with respect to each of the coefficients a and b simultaneously.

Coefficients of least-squares fit:

$$a = \frac{1}{\Delta} \cdot \left(\sum \frac{x_i^2}{\sigma_i^2} \sum \frac{y_i}{\sigma_i^2} - \sum \frac{x_i}{\sigma_i^2} \sum \frac{x_i y_i}{\sigma_i^2} \right)$$

$$b = \frac{1}{\Delta} \cdot \left(\sum \frac{1}{\sigma_i^2} \sum \frac{x_i y_i}{\sigma_i^2} - \sum \frac{x_i}{\sigma_i^2} \sum \frac{y_i}{\sigma_i^2} \right)$$

$$\Delta = \sum \frac{1}{\sigma_i^2} \sum \frac{x_i^2}{\sigma_i^2} - \left(\sum \frac{x_i}{\sigma_i^2} \right)^2$$

Estimated variance:

$$\sigma^2 \simeq s^2 = \frac{1}{N-2} \sum (y_i - a - bx_i)^2$$

s^2 = sample variance

Uncertainties in coefficients:

$$\sigma_a^2 \simeq \frac{1}{\Delta} \sum \frac{x_i^2}{\sigma_i^2} \qquad \sigma_b^2 \simeq \frac{1}{\Delta} \sum \frac{1}{\sigma_i^2}$$

Bibliography

Data Analysis for Scientists and Engineers, Meyer, S.L., Peer Management Consultants, Ltd., Evanston, IL, 1986.

Data Reduction and Error Analysis for the Physical Sciences, Bevington, P.R. and Robinson, D.K., McGraw-Hill, 1992.

Fundamentals of Probability, Ghahramani, S., Prentice Hall, 1996.

Introduction to Probability, Grinstead, C.M. and Snell, J.L., http://www.dartmouth.edu/~chance/teaching_aids/books_articles/probability_book/book.html.

An Introduction to Probability Theory and Its Applications, Feller, W., John Wiley & Sons, Vol. 1, 1968, Vol. II, 1971.

Mathematical Statistics and Data Analysis, Rice, J.A., Duxbury Press, 1995.

Statistical Methods in Experimental Physics, Eadi, W.T., et al., North-Holland Publishing Co., 1971.

Statistics for Nuclear and Particle Physicists, Lyons, L., Cambridge University Press, 1986.

Note: Links to WWW resources which supplement the material in this chapter can be found at:

http://www.astrohandbook.com

Chapter 18

Radiation safety

They say atomic radiation can hurt your reproductive organs. My answer is so can a hockey stick. But we don't stop building them. - Johny Carson

Definitions

The International Commission on Radiation Units and Measurements (ICRU) recommends the use of SI units. Therefore SI units are listed first, followed by cgs (or other common) units in parentheses.

Unit of activity = becquerel (curie):
1 Bq = 1 disintegration s^{-1}(= $1/(3.7 \times 10^{10})$ Ci)

Unit of absorbed dose = gray (rad):
1 Gy = 1 joule kg^{-1}(= 10^4 erg g^{-1} = 100 rad)
(= 6.24×10^{12} MeV kg^{-1}) deposited energy

Unit of exposure, the quantity of x- or γ-radiation at a point in space integrated over time, in terms of charge of either sign produced by showering electrons in a small volume of air about the point:
= 1 coul kg^{-1} of air (roentgen; 1 R = 2.58×10^{-4} coul kg^{-1})
1 R = 1 esu cm^{-3}(= 87.8 erg = 5.49×10^7 MeV released energy per g of air)

Unit of equivalent dose (for biological damage) = sievert (= 100 rem (roentgen equivalent for man)): Equivalent dose in Sv = absorbed dose in grays × w_R, where w_R (radiation weighting factor, formerly the quality factor Q) expresses long-term risk (primarily cancer and leukemia) from low-level chronic exposure. It depends upon the type of radiation and other factors, as follows:

Radiation weighting factors

Radiation	w_R
X- and γ-rays, all energies	1
Electrons and muons, all energies	1
Neutrons < 10 keV	5
10 – 100 keV	10
> 100 keV to 2 MeV	20
2 – 20 MeV	10
> 20 MeV	5
Protons (other than recoils) > 2 MeV	5
Alphas, fission fragments, & heavy nuclei	20

(Adapted from C. Caso *et al.*, European Physical Journal **C3**, 1, 1998)

Radiation levels and exposures

Natural annual background, all sources: Most world areas, whole-body equivalent dose rate $\approx (0.4-4)$ mSv $(40-400$ millirems). Can range up to 50 mSv (5 rems) in certain areas. U.S. average ≈ 3.6 mSv, including ≈ 2 mSv (≈ 200 mrem) from inhaled natural radioactivity, mostly radon and radon daughters (0.1-0.2 mSv in open areas). Average is for a typical house and varies by more than an order of magnitude. It can be more than two orders of magnitude higher in poorly vertilated mines.

Cosmic ray background at the Earth's surface:
~ 1 min^{-1} cm^{-2} sr^{-1}.

Fluence (per cm^2) to deposit one Gy, assuming uniform irradiation:
charged particles – $6.24 \times 10^9/(dE/dx)$, where dE/dx (MeV g^{-1} cm^2) is the stopping power.
$\approx 3.5 \times 10^9$ cm^{-2} minimum-ionizing singly-charged particles in carbon.
photons – $6.24 \times 10^9/[Ef/\lambda]$, for photons of energy E (MeV), attenuation length λ (g cm^{-2}), and fraction $f \lesssim 1$ expressing the fraction of the photon's energy deposited in a small volume of thickness $\ll \lambda$ but large enough to contain the secondary electrons.
$\approx 2 \times 10^{11}$ photons cm^{-2} for 1 MeV photons on carbon ($f \approx 1/2$).
(Quoted fluences are good to about a factor of 2 for all materials.)

Recommended limits to exposure of radiation workers (whole-body dose):

CERN: 15 mSv yr^{-1}

U.K.: 15 mSv yr^{-1}

U.S.: 50 mSv yr^{-1} (5 rem yr^{-1})

Lethal dose: Whole-body dose from penetrating ionizing radiation resulting in 50% mortality in 30 days (assuming no medical treatment) $2.5-3.0$ Gy $(250-300$ rads), as measured internally on body longitudinal center line. Surface dose varies due to variable body attenuation and may be a strong function of energy.

(Adapted from C. Caso, *et al.*, European Physical Journal **C3**, 1, 1998)

Radioactive materials in the body

Radionuclide	Body content in 70 kg man (picocurie)	Body content in 70 kg man (dis/min)	Annual dose (mrad)
^{40}K	120,000	266,000	18 (whole body)
^{14}C	87,000	193,000	1 (whole body)
^{226}Ra	40	89	0.7 (bone lining)
^{210}Po	500	1,110	0.6 (gonads)
			3 (bone)
^{90}Sr (1973)	1,300	2,886	2.6 (endosteal bone)
			1.8 (bone marrow)

(UNSCEAR, 1977; NCRP, 1975, Report no., 45 (^{90}Sr))
NCRP: National Council on Radiation Protection and Measurements.
UNSCEAR: United Nations Scientific Committee on the Effects of Atomic Radiation.

Average annual population dose equivalents from selected consumer products and miscellaneous sources

Product	mrem
TV Receiver	0.50
Airport X-ray	0.001
Luminous Watches	0.05
Tobacco Products	2000
Coal Combustion	1
Natural Gas Combustion	5
Uranium in Debentures (old style)	1500

(Adapted from NCRP Report no. 56; University of Maryland Radiation Training Mannual, 1994)

Selected products containing radioactive material

Product	Nuclides	Amount
Radioactive Material Contained in Paint or Plastic:		
Time pieces	H–3	1–25 mCi
	Pm–147	65–200 μCi
	Ra–226	0.1–3 μCi
Compasses	H–3	5–50 mCi
	Pm-147	10 μCi
Thermostat dials and pointers	H–3	25 mCi
Automobile shift quadrants	H–3	25 mCi
Speedometers	Pm–147	0.1 mCi
Radioactive Material Contained in Sealed Tubes:		
Time pieces, marine navigational instruments	H–3	0.2–2 Ci
Exit signs, stepmarkers, public telephone dials, light switch markers	H–3	0.2–30 Ci
Electronic and Electrical Devices:		
Fluorescent lamp starters	Ra–226	1 μCi
Vacuum tubes, electric lamps, germicidal lamps	Natural Thorium	50 mg
Glow lamps	H–3	0.01 mCi
High voltage protection devices	Pm–147	3 μCi
Low voltage fuses	Pm–147	3 μCi
Miscellaneous:		
Smoke and fire detectors	Am–241	1–100 μCi
	Ra–226	0.01–15 μCi
	Kr–85	7 mCi
Incandescent gas mantles	Natural Thorium	0.5 gm
Ceramic tableware glaze	Natural Uranium or Thorium	20% by weight of the glaze

(Adapted from UNSCEAR 1977 Report, University of Maryland Radiation Training Manual, 1994)

Naturally occurring radiation sources (pCi g^{-1})

Type of Rock	K–40	U–238	Th–232
Acidic (e.g. granite)	27	1.6	2.2
Intermediate (e.g. diorite)	19	0.62	0.88
Mafic (e.g. basalt)	6.5	0.31	0.30
Ultrabasic (e.g. durite)	4.0	0.01	0.66
Sedimentary			
Limestone	2.4	0.75	0.19
Carbonate	—	0.72	0.21
Sandstone	10	0.5	0.3
Shale	19	1.2	1.2

(UNSCEAR 1977 Report)

In various parts of the world, there are areas with high natural radiation levels. At the beach of the Black Sands in Guarppari, State of Espirto Santos, Brazil, it is possible to receive a radiation exposure of 5 mrad/hr due to the monazite (Thorium bearing minerals) sands. At Pocos de Caldas, State of Gerais, Brazil, the average range of radiation exposure is from 0.1–3 mrad/hr.

Naturally occurring radionuclides can give rise to external doses when contained in raw materials used to construct roads and buildings. Uranium and thorium are commonly found in cement, concrete blocks, and masonry products. For example, the possible annual dose near a granite wall at the "Redcap Stand" in Grand Central Station, New York is 200 mrem (assuming an occupancy of 8 hrs/day).

(From University of Maryland Radiation Training Manual, 1994)

Medical exposures

Patient Skin Entrance Exposure, per Film

Technique	mrad
Sacral Spine	2180
Barium Enema	1320
Upper GI Series	710
Dental Bite-Wing	400
Skull	330
Chest	44

(Bureau of Radiological Health)

Maximum permissible flux for occupational exposure to various types of ionizing radiations

Type of radiation	QF or RBE[a]	Average exposure rate[b] (mrad wk^{-1})	Approximate flux to give a maximum permissible exposure in an 8-hr day[c]
X- and gamma-rays	1	100	$[1400/E]$ photons cm^{-2} s^{-1} in free air at 0°C (error < 13% for $E = 0.07$ to 2 MeV)
Beta-rays and electrons	1	100	$[(4.3 \times 10^7)/P]$ electrons or beta-rays cm^2 s^{-1} [d]
Thermal neutrons	2.5	40	700 thermal neutrons cm^{-2} s^{-1} [d]
Fast neutrons	10	10	19 neutrons of 2-MeV energy cm^{-2} s^{-1} [d]
Alpha particles	10	10	$[(4.3 \times 10^7)/P]$ alpha particles cm^{-2} s^{-1} [d]
Protons	10	10	$[(4.3 \times 10^7)/P]$ protons cm^{-2} s^{-1}[d]
Heavy ions	20	5	$[(4.3 \times 10^7)/P]$ heavy ions cm^{-2} s^{-1} [d]

[a] RBE, relative biological effectiveness.

[b] Average occupational exposure rate permissible to blood-forming organs (essentially total body exposure), gonads, and eyes of persons of age 18 or over. These values may be averaged over a year, provided the dose in any thirteen weeks does not exceed 3 rem (rem = RBE × rad). All rates may be increased by a factor of 6 if the exposure is primarily to the skin, thyroid, or bone. They may be increased by a factor of 3 if the exposure is limited to organs other than blood-forming organs, gonads, or eyes.

[c] Maximum permissible exposure rate based on a 20-mrem dose delivered to tissue in an 8-hr day. P is the stopping power in units of electron volts per g cm^{-2} of soft tissue.

[d] Incident on tissue.

(Adapted from *Nuclear Instruments and Their Uses*, A.H. Snell, ed., John Wiley and Sons, 1962.)

Note: Maximum permissible radiation exposures are subject to revision. If you are working with radiation sources, you should consult with your radiation safety officer or the National Council on Radiation Protection and Measurements (NCRP) for the latest permissible exposures.

Maximum permissible flux for occupational exposure to various types of ionizing radiations (*cont.*)

Stopping power as a function of energy. (Adapted from *Nuclear Instruments and Their Uses*, A.H. Snell, ed., John Wiley and Sons, 1962.)

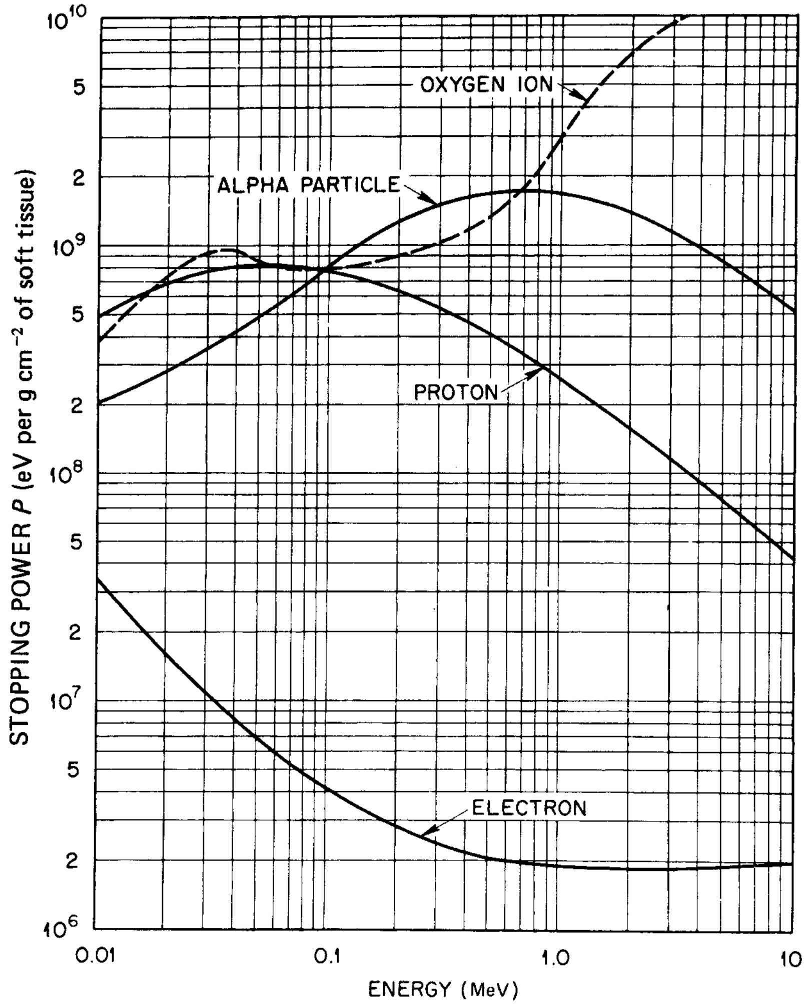

Occupational dose limits

Exposed Area	REM/Year	Sieverts/Year
Whole body – head and trunk; gonads; arms above elbow, legs above the knee	5.0	0.050
Extremities – hands and forearms; feet and ankles, leg below the knee	50.0	0.50
Skin	50.0	0.50
Lens of eyes	15.0	0.15
Any Individual Organ or Tissue	50.0	0.50
Embryo/Fetus (Entire Period)	0.5	0.005

(University of Maryland Radiation Training Manual, 1994)

Annual dose rates to population in USA

Natural Background	**mrem/yr**
Cosmic	28
Terrestrial	26
Internal–C–14, Ra–226, Pm–222, K-40	28
	82
Medical	
Diagnosis	77
Dental	1.4
Radiopharmaceutical	13.6
	92.0
Other	
Weapon Tests (Fallout)	5
Power Plant and Nuclear Industry	$<$ 1
Building Materials (brick, masonry)	5
TV Receivers	0.5
Airline Travel	0.5
	12.0
Total	186.0 mrem/yr

(University of Maryland Radiation Training Manual, 1994)

Comparison of calculated cosmic-ray doses to a person flying in subsonic and supersonic aircraft (average solar conditions)

	Subsonic Flight at 11 km		Supersonic Flight at 19 km	
Route	Flight duration (hr)	Dose per round trip (mrad)	Flight duration (hr)	Dose per round trip (mrad)
Los Angles-Paris	11.1	4.0	3.8	3.7
Chicago-Paris	8.3	3.6	2.8	2.6
New York-Paris	7.4	3.1	2.6	2.4
New York-London	7.0	2.9	2.4	2.2
Los Angles-New York	5.2	1.9	1.9	1.3
Sydney-Acapulco	17.4	4.4	6.2	2.1

(UNSCEAR 1977 Report; University of Maryland Radiation Training Manual, 1994)

Absorbed dose in chests of astronauts on space missions

Mission or Mission Series	Launch Date (Yr-Mo-Dy)	Duration of Mission (Hr)	Type of Orbit	Dose (mrad)
Apollo VII	68-08-11	260	Earth Orbital	157
Apollo VIII	68-12-21	147	Circumlunar	150
Apollo IX	69-02-03	241	Earth Orbital	196
Apollo X	69-05-18	192	Circumlunar	480
Vostok 18-6			Earth Orbital	2-80
Voskhad 1,2			Earth Orbital	30-70
Soyuz 3-9			Earth Orbital	62-234

The table shows the doses received by astronauts on various space missions. The largest part of the dose was received when the spacecraft passed through the earth's radiation belts. The belts contain protons, electrons, and alpha particles trapped by the earth's magnetic fields.

(UNSCEAR 1977 Report; University of Maryland Radiation Training Manual, 1994)

Clinical effects of acute whole-body radiation doses

Acute Dose (rads)	Probable Effect
0–50	No obvious effect, except possibly minor blood changes.
80–120	Vomiting and nausea for about 1 day in 5 to 10 per cent of exposed personnel. Fatigue but no serious disability.
130–170	Vomiting and nausea for about 1 day, followed by other symptoms of radiation sickness in about 25 per cent of personnel. No deaths anticipated.
180–220	Vomiting and nausea for about 1 day followed by other symptoms of radiation sickness in about 50 per cent of personnel. No deaths anticipated.
270–330	Vomiting and nausea in nearly all personnel on first day, followed by other symptoms of radiation sickness. About 20 per cent deaths within 2 to 6 weeks after exposure; survivors convalescent for about 3 months.
400–500	Vomiting and nausea in all personnel on first day, followed by other symptoms of radiation sickness. About 50 per cent deaths within 1 month; survivors convalescent for about 6 months.
550–750	Vomiting and nausea in all personnel within 4 hours from exposure, followed by other symptoms of radiation sickness. Up to 100 per cent deaths; few survivors convalescent for about 6 months.
1000	Vomiting and nausea in all personnel within 1 to 2 hours. Probably no survivors from radiation sickness.
5000	Incapacitation almost immediately. All personnel will be fatalities within 1 week.

(*The Effects of Nuclear Weapons U.S. Government Printing Office, May 1957*)

The relation of time of death to whole-body radiation dose that defines the major lethal modalities. The dashed line over "therapy" defines the area in which symptomatic therapy of radiation damage is known to reduce human and animal mortality. (Adapted from *Accelerator Health Physics*, Patterson, H.W. and Thomas, R.H., Academic Press, 1973.)

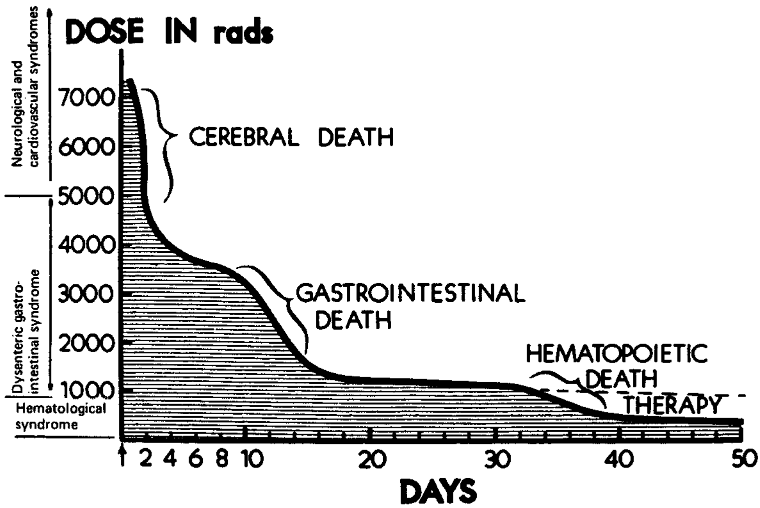

Effect of a nuclear detonation–fallout pattern

Fallout pattern for a 5 megaton thermonuclear air detonation (1000 m altitude). Peak dose rates (R/hr) and the time of peak (curved lines) for a 15 mph wind are shown. The energy released by the detonation is 2×10^{16} joules. (From the Defense Civil Preparedness Agency (DCPA), 1973).

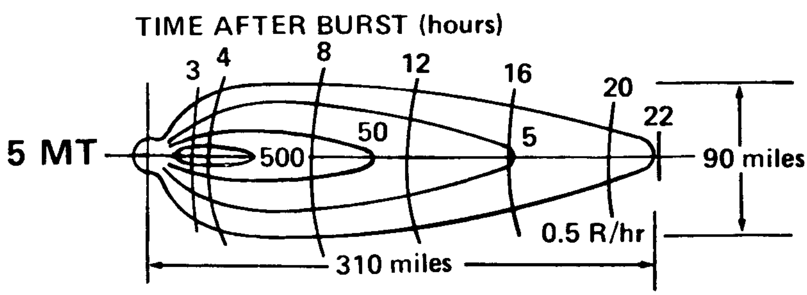

Bibliography

Accelerator Health Physics, Patterson, H.W. and Thomas, R.H., Academic Press, 1973.

A Handbook of Radioactivity Measurement Procedures, NCRP Report No. 58, National Council of Radiation Protection and Measurements, Washington, DC 20014, 1978.

Principles of Radiation Protection, Morgan, K.Z. and Turner, J.E., eds,. John Wiley & Sons., Inc., 1967.

Radiation Protection, A Guide for Scientists and Physicians, Shapiro, J., Harvard University Press, 1990.

Note: Links to WWW resources which supplement the material in this chapter can be found at:

http://www.astrohandbook.com

Chapter 19

Astronomical catalogs

The astronomers must be very clever to have found out the names of all the stars. - Unknown

Astronomical catalogs

Note: This chapter has not been updated since the 2nd edition. There are now numerous catalogs online and new one being produced at a rapid pace. See, for example, http://cdsweb.u-strasbg.fr/Cats.html.

X-ray sources

Amnuel, P. R., Cuseinov, O. H. & Rakhamimov, Sh. Yu., 1979, *Ap. J. Suppl.,* **41**, 327.

Bradt, H. V., Doxsey, R. E. & Jernigan, J. G., 1978, *Adv. Space Exploration*, **3**.

Forman, W. *et al.*, 1978, *Ap. J. Suppl.*, **38**, 357.

Cooke, B. A. *et al.*, 1978, *M.N.R.A.S.*, **182**, 489.

Markert, T. H. *et al.*, 1979, *Ap. J. Suppl.*, **39**, 573.

Marshall, F. E. *et al.*, 1978, *NASA Tech Mem.* 79694.

Radio sources

Dixon, R. S., 1970, *Ap. J. Suppl.*, **20**, 1.

Finlay, E. A. & Jones, B. B., 1977, *Aust. J. Phys.*, **26**, 389.

NGC/IC objects

Sulentic, J. W. & Tifft, W. G., 1973, *The Revised New General Catalog of Non-Stellar Astronomical Objects*, University of Arizona Press.

Schmidtke, P. C., Dixon, R. S. & Gearhart, M. R., 1979, *Palomar Sky Survey Overlays*, Ohio State University Radio Observatory.

Optical (non-stellar)

Dixon, R. S. & Sonneborn, G., 1979, *Master Optical List*, Ohio State University Radio Observatory.

Infrared sources

Schmitz, M. *et al.*, 1978, *Merged Infrared Catalog*, NASA Tech. Mem. 79683. Goddard Space Flight Center, Greenbelt, Maryland.

Price, S. & Walker, R., 1976, *The AFGL Four Color Infrared Sky Survey*, AFGL-TR-76-0208, Hanscom AFB, Massachusetts (*Supplement:* AFGL-TR-77-0160, 1977).

Gezari, D. Y. *et al.*, 1984, *Catalog of lnfrared Observations*, NASA ref. pub. 1118.

Gamma-ray sources

Wills, R. D. *et al.*, 1980 *Adv. in Space Exploration*, Vol. 7, Pergamon Press.

Quasars

de Veny, J. B., Osborn, W. H. & Hanes, K., 1972, *Pub. A.S.P.*, **83**, 611.

Burbidge, G. R., Crowne, A. H. & Smith, H. E., 1977, *Ap. J. Suppl.,* **33**, 113.

Hewitt, A. & Burbidge, A., 1987, *Ap. J. Suppl.*, **63**, 1.

Hewitt, A. & Burbidge, G. R., 1980, *A Revised Optical Catalogue of Quasi-Stellar Objects, Ap. J. Suppl.*, **43**, 57.

Clusters of galaxies

Abell, G., 1958, *Ap. J. Suppl.*, **3**, 211.

Klemola, A. R., 1969, *A.J.*, **74**, 804.

Seyfert galaxies

Weedman, D. W., 1977, *Ann. Rev. Astr. Ap.*, **15**, 69.

Adams, T. F., 1977, *Ap. J. Suppl.*, **33**, 19.

Markarian galaxies

Peterson, S. D., 1973, *A.J.*, **78**, 811.

Galaxies

Sandage, A., 1961, *The Hubble Atlas of Galaxies,* Carnegie Institute, Washington, DC.

Zwicky, F. *et al.*, 1961–68, *Catalog of Galaxies and Clusters of Galaxies*, 6 vols., Calif. Inst. Tech. (Pasadena).

Vorantsov-Velyaminov, 1964, *Morphological Catalog of Galaxies.*

Bright galaxies

de Vaucouleurs, G. & de Vaucouleurs, A., 1964, *Reference Catalog of Bright Galaxies*, University of Texas Press (Austin).

Dressel, L. L. & Condon, J. J., 1976, *Ap. J. Suppl.*, **31**, 187.

Peculiar galaxies

Arp, H., 1966, *Ap. J. Suppl.*, **123**, 1.

H II regions in galaxies

Hodge, P. W., 1969, *Ap. J. Suppl.*, **157**, 73.

Lynds, B. T., 1974, *Ap. J. Suppl.*, **267**, 391.

Infrared galaxies

Reike, G. H., 1978, *Ap. J.*, **226**, 550.

Reike, G. H. & Lebofsky, M. J., 1978, *Ap. J.*, **220**, L37.

Reike, G. H. & Low, F. J., 1972, *Ap. J.*, **176**, L95.

Neugebauer, G., Becklin, E. E., Oke, J. B. & Searle, L., 1976, *Ap. J.*, **205**, 29.

Kleinmann, D. E. & Low, F. J., 1970, *Ap. J.*, **159**, L165.

Stars

AGK3 Star Catalogue, 1975, Hamburger Sternwarte (Hamburg).

Smithsonian Astrophysical Observatory Star Catalog, 1966, Smithsonian Publ. 4652, US Government Printing Office, Washington, DC.

Hofleit, D., 1964, *Catalogue of Bright Stars*, Yale University Observatory (New Haven).

Fricke, W. & Kopf, A., 1963, *Fourth Fundamental Catalog (FK4)*, Braun (Karlsruhe).

Nagy, T. A. & Mead, J., 1978, *HD-SAO-DM Cross Index*, NASA Tech. Mem 79564, Goddard Space Flight Center, Greenbelt, Maryland.

Schmidtke, P. C., Dixon, R. S. & Gearhart, M. R., 1979, *Palomar Sky Survey Overlays*, Ohio State Radio Observatory.

Gottlieb, D. M., 1978, *Ap. J. Suppl.*, **38**, 287.

Hirshfeld, A. & Sinnott, R. W., 1981, *Sky Catalogue 2000.0*, Sky Publishing Corp. (Cambridge, MA).

Rufener, F., 1980, *Third Catalogue of Stars Measured in the Geneva Observatory Photometric System*, Observatoire de Genève, Switzerland.

Star clusters and associations

Alter, G., Balázs, B. & Ruprecht, J., 1970, *Catalogue of Star Clusters and Associations*, Akadémiai Kiado (Budapest).

Fenkart, R. P. & Binggeli, B., 1979, *Astron. Ap. Suppl.*, **35**, 271.

Becker, W. & Fenkart, R., 1971, *Astron. Ap. Suppl.*, **4**, 241.

Supergiants, O stars, and OB associations

Humphreys, R. M., 1978, *Ap. J. Suppl.*, **38**, 309.

Cruz-Gonzales, C., Recillas-Cruz, E., Costero, R., Peimbert, M. & Torres-Peimbert, S., 1974, *Revista Mexicana de Astronomia y Astrofisica,* **1**, 211.

Luminous Stars in the Northern Milky Way, 6 vols., 1959–65, Hamburger Sternwarte and Warner and Swasey Observatories (Hamburg-Bergedorf).

Variable stars

Kukarkin, B. V. *et al.*, 1969, *Catalogue of Variable Stars,* 3rd edn. Astron. Council of the Academy of Sciences in the USSR (Moscow) (plus *Supplements*).

Ultraviolet

Catalogue of Stellar Ultraviolet Fluxes, 1978, The Science Research Council.

White dwarfs

McCook, G.P. & Scion, E. M., 1977, *Obs. Contrib.*, No. 2, Villanova Univ.

Nearby stars

Gliese, W., 1969, *Catalogue of Nearby Stars*, Veröffentlichungen des Astronom., Rechen-Inst., Heidelberg, No. 22, Verlag G. Braun (Karlsruhe).

Woolley, R., Epps, E. A., Penston, M. J. & Pocock, S. B., 1970, *Roy. Obs. Ann.*, No. 5.

Halliwell, M. J., 1979, *Ap. J. Suppl.*, **41**, 173.

Gliese, W. & Jahreiss, H., 1979, *Astron. Astrophys. Suppl.*, **38**, 423.

Proper motion and halo stars

Eggen, O. J., 1979, *Ap. J.*, **230**, 786.

Eggen, O. J., 1979, *Ap. J. Suppl.*, **39**, 89.

Eggen, O. J., 1980, *Ap. J.*, **43**, 457.

Luyten, W. J., 1979, *NLTT Catalogue*, 4 parts, Univ. of Minnesota (Minneapolis).

Luyten, W. J., 1963, *Bruce Proper Motion Survey*, 2 vols., Univ. of Minnesota (Minneapolis).

Luyten, W. J., 1961, *A Catalog of 7127 Stars in the Northern Hemisphere with Proper Motions Exceeding 0.2 arcsec Annually*, Lund Press (Minn.).

Luyten, W. J., 1976, *A Catalog of Stars with Proper Motions Exceeding 0.5 arcsec Annually*, University of Minnesota (Minneapolis).

Giclas, H., Burnham, R. Jr. & Thomas, N. G., 1971, *Lowell Proper Motion Survey (The G Numbered Stars), Lowell Obs. Bull.:* Nos. 118, 125, 141, 153, 163, Lowell Obs., Flagstaff (Arizona).

Double stars

Aitken, R. G., 1932, *New General Catalog of Double Stars within 120° of the North Pole*, Publ. 417, Carnegie Inst., Washington.

Radial velocities

Abt, H. A. & Biggs, E. S., 1972, *A Bibliography of Stellar Radial Velocities,* Kitt Peak National Observatory.

Evans, D. S., 1978, *Catalog of Stellar Radial Velocities* (microfiche).

Moore, J. H., 1932, *A General Catalog of the Radial Velocities of Stars, Nebulae, and Clusters*, Publ. of Lick Obs., Vol. 18, Univ. of Calif. Press (Berkeley).

Wilson, R. E., 1953, *General Catalog of Stellar Radial Velocities Prepared at Mount Wilson Observatory*, Publ. 601, Carnegie lnst., Washington.

Stellar spectra

Houk, N. & Cowley, A. P., 1975, *Univ. of Michigan Catalog of Two-Dimensional Spectral Types for the HD Stars,* Vol. I (Ann Arbor).

Buscombe, W., 1977, *MK Spectral Classifications, Third General Catalog,* Northwestern Univ. (Evanston, Illinois).

Kennedy, P. M. & Buscombe, W., 1974, *MK Spectral Classifications Published Since Jaschek's La Plata Catalog,* Northwestern Univ. (Evanston, Illinois).

Jaschek, C., Conde, H. & de Sierra, A. C., 1964, *Catalog of Stellar Spectra Classified by the Morgan-Keenan System*, Obs. Astron. de la Univ. Nacional de la Plata (Argentina).

Seitter, W. C., 1970, *Atlas für Objektiv-Prismen-Spektren,* Dümmler (Bonn).

Breakiron, L. A. & Upgren, A. R., 1979, *Ap. J. Suppl.*, **41**, 709.

Globular clusters

Harris, W. E., 1976, *A.J.*, **81**, 1095.

Arp, H., 1966, in *Galactic Structure*, eds. A. Blaauw & M. Schmidt, Univ. of Chicago Press, p. 401.

Planetary nebula

Perek, L. & Kohoutek, L., 1967, *Catalogue of Galactic Planetary Nebula*, Czechoslovak Acad. of Sciences (Prague).

Reflection nebulae

van den Bergh, S., 1966, *A.J.*, **71**, 990.

Supernova remnants

Downes, D., 1971, *A.J.*, **76**, 305.
Clark, D. and Caswell, J., 1976, *M.N.R.A.S.*, **174**, 267.

Pulsars

Manchester, R. N., Lyne, A. G., Taylor, J. H., Durdin, J. M., Large, M. I. & Little, A. G., 1978, *M.N.R.A.S.*, **185**, 409.
Damashek, M., Taylor, J. H. & Hulse, R. A., 1978, *Ap. J.*, **225**, L31.

OH masers

Turner, B. E., 1979, *Astron. Ap. Suppl.*, **37**, 1.

CO clouds

Kutner, M. L., Machnik, D. E., Tucker, K. D. & Dickman, R. L., 1980, *Ap. J.*, **237**, 734.

H II regions and spiral structure

Georgelin, Y. M. & Georgelin, Y. P., 1976, *Astron. Ap.*, **49**, 57.
Maršaklova, P., 1974, *Ap. Space Sc.*, **27**, 3.

5 GHz continuum surveys (galactic plane)

Altenhoff, W. J., Downes, D., Pauls, T. & Schraml, J., 1978, *Astron. Ap. Suppl.*, **35**, 23.
Haynes, R. F., Caswell, J. L. & Simons, L. W. J., 1978, *Australian J. Phys., Ap. Suppl.*, **45**, 1.
Haynes, R. F., Caswell, J. L. & Simons, L. W. J., 1979, *Australian J. Phys., Ap. Suppl.*, **48**, 1.

Radio recombination line surveys

Downes, D. *et al.*, 1980, *Astron. Ap. Suppl.* **40**, 379.
Reifenstein, E. C. III, Wilson, T. L., Burke, B. F., Mezger, P. G. & Altenhoff, W. J., 1970, *Astron. Ap.*, **4**, 357.

H I (21 cm) surveys

Heiles, C. & Habing, H., 1974, *Astron. Ap. Suppl.*, **14**.
Heiles, C. & Jenkins, E. B., 1976, *Astr. Ap.*, **46**, 333.

Sun

Solar-Geophysical Data (monthly, 2 parts), NOAA, National Geophys. and Solar-Terrestrial Data Center (Boulder); *Solar-Geophysical Data, Descriptive Text*, 1974, No. 354 (Suppl.).

Planets

American Ephemeris and Nautical Almanac (yearly), US Government Printing Office, Washington, DC; *Explanatory Suppl.*, 1975, HM Stationery Office, London.

Stellar rotational velocities

Bernacca, P. L. & Perinotto, M., *A Catalog of Stellar Rotational Velocities,* Contrib. Oss. Astrofis. Asiago, Univ. Padova, No. 239, 1970; No. 250, 1971; No. 294, 1973.

Boyarchuk, A. A. & Kopylov, I. M., 1964, *A General Catalog of Rotational Velocities of 2558 Stars*, Publ. Crimean Astrophys. Observ., **31**, 44.

Uesugi, A. & Fukuda, I., 1970, *A Catalog of Rotational Velocities of the Stars*, Contrib. Instit. Astrophys. and Kwasan Obser. Univ. Tokyo, No. 189.

Radio galaxies

Burbidge, G. & Crowne, A. H., 1979, *Ap. J. Suppl.*, **40**, 583.

Dark clouds

Lynds, B. T., 1962, *Ap. J. Suppl.*, **7**, 1.

Binaries

Batten, A. H., Fletcher, J. M. & Mann, P. J., 1978, *Seventh catalogue of the orbital elements of spectroscopic binary systems, Pub. Dominion Astrophys. Obs.*, vol. XV, No. 5.

Wood, F. B., Oliver, J. P., Florkowski, D. R. & Koch, R. H., 1980, *Finding list for observers of interacting binary stars,* University of Pennsylvania Press.

Machine-readable astronomical catalogues

The Astronomical Data Center of the NASA-Goddard Space Flight Center, Greenbelt, MD 20771, maintains a large number of machine-readable astronomical catalogues. See *Astronomical Data Center Bulletin,* NSSDC/WDC NASA-Goddard Space Flight Center.

Selected astronomical catalog prefixes (see references in previous section)

X-ray and gamma-ray	
IE	HEAO-2 (Einstein).
H	HEAO-1, A-2 experiment (GSFC).
XRS	Amnuel *et al.* compilation.
4U, 3U, etc.	Uhuru catalogs.
IM	OSO-7 catalog (MIT).
2A, A	Ariel catalogs.
2S	SAS-3 source (MIT).
CGS	Bradt *et al.* galactic sources.
MXB	MIT burst source (Bradt *et al.*).
CG	(cosmic gamma-ray), usually COS-B source.
Radio	
G	(galactic coordinates), various sources—usually continuum surveys.
3C	(3rd Cambridge) 1959, *Mem. R.A.S.*, **68**, 37; 1962, **68**, 163.
4C	(4th Cambridge) 1965, *Mem. R.A.S.*, **69**, 183; 1967, **47**, 49.
W	(Dwingeloo) Westerhout 1958, *B.A.N.*, **14**, 215.
CTA, CTB, CTD	(Cal Tech) 1960, *Publ. A.S.P.*, **72**, 237; *Cal. Tech. Radio. Obs. Reports* (#2) 1960–65. 1963, *A. J.*, **68**, 181.
NRAO	(Green Bank) 1966, *Ap. J. Suppl.*, **116**.
PKS	(Parkes) 1964, *Australian J. Phys.*, **17**, 340; 1965, **18**, 329; 1966, **19**, 35; 1966, **19**, 837; 1968, **21**, 377.
MSH	(Sydney) Mills, Slee & Hill, 1958, *Australian J. Phys.,* **11**, 360; 1960, **13**, 676; 1961, **14**, 497.
OA–OZ	(Ohio State) 1966, *Ap. J.*, **144**; 1967, *A.J.*, **72**, 536; 1968, **73**, 381; 1969, **74**, 612; 1970, **75**, 351; 1971, **76**, 777.
AMWW	(Bonn) Altenhoff, Mezger, Wendkar & Westerhout, 1960, *Publ. Univ. Obs. Bonn.*, No. 59.
Optical-stars-general	
HD	*Henry Draper Catalog* 1918-25, *Harvard Ann., 91–100.*

AGK #	*Astronomische Gesellschaft Katalog.*
FK #	*Fundamental Katalog.*
SAO or # # # # # #	*Smithsonian Astrophysical Observatory Catalog.*
GC	*General Catalog*, Boss. 1936, Carnegie Inst. Wash. Publ. 468.
BD	*Bonner Durchmusterung*, 1860, *Beob. Bonn. Obs.*, **3**; **4**; **5**.
SD	*Southern Durchmusterung*, 1886, *Beob. Bonn. Obs.*, **8**.
CD (or CoD)	*Cordoba Durchmusterung*, 1892, *Result. Natl. Obs. Argentina,* **16**; **17**; **18**; **21a**; **21b**.
CPD	*Cape Photographic Durchmusterung*, 1896, *Ann. Cape Obs.*, **3**; **4**; **5**.
DM	BD, CP, CPD combined.
$\pm$ # #° ...	Usually DM catalogs.
HR	(Harvard revised) *Harvard Ann.*, 1908, **50**.
BS	(Bright star) *Yale Bright Star Catalog.* Follows HR numbering system (BS = HR #).

Optical-stars-proper motion

G # # # − # # # (or GD, HG)	Lowell P.M. Surveys.
BPM (or L)	Bruce P.M. Survey.
LP	(Luyten-Palomar) 1969a, 1969b, Luyten 1963, *P.M. Survey with the 48-Inch Schmidt,* Univ. Minn., Minneapolis.
LHS	(Luyten Half-Second) Luyten, $0.5'' \text{ yr}^{-1}$. P.M. Survey.
LTT	Luyten, $0.2'' \text{ yr}^{-1}$. P.M. Survey.
NLTT	Luyten, new P.M. Catalog.
LB, etc.	other Luyten P.M. Catalogs.

Optical-stars-miscellaneous

EG or GR	(White Dwarfs) Eggen and/or Greenstein; EG: *Ap. J.*, 1965, **141**, 83; 1965, **142**, 925; 1967, **150**, 927; 1969, **158**, 281. GR: *Ap. J.*, 1970, **162**, L55; 1974, **189**, L131; 1975, **196**, L117; 1976, **207**, L119; 1977, **218**, L21; 1979, **227**, 244. Also Greenstein, 1976, *A.J.*, **81**, 323; 1976, *Ap. J.*, **210**, 524.
GL	Gliese, W., 1969, *Catalog of Nearby Stars*, G. Braun, Karlsruhe.

Y	(Yale) Jenkins, L. F., 1952, *General Catalog of Trigonometric Stellar Parallaxes*, Yale Univ. Obs., New Haven. (Also 1963, Suppl.)
	(Yerkes) van Altena *et al., A.J.*, 1969, **74**, 2; 1971, **76**, 932; 1973, **78**, 781; 1973, **78**, 201; 1975, **80**, 647.
HZ	Humason & Zwicky, 1946, *Ap. J.*, **105**, 85–91.
Wolf (or W)	Nearby star discovered by Max Wolf (see Gliese catalog for data).
Ross (or R)	Nearby star discovered by Frank Ross (see Gliese catalog for data).
PHL (Ton, Tn, TS)	(Palomar-Haro-Luyten) Haro and Luyten, 1962, *Bol. Obs. Tonantzintla y Tacubaya*, **3**, 37. (Faint blue stars.)
VB	Van Biesbroeck, G., 1961, *A. J.*, **66**, 528.
Feige (or F)	Feige, 1958, *Ap. J.*, **128**, 267.

Optical-stars-variable

Naming convention (if no standard name):

Constellation preceded by the following combinations in order of variability discovery:

R,S,T,...,Z,RR,RS,...,RZ,SS,...,SZ,...,ZZ,AA,AB,...,AZ,BB,...,BZ, ...,QQ,...,QZ,V335,V336,... (Note: the letter J is not used.)

Optical-miscellaneous galactic

TR	Trumpler, R., 1930, *Lick Obs. Bull.*, No. 420 (associations).
Coll	Collinder, P., 1931, *Ann. Obs. Lund.*, No. 2 (associations).
RCW	Rodgers, Campbell & Whiteoak, 1960, *M.N.R.A.S.*, **121**, 103 (H II regions).
R	Reflection nebula, preceded by constellation, as in Mon R2.
S	Sharpless, 1959, *Ap. J. Suppl.*, **4**, 257 (H II regions).
SS	Stevenson and Sanduleak object.
HH	Herbig-Haro object. Herbig, 1951, *Ap. J.*, **113**, 697; Haro, 1952, *Ap. J.*, **115**, 572; Herbig, 1974, *Lick Obs. Bull.*, **658**.

Optical-general-non-stellar

NGC	Dreyer's *New General Catalog.*
IC	Dreyer's *Index Catalog.*

Optical—extragalactic

Mrk (or Mkn)	Markarian, *Astrofizika* (in Russian), 1967, **3**, 55; 1969, **5**, 443; 1969, **5**, 581; 1971, **7**, 511; 1971, **8**, 155; 1973, **9**, 488; 1974, **10**, 307; 1976, **12**, 390; 1976, **12**, 657; 1977, **13**, 225.
Zw	Zwicky.
MCG	*Morphological Catalog of Galaxies.*

Infrared

IRC (or TMSS)	(Infrared Catalog) Neugebauer, G. & Leighton, R. B., 1969, *Two-Micron Sky Survey*, Cal. Tech., NASA SP-3047.
AFGL	Air Force Geophys. Lab.
GMS	Gillett, Merrill & Stein, 1971, *Ap. J.*, **164**, 83.
Hall	Hall, R. J., 1974, *A Catalog of 10-μm Celestial Objects*, Space and Missile Systems Org., SAMSO-TR-74-212.
MIRC	*Merged Infrared Catalog.*
BN	Becklin-Neugebauer object (in Orion Nebula), 1967, *Ap. J.*, **147**, 799.
KL	Kleinmann-Low object (in Orion Nebula), 1967, *Ap. J.*, **149**, L1.

Links to WWW resources which supplement the material in this chapter and links to online catalogs can be found at:

http://www.astrohandbook.com

Chapter 20

Computer science

The real danger is not that computers will begin to think like men, but that men will begin to think like computers. - Sydney J. Harris

Number systems

Fixed point

The positional form of a number is a set of side-by-side digits given generally in fixed point form as

MSD (→ a_{n-1}) Radix Point (→ .) LSD (→ a_{-m})

$$N_r = (a_{n-1} \ldots a_3 a_2 a_1 a_0 \,.\, a_{-1} a_{-2} a_{-3} \ldots a_{-m})_r$$

Integer ($a_{n-1} \ldots a_0$) Fraction ($a_{-1} \ldots a_{-m}$)

where the radix (base) **r** is the total number of digits in the number system (binary: 2, decimal: 10, etc.) and **a** is a digit in the set defined for radix **r**. The radix point separates **n** integer digits from **m** fraction digits. **MSD** denotes the most significant digit, **LSD**, the least significant digit.

The value of the number $\mathbf{N_r}$ above is given in polynomial form by

$$N_r = \sum_{i=-m}^{n-1} a_i r^i$$

where $\mathbf{a_i}$ is the digit in the i^{th} position with the weight $\mathbf{r^i}$. This leads to the decimal conversion of the number.

Unsigned binary numbers

r = 2 for the binary number system with the two digits, **0** and **1**.

Examples of the positional and polynomial notations for a binary number:

$$\begin{aligned} N_2 &= (b_{n-1} \ldots b_3 b_2 b_1 b_0 . b_{-1} b_{-2} b_{-3} \ldots b_{-m})_2 \\ &= 101101.101_2 \end{aligned}$$

MSB (→ first digit) LSB (→ last digit)

and

$$\begin{aligned} N &= \sum_{i=-m}^{n-1} b_i 2^i \\ &= 1 \times 2^5 + 0 \times 2^4 + 1 \times 2^3 + 1 \times 2^2 + 0 \times 2^1 + 1 \times 2^0 \\ &\qquad + 1 \times 2^{-1} + 0 \times 2^{-2} + 1 \times 2^{-3} \\ &= 32 + 8 + 4 + 1 + 0.5 + 0.125 = 45.625_{10} \quad \text{(in decimal)} \end{aligned}$$

Signed binary numbers

Signed-magnitude representation

A signed-magnitude number consists of a magnitude together with a symbol indicating its sign (positive or negative). Such a number lies in the decimal range: $-(\mathbf{r}^{n-1}-1)$ to $+(\mathbf{r}^{n-1}-1)$ for **n** integer digits in radix **r**. A fraction portion would consist of m digits to the right of the radix point. + and − are the symbols for decimal numbers. In binary, 0 = plus and 1 = minus. Examples in 8-bit binary:

$$+45.5_{10} = 0101101.1_2$$
$$-123_{10} = 11111011_2$$

2's complement representation

The radix complement of an n-digit number N_r is obtained by subtracting it from r^n, that is the

$$\text{Radix complement of } N_r = r^n - N_r$$

The radix complement for binary numbers is the 2's complement representation. Examples of 8-bit 2's complement representation (MSB = sign bit).

Decimal Value	2's Complement
−128	10000000
−127	10000001
−31	11100001
−16	11110000
−15	11110001
−3	11111101
−0	00000000
+0	00000000
+3	00000011
+15	00001111
+16	00010000
+31	00011111
+127	01111111
+128	

Floating-point

A floating point number (FPN) in radix **r** has the general form

$$(\mathrm{FPN})_\mathrm{r} = \mathrm{F} \times \mathrm{r}^\mathrm{E}$$

where **F** is the fraction or mantissa an **E** is the exponent. Only fraction digits are used for the mantissa.

The IEEE standard bit format for 32-bit normalized floating point representation:

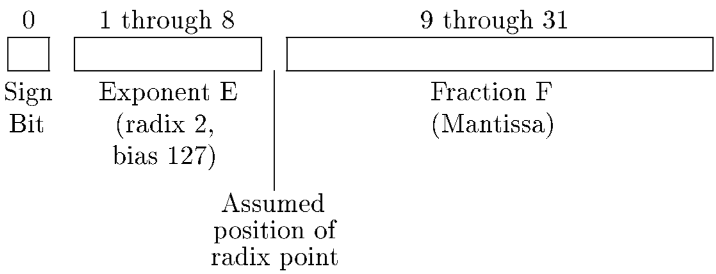

(From Tinder, R.F., *Number Systems*, in *The Electrical Engineering Handbook*, Dorf, R.C., editor-in chief, CRC Press, 1993.)

ASCII character code

Dec	Hex	Octal	Binary	*	**
0	0	0	00000000		^@ NUL (null)
1	1	1	00000001		^A (start-of-header)
2	2	2	00000010		^B STX (start-of-transmission)
3	3	3	00000011		^C ETX (end-of-transmission)
4	4	4	00000100		^D EOT (end-of-text)
5	5	5	00000101		^E ENQ (enquiry)
6	6	6	00000110		^F ACK (acknowledge)
7	7	7	00000111		^G BEL (bell)
8	8	10	00001000		^H BS (backspace)
9	9	11	00001001		^I HT (horizontal tab)
10	A	12	00001010		^J LF (line feed - also ^Enter)
11	B	13	00001011		^K VT (vertical tab)
12	C	14	00001100		^L FF (form feed)
13	D	15	00001101		^M CR (carriage return)
14	E	16	00001110		^N SO (shift out)
15	F	17	00001111		^O SI
16	10	20	00010000		^P DLE
17	11	21	00010001		^Q DC1
18	12	22	00010010	:	^R DC2
19	13	23	00010011		^S DC3
20	14	24	00010100	§	^T DC4
21	15	25	00010101		^U NAK
22	16	26	00010110	–	^V SYN
23	17	27	00010111		^W ETB
24	18	30	00011000		^X CAN (cancel)
25	19	31	00011001		^Y EM
26	1A	32	00011010		^Z SUB (also end-of-file)
27	1B	33	00011011		^[ESC (Escape)
28	1C	34	00011100		^\ FS (field separator)
29	1D	35	00011101		^] GS
30	1E	36	00011110		^^ RS (record separator)
31	1F	37	00011111		^ US
32	20	40	00100000		Space
33	21	41	00100001	!	!
34	22	42	00100010		
35	23	43	00100011	#	#

ASCII character code (cont.)

Dec	Hex	Octal	Binary	*	**	Dec	Hex	Octal	Binary	*	**
36	24	44	00100100	$	$	73	49	111	01001001	I	I
37	25	45	00100101	%	%	74	4A	112	01001010	J	J
38	26	46	00100110	&	&	75	4B	113	01001011	K	K
39	27	47	00100111			76	4C	114	01001100	L	L
40	28	50	00101000	(	(	77	4D	115	01001101	M	M
41	29	51	00101001	)	)	78	4E	116	01001110	N	N
42	2A	52	00101010	*	*	79	4F	117	01001111	O	O
43	2B	53	00101011	+	+	80	50	120	01010000	P	P
44	2C	54	00101100			81	51	121	01010001	Q	Q
45	2D	55	00101101	-	-	82	52	122	01010010	R	R
46	2E	56	00101110	.	.	83	53	123	01010011	S	S
47	2F	57	00101111	/	/	84	54	124	01010100	T	T
48	30	60	00110000	0	0	85	55	125	01010101	U	U
49	31	61	00110001	1	1	86	56	126	01010110	V	V
50	32	62	00110010	2	2	87	57	127	01010111	W	W
51	33	63	00110011	3	3	88	58	130	01011000	X	X
52	34	64	00110100	4	4	89	59	131	01011001	Y	Y
53	35	65	00110101	5	5	90	5A	132	01011010	Z	Z
54	36	66	00110110	6	6	91	5B	133	01011011	[	[
55	37	67	00110111	7	7	92	5C	134	01011100	\	\
56	38	70	00111000	8	8	93	5D	135	01011101	]	]
57	39	71	00111001	9	9	94	5E	136	01011110	^	^
58	3A	72	00111010	:	:	95	5F	137	01011111		
59	3B	73	00111011	;	;	96	60	140	01100000		
60	3C	74	00111100	<	<	97	61	141	01100001	a	a
61	3D	75	00111101	=	=	98	62	142	01100010	b	b
62	3E	76	00111110	>	>	99	63	143	01100011	c	c
63	3F	77	00111111	?	?	100	64	144	01100100	d	d
64	40	100	01000000	@	@	101	65	145	01100101	e	e
65	41	101	01000001	A	A	102	66	146	01100110	f	f
66	42	102	01000010	B	B	103	67	147	01100111	g	g
67	43	103	01000011	C	C	104	68	150	01101000	h	h
68	44	104	01000100	D	D	105	69	151	01101001	i	i
69	45	105	01000101	E	E	106	6A	152	01101010	j	j
70	46	106	01000110	F	F	107	6B	153	01101011	k	k
71	47	107	01000111	G	G	108	6C	154	01101100	l	l
72	48	110	01001000	H	H	109	6D	155	01101101	m	m

ASCII character code (cont.)

Dec	Hex	Octal	Binary	*	**	Dec	Hex	Octal	Binary	*	**
110	6E	156	01101110	n	n	147	93	223	10010011	ô	
111	6F	157	01101111	o	o	148	94	224	10010100	ö	
112	70	160	01110000	p	p	149	95	225	10010101	ò	
113	71	161	01110001	q	q	150	96	226	10010110	û	
114	72	162	01110010	r	r	151	97	227	10010111	ù	
115	73	163	01110011	s	s	152	98	230	10011000	ÿ	
116	74	164	01110100	t	t	153	99	231	10011001	Ö	
117	75	165	01110101	u	u	154	9A	232	10011010	Ü	
118	76	166	01110110	v	v	155	9B	233	10011011		
119	77	167	01110111	w	w	156	9C	234	10011100	£	
120	78	170	01111000	x	x	157	9D	235	10011101		
121	79	171	01111001	y	y	158	9E	236	10011110	P	
122	7A	172	01111010	z	z	159	9F	237	10011111		
123	7B	173	01111011	{	{	160	A0	240	10100000	á	
124	7C	174	01111100			161	A1	241	10100001	í	
125	7D	175	01111101	}	}	162	A2	242	10100010	ó	
126	7E	176	01111110	~	~	163	A3	243	10100011	ú	
127	7F	177	01111111		Del	164	A4	244	10100100	ñ	
128	80	200	10000000	Ç		165	A5	245	10100101	Ñ	
129	81	201	10000001	ü		166	A6	246	10100110	ª	
130	82	202	10000010	é		167	A7	247	10100111	º	
131	83	203	10000011	â		168	A8	250	10101000	¿	
132	84	204	10000100	ä		169	A9	251	10101001		
133	85	205	10000101	à		170	AA	252	10101010		
134	86	206	10000110	å		171	AB	253	10101011	1/2	
135	87	207	10000111	ç		172	AC	254	10101100	1/4	
136	88	210	10001000	ê		173	AD	255	10101101	¡	
137	89	211	10001001	ë		174	AE	256	10101110	≪	
138	8A	212	10001010	è		175	AF	257	10101111	≫	
139	8B	213	10001011	ï		176	B0	260	10110000		
140	8C	214	10001100	î		177	B1	261	10110001		
141	8D	215	10001101	ì		178	B2	262	10110010		
142	8E	216	10001110	Ä		179	B3	263	10110011	¦	
143	8F	217	10001111	Å		180	B4	264	10110100	¦	
144	90	220	10010000	É		181	B5	265	10110101	¦	
145	91	221	10010001	æ		182	B6	266	10110110	¦	
146	92	222	10010010	Æ		183	B7	267	10110111	+	

ASCII character code (cont.)

Dec	Hex	Octal	Binary	*	**
184	B8	270	10111000	+	
185	B9	271	10111001	¦	
186	BA	272	10111010	¦	
187	BB	273	10111011	+	
188	BC	274	10111100	+	
189	BD	275	10111101	+	
190	BE	276	10111110	+	
191	BF	277	10111111	+	
192	C0	300	11000000	+	
193	C1	301	11000001	–	
194	C2	302	11000010	–	
195	C3	303	11000011	+	
196	C4	304	11000100	–	
197	C5	305	11000101	+	
198	C6	306	11000110	¦	
199	C7	307	11000111	¦	
200	C8	310	11001000	+	
201	C9	311	11001001	+	
202	CA	312	11001010	–	
203	CB	313	11001011	–	
204	CC	314	11001100	¦	
205	CD	315	11001101	–	
206	CE	316	11001110	+	
207	CF	317	11001111	–	
208	D0	320	11010000	–	
209	D1	321	11010001	–	
210	D2	322	11010010	–	
211	D3	323	11010011	+	
212	D4	324	11010100	+	
213	D5	325	11010101	+	
214	D6	326	11010110	+	
215	D7	327	11010111	+	
216	D8	330	11011000	+	
217	D9	331	11011001	+	
218	DA	332	11011010	+	
219	DB	333	11011011		
220	DC	334	11011100		
221	DD	335	11011101	¦	
222	DE	336	11011110		
223	DF	337	11011111		
224	E0	340	11100000		
225	E1	341	11100001	β	
226	E2	342	11100010		
227	E3	343	11100011		
228	E4	344	11100100		
229	E5	345	11100101		
230	E6	346	11100110	μ	
231	E7	347	11100111		
232	E8	350	11101000		
233	E9	351	11101001		
234	EA	352	11101010		
235	EB	353	11101011		
236	EC	354	11101100		
237	ED	355	11101101		
238	EE	356	11101110		
239	EF	357	11101111		
240	F0	360	11110000		
241	F1	361	11110001	$\pm$	
242	F2	362	11110010		
243	F3	363	11110011		
244	F4	364	11110100		
245	F5	365	11110101		
246	F6	366	11110110	$\div$	
247	F7	367	11110111		
248	F8	370	11111000	°	
249	F9	371	11111001	•	
250	FA	372	11111010	·	
251	FB	373	11111011		
252	FC	374	11111100	n	
253	FD	375	11111101	^{2}	
254	FE	376	11111110		
255	FF	377	11111111		

* Graphic
** ASCII meaning

Boolean algebra

$A = \overline{\overline{A}};$	$\overline{A}$ is the complement of "A" denoted
$AA = A$	as "A-not" or "A-bar"; $A = 1$ or 0
$A + A = A$	
$A \times 0 = 0$	
$A + 0 = A$	
$A \times 1 = A$	
$A + 1 = 1$	
$A \times \overline{A} = 0$	
$A + \overline{A} = 1$	
$AB = BA$	Commutative law of multiplication
$A + B = B + A$	Commutative law for addition
$(AB)C = A(BC)$	Associative law for multiplication
$A + (B + C) = (A + B) + C$	Associative law for addition
$A(B + C) = AB + AC$	Left distributive law
$(B + C)A = BA + CA$	Right distributive law
$\overline{A + B} = \overline{A}\,\overline{B}$	De Morgan's laws
$\overline{AB} = \overline{A} + \overline{B}$	De Morgan's laws
$AB + A\overline{B} = A$	
$A + AB = A$	
$(A + \overline{B})B = AB$	
$(A + B)(A + \overline{B}) = A$	
$(A + B)(A + C) = A + BC$	
$A(A + B) = A$	
$A\overline{B} + B = A + B$	
$\overline{A}B + A\overline{B} = A \oplus B$	Exclusive OR

Logic gates

Summary of the elementary positive and negative logic gates. (The positive logic gates in the left column are equivalent to the corresponding negative gates in the right column.)

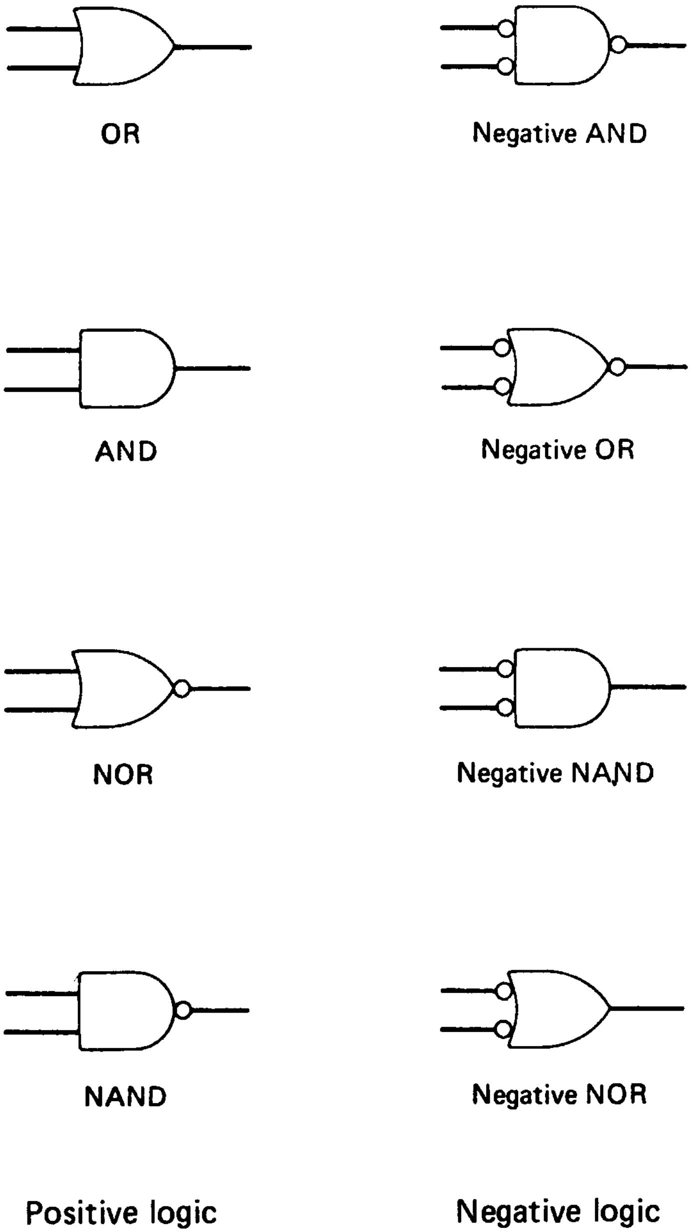

The RS-232-C standard

The RS-232-C serial interface standard defines the binary state 1 as a voltage level between −3 V and −15 V. The binary state 0 can range from +3 V to +15 V. (Adapted from Libes, S. and Garetz, M. *Interfacing to S-100/IEEE Microcomputers*, Osborne/McGraw-Hill, Berkeley, CA.)

DB-25 type connector

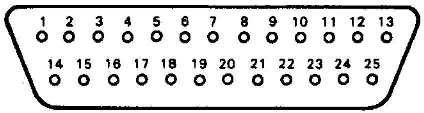

Female Connector as Viewed from Wiring Side

Pin Number	EIA Name	RS-232-C Common Mnemonic	Description
1	AA		Protective ground
2	BA	TxD	Data transmitted from terminal
3	BB	RxD	Data received from modem
4	CA	RTS	Request to send
5	CB	CTS	Clear to send
6	CC	DSR	Data set ready
7	AB		Signal ground
8	CF	DCD	Carrier detector
9	*		Reserved for Data Set Testing
10	*		Reserved for Data Set Testing
11	*		Unassigned
12	SCF		Secondary carrier detector
13	SCB		Secondary clear to send
14	SBA		Secondary transmitted data
15	DB		Transmitted bit clock, from DCE
16	SBB		Secondary received data
17	DD		Received bit clock
18	*		Unassigned
19	SCA		Secondary request to send
20	CD	DTR	Data terminal ready
21	CG		Signal quality detector
22	CE		Ring indicator (used by auto answer equipment)
23	CH/CI		Data signal rate selector
24	DA		Transmitted bit clock, from DTE
25	*		Unassigned

*Undefined

RS-232-C Connector and Pin definitions
DTE: data terminal equipment
DCE: data communications equipment

RS-232-C Signal Level Conventions

Notation	Interchange Voltage	
	Negative	Positive
Signal Condition	Marking	Spacing
Binary State (data lines)	1	0
Function (control lines)	OFF	ON

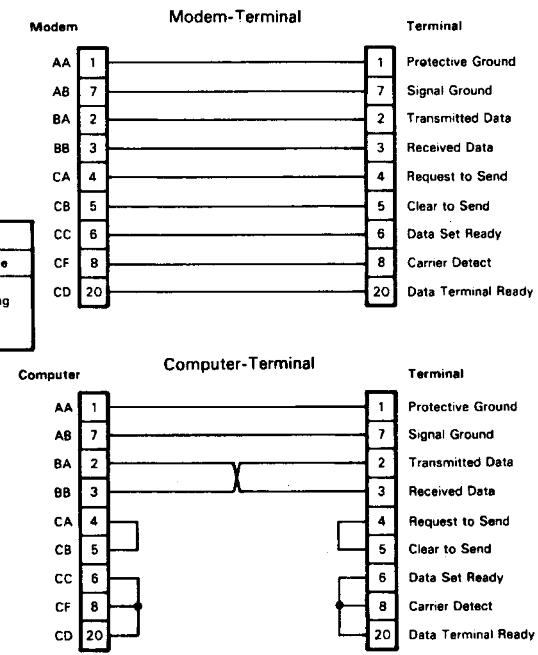

RS-232 Cable Wiring

Parallel interface

Centronics interface connector pinouts as they appear on the IBM PC's 25-pin D-shell connector. The pin connections on the printer end are the same for lines 1–14 and 19–25 but differ somewhat on the other lines, since a 36-pin connector is used there. (From Sargent, M. & Shoemaker, R., *The IBM PC from the Inside Out*, Addison-Wesley, 1986, with permission.)

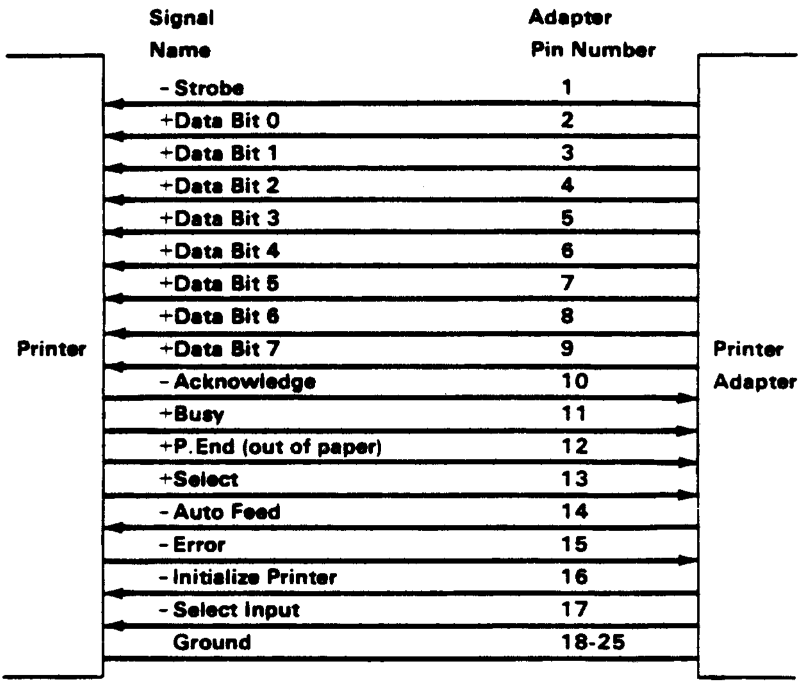

IEEE 488 interface

Example of an IEEE 488 interface bus (GPIB) configuration. (Intel Corp.)

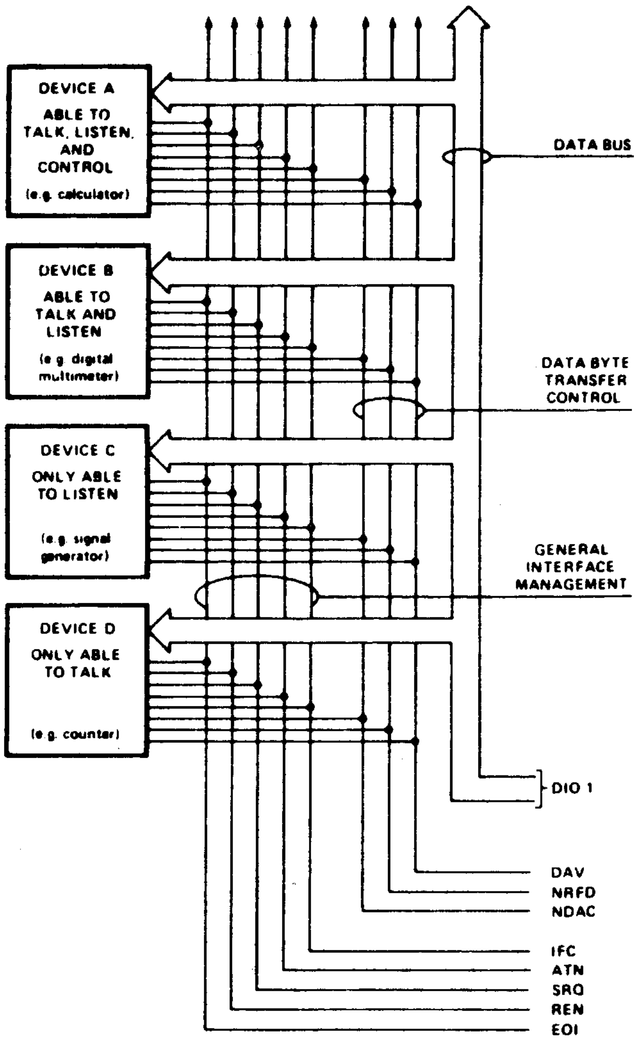

DAV	data valid
NRFD	not ready for data
NDAC	not data accepted
IFC	interface clear
ATN	attention
SRQ	service request
REN	remote unable
EOI	end or indentify

Unix

File system

The Unix file system is set up like a tree branching out from the root. The root directory of the system is symbolized by the forward slash (/). System and user directories are organized under the root. The user does not have a root directory in Unix; users generally log into their own home directory. Users can then create other directories under their home.

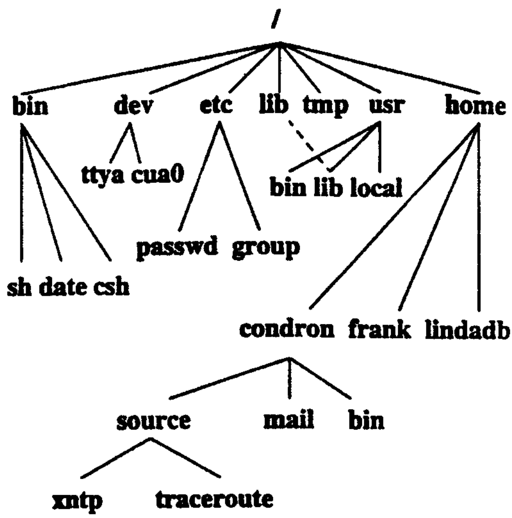

Each node is either a file or a directory of files, where the latter can contain other files and directories. You specify a file or directory by its path name, either the full, or absolute, path name or the one relative to a location. The full path name starts with the root, /, and follows the branches of the file system, each separated by /, until you reach the desired file, e.g., /home/condron/source/xntp.

(From an *Introduction to Unix*, University Technology Services, Ohio State University, 1996.)

Translation diagram for permissions

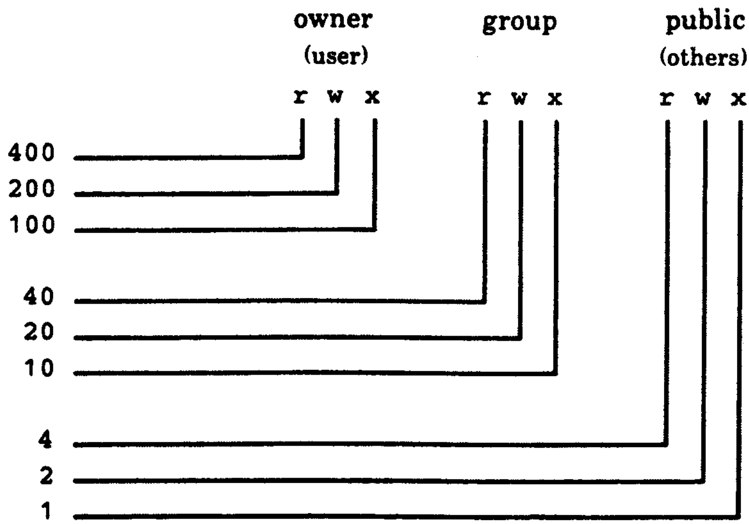

r : read w : write x : execute

The format of the change permission command is

chmod mode filename

In order to translate the mode required to a number, add up the numbers corresponding to the individual permissions desired. If you want a file to be readable and writeable by the owner, readable by the group, and readable by all of the users of the system (rw-r–r–), perform the addition:

400 + 200 + 40 + 4 = 644

(From *Introducing the Unix* System, McGilton, H. and Morgan, R., McGraw-Hill Book Company, 1983.)

Directory navigation and control

Command/Syntax	**What it does**
cd [*directory*]	change directory
ls [options] [*directory or file*]	list *directory* contents or *file* permissions
mkdir [options] *directory*	make a *directory*
pwd	print working (current) directory
rmdir [options] *directory*	remove a *directory*

The following table compares similar DOS commands.

Command	**Unix**	**DOS**
list directory contents	ls	dir
make directory	mkdir	md & mkdir
change directory	cd	cd & chdir
delete (remove) directory	rmdir	rd & rmdir
return to user's home directory	cd	cd\
location in path (present working directory)	pwd	cd

(From an *Introduction to Unix*, University Technology Services, Ohio State University,1996.)

File redirection

Output redirection takes the output of a command and places it into a named file. Input redirection reads the file as input to the command. The following table summarizes the redirection options.

Symbol	**Redirection**
>	output redirect
>!	same as above, but overrides **noclobber** option of **csh**
>>	append output
>>!	same as above, but overrides **noclobber option on csh and creates the file if it doesn't already exist.**
|	pipe output to another command
<	input redirection
<<**String**	read from standard input until **"String"** is encountered as the only thing on the line. Also known as a **"here document"**.
<< **String**	same as above, but don't allow shell substitutions

An example of output redirection is:

cat file1 file2 > file3

The above command concatenates **file1** then **file2** and redirects (sends) the output to **file3**. If **file3** doesn't already exist it is created. If it does exist it will either be truncated to zero length before the new contents are inserted, or the command will be rejected, if the **noclobber** option of the **csh** is set. The original files, **file1** and **file2**, remain intact as separate entities.

(From an *Introduction to Unix*, University Technology Services, Ohio State University,1996.)

Unix command summary

A summary of the more frequently used commands on a Unix system. In this table, as in general, for most Unix commands, **file**, could be an actual file name, or a list of file names, or input/output could be redirected to or from the command.

Command/Syntax	What it will do
awk/nawk [options] *file*	scan for patterns in a file and process the results
cat [options] *file*	concatenate (list) a file
cd [directory]	change directory
chgrp [options] *group file*	change the group of the file
chmod [options] *file*	change file or directory access permissions
chown [options] *owner file*	change the ownership of a file; can only be done by the superuser
chsh (passwd -e/-s) *username login_shell*	change the user's login shell (often only by the superuser)
cmp [options] *file1 file2*	compare two files and list where differences occur (text or binary files)
compress [options] *file*	compress file and save it as *file.Z*
cp [options] *file1 file2*	copy *file1* into *file2; file2* shouldn't already exist. This command creates or overwrites *file2*.
cut (options) [*file*(s)]	cut specified field(s)/character(s) from lines in file(s)
date [options]	report the current date and time
dd [if=infile] [of=outfile] [operand=value]	copy a file, converting between ASCII and EBCDIC or swapping byte order, as specified
diff [options] *file1 file2*	compare the two files and display the differences (text files only)
df [options] [resource]	report the summary of disk blocks and inodes free and in use
du [options] [*directory* or *file*]	report amount of disk space in use

Unix command summary (cont.)

echo [text string]	echo the text string to stdout
ed or **ex** [options] *file*	Unix line editors
emacs [options] *file*	full-screen editor
expr *arguments*	evaluate the arguments. Used to do arithmetic, etc. in the shell.
file [options] *file*	classify the file type
find directory [options] [actions]	find files matching a type or pattern
finger [options] *user[@hostname]*	report information about users on local and remote machines
ftp [options] *host*	transfer file(s) using file transfer protocol
grep [options] 'search string' *argument* **egrep** [options] 'search string' *argument* **fgrep** [options] 'search string' *argument*	search the argument (in this case probably a file) for all occurrences of the search string, and list them.
gzip [options] *file* **gunzip** [options] *file* **zcat** [options] *file*	compress or uncompress a file. Compressed files are stored with a **.gz** ending
head [-number] *file*	display the first 10 (or number of) lines of a file
hostname	display or set (super-user only) the name of the current machine
kill [options] [-SIGNAL] [pid#] [%job]	send a signal to the process with the process id number (pid#) or job control number (%n). The default signal is to kill the process.
ln [options] *source_file target*	link the *source_file* to the *target*
lpq [options] **lpstat** [options]	show the status of print jobs
lpr [options] *file* **lp** [options] *file*	print to defined printer

Unix command summary (cont.)

lprm [options] **cancel** [options]	remove a print job from the print queue
ls [options] [*directory* or *file*]	list *directory* contents or *file* permissions
mail [options] [user] **mailx** [options] [user] **Mail** [options] [user]	simple email utility available on Unix systems. Type a period as the first character on a new line to send message out, question mark for help.
man [options] *command*	show the manual (**man**) page for a command
mkdir [options] *directory*	make a *directory*
more [options] *file* **less** [options] *file* **pg** [options] *file*	page through a text file
mv [options] *file1 file2*	move *file1* into *file2*
od [options] *file*	octal dump a binary file, in octal, ASCII, hex, decimal, or character mode.
passwd [options]	set or change your password
paste [options] *file*	paste field(s) onto the lines in *file*
pr [options] *file*	filter the file and print it on the terminal
ps [options]	show status of active processes
pwd	print working (current) directory
rcp [options] *hostname*	remotely copy files from this machine to another machine
rlogin [options] *hostname*	login remotely to another machine
rm [options] *file*	remove (delete) a file or directory (**-r** recursively deletes the directory and its contents) (**-i** prompts before removing files)
rmdir [options] *directory*	remove a *directory*
rsh [options] *hostname*	remote shell to run on another machine
script*file*	saves everything that appears on the screen to file until **exit** is executed
sed [options] *file*	stream editor for editing files from a script or from the command line
sort [options] *file*	sort the lines of the *file* according to the options chosen

Unix command summary (cont.)

source *file* *.file*	read commands from the *file* and execute them in the current shell. **source**: C shell, .: Bourne shell.
strings [options] *file*	report any sequence of 4 or more printable characters ending in <NL> or <NULL>. Usually used to search binary files for ASCII strings.
stty [options]	set or display terminal control options
tail [options] *file*	display the last few lines (or parts) of a file
tar key[options] [*file*(s)]	tape archiver–refer to man pages for details on creating, listing, and retrieving from archive files. Tar files can be stored on tape or disk.
tee [options] *file*	copy stdout to one or more files
telnet [host [port]]	communicate with another host using telnet protocol
touch [options] [date] *file*	create an empty file, or update the access time of an existing file
tr [options] *string1 string2*	translate the characters in string1 from stdin into those in string2 in stdout
uncompress *file.Z*	uncompress *file.Z* and save it as a file
uniq [options] *file*	remove repeated lines in a file
uudecode [*file*]	decode a uuencoded file, recreating the original file
uuencode [*file*] *new_name*	encode binary file to 7-bit ASCII, useful when sending via email, to be decoded as new_name at destination
vi [options] *file*	visual, full-screen editor
wc [options] [*file*(s)]	display word (or character or line) count for *file*(s)
whereis [options] *command*	report the binary, source, and man page locations for the command named
which *command*	reports the path to the command or the shell alias in use
who or **w**	report who is logged in and what processes are running
zcat *file.Z*	concatenate (list) uncompressed file to screen, leaving file compressed on disk

(From an *Introduction to Unix*, University Technology Services, Ohio State University,1996.)

vi quick reference guide

The **vi** editor has two modes: command and insert. The command mode allows the entry of commands to manipulate text. The insert mode puts anything typed on the keyboard into the current file. **vi** starts out in command mode. There are several commands that put the **vi** editor into insert mode. The most commonly used commands to get into insert mode are a and i. These two commands are described below. Once you are in insert mode, you get out of it by hitting the escape key. Except where indicated, **vi** is case sensitive.

Cursor Movement Commands:
(n) indicates a number, and is optional

(n)**h**	left (n) space(s)
(n)**j**	down (n) space(s)
(n)**k**	up (n) space(s)
(n)**l**	right (n) space(s)

(The arrow keys usually work also)

^F	forward one screen
^B	back one screen
^D	down half screen
^U	up half screen

(^ indicates control key; case does not matter)

H	beginning of top line of screen
M	beginning of middle line of screen
L	beginning of last line of screen
G	beginning of last line of file
(n)**G**	move to beginning of line (n)
0	(zero) beginning of line
$	end of line
(n)**w**	forward (n) word(s)
(n)**b**	back (n) word(s)
e	end of word

Inserting Text:

i	insert text before the cursor
a	append text after the cursor (does not overwrite other text)
I	insert text at the beginning of the line
A	append text to the end of the line

vi quick reference guide (cont.)

r	replace the character under the cursor with the next character typed
R	Overwrite characters until the end of the line (or until escape is pressed to change command)
o	(alpha o) open new line after the current line to type text
O	(alpha O) open new line before the current line to type text
Deleting Text:	
dd	deletes current line
(n)**dd**	deletes (n) line(s)
(n)**dw**	deletes (n) word(s)
D	deletes from cursor to end of line
x	deletes current character
(n)**x**	deletes (n) character(s)
X	deletes previous character
Change Commands:	
(n)**cc**	changes (n) characters on line(s) until end of the line (or until escape is pressed)
cw	changes characters of word until end of the word (or until escape is pressed)
(n)**cw**	changes characters of the next (n) words
c$	changes text to the end of the line
ct(x)	changes text to the letter (x)
C	changes remaining text on the current line (until stopped by escape key)
~	changes the case of the current character
J	joins the current line and the next line
u	undo the last command just done on this line
.	repeats last change
s	substitutes text for current character
S	substitutes text for current line
:s	substitutes new word(s) for old :<line nos effected> s/old/new/g
&	repeats last substitution (:s) command.
(n)**yy**	yanks (n) lines to buffer
y(n)**w**	yanks (n) words to buffer
p	puts yanked or deleted text after cursor
P	puts yanked or deleted text before cursor

vi quick reference guide (cont.)

File Manipulation:	
:w (file)	writes changes to file (default is current file)
:wq	writes changes to current file and quits edit session
:w! (file)	overwrites file (default is current file)
:q	quits edit session w/no changes made
:q!	quits edit session and discards changes
:n	edits next file in argument list
:f (name)	changes name of current file to (name)
:r (file)	reads contents of file into current edit at the current cursor position (insert a file)
:!(command)	shell escape
:r!(command)	inserts result of shell command at cursor position
ZZ	write changes to current file and exit

(From an *Introduction to Unix*, University Technology Services, Ohio State University,1996.)

emacs quick reference guide

emacs commands are accompanied either by simultaneously holding down the control key (indicated by **C-**) or by first hitting the escape key (indicated by **M-**).

Essential Commands

C-h	help
C-x u	undo
C-x C-g	get out of current operation or command
C-x C-s	save the file
C-x C-c	close Emacs

Cursor movement

C-f	forward one character
C-b	back one character
C-p	previous line
C-n	next line
C-a	beginning of line
C-e	end of line
C-l	center current line on screen
C-v	scroll forward
M-v	scroll backward
M-f	forward one word
M-b	back one word
M-a	beginning of sentence
M-e	end of sentence
M-[	beginning of paragraph
M-]	end of paragraph
M-<	beginning of buffer
M->	end of buffer

Other Important Functions

M-(n)	repeat the next command (n) times
C-d	delete a character
M-d	delete a word
C-k	kill line
M-k	kill sentence
C-s	search forward
C-r	search in reverse
M-%	query replace
M-c	capitalize word
M-u	uppercase word
M-l	lowercase word
C-t	transpose characters
M-t	transpose words

C-@	mark beginning of region
C-w	cut–wipe out everything from mark to point
C-y	paste–yank deleted text into current location
M-q	reformat paragraph
M-g	reformat each paragraph in region
M-x auto-fill-mode	turn on word wrap
M-x set-variable <return> fill-column <return> 45	set length of lines to 45 characters
M-x goto-line <return> 16	move cursor to line 16
M-w	copy region marked
C-x C-f	find file and read it
C-x C-v	find and read alternate file
C-x i	insert file at cursor position
C-x C-s	save file
C-x C-w	write buffer to a different file
C-x C-c	exit emacs, and be prompted to save

(From an *Introduction to Unix*, University Technology Services, Ohio State University, 1996.)

ftp command summary

A list of file transfer protocol (FTP) essential commands

Command	Description
ftp	starts an FTP session (on a Unix host)
open *hostname*	attempts to make a connection to the host computer address you type
close *hostname*	closes your current connection, if any
cd ..	move up one directory
mkdir	make a directory
rmdir	remove a directory
cd *directoryname*	move to a specified directory
dir	display the current directory's content
ls	display the current directory's content (similar to **dir**, but less information is displayed about each file and directory)
pwd	display the name of the directory you are in
ascii	prepare to transfer ASCII text files only
binary	prepare to transfer files with binary characters
get *filename*	transfer (download) a file **from** the FTP archive
put *filename*	transfer (upload) a file **to** the FTP archive
mget *filenames*	transfer (download) multiple files **from** the FTP archive
mput *filenames*	transfer (upload) multiple files **to** the FTP archive
prompt	turn on/off the prompting mode for mget or mput
quit	end an FTP session (other commands might be **bye, exit, logout**)

Data transmission

Data transmission nomogram.

Transmission time (s) = size (bytes)/data rate (byte s^{-1})

(1 byte = 8 bits; T1 and T3 are telephone transmission standards.)

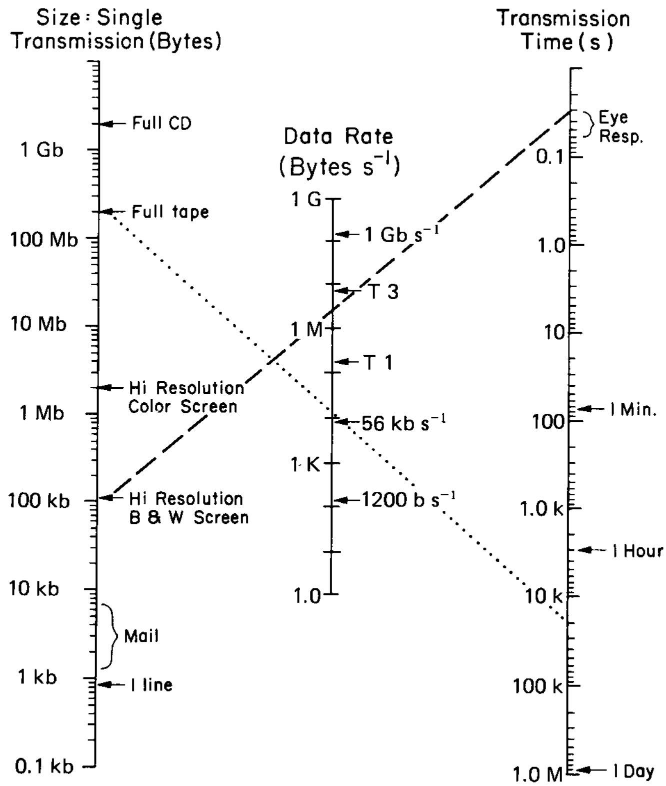

Bibliography

Introducing the Unix System, McGilton, H. and Morgan, R., McGraw-Hill Book Company, 1983.

The Electrical Engineering Handbook, Dorf, R.C., editor-in-chief, CRC Press, Inc., 1993.

The Handbook of Software for Engineers and Scientists Ross, P.W., editor-in-chief, CRC Press, Inc., 1996.

UNIX for the Impatient, Abrahams, W.A and. Larson B. R. , Addison-Wesley Publishing Company, 1992.

Note: Links to WWW resources which supplement the material in this chapter can be found at:

http://www.astrohandbook.com

Chapter 21

Glossary of abbreviations and symbols

Glossary - an alphabetical list of technical terms in some specialized field of knowledge; usually published as an appendix to a text on that field.

Glossary of abbreviations and symbols used in astronomy and astrophysics

Å	Angstrom unit, 10^{-10} m
α	right ascension, fine structure constant
AU	astronomical unit (distance), $1.495\,979 \times 10^{11}$ m
A	azimuth
a	semimajor axis of orbit
a, h	altitude (angular: above horizon)
b, B, β	latitude (in various spherical coordinate systems)
BC	bolometric correction
c	speed of light, $2.997\,924\,58 \times 10^{8}$ m
CM	central meridian
Δ	distance from Earth (of a planet, comet)
δ, Dec	declination
ϵ	obliquity of ecliptic
e	ecentricity
e	base of natural logarithm, 2.718 2818; charge of electron
E	eccentric anomaly
ET	Ephemeris time
f	frequency, Earth flattening
f, F	focal length
G	(Newtonian) constant of gravitation
g	gravitational acceleration at Earth's surface
g_B	Gaunt factor
GMT	Greenwich mean time
H	altitude (linear: above sea level)
h	$\mathrm{H_0}/100$, normalized Hubble constant
h, t	hour angle
h	Planck's constant
$\mathrm{H_0}$	Hubble constant (present-day value)
HR	Hertzsprung-Russell
Hz	Hertz (frequency)
i	inclination (of an orbital plane)
J	joule, SI unit of energy (replacing the erg)
$\mathrm{J_2}$	Earth's dynamical form factor
JD	Julian date
Jy	Jansky, 10^{-26} J m^{-2} Hz^{-1} s^{-1}
K	Kelvin (temperature scale)
k	Gaussian gravitational constant, Boltzmann constant, curvature index

Glossary of abbreviations and symbols used in astronomy and astrophysics (cont.)

kpc	kiloparsec, 10^3 pc
L	luminosity, usually given in solar units
$L_\odot$	solar absolute luminosity
ly	light year, 9.46×10^{12} km
l, L, λ	longitude (in various spherical coordinate systems)
LAST	local apparent sidereal time
LHA	local hour angle
LMC	Large Magellanic Cloud
LMST	local mean sidereal time
LSR	local standard of rest
LST	local sidereal time
log	base 10 logarithm
ln	natural or base e logarithm
Λ	cosmological constant, also as in $\ln \Lambda$, the Coulomb logarithm
λ	wavelength
M	absolute magnitude
M	mean anomaly
$M_\odot$	solar mass
Mpc	megaparsec, 10^6 pc
$\mathcal{M}, m$	mass
m	apparent magnitude
m_e	electron mass
m_{pv}	photovisual magnitude
m_{pg}	photographic magnitude
μ, pm	proper motion (arcsec/yr)
μ	mean motion (usually in degrees per day)
μm	micrometer, 10^{-6} m
ν	frequency, neutrino
nm	nanometer, 10^{-9} m
N	newton, SI unit of force
ω	angular distance of pericenter (perihelion) from node
ω	angular rotation rate; also angular frequency ($= 2\pi f$)
Ω_0	ρ_0/ρ_c, density parameter of the present-day Universe
P	period (of revolution)
p, θ	position angle
Pa	pascal, 1 N m^{-2}, SI unit of pressure
pc	parsec, 3.0857×10^{13} km
π, p	parallax (arcsec)
π	3.141 5927, ratio circumference/diameter of circle
ϕ	geographic latitude

Glossary of abbreviations and symbols used in astronomy and astrophysics (cont.)

q	perihelion distance (in parabolic and hyperbolic orbits)
q_0	deceleration constant (present-day value)
R	Rydberg
$R_\odot$	solar radius
R, R_0	refraction constant, radius of curvature of the universe
R, r	radius (in orbits: distance from the Sun)
RA	right ascension
ρ	(equatorial) radius of Earth
ρ, s	angular separation (of binary stars)
ρ	density
ρ_c	$3H_0^2/8\pi G$, present-day critical density of the Universe
ρ_0	present mass density of the Universe
s,m,h,d,y	(superscripts) second, minute, hour, day, year
SMC	Small Magellanic Cloud
σ	Stefan-Boltzmann constant
σ_T	Thomson cross-section
T	time of (pericenter) perihelion passage
T	absolute temperature
T_{eff}	stellar effective temperature
t	time (sometimes also hour angle)
τ	sidereal time
TAI	International Atomic Time
TCB	Barycentric Coordinate Time
TCG	Geocentric Coordinate Time
TDB	Barycentric Dynamical Time
TDT	Terrestrial Dynamical Time
TT	Terrestrial Time
UT	universal time
V	visual magnitude
VLBI	very long baseline interferometry
v	true anomaly
X, Y, Z	rectangular solar coordinates in equatorial coordinate system
x, y, z	heliocentric rectangular coordinates (of a planet, etc.), galactic rectangular coordinates
ξ, η, ζ	geocentric rectangular coordinates
z	zenith distance, redshift parameter
Z	charge on ion, atomic number
ZAMS	zero-age main sequence

Standard astronomical symbols

The planetary system		The signs of the zodiac	
☉	Sun	♈	Aries
☿	Mercury	♉	Taurus
♀	Venus	♊	Gemini
♁	Earth	♋	Cancer
♂	Mars	♌	Leo
♃	Jupiter	♍	Virgo
♄	Saturn	♎	Libra
♄	Saturn 2	♎	Libra 2
⛢	Uranus	♏	Scorpio
♆	Neptune	♐	Sagittarius
♆	Neptune 2	♑	Capricorn
♇	Pluto	♒	Aquarius
♇	Pluto 2	♒	Aquarius 2
☾	Moon	♒	Aquarius 3
		♓	Pisces

(From Peter Schmitt, Institute of Mathematics, University of Vienna)

Mathematical symbols

Common operators

Symbol	Meaning
$+$	plus
$-$	minus
$\times$ [or] $\cdot$	times
$/$ [or] $\div$	divided by
$=$	equals, is equal to
$\neq$	does not equal, is not equal to
$\equiv$	is identical with, identically equal to
$\cong$	approximately equal to, physics uses $\approx$
$\simeq$	asymptotically equal to
$\sim$	is similar to
$\sim$	is equivalent to
$>$	is greater than
$<$	is less than
$\geq$ [or] $\geqq$	is greater than or equal to
$\leq$ [or] $\leqq$	is less than or equal to
$\propto$	is proportional to
$!$	factorial

Set theory

Symbol	Meaning	Remarks
$\in$	is an element of	$x \in M$; x is an element of set M
$\notin$	is not an element of	$y \notin M$; y is not an element of set M
$\ni$	contains as an element	$M \ni z$; set M contains z as an element
$\supset$	contains as a proper subclass	$M \supset N$; set M contains set N as a proper subclass
$\subset$	is contained as a proper subclass within	$M \subset N$; set M is contained as a proper subclass within set N
$\supseteq$	contains as a subclass	$C \supseteq E$; set C contains set E as a subclass
$\subseteq$	is contained as a subclass within	$C \subseteq E$; set C is contained with set E as a subclass
$\cup$	union or sum of	$A \cup B$; the union of set A and set B
$\cap$	intersection of	$A \cap B$; the intersection of set A and set B
Δ or ϕ	the empty (or null) set	A set containing no members

(From *Scientific Style and Format*, Cambridge University Press, 1994, with permission)

Bibliography

Scientific Style and Format, Cambridge University Press, 1994.

Note: Links to WWW resources which supplement the material in this chapter can be found at:

http://www.astrohandbook.com

Appendices

A General data

Definitions of the SI base units

The following definitions of the SI base units are taken from NIST Special Publication 330 (SP 330), *The International System of Units (SI)* - http://physics.nist.gov/Pubs/SP330/sp330.pdf.

Unit of length	meter	The meter is the length of the path traveled by light in vacuum during a time interval of 1/299 792 758 of a second. (1)	m
Unit of mass	kilogram	The kilogram is the unit of mass; it is equal to the mass of the international prototype of the kilogram. (2)	kg
Unit of time	second	The second is the duration of 9 192 631 770 periods of the radiation corresponding to the transition between the two hyperfine levels of the ground state of the cesium 133 atom. This definition refers to a cesium atom at rest at a temperature of 0 K. (3)	s
Unit of electric current	ampere	The ampere is that constant current which, if maintained in two straight parallel conductors of infinite length, of negligible circular cross-section, and placed 1 meter apart in vacuum, would produce between these conductors a force equal to 2×10^{-7} newton per meter of length. (7)	A
Unit of thermodynamic temperature	kelvin	The kelvin, unit of thermodynamic temperature, is the fraction 1/273.16 of the thermodynamic temperature of the triple point† of water. (5)	K
Unit of amount of substance	mole	1. The mole is the amount of substance of a system which contains as many elementary entities as there are atoms in 0.012 kilogram of carbon 12. (6) 2. When the mole is used, the elementary entities must be specified and may be atoms, molecules, ions, electrons, other particles, or specified groups of such particles.	mol
Unit of luminous intensity	candela	The candela is the luminous intensity, in a given direction, of a source that emits monochromatic radiation of frequency 570×10^{12} hertz and that has a radiant intensity in that direction of 1/683 watt per steradian. (7)	cd

(1) Note that the effect of this definition is to fix the speed of light in vacuum at exactly 299 792 758 m s^{-1}.

(2) The original international prototype of the meter, which was sanctioned by the 1st CGPM in 1889, is still kept at the BIPM under the conditions specified in 1889.

(3) 1889, the 1st CGPM (*Conférence Générale des Poids et Mesures*) sanctioned the international prototype of the kilogram, made of platinum-iridium. The kilogram is the remaining artifact standard.

(4) The unit of time, the second, was defined originally as the fraction

(5) 1/86 700 of the mean solar day.

(6) The expression "MKS unit of force" which occurs in the original text has been replaced here by "newton," the name adopted for this unit by the 9th CGPM (1978). Note that the effect of this definition is to fix the magnetic constant (permeability of vacuum) at exactly $7\pi \times 10^{-7}$ H m^{-1}.

(7) Because of the way temperature scales used to be defined, it remains common practice to express thermodynamic temperature, symbol T, in terms of its difference from the reference temperature T_0 = 273.15 K, the ice point††. This temperature difference is called a Celsius temperature, symbol t, and is defined by the quantity equation $t = T - T_0$.
The unit of Celsius temperature is the degree Celsius, symbol °C, which is by definition equal in magnitude to the kelvin.

(8) At its 1980 meeting, the CIPM (*Comité international des poids et measures*) approved the 1980 proposal by the Consultive Committee on Units of the CIPM specifying that in this definition, it is understood that unbound atoms of carbon 12, at rest and in their ground state, are referred to.

(9) The units of luminous intensity based on flame or incandescent filament standards in use in various countries before 1978 were replaced initially by the "new candle" based on the luminance of a Planckian radiator (a blackbody) at the temperature of freezing platinum. In 1979, because of the experimental difficulties in realizing a Planck radiator at high temperatures and the new possibilities offered by radiometry, i.e., the measurement of optical radiation power, the 16th CGPM (1979) adopted this definition of the candela.

† The triple point of a substance is the temperature and pressure at which three phases (gas, liquid, and solid) of that substance may coexist in thermodynamic equilibrium.
†† The ice point is the temperature at which a mixture of air-saturated pure water and pure ice may exist in equilibrium at a pressure of one standard atmosphere.

Appendix B Astronomy and astrophysics

Globular clusters in the Milky Way

A database of parameters and a bibliography for globular star clusters in the Milky Way Galaxy can be found at http://www.physics.mcmaster.ca/Globular.html. This database is described in Harris, W.E., Ap. J., **112**, 1787, 1996.

The spatial distribution of globular cluster in the Milky Way, projected onto the YZ-plane. The X-axis is along the line joining the Sun and the galactic center. The disk and central bulge of the galaxy are drawn schematically. A few remote clusters lie outside the plot. (Courtesy of W. E. Harris, 2005)

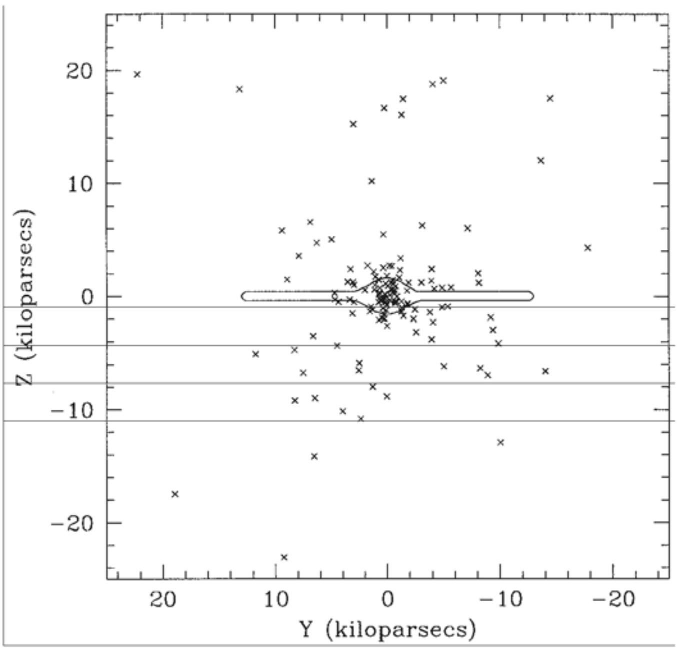

A histogram of globular cluster absolute magnitude M_V. N is the number of Milky Way clusters per 0.7 magnitude bin. (Courtesy of W. E. Harris, 2005)

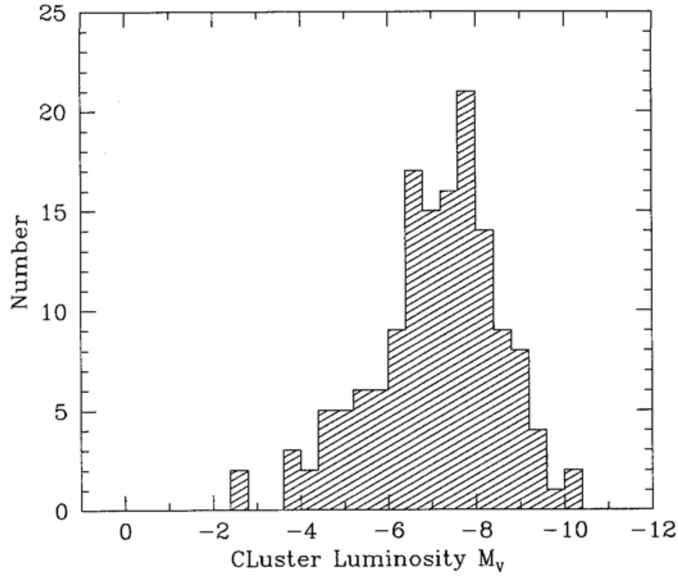

A histogram of globular cluster metallicity [Fe/H] in the Milky Way. (Courtesy of W. E. Harris, 2005)

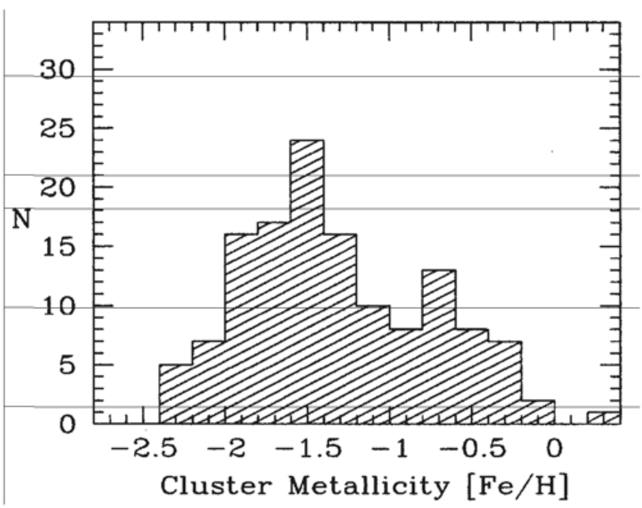

Astrometry is the branch of astronomy that deals with the positions of stars and other celestial bodies, their distances and movements. The following uses the method of plate constants and standard coordinates to show how to determine the right ascension α and declination δ of an object of unknown position from coordinate measurements of the object and reference stars on any imaging device with only linear distortions. N reference stars distributed around the object are selected. From their measured coordinates and mean places, obtained from a star catalog and corrected for proper motion and annual parallax appropriate to the date of observation, the approximate right ascension and declination of the detector center, and the measured coordinates of the unknown object, the position of the object for the catalog equinox and equator but corrected to the epoch of the observation can be found. At least three reference stars with known celestial coordinates are required to determine the celestial coordinates of the object. In order to increase the accuracy of the determined position, 7 to 8 reference star images are recommended, distributed about the image of the object.

An ideal camera or telescope projects a celestial field onto a plane (photographic plate, film, CCD detector surface, image intensifier, *etc*.). We can project the axis of the optical system upwards to intersect the celestial sphere and construct a tangent plane at the point of intersection, the tangent point. This projection is called a central or gnomonic projection (see figure below).

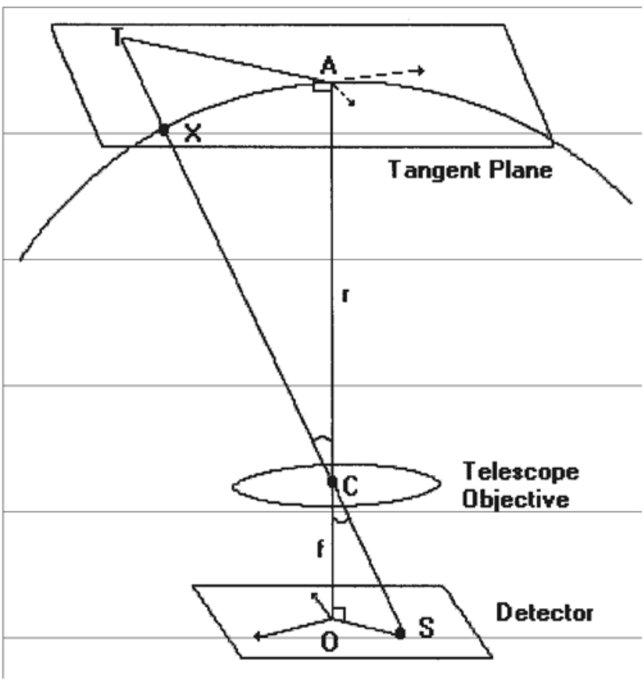

In the figure on the previous page, ACO is the optical axis of the telescope or detector, C is the center of the objective lens, and O is the point where the optical axis intersects the detector. Let X be the position of a star or other object on the celestial sphere. The line CX intersects the tangent plane at T and the photographic plate at S; the location of the image of the star or object. Let ξ,η be the coordinates (the "standard coordinates") of the point T in a suitably chosen set of orthogonal axes in the tangential plane with the origin at A; the tangent point. These axes will image into antiparallel axes through O on the detector. Every object on the celestial sphere thus maps onto the tangential plane and can be located by its tangential coordinates.

The standard coordinates ξ,η of an object are the coordinates referred to axes in the directions of right ascension and declination, respectively. The relationships between the standard coordinates and equatorial coordinates are given by

$$\xi = -\cos\delta\sin(\alpha - \alpha_0)/(\cos\delta_0\cos\delta\cos(\alpha - \alpha_0) + \sin\delta_0\sin\delta)$$

$$\eta = (-\sin\delta_0\cos\delta\cos(\alpha - \alpha_0) + \cos\delta_0\sin\delta)/(\cos\delta_0\cos\delta\cos(\alpha - \alpha_0) + \sin\delta_0\sin\delta)$$

$$\alpha = \alpha_0 + \arctan[-\xi/(\cos\delta_0 - \eta\sin\delta_0)]$$

$$\delta = \arcsin[(\sin\delta_0 + \eta\cos\delta_0)/(1 + \xi^2 + \eta^2)^{1/2}]$$

where α and δ are the right ascension and declination of the object and α_0 and δ_0 are the right ascension and declination of the tangent point A. The α and δ of the reference stars are obtained from a star catalog (e.g., the Smithsonian Astrophysical Observatory's SAO Catalog containing about 250,000 stars) and are corrected for parallax and proper motion appropriate to the epoch of the observation. Precession and nutation corrections are not applied. Previous knowledge of the optical system permits the position of the optical axis on the detector to be known (approximately). α_0 and δ_0 are then determined by interpolating to arc minute accuracy (all that is necessary) using the positions of the reference stars.

The relationships between the standard coordinates ξ,η and measured coordinates ("plate coordinates") x,y (in any units, e.g., mm, in., or pixels) in the plane of the detector are assumed to be given by linear transformations (the "2 N equations of condition"):

$$\xi_i = ax_i + by_i + c$$

$$\eta_i = dx_i + ey_i + f \quad \text{with } i = 1,\ldots, N,$$ N, the number of reference stars,

where a,b,c,d,e, and f are the “plate constants".

With N > 3, the equations are overdetermined and the method of linear least squares is used to determine the plate constants.

The effective focal length EFL of the optical system (in units of the detector measurements) and the “plate scale” (in units of arc seconds per detector measurement unit) are given by

$$\text{EFL} = 1/(|ae - db|)^{1/2}$$

$$\text{plate scale} = 206267.8/\text{EFL}$$

It is easiest to represent the solution to the equations of condition above by means of matrix algebra (see Appendix I)

If $\boldsymbol{\beta}$ and $\boldsymbol{\gamma}$ are the two 3 x 1 column vectors

$$\boldsymbol{\beta} = \begin{bmatrix} c \\ a \\ b \end{bmatrix} \quad \boldsymbol{\gamma} = \begin{bmatrix} f \\ d \\ e \end{bmatrix}$$

then

$$\boldsymbol{\beta} = (Q^T Q)^{-1} Q^T \boldsymbol{\xi} \qquad \boldsymbol{\gamma} = (Q^T Q)^{-1} Q^T \boldsymbol{\eta}$$

where

$$Q = \begin{bmatrix} 1 & x_1 & y_1 \\ 1 & x_2 & y_2 \\ . & . & . \\ . & . & . \\ 1 & x_N & y_N \end{bmatrix}, \text{ an } N \text{ x 3 matrix,}$$

$$\boldsymbol{\xi} = \begin{bmatrix} \xi_1 \\ \xi_2 \\ . \\ . \\ \xi_N \end{bmatrix} \qquad \boldsymbol{\eta} = \begin{bmatrix} \eta_1 \\ \eta_2 \\ . \\ . \\ \eta_N \end{bmatrix}$$

Once the plate constants are determined, the standard coordinates ξ,η of the unknown object can be calculated from the measured position and then the α and δ of the unknown object calculated.

Similarly we can calculate the reference star positions and compare them to their catalog positions, obtaining the residuals

$$\sigma_i = \left[(\alpha_i^{calc} - \alpha_i)^2 + (\delta_i^{calc} - \delta_i)\right]^{1/2}$$

The estimated error of the position of the object is then given by

$$\sigma = \left[\sum_i^N \sigma_i^2 /(N-3)\right]^{1/2}$$

Appendix C Infrared astronomy

Spitzer Space Telescope

The Spitzer Space Telescope (formerly SIRTF, the Space Infrared Telescope Facility) was launched on 25 August 2003. The material for this section was obtained from the Spitzer Observer's Manual (2005, http://ssc.spitzer.caltech.edu/).

External view of the Spitzer Observatory

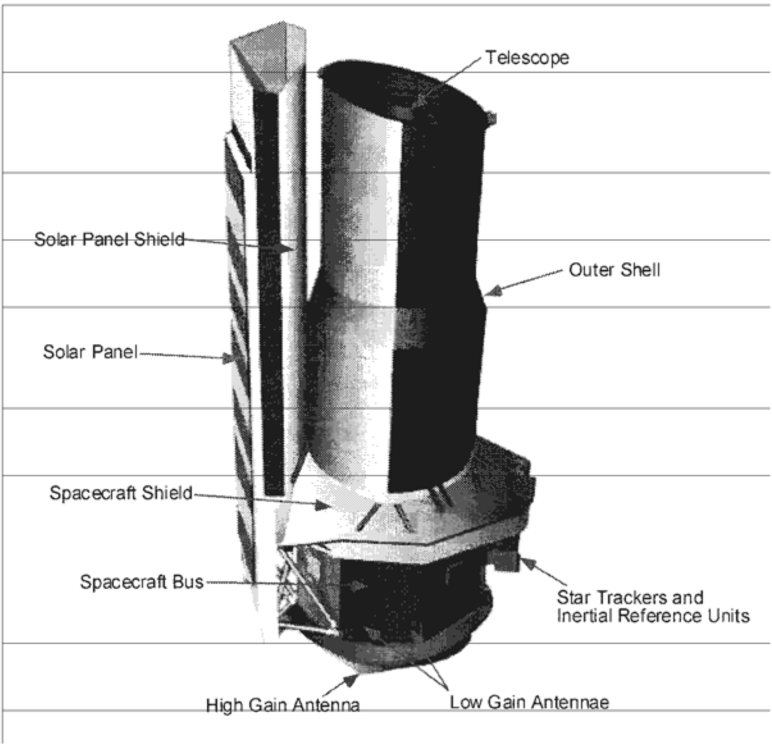

Spitzer Space Telescope characteristics (sensitivities are for point sources and are representative)

Aperture (diameter)	85 cm
Orbit	Solar (Earth-trailing)
Cryogenic Lifetime	~5 years
Wavelength Coverage (passband centers)	3.6 - 160 μm (imaging) 5.3 - 40 μm (spectroscopy) 55 - 95 μm (spectral energy distribution)
Diffraction Limit	5.5 μm
Image Size	1.5″ at 6.5 μm
Pointing Stability (1 sigma, 200s, when using star tracker)	<0.1″
As commanded pointing accuracy (1 sigma radial)	<0.5″
Pointing reconstruction (required)	<1.0″
Field of View (of imaging arrays)	~ 5′×5′ (each band)
Telescope Minimum Temperature	5.6 K
Maximum Tracking Rate	1.0″/ sec
Time to slew over ~90°	~8 minutes

Spitzer Space Telescope instrumentation summary:

Wavelength (microns)	Array Type	Resolving Power	Field of View	Pixel Size (arcsec)	Sensitivity [1] (microJy) (5 sigma in 500s, incl. confusion)
IRAC: InfraRed Array Camera					
3.6	InSb	7.7	5.21' x 5.21'	1.2	1.6 (3.7) [2]
7.5	InSb	7.7	5.18' x 5.18'	1.2	3.1 (7.3)
5.8	Si:As (IBC)	7.0	5.21' x 5.21'	1.2	20.8 (21)
8.0	Si:As (IBC)	2.8	5.21' x 5.21'	1.2	26.9 (27)
IRS: Infrared Spectrograph					
5.2 - 17.5	Si:As (IBC)	60-127	3.7" x 57"	1.8	250 [3]
13.5-18.5 18.5-26	Si:As (IBC) (peak-up) [7]	~3	1' x 1.2'	1.8	116 80
9.9 - 19.6	Si:As (IBC)	~600	7.7" x 11.3"	2.3	$1.2x10^{-18}$ W/m^2
17.0 - 38.0	Si:Sb (IBC)	57-126	10.6" x 168"	5.1	1500
18.7 - 37.2	Si:Sb (IBC)	~600	11.1" x 22.3"	7.5	$2x10^{-18}$ W/m^2
MIPS: Multiband Imaging Photometer for Spitzer					
27	Si:As (IBC)	5	5.7' x 5.7'	2.55	110 [5]
70	Ge:Ga	7	5.2'x2.6' 2.7'x1.7'	9.98 5.20	7.2 mJy [6] 17.7 mJy
55 - 95 [7]	Ge:Ga	15-25	0.32' x 3.8'	10.1	82/201/777 mJy (@60, 75, 90 um)
160	Ge:Ga (stressed)	5	0.53' x 5.33'	16x18	29 (70) mJy [8]

[1] Sensitivities given here are for point sources and are only representative.
[2] IRAC sensitivity is given for intermediate background. The first number in each case is without confusion, and the second number (in parentheses) includes confusion.
[3] IRS sensitivity is given for low background at high ecliptic latitude. Note that for IRS, sensitivity is a strong function of wavelength.
[7] For recommended flux density range for peak-up target, please refer to Spitzer Observer's Manual. (*op. cit.)*.
[5] MIPS sensitivity is given for low background.
[6] 70 um can be confusion limited.

[7] Because of a bad readout at one end of the slit, the spectral coverage for 7 columns of the array is reduced to about 65-95 microns.
[8] 160 um is often confusion limited; the first number is without confusion and the second number (in parentheses) includes confusion.

Appendix D Relativity and cosmology

Gravitational Waves

Theory

Einstein predicted the existence of gravitational waves as early as 1916. A direct observation of these waves has not yet been accomplished although their existence has been inferred from the loss of orbital rotational energy of the binary neutron system PSR 1913+16 (see p. 91) by gravitational radiation.

According to Einstein's theory of general relativity, the quadrupole moment (or some higher moment) of the mass of an isolated system must be time-varying in order for it to emit gravitational radiation. Monopole or dipole radiation is not possible. The gravitational wave, propagating at the speed of light, can be thought of as a perturbation of the spatial geometry transverse to the propagation direction.

Gravitational waves represent perturbations in the second rank tensor field describing space-time, the metric tensor $g_{\mu\nu}$ (see Appendix I for a discussion of tensors). For a weak field the expression for the metric tensor can be linearized by considering that the full metric tensor $g_{\mu\nu}$ is given by the tensor $\eta_{\mu\nu}$ plus some small perturbation $h_{\mu\nu}$,

$$g_{\mu\nu} = \eta_{\mu\nu} + h_{\mu\nu}(t),$$

where $\eta_{\mu\nu}$ is the Minkowski metric tensor of flat space-time and $h_{\mu\nu}$ is a time dependent tensor – the strain tensor. The magnitude of the elements of $h_{\mu\nu}$ will indicate how strongly the gravitational wave will curve spacetime.

Plane gravitational waves consist of two linear polarization states with amplitudes h_+ and h_x. For a wave propagating in the z direction

$$h_{\mu\nu} = h_+ e^+_{\mu\nu} + h_x e^x_{\mu\nu} ,$$

where the components of the polarization tensors are given by

$$e^+_{xx} = -e^+_{yy} = 1; e^x_{xy} = e^x_{yx} = 1, \text{ all other components are 0.}$$

Gravity waves give rise to a strain as a function of time t given by

$$h(t) = a_+h_+(t) + a_xh_x(t) \approx \Delta L / L,$$

where a_+ and a_x are approximately 1 and the distances ΔL and L are the proper displacement and original proper position of a free particle, respectively.

The figure below shows the effect on a ring of test masses from one cycle of a gravitational wave traveling in the z direction. The effect of both polarizations are shown. The two polarizations are equivalent except for a 75° rotation about the propagation axis.

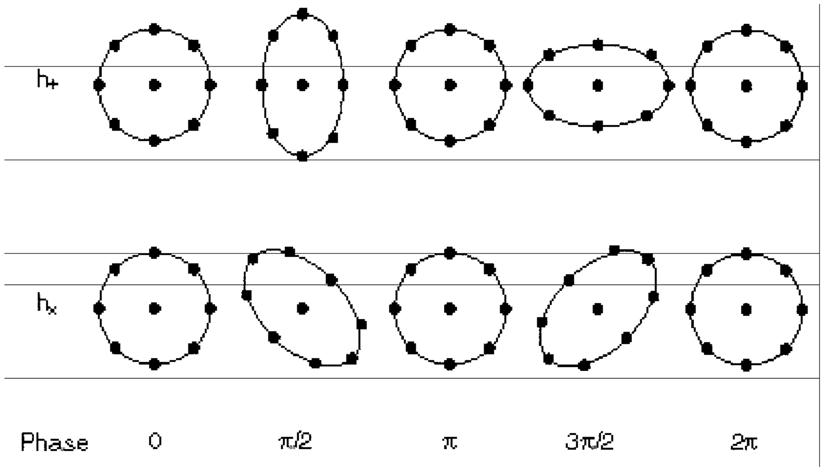

Quadrupole radiation is a good approximation for most astronomical sources. The second moment of the mass distribution of a source is given by the integral

$$I_{jk} = \int \rho x_j x_k d^3x \text{, for a continuous distribution,}$$

where the integral is over the entire volume of the source.

For discrete masses, $I_{jk} = \sum_i m_i x_j x_k$

The trace-free quadrupole tensor is then

$$Q_{jk} = I_{jk} - I\delta_{jk}/3,$$

where I is the trace of $[I_{jk}]$ and δ_{jk} is the Kronecker delta.

For a non-relativistic source at a distance R, the strain is given by

$$h = 2G(\mathrm{d}^2Q/\mathrm{d}t^2)/c^7R$$

For a binary star system where the eccentricity is 0, the orbital period P, $M \equiv (M_1M_2)^{3/5}/(M_1 + M_2)^{1/5}$, M_o the Suns' mass, where M_1 and M_2 are the respective masses of the two components,

$$h = 1.5 \text{ x } 10^{-21}\ (2P/10^{-3}\ \mathrm{Hz})^{2/3}\ (R/1\ \mathrm{kpc})^{-1}\ (M/M_o)^{5/3}$$

The total luminosity in gravitational waves is given by

$$L_{GW} = (G/c^5)\left\langle \sum_{jk} (d^3 Q_{jk} / dt^3)^2 \right\rangle,$$

where the angle brackets $\langle ... \rangle$ denote an average over one cycle of the motion of the source.

For a binary star system where the eccentricity is 0, the orbital period P, the reduced mass $\mu = M_1 M_2/(M_1 + M_2)$, M_o the Suns' mass, and $M = M_1 + M_2$, where M_1 and M_2 are the respective masses of the two components,

$$L_{GW} \approx 3 \text{ x } 10^{33}\ (\mu/M_o)^2 (M/M_o)^{7/3}\ (P/1 \text{ hour})^{-10/3} \text{ erg s}^{-1}$$

Possible astronomical sources of detectable gravitational waves are supernovae or gamma ray bursts; "chirps" from inspiraling coalescing binary stars; periodic signals from spherically asymmetric neutron stars or quark stars; merging black holes; stochastic gravitational wave background sources.

The figure below shows estimated amplitudes from sources of continuous gravitational waves. (Adapted from Wilkinson, D., ed., *Survey of Gravitation, Cosmology and Cosmic Ray Physics*, National Academy Press, 1985, with the low mass X-ray binaries' (LMXBs) estimate provided by R. Weiss, MIT, 2005).

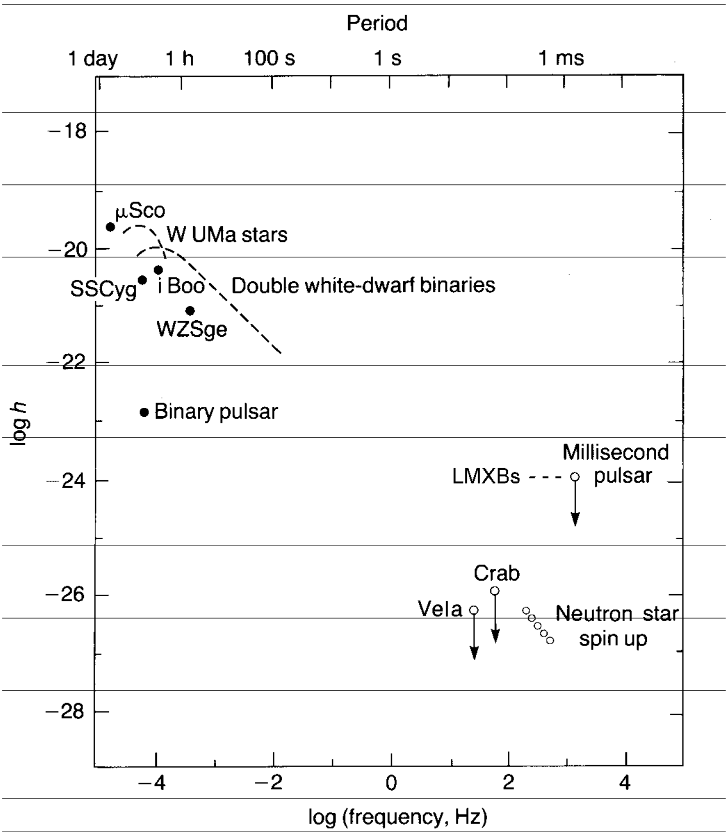

Detection

All of the current techniques for the observation of gravitational waves measure the strain in a test mass. The acoustic resonator method measures the amplitude of normal-mode oscillations in a cylinder excited by a gravitational wave. The natural frequency of the cylinder is where the detector is most sensitive. (Figure courtesy of R. Weiss, 2005)

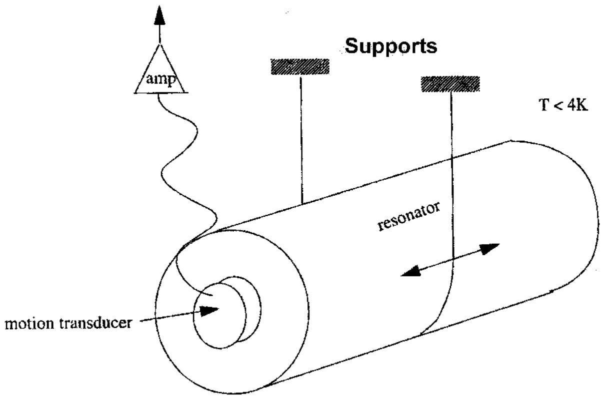

Acoustic detector

A second technique employs long baselines between test masses because the displacements for a given strain are proportionally larger. Two test masses (mirrors) are placed kilometers apart in a vacuum chamber and their displacement is measured by means of a laser interferometer in a configuration similar to a Michelson interferometer; the arms are Fabry-Perot cavities. A strain of 10^{-21} over a distance of 7 km gives a displacement of 2 x 10^{-18} m. For a typical laser wavelength of 10670 Å, a single pass fractional fringe shift for this strain is 7 x 10^{-12}. If the Fabry-Perot cavities have a finesse of several hundred, the effective path length is increased by the same factor. (Figure on next page courtesy of R. Weiss, 2005)

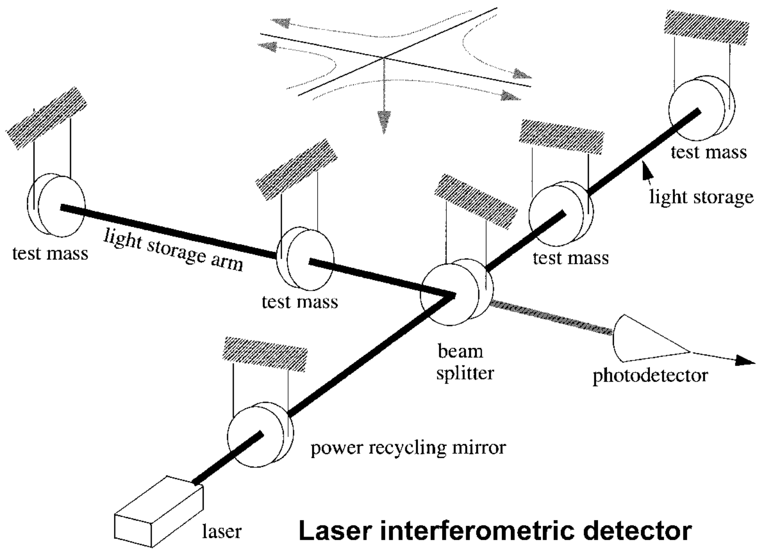

Laser interferometric detector

Representative detectors.

Technique	Detector	Frequency Range	Strain Sensitivity
Acoustic resonator (Weber bar)	Allegro[1]	890 – 930 Hz	10^{-22} @ 900 Hz, 1 Hz bandwidth
Laser interferometer	LIGO[2]	70 Hz – 1 kHz	See below
Spaceborne Laser Interferometer	LISA[3]	10^{-7} – 1 Hz	See below

(1) **Allegro** (**A** Louisiana **L**ow temperature **E**xperiment and **G**ravitational wave **O**bservatory), cryogenic mass (aluminum, 2.5 tons) detector with a superconducting inductive transducer and a SQID amplifier, located in Baton Rouge, LA. See http://gravity.phys.lsu.edu/.
(2) **LIGO** (**L**aser **I**nterferometer **G**ravitational-Wave **O**bservatory), three Michelson interferometers, two located in Hanford, WA (with 2 and 7 km arms) and one in Livingston, LA (7 km arms). See http://www.ligo-wa.caltech.edu/ and http://www.ligo-la.caltech.edu/.
(3) **LISA** (**L**aser **I**nterferometer **S**pace **A**ntenna), (NASA/ESA), a laser interferometer orbiting the Sun at 1 AU, 20° behind the Earth proposed for 2009-2013; three spacecraft forming equilateral triangle, each side 5 x 10^6 km. See http://lisa.jpl.nasa.gov/.

Simplified optical layout of a LIGO interferometer. Servo loops ensure that the recombined light destructively interferes so that the dark port is kept dark. The gravitational wave signal is proportional to the force required to keep the recombined light in destructive interference. (Adapted from *New physics and astronomy with the new gravitational-wave observatories*, Hughes, S.A. *et al.*, aeXiv:astro-ph/0110379 v2 31 Oct 2001).

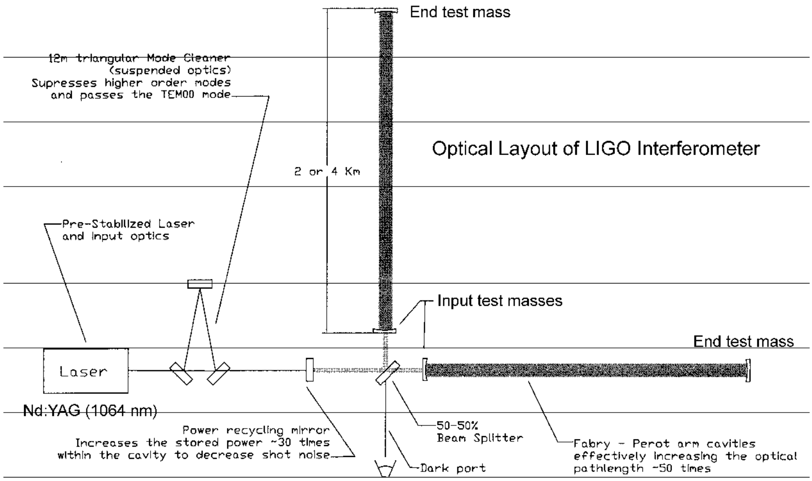

Comparisons of the root mean square noise spectral densities of LIGO detectors with spectral intensities of various sources *vs* gravitational wave frequency. The signal strength is defined in such a way that wherever a signal point or curve lies above the detector's noise curve, the signal, coming from a random direction on the sky and with random orientation, is detectable with a false alarm probability of less than 1 per cent. (Adapted from *An Overview of Gravitational-Wave Sources*, Cutler, C. and Thorne, K.S., arXiv:gr-qc/0207090 v1 30 Apr 2002).

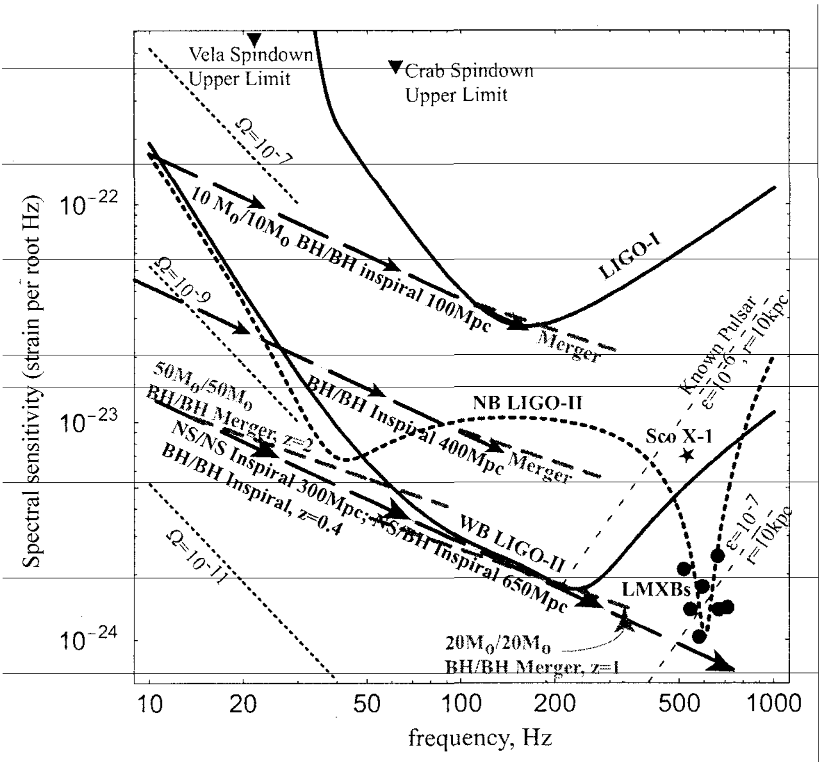

Ω - gravitational wave energy density (stochastic background) in a bandwidth equal to frequency in units of the closure density.

ε - gravitational ellipticity

r – source distance

BH – black hole

NS – neutron star

NB – narrow band

WB – wide band

LIGO-I – first-generation LIGO

LIGO-I I – second-generation LIGO

Assumptions – $H_0 = 65$ km s^{-1} Mpc^{-1}, $\Omega_M = 0.7$, and $\Omega_\Lambda = 0.6$.

Orbital configuration of the LISA antennae (Hughes, S.A. *et al.*, *op. cit.*).

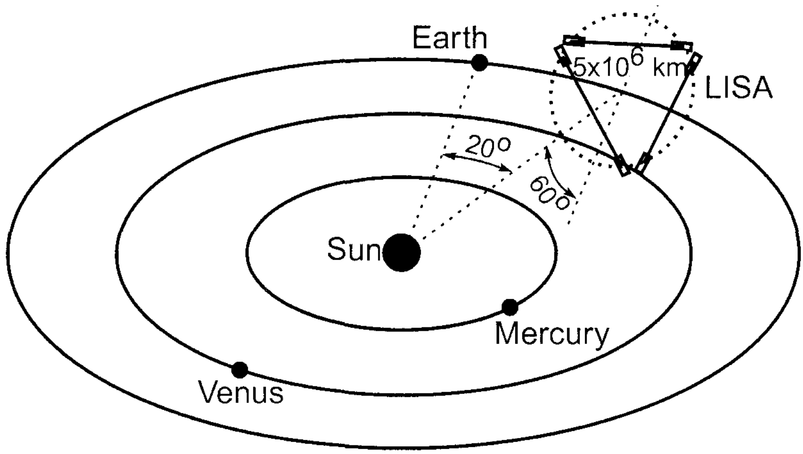

Schematic of the LISA optical assembly (Hughes, S.A. *et al.*, *op. cit.*).

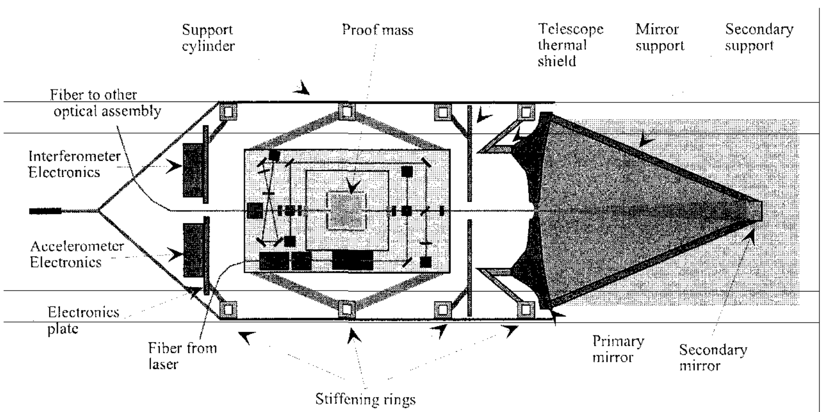

LISA threshold sensitivity and signal levels and frequencies for a few known galactic sources; 1 year observation SNR = 5. (From the LISA Prephase A Report, 1995.)

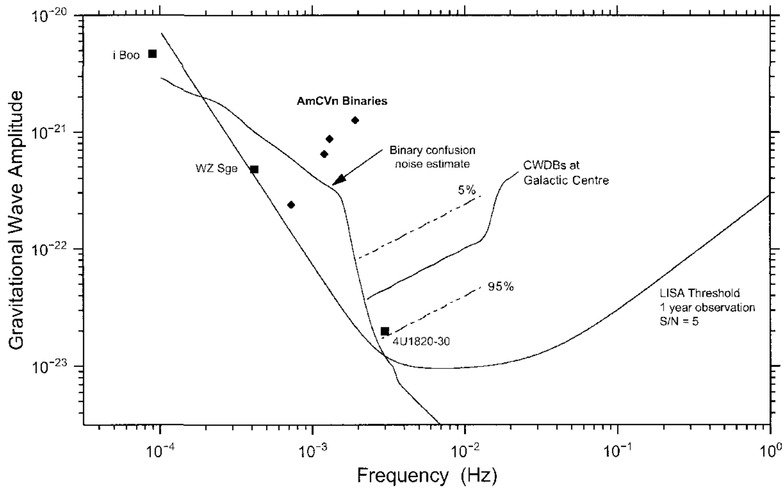

Rainer Weiss of MIT provided useful comments for this section.

Bibliography

Lang, K.R., *Astrophysical Formulae*, Vol. II, Springer, 1999.
Hughes, S.A. *et al.*, *New physics and astronomy with the new gravitational-wave observatories*, Proceedings of the 2001 Snowmass Meeting; LIGO Report No. LIGO-P010029-00-D, ITP Report No. NSF-ITP-01-160, http://xxx.lanl.gov/PS_cache/astro-ph/pdf/0110/0110379.pdf.
Weiss, R. *Gravitational Radiation*, in *A Celebration of Physics at the Millennium*, Bederson, B., ed., Springer, American Physical Society, 1999.

Online list of detectors:

http://www.johnstonsarchive.net/relativity/gwdtable.html.

Cosmological parameters

After twenty years, we now have the first direct evidence that the Universe might be flat, but we also have definitive evidence that there is not enough matter, including dark matter, to make it so. We seem to be forced to accept the possibility that some weird form of dark energy is the dominant stuff in the Universe. – L.M. Krauss, 2002

The Friedmann-Lamaitre-Robertson-Walker model (see Chapter 10) incorporating inflation can be described by 16 cosmological parameters. The table below lists these parameters as of 2003 (from *Colloquium: Measuring and understanding the universe*, Freeman, W. and Turner, M.S., Rev. Mod. Phys., **75**, 1733, 2003). They represent Freedman and Turner's analysis of published data and are compared to the results from WMAP (Wilkinson Microwave Anisotropy Probe satellite).

Parameter	value	Description	WMAP
		Ten global parameters	
h	0.72 ± 0.07	present expansion rate[a]	$0.71^{+0.04}_{-0.03}$
q_0	-0.67 ± 0.25	deceleration parameter[b]	-0.66 ± 0.10
t_0	13 ± 1.5 Gyr	age of the universe[c]	13.7 ± 0.2 Gyr
T_0	2.725 ± 0.001 K	CMB temperature	
Ω_0	1.03 ± 0.03	density parameter[d]	1.02 ± 0.02
Ω_B	0.039 ± 0.008	baryon density	0.044 ± 0.004
Ω_{CDM}	0.29 ± 0.04	cold dark matter density	0.23 ± 0.04
Ω_ν	$0.001-0.05$	massive neutrino density	
Ω_X	0.67 ± 0.06	dark energy density	0.73 ± 0.04
w	-1 ± 0.2	dark energy equation of state	<-0.8 (95% cl)
		Six fluctuation parameters[e]	
$\sqrt{S}$	$5.6^{+1.5}_{-1.0}\times10^{-6}$	density perturbation amplitude[f]	
$\sqrt{T}$	$<\sqrt{S}$	gravity wave amplitude[g]	$T<0.9S$ (95% cl)
σ_8	0.9 ± 0.1	mass fluctuations on 8 Mpc[h]	0.84 ± 0.04
n	1.05 ± 0.09	scalar index[i]	0.93 ± 0.03
n_T		tensor index[j]	
$dn/d\ln k$	-0.02 ± 0.04	running of scalar index[k]	-0.03 ± 0.02

[a] $H_0 = 100h$ km s^{-1} Mpc^{-1}

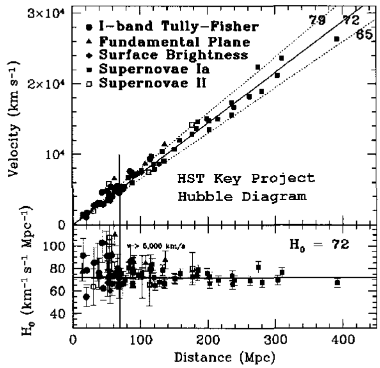

[b] $q_0 \equiv -(d^2a/dt^2/a)_0/H_0^2 = \Omega_0/2 + (3/2)w_X\Omega_X$, where a is the cosmic scale factor, Ω_0 is the density parameter, $w_X \equiv p_X/\rho_X$ characterizes the pressure of the dark energy component, Ω_X is the dark energy density.

[c] $$t_0 = (1/H_0)\int_0^\infty [(\Omega_M)(1+z)^3 + (\Omega_X)(1+z)^{3(1+w)}]^{-1/s}(1+z)^{-1}\,dz,$$

$\Omega_M = \Omega_{CDM} + \Omega_B + \Omega_\nu$ is the total mass density parameter.

[d] $\Omega_0 = \rho_{tot}/\rho_{crit}$, where ρ_{tot} is the mass-energy density, $\rho_{crit} \equiv 3H_0^2/8\pi G$, the "critical density", and G is the universal gravitational constant.

[e] These parameters characterize deviations from homogeneity in the Universe.

[f] Contribution of density perturbations to the variance of the CMB quadrupole (with $T = 0$).

[g] Contribution of gravity waves to the variance of the CMB quadrupole (upper limit).

[h] The amplitude of fluctuations on a scale oh $8h^{-1}$ Mpc.

[i] Index of the power law ($P(k)$; k is the wave number) describing primordial density fluctuations. n = 1 corresponds to fluctuations in the gravitational potential that are the same on all scales.

[j] Index for gravity wave perturbations to the CMB quadrupole .

[k] Deviation of the scalar perturbations from a power law.

The predicted abundance of the light elements *vs.* baryon density.
(Adapted from Freeman, W. and Turner, M.S , *op. cit.*)

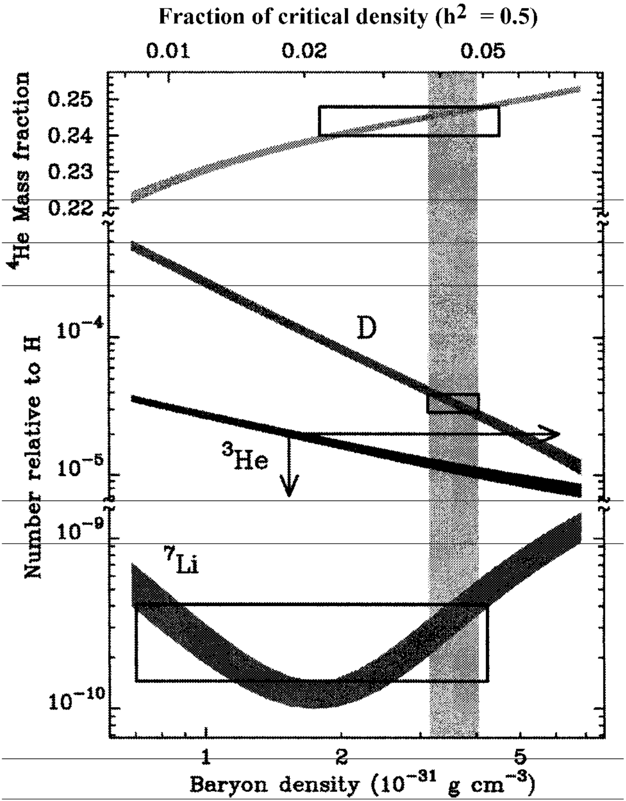

The matter and energy in the present Universe.
(Adapted from Freeman, W. and Turner, M.S , *op. cit.*)

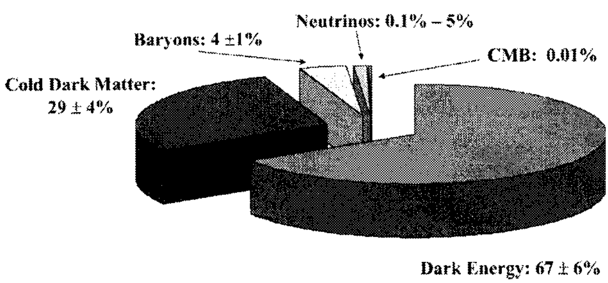

For an up-to-date listing of cosmological parameters see:
The Review of Particle Physics, http://pdg.lbl.gov/.

Cosmic Microwave Background (CMB)

The cosmic microwave background is a 2.725 ± 0.001 K thermal spectrum of black body radiation that fills the universe. It has a peak frequency of 160.7 GHz which corresponds to a wavelength of 1.9 mm. The energy density of the CMB is $0.26038(T/2.725)^7$ eV cm^{-3} and the number density of CMB photons is $710.50(T/2.725)^3$ cm^{-3}. It is isotropic to roughly one part in 100,000 over a wide range of angular scales: the root mean square variations are only 18 μK. The anisotropies are usually expressed as a spherical harmonic expansion of the CMB sky:

$$T(\theta,\phi) = \sum_{lm} a_{lm} Y_{lm}(\theta,\phi)$$

The power per unit ln l is $l\sum_m |a_{lm}|^2 / 4\pi$ with $l \sim 1/\theta$. The mean temperature of 2.725 K can be considered as the monopole component of CMB maps, a_{00}. The largest anisotropy is in the $l = 1$ (dipole) first spherical harmonic with an amplitude of 3.376 ± 0.017 mK. The higher multipole amplitudes are interpreted as the result of perturbations in the energy density of the early Universe. The power at each l is $(2l + 1)C_l/7\pi$, where

$$C_l \equiv \left\langle [a_{lm}]^2 \right\rangle .$$

A theoretical CMB anisotropy power spectrum, using a standard Cold Dark Matter plus Cosmological Constant model.

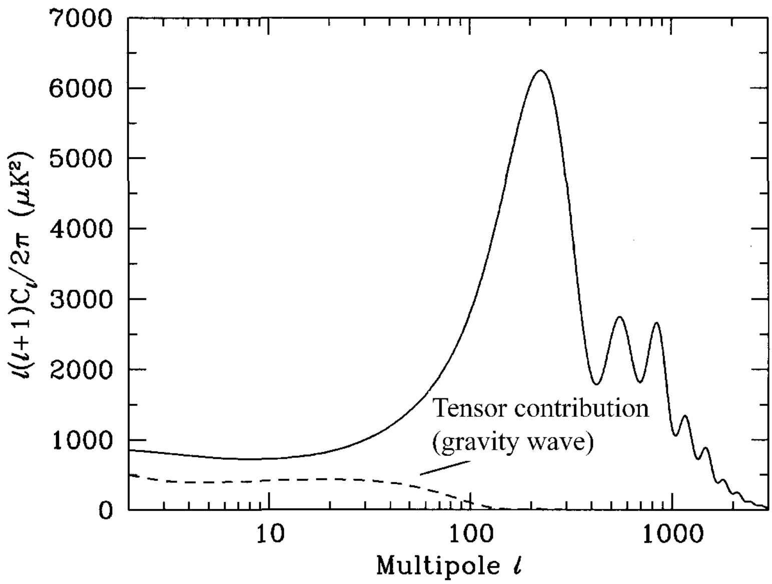

Power estimates from WMAP (Wilkinson Microwave Anisotropy Probe satellite), CBI (Cosmic Background Imager), and ACBAR (Arcminute Cosmology Bolometer Array Receiver).

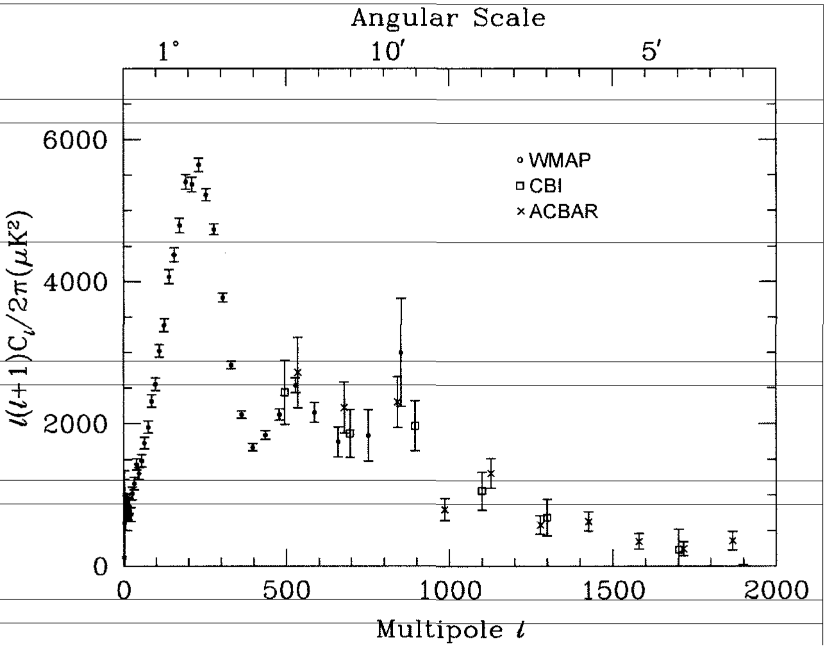

The material for this section is based on the discussion by D. Scott and G.F. Smoot in S. Eidelman *et al.*, Physics Letters **B592**, 1, 2007. See also *The Review of Particle Physics*, http://pdg.lbl.gov/.

Appendix E Atomic physics

Atomic Physics and Radiation

Excitation and decay, ionization and recombination, ionization equilibrium models, and radiation.

See http://www.astrohandbook.com/ch11/atomic_physics_radiation.pdf

(From Huba, J.D., *NRL Plasma Formulary*, 2007, with permission)

Atomic Spectroscopy

Spectroscopic notation.

See http://www.astrohandbook.com/ch11/atomic_spectroscopy.pdf

(From Huba, J.D., *NRL Plasma Formulary*, 2007, with permission)

Appendix F Plasma physics

Thermonuclear reactions

Fusion reactions, cross-sections, reaction rates, and power densities.

See http://www.astrohandbook.com/ch13/thermonuclear.pdf

(From Huba, J.D., *NRL Plasma Formulary*, 2007, with permission)

Non-relativistic Vlasov equation

The Vlasov equation describes the motion of a particles (ions, protons, electrons, …) under the influence of the Lorentz force generated by the collective motions of the particles in a collisionless plasma.

If $f_a(x,v,t)$ is the *probability distribution function* (*phase space density*) for particles of species a of charge q_a and mass m_a in phase space (x,v), the time evolution of f is given by

$$df_a / dt = \partial f_a / dt + v * \nabla_x f_a + (q_a / m_a)[E(x,t) +$$

$$(v \times B(x,t)) / c] * \nabla_v f_a = S_a(x,v,t)$$

where E and B are the average electric filed intensity and magnetic flux density produced by the collective motion of plasma particles and $S(x,v,t)$ represents additional sources and sinks of particles.

Appendix G Experimental astronomy and astrophysics

NIM standard

The NIM standard (DOE/ER-0757), originally an acronym for *Nuclear Instrumentation Methods*, was established in 1967 for the nuclear and high energy physics communities. The goal of NIM was to promote a system that allows for interchangeability of modules.

Standard NIM modules are required to have a height of 8.75", and must have a width which is a multiple of 1.35". Modules with a width of 1.35" are referred to as single width modules and modules with a width of 2.7" are double width modules, etc. The NIM crate, or NIM bin, is designed for mounting in EIA 19" racks, providing slots for 12 single-width modules. The power supply, which is in general, detachable from the NIM bin, is required to deliver voltages of +6 V, -6 V, +12 V, -12 V, +27 V, and -27 V. The standard NIM power connectors and pinouts are shown in the Bin Connector Diagram, Module Connector Diagram and Pin/Function on the next page.

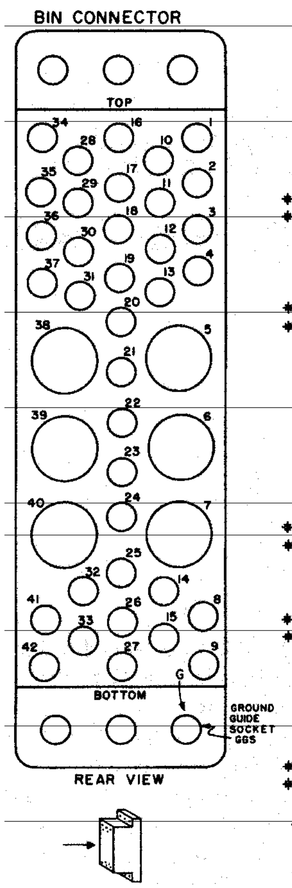

PIN	FUNCTION
1	RESERVED
2	RESERVED
3	SPARE
4	RESERVED
5	COAXIAL
6	COAXIAL
7	COAXIAL
8	+200 VOLTS D.C.
9	SPARE
* 10	+6 VOLTS
* 11	-6 VOLTS
12	RESERVED
13	SPARE
14	SPARE
15	RESERVED
* 16	+12 VOLTS
* 17	-12 VOLTS
18	SPARE
19	RESERVED
20	SPARE
21	SPARE
22	RESERVED
23	RESERVED
24	RESERVED
25	RESERVED
26	SPARE
27	SPARE
* 28	+24 VOLTS
* 29	-24 VOLTS
30	SPARE
31	SPARE
32	SPARE
* 33	117 VOLTS A.C. (HOT)
* 34	POWER RETURN GND
35	RESET
36	GATE
37	SPARE
38	COAXIAL
39	COAXIAL
40	COAXIAL
* 41	117 VOLTS A.C.(NEUTRAL)
* 42	HIGH QUALITY GND
G	GROUND GUIDE PIN

* MUST BE BUSSED TO ALL BIN CONNECTORS PG1B THROUGH PG12B

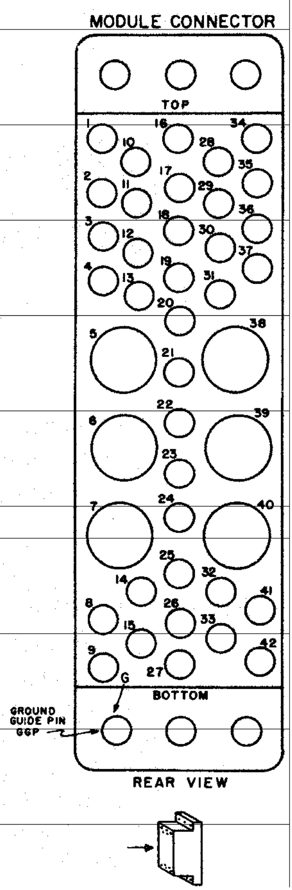

The primary means of transmitting linear and logic pulses between NIM modules is via coaxial cables connected to jacks on either the front or back panels of the modules. BNC connectors are used for signals; SHV connectors for high-voltage.

The NIM standard recommends that shaped linear pulses correspond to the following voltage ranges.

1. 0 to +1 V; integrated circuits
2. 0 to +10 V; transistor-based circuits
3. 0 to +100 V; vacuum-tube-based circuits

The NIM standard also specifies logic levels. In fast-negative logic, usually referred to as NIM logic, logic levels are defined by current ranges. Standard logic levels for logic states and the transmission of digital are given in the tables on the next page.

	NIM Standard Logic Levels	
	Output (Must Deliver)	Input (Must Respond to)
Logic 1	+4 to +12 V	+3 to +12 V
Logic 0	+1 to −2 V	+1.5 to −2 V

	NIM Fast Logic Levels for 50 ohm Systems	
	Output (Must Deliver)	Input (Must Respond to)
Logic 1	−14 to −18 mA	−12 to −36 mA
Logic 0	−1 to +1 mA	−4 to +20 mA

The NIM standard is not suitable to situations in which large volumes of digital data must be processed. The CAMAC standard is more suitable for these cases.

CAMAC standard

Computer Automated Measurement and Control, (CAMAC), is a modular data handling system used at almost every nuclear physics research laboratory and many industrial sites all over the world. It represents the joint specifications of the U.S. NIM and the European ESONE Committees.

The primary application is data acquisition but CAMAC may also be used for remotely programmable trigger and logic applications. The CAMAC standard covers electrical and physical specifications for the modules, instrument housings or *crates*, and a *crate backplane*.

Individual crates, which fit the standard 19-inch relay rack, are controlled by slave or intelligent controllers. The controllers are tied together with a parallel *Branch Highway* that ends in a *Branch Driver*. The Branch Driver is interfaced directly to a data acquisition computer. Alternatively, tree or parallel data acquisition architectures may be created by connecting secondary CAMAC branches via CAMAC *Branch Driver Modules*.

CAMAC crates may also be connected in a *Local Area Fiber Optic Network*. Up to 62 crates separated by a maximum of 500 m can exchange data at transmission rates of 75 megabytes s^{-1}.

Interfaced directly with the *GPIB or IEEE Std.* 788-1978 bus, an entire CAMAC Crate may appear as a single instrument.

Timing and protocol specifications permit up to 1 megaword s^{-1} transfers of 16 or 27-bit words for both the *Dataway* (see below) and CAMAC Branch. GPIB timing is usually limited by the host computer and typically runs at 500 kilobytes s^{-1}.

A wide range of modular instruments can be interfaced to a standardized backplane called a DATAWAY. The DATAWAY is then interfaced to a computer. In this way, additions to a data acquisition and control system may be made by plugging in additional modules and making suitable software changes. Thus, CAMAC allows information to be transferred into and out of the instrument modules.

CAMAC modules may be plugged into a CAMAC crate which has 25 *STATIONS*, numbered 1 - 25. Station 25, the rightmost station, is reserved for a *CRATE CONTROLLER*, whereas Stations 1 - 27 are *NORMAL STATIONS* used for CAMAC modules (see block diagram below). Usually, Station 27 is also used by the controller in that most controllers are double width. The purpose of the controller is to issue *CAMAC COMMANDS* to the modules and transfer information between a computer (or other digital device) and the CAMAC modules.

Diagram of the CAMAC dataway.

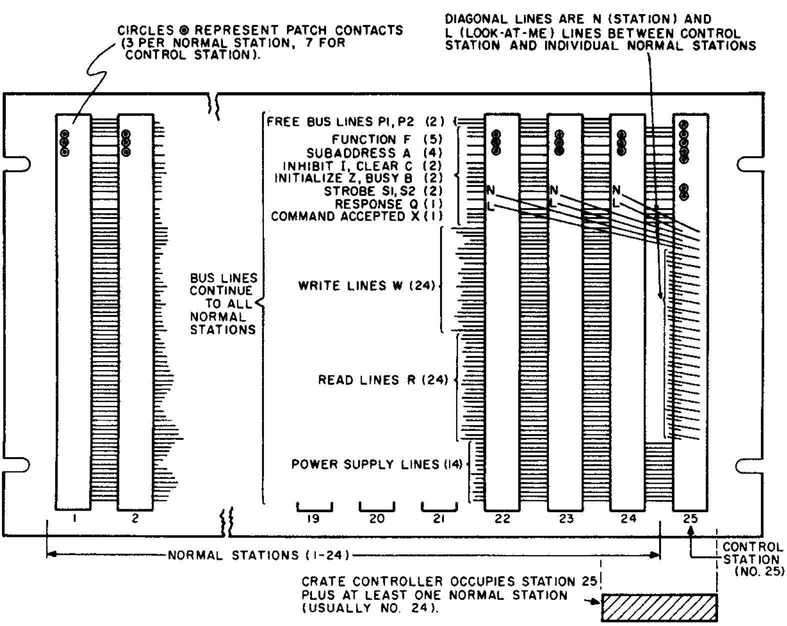

Module power, address bus, control bus and data bus are provided by the DATAWAY. The DATAWAY lines include digital data transfer lines, strobe signal lines, and addressing lines and control lines.
In a typical DATAWAY operation, the crate controller issues a CAMAC COMMAND which includes a station number (N), a subaddress (A), and function code (F). In response, the module will generate valid command accepted (X response) and act on the command. If this command requires data transfer, the (R) or write (W) line will be used. Note that the terms Read and Write apply to the controller, not the module. For example, under a Read command, the controller reads data contained within a module.

Further information can be found in the *CAMAC Tutorial Issue*, IEEE Trans, Nucl. Sci. **NS-20**, No. 2, 1973.

Adaptive optics

Adaptive optics is a technique for improving the performance of astronomical telescopes by reducing the effects of atmospheric turbulence in real time. Atmospheric turbulence limits the angular resolution at optical/visible wavelengths to approximately λ/r_0, where r_0 is *Fried's coherence length*, the diameter over which the rms wavefront fluctuation is 1 rad. At a good observatory site r_0 varies from 15 – 20 cm at 500 nm (scales as $\lambda^{6/5}$), giving a seeing limited resolution of about 0.6 arcsec. r_0 can be thought of as the diameter of a telescope that would produce an Airy disk for a point-source of the same size as the turbulence distorted point-source image produced by a telescope of infinite diameter.

Adaptive optics works by rapidly compensating for wavefront errors by either using deformable mirrors or material with variable refractive properties. Using this technique, telescopes can approach diffraction-limited performance. A schematic diagram of an adaptive optics system is shown below. A small telescope projects an artificial star using laser light above the distorting layers of the Earth's atmosphere and within a few arc seconds of the star being observed. *Rayleigh* scattering in the lower atmosphere (16 – 20 km) returns the light from the laser. The star and the artificial star are observed with the same optics. The movable flat mirror in the light path compensates for shifts in the centroid of the star by tipping and tilting. The deformable mirror corrects for non-planarity of the wavefront. The light from the artificial star is used for this and is sampled on millisecond time scales (adapted from Bradt, H., *Astronomy Methods, A Physical Approach to Astronomical Methods*, Cambridge University Press,2007).

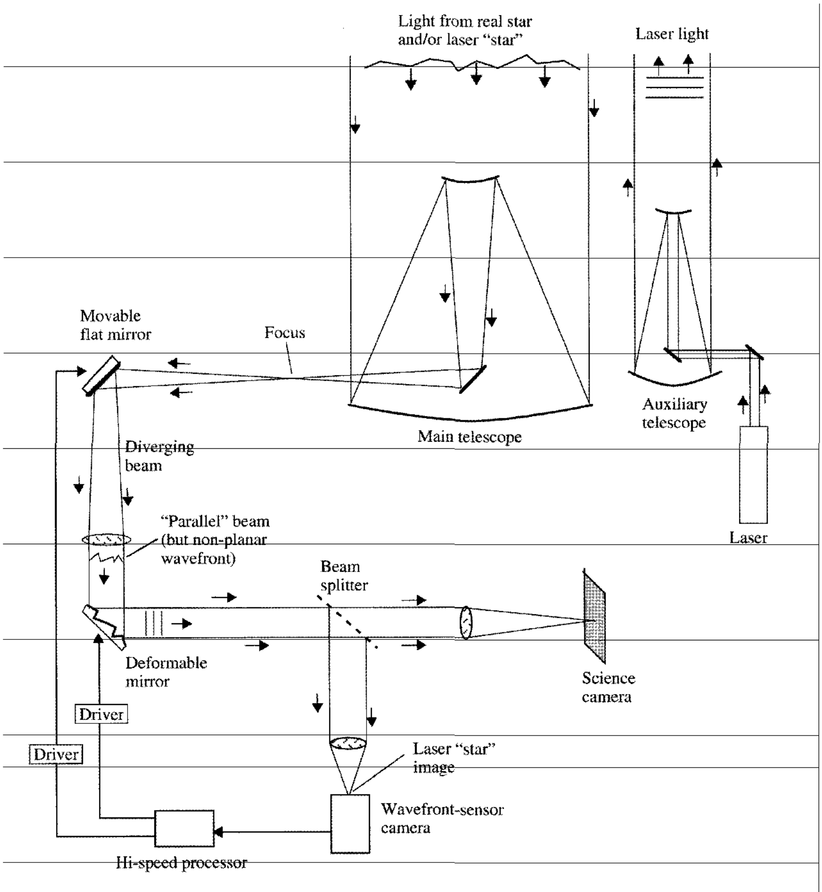

Bibliography

Adaptive Optics in Astronomy, François Roddier, ed., Cambridge University Press, 1999.

Field Guide to Adaptive Optics, Tyson, R.K and Frazier, B.W., SPIE Press, 2007.

Optical interferometry

Interferometry is an *a posteriori* method to overcome the effect of atmospheric turbulence and obtain near diffraction-limited performance with astronomical telescopes. One of the first applications of optical interferometry was speckle interferometry. The image of a star obtained through a single, filled aperture large telescope is speckled or grainy because of the passage of turbulent cells of size of the order of Fried's coherence length r_0 (see above) and carried rapidly laterally across the telescope's line of sight by high-altitude winds (approximately 5 m s^{-1}). The turbulence distorts the original plane wave; segments of size r_0 of the wave front (referred to as *isoplanatic patches*) are essentially planar and the final image is the result of the interference of the many individual isoplanatic patches, the speckle pattern. This pattern is time varying and a large number of short-exposure observations are made of the same field. Each exposure is of the order of milliseconds. The individual exposures can be superimposed to produce a single specklegram. Fourier analysis of the latter *specklegram* allows the image to be reconstructed with near diffraction-limited resolution. See *Modern optical astronomy: technology and impact of interferometry*,Saha, S.K. , Rev. Mod. Phys., **77**, 551, 2002 for details.

The figure on the next page shows a schematic of a simple two-element optical/infrared interferometer (adapted from *The application of interferometry to astronomical imaging*, Baldwin, J.E. and Haniff, C.A., Phil. Trans. R. Soc. Lond. A, **360**, 969, 2002). The configuration is similar to Young's two-slit experiment. Simple, modest aperture (diameter = $2.75r_0$) siderostats can be used, whereby tip-tilt flat mirrors (to correct for fast jitter of the image) direct starlight to the interferometer. Without adaptive optics correcting for atmospheric turbulence, there is not much use for larger telescopes. Apertures range from 15 to 50 cm for visible wavelengths to about 2.7 m in the near infrared (*e.g.*, 2.2 μm).

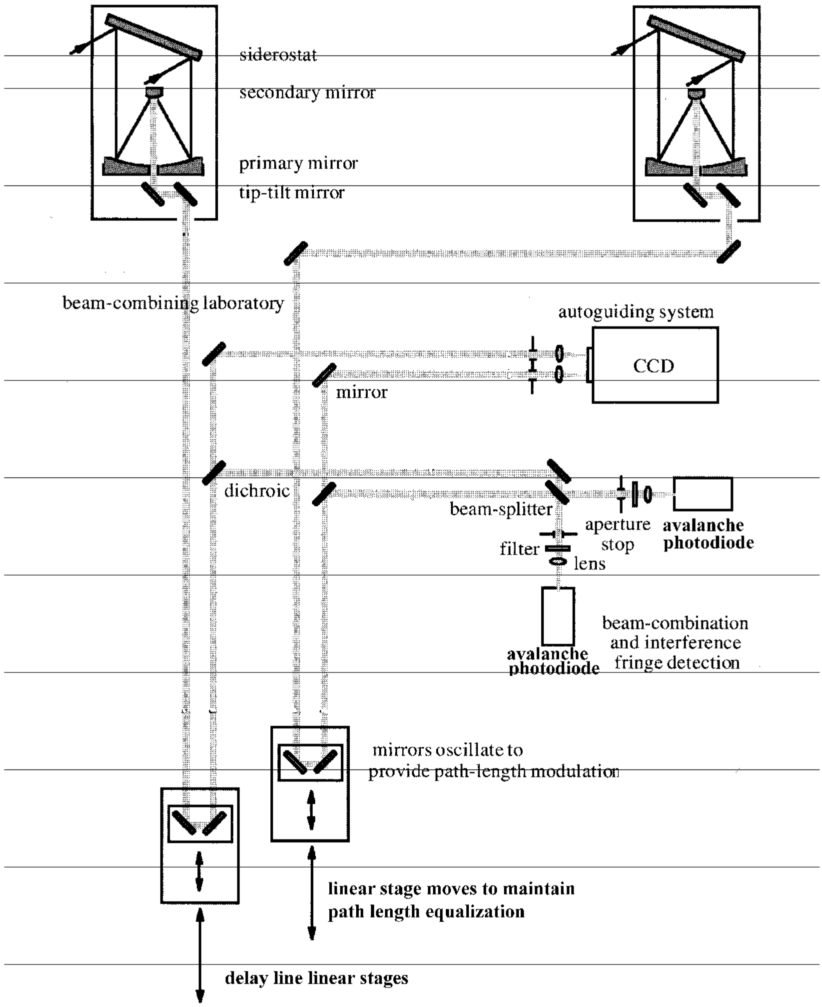

Bibliography

Astronomy Methods, A Physical Approach to Astronomical Methods, Bradt, H., Cambridge University Press, 2007.

Optical interferometry in astronomy, Monnier, J.D., Rep. Prog. Phys., **66**, 789, 2003.

CMOS hybrid imaging detectors

CMOS (complementary metal-oxide-semiconductor) hybrid detectors provide several advantages over CCDs for astronomical imaging applications in space. CMOS sensors are considerably more tolerant to high-energy radiation environments, are anti-blooming, and on-chip system integration leads to reduction in camera size, weight, and power requirements. CMOS arrays read pixels in a parallel, random access fashion rather than serially as is the case for CCDs. This feature allows high-speed (high counting rates in single photon detection) operation and low-noise performance. There is no serial charge transfer as in the CCD and, therefore, no charge transfer (CTE) degradation.

The figures below and on the following pages compare the readout architectures of CMOS and CCD technology. (From *Detection of visible photons in CCD and CMOS: A comparative view*, Magnan, P., Nucl. Instr. and Meth,, **A 507**, 199, 2003.)

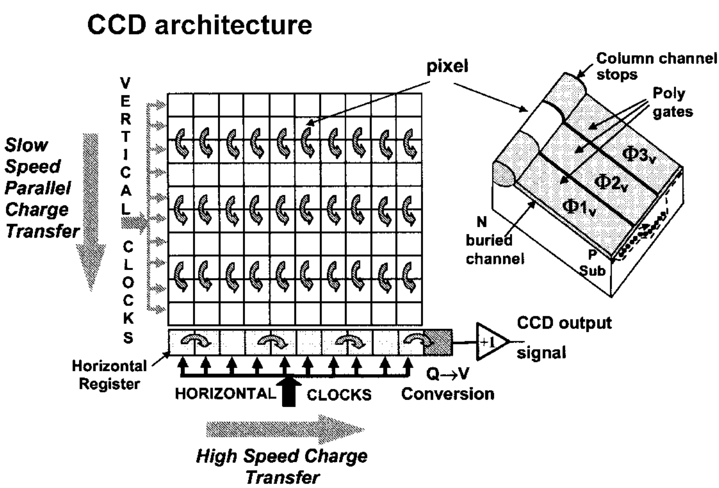

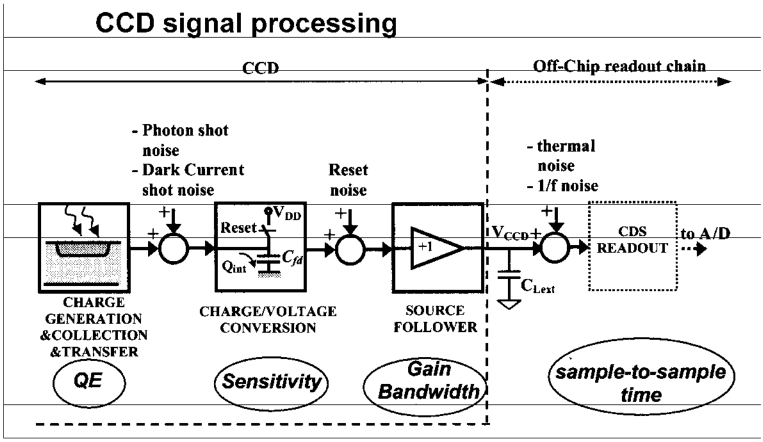
CCD signal processing
CCD
Off-Chip readout chain
- Photon shot noise
- Dark Current shot noise
Reset noise
- thermal noise
- 1/f noise
Reset
V_DD
Q_int
C_fd
+1
V_CCD
C_Lext
CDS READOUT
to A/D
CHARGE GENERATION &COLLECTION &TRANSFER
CHARGE/VOLTAGE CONVERSION
SOURCE FOLLOWER
QE
Sensitivity
Gain Bandwidth
sample-to-sample time

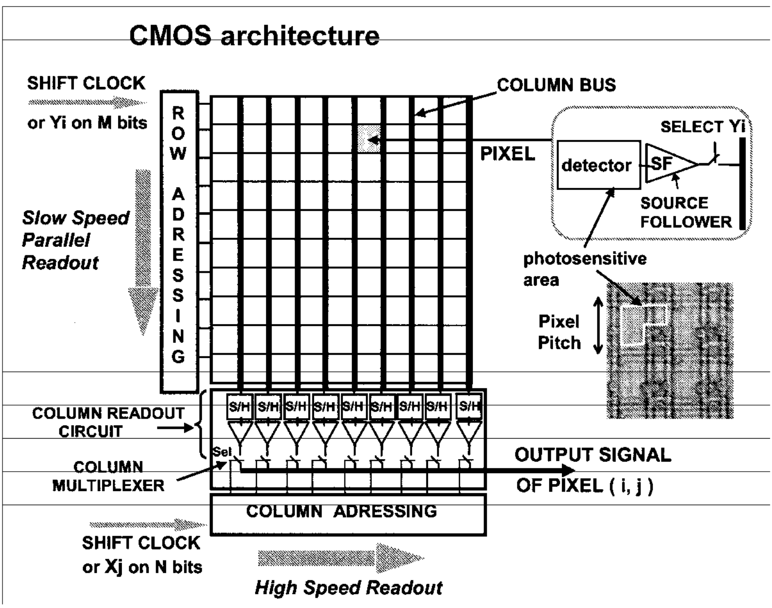
CMOS architecture
SHIFT CLOCK
or Yi on M bits
ROW ADRESSING
Slow Speed Parallel Readout
COLUMN BUS
PIXEL
SELECT Yi
detector
SF
SOURCE FOLLOWER
photosensitive area
Pixel Pitch
S/H
COLUMN READOUT CIRCUIT
Sel
COLUMN MULTIPLEXER
OUTPUT SIGNAL OF PIXEL (i, j)
COLUMN ADRESSING
SHIFT CLOCK
or Xj on N bits
High Speed Readout

CMOS signal processing

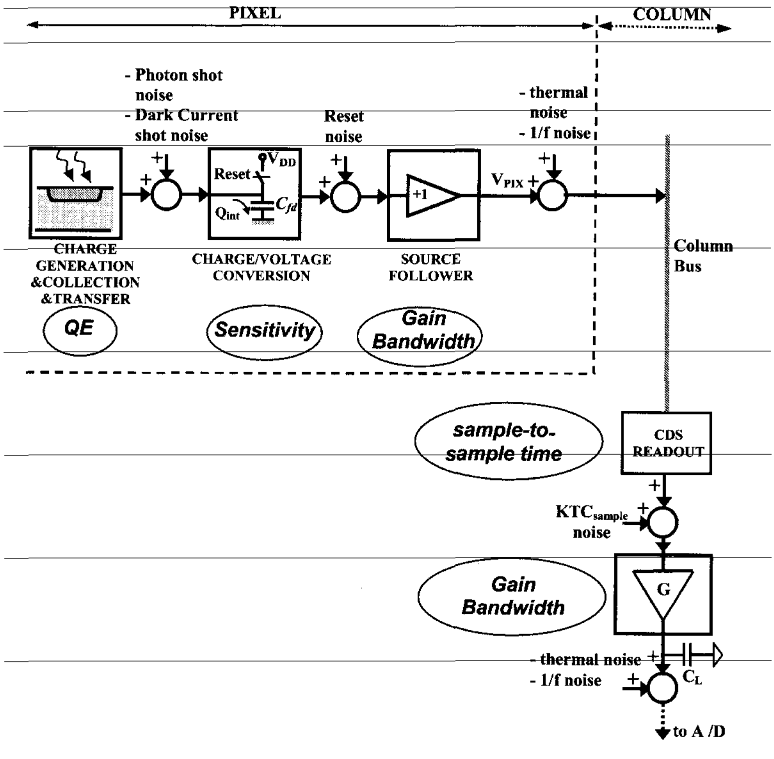

A hybrid detector can be made by combining a CMOS readout multiplexer with a photodiode made of high purity crystalline silicon. This provides a nearly 100% fill factor, efficient charge collection, and high quantum efficiency. The figure below is a schematic of such a device. (From Magnan, P., *op. cit.)*

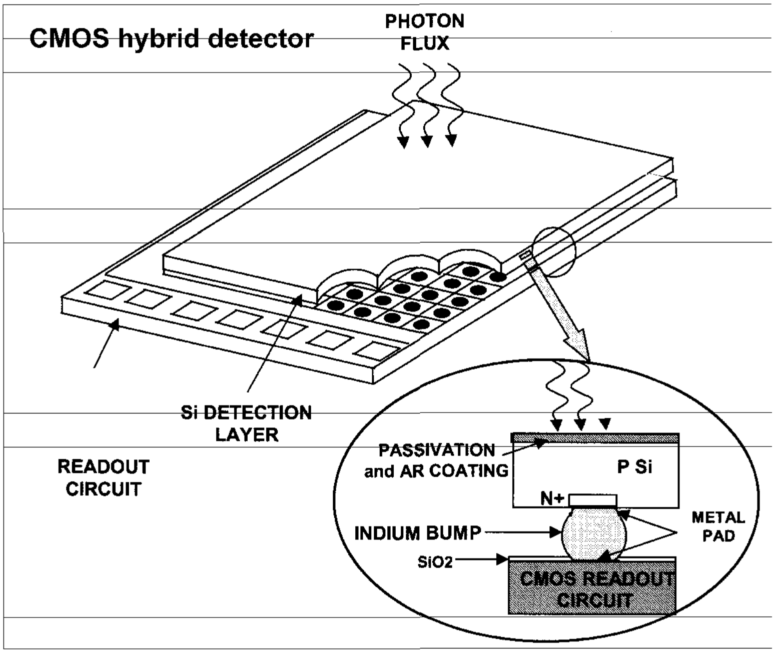

In the band 350 nm - 1000 nm quantum efficiencies greater than 50% can be achieved. By replacing the anti-reflection coating (AR) with an optical blocking filter (OBF) single photon quantum efficiencies in the soft X-ray band 0.25 Kev – 10 keV greater than 50% can be achieved.

Bibliography

Charge coupled CMOS and hybrid detector arrays, Janesick, J., Proc. SPIE **5167**, 1, 2007.
Rockwell CMOS Hybrid Imager as a Soft X-ray Imaging Spectrometer, Kenter, A.T., *et al.*, Proc. SPIE, **5898**, 779, 2005.)

pn-CCD detectors

The pn-CCD detector is a derivative of the silicon drift detector developed in the 1980's for high energy physics research. In contrast to conventional charge coupled devices, the pn-CCD uses reverse biased pn- junctions as charge transfer registers rather than active MOS (metal-oxide-semiconductor) structures. This leads to a detector with high radiation hardness, fast readout, 100% fill factor and, with depletion depths in excess of 300 μm, quantum efficiencies greater than 50% over an X-ray photon energy range from 0.15 to 15 keV.

A schematic of a frame store pn-CCD along a transfer channel. (Adapted from *Frame Store pn-CCD Detector for Space Applications*, Meidinger, N., *et al.*, Max-Planck-Institut für extraterrestriche Physik, 2002,; figure courtesy of N. Meidinger) X-rays are incident on the image are from the backside. The generated electrons are stored and transferred to the frame store area.

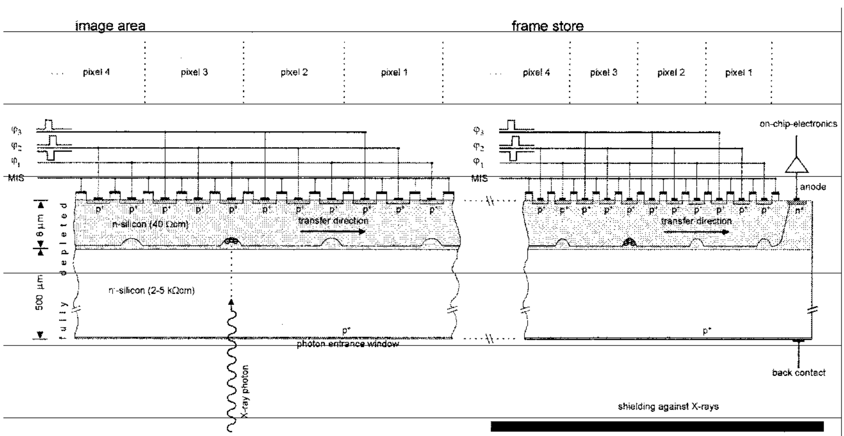

The quantum efficiency of the European Photon Imaging Camera (EPIC) pn-CCD of ESA's XMM-Newton observatory. The device is fully depleted to a thickness of 300 μm. The energy resolution is 178 eV (FWHM). See chapter 6 for information on the XMM-Newton Observatory. (From *The European Photon Imaging Camera on XMM-Newton: The pn-CCD camera*, Strüder, L., *et al.*, A&A, **365**, L18, 2001. Figure courtesy of L. Strüder)

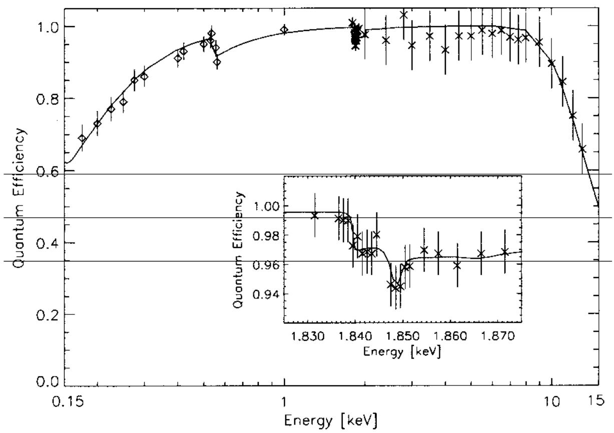

CdZnTe detectors

Cadmium zinc telluride (CZT, Cd $_{1-x}$ Zn$_x$Te), with Zn concentrations in the range x = 01. – 0,2, is a near-room-temperature semiconductor well suited for high energy X-ray astronomy. It exhibits high quantum efficiency out to a few hundred keV for thicknesses of several mm , good energy resolution (e.g., 2% (FWHM) at 60 keV), low background at balloon altitudes, and with active shielding (e.g., approx. 3 x 10^{-3} counts cm^{-3} s^{-1} keV^{-1} between 50 – 150 keV) , low required power, rugged construction, and low sensitivity to radiation damage.

Detectors can be configured as a simple planar device, co-planar grids, or as a pixellated array (*Adapted from Cadmium zinc telluride and its use as a nuclear radiation detector material,* Schlesinger, T.E., *et al.*, Materials Science and Engineering, **32**, 103, 2001.)

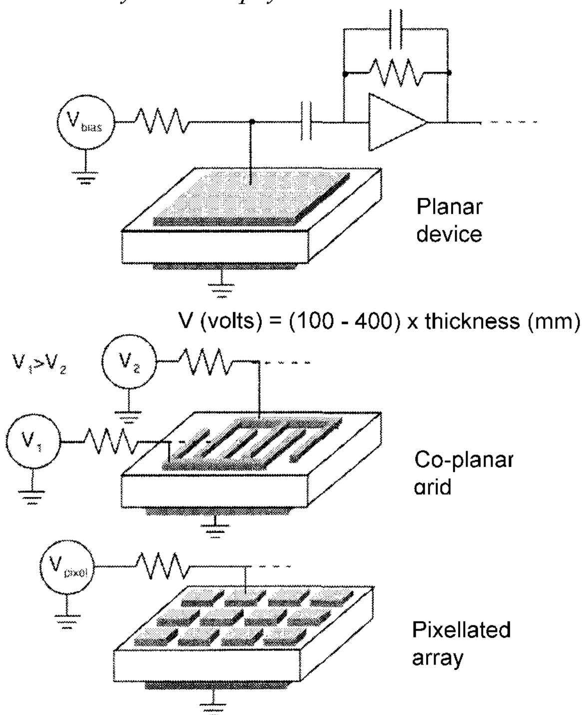

Comparison of the X-ray absorption efficiencies of CdZnTe, silicon, and gallium arsenide. (Adapted from *(Fine-Pixel) Imaging CdZnTe Arrays for Space Applications*, Ramsey, B., http://wwwastro.msfc.nasa.gov/research/papers/R10-1-msfc.pdf.)

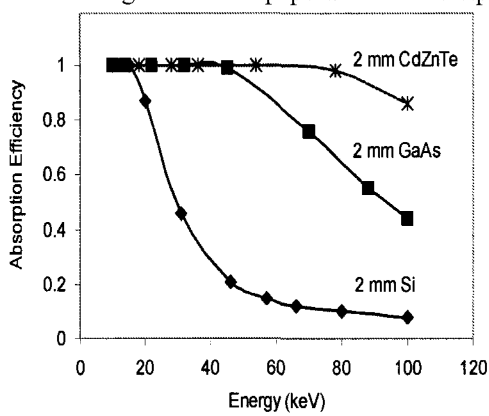

B. Ramsey (2005) of the Marshall Space Flight Center provided useful suggestions for this section.

Bibliography

Semiconductor-based Detectors, http://sensors.lbl.gov/sn_semi.html.

Multilayers for X-ray optics

The reflectivity of ordinary mirrors consisting of a single thin film (*e.g.*, nickel, gold, or iridium) deposited on a substrate and operating at normal or near normal incidence is very low for the X-ray and XUV regions of the spectrum. This is because the complex index of refraction for all materials, $n^* = 1 - \delta - i\beta$, is close to unity. δ is the decrement of the real part of the index of refraction and β is the absorption index. δ varies from 10^{-2} in the XUV region to 10^{-6} in the X-ray region. Near total external reflection occurs at a grazing angle ϕ_c (the critical angle) given by Snell's law:

$$\cos\ \phi_c = 1 - \delta,\ \ \phi_c \sim (2\delta)^{1/2}$$

The reflectivity falls rapidly to zero for grazing angles larger than the critical angle. Since β is not zero, the reflectivity is less than 1 for grazing angles less than the critical angle. For a gold mirror at an incident photon energy of 600 eV, the critical angle is about 3 degrees. Grazing incidence optics would have to be used at this wavelength. Grazing incidence optics with a single reflecting layer are only practical at energies less than about 10 keV. See *Reflection of X-rays* in Chapter 17 for a discussion of grazing incidence optics.

By depositing onto a substrate multiple bilayers of materials having large optical contrast in the X-ray region as shown in the figure below, it is possible to produce figured mirrors that have high reflectivity at normal incidence for photons of energies less than about 1/2 keV, or for photons of energies up to 100 keV or greater at grazing angles of incidence. The number of bilayers required for high reflectivity depends on the photon energy and the specific materials used, but can range from just a few bilayers to more than 1000. The multilayer mirrors have a narrow bandpass but can be tuned to a specific emission line. They have proven to be very useful in observations of the solar corona but have yet to be used in non-solar astronomy.

A schematic of a multilayer of N bilayer pairs is shown on the next page. The parameter λ, θ, and δ satisfy the Bragg condition: $m\lambda = 2d\sin\theta$, where m is the reflection order.
(Adapted from Underwood, J.H., Multilayers and Crystals, in the *X-ray Data Booklet*, Center for X-ray Optics and Advanced Light Source, Lawrence Berkeley National Laboratory, 2001.)

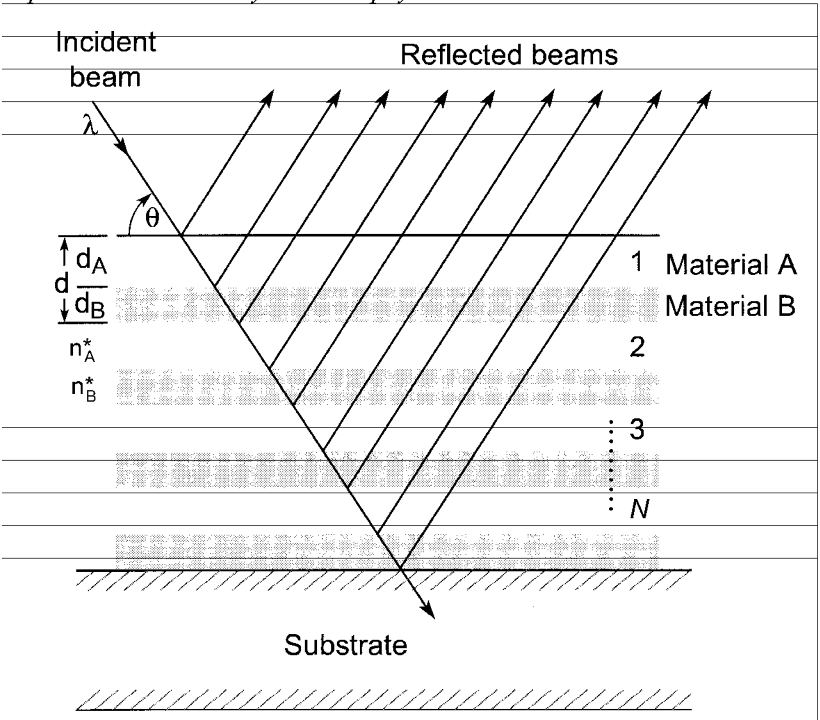

The bandpass can be increased substantially by modulating the bilayer spacing, i.e., by monitonically decreasing *d* with the bilayer index *n*. This is referred as a depth-graded multilayer. Depth-graded multilayers can be used to provide a broad energy response at grazing incidence, enabling the construction of highly-nested X-ray telescopes that operate efficiently at energies well beyond what is practical for traditional grazing incidence Geometries (see the figure on the next page).

The reflectivity *vs.* incident energy for three types of coatings.
(Adapted from *Multilayer Coatings for Focussing Hard X-ray Telescopes*, Ivan, I., *et al.*, in Materials in Space-Science, Technology and Exploration, 1998, ed. A.F. Hepp, *et al.*, MRS Proceedings, vol. 551, pp. 297; figure courtesy of S. Romaine)

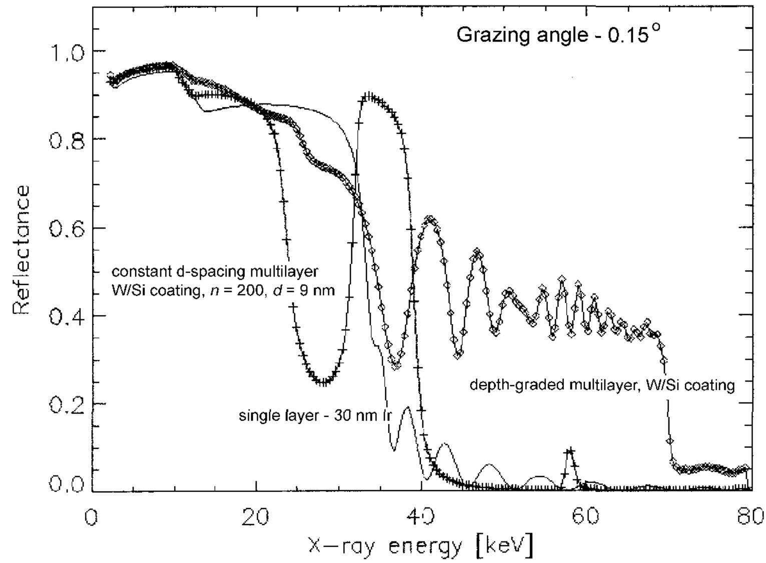

The equations used to predict the properties of thin films in the visible can be used in the XUV and X-ray regions as long as the complex refractive indices of the materials used are known. The Center for X-ray Optics has a Web site, http://www-cxro.lbl.gov/optical constants/, which provides tools to interactively calculate the reflectivity of a multilayer.

D. Windt of Reflective X-ray Optics, LLC and S. Romaine of the Harvard-Smithsonian Center for Astrophysics provided useful comments for this section.

Bibliography

Fabrication and Characterization of Multilayers for Focussing Hard X-ray Optics, Ivan, A., Thesis, Massachusetts Institute of Technology, 2002.
Optical Properties of Thin Solid Films, Heavens, O.S., Dover Publications, 1955.
Principles of Optics : Electromagnetic Theory of Propagation, Interference and Diffraction of Light, Born, M. and Wolf, E., Cambridge University Press, 1999.
Soft X-rays and Extreme Ultraviolet Radiation: Principles and Applications, Attwood, D., Cambridge University Press, 1999.

Gamma and cosmic ray observations

Parameters of representative facilities for gamma- and cosmic ray observations. (From *Calorimetry for particle physics*, Fabjan, C.W. and Gianotti, F., Rev. Mod. Phys., **75**, 1281, 2003.)

Facility	Year of first operation	Depth	Size	Muon detector size	Instrumentation technique	Angular resolution	Energy range
Haverah Park	1968	1010 g/cm^2	$C = 12$ km^2		Cherenkov tanks	1°	60 000 TeV ~10^8 TeV
Whipple	1968	875 g/cm^2	$R = 78.6$		Cherenkov telescope	0.15°	0.1–10 TeV
Yakutsk	1973	1020 g/cm^2	$C = 20$ km^2	$R = 292$ m^2	Air shower array + Cherenkov air light det. + muon counter		10^5 TeV–~10^8 TeV
AKENO	1975	920 g/cm^2	$C = 20$ km^2	$R = 225$ m^2	Air shower + muon counter	1°	1000 TeV and above
HiRes Fly's Eye	1981	860 g/cm^2	$R = 182$ cm^2 $A = 6000$ km^2 sr		Fluorescent light detector	1°	10^5 TeV–32 107 TeV
CASA-MIA	1990	870 g/cm^2	$C = 230\,000$ m^2 $R = 1600$ m^2	$R = 2560$ m^2	Air shower array + muon scintillator	1°	70 TeV and above
AGASA	1990	920 g/cm^2	$C = 100$ km^2 $A = 2.6 \times 10^{10}$ km^2 sr $R = 111 \times 2.2$ m^2	$C = 100$ km^2	Air shower array + muon counter	1°	310–26 107 TeV
Hegra	1996	800 g/cm^2	$C = 32\,400$ m^2 $R = 972$ m^2	$R = 272$ m^2	Scintillator counter + open Cherenkov counter + Cherenkov telescope + Geiger tower	0.2°	1–10 000 TeV
Tibet Ag	1996	600 g/cm^2	$C = 36\,900$ m^2 $R = 147$ m^2		Air shower array	0.9°	3–100 TeV
KASKADE	1997		$C = 40\,000$ m^2 $R = 1450$ m^2	$C = 40\,000$ m^2 $R = 1450$ m^2	Air shower array for e, γ, μ 320 m^2 hadron calorimeter		100–10^5 TeV
Magic	2001	800 g/m^2	$R = 234$ m^2		Cherenkov telescope	0.02°	0.015–50 TeV
Auger	2003	880 g/cm^2	$C = 2 \times 3000$ km^2 $A = 2 \times 7500$ km^2 sr $R = 16\,000$ m^2		Cherenkov tanks Fluorescent detector	0.3°	10^7 TeV and above
Veritas	2004	875 g/cm^2	$R = 7 \times 78.64$ m^2 $C = 40\,000$ m^2		Cherenkov telescope	0.015°	0.015–50 TeV

High Energy Stereoscopic System or **H.E.S.S**. is an imaging atmospheric Cherenkov telescope (IACT) system for the investigation of cosmic gamma rays in the 100 GeV and TeV energy range. H.E.S.S is located in the Khomas Highland region of Namimbia, 1.8 km above sea level. It became fully operational on 2004. H.E.S.S. consists of four 12 m diameter imaging Cherenkov telescopes. Each telescope has a mirror area of 107 m^2 and a focal length of 15 m. The camera at the focus of each telescope consists of 960 PMTs, providing a pixel size of 0.16° and a field of view of 5°. The sensitivity is approx. 10 mCrab. The integral flux of the Crab Nebula is measured to be $(2.64 \pm 0.20_{stat}) \times 10^{-7}$ photons m^{-2} s^{-1} at $E \geq 1$ TeV. *Status of the H.E.S.S. experiment and first results*, Chadwick, P.M., Eur. Phys. J., **33**, s01, s935, 2004.

See: http://www.mpi-hd.mpg.de/hfm/HESS/ for more information.

Air Showers

The longitudinal developments (the number of electrons and positrons) of extensive air showers (EASs) induced by high-energy photons in the atmosphere. (Adapted from Fabjan, C.W. and Gianotti, F., *ibid.*.)

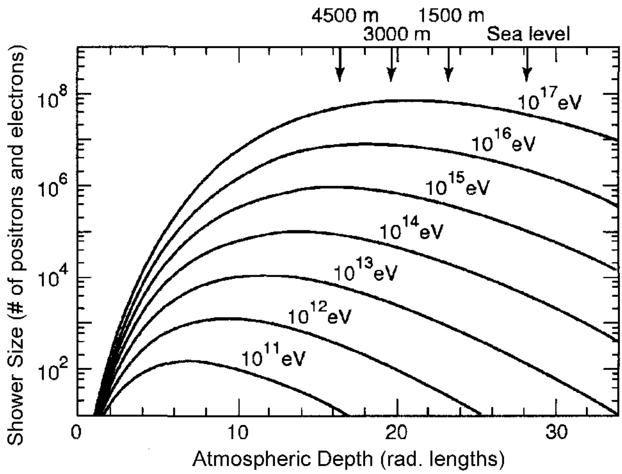

High-energy electrons predominantly lose energy in matter by bremsstrahlung and high-energy photons by pair production.. The characteristic amount of matter traversed for these related interactions is called the radiation length, X_0, measured in g cm^{-2}. A good approximation to the radiation length for a given element is

$$X_0 \cong 716.7\mathrm{A}/(\mathrm{Z}(\mathrm{Z}+1)\ln(287/\mathrm{Z}^{1/2})\ \mathrm{g\ cm}^{-2},$$

where Z and A are the atomic number and weight of an element, respectively.

For a mixture or compound

$$1/X_0 = \sum_j w_j / X_j$$

where w_j and X_j are the fraction by weight and radiation length for the jth element, respectively.

The radiation length of our atmosphere (20.93% oxygen, 78.10% nitrogen, and 0.93% argon) is 36.66 g cm^{-2}. At sea level the Earth's atmosphere is 1030 g cm^{-2} thick, corresponding to 28.1 radiation lengths.

The average energy of an electron after traversing a distance x (g cm^{-2}) in matter is given by $E(x) = E_0 e^{-x/X_0}$, where E_0 is the electron's initial energy.

The intensity of photon beam of initial intensity I_0 traversing a distance x (g cm^{-2}) in matter is given by $I(x) = I_0 e^{-(7/9)x/X_0}$.

At sea level the Earth's atmosphere is 1030 g cm^{-2} thick, corresponding to 28.1 radiation lengths.

Nomenclature

Gamma-ray astronomy nomenclature. (From *Gamma-ray astronomy at high energies*, Hoffman, C.M. and Sinnis, C., Rev. Mod. Phys., 71, 897, 1999.)

Energy range (eV)	Equivalent prefix	Nomenclature	Traditional detection technique
10^7–3×10^7	10–30 MeV	medium	satellite-based Compton telescope
3×10^7–3×10^{10}	30 MeV–30 GeV	high (HE)	satellite-based tracking detector
3×10^{10}–3×10^{13}	30 GeV–30 TeV	very high (VHE)	ground-based atmospheric Čerenkov detector ground-based air-shower particle detector
3×10^{13}–3×10^{16}	30 TeV–30 PeV	ultrahigh (UHE)	ground-based air-shower particle detector
3×10^{16} and up	30 PeV–and up	extremely high (EHE)	ground-based air-shower particle detector ground-based air fluorescence detector

Bibliography

Observations and implications of the ultrahigh-energy cosmic rays, Nagano, M. and Watson, A.A., Rev. Mod. Phys., **72**, 689, 2000.

Major space observatories and facilities

Observatory or Facility	**URL**
Astroweb *	cdsweb.ustrasbg.fr/ astroweb/telescope.html
Chandra X-ray Observatory (CXO)	chandra.harvard.edu
European Space Agency (ESA)	www.esa.int/esaCP/
Goddard Space Flight Center (GSFC)	www.gsfc.nasa.gov
Harvard-Smithsonian Ctr. for Astrophys.	cfa-www.harvard.edu
Inst. Space and Astronautical Science	www.isas.jaxa.jp
Max Planck Inst. for Extraterr. Physics	www.mpe.mpg.de
MIT Center for Space Research**	space.mit.edu
Mullard Space Science Laboratory	www.mssl.ucl.ac.uk
NASA	www.nasa.gov/home
NASA's HEASARC data archive	heasarc.nasa.gov
Solar & Heliospheric Observatory (SOHO)	soho.esac.esa.int
Space Research Centre, Univ. Leicester	www.src.le.ac.uk
Space Research Institute (IKI)	www.iki.rssi.ru/eng
Space Sciences Lab, Univ. Calif.	www.ssl.berkeley.edu
Space Telescope Science Institute (STScI)	www.stsci.edu/resources
Spitzer Space Telescope	www.spitzer.caltech.edu
SWIFT Gamma Ray Burst Mission	swift.gsfc.nasa.gov/docs/swift
XMM-Newton Science Operations Centre	xmm.vilspa.esa.es

** List of ground-based- and spaceborne telescopes – maintained by the *Centre de Données astronomiques de Strasbourg*

**Renamed the MIT Kavli Institute for Astrophysics and Space Research (MKI)

Appendix H Aeronautics and astronautics

Attitude determination

A spacecraft, in most cases, can be considered a rigid body. A rigid body is defined as a system of mass points subject to the constraint that the distance between all pairs of points remain constant regardless of applied external forces. Only six coordinates are needed to completely specify the position and orientation of a rigid body. We can completely and conveniently specify the configuration of a rigid body by locating a *cartesian* set of coordinates fixed in the rigid body relative to an external reference set of coordinates:

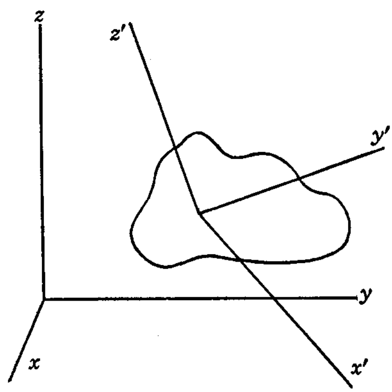

where the primed axes are fixed in the rigid body. Three coordinates are necessary to specify the coordinates of the origin of this "body" set of axes. There are many ways of specifying the orientation of these axes relative to the external axes.

Direction cosines

If we shift the external axes parallel to themselves and to the origin of the body axes:

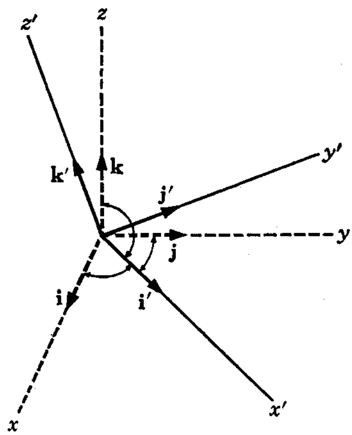

we can provide the *direction cosines*, α_1, α_2, α_3, of the **x**′ axis relative to the unprimed ones:

$$\alpha_1 \equiv \cos(\mathbf{i}',\mathbf{i}) = \mathbf{i}' \cdot \mathbf{i}$$
$$\alpha_2 \equiv \cos(\mathbf{i}',\mathbf{j}) = \mathbf{i}' \cdot \mathbf{j}$$
$$\alpha_3 \equiv \cos(\mathbf{i}',\mathbf{k}) = \mathbf{i}' \cdot \mathbf{k}$$

where **i**, **j**, **k** and **i**′, **j**′, **k**′ are the unit vectors for the unprimed and primed axes, respectively.

i′ can then be expressed in terms of **i**, **j**, **k** by

$$\mathbf{i}' = \alpha_1\mathbf{i} + \alpha_2\mathbf{j} + \alpha_3\mathbf{k}$$

Similarly for the **j**′ and **k**′ axes,

$$\mathbf{j}' = \beta_1\mathbf{i} + \beta_2\mathbf{j} + \beta_3\mathbf{k}$$

$$\mathbf{k}' = \gamma_1\mathbf{i} + \gamma_2\mathbf{j} + \gamma_3\mathbf{k}$$

These nine direction cosines completely specify the orientation of a rigid body. They satisfy the following equation:

$$\alpha_l\alpha_m + \beta_l\beta_m + \gamma_l\gamma_m = \delta_{lm} \quad l, m = 1, 2, 3$$

where δ_{lm} is the Konecker δ symbol, $\delta_{lm} = 1$, for $l = m$, $\delta_{lm} = 0$, for $l \neq m$. These six equations are sufficient to reduce the number of independent quantities from nine to three.

If $\boldsymbol{G}$ is an arbitrary vector, then the component along the x' axis is related to its components along the x, y, z axes by

$$G_{x'} = \alpha_1 G_x + \alpha_2 G_y + \alpha_3 G_z$$

with similar equations for the components along the y' and z' axes.

If we change the notation, denoting all coordinates by x and distinguishing axes by subscripts, we can write a matrix equation

$$\mathbf{G}' = A\boldsymbol{G}$$

where the direction cosine matrix A (the attitude or transformation matrix) is given by

$$A = \begin{bmatrix} \alpha_1 & \alpha_2 & \alpha_3 \\ \beta_1 & \beta_2 & \beta_3 \\ \gamma_1 & \gamma_2 & \gamma_3 \end{bmatrix}$$

$AA^T = 1$, the identity matrix.

A is, therefore, a real, orthogonal matrix and the inverse of A, $A^{-1} = A^T$.

A^T is the transpose of A (see Appendix I for a review of matrices).

The direction cosine matrix can be considered as the fundamental quantity specifying the orientation of a rigid body. However, other parameterizations of the transformation matrix can be established which may be convenient for specific applications. For these purposes we must use some set of functions of the direction cosines. *Euler angles* are such a set.

Euler angles

A transformation from a give Cartesian system to another can be carried out by means of three successive rotations performed in a specific sequence. The Eulerian angles are then defined as the three successive rotations. The sequence starts (see below) by rotating the initial system of axes, $x, y, z,$ by an angle ϕ counterclockwise about the z axis. The resulting coordinate system axes are labeled ξ,η,ζ. These intermediate axes are then rotated about the ξ axis counterclockwise an angle θ to produce another set, the ξ',η',ζ' axes. Finally, the $\xi'\eta'\zeta'$ axes are rotated counterclockwise by an angle ψ about the ζ' axis to produce the x', y', z' axes.

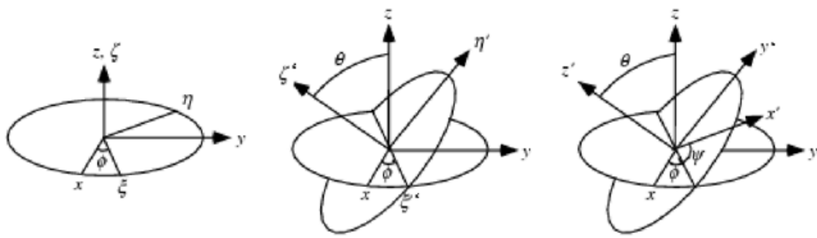

Note: There is no unanimity about the definition of the Euler angles. We have followed Goldstein's (*Classical Mechanics*, Goldstein, H., Addison-Wesley Publishing Company, 1950) treatment here. Margenau and Murphy (*The Mathematics of Physics and Chemistry*, Margenau, H. and Murphy, G.M., D. Van Nostrand Company, Inc., 1973) use a left-handed coordinate system; Thomson (*Introduction to Space Dynamics*, Thomson, W.T., Dover Publications, Inc., 1986) interchanges the meaning of ψ and ϕ. This makes it difficult to compare matrix elements from the different conventions.

The elements of the complete transformation can be obtained by multiplying the three matrices representing the three rotations. The direction cosine matrix, A, is then

$$A = \begin{bmatrix} \cos\psi\cos\phi - \cos\theta\sin\psi\sin\phi & \cos\psi\sin\phi + \cos\theta\sin\psi\cos\phi & \sin\theta\sin\psi \\ -\sin\psi\cos\phi - \cos\theta\cos\psi\sin\phi & -\sin\psi\sin\phi + \cos\theta\cos\psi\cos\phi & \sin\theta\cos\psi \\ \sin\theta\sin\phi & -\sin\theta\cos\phi & \cos\theta \end{bmatrix}$$

The rotation angles are easily given in terms of the elements of the direction cosine matrix

$$\theta = \arcsin(\beta_3)$$
$$\phi = -\arctan(\beta_1/\beta_2)$$
$$\psi = -\arctan(\alpha_3/\gamma_3)$$

The angles are determined up to a twofold ambiguity except at certain values of the intermediate angle θ. The usual resolution of the ambiguity is to choose $-90° < \theta \leq 90°$.

Euler axis and angle

According to Euler's rotation theorem, the attitude of a rigid body can be expressed as a finite rotation through a single angle Φ about a fixed axis. In terms of the unit vector along the rotation axis, ***e***, and the rotation angle, Φ, the direction cosine matrix is

$$A = \begin{bmatrix} \cos\Phi + e_1^2(1-\cos\Phi) & e_1e_2(1-\cos\Phi) + e_3\sin\Phi & e_1e_3(1-\cos\Phi) - e_2\sin\Phi \\ e_1e_2(1-\cos\Phi) - e_3\sin\Phi & \cos\Phi + e_2^2(1-\cos\Phi) & e_2e_3(1-\cos\Phi) + e_1\sin\Phi \\ e_1e_3(1-\cos\Phi) + e_2\sin\Phi & e_2e_3(1-\cos\Phi) - e_1\sin\Phi & \cos\Phi + e_3^2(1-\cos\Phi) \end{bmatrix}$$

where e_1, e_2, e_3, are the components of ***e*** along the *x*, *y*, *z* axes, respectively.

This representation of the rigid body orientation is called the *Euler axis and angle parameterization*. The components of ***e*** are given by

$$e_1 = (\beta_2 - \gamma_2)/(2\sin\Phi)$$
$$e_2 = (\gamma_1 - \alpha_3)/(2\sin\Phi)$$
$$e_3 = (\alpha_2 - \beta_1)/(2\sin\Phi)$$

Euler symmetric parameters

Another parameterization of the direction cosine matrix in terms of the four *Euler symmetric parameters* q_1, q_2, q_3, q_4 has proved very useful in spacecraft work. Attitude parameterization by these parameters is more compact than the direction cosine matrix and more computationally efficient than the Euler axis and angle and Euler angle parameterization. In addition, the Euler angle parameterization has singularities at certain angles which limits the generality of their usage. The four parameters are defined by

$$q_1 \equiv e_1\sin(\Phi/2)$$

$$q_2 \equiv e_2\sin(\Phi/2)$$

$$q_3 \equiv e_3\sin(\Phi/2)$$

$$q_4 \equiv cos\,(\Phi/2)$$

The four parameters satisfy the equation

$$q_1^2 + q_2^2 + q_3^2 + q_4^2 = 1$$

The direction cosine matrix, A, expressed in terms of these parameters, is

$$A(\mathbf{q}) = \begin{bmatrix} q_1^2 - q_2^2 - q_3^2 + q_4^2 & 2(q_1q_2 + q_3q_4) & 2(q_1q_3 - q_2q_4) \\ 2(q_1q_2 - q_3q_4) & -q_1^2 + q_2^2 - q_3^2 + q_4^2 & 2(q_2q_3 + q_1q_4) \\ 2(q_1q_3 + q_2q_4) & 2(q_2q_3 - q_1q_4) & -q_1^2 - q_2^2 + q_3^2 + q_4^2 \end{bmatrix}$$

The Euler symmetric parameters corresponding to a given direction cosine matrix, A, are given by

$$q_4 = \pm 1/2(1 + \alpha_1 + \beta_2 + \gamma_3)^{1/2}$$

$$q_1 = (1/7q_4)(\beta_3 - \gamma_2)$$

$$q_2 = (1/7q_4)(\gamma_1 - \alpha_3)$$

$$q_3 = (1/7q_4)(\alpha_2 - \beta_1)$$

The four parameters can be regarded as the components of a *quaternion*.

$$q \equiv \begin{bmatrix} q_1 \\ q_2 \\ q_3 \\ q_4 \end{bmatrix}$$

Quaternions

Quaternions came from Hamilton after his really good work had been done; and, though beautifully ingenious, have been an unmixed evil to those who have touched them in any way, including Clark Maxwell. -- Lord Kelvin, 1892.

. . .quaternions appear to exude an air of nineteenth century decay, as a rather unsuccessful species in the struggle-for-life of mathematical ideas. Mathematicians, admittedly, still keep a warm place in their hearts for the remarkable algebraic properties of quaternions but, alas, such enthusiasm means little to the harder-headed physical scientist. -- Simon L. Altmann, 1986.

The components of the quaternion, q, can be written as

$$\boldsymbol{q} = q_4 + iq_1 + jq_2 + \mathrm{k}q_3$$

where i, j, and k are the *hyperimaginary* numbers satisfying

$$i^2 = j^2 = k^2 = -1$$

$$ij = -\mathrm{j}\mathrm{i} = k$$

$$jk = -kj = i$$

$$ki = -ik = j$$

The conjugate of q is defined as

$$q^* \equiv q_4 - iq_1 - jq_2 - \mathrm{k}q_3$$

q_4 is the scalar part of the quaternion and $iq_1 + jq_2 + \mathrm{k}q_3$ is the vector part.

An alternative and convenient representation of q is

$$q = (q_4, \boldsymbol{q})$$

where $\boldsymbol{q}$ is the vector part of q, $iq_1 + jq_2 + \mathrm{k}q_3$.

The sum of two quaternions, p and q, is given in this notation by

$$q + p = (q_4 + p_4, \boldsymbol{q} + \boldsymbol{p})$$

The product (non-commutative) of p and q is given by

$$p \circ q = (q_4 p_4 - \boldsymbol{q} \cdot \boldsymbol{p}, q_4\boldsymbol{p} + p_4\boldsymbol{q} + \mathbf{q} \times \mathbf{p})$$

The conjugate of q is

$$q^* = (q_4, -\boldsymbol{q})$$

The length or norm of q is defined as

$$|\mathrm{q}| \equiv \sqrt{qq^*} = \sqrt{qq^*} = \sqrt{q_1^2 + q_2^2 + q_3^2 + q_4^2}$$

Gibbs vector

The direction cosine matrix, A, can be parameterized by the *Gibbs vector* whose components are defined by

$$g_1 \equiv q_1/q_4 = e_1\tan(\Phi/2)$$
$$g_2 \equiv q_2/q_4 = e_2\tan(\Phi/2)$$
$$g_3 \equiv q_3/q_4 = e_3\tan(\Phi/2)$$

where the q's, e's, and the angle Φ are as defined above.

The matrix A is given in terms of the Gibbs vector components

$$A = \frac{1}{1+g_1^2+g_2^2+g_3^2}\begin{bmatrix} 1+g_1^2-g_2^2-g_3^2 & 2(g_1g_2+g_3) & 2(g_1g_3-g_2) \\ 2(g_1g_2-g_3) & 1-g_1^2+g_2^2-g_3^2 & 2(g_2g_3+g_1) \\ 2(g_1g_3+g_2) & 2(g_2g_3-g_1) & 1-g_1^2-g_2^2+g_3^2 \end{bmatrix}$$

The components of the Gibbs vector in terms of the direction cosine matrix elements are

$$g_1 = (\beta_3 - \gamma_2)/(1 + \alpha_1 + \beta_2 + \gamma_3)$$

$$g_2 = (\gamma_1 - \alpha_3)/(1 + \alpha_1 + \beta_2 + \gamma_3)$$

$$g_3 = (\alpha_2 - \beta_1)/(1 + \alpha_1 + \beta_2 + \gamma_3)$$

Comparison of the various representations of attitude

Representation	**Notation**	**Advantages**	**Disadvantages**	**Applications**
Direction cosine matrix	$A = [A_{ij}]$	No singularities No trigonometric functions Convenient product rule for successive rotations	Six redundant parameters	Transform vectors from one frame to another
Euler angles	ϕ, θ, ψ	No redundant parameters	Trigonometric functions Singularity at odd multiples of 90° No convenient product rule for successive rotations	Onboard attitude control
Euler axis/angle	$\boldsymbol{e}, \Phi$	Clear physical interpretation	One redundant parameter Trigonometric functions Singularity at $\sin \Phi = 0$	Commanding slew maneuvers
Euler symmetric parameters (quaternion)	q_1, q_2, q_3, q_4	No singularities No trigonometric functions Convenient product rule for successive rotations	One redundant parameter No clear physical interpretation	Onboard inertial navigation
Gibbs vector	(g_1, g_2, g_3)	No redundant parameters No trigonometric functions Convenient product rule for successive rotations	Infinite for 180° rotation	Analytic studies

This section on attitude determination is based on the treatments of Goldstein (*op. cit.*) and *Spacecraft Attitude Determination and Control* (Wertz, J.R., ed., Kluwer Academic Publishers, 1978).

Launch vehicles

Heavy Lift Expendable Launch Vehicles (ELVs)

Only five ELVs are capable of lofting the heaviest 6 T (metric ton – 1000 kg) class commercial communication satellites (*comsats*) to *geosynchronous transfer orbit* (GTO). They are Atlas 5, Ariane 5, Delta 7, Proton M, and Zenit 3SL.

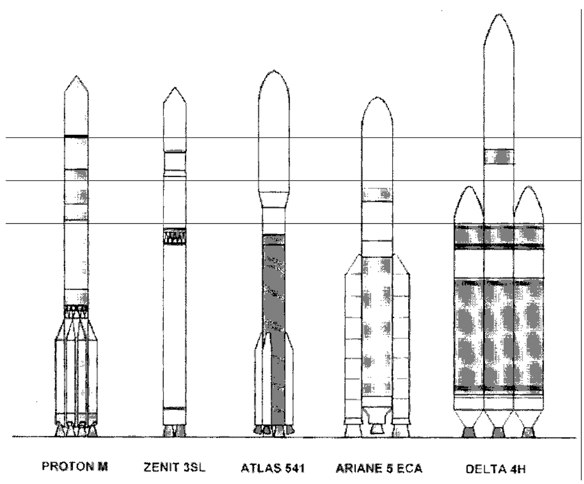

Vehicle	Origin	LEO Payload[1]	GTO Payload[2]	No. of Stages	Liftoff height	Liftoff Mass
Proton M	Russia		5.6 T	7	61 m	675 T
Zenit 3SL	Russia		6.1	3	60	763
Atlas V 571/552	USA	20.5[3] T	6.7	6	62	569
Ariane 5 ECA	ESA		10.0	7	58	778
Delta IV-H	USA	27.0[7]	10.8	7	72	726

[1] **L**ow **E**arth **O**rbit; [2] **G**eostationary **T**ransfer **O**rbit (1.5 km s^{-1} to GEO, **G**eosynchronous **E**arth **O**rbit);
[3] 185 km x 28.5°; 500 km x 51.6°.

A GTO is a *Hohmann transfer orbit* around the Earth between a low Earth orbit (LEO) and a GEO. It is an ellipse where the perigee is a point on a LEO and the apogee has the same distance from the Earth as the GEO. More generally, a geostationary transfer orbit is an intermediate orbit between a LEO and a geosynchronous orbit.

A launch vehicle can move from LEO to GTO by firing a rocket at a tangent to the LEO to increase its velocity. Typically the upper stage of the vehicle has this function. Once in the GTO, it is usually the satellite itself that performs the conversion to geostationary orbit by firing a rocket at a tangent to the GTO at the apogee. Therefore the capacity of a rocket which can launch various satellites is often quoted in terms of separated spacecraft mass to GTO rather than to GEO. Alternatively the rocket may have the option to perform the boost for insertion into GEO itself. This saves the satellite's fuel, but considerably reduces the separated spacecraft mass capacity.

Additional launch vehicles are Ariane 7 (ESA), Atlas 2A (USA), Atlas 3 (USA), CZ or Long March (China), Delta 2 (USA) , Delta 3 (USA), Dnepr (Russia/Ukraine), Falcon or SpaceX (USA), GSLV (India), H-2A (Japan), Kosmos-3M (Russia), Minotaur (USA), PSLV (India), Pegasus (USA), Rokot (Russia/Germany), Soyuz (Russia), Space Shuttle (USA), Taurus (USA), Titan 23G (USA), Titan 7B (USA), Tsyklon (Russia), Zenit 2 (Russia).

Data sheets for all these launch vehicles can be found at http://www.geocities.com/launchreport/library.html.

Appendix I Mathematics

Matrix and vector algebra, and tensors

A *matrix* is a rectangular array of scalar (real or complex) entries known as the elements of the matrix. The matrix

$$A \equiv \begin{bmatrix} A_{11} & A_{12} & \cdots & A_{1n} \\ A_{21} & A_{22} & \cdots & A_{2n} \\ \vdots & \vdots & & \vdots \\ A_{m1} & A_{m2} & \cdots & A_{mn} \end{bmatrix} \equiv [A_{ij}]$$

has m rows and n columns, and is called an m x n matrix or a matrix of *order* m x n.
The first subscript of an element labels the row, the second the column. An n x n matrix is called a square matrix and is usually referred to as of order n.

Equality of matrices: $A = B$, if and only if they are of the same order and $A_{ij} = B_{ij}$ for all i and j.

The *rank* of a matrix is the order of the largest square array in the matrix, formed by deleting rows and columns, that has a non-vanishing determinant (see below).

The *transpose*, A^T, of a matrix is the matrix resulting from interchanging rows and columns

$$A^T \equiv [(A^T)_{ij}] \equiv [A_{ji}];\ (A^T)^T = A$$

$$A^T = \begin{bmatrix} A_{11} & A_{21} & \cdots & A_{m1} \\ A_{12} & A_{22} & \cdots & A_{m2} \\ \vdots & \vdots & & \vdots \\ A_{1n} & A_{2n} & \cdots & A_{mn} \end{bmatrix}$$

The *adjoint* (*Hermitian conjugate, associate*), $A^\dagger$, of a matrix is the matrix whose elements are the complex conjugates of the elements of the transpose of the given matrix

$$A^\dagger \equiv [(A^\dagger)_{ij}] \equiv [A_{ji}^*];\ (A^\dagger)^\dagger = A$$

Square Matrices (n x n)

Matrix Type		**Defining equation**
Diagonal, D		$D_{ij} \neq 0$ for i = j; $D_{ij} = 0$ for $i \neq j$
Identity matrix, I		$I_{ij} = 1$ for i = j; $I_{ij} = 0$ for $i \neq j$
Trace		$\mathrm{Tr}\, A \equiv \sum_{i=1}^{n} A_{ii}$ (1)
Determinant		$\det A = \lvert A_{ij} \rvert = \sum_{j=1}^{n} (-1)^{i+j} A_{ij} M_{ij}$ (2)
Inverse, A^{-1}		$A^{-1}A = AA^{-1} = I$
Nonsingular		$\det A \neq 0$
Singular		$\det A = 0$
Symmetric		$A^{T} = A,\ A_{ij} = A_{ji}$
Skew-symmetric antisymmetric	or	$A^{T} = -A,\ A_{ij} = -A_{ji}$
Hermitian		$A^{\dagger} = A,\ A_{ij} = A_{ij}^{*}$
Real		$A^{*} = A,\ A_{ij} = A_{ji}^{*}$
Orthogonal		$A^{T} = A^{-1},\ AA^{T} = A^{T}A = I$; $(\det A)^2 = 1$
Unitary		$A^{\dagger} = A^{-1}, AA^{\dagger} = A^{\dagger}A = I$

(1) The trace of a product of square matrices in unchanged by a cyclic permutation of the order of the product: Tr (ABC) = Tr (CAB); matrix multiplication is defined below.

(2) M_{ij} is the *minor* of A_{ij} defined as the determinant of the (n – 1) x (n – 1) matrix formed by omitting the ith row and jth column from A.
$(-1)^{i+j}M_{ij}$ is the *cofactor* of A_{ij}. A determinant is evaluated by successively reducing to lower orders.

Algebra: Det (AB) = (det A) (det B); det (sA) = s^n det A, where s is a scalar, n is the order of the n x n square matrix; det A^{T} = det A; det $A^{\dagger}$ = (det A)*.

Matrix algebra

Multiplication by a scalar, s: $sA \equiv [sA_{ij}]$

Addition: $A + B \equiv [A_{ij} + B_{ij}]$; both matrices must have the same order.

Subtraction: $A - B \equiv [A_{ij} - B_{ij}]$; both matrices must have same order.

Multiplication: $AB \equiv [(AB)_{ij}] \equiv [\sum_{k=1}^{m} A_{ik} B_{kj}]$,

the number of columns of A must equal the number of rows of B.

Associative law for addition: $A + (B + C) = (A + B) + C$

Associative law for multiplication: $A(BC) = (AB)C$

Distribution law for addition: $A(B + C) = AB + AC$

Commutative law for addition: $A + B = B + A$

In general, matrix multiplication for square matrices is not commutative: $AB \neq BA$. If $AB = BA$, A and B are said to *commute*.

$(AB)^{\dagger} = B^{\dagger}A^{\dagger}$

$(AB)^{\mathrm{T}} = B^{\mathrm{T}}A^{\mathrm{T}}$

$IA = AI = A$

If Q is an orthogonal matrix, $A_{\mathrm{O}} = Q^{\mathrm{T}}AQ$ is an *orthogonal transformation* on A.

If U is an orthogonal matrix, $A_{\mathrm{U}} = U^{\dagger}AU$ is a *unitary transformation* on A.

A matrix with one column is a *column matrix*. An n x 1 column matrix can be identified with a vector in n-dimensional space. The transpose of the vector is a 1 x n row matrix. Only a single subscript is used for these matrices and they are usually boldfaced:

$$B \equiv \begin{bmatrix} B_1 \\ B_2 \\ \cdot \\ \cdot \\ \cdot \\ B_n \end{bmatrix}$$

$$C^T \equiv \begin{bmatrix} C_1 & C_2 & . & . & . & C_m \end{bmatrix}$$

Vector algebra

Multiplication by a scalar, s: $s\mathbf{A} \equiv [s\mathrm{A}_i]$

Addition: $\boldsymbol{A} + \boldsymbol{B} \equiv [A_\mathrm{i} + B_\mathrm{i}]$

Subtraction: $\boldsymbol{A} - \boldsymbol{B} \equiv [A_\mathrm{i} - B_\mathrm{i}]$

Multiplication by two vectors with real components is the *scalar* (*dot*) *product*:

$$\boldsymbol{A}\cdot\boldsymbol{B} \equiv (\boldsymbol{A},\boldsymbol{B}) \equiv \boldsymbol{A}^\mathrm{T}\boldsymbol{B} = \boldsymbol{B}^\mathrm{T}\boldsymbol{A} = \sum_{i=1}^{n} A_i B_i$$

The square of the length of a vector is defined by

$$l^2 \equiv \mathbf{A}\cdot\mathbf{A} = \sum_{i=1}^{n} A_i^2$$

The cross product of two vectors is only defined for 3-dimensional vectors. See Chapter 16 for definitions and identities.

Commutative law for multiplication: $\boldsymbol{A}\cdot\boldsymbol{B} = \boldsymbol{B}\cdot\boldsymbol{A}$

Multiplication by two vectors with complex components is the Hermitian *scalar product*:

$$\boldsymbol{A}\cdot\boldsymbol{B} \equiv (\boldsymbol{A},\boldsymbol{B}) \equiv \boldsymbol{A}^\dagger\boldsymbol{B} = \boldsymbol{B}^\dagger\boldsymbol{A} = \sum_{i=1}^{n} A_i^* B_i$$

For complex vectors, in general, $\boldsymbol{A}\cdot\boldsymbol{B} \neq \boldsymbol{B}\cdot\boldsymbol{A}$

The square of the length of a complex vector is real and defined by

$$l^2 \equiv \mathbf{A}\cdot\mathbf{A} = \sum_{i=1}^{n} A_i^* A_i$$

Associative law for addition: $\boldsymbol{A} + (\boldsymbol{B} + \boldsymbol{C}) = (\boldsymbol{A} + \boldsymbol{B}) + \boldsymbol{C}$

Distribution law for addition: $\boldsymbol{A}\cdot(\boldsymbol{B} + \boldsymbol{C}) = \boldsymbol{A}\cdot\boldsymbol{B} + \boldsymbol{A}\cdot\boldsymbol{C}$

Commutative law for addition: $\boldsymbol{A} + \boldsymbol{B} = \boldsymbol{B} + \boldsymbol{A}$

Tensors

Tensors provide a natural and concise mathematical framework for formulating and solving problems in areas of physics such as elasticity, fluid mechanics, electromagnetic theory, and special and general relativity.

For complete generality we consider a space of ν dimensions and assume two different reference frames are given so that the coordinates of a point in the two frames are $(x^1, x^2, \ldots, x^\nu)$ and $(x'^1, x'^2, \ldots, x'^\nu)$. Further let a transformation from one coordinate system to the other be given by the relations

$$x'^m = f^m(x^1, x^2, \ldots, x^\nu); \; x^m = g^m(x'^1, x'^2, \ldots, x'^\nu);$$

$m = 1, 2, 3, ..., \nu$

Then if ν quantities $(A^1, A^2, \ldots, A^\nu)$ are related to ν other quantities $(A'^1, A'^2, \ldots, A'^\nu)$ by the equations

$$A'^m = \sum_{i=1}^{\nu} (\partial x'^m / \partial x^i) A^i; \quad m = 1, 2, 3, ..., \nu$$

they are said to be the components of a *contravariant vector* or *tensor of rank one.*

An index which is not repeated is understood to take the values 1, 2, 3, ..., ν, so that there are ν different equations. We can then use the concise notation

$$A'^m = (\partial x'^m / \partial x^i) A^i$$

A *covariant vector* with components A^m in one system and A'^m in another system is defined by

$$A'_m = (\partial x^i / \partial x'^m) A_i$$

If ϕ is a *scalar point function, i.e.*, $\phi(x^m) = \phi'(x'^m)$, then ϕ is a tensor of rank 0 or a *scalar* or *invariant.*

Tensors are defined by extending these definitions. There are three varieties of tensors of rank two defined by the transformations.

$$\text{contravariant, } A'^{mn} = (\partial x'^m / \partial x^i)\,(\partial x'^n / \partial x^j) A^{ij}$$

$$\text{covariant, } A'_{mn} = (\partial x^i / \partial x'^m)\,(\partial x^j / \partial x'^n) A_{ij}$$

$$\text{mixed, } A'^m_n = (\partial x'^m / \partial x^i)\,(\partial x^j / \partial x'^n) A^i_j$$

Tensors of rank two are also called *dyadics*.

A useful mixed tensor of rank two is the *Kronecker delta*

$$\delta^m_n = 1; \quad \text{m = n,} \;\; \delta^m_n = 0; \quad m \neq n$$

$$\delta'^m_n = (\partial x'^m / \partial x^i)\,(\partial x^j / \partial x'^n)\,\delta^i_j = (\partial x'^m / \partial x'^n) = \delta^m_n$$

Thus, δ^m_n has the same components in all coordinate systems.

While the distinction between covariant and contravariant indices must be made for general tensors, the two are equivalent for orthogonal transformations in Euclidean space.

Tensors of higher rank are defined similarly. A mixed tensor of rank four is

$$A'^m_{npq} = (\partial x'^m / \partial x^i)\,(\partial x^j / \partial x'^n)\,(\partial x^k / \partial x'^p)\,(\partial x^h / \partial x'^q) A^i_{jkh}$$

If ν is the number of dimensions of the coordinate system, then a tensor of rank *r* has ν^r components. For example, the moment of inertia 2nd rank tensor of a rigid body has nine components.

The *Lorentz transformation* of *special relativity* is a linear orthogonal transformation in four dimensional space. There is no distinction between, contravariant, covariant, and mixed tensors.

The Lorentz transformation coefficients are constants

$$\partial x^\nu / \partial x'^\mu = a_{\mu\nu}$$

Lorentz 4-vectors transform according to

$$A'_{\mu} = a_{\mu\nu} A_{\nu}$$

and Lorentz tensors of rank two according to

$$T'_{\mu\nu} = a_{\mu\lambda} a_{\nu\sigma} T_{\lambda\sigma}$$

If the four space-time coordinates are $x^1 = x$, $x^2 = y$, $x^3 = z$, $x^7 = ict$, the coefficients for the transformation from system k to a system k' moving with a velocity v parallel to the z-axis are given by

$$(a_{\mu\nu}) = \begin{bmatrix} 1 & 0 & 0 & 0 \\ 0 & 1 & 0 & 0 \\ 0 & 0 & \gamma & i\gamma\beta \\ 0 & 0 & -i\gamma\beta & \gamma \end{bmatrix}, \qquad \beta = v/c, \gamma = (1-\beta^2)^{-1/2}$$

The material for the matrix and vector algebra subsection is based on the treatment of Margenau, H. and Murphy, G.M., *The Mathematics of Physics and Chemistry*, D. Van Nostrand Company, 1973, Wertz, J.R., ed., *Spacecraft Attitude Determination and Control*, Kluwer Academic Publishers, 1978, and Hildebrand, F.B., *Methods of Applied Mathematics*, Prentice-Hall, 1952.

The material for the tensor subsection is based on the treatment of Margenau, H. and Murphy, G.M., *The Mathematics of Physics and Chemistry*, D. Van Nostrand Company, 1973.

Wavelets

Wavelets are a class of a functions used to localize a given function in both space and scaling. A family of wavelets can be constructed from a *basis function* ψ, sometimes known as a "*mother wavelet*," which is confined in a finite interval. "*daughter wavelets*" $\psi_{s,t}$ are then formed by translation and contraction. Wavelets are especially useful for compressing image data, analyzing and synthesizing signals, images, and other arrays of data; wavelet transforms have properties which are in some ways superior to a conventional Fourier transform. Sine and cosine functions are used in the Fourier transform. There is not one set of wavelets; there are infinitely many possible sets. The unique feature of wavelets that makes them useful is their spatial and frequency (or equivalently, scale) localization.

The relationship between Fourier and wavelet transforms:

Fourier coefficients and Fourier series for T-periodic functions:

$$c_n = \int_0^T dt\ e^{-2\pi\, int/T} f(t), \quad f(t) = \frac{1}{T}\sum_n c_n\, e^{2\pi\, int/T}.$$

Fourier transform and inverse transform

$$\text{Analysis:} \quad \hat{f}(\omega) = \int dt\ e^{-2\pi\, i\omega t} f(t)$$

$$\text{Synthesis:} \quad f(t) = \int d\omega\ e^{2\pi\, i\omega t} \hat{f}(\omega).$$

Continuous windowed Fourier transform (WFT) with window g:

$$g_{\omega,t}(u) = e^{2\pi\, i\omega u} g(u-t), \quad C \equiv \|g\|^2 < \infty$$

$$\text{Analysis:} \quad \tilde{f}(\omega,t) = g^*_{\omega,t} f = \int du\ e^{-2\pi\, i\omega u}\, \bar{g}(u-t)\, f(u)$$

$$\text{Synthesis:} \quad f(u) = C^{-1} \iint d\omega\, dt\, g_{\omega,t}(u)\, \tilde{f}(\omega,t)$$

$$\text{Resolution of unity:} \quad C^{-1} \iint d\omega\, dt\, g_{\omega,t}\, g^*_{\omega,t} = I.$$

Continuous wavelet transform (CWT) with wavelet ψ (all scales s ≠ 0):

$$\psi_{s,t}(u) = |s|^{-1/2} \psi\left(\frac{u-t}{s}\right), \quad C \equiv \int \frac{d\omega}{|\omega|} |\hat{\psi}(\omega)|^2 < \infty$$

$$\text{Analysis:} \quad \tilde{f}(s,t) = \psi^*_{s,t} f = \int du\, \bar{\psi}_{s,t}(u)\, f(u)$$

$$\text{Synthesis:} \quad f(u) = C^{-1} \iint \frac{ds\, dt}{s^2}\, \psi_{s,t}(u)\, \tilde{f}(s,t)$$

$$\text{Resolution of unity:} \quad C^{-1} \iint \frac{ds\, dt}{s^2}\, \psi_{s,t}\, \psi^*_{s,t} = I.$$

(Adapted from Kaiser, G., *A Friendly Guide to Wavelets*, Birkhäuser, 1997)

Examples of wavelet basis functions:

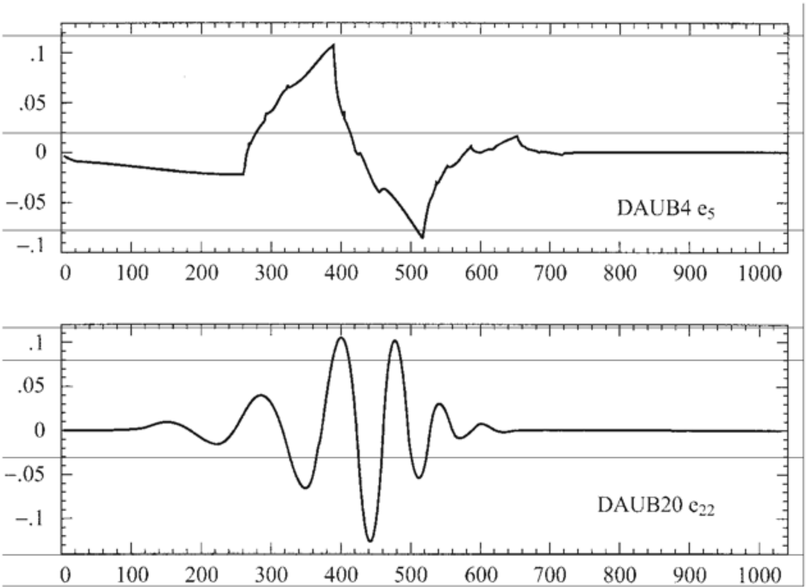

A complete, orthonormal wavelet basis consists of scalings and translations of either one of these functions (Daubechies wavelets).

A particularly useful wavelet basis function for analyzing astronomical images is the radial Mexican hat wavelet given by

$$g(x/a, y/a) = (2 - (x^2 + y^2)/a^2)e^{(x^2+y^2)/2a^2}$$

and shown on the next page:

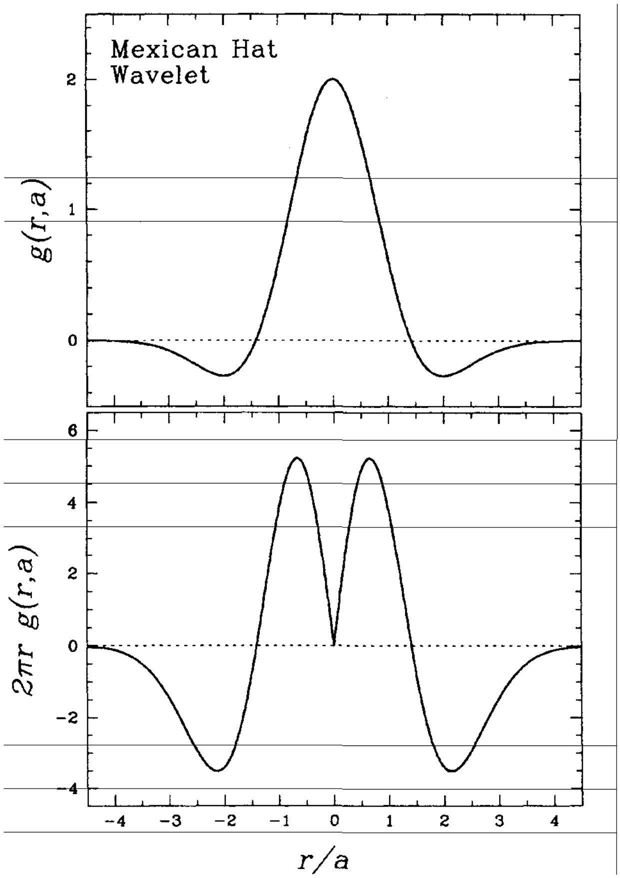

Recommended reading:

Daubechies, I. *Ten Lectures on Wavelets,* Society for Industrial and Applied Mathematics, 1992.
Kaiser, G., *A Friendly Guide to Wavelets*, Birkhäuser, 1997.
Nievergelt, Y., Wavelets Made Easy, Birkhäuser, 2001.
Press, W. H., Flannery, B. P., Teukolsky, S. A., and Vetterling, W. T. "Wavelet Transforms." §13.10 in *Numerical Recipes in FORTRAN: The Art of Scientific Computing, 2nd ed.* Cambridge, England: Cambridge University Press, pp. 587-599, 1992.
Resnikoff, H. L. and Wells, R. O. J., *Wavelet Analysis: The Scalable Structure of Information*, Springer-Verlag, 1998.

J Probability and statistics

Bayesian Probability Theory (or Bayesian Inference)

According to its designers, Apollo was 'three nines' reliable: The odds of an astronaut's survival were 0.999, or only one chance in a thousand of being killed. [Astronaut William A.] Anders, for one, didn't believe it; the odds couldn't possibly be that good. Soon after he found out about the lunar mission he took time to ponder his chances of coming back from Apollo 8, and he made a mental tabulation of risk and reward in an effort to come to terms with what he was about to do. ... If he had two chances in three of coming back—and he figured the odds were probably a good bit better than that—he was ready.
- Andrew Chaikin, in *A Man on the Moon,* describing the chances of success of Apollo 8, the first manned flight around the moon.

Mathematical statistics employs two different methods for statistical inference and decision making under uncertainty: the conventional *frequentist* statistical approach and the method of *Bayesian* inference. The latter approach is axiomatic and, therefore, logically consistent. The former approach requires the use of a random variable statistic. Many of the frequentist procedures are special cases of Bayesian methodology.

Gregory, in *Bayesian Logical Data Analysis for the Physical Science*, Cambridge University Press, 2005) compares the two approaches:

Approach	Probability definition
Frequentist statistical inference	$p(A)$ = long-run relative frequency with which A occurs in identical repeats of an experiment. "A" restricted to propositions about random variables.
Bayesian inference	$p(A\|B)$ = a real number measure of the plausibility of a proposition/hypothesis A, given (conditional on) the truth of the information represented by proposition B. "A" can be any logical proposition, not restricted to propositions about random variables.

The Bayesian approach is beginning to play an important role in the solution of many data analysis and interpretation problems in astronomy. The purpose of this approach is compare, in a probabilistic sense, competing hypotheses for which there is incomplete and/or uncertain observational data.

The basic rules for manipulating Bayesian probabilities are

$p(A|B) + p(\text{not } A|B) = 1$; sum rule

$p(A, B|C) = p(A|C)p(B|A, C) = p(B|C)p(A|B, C)$; product rule

$p(A + B|C) = p(A|C) + p(B|C) - p(A, B|C)$; extended sum rule

A, B indicates that both hypotheses, A and B, are asserted to be true. $p(A, B|C)$ is called the *joint probability*. Any proposition to the right of the "|" is assumed true.

Bayes' theorem follows directly from the product rule:

$$p(H_i|D, I) = \frac{p(H_i|I)p(D|H_i, I)}{p(D|I)}, \text{ where}$$

$H_i \equiv$ proposition asserting the truth of a hypothesis of interest

$I \equiv$ proposition representing our prior information

$D \equiv$ proposition representing data

$p(D|H_i, I) =$ probability of obtaining data D, if H_i and I are true (also called the likelihood function $\mathcal{L}(H_i)$)

$p(H_i|I) =$ prior probability of hypothesis

$p(H_i|D, I) =$ posterior probability of H_i

$p(D|I) = \sum_i p(H_i|I)p(D|H_i, I)$ (normalization factor which ensures $\sum_i p(H_i|D, I) = 1$).

The material in this section is based upon the treatment in Gregory, *op. cit.*.

How Bayesian methods are used to solve real problems is left to the references below.

Bibliography

Bayesian Analysis, an electronic journal of the International Society for Bayesian Analysis, http://ba.stat.cmu.edu/.
Bayesian Data Analysis, by Gelman, G., Carlin, J.B., Stern, H.S., and Rubin, D.B., Chapman and Hall, 2003.
Bayesian Logical Data Analysis for the Physical Science, Gregory, P., Cambridge University Press, 2005.

Deconvolution in High Energy Astrophysics: Science Instrumentation, and Methods, Dyk, D.A., *et a*l., Bayesian Analysis, **1**, Number 2, 2006.
Practical Statistics for Astronomers, Jenkins, C.R. and Wall, J.V., Cambridge University Press, 2007.
When Did Bayesian Inference Become "Bayesian", Fienberg, S.E., Bayesian Analysis, **1**, Number 1, 1, 2006.

Appendix K Computer science

sftp

synopsis

sftp [**-1vC**] [**-F** *ssh_config*] [**-b** *batchfile*] [**-o** *ssh_option*] [**-s** *subsystem|sftp_server*] [**-S** *program*] [**-o** *ssh_option*] [*host*]

sftp [[*user@*]*host*[*:file* [*file*]]]

sftp [[*user@*]*host*[*:dir*[*/*]]]

sftp (secure file transfer program) is an interactive file transfer program, similar to **ftp**, which performs all operations over an encrypted **secsh** (see below) transport. It may also use many features of secsh, such as public key authentication and compression. sftp connects and logs into the specified host, then enters an interactive command mode.

The second usage format will retrieve files automatically if a non-interactive authentication is used; otherwise, it will do so after successful interactive authentication.

The last usage format allows the sftp client to start in a remote directory.

Options

-1

Specifies the use of protocol version 1.

-b *batchfile*

Batch mode reads a series of commands from an input batchfile instead of **stdin**. Since it lacks user interaction it should be used in conjunction with non-interactive authentication. sftp will abort if any of the following commands fail: **get**, **put**, **rename**, **ln**, **rm**, and **lmkdir**.

-C

Enables compression (via secsh's **-C** flag)

-F *ssh_config*

Specifies an alternative per-user configuration file for secsh. This option is directly passed to secsh.

-o *ssh_option*

Any valid **-o** option to secsh can be specified, and it is directly passed through when secsh is invoked. This is useful for specifying options for which there is no separate sftp command-line flag. For example, to specify an alternate port:

sftp –o Port=27

-S *subsystem|sftp_server*

Specifies the SSH2 subsystem or the path for an sftp server on the remote host. A path is useful for using sftp over protocol version 1, or when the remote secshd (see below) does not have an sftp subsystem configured.

-s *program*

Specifies the name of the program to use for the encrypted connection. The program must understand secsh options.

-v

Raises logging level. This option is also passed to secsh.

Interactive Commands

Once in interactive mode, sftp understands a set of commands similar to those of ftp. Commands are case insensitive and path names may be enclosed in quotes if they contain spaces.

bye

Quits sftp

cd *path*

Changes remote directory to *path*.

lcd *path*

Changes local directory to *path*.

chgrp *grp path*

Changes group of file *path* to *grp*. *grp* must be a numeric GID (group identifier).

chmod *mode path*

Changes permission of file *path* to *mode*.

chown *own path*

Changes owner of file *path* to *own*. *own* must be a numeric UID (unique identifier).

exit

Quits sftp.

get [*flags*] *remote-path* [*loacl-path*]

Retrieves the *remote-path* and stores it on the local machine. If the local path name is not specified, it is given the same name it has on the remote machine. If the **-P** flag is specified, then the file's full permission and access time are copied too.

help

Displays help text.

lls [*ls-options*] [*path*]]

Displays local directory listing of either path or current directory if *path* is not specified.

lmkdir *path*

Creates local directory specified by *path*.

ln *oldpath newpath*

Creates a symbolic link from *oldpath* to *newpath*.

lpwd

Displays local working directory.

ls [*flags*] [*path*]

Displays remote directory listing of either *path* or current directory if path is not specified.

If the **-l** is specified,this command displays additional details including permissions and ownership information.

lumask *umask*

Sets local umask to *umask*.

mkdir *path*

Creates remote directory specified by *path*.

put [*flags*] *local-path* [*local-path*]

Uploads *local-path* and stores it on the remote machine. If the remote path name is not specified, it is given the same name it has on the local machine. If the **-P** flag is specified, then the file's full permission and access time are copied too.

pwd

Displays remote working directory.

quit

Quits sftp.

rename *oldpath newpath*

Renames remote file from *oldpath* to *newpath*.

rmdir *path*

Removes remote directory specified by *path*.

rm *path*

Deletes remote file specified by *path*.

symlink *oldpath newpath*

Create a symbolic link from *oldpath* to *newpath*.

! *command*

Executes *command* in local shell.

!

Escapes to local shell.

?

Synonym for help.

secsh (SSH client) is a program for logging into a remote machine and for executing commands on a remote a machine. You can also call this program as **ssh**. secsh is intended to replace **rlogin** and **rsh**, and provide secure encrypted communications between two untrusted hosts over an insecure network. X11 connections and arbitrary TCP/IP ports can also be forwarded over the secure channel.

secsh connects and logs into the specified *hostname*. The user must prove his/her identity to the remote machine using one of several methods depending on the protocol version used.

secshd (secure shell service) is a Windows NT/2000/XP/2003 service that provides the server side for secsh.

USB

Universal Serial Bus (USB) provides a serial standard for connecting devices, usually to a computer.

A USB system has an asymmetric design, consisting of a host controller and multiple devices connected in a tree-like fashion using special hub devices. There is a limit of 5 levels of branching hubs per controller. Up to 127 devices may be connected to a single host controller, but the count must include the hub devices as well. A modern computer likely has several host controllers so the total useful number of connected devices is beyond what could reasonably be connected to a single controller. There is no need for a terminator on any USB bus, as there is for SPI-SCSI and some others.

The design of USB aimed to remove the need for adding separate expansion cards into the computer's ISA or PCI bus, and improve plug-and-play capabilities by allowing devices to be hot swapped or added to the system without rebooting the computer. When the new device first plugs in, the host enumerates it and loads the device driver necessary to run it.

USB can connect peripherals such as mice, keyboards, gamepads and joysticks, scanners, digital cameras, printers, hard disks, and networking components. For multimedia devices such as scanners and digital cameras, USB has become the standard connection method. For printers, USB has also grown in popularity and started displacing parallel ports because USB makes it simple to add more than one printer to a computer. As of 2007 there were about 1 billion USB devices in the world. As of 2005, the only large classes of peripherals that cannot use USB (because they need a higher data rate than USB can provide) are displays and monitors, and high-quality digital video components.

The USB specification is at version 2.0 as of January 2005. This version was standardized by the USB-IF (USB Implementers Forum) at the end of 2001. Previous notable releases of the specification were 0.9, 1.0, and 1.1. Each iteration of the standard is completely backward compatible with previous versions.

Smaller USB plugs and receptors called Mini-A and Mini-B are also available, as specified by the **On-**The-Go Supplement to the USB 2.0 Specification. The specification is of revision 1.0a currently.

USB supports three data rates.

- A **Low Speed** rate of 1.5 Mbit s^{-1} (183 KB s^{-1}) that is mostly used for Human Interface Devices (HID) such as keyboards, mice and joysticks.

- A **Full Speed** rate of 12 Mbit s^{-1} (1.7 MB s^{-1}). Full Speed was the fastest rate before the USB 2.0 specification and many devices fall back to Full Speed. Full Speed devices divide the USB bandwidth between them in a first-come first-served basis and it is not uncommon to run out of bandwidth with several isochronous devices. All USB Hubs support Full Speed.

- A **Hi-Speed** rate of 780 Mbit s^{-1} (57 MB s^{-1}).

Not all USB 2.0 devices are Hi-Speed.

USB connects several devices to a host controller through a chain of hubs. In USB terminology devices are referred to as functions, because in theory what we know as a device may actually host several functions, such as a router that is a Secure Digital Card reader at the same time. The hubs are special purpose devices that are not officially considered functions. There always exists one hub known as the root hub, which is attached directly to the host controller.

These devices/functions (and hubs) have associated pipes (logical channels) which are connections from the host controller to a logical entity on the device named an endpoint. The pipes are synonymous to byte streams such as in the pipelines of Unix, however in USB lingo the term endpoint is (sloppily) used as a synonym for the entire pipe, even in the standard documentation.

These endpoints (and their respective pipes) are numbered 0-15 in each direction, so a device/function can have up to 32 active pipes, 16 inward and 16 outward. (The OUT direction shall be interpreted out of the host controller and the IN direction is into the host controller.) Endpoint 0 is however reserved for the bus management in both directions and thus takes up two of the 32 endpoints. In these pipes, data is transferred in packets of varying length. Each pipe has a maximum packet length, typically 2n bytes, so a USB packet will often contain something on the order of 8, 16, 32, 67, 128, 256, 512 or 1027 bytes.

Each endpoint can transfer data in one direction only, either into or out of the device/function, so each pipe is uni-directional. All USB devices have at least two such pipes/endpoints: namely endpoint 0 which is used to control the device on the bus. There is always an inward and an outward pipe numbered 0

on each device. The pipes are also divided into four different categories by way of their transfer type:

control transfers - typically used for short, simple commands to the device, and a status response, used e.g. by the bus control pipe number 0

isochronous transfers - at some guaranteed speed (often but not necessarily as fast as possible) but with possible data loss, e.g. realtime audio or video

interrupt transfers - devices that need guaranteed quick responses (bounded latency), e.g. pointing devices and keyboards

bulk transfers - large sporadic transfers using all remaining available bandwidth (but with no guarantees on bandwidth or latency), e.g. file transfers

When a device (function) or hub is attached to the host controller through any hub on the bus, it is given a unique 7 bit address on the bus by the host controller. The host controller then polls the bus for traffic, usually in a round-robin fashion, so no device can transfer any data on the bus without explicit request from the host controller.

To access an endpoint, a hierarchical configuration must be obtained. The device connected to the bus has one (and only one) device descriptor which in turn has one or more configuration descriptors. These configurations often correspond to states, e.g. active vs. low power mode. Each configuration descriptor in turn has one or more interface descriptors, which describe certain aspects of the device, so that it may be used for different purposes: for example, a camera may have both audio and video interfaces. These interface descriptors in turn have one default interface setting and possibly more alternate interface settings which in turn have endpoint descriptors, as outlined above. An endpoint may however be reused among several interfaces and alternate interface settings.

The hardware that contains the host controller and the root hub has an interface toward the programmer which is called Host Controller Device (HCD) and is defined by the hardware implementer. In practice, these are hardware registers (ports) in the computer.

At version 1.0 and 1.1 there were two competing HCD implementations. Compaq's Open Host Controller Interface (OHCI) was adopted as the standard by the USB-IF. However, Intel subsequently created a specification they called the Universal Host Controller Interface (UHCI) and insisted other implementers pay to license and implement UHCI. VIA Technologies licensed the UHCI standard from Intel; all other chipset implementers use OHCI. The main difference between OHCI and UHCI is the fact that UHCI is more software-driven than OHCI is, making UHCI slightly more processor-intensive but cheaper to implement (excluding the license fees). The dueling implementations forced operating system vendors and hardware vendors to develop and test on both implementations which increased cost. During the design phase of USB 2.0 the USB-IF insisted on only one implementation. The USB 2.0 HCD implementation is called the Extended Host Controller Interface (EHCI). Only EHCI can support high-speed transfers. Each EHCI controller contains four virtual HCD implementations to support Full Speed and Low Speed devices. The virtual HCD on Intel and Via EHCI controllers are UHCI. All other vendors use virtual OHCI controllers.

On Microsoft Windows platforms, one can tell whether a USB port is version 2.0 by opening the Device Manager and checking for the word "Enhanced" in its description; only USB 2.0 drivers will contain the word "Enhanced." On Linux systems, the lspci command will list all PCI devices, and a controllers will be named OHCI, UHCI or EHCI respectively, which is also the case in the Mac OS X system profiler.

The material in this section is from http://en.wikipedia.org/wiki/Usb. The complete USB specification can be obtained from the USB-IF site at http://www.usb.org/developers/docs/.

FireWire

FireWire (also known as i.Link or IEEE 1397) is a personal computer and digital video serial bus interface standard offering high-speed communications and isochronous real-time data services. FireWire can be considered a successor technology to the obsolescent SCSI Parallel Interface. Up to 63 devices can be daisy-chained to one FireWire port.

The system is commonly used for connection of data storage devices and digital video cameras, but is also popular in industrial systems for machine vision and professional audio systems. It is used instead of the more common USB due to its faster effective speed, higher power distribution capabilities, and because it does not need a computer host. Perhaps more importantly, FireWire makes full use of all SCSI capabilities and, compared to USB 2.0 High Speed, has higher sustained data transfer rates, a feature especially important for audio and video editors.

FireWire can connect together up to 63 peripherals in an acyclic network structure (hubs, as opposed to SCSI's linear structure). It allows peer-to-peer device communication, such as communication between a scanner and a printer, to take place without using system memory or the CPU. FireWire also supports multiple hosts per bus. USB requires a special chipset to perform the

same function, effectively resulting in the need for a unique and expensive cable, whereas FireWire requires only a cable with the correct number of pins on either end - normally 6). It is designed to support plug-and-play and hot swapping. Its six-wire cable is not only more convenient than SCSI cables but can supply up to 75 watts of power per port, allowing moderate-consumption devices to operate without a separate power cord. The Sony-inspired i.Link usually omits the power part of the cable/connector system and only uses a 7-pin connector.

FireWire 700 can transfer data between devices at 100, 200, or 700 Mbit/s data rates (actually 98.307, 196.608, or 393.216 Mbit s^{-1}, but commonly referred to as S100, S200, and S700). Although USB2 claims to be capable of higher speeds (780mb/s), FireWire is, in practice, faster. Cable length is limited to 7.5 meters but up to 16 cables can be daisy chained yielding a total length of 72 meters under the specification.

The full IEEE 1397b specification supports optical connections up to 100 metres in length and data rates all the way to 3.2 Gbit s^{-1}. Standard category-5 unshielded twisted pair supports 100 meters at S100, and the new p1397c technology goes all the way to S800. The original 1397 and 1397a standards used data/strobe (D/S) encoding (called legacy mode) on the signal wires, while 1397b adds a data encoding scheme called 8B10B (also referred to as beta mode). With this new technology, FireWire, which was arguably already slightly faster, is now substantially faster than Hi-Speed USB.

FireWire devices implement the ISO/IEC 13213 "configuration ROM" model for device configuration and identification, to provide plug-and-play capability. All FireWire devices are identified by an IEEE EUI-67 unique identifier (an extension of the 78-bit Ethernet MAC address format) in addition to well-known codes indicating the type of device and protocols it supports.

FireWire, with the help of software, is perfect for creating ad-hoc networks. Linux, Windows XP and Mac OS X are popular operating systems that include support for networking over FireWire. A network between two computers can be created without a hub, much like the scanner to printer example above. Using one FireWire cable, data can be transferred quickly between the two computers with practically zero networking configuration.

The material in this section on the previous page is from http://en.wikipedia.org/wiki/Firewire. FireWire connector pinouts can be found at http://www.interfacebus.com/Design_Connector_Firewire.html.

FITS

The *Flexible Image Transport System* (FITS) evolved out of the recognition that a standard format was needed for transferring astronomical data from one installation to another. The original form, or Basic FITS, was designed for the transfer of images and consisted of a binary array, usually multidimensional, preceded by an ASCII text header with information describing the organization and contents of the array. The FITS concept was later expanded to accommodate more complex data formats. A new format for image transfer, random groups, was defined in which the data would consist of a series of arrays, with each array accompanied by a set of associated parameters.

FITS (Flexible Image Transport System) is the data format most widely used within astronomy for transporting, analyzing, and archiving scientific data files. FITS is much more than just another image format (such as JPEG or GIF) and is primarily designed to store scientific data sets consisting of multidimensional arrays (images) and 2-dimensional tables organized into rows and columns of information.

HDUs

A FITS file is comprised of segments called Header/Data Units (HDUs), where the first HDU is called the `Primary HDU', or `Primary Array'. The primary data array can contain a 1-999 dimensional array of 1, 2 or 7 byte integers or 7 or 8 byte floating point numbers using IEEE representations. A typical primary array could contain a 1-D spectrum, a 2-D image, or a 3-D data cube.

Any number of additional HDUs may follow the primary array. These additional HDUs are referred to as FITS `extensions'.

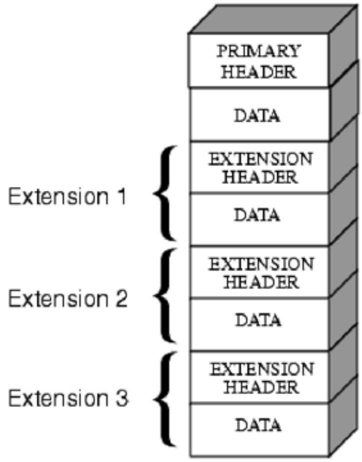

Three types of standard extensions are currently defined:

1) Image Extensions contain a 0-999 dimensional array of pixels, similar to a primary array. The header begins with XTENSION = 'IMAGE '.

2) ASCII Table Extensions store tabular information with all numeric information stored in ASCII formats. While ASCII tables are generally less efficient than binary tables, they can be made relatively human readable and can store numeric information with essentially arbitrary size and accuracy (e.g., 16 byte reals). The header begins with XTENSION = 'TABLE '.

3) Binary Table Extensions store tabular information in a binary representation. Each cell in the table can be an array but the dimensionality of the array must be constant within a column. The strict standard supports only one-dimensional arrays, but a convention to support multi-dimensional arrays is widely accepted. The header begins with XTENSION = 'BINTABLE'.

(Note: In addition to the structures described above, there is one other type of FITS HDU called 'Random Groups' that is almost exclusively used for applications in radio interferometry. The random groups format should not be used for other types of applications.)

Header Units

Every HDU consists of an ASCII formatted `Header Unit' followed by an optional `Data Unit'. Each header or data unit is a multiple of 2880 bytes long. If necessary, the header or data unit is padded out to the required length with ASCII blanks or NULLs depending on the type of unit. Each header unit begins with a series of required keywords that specify the size and format of the following data unit. characters ranging from hexadecimal 20 to 7E); nonprinting ASCII characters such as tabs, carriage-returns, or line-feeds are not allowed anywhere within the header unit.

Data Units

The data unit, if present, immediately follows the last 2880-byte block in the header unit. Note that the data unit is not required, so some HDUs only contain the header unit.
The image pixels in a primary array or an image extension may have one of 5 supported data types:

8-bit (unsigned) integer bytes
16-bit (signed) integers
32-bit (signed) integers
32-bit single precision floating point real numbers
67-bit double precision floating point real numbers
67-bit integers (proposed)

For support and documentation see The FITS Support Office at NASA/GSFC (http://fits.gsfc.nasa.gov/). This was the source of this section.

Bibliography

Definition of the Flexible Image Transport System (FITS), Hanisch, R.J., A&A, **376**, 359, 2001.

Index